THE ORIGIN OF RECUMBENT FOLD NAPPES: THE LOCHALSH FOLD AS THE MAIN EXAMPLE.

by Graham John Potts

Submitted in fulfilment of the requirements for the degree of Doctor of Philosopy.

Department of Earth Sciences
The University of Leeds
Leeds

Submitted January 1983.

Abstract

This thesis describes structural studies of the Kishorn and Balmacara Nappes of Northwest Scotland and the Mellene Nappe of southern central Norway. These studies have involved the mapping of the orientation, age and distribution of cleavages related to recumbent folding. Using a variety of techniques, including grain shape analysis, measurement of conglomerate pebbles, magnetic anisotropy and palaeomagnetism strain patterns have been obtained for these nappes.

Different rock types control the style of folding, and, in part, the sequence of structures developed. The development of each recumbent fold is a multistage process and prior to each change of mechanism the rate of the current mechanism declines. It is suggested that each change of mechanism is an attempt by the developing structure to maintain the displacement rate required by the thrust belt as a whole. The suggested model for the development of the bedding parallel fabric seen in these nappes indicates the dominance of simpe shear deformation on the overturned limbs of recumbent folds.

In recumbent fold nappes the passage of the thrust tip into undeformed strata is preceded by folding. The relative ease of lateral propagation may be indicated by the presence or absence of extension parallel to the fold axis or, the presence of layer normal shear strains depending upon the style of folding. The Skarvemellen Anticline or the Mellene Nappe is a non-cylindrical fold with a marked extension lineation parallel to the fold axis. It is thought that this extension lineation results from restriction to the lateral propagation of the fold and thrust. There is an average of 40% extension parallel to the fold axis of the Skarvemellen Anticline in contrast to the Lochalsh Syncline which is a relatively cylindrical fold with relatively little extension parallel to the fold axis, less than 10%.

Acknowledgements

I would like to thank all members of the Department of Earth Sciences (University of Leeds), both academic and technical, for their assistance and support throughout this project. In particular, Professor J.C. Briden and Dr. R.J. Knipe for their interest and discussion.

The active encouragement of my work in Norway by Drs. J. Hossack and R. Nickelsen was warmly appreciated. My thanks are also extended to the Department of Physics, University of Newcastle for the use of their equipment.

I would like to thank Mike Coward, my supervisor, for his help and encouragement throughout the project. His persistent provocation and discussion helped to broaden and strengthen my ideas and for this I will always be grateful. An equal contribution was made to the project by my wife, Susan, whose patience throughout the project has been immense, especially in the last year while typing the draft and final copies of the thesis. Throughout the period of this study she has provided both encouragement and sympathy.

The work was undertaken during a Natural Environmental Research Council Studentship and receipt of this grant is gratefully acknowledged.

Symbols used

P, Q, R,	The lengths of pebble axes measured in the field, where P>Q>R.
Ap, Bp	Ap= P/Q Bp= Q/R.
Kp	Kp= Ap/Bp.
a, b,	The lengths of grain axes measured on any plane where, a>b.
Rf	Final grain shape ratio (Rf= a/b).
Ri	Initial grain shape ratio.
ϕ	Final orientation of a grain long axis.
θ	Initial orientation of a grain long axis
N	Population sampled.
H	Harmonic mean of grain axial ratios Lisle 1977a, b).
Rs	Finite strain ratio.
X, Y, Z,	Principal semi-axes of the finite strain ellipsoid where, X>Y>Z ($X=\sqrt{\lambda_1}$ etc. following Ramsay 1967).
Xt, Yt, Zt	Tectonic axes, perpendicular axes chosen to bear a simple relationship to the structural features of an area e.g. bedding, cleavage, fold axis. The axes have no conotations of flow direction and no fixed relationship to the finite strain axes.
εi	Logarithmic, natural or true strain $\varepsilon= \ln\sqrt{\lambda_i}$.
ε_x ε_y ε_z	Natural strain parallel to the tectonic axes Xt, Yt and Zt respectively.
ε_1 ε_2 ε_3	Natural strain where $\varepsilon_1 > \varepsilon_2 > \varepsilon_3$.
A, B,	Flinn parameters after Ramsay (1967) where, A= ln (X/Y) and B= ln (Y/Z).
D	Declination (degrees to the east of north).
I	Inclination (positive downwards).
R	Length of the resultant vector associated with the mean direction of orientation data.

κ	Best estimate of the precision parameter given by $\kappa = (N-1)/(N-R)$.
α_{95}	Cone of confidence at the 95% level around a mean direction $\alpha_{95} \simeq 140/\sqrt{(\kappa N)}$.
dp, dm,	Polar error or oval of 95% confidence about a pole position $dp = \frac{1}{2}\alpha_{95}(1+3\cos^2 \rho)$ and $dm = \alpha_{95} \sin \rho / \cos I$. ρ ancient co-latitude.
Mo	The intensity of the NRM.
Mn	Normalized intensity after each demagnetizing step such that $Mn = M/Mo$.
η	Orientation of the long axis of the strain ellipse relative to the shear direction.
γ	Shear strain.
ψ	Angular shear strain.
β	Dip of the kink band boundary.
ν	Dip of the layering within a kink band.
α	An angle generally the dip of the bedding before deformation.
α'	Orientation of the bedding after deformation.
J	Induced magnetization.
H	Applied magnetic field.
k	Magnetic susceptibility with principal axes $k_1 > k_2 > k_3$.
$\bar{k}$	$(k_1+k_2+k_3)/3$.
kv	$(k_1 \cdot k_2 \cdot k_3)^{\frac{1}{3}}$
k_i'	$k_i/\bar{k}$ or k_i/kv
Am, Bm,	Flinn type parameters such that $Am = \ln (k_1/k_2)$ and $Bm = \ln (k_2/k_3)$
Hs	$\frac{2}{3}\left((k_1'-k_2')^2 + (k_2'-k_3')^2 + (k_3'-k_1')^2 \right)^{\frac{1}{2}}$
Es	$\frac{2}{3}\left((\varepsilon_1-\varepsilon_2)^2 + (\varepsilon_2-\varepsilon_3)^2 + (\varepsilon_3-\varepsilon_1)^2 \right)^{\frac{1}{2}}$
Mi	$(k_i-\bar{k})/\bar{k}$
Km	$Km = Am/Bm$.
K	K=

Contents

Chapter 1 Introduction

Definition of a Recumbent Fold Nappe

A typical recumbent fold is shown in Figure 1.A.1.. This diagram is after Read and Watson (1962) and it shows the relationship of the folds to the thrust plane and the age relationship of the beds within the folds. The inverted limb of the fold structure has been replaced by a thrust due to thinning of the inverted limb. This diagram was chosen because it shows clearly the relationship of the beds to the thrust plane. It is these relationships which are expressed in the definition of recumbent fold nappes given by McClay (1981), "A fold nappe is an allochthonous tectonic unit which exhibits large scale stratigraphic inversion and may have initiated from large recumbent folds. The underlying limbs of these folds may be sheared out into thrust faults.". This definition is useful since it was constructed to avoid any reference to the actual dimensions of the folds and the amount of displacement on the thrust plane. Therefore, structures which have the geometry shown in Figure 1.A.1. may be grouped together irrespective of size. It has been shown, Coward and Potts (in press a) that within the Moine Thrust Zone structures with the relationship shown in Figure 1.A.1. may range in dimensions from a few metres to several tens of kilometres but they are essentially the same structure and they were formed by a common process.

Conventionally a recumbent fold is any fold in which the axial plane dips at less than 10 degrees (Fleuty 1964). However, many of the folds which will be described in this thesis do not conform to this description. Any constraint on the dip of the axial plane was excluded from the above definition as it was recognised (McClay 1981), that many structures within mountain

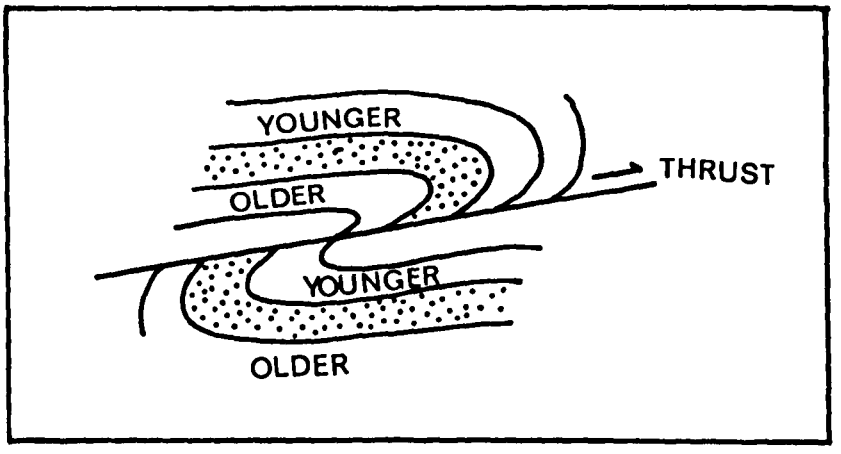

Figure 1.A.1. A typical recumbent fold (after Read and Watson 1962) showing the relationship of the folding to the thrust plane.

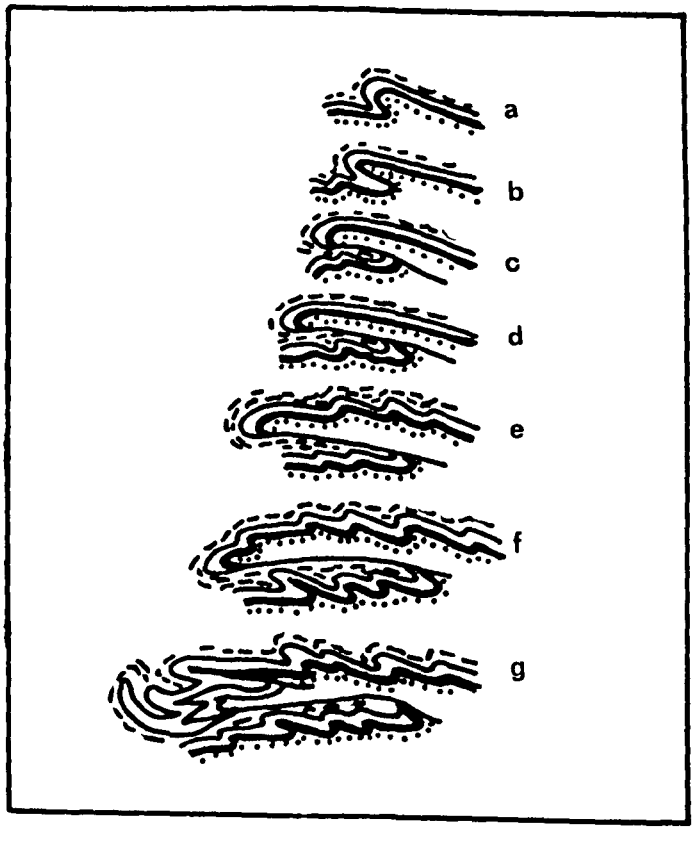

Figure 1.A.2. A series of diagrams illustrating the model proposed by Heim (1922) for the development of recumbent fold nappes.

belts are refolded by later structures and in such cases the dip of the axial plane is meaningless. Any definition of fold nappes should not include a restriction regarding the interlimb angles of the folds as a wide range of interlimb angles are possible without affecting the relationships shown in Figure 1.A.1. (Coward and Potts in press a)

Origin of Recumbent Fold Nappes, a Review of Previous Work

The concept of recumbent fold nappes developed from the study of the Swiss Alps during the last century,. Recumbent fold nappes were first described by Heim (1878) whos descriptions established the common features of recumbent fold nappes, generally flat lying folds in which the lower limb is sheared out and partly, or wholly, replaced by a thrust. In the years that followed this work, arguments developed reagrding the presence or absence of such structures within the Alps. These discussions formed part of a general argument regarding the possible origins of the Alps. Important workers in the establishment of fold nappes within the Alps include, Bertrand (1884) and Lugeon (1901, 1903).

Heim (1922) suggested a model for the development of recumbent fold nappes. A translation of his description is given by Heritsch (1929). The proposed model is shown in Figure 1.A.2. and Heim's description is as follows, (a) a fold arises; (b) it begins to grow longitudinally; (c) it becomes recumbent towards the foreland; (d) the reversed middle limb becomes more and more reduced in the now recumbent fold; (e) as a result of the movement, even the oldest beds of the series may be stripped off; (f) the recumbent fold becomes an overfold and an overfolded nappe; (g) the horizontal thrust continues, the friction

on the underside becomes greater and further sliding movement is retarded; (h) a new fold arises at the place of least resistance, that is, in the back of the overfolded nappe, and this develops in the same way into a new and higher nappe. In essence, this description is correct and has not been improved since.

Haug (1900) described a nappe as a recumbent anticline, the reversed limb of which has partly disappeared due to stretching. Subsequent work, for example Collet (1927), distinguished between recumbent anticlinal nappes and "true nappes", which lie above clean cut thrust planes, but work of this type made little or no contribution to the origin of recumbent fold nappes.

During this century the research in thrust tectonics changed in emphasis and concerned the mechanisms by which large rock masses could be translated, the so called "overthrust paradox". This line of study was based on the observation of Smoluchowski (1909), "we may press the block (thrust sheet) with whatever force: we may eventually crush it, but we cannot succeed in moving it, ". This analysis was followed by several workers, notably Hubbert and Rubey (1959), Hsu (1969) and Elliott (1976b). A useful review of this controversy is provided by Voight (1976). In essence it concerns the ability of a thrust sheet or wedge to withstand the forces necessary to produce the translation which it has undergone. These studies suggest that a weak basal layer is necessary for thrust movement and while it was active, the thrust plane must have dipped towards the foreland. In this situation of gravity sliding or gliding, recumbent folds developed due to drag on the thrust plane. Clearly this model is unacceptable in view of recent evidence that, during their development, the thrust planes dip away from the foreland (Rich 1934, Douglas 1950, Elliott and

Johnson 1980).

For further advances on the origin of recumbent fold nappes it is necessary to follow their study in North America. Willis (1891) defined four types of thrust fault and their relationship to associated folds, the two most important of these being, the "break thrust" and the "stretch thrust" (see Figure 1.A.3.). A break thrust develops when "the strata forms first an anticline, so conditioned that in process of development folding soon becomes more difficult than breaking, followed by overthrust on the fracture plane". Willis (1891) noted that this was a common form of thrust in the Appalachians. A stretch thrust "is the result of extreme folding, with the development of an overturned limb, which is stretched by the opposite pressures of the roof and floor". He found confirmation of his classification of thrust faulting in analogue models and the Appalachians. Though, these descriptions were meant to provide a classification of thrusts, they give an indication of the different relationships of folding to thrusting which may be seen in natural examples.

Busk (1929) recognised that folds which have been formed at a high structural level have nearly constant orthogonal bed thickness. Any curve may be approximated by a series of tangential circular arcs, and this provides a geometrical method for the construction of parallel folds in geological cross sections. The method is often termed the Busk construction. This was taken further with the concept of balanced cross sections, established by workers in the North American thrust belts. Dahlstrom (1969 and 1970) formalised the methods of balancing sections and summarised the geometrical rules concerning the development of thrusts. A geometrical consequence of the Busk construction is that the folds must die out with depth to some decollment horizon, Bucher (1933)

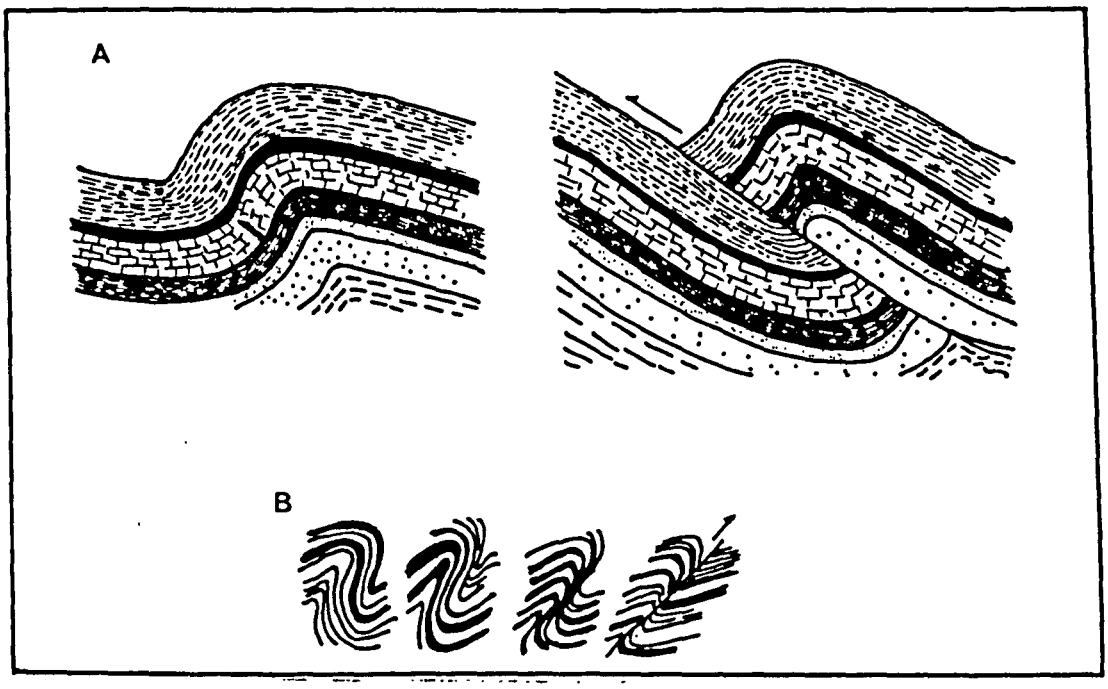

Figure 1.A.3. A. a "break thrust" which developed from the fracture within the limestone unit. B. a "stretch thrust" produced by intense folding. Both diagrams are after Willis (1891).

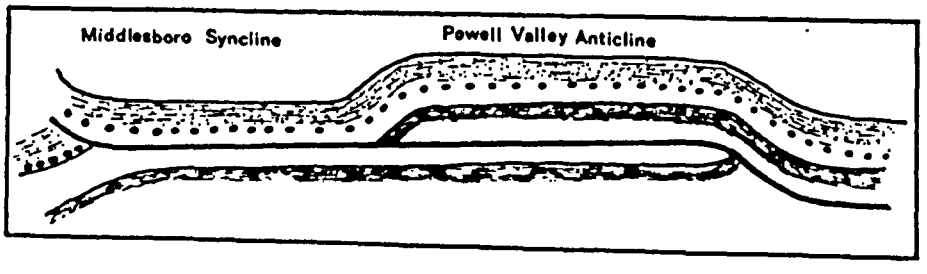

Figure 1.A.4. Geological cross section through the Pine Mountain Cumberland Thrust Block. The section is after Rich (1934) and shows clearly the flat topped Powell Valley Anticline.

found that the decollement horizons obtained from Busk constructions corresponded to well known decollement horizons within the Jura Mountains. When bed lengths around a parallel fold, constructed by the Busk method, are compared, there is a greater amount of shortening in the upper layers of the fold than those close to the decollement horizon. Geological structures must be introduced in order to balance the sections. One such method is to introduce more complex folding at depth and obtain the extra bed lengths. An alternative method is to introduce a thrust fault on one of the limbs of the fold. This suggests a genetic relationship between the two structures, folds and thrusts, geometrically a parallel fold requires a thrust plane in order to balance and by implication conserve displacement throughout the thrust sheet.

Rich (1934) showed that thrusts had a "staircase geometry" composed of ramps and flats. Flats are thrust planes which are parallel to the bedding and in general they tend to follow horizons of easy slip. Successive flats are joined by ramps which cut across the more competent horizons. Rich's (1934) concept originated from the study of cross sections through the Pine Mountain Cumberland Thrust Block in Virginia, Kentucky and Tennessee. The folds in the blocks are characterised by a large flat topped anticline, the Powell Valley Anticline, separated from the hinge of the Middlesborough Syncline by a short, steeply dipping, limb (see Figure 1.A.4.). Rich (1934) considered this fold to be a natural consequence of the transport of a thrust block over a ramp. Subsequent papers in Appalachian geology have verified the essential features of the Rich model (Harris 1970, Harris and Milici 1977) and comparable fold mechanisms have been applied to explain structures in the Rocky Mountains (Douglas 1950, Dahlstrom 1970) and in the Moine Thrust Zone of Scotland (Elliott and Johnson 1980). Boyer and Elliott (1982) have advanced

our thinking on the geometrical consequences of ramp climb permitting the calculation of displacement and the number of imbricates within a thrust system.

In the Rich model (Rich 1934) and similar subsequent models (Boyer and Elliott 1982) the dip of the beds in the fold is equal to the ramp angle. Berger and Johnson (1980) noted that the short limbs of these folds are much steeper and often overturned. They show how recumbent anticlinal folds may be generated by a component of drag on the ramp surface. In the models of Rich (1934) and Berger and Johnson (1980) no syncline is formed in the footwall of the thrust. Coward and Potts (in press) have shown that synclines generally occur in the footwalls of thrusts and that the development of the thrust is associated with the development of the recumbent folds.

The aims of this thesis are; (a) to examine the models described above in the light of evidence obtained from two natural examples and (b) by the use of strain patterns obtained from these examples define more accurately the processes of "reduction"(Heim 1922), "stretching" (Haug 1900) and "shearing and thinning" (Read and Watson 1962) which affect the overturned limbs of the recumbent folds. The nappes studied in this thesis are the Kishorn Nappe of northwest Scotland and the Mellene Nappe of southern central Norway.

The Kishorn Nappe is dominated by the recumbent Lochalsh fold or Lochalsh Syncline and it forms the lowest of a stack of nappes at the southern end of the Moine Thrust Zone (see Figure 1.A.5.). The Zone is of Caledonian age which involves the thrusting to the west-northwest, of Upper Proterozoic Moine Schists over Lower Proterozoic Lewisian Gneisses with their cover of Upper Proterozoic Torridonian and Cambro-Ordovician sediments. The Torridonian is a several kilometres thick sequence of

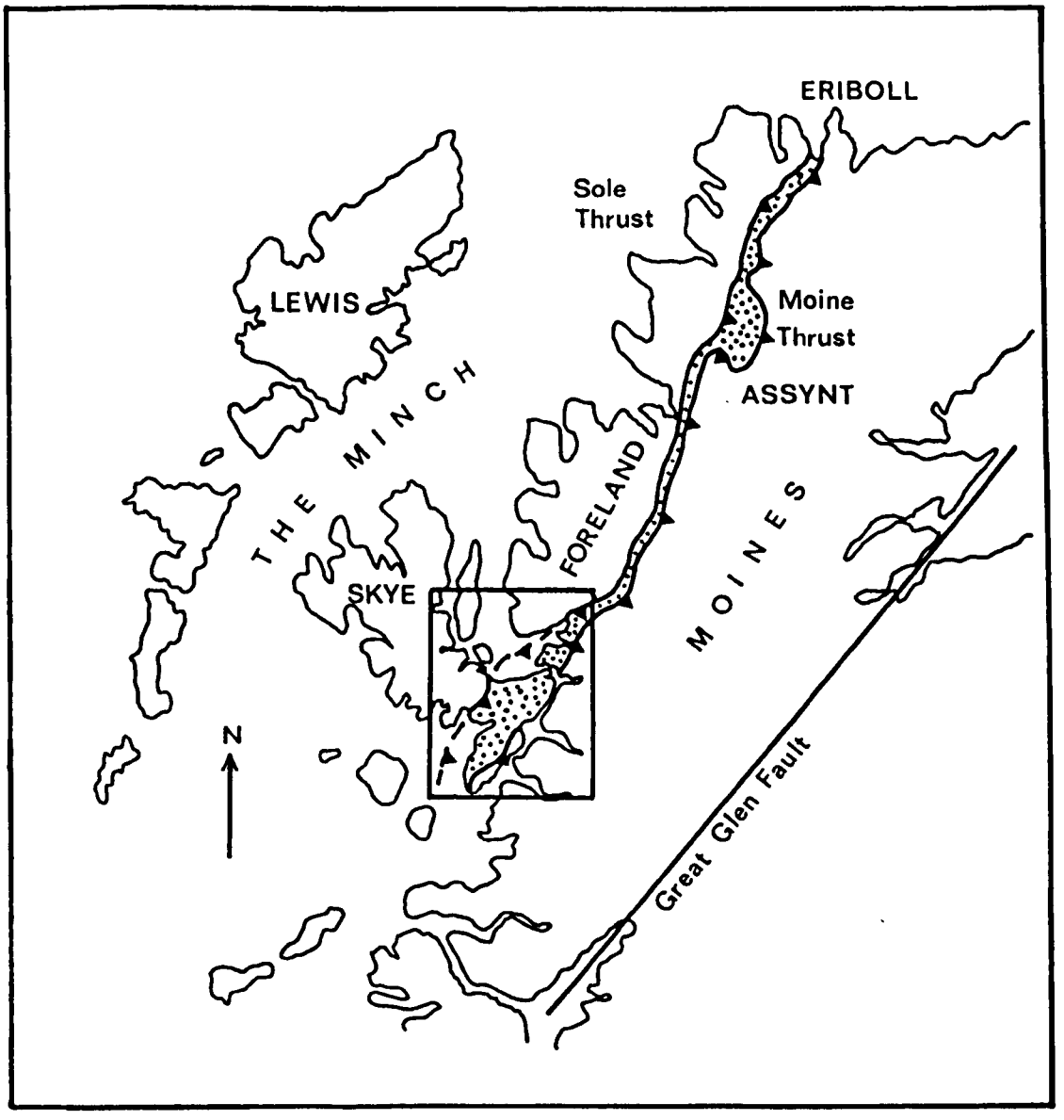

Figure 1.A.5. Simplified geological map of northern Scotland showing the extent of the Moine Thrust Zone. The area studied is enclosed in the rectangle.

monotonous grits, sandstones and shales, divided into a series of groups, many of which show only a regional development (Stewart 1966). The Cambrian consists of a basal quartz sandstone, the upper part of which (the Pipe Rock Member) is bioturbated by worm tubes or pipes. This overlain by a mixed series of dolomitic shales (the Fucoid Beds Member) and quartz rich sandstones (the Serpulite Grits Member) and then by a thick sequence of limestones (the Durness Limestone).

The thrust sheets or nappes of the Moine Thrust Zone vary in thickness from several hundred metres, where they involve Lewisian Gneisses and their cover of Proterozoic and Phanerozoic rocks, to several metres or tens of metres where they involve thin zones of the Phanerozoic rocks. A full account of the Moine Thrust Zone is provided by Peach et al (1907) and useful recent reviews include MacIntyre (1954), McClay and Coward (1981) and Elliott and Johnson (1980). A full reference list and review of published work which is relevant to the area studied will be given in chapter 2..

The Mellene Nappe forms part of the Valdres Group of nappes. These nappes lie beneath the Jotun Thrust, the highest thrust in southern central Norway. The Valdres Nappes involve both pre-Cambrian basement gneisses and their cover of Vendian to Ordovician rocks, they were translated to the southeast during Caledonian times over a series of imbricate zones of Vendian to Silurian sediments. A thin autochthonous sequence of shale overlies the gneisses of the Foreland. The structural geology and stratigraphy of the area has been reviewed by Hossack et al (1981) and Nickelsen et al (1981), a full description and review will be given in chapter 7..

These nappes were chosen in preference to the more well known and perhaps more spectacular examples of recumbent fold nappes such as the Morcles Nappe of the western Alps, or the Tay Nappe of Scotland, for the following reasons; (a) the Kishorn and Mellene Nappes have much smaller areas of outcrop which allows a much larger proportion of the structure to be studied and this provides more details on the origin of these structures, (b) within the Kishorn and Mellene Nappes the cleavage development is relatively weak and early fabric related to initial stages of folding have not been obliterated, (c) the work of Coward and Whalley (1979) showed that a variety of techniques could be applied, successfully, to the rocks of the Kishorn Nappe to determine the possible origins of the cleavages related to the Lochalsh Fold.

The Kishorn Nappe was studied during three field seasons on the Isle of Skye and the adjacent mainland of Scotland. Principally the Lochalsh Fold or Syncline was studied, but around the villages of Ord and Tarskavaig several other recumbent folds are present and these were also studied in detail. The adjacent nappes, the Balmacara and Tarskavaig Nappes were studied to determine the relationship of the Kishorn Nappe to the remainder of the thrust zone. Detailed structural mapping, the results of which are described in chapter 2., provided a framework and defined critical areas from which samples were collected for laboratory work. The Laboratory work is described in chapters 3. to 6., each chapter describes a different aspect of this work. Four techniques were used, X-ray diffraction (chapter 3.), thin section study for both mineralogy and finite strain (chapters 3. and 4.), palaeomagnetism (chapter 5.) and magnetic anisotropy (chapter 6.). The X-ray diffraction work was intended to provide information regarding metamorphic grade of the Kishorn Nappe. The studies of finite strain,

palaeomagnetism and magnetic anisotropy were undertaken to obtain strain patterns and possible mechanisms of formation related to the recumbent folds of the Kishorn Nappe.

The laboratory work was undertaken at the Department of Earth Sciences the University of Leeds , with the exception of the magnetic anisotropy which was measured in the Department of Physics at the University of Newcastle-Upon-Tyne.

The Mellene Nappe was mapped in detail during one short field season. The samples collected were analysed in exactly the same way as those from Scotland. The results of this study are described in chapter 7. and they provide a comparison to the main study area. During this field season it was possible to follow part of an excursion related to the Uppsala Caledonide Symposium (1982) and the series of nappes between the Foreland and the Jotun Nappe were studied. This provided a regional framework into which the Mellene Nappe could be placed.

Chapter 8. provides an analysis of the field and laboratory data, and compares these results to the models of fold formation described earlier and suggest possible mechanisms for the development of recumbent fold nappes. The conclusions which may be drawn from this study are summarised briefly in chapter 9..

Chapter 2 Structural Geology of the Kishorn and Balmacara Nappes

The purpose of this chapter is to describe the structural geology of the Kishorn and Balmacara Nappes. Previous work on these Nappes will be reviewed in the early part of the chapter, the remainder of the chapter providing a description of the structures within the Kishorn and Balmacara Nappes. A sequence has been established for these structures and the proposed sequence is compared with those of previous workers in the area.

The structural geology of the Kishorn and Balmacara Nappes will be described separately. This distinction is purely for convenience as it will be shown that the Kishorn and Balmacara Nappes are closely related structures.

Section 2A Stratigraphy

All the nappes at the southern end of the Moine Thrust Zone contain Lewisian Gneiss or mylonitic rocks derived from this Gneiss. A wide variety of rock types are seen within the Moine Nappe (Peach et al 1907 and Barber 1969), however only a limited number of rock types are seen within the Kishorn, Balmacara and Tarskavaig Nappes. The dominant rock types within these nappes are chlorite schists, acid gneisses and hornblende gneisses (Peach et al 1907, Cheeney and Matthews 1965, Matthews and Cheeney 1968 and Barber 1969). The Lewisian rocks are the basement to many sedimentary and metasedimentary sequences within the Moine Thrust Zone and on the Foreland.

Stewart (1969) has reviewed the stratigraphy of the Torridonian succession of northwest Scotland and applied a terminology which conforms to the American

Code of Stratigraphic Nomenclature (1961, article 6). This revised stratigraphy will be used throughout this thesis and where necessary substituted for the nomenclature used by previous authors (see table 2.A.1.).

The Sleat Group (Stewart 1969) forms the main portion of the Torridonian rocks of the Kishorn Nappe on Sleat, Lochalsh and Lochcarron. No comparable sequence of Torridonian age is seen on the Foreland. The rocks of the Sleat Group were originally included in the 'Diabaig Formation' by Peach et al (1907) but this correlation has been questioned by Stewart (1966). The rocks of the Sleat Group have been described in detail by Peach et al(1907) and Sutton and Watson (1960 and 1964). The fourfold subdivision proposed by Peach et al (1907) was retained by Stewart (1969) and is given in table 2.A.1.. This division is accepted by the author but has not been used in this study as in the field the boundaries between the upper formations are not distinct. However, the upper boundary of the Epidotic Grit was mapped as it is generally clear. The upper boundary of the Sleat Group was only mapped to the south of the Loch Eilean Fault, see Figure 2.A.1. (Peach et al 1907) where it could be clearly seen and the boundary was useful in establishing the structure around the Ord Window. During this work no rocks, which could be assigned to the Diabaig Formation of the Foreland (Stewart 1969) were seen. Stewart (1969) suggests that rocks immediately beneath the Applecross Formation should be assigned to the Diabaig Formation. However, these units are not highly carbonaceous as suggested by Stewart (1969) and the rocks immediately beneath the Applecross Formation were assigned to the Kinloch Formation of the Sleat Group.

Stewart (1969) shows two models for the relationship of the Torridon Group to the Sleat Group within the Kishorn Nappe. His first model shows a transitional change of

Table 2.A.1.

Peach et al 1907		Following Swett 1967	
Ben Suardal Limestone Strath Suardal and Beinn an Dubhaich Limestones Sangomore Limestone Sailmhor Limestone Eilean Dubh Limestone Ghrudaidh Limestone	CALCAREOUS SERIES	Ben Suardal Member Strath Suardal and Beinn an Dubhaich Member Sangomore Member Sailmhor Member Eilean Dubh Member Ghrudaidh Member	Durness Limestone
Serpulite Grit Fucoid Shales		Surpulite Grit Member Fucoid Beds Member	An t-Sron Formation
Upper Quartzite or Pipe Rock Lower or false bedded Quartzite	QUARTZITE	Pipe Rock Member Lower Member	Eriboll Sandstone

Peach et al 1907		Stewart 1969	
Applecross Group		Applecross Formation Diabaig Formation	Torridon Group
Kinloch Beds (sub-division) Beinn na Seamaraig Grits Loch na Dal Beds	Diabaig Formation	Kinloch Formation Beinn na Seamaraig Formation Loch na Dal Formation	Sleat Group
Epidotic Grits and Conglomerates		Epidotic Grit and Conglomerates	

Table 2.A.2.

Stratigraphic Unit	Peach et al (1907) Skye (metres)	Peach et al (1907) Lochalsh (metres)	Sutton & Watson Skye (metres)
Sailmhor Member	82 (Ord)		
Ellean Dubh Member	152 (Ord)		
Ghrudaidh Member	35 (e, Ord)		
Serpulite Grit Member	15 (Ord Glen)		
Fucoid Beds Member	18 (Ord Glen)		
Pipe Rock Member	82 (Rudha Dubh Ard)		
Lower Member	100 (Rudha Dubh Ard)		
Applecross Formation	1524 (Skulamus)		457
Kinloch Formation	1067 (Glen Arroch)[2]	823	393
Beinn na Seamraig Formation	792 (e)	366	320
Loch na Dal Formation	183 (Dun Ruaige)[1]	152	76(Ardnameacan)
Epidotic Grits	91	18(Carn a Bhealaich Mhoir)	36(Rubha Guail)

(1) Measured at Dun Ruaige but the thickness of the Formation may double when traced southwards to Loch na Dal.

(2) Measured at Glen Arroch but the Formation may thicken southwards.

(e) Denotes Estimate

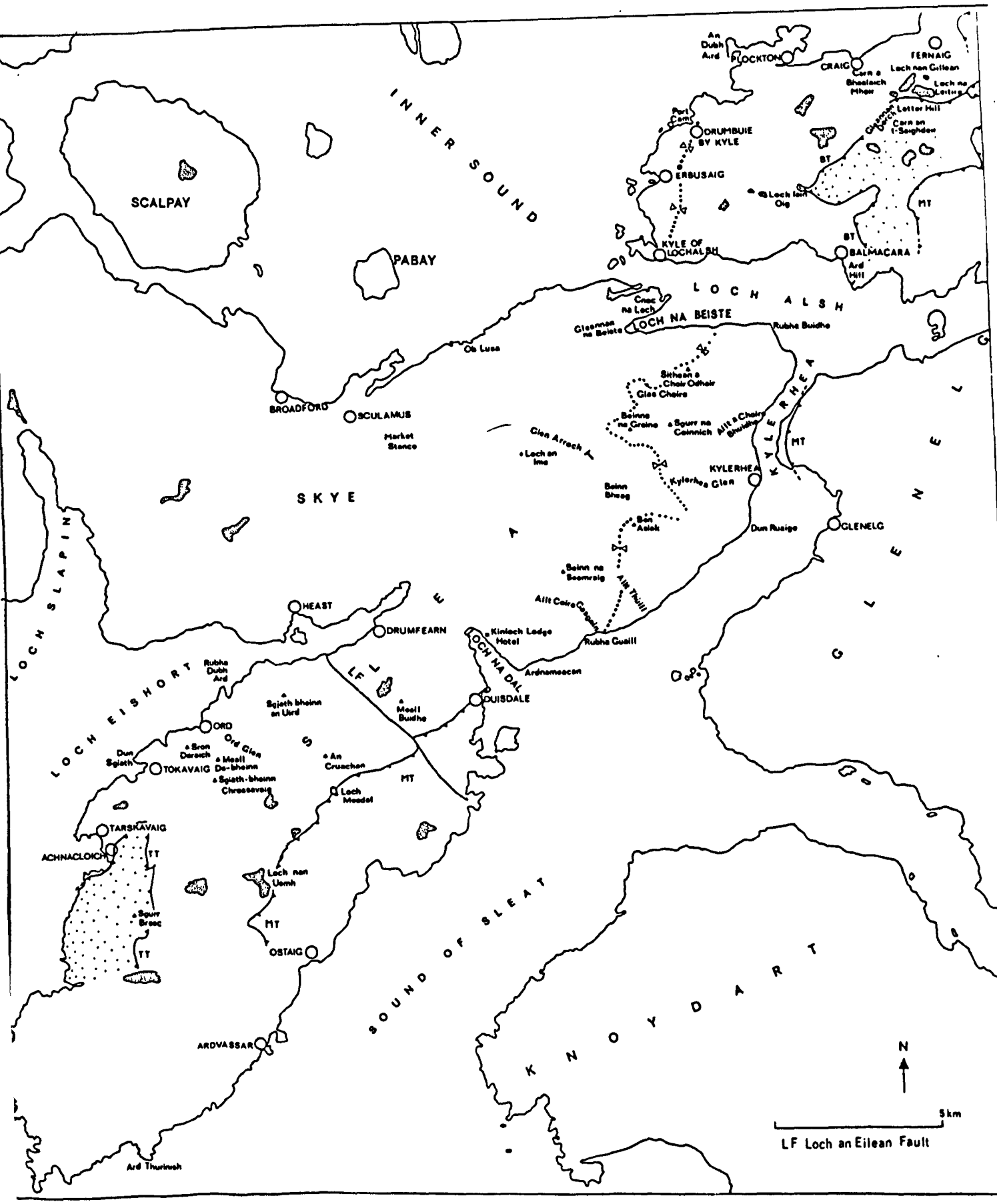

Figure 2.A.1. A locality map of Skye and the adjacent mainland of northwest Scotland. The Figure will be used throughout this chapter.

sedimentary facies marked by the presence of a shaly Diabaig Formation. Thus the Sleat Group and the Torridon Group are of a similar age. His second model suggests that the Diabaig Formation represents a stratigraphic marker between the older Sleat Group and the younger Torridon Group. Neither of these models is accepted here. On southern Sleat the boundary is transitional; around Tokavaig and Tarskavaig, red sandstones can be seen in the upper parts of the Sleat Group which pass laterale into a continuous sequence of red sandstones at Sron Daraich, see Figure 2.A.1.. Further to the north on Sleat and the Kyle of Lochalsh, the base of the Torridon Group is not transitional but appears to be conformable. This boundary appears to represent the northward migration of a change in sedimentary facies not marked by the presence of the Diabaig Formation.

Within the Kishorn Nappe the thickness of both the Sleat and Torridon Groups is extremely variable and the various thicknesses suggested by several authors are shown in table 2.A.2.. The complex folding and variable finite strain of the Sleat Group makes an accurate determination of thickness difficult. Further, the base of the Sleat Group may have been undulose as it was deposited on an eroded surface of Lewisian Gneiss. The thickness of the Applecross Formation decreases to the south and around Ord it is only 200 feet thick (Bailey 1939). Stewart (1969) suggests that this variation is due to erosion prior to the deposition of the Cambro-Ordovician sequence, as proposed by Soper and Barber (1979) for the Assynt area.

Swett (1969) has proposed a revision of the Cambro-Ordovician sequence based principally on the sequence described by Peach et al (1907) for Sutherland. Clough in Peach et al (1907) gave a sequence for the Cambro-

Ordovician succession on Skye and a proposed revision of this sequence is shown in table 2.A.1.. This follows Swett's (1969) revision in Sutherland and adheres to the American Code of Stratigraphic Nomenclature (1961, article 6.) and will be used in this thesis.

Suggested thicknesses for the Cambro-Ordovician sequence are shown in table 2.A.2.. While the base of the Eriboll Sandstone is very probably planar, the base of the Pipe Rock Member is poorly defined. During mapping, the base of the Pipe Rock Member was taken to be marked by the presence of 3mm diameter pipes. These pipes are often difficult to see and may not always have been recognised. To a certain extent the appearance of any kind of pipe may be controlled not only by the stratigraphical horizon but by the grain size of the sediment. The Pipe Rock Member was not divided into zones as proposed by Clough in Peach et al (1907) but the sequence given (Peach et al 1907 page 418) is common throughout the Ord Window and was often used to distinguish the way up of a continuous series of beds. Three types of pipe were distinguished during the mapping, 3mm diameter cylindrical pipes which correspond to the 1/8 inch diameter pipes of Peach et al (1907), 1cm diameter pipes equivalent to the 1/4 inch diameter pipes (op cit) and the trumpet pipes. The former two types have been given the generic name Skolithos linearis by Hallam and Swett (1966) and the trumpet pipes the generic name Monocraterion.

The upper boundary of the Pipe Rock Member is well defined due to the rapid change into dolomitic shales of the Fucoid Beds Member. The thickness of the An t-Sron Formation is variable due to the omission of the Fucoid Beds Member to the west of Sgaith Bheinn Tokavaig and repetition by imbrication at Rubha Dubh Ard.

The base of the Durness Limestone may be transitional with the underlying Serpulite Grit Member but is generally well defined and can be accurately mapped. The top of the Durness Limestone is never seen. During mapping, the Durness Limestone was not divided into the zones given in table 2.A.1. due to the highly altered nature of the rock.

During field work the following stratigraphical boundaries were mapped, the sub-Torridonian unconformity of eroded and tectonised Lewisian Gneiss, the top of the Epidotic Grit and the base of the Applecross Formation (to the south of the Loch An Eilean Fault (Peach et al 1907)). Within the Cambro-Ordovician succession the bases of each of the following stratigraphical units were mapped, the Eriboll Sandstone, Pipe Rock Member, Fucoid Beds Member, the Serpulite Grit Member and the Durness Limestone.

In this section emphasis has been placed on stratigraphical thicknesses as they are important in the construction of balanced cross sections (Dalhstrom 1970). From the contrasting estimates of stratigraphical thickness given in table 2.A.2. it is clear that these are only known with any accuracy for the Cambro-Ordovician succession.

The variable estimates of thickness for the Sleat Group may reflect changes in the depth of the sedimentary basin (see Sutton and Watson 1964, Black and Welsh 1961 and Stewart 1969). If this is the case, then prior to the development of Caledonian structures the sedimentary sequence in this area was not a "simple layer cake" (cf. Elliott and Johnson 1981) and this presents problems in the construction of balanced cross sections, as does the pre-Cambrian folding which appears to be present at Ord.

The Balmacara Nappe is composed mainly of mylonites after Lewisian Gneiss. However, around Letter Hill (Figure 2.A.1.) the lowest portion of the Sleat Group is exposed within the Nappe.

Section 2B Previous Work

The Lochalsh Syncline was first recognised by Peach and Horne in Peach et al (1907) who wrote (p565), "the most striking feature of the belt of complication in the ground now to be described (Lochcarron and Lochalsh) is the stupendous inversion of the Torridon Sandstone and the Lewisian rocks above the Kishorn Thrust Plane ". They recognised many of the main tectonic features present within the nappes beneath the Moine Thrust (the highest thrust in the area) including the highly deformed nature of the lower portion of the Sleat Group, in particular the basal conglomerate exposed between Fernaig and Gleannan Dorch (see Figure 2.A.1.) and the development of a strong Caledonian fabric in the Lewisian Gneiss of both the Kishorn and Balmacara Nappes. In Figures 56 and 66 of Peach et al (1907), the Kishorn Nappe is shown as a large sheet containing gently dipping but inverted Sleat Group overlain by Lewisian rocks immediately beneath the Moine Thrust. At Loch Kishorn the Kishorn Thrust is underlain by imbricated rocks of Cambrian age.

Peach and Horne (Peach et al 1907) suggest that the trace of the Lochalsh Syncline passes northwards into Loch Carron at An Dubh Aird, exposing beds of the normal limb which dip gently westwards. The normal limb is exposed between An Dubh Aird and Kyle of Lochalsh to the west of the axial trace (see Figure 2.A.1.).

The geology of Sleat and the Isle of Skye was described by Clough in Peach et al (1907 page 574), where he

hoted the dominance of recumbent folding over imbrication and that this folding is characteristic of the southern end of the exposed Moine Thrust Zone. "The much greater thickness of the Torridonian series in this island than on the mainland to the north of Loch Alsh has doubtless led to a striking manifestation of the characters of this belt of complication among the members of that series. The great Torridonian inversion so clearly displayed on the opposite mainland crosses into the district of Sleat,....., over folding of the strata appears to be more prevalent than reversed faults in front of the great thrusts".

The amount of Lewisian rock on the Isle of Skye is extremely limited and the Sleat Peninsula is composed almost entirely of Torridonian rocks. The Moine Thrust is present on Glenelg and on Skye between Duisdale and Ard Thuirnish (see Figure 2.A.1.).

Clough in (Peach et al 1907) described the nature of the Lochalsh inversion (Lochalsh Syncline) on the northern part of Sleat, noting the presence of the axial planar cleavage on Sgurr na Coinnich, Ben Aslak and Beinn na Seamraig. He noted the increase in deformation to the east, with the development of a strong grain shape lineation and the general decrease in deformation to the southwest, to such an extent that, to the south of Loch na Dal, no cleavages can be seen.

Figure 61 in Peach et al (1907) shows the Ben Suardal Thrust carrying Torridonian rocks over Durness Limestone in the area to the south of Broadford. The Ben Suardal Thrust was correlated with the Sgiath bheinn Tokavaig Thrust by Clough (page 580, Peach et al 1907) see Figure 2.B.1.. The Sgiath bheinn Tokavaig Thrust is a thrust exposed to the east of Ord where Cambrian rocks form a structural outlier

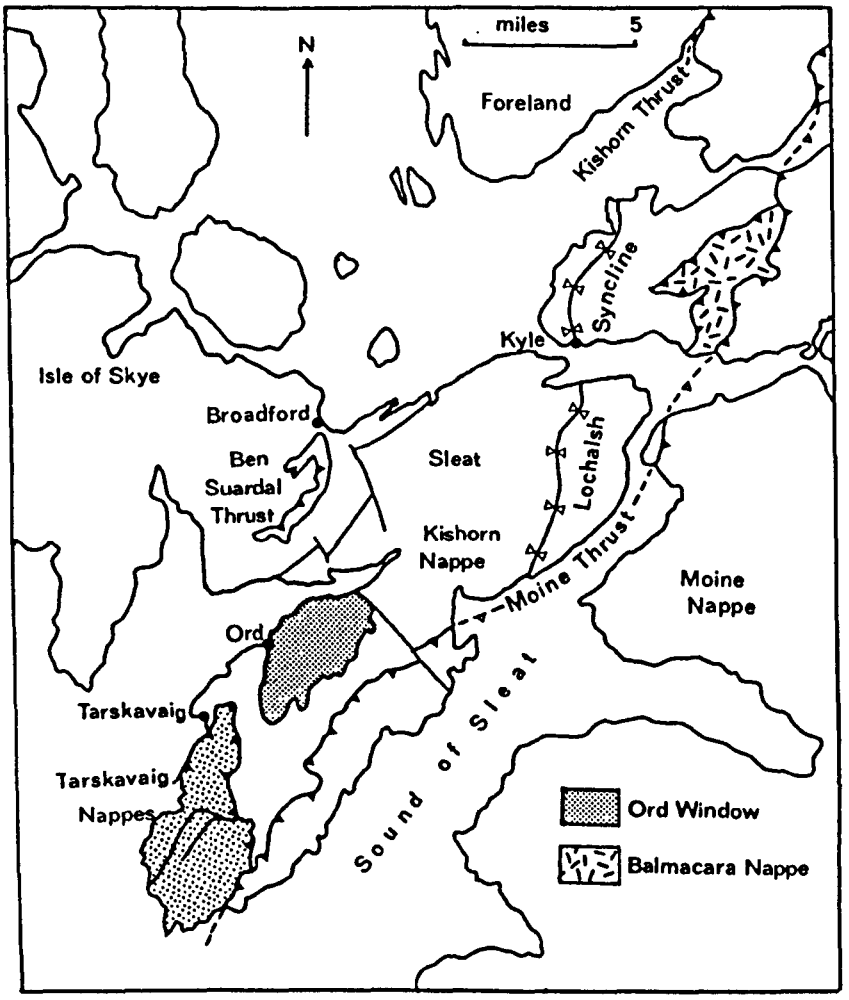

Figure 2.B.1. A simplified geological map of Skye and the adjacent mainland of Scotland showing the nappes and major structural features of the area.

surrounded and overlain by Torridonian rocks (see Figure 2.B.1.). Clough (Peach et al 1907) suggested that the repetition of thrust planes and Cambrian rocks seen to the east of Ord was achieved by folding of the thrust planes into a large anticline. Clough (Peach et al 1907) shows that within the Cambrian rocks there are two major thrust planes: the lower, Sgiath bheinn an Uird Thrust and the higher, Sgiath bheinn Tokavaig Thrust (see Figure 2.B.2.). Between these thrusts the Cambrian rocks, mainly quartzites, are strongly folded and affected by minor thrusts. In contrast to the Cambrian rocks seen further north in the Moine Thrust Zone they are relatively undeformed a fact noted by Clough (page 584, Peach et al 1907): "below the Sgiath bheinn an Uird Thrust strata are not cleaved, nor is there any noticeable distortion of the pipes in the Pipe Rock.".

Between Ord Bay and Dun Sgiath (Figure 2.A.1.) the unconformity between the Applecross Formation and the younger Eriboll Sandstone is clearly seen but it is inverted. Clough (Peach et al 1907) suggested that it formed the overturned, upper limb, of a recumbent syncline with an axial plane that dipped to the south-east.

To the south of Tarskavaig, Clough (Peach et al 1907) recognised the Tarskavaig Thrust which carries mylonitic Lewisian Gneiss and its cover of arkosic sandstones over sandstones and shales of the Kinloch Formation. He suggested that they, the Tarskavaig Moines, represented altered and deformed Torridonian sandstones equivalent to the Sleat Group but of a different sedimentary facies and that they may be intermediate both in deposition and deformation between unaltered Torridonian rocks and the true Moine metasediments which lie above the Moine Thrust.

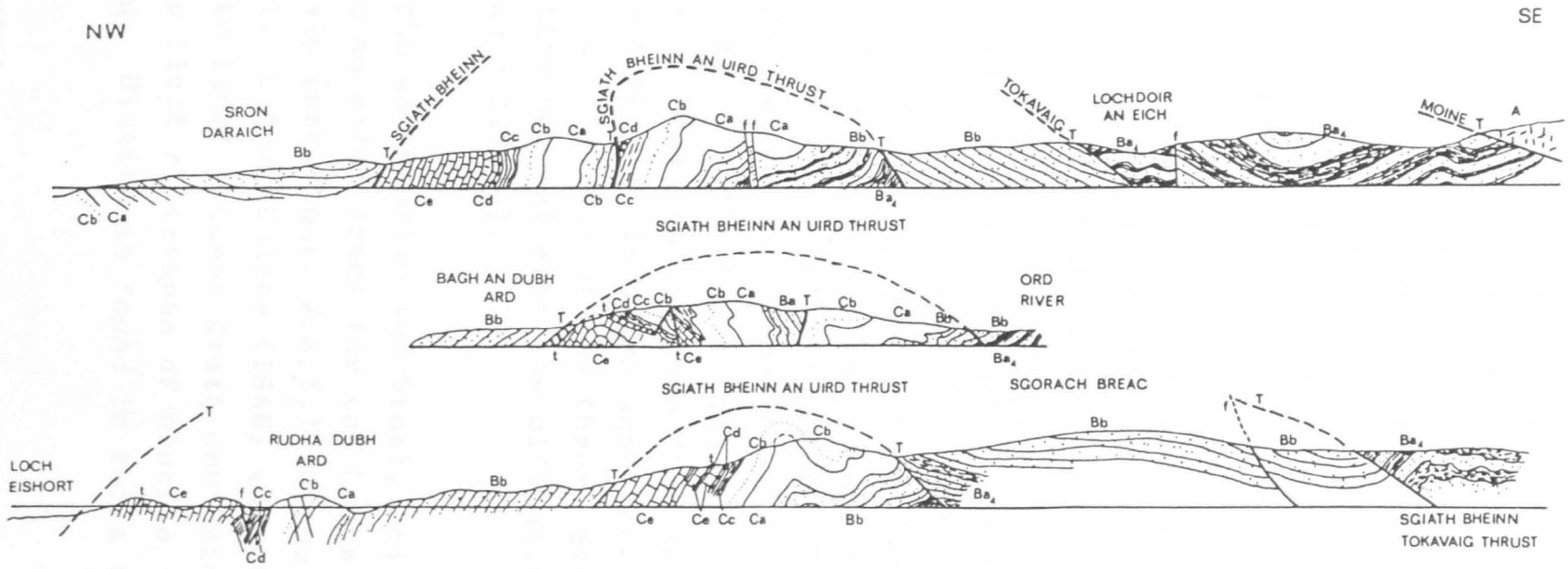

Figure 2.B.2. Three sections through the Ord Window after Clough (in Peach et al 1907). A = Lewisian, Ba_4 = Kinloch Formation, Bb = Applecross Formation, Ca = Lower Member (Eriboll Sandstone), Cb = Pipe Rock Member, Cc = Fucoid Beds Member, Cd = Serpulite Grit Member and Ce = Durness Limestone. T = Thrust and t = Minor Thrust. The sections show the folded thrusts of Clough's original interpretations.

The Tarskavaig Thrust is folded by a Syncline (Figure 2.B.2.) and Clough (Peach et al 1907) described the trace of the fold from the Tarskavaig Nappe in the south to the coast of Loch Eishort, slightly to the west of Ord. Clough (op cit) also presents a comprehensive account of the Tarskavaig Nappes and describes the numerous thrusts present within this group of nappes.

The next contribution to the geology of the Kishorn Nappe was made by Bailey (1939, 1955). On the basis of its "great persistence northwards" Bailey (op cit) correlated the Kishorn Thrust with the Suardal Thrust on Skye (Figure 2.B.1.) and by implication the thrusts of the Ord Window. The Kishorn Thrust is the lowest thrust on the mainland. Specifically Bailey correlated the Kishorn Thrust with the Sgiath bheinn an Uird Thrust (the lowest of the Ord thrusts), thus dividing the Window into foreland and nappe (Figure 2.B.3.). To the western limb of the folded Sgiath bheinn Tokavaig Thrust, Bailey assigned the name "Ord Thrust". The Ord Syncline is formed of Cambrian aged rocks and it lies immediately to the east of the thrust plane. This interpretation necessitated the bification of the Kishorn Thrust (Figure 2.B.3.).

Further north on Lochalsh and Sleat, Bailey (1939) established an axial trace for the Lochalsh Syncline, from Erbusaig (see Figure 2.A.1.) to the area north of Loch na Dal. Later, Bailey (1948) was able to construct his "biotite line" between Craig and Balmacara which records the first appearance of biotite in rocks of the Sleat Group. Biotite is found in rocks to the east of the line.

Kennedy (1954) suggested that the Sleat Peninsula consists of a recumbent syncline of Cambrian and Torridonian rocks disrupted by clean cut thrusts and

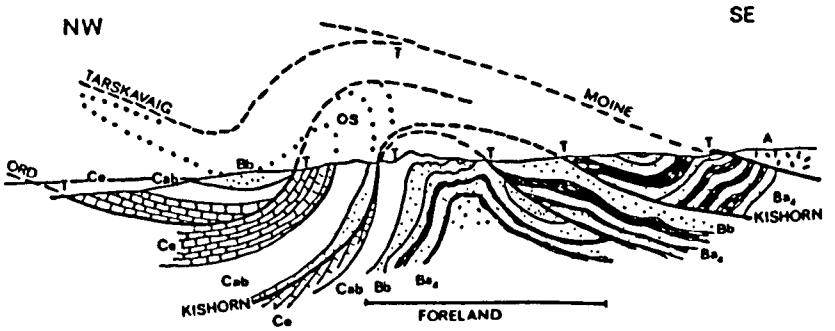

Figure 2.8.3. A section through the Ord Window after Bailey (1939). The section is based on a reassessment of Clough's original work.

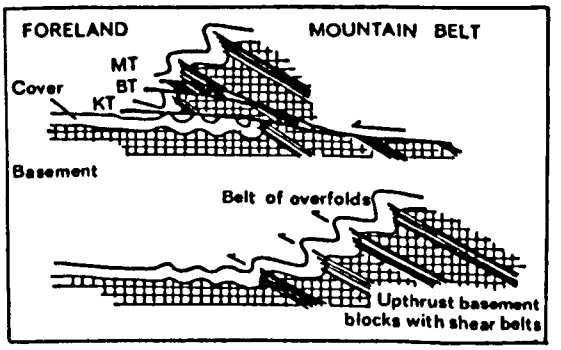

Figure 2.8.4. Two sections showing the evolution of the Lochalsh Syncline and the adjacent portions of the Moine Thrust Zone (after Barber 1965).

that the recumbent folding predated the thrusting.

Johnson (1955a, 1955b, 1956, 1957, 1960a and 1960b) presented a series of papers which record in detail the minor structures seen in the Kishorn Nappe on Lochcarron and to the north in the Coulin Forest area. He established a general time sequence of linear structures, including fold axes, of both "Caledonoid" (north-south to northeast-southwest) and "cross" (east-west to northwest-southeast) trend. Within the Kishorn Nappe this sequence is as follows:

Phase 1. Formation of recumbent Caledonoid Syncline (Lochalsh Syncline)
Phase 2. Formation of cross folds which plunge to the east-southeast and the development of a mineral lineation which plunges down dip on the axial plane of the isoclinal folds.
Phase 3. Caledonoid folds which are generally small scale recumbent folds.
Phase 4. Formation of conjugate cross folds. Kink bands, monoclines and box folds.
Phase 5. Thrusting to the northwest on clean cut thrust planes.
Phase 6. Open cross folds.

Kanungo (1956) working in the Lochalsh area remapped the axial trace of the Lochalsh Syncline using way up criteria and obtained a trace similar to that obtained by Peach and Horne (Peach et al 1907). He also recorded the existence of several minor folds related to the Lochalsh Syncline and noted their associated cleavages. Kanungo (1956) showed that there are several cleavages, a shallowly dipping S_2 axial planar cleavage and a steeper S_3 fracture cleavage which is irregularily distributed. Both cleavages are seen around the hinge of the Syncline. In the east of the Nappe, Kanungo

(1956) recognised a bedding fissility with a related east-southeast mineral lineation which obliterates sedimentary features and a S_4 cleavage which is steeper than bedding on the overturned limb of the Lochalsh Syncline. The latter he termed a "thrust cleavage". Within the mylonites to the east of the area he was able to map regions of unmylonitised Lewisian Gneiss preserving its Laxfordian trend.

Barber (1965, 1969) working around Balmacara was able to establish, independently, a structural sequence similar to that of Johnson (1955a) and related to that of May (1959). This sequence is:

1. Mylonitisation often within narrow localised bands.
2. Isoclinal folding on east-southeast axes.
3. Recrystallization resulting in the dominant foliation and lineation in the mylonites.
4. Asymmetrical folding on the north-south axes.
5. Monoclinal folding on variable axes.
6. Thrusting, the development of clean cut thrusts planes which cut earlier structures.
7. Post thrusting, flexing of the thrust planes.

Barber (1965) was the first to suggest a model for the development of the Lochalsh Syncline which showed the fold to develop above basement shear zones. The fold train was disrupted by thrusting to produce the outcrop pattern seen (Figure 2.B.4.).

Sutton and Watson (1960 and 1964) working on Sleat immediately to the north of Loch na Dal revised the stratigraphy and sedimentology of the Sleat Group, in particular that of the Epidotic Grit. They gave an accurate map of the trace of the Lochalsh Syncline. between Ben Aslak and Rubha Guail (Figure 2.A.1.).

Recently, Coward and Whalley (1979) applied structural techniques, texture goniometery and magnetic anisotropy to determine the nature and origin of the various cleavages seen within parts of the Kishorn Nappe relating these to the increase in the deformation towards the east.

The geology of the Tarskavaig Nappes was first described by Clough in Peach et al (1907). Subsequent work has included that of Phillips (1939), Bailey (1939, 1955), Cheeney (1965), Cheeney and Matthews (1965) and Matthews and Cheeney (1968). Their work suggests that a stack of nappes are present folded into a synform and truncated by the overlying Moine Thrust.

Section 2C Major Structures of the Kishorn Nappe

The recumbent folds of the Kishorn Nappe, in particular the Lochalsh Syncline, have been mapped at a scale of 1:10,000 between the southern shore of Loch Carron and a line between Ostaig and Sgurr Breac on Skye. This area includes the northern part of the Tarskavaig Nappe. Several excursions were made outside this area to facilitate the correlation of minor structures with those recorded by Johnson (1955a) on Lochcarron and Cheeney (1965) within the Tarskavaig Nappes.

The major structures of the Kishorn Nappe will be discussed in three areas. Within each area slightly different structural levels are exposed. The three areas are shown in figure 2.C.1..

The northern area lies to the north of a major fault, the Loch na Beiste Fault. On aerial photographs of northern Sleat a marked linear feature may be seen which runs east-west along Gleannan na Beiste between Market Stance and Loch na Beiste (Figure 2.C.1.) and it is suggested that this is the trace of a major fault

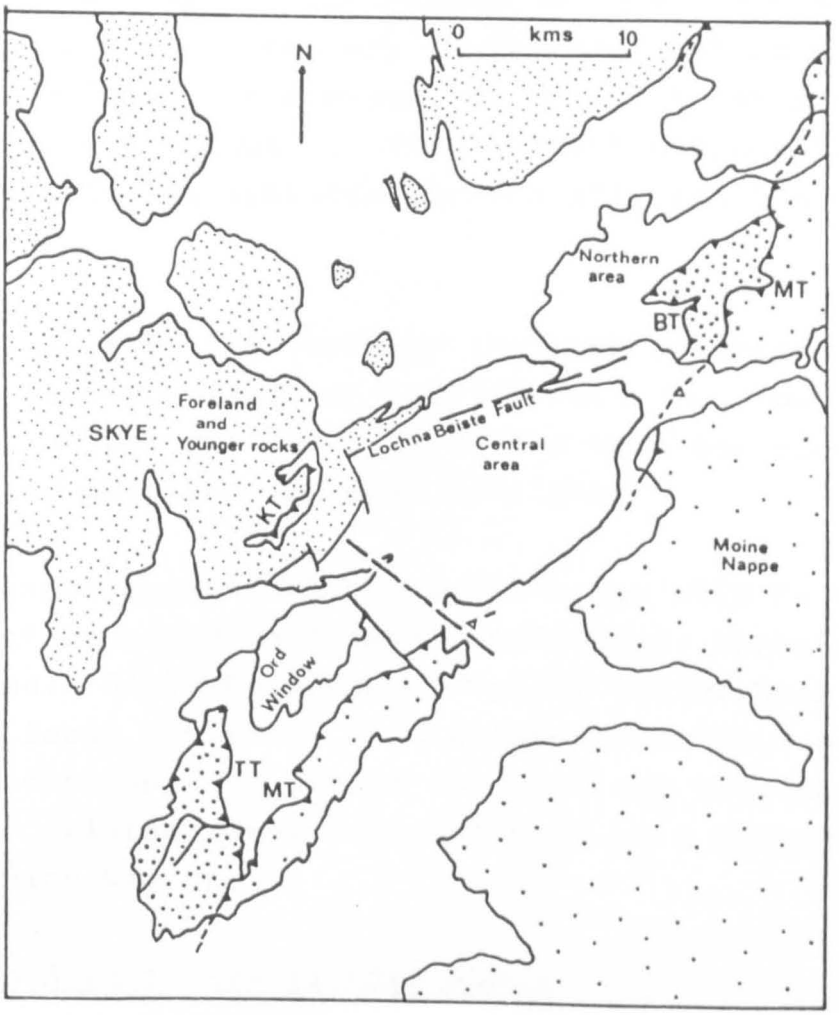

Figure 2.C.1. A simplified geological map of Skye and the adjacent mainland of Scotland. The map shows the position of the Loch na Beiste Fault which forms one of the boundaries to the regions of the Kishorn Nappe which are described in this thesis. MT = Moine Thrust, BT = Balmacara Thrust, TT = Tarskavaig Thrust.

which runs into Loch Alsh. The structure of Cnoc na Loch bears a closer relationship to those seen around Kyle than those immediately to the south of Loch na Beiste. Offset of the hinge of the Lochalsh Syncline across the fault suggests displacement components of approximately 3Km sinistral strike slip and 1Km dip slip.

The central area lies between the Loch na Beiste Fault and the southern shore of Loch na Dal. The southern boundary of the central area is the cleavage front associated with the Lochalsh Syncline.

During mapping, particular attention was paid to the way up of beds and in general sedimentary structures were used. Since Coward and Whalley (1979) have shown that at least one phase of cleavage production within the Kishorn Nappe postdates the folding, bedding-cleavage relationships were not used as a method of determining way up.

Northern Area of the Kishorn Nappe

The northern area consists mainly of the inverted limb of the Lochalsh Syncline. The axial trace of this fold may be followed from Cnoc na Loch north through Kyle of Lochalsh towards Drumbuie by Kyle (see Figure 2.A.1.). Certain parts of the axial trace are ill defined due to the poorly bedded nature of the Applecross Formation in which it is exposed and the strongly developed faulting and jointing around Drumbuie and Plockton.

Rocks of the normal limb lie to the west of the axial trace and dip gently to the northwest, as seen on the north coast of Sleat to the north of Kyle. Beds of the inverted limb dip to the east and southeast and the dip gradually decreases from vertical to around 20 degrees.

Locally, such as to the south of Loch Iain Oig, beds become flat lying or dip gently to the west but remain inverted. The axial trace obtained broadly corresponds to that obtained by Peach et al (1907), Bailey (1939) and Kanungo (1956).

The stereogram of poles to bedding shown in figure 2.C.2. indicates a fold axis plunging at 10 degrees to 045 degrees. The stereogram shows two well defined maxima corresponding to the limbs of the Lochalsh Syncline which appears to be a fairly straight limbed, almost angular fold (assuming that the sampling of the bedding values was homogeneous over the entire area).

The occurrence of minor folds related to the Lochalsh Syncline is extremely limited and only three were seen in the northern area;

1. Plockton (NG 79903421)
2. Port Cam (NG 76853130)
3. Erbusaig (NG 75663005)

The stereograms of poles to bedding (and cleavage) around these minor folds are shown in Figure 2.C.3. and they correspond closely to those in Figure 2.C.2. suggesting that they are related. Kanungo (1956) lists the occurrence of six such minor folds. Of his six hinges (vi) was not visited and (ii) and (iii) could not be found.

The minor folds occur in fault bounded blocks which may be up to thirty metres in length. In profile the minor folds show small curved hinge zones and relatively straight limbs and as shown in the section through Cnoc na Loch Figure 2.C.4. the main hinge of the Lochalsh Syncline appears to be relatively rounded.

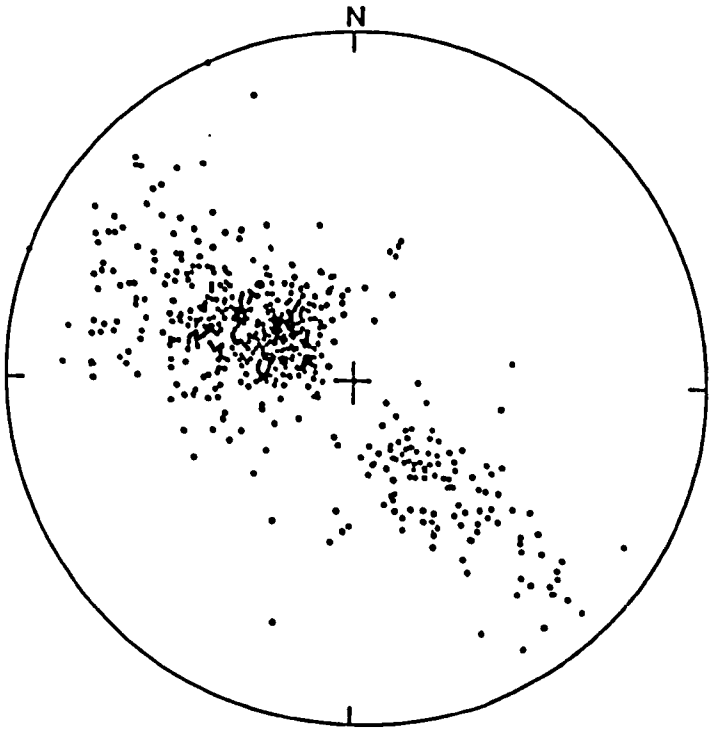

Figure 2.C.2. A stereogram of poles to bedding from the northern area of the Kishorn Nappe.

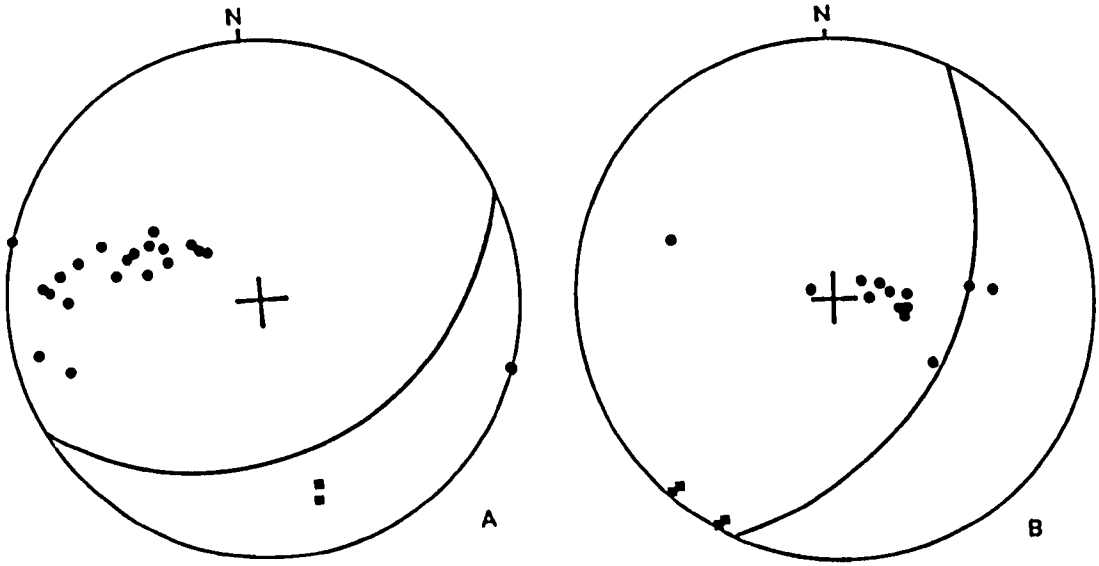

Figure 2.C.3. π-pole diagrams of the minor folds at Plockton (A) and Port Cam (B). ● = pole to bedding and ■= bedding cleavage intersection lineations. The great circle marks the position of the dominant cleavage, at Plockton this is the axial planar cleavage but at Port Cam it is the transverse cleavage. Data from the fold at Erbusaig is not shown.

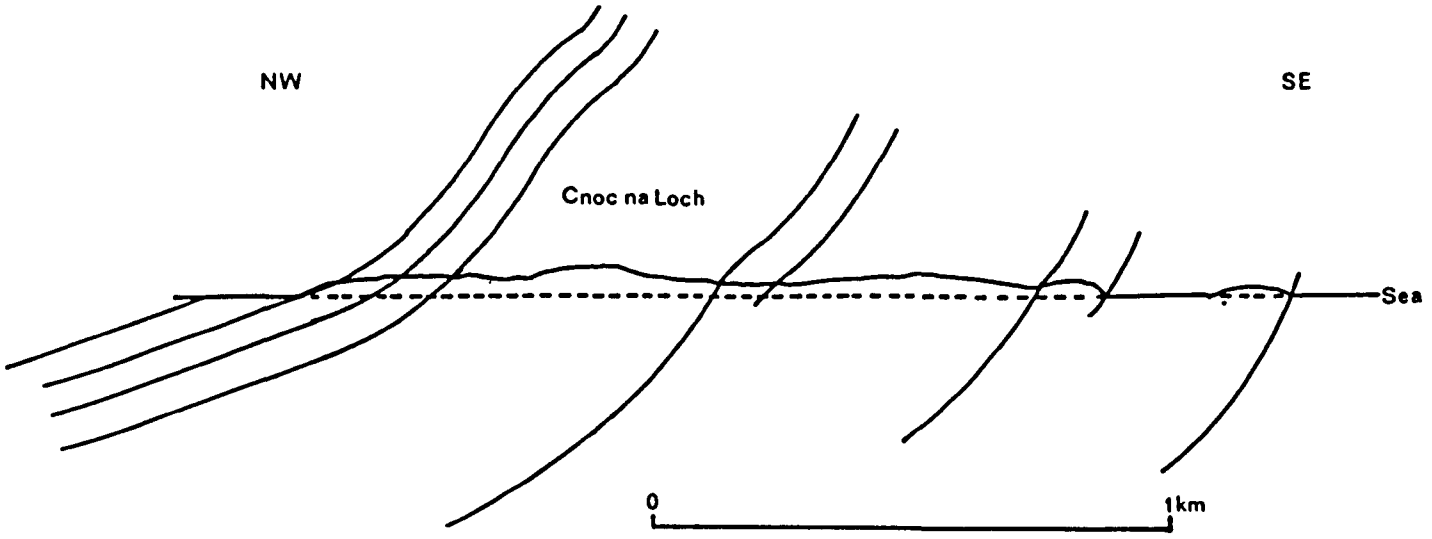

Figure 2.C.4. A cross section through Cnoc na Loch showing the relatively rounded hinge zone of the Lochalsh Syncline. The limbs of the fold are relatively long and straight producing, overall, an angular profile. The section was drawn from field maps of the area.

A

B

Figure 2.C.5. A. A photograph (looking north) of the fold profile at Plockton (NG 79903421). The outcrop is approximately 2 metres high. B. Looking south at a small minor fold related to the fold profile shown in A.

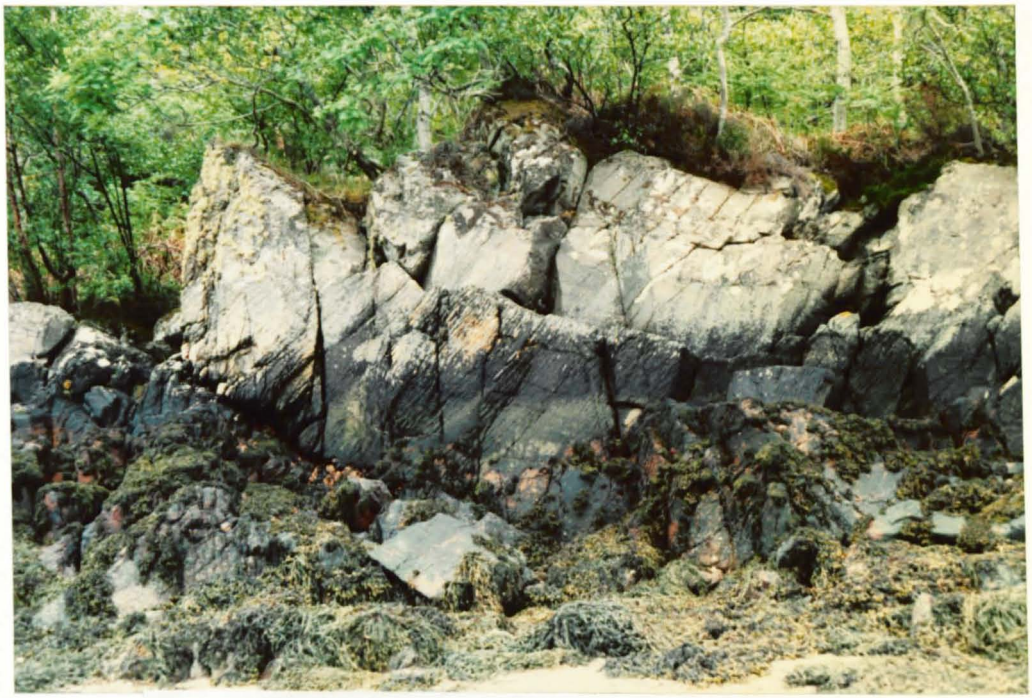

Figure 2.C.6. Looking south at the minor fold exposed at Port Cam (NG 76853130). The strong cleavage in the photograph is the transverse cleavage.

The hinge of the minor fold at Plockton has several related asymmetric minor folds of around 20cm limb length and they suggest that the section is on the overturned limb of a large syncline (see Figure 2.C.5.). This fold occurs within the hinge zone of the Lochalsh Syncline,to the east of the axial trace and is parasitic to the Syncline. The hinge at Port Cam is shown in Figure 2.C.6., the fold at Erbusaig is identical,both are gentle arcs of bedding concave westwards and these lie to the west of the main hinge and axial trace of the Lochalsh Syncline (see Figure 2.A.1.). Figure 2.C.7. shows two sections through the Lochalsh Syncline, one along the north coast of Sleat and south coast of Lochalsh and the second along the south coast of Loch Carron. These were drawn using field data and isogon patterns (Ramsay 1967) obtained from the minor fold at Plockton.

On the highest part of the overturned limb of the Lochalsh Syncline at Carn a Bhealaich Mhoir, Lewisian Gneiss is exposed. The gneisses form a prominent ridge which dips gently away to the southeast. Around Loch nan Gillean and Loch na Leitire, Epidotic Grit is exposed in a series of small folds but as shown in Figure 2.C.7. there is little evidence for folding of the fabric in this region and the outliers may represent a gentle warp of the fabric exposed by erosion.

Central Area of the Kishorn Nappe

The northern part of Sleat (Figure 2.A.1.) consists mainly of rocks attributed to the Sleat Group with some rocks of the Torridon Group in the west. Within this central area both limbs of the Lochalsh Syncline are well exposed. The axial trace of the Syncline may be followed from Allt Mor a Ghaidh southwards across the ridges of Sithean a Choire Odhair, Glas Choire

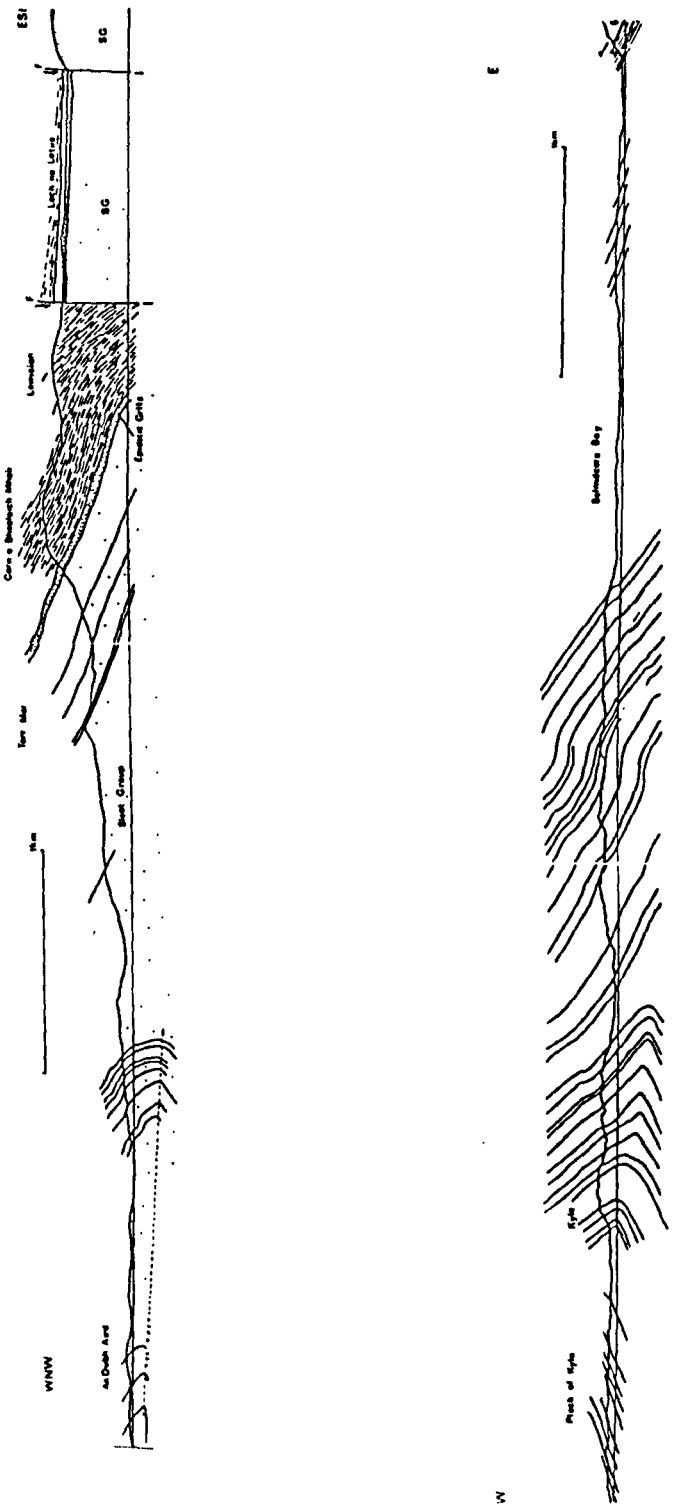

Figure 2.C.7. Two sections through the Lochalsh Syncline between, A. An Dubh Aird and Loch na Letire and B. Kyle of Lochalsh and Balmacara. The sections are based on mapping for this thesis.

and Beinne na Greine where it abruptly changes trend and runs in a more easterly direction towards Coire na Coinnich (see Figure 2.A.1.). This change in trend on the northern side of Kylerhea Glen suggests that the axial plane dips gently eastwards.

From NG 770200 in Kylerhea Glen southwards, the axial trace is marked by an abrupt change in topographic slope and frequently the change from normal to inverted limb is so rapid that the hinge appears to be marked by a thrust. The thrust plane is never exposed, but may be mapped in the field using the orientation of the bedding and changes in topographic slope. As shown in Figure 2.C.8. the thrust is restricted to the inner arc of the Lochalsh Syncline. The thrust is not present at all points along the axial trace of the Syncline and where it is absent, the bedding curves gently around the fold. It is thought that this thrust represents an out-of-syncline thrust, which is a thrust plane that develops due to the lack of space in the core of a growing syncline. The position of the thrust within the Lochalsh Syncline suggests that it may be an out-of-syncline thrust. However, the outcrop is insufficient to distinguish whether the thrust is a true out-of-syncline thrust or a climbing thrust which has followed the axial plane of the fold. From the close association of the two structures it is thought to be an out-of-syncline thrust and will be described as such in the remainder of the thesis. (See Figure 2.C.9).

The thrust is particularily well developed on Ben Aslak. From Ben Aslak the axial trace runs in a southerly direction towards the north end of Rudha Guaill. The portion of the axial trace mapped to the south of Kylerhea Glen (Figure 2.A.1.)

SEE BACK POCKET FOR MAP

Figure 2.C.8. A geological map of northern Sleat showing the out of syncline thrust which is related to the Lochalsh Syncline. A large proportion of the original data has been omitted for clarity.

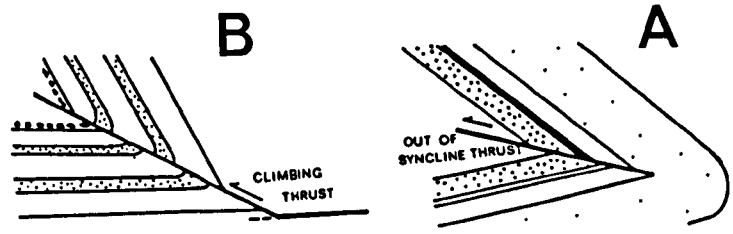

Figure 2.C.9. A. A true out of syncline thrust, at the lower end the thrust plane forms a tip. B. A thrust which has followed the axial plane of a recumbent syncline, at its lower end the thrust joins another fault.

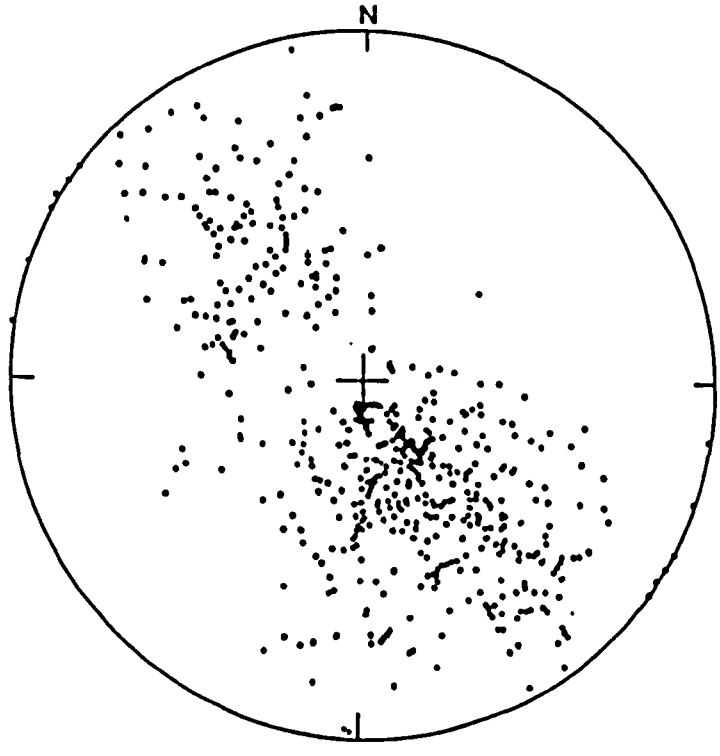

Figure 2.C.10. A stereogram of poles to bedding from the central area of the Kishorn Nappe.

corresponds well with those mapped by Peach et al (1907), Bailey (1939) and Sutton and Watson (1964). However, to the north of the Glen the trace of the fold is much simpler than that obtained by Bailey (1939) who shows a highly sinuous trace. The recognition of the Loch na Beiste Fault removes the need for such a complex trace.

The stereogram of poles to bedding (Figure 2.C.10.) indicates a fold axis plunging at 10 degrees towards 045 degrees. The stereogram shows two well defined maxima corresponding to the relatively straight limbs of the Lochalsh Syncline but in contrast to the northern area, the girdle is much more diffuse and this may be due to a larger sample of the hinge zone.

In general,,to the east of the axial trace the beds dip moderately of gently to the southeast and are inverted. However, to the north of Carn an t-Seachrain (see Figure 2.C.8.) and along the coast of Kylerhea from Rubha Buidhe to Allt a Choire Buidhe, beds of the right way up limb are exposed to the east of the main axial trace, see Figure 2.C.8.. At several localities within this area way up evidence has been found indicating that the beds form part of the normal limb of the Lochalsh Syncline. It is thought that this represents a portion of the normal limb surrounded by the out-of-syncline thrust. The thrust plane dips very gently eastwards and may be followed around Carn an t-Seachrain but it is never exposed.

Figure 2.C.11. shows a cross section through Carn an t-Seachrain to Kyle Rhea which indicates the position of the out-of-syncline thrust. The gently dipping beds of the normal limb at the north west end of the section steepen slightly beneath the thrust. A similar section may be drawn for Sithean a Choire Odhair, but the evidence for the thrust at the northwest end of

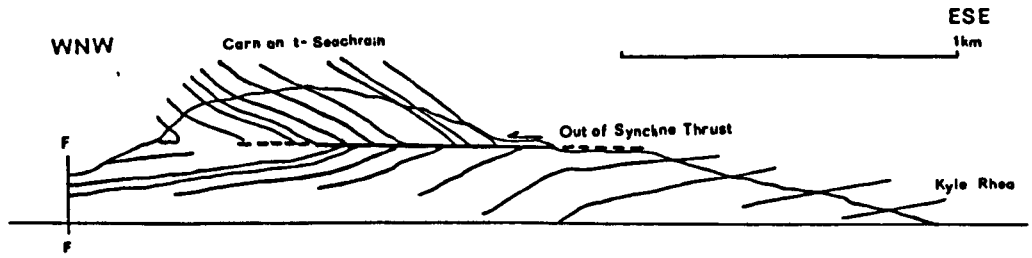

Figure 2.C.11. A geological cross sections through Carn na t-Seachrain showing the position of the out of syncline thrust. The sections was drawn from field maps.

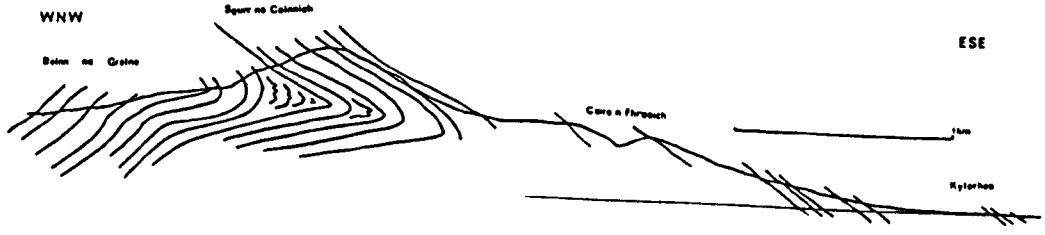

Figure 2.C.12. A geological cross section through Beinne na Greine.

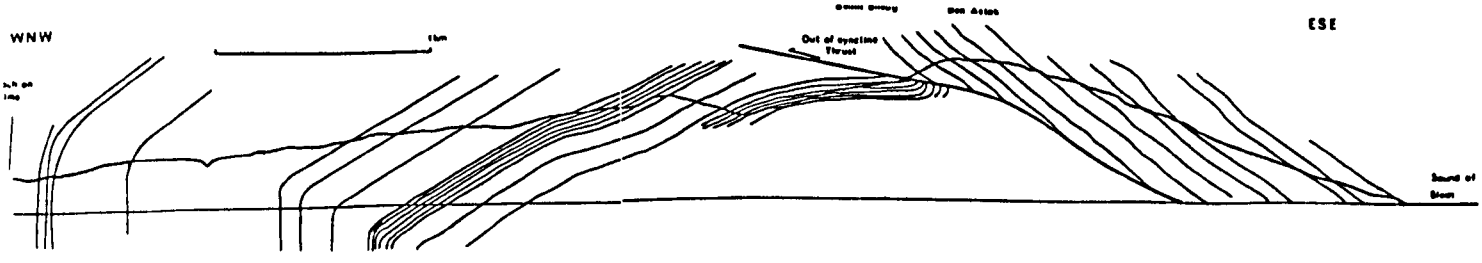

Figure 2.C.13. A cross section through Beinn Bheag and Ben Aslak showing the position of the out of syncline thrust.

the section is limited.

The section shown in Figure 2.C.12. corresponds to Figure 59 of Peach et al (1907) and is in broad agreement with it. The beds of the normal limb dip to the northwest and the dip increases gradually from 30 degrees to 60 degrees, then dip gently to the northeast before becoming overturned. The fold profile appears to be very similar to that of the northern region, with relatively long straight limbs separated by a small rounded hinge zone.

A section through Ben Aslak (Figure 2.C.13.) shows the position of the out-of-syncline thrust within the hinge of the Lochalsh Syncline and more clearly the gradual increase in dip of the normal limb into the hinge as seen on Beinn Bheag. This section also shows the presence of a large angular fold around Loch an Ime which cannot be followed to the north of Glen Arroch, suggesting the presence of a large fault (Figure 2.C.8.) which may have been active during the development of the recumbent folding. The out-of-syncline thrust on Ben Aslak cannot be traced to the rocks immediately to the north of Kylerhea Glen where the hinge of the Lochalsh Sycnline is more rounded. The lateral persistence of the thrust may be controlled by compartmental faults. Such faults were first described by Dahlstrom (1970) and are in general parallel to the movement direction of the thrust belt. Many of the streams such as Allt Thuill and Allt Coire Gasgain (Figure 2.A.1.) appear to follow fault traces (north-west-southeast) and many of these faults may be compartmental in origin. Such faults may exist within the northern region but are much more difficult to define.

Between Allt Thuill and Allt Coire Gasgain, the fold

profile of the Lochalsh Syncline changes and the section is shown in Figure 2.C.14.. This section corresponds to Figure 60 of Peach et al (1907). The very angular portion of the hinge exposed on the beach at NG 741159 is shown in Figure 2.C.15.. No evidence for a large out-of-syncline thrust is present in this area, but on the beach the hinge of the fold appears to have been thrust out.

To the south of Allt Coire Gasgain only the normal limb of the Lochalsh Syncline is exposed as the axial trace passes into the Sound of Sleat at NG 741159. Beneath the Sound of Sleat the hinge of the Syncline probably passes under the Moine Thrust in a similar manner to the northern region at Fernaig.

Within the central area, in contrast to the northern region, a much larger number of folds related to the Lochalsh Syncline are exposed, but really for the large area of fold exposed, the number of minor folds is small. The minor folds related to the Lochalsh Sycnline in the central area are of two types; (a) the fold axes measured in the field or constructed from stereograms are generally parallel to the major fold and the folds tend to occur close to the axial trace. (b) the fold axes of bedding plunge to the east-southeast, parallel to a strong grain shape fabric within the rock. These tend to occur on the overturned limb of the Lochalsh Syncline. Both types of minor folds have limb lengths of approximately 1-10 metres. The type (a) folds generally have fold profiles which are similar to the major fold profile obtained from cross sections.

Minor Folds of Type (a) in the Central Area

On Beinne na Greine (Figure 2.A.1.) close to the hinge of the major fold, several minor folds can be seen and these are shown in Figure 2.C.16., the fold profiles

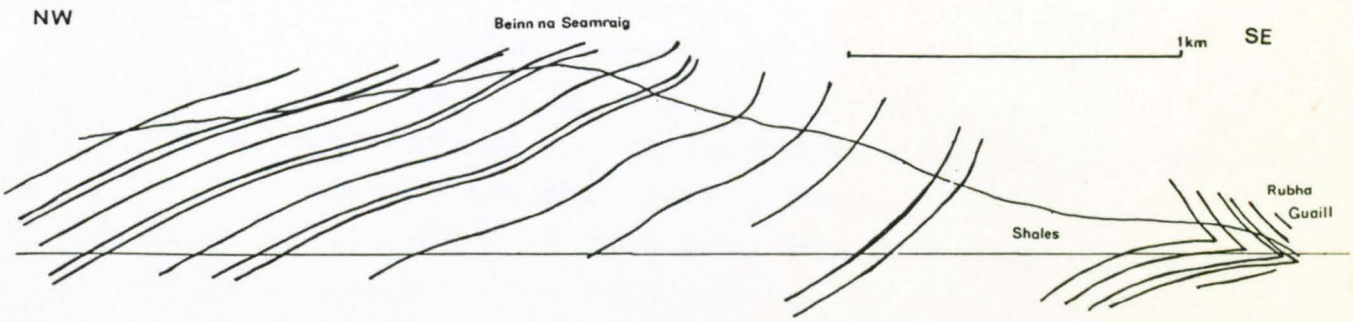

Figure 2.C.14. A cross section through the hinge of the Lochalsh Syncline between Beinn na Seamraig and Rubha Guaill. The section was drawn from field maps.

Figure 2.C.15. A photograph, looking to the northeast, at the hinge of the Lochalsh Syncline exposed at the north end of Rubha Guaill (NG 741159).

are very similar to Figure 2.C.12 and Figure 59 of Peach et al (1907). However, as shown in Figure 2.C.16 the cleavage is not axial planar to the fold and as the cleavage is not folded it must postdate it. Thus the only inaccuracy in the original section of Peach et al (1907) is that they show the cleavage to be axial planar. The fold profile in this area is very similar to that of the Plockton hinge described previously. The bedding values from around the minor fold on Beinne na Greine define a fold axis very close to that defined by the poles to the bedding for the whole of the central region. The asymmetry of the folds on Beinnenna Greine suggests that they lie beneath the main hinge of the Lochalsh Syncline and that the axial plane dips gently to the east.

On the Forestry Commission track to the north of the Kinloch Lodge Hotel (Figure 2.A.1.) several minor folds of several metres limb length are seen and some typical examples are shown in Figure 2.C.17.. Measurement of bed thickness around the folds indicate that they are chevron in style (Ramsay 1967, 1974). These folds have cleavages of variable intensity. Sometimes the cleavage is developed only in the hinge of the folds. Elsewhere a strong cleavage is present, but often it appears to cut across the folds and therefore post-dates them. Figure 2.C.17. shows stereograms of bedding and fold axes which are very similar to those obtained for the whole area. These minor folds are very similar to the larger folds on both shores of Loch na Dal which are revealed by mapping and shown in Figure 2.C.18..

Withinthe Epidotic Grits at NG 72511508, NG 72421508, NG 72561508 and NG 72681518 minor folds of type (a) are present which are much more rounded in profile and have fold axes parallel to the main fold with a gently southeasterly dipping axial plane. Locally

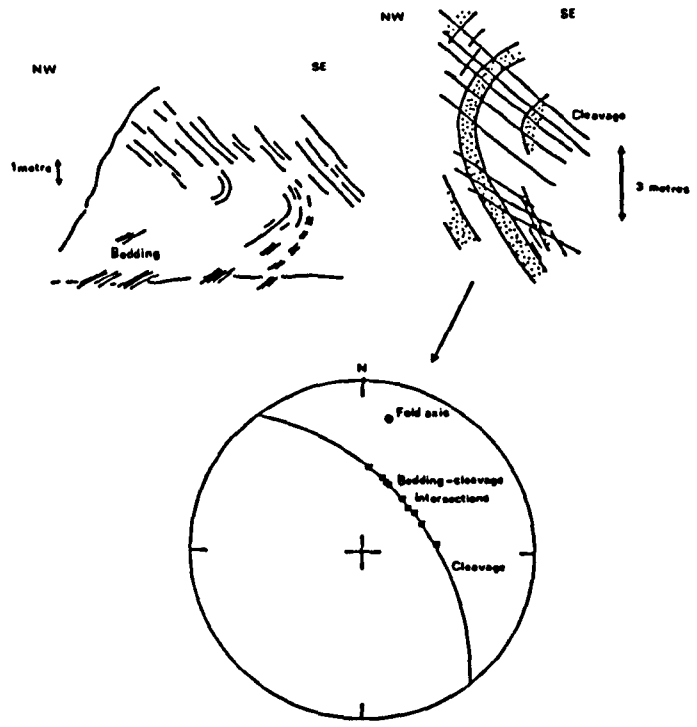

Figure 2.C.16. Field sketches of two of the minor folds which are exposed on Beinne na Greine in the hinge of the Lochalsh Syncline. The orientation of the bedding and cleavage in these folds is shown on the stereograms.

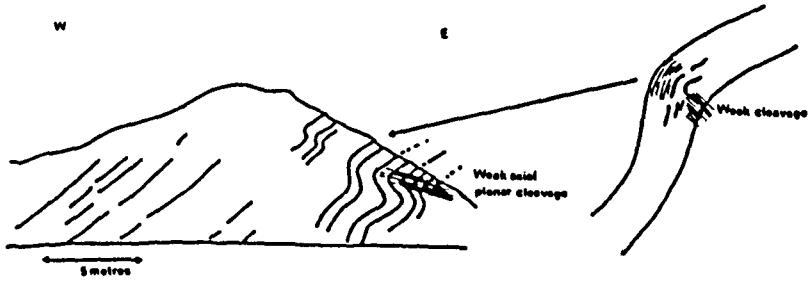

Figure 2.C.17. A field sketch from NG 71301536 showing fold profiles typicel of this area. The cleavage is only weakly developed in the hinges of the folds.

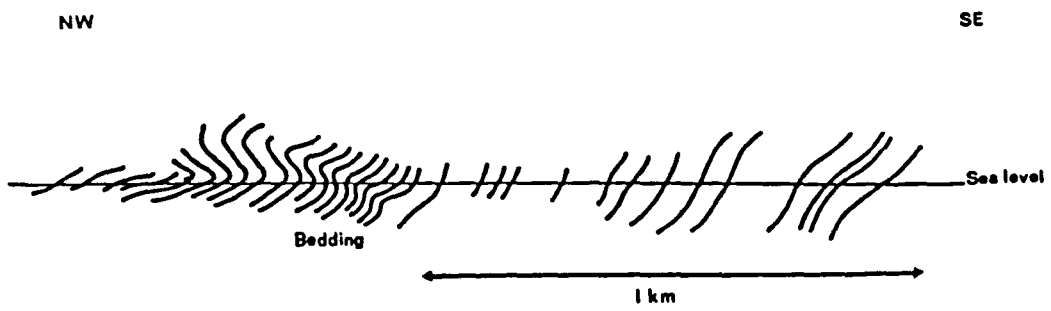

Figure 2.C.18. A cross section along the southern shore of Loch na Dal showing the style of folding. Here, the cleavage is not axial planar to the folds.

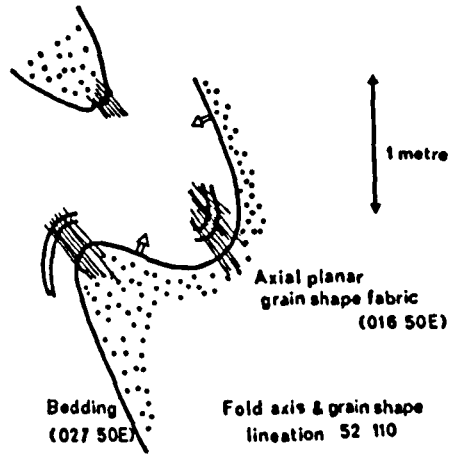

Figure 2.C.19. A field sketch of the minor fold exposed at NG 74681616 . The cleavage developed in the hinges of the folds is axial planar to the folds.

developed weak axial planar fabrics are present. The folds have no real sense of asymmetry and in in any cases they are disharmonic.

Minor Folds of Type (b) in the Central Area

At NG 74681616 and NG 76911774 the folds of type (b) are clearly seen and a field sketch is shown in Figure 2.C.19.. The fold axes plunge to the east-southeast. These folds are restricted to the most eastern portion of the overturned limb and the fold profiles are often irregular, particularly the large folds at NG 76911774. They generally show highly thickened hinges within which the rocks have a weak fabric parallel to the axial planes.

At Dun Ruaige (Figure 2.A.1.) a small area of green chloritic pelite is exposed, it overlies the Epidotic Grits of the overturned limb of the Lochalsh Syncline. The pelite or "Dun Rock" (Peach et al 1907) is very similar in structure and appearance to the mylonitic Lewisian rocks within the Balmacara Nappe at Ard Hill. (Figure 2.A.1.). It is thought that this represents a small sliver of the Balmacara Nappe or some similar nappe which lies in an equivalent structural position. There appears to be some evidence of brecciation beneath the Dun Ruaige Thrust.

Southern Region of the Kishorn Nappe

The southern region lies to the south of Loch na Dal and consists of the remainder of Sleat until the outcrop of the structurally higher Tarskavaig Nappes. Around Ord (Figure 2.A.1. and 2.B.1.) a small outlier of Cambro-Ordovician rocks is exposed and has been termed the "Ord Window" by Bailey (1939). A structural reinterpretation has been made for this area and it will be presented in this thesis. The reinterpretation of the major structure will be described first and then

detailed description of the structures present.

No cleavages are seen within the Kishorn Nappe in the southern region and no portion of the overturned limb of the Lochalsh Syncline is exposed. Beneath the Moine Thrust and westwards to the Ord Window and Tarskavaig Nappes the normal limb of the Lochalsh Syncline is exposed. Several large angular folds are seen on this limb and generally they have short slightly overturned limbs which young to the north-west. They can be traced over several kilometres along strike on the basis of bedding orientation or the presence of minor folds or one metre or a few centimetres limb length. These minor folds are restricted to the hinges of the large folds. The traces of the large folds generally run northeast southwest and the fold axes plunge gently to the northeast or southwest.(Figure 2.C.20.).

Figure 2.C.21. shows poles to bedding for these angular folds, which from mapping appear to have limb lengths of 1 to 2 kilometres and an asymmetry which suggests that they lie on the normal limb of a larger recumbent syncline. The limbs of the large angular folds are relatively straight with only slight undulations, particularily on the flat limb and there are very few minor folds. The smallest of the minor folds seen in the field are of 1 to 2 centimetres limb length, usually they affect silty and sandy laminae within shale units and reflect the geometry of the 1 and 2 metre folds which generally affect the bedding as a whole, as shown in Figure 2.C.22.. The minor folds of all sizes show a chevron style (Ramsay 1974) and this has also been inferred for the larger folds during construction of the sections shown in Figure 2.C.23..

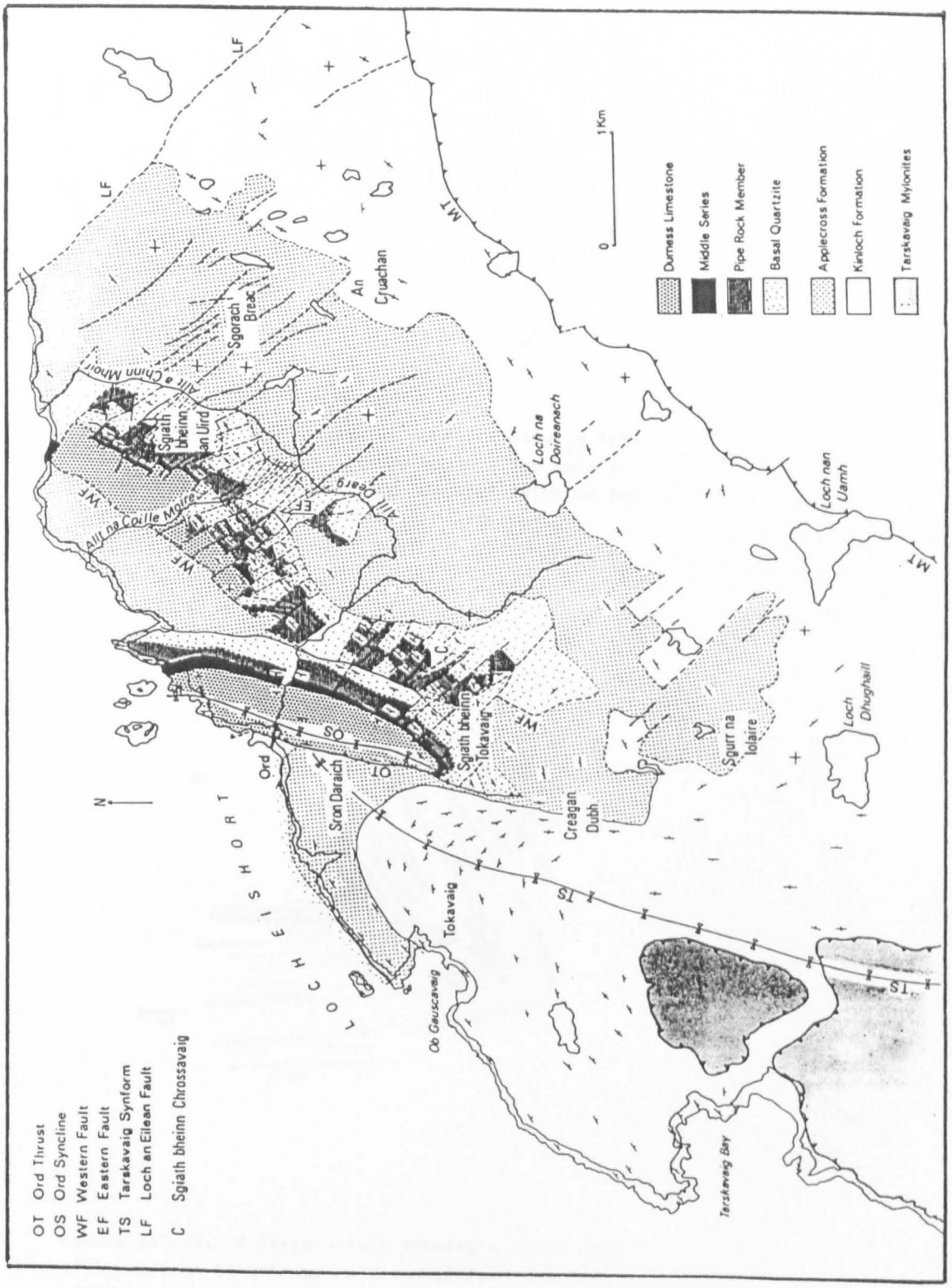

Figure 2.C.20. A geological map of southern Sleat showing the area to the south of the Loch an Eilean Fault. The large angular folds will be followed between An Cruachan and Loch Dhughaill.

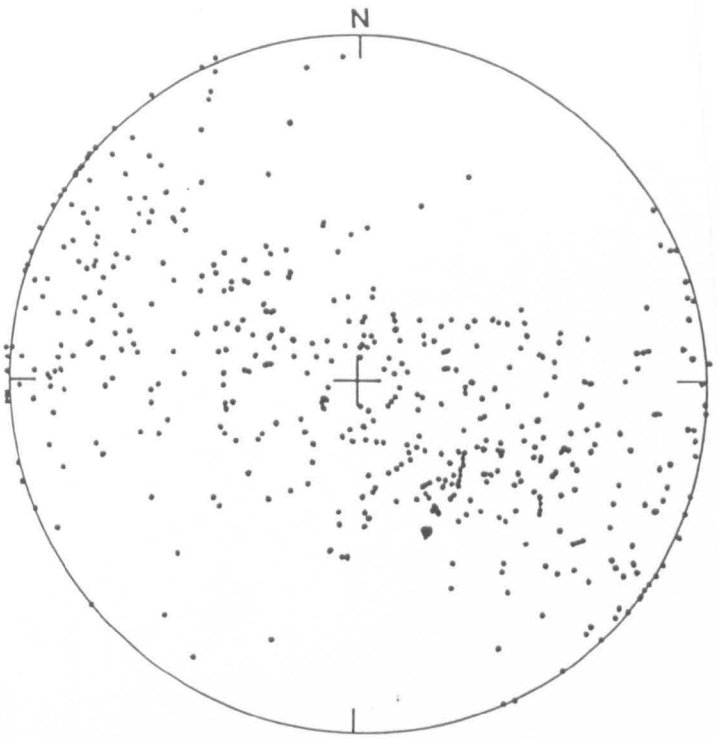

Figure 2.C.21. A stereogram of poles to bedding from the southern area of the Kishorn Nappe. The data in this diagram refers to the large angular folds on the correct way up limb of the Lochalsh Syncline.

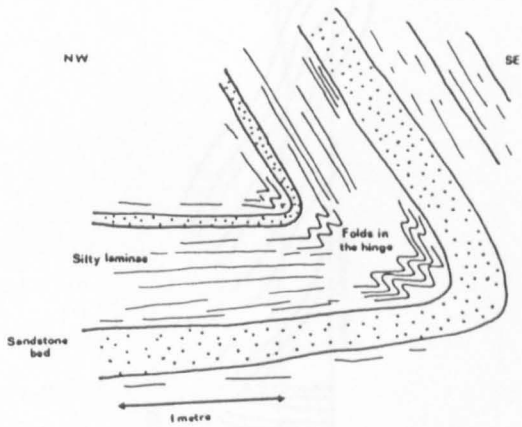

Figure 2.C.22. A field sketch showing a minor fold of 1-2 metres limb length and associated folds of 10-20 centimetres limb length. These folds outcrop as linear zones in the hinges of the major folds.

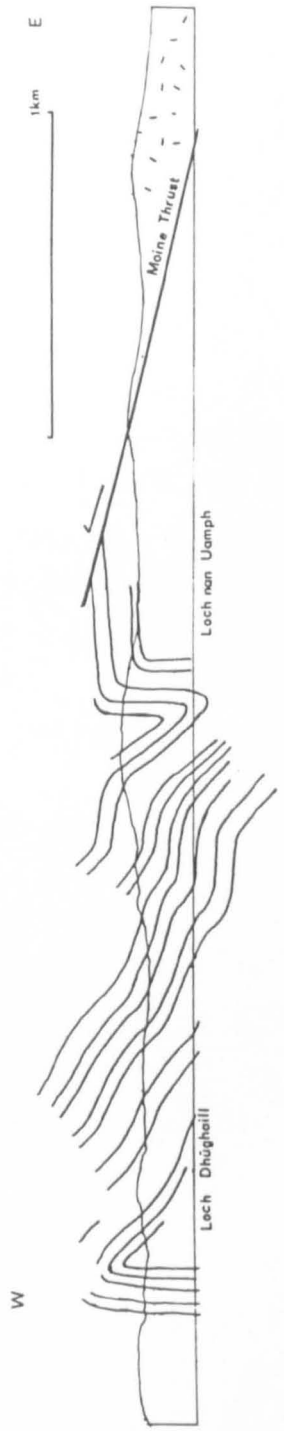

Figure 2.C.23. A cross section, to the north of Loch Dhughaill, showing the large angular fold on the correct way up limb of the Lochalsh Syncline.

Revision of the Ord Window

In this thesis the term "Ord Window" will be used to denote all of the Cambrian rocks of the structural outlier east of Ord. Bailey (1939,1955) suggested that portions of the Ord Window formed part of the Foreland (Figure 2.B.3.). However, results will be presented which indicate that all the rocks within the Window form part of the Kishorn Nappe and none may be considered as part of the Foreland. The Ord Window is composed of a series of fault bounded blocks, several structures and contacts are crucial in the interpretation presented here.and these will be described in detail. A fault, the Ord Fault (Figure 2.C.20.) runs south from the beach at Ord along the west side of Sgiath Bheinn Tokavaig for a distance of 2Km.. At Creagan Dubh the Fault passes into or under an angular antiform,part of the overlying normal limb of the Lochalsh Syncline. A steep to vertical dip is inferred for the Fault from its relatively straight outcrop and the steep sided narrow valley which it occupies. The Fault throws rocks of Cambrian age against red sandstones of Torridonian age and it forms the western limit to the Window.

Along the coast between the villages of Ord and Tokavaig the basal quartzite can be seen to underlie Torridonian sandstones of the Applecross Formation. The outcrop of the unconformity lies close to the low water mark and it strikes NE-SW and dips gently southwards. From Tokavaig to Tarskavaig Bay (Figure 2.C.20.) the inversion may be followed by the use of sedimentary structures. The rocks of the inversion form the overturned limb of a recumbent anticline, the Eishort Anticline. The axial trace of the anticline may be followed northwestwards for 6Km from Tarskavaig Bay to the south of Sron Daraich where it is truncated

by the Ord Fault (Figure 2.C.20.). This period of recumbent folding must predate the faulting.

To the south of Sron Daraich, the axial trace of the Eishort Anticline is folded by an open synformal fold, the Tarskavaig Synform which plunges gently to the south. The axial trace may be followed south-westwards in sandstones and shales of the Kinloch Formation into the overlying Tarskavaig Nappe where it folds the fabric and the thrust plane. At its northern end the axial trace of the Tarskavaig Synform is truncated by the Ord Fault and must predate, perhaps only slightly, the faulting, but postdate the recumbent folding.

Two major northeast-southwest striking faults crop out to the east of Ord village, the most westerly of these faults named the Western Fault in Figure 2.C.20. (this name will be used throughout this thesis) may be followed from the coast of Loch Eishort southwards down the west side of Sgiath bheinn Chrossavaig, a distance of approximately 6Km. Its outcrop is slightly curved, convex westwards. The trace of the Fault pays little attention to the topography and a steep to vertical dip is inferred. The curvature of the fault trace suggests that the Fault could dip eastwards with listric geometry (McClay 1981). A similar geometry is inferred for the most easterly fault (the Eastern Fault in Figure 2.C.20.) which can be traced for approximately 1Km between the head of Allt na Coille Moire and the road in Ord Glen. The above fault together with the Ord Fault bound a series of strike parallel blocks or slices of previously folded Torridonian and Cambrian rocks. To the east of the Ord Fault the slice contains a major syncline, the Ord Syncline (Bailey 1939) which contains a core of Durness Limestone and an envelope of Eriboll Sandstone. The fold is truncated by the Ord and Western Faults and its axial

trace runs north-south.

In the Basal Quartzite and the Pipe Rock Member which form the hill Sgiath Bheinn an Uird (Figure 2.A.1. and 2.C.20.) a synclinal fold may be recognised by the use of way up criteria. The longer upper limb is overturned and dips moderately to the east. The hinge of the syncline may be seen along the west side of Sgiath Bheinn an Uird where it is faulted by northwest-southeast striking faults of near vertical dip. Around the south end of Sgiath Bheinn an Uird the shorter normal limb is flat lying and partially cut out by the Eastern Fault. The offset of the Pipe Rock Member suggests that the Eastern Fault has a normal fault displacement and the hanging wall is downthrown to the southeast. Southwards the quartzite ridge occupies an overturned fold limb which dips to the east but youngs westwards. To the south of the road in Ord Glen the quartzite can be traced into several synclinal folds similar to those described above. A stereogram of poles to bedding (Figure 2.C.24.) shows that the plunge of the folds is almost horizontal. The form and asymmetry of the folds suggest that the main synclinal hinge lies below the present erosion level and that the eastern quartzite ridge forms the upper, overturned limb of that fold. The axial plane dips eastwards or southeastwards.

Along the east side of Sgiath Bheinn an Uird the stream Allt a Chinn Mhoir runs along a fault surface which dips moderately to steeply eastwards. The western footwall is formed of Cambrian Quartzite (s.l.) and the hanging wall consists of red sandstones of the Applecross Formation which dip gently southwards. These sandstones form part of a flat-lying limb of one of the large folds on the normal limb of the Lochalsh Syncline. The fault surface forms the eastern limit to the Window and it is apparent that the

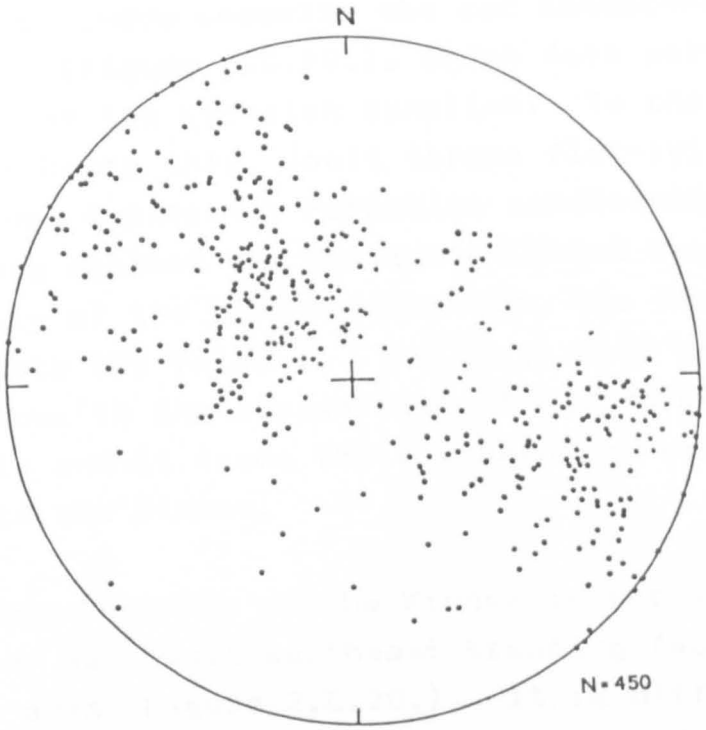

Figure 2.C.24. A stereogram of poles to bedding for all of the rock types exposed within the Ord Window.

Figure 2.C.25. A map of the area around Allt na Coille Moire (A). Ornamentation as for Figure 2.C.20. The northwest-southeast trending faults must have been active at a comparable time to the Western Fault to have offset the base of the Durness Limestone without affecting the Western Fault. S = Loch Starsaich.

rocks of the Window underlie the red sandstones of Sgorach Beag (Figure 2.C.20.), which form part of the normal limb of the Lochalsh Syncline. To the south around Allt Dearg this fault throws flat-lying , right way up, Applecross Formation sandstones of Sgorach Beag against the overturned Basal Cambrian unconformity of the Window therefore, the Fault must postdate the folding. The fault must be present close to the stream east of Sgiath bheinn Chrossavaig and it forms the southern and eastern boundary to the Window.

The northern boundary of the Window is formed by one of the many northwest-southeast trending faults which cross the area (Figure 2.C.20.). It is difficult to assess whether the faults are entirely of Caledonian or Tertiary age. But, as shown in figure 2.C.25. the faults must have been active during folding to produce the offset seen in the Durness Limestone around Allt na Coille Moire. Similar faults which are parallel to the transport direction of the thrust zone were described in the central area. Their association with the folding is more clearly seen in the Window. However, it is possible that some Tertiary displacements have occurred on these faults. On southern Sleat the Tertiary dykes trend parallel to the faults which suggests that the faults may form part of a fracture pattern of Tertiary age. It is reasonable to expect the dykes to follow earlier regional fracture patterns if the fractures are close to those required by the development of the volcanic complex. It is thought, that the Tertiary dykes follow,in part, an inherited pattern of fractures which were compartmental faults (Dahlstrom 1970) developed during the recumbent folding on southern Sleat.

From the above description it is apparent that a period of fecumbent folding affecting both Cambrian

and Torridonian rocks predated the Tarskavaig Synform and both the recumbent folding and the Tarskavaig Synform were affected by later thrusting and faulting.

Bailey (1939) stated that "it (the Ord Syncline) almost certainly originated as a recumbent syncline closing downwards to the southeast with its upper limb largely replaced by a recumbent thrust (the Ord Thrust)". He suggested that the syncline now closes upwards due to reorientation during the uplift of the Window and is related to the Ord Inversion to the west of the Ord Thrust (see Figure 2.B.3.). There is no field evidence to suggest whether the Ord Syncline is an antiformal (Figure 2.B.3.) or a synformal syncline (Figure 2.C.26.). It is suggested that the Ord Syncline is synformal as evidence presented for the eastern quartzite ridge suggests that a synformal syncline is present in the Cambrian rocks of the Window. It is thought that prior to the faulting, the Ord Syncline was a much larger fold than that described by Bailey (1939) and the main hinge is present in the slice immediately to the east of Ord and that the overturned limb is exposed on Sgiath Bheinn and Uird and Sgiath Bheinn Chrossavaig (see Figure 2.C.26.). As the rocks of the Window are structurally lower than the surrounding Torridonian sandstones and a period of recumbent folding is recognised prior to the faulting, it seems logical to link the structurally lower Ord Syncline to the overlying Lochalsh Syncline by the Eishort Anticline which outcrops at a intermediate structural level (Bailey 1939).

The dip of the major north-south faults can only be inferred, as described above. Clough in Peach et al (1907) gives conflicting evidence for the dip of the Ord Thrust from zones of brecciation to the east of Sgiath Bheinn Tokavaig. Both Peach et al (1907) and Bailey (1939,1955) concluded that the faults traced

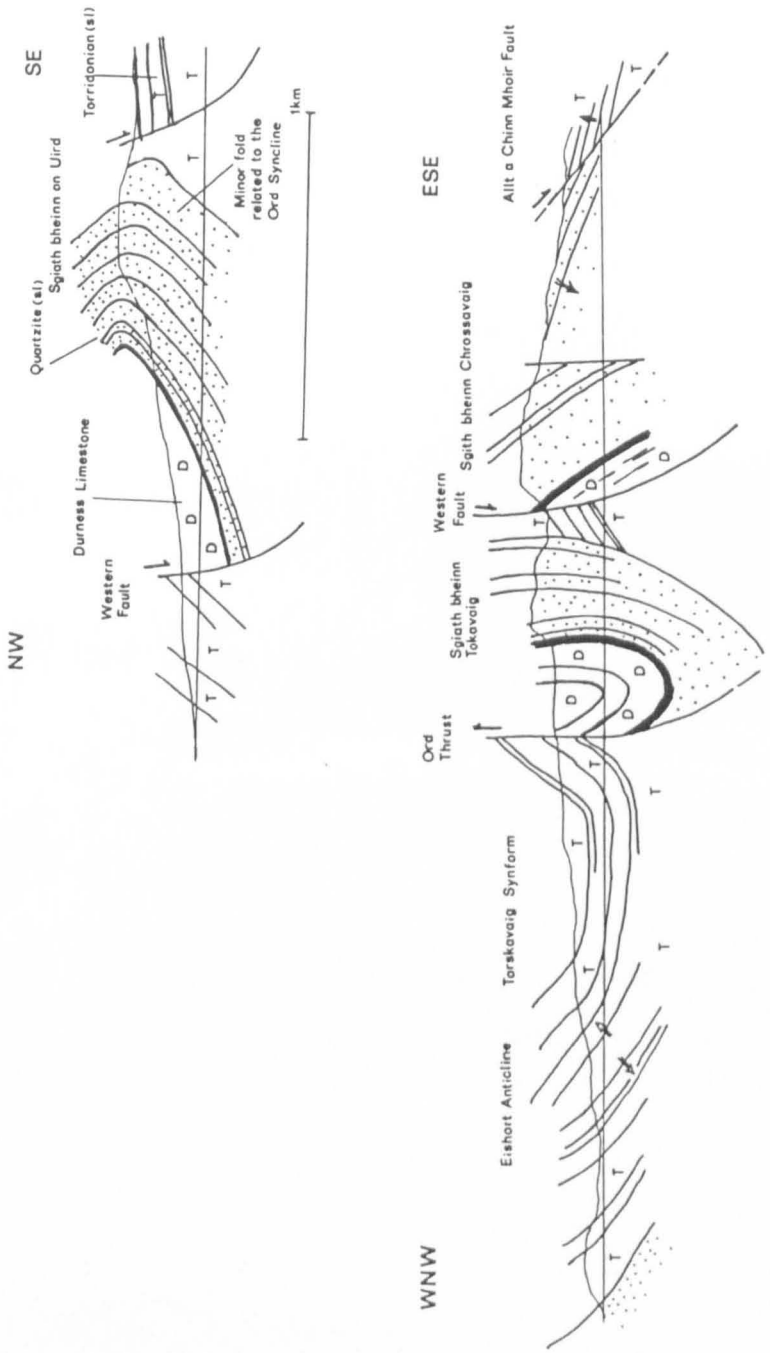

Figure 2.C.26. Cross sections through the Ord Window produced as a result of the recent mapping of the Kishorn Nappe for this thesis.

out antiforms and had been folded during uplift of the central portion of the Window. The work presented in this thesis suggests that the major faults have steep easterly dips. Three possiblilities exist for the movement direction on the faults:

1. Reverse or thrust movement to the northwest. The faults may represent imbricate thrusts similar to structures described further north in the thrust zone (Peach et al 1907, Elliott and Johnson 1980). By analogy with Dahlstrom (1970) it is thought that the Tarskavaig Synform formed to the west of the Ord Fault (Ord Thrust of Bailey 1939) as a footwall structure beneath the Fault, thus indicating a thrust sense of movement. Further, during thrust fault movement fault slices would uplift portions of the structurally lower Ord Syncline through the overlying limb of the Lochalsh Syncline. This agrees with the field observations above. However, a thrust sense of movement cannot be demonstrated on the Eastern and Western Faults. The overturned limb of the Ord Syncline lies to the east of the main hinge at the same structural level (see Figure 2.C.26.). Imbrication of a pre-existing recumbent syncline could not place the overturned limb in such a position, see Figure 2.C.27.. Further, cross sections which assume thrust imbrication of a pre-existing syncline cannot be balanced (Dahlstrom 1970) and lead to an excess of Basal Quartzite and Pipe Rock Member compared with the overlying Durness Limestone.

2. All three faults may be normal faults downthrown to the southeast, dropping a structurally higher syncline down into its present position. This model concurs with some field evidence. It has been shown that the Eastern Fault has a hanging wall which is downthrown to the east. Following the argument above (Figure 2.C.27.) normal faults could place the overturned limb of a pre-

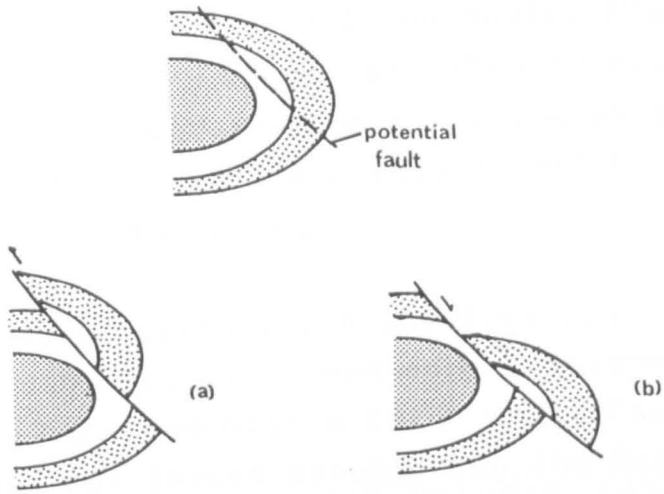

Figure 2.C.27. A recumbent syncline with a potential fault surface. Case (a) thrusting cannot place the overturned limb at the same structural level as the core of the fold. Case (b) normal faulting can place the overturned limb at the same level as the core of the fold.

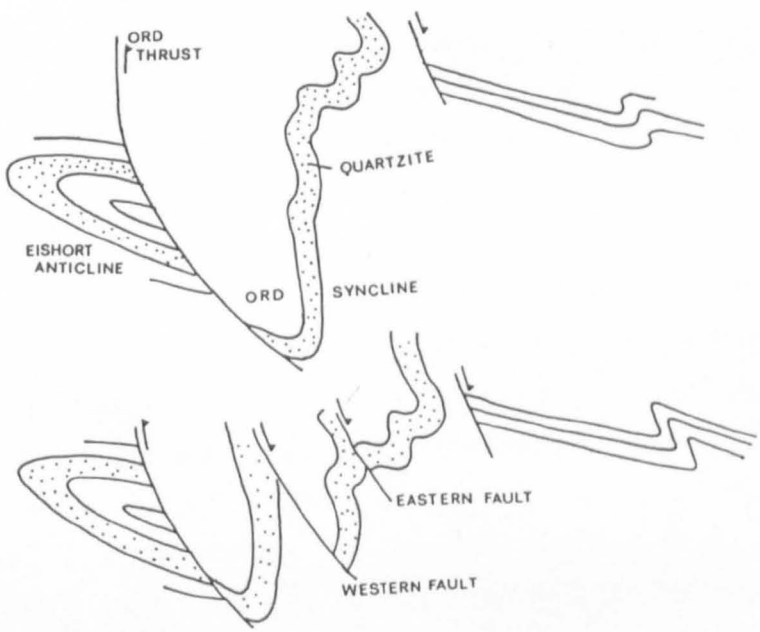

Figure 2.C.28. A series of schematic sections showing the development of the Ord Window and the adjacent structures of southern Sleat.

existing syncline to the east of its hinge. However, all the four major faults shown in Figure 2.C.20. cannot be normal faults as thrust movement can be demonstrated on the Ord Fault. It is clear that from the fault contact at Allt a Chinn Mhoir, that the Cambrian rocks of the Window are structurally lower than the Torridonian sandstones and shales in the hanging wall to the east and this cannot be incorporated in this model.

3. A compromise model, which involves reverse or thrust movement on the Ord Fault and normal movement on the Eastern, Western and Allt a Chinn Mhoir Faults. This model allows for thrust movement on the Ord Fault, as suggested by the form and position of the Tarskavaig Synform and uplift of the Ord Syncline in the hanging wall of the Ord Thrust. The model also allows southeasterly directed normal movement on the Eastern and Western Faults as described above.

The proposed model (that of 3. above) is in conflict with interpretations of both Clough in Peach et al (1907) and Bailey (1939,1955) (Figures 2.B.2. and 2.B.3.). Of Clough's original work the main conflict arises over the nature and position of the eastern boundary of the Window,he took this to be the contact between the Kinloch and the Applecross Formations and interpreted it as a thrust, the eastern limb of the Sgiath Bheinn Tokavaig Thrust (see Figure 2.B.2.). The author feels that Clough was misled by the nature of the contact which in his sections he shows dipping eastwards. It is offset by the northwest-southeast trending faults (Figure 2.C.20.). At several points along its outcrop it can be demonstrated that the boundary dips to the northwest i.e. the Kinloch Formation underlies the Applecross Formation. In other areas the boundary is complicated by folding; the Applecross Formation tends to be flat-lying with a gentle southward dip while the Kinloch Formation is almost vertical about a northeast-southwest strike and it youngs to the northwest. To the northeast of An

Cruachan (Figure 2.C.20.) the Kinloch Formation tends to form the high ground to the east of the boundary and it appears, incorrectly, that the Kinloch Formation overlies the Applecross Formation and the contact dips to the southeast. It is suggested here that the contact is the stratigraphic boundary between the Kinloch Formation and the overlying younger Applecross Formation. The boundary is however, affected by one of the large angular folds shown in Figure 2.C.23.. Such folds are present on Meall Buidhe and to the south of Creagan Dubh. South of Ord Glen, particularily around Sgurr na Iolaire (Figure 2.C.20.), the Applecross Formation forms the tops of the hills underlain by the Kinloch Formation. This boundary is further complicated in that between Sron 'Daraich and Creagan Dubh the boundary between the Kinloch and Applecross Formations represents a transitional change in sedimentary facies, It is apparent therefore that the boundary between the Kinloch and Applecross Formations does not represent a tectonic contact and that the eastern boundary of the Window is formed by the Allt a Chinn Mhoir Fault (Figure 2.C.20.) and its continuation to the south of Ord Glen.

Bailey (1939) extended the trace of what he termed the Ord Thrust south to Loch Dhughaill and modified the maps of Clough (Peach et al 1907). The mapping for this thesis agrees with Clough's interpretation that the boundary between the Kinloch and Applecross Formations is continuous around Sgurr na Iolaire to Creagan Dubh (see Figure 3. Bailey 1939). The prominent scarp taken by Bailey (1939) to be the Ord Thrust is in fact, nearly vertical bedding surface in an angular anticline of the type previously described and this forms part of the normal limb of the Lochalsh Syncline.

The Cambrian age rocks of the Window represent a structurally lower syncline, the Ord Syncline which was uplifted through the overlying normal limb of the

Lochalsh Syncline by the Ord Thrust (Figure 2.C.28.). The Ord Syncline is also affected by three listric extensional faults the Eastern, Western and Allt a Chinn Mhoir Faults. The Eastern and Western Faults affect rocks within the Window and it is thought that they have a common sole fault with the Ord Thrust. The Allt a Chin Mhoir Fault forms a contact between the rocks of the Window and the overlying Lochalsh Syncline. Both thrust and normal faulting appear to have operated at a similar time and as a result the Ord Syncline lies at the same structural level as the Eishort Anticline.

The Tarskavaig Synform formed as a footwall syncline during the development of the Ord Thrust, being eventually cut out by the Thrust. The Ord Thrust possesses a very steep dip much greater than ramps seen in other areas of recumbent folding related to thrusting and it is thought that it was reorientated by shortening due to the development of the thrust beneath.

The term "Window" in the case of Ord requires some qualification as the structural outlier is not exposed through a thrust plane. The boundary of the Ord Window (Figure 2.C.20.) is formed by the Ord Thrust in the west but in the east and south by the Allt a Chinn Mhoir Fault which is a normal fault. Since the faults of the Ord Window cannot be related to the Kishorn Thrust, it is clear that an early period of recumbent folding occurred entirely within the Kishorn Nappe and that all the rocks of the Window form part of the Kishorn Nappe.

Having established the major structure of southern Sleat the geometry of the folds will be described in detail. It is thought that the three recumbent folds, the Lochalsh Syncline, the Eishort Anticline and the Ord Syncline formed a single continuous fold train,

the Lochalsh Syncline being the structurally highest of these folds. The fold train on Sleat was disrupted by subsequent thrusting and faulting.

Geometry of the Eishort Anticline, Ord Syncline and the Tarskavaig Synform

Between the villages of Ord and Tarskavaig the hinge of a recumbent anticline is exposed (the Eishort Anticline). This fold has a core of Kinloch Formation and an envelope of Applecross Formation and the Cambro-Ordovician sequence (Figure 2.C.20.). The fold axis of the Eishort Anticline is very nearly horizontal as shown in Figure 2.C.29., a stereogram of poles to bedding for this area. The axial plane dips gently to the south east and the overturned limb dips at 20 to 30 degrees to the south-east, whereas the normal limb dips very gently to the northeast. The axial trace may be followed by means of way up evidence from Tarskavaig Bay through Tarskavaig village, to the south of Tokavaig and to the south of Sron Daraich, where it is truncated against the Ord Window.

The Applecross Formation and Cambro-Ordovician sequence have no minor folds but the sandstones and the shales of the Kinloch Formation beneath are intensely folded. However, these minor folds only occur within the core of the Eishort Anticline and relatively few minor folds are seen on the limbs of the fold.

On Tarskavaig Point and through Tarskavaig village, the hinge of the Eishort Anticline is well exposed. The minor folds show a chevron style and appear to have the same geometry and orientation as the Eishort Anticline (Figure 2.C.29.). Many box folds and kink bands are present, the orientation of which are shown in Figure 2.C.30.. The kink bands and box folds tend to modify the earlier chevron folds which can be related to the

A

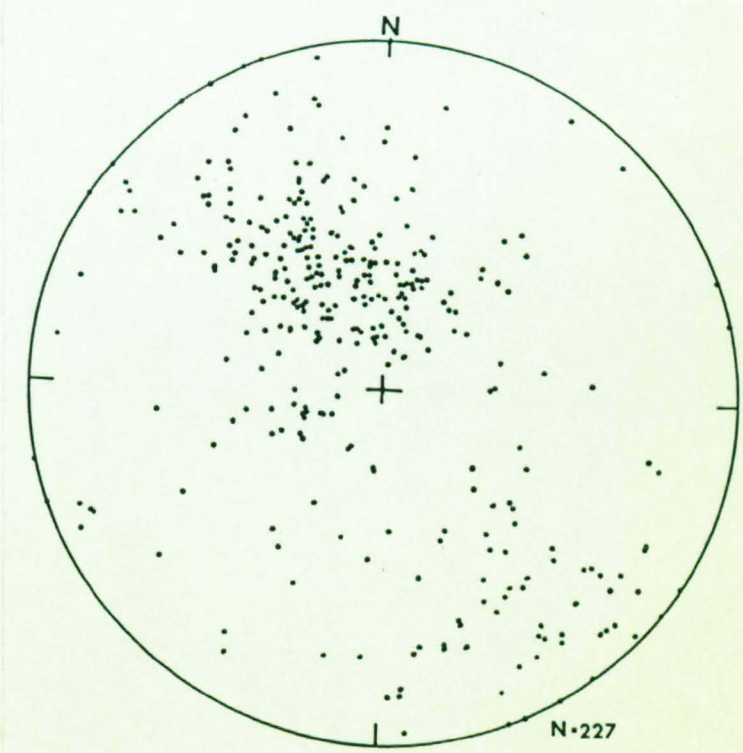

Figure 2.C.29. A. A minor fold on Tarskavaig beach (looking east) showing the chevron style of fold profile and a stereogram of poles to bedding (B) from around the Eishort Anticline.

A

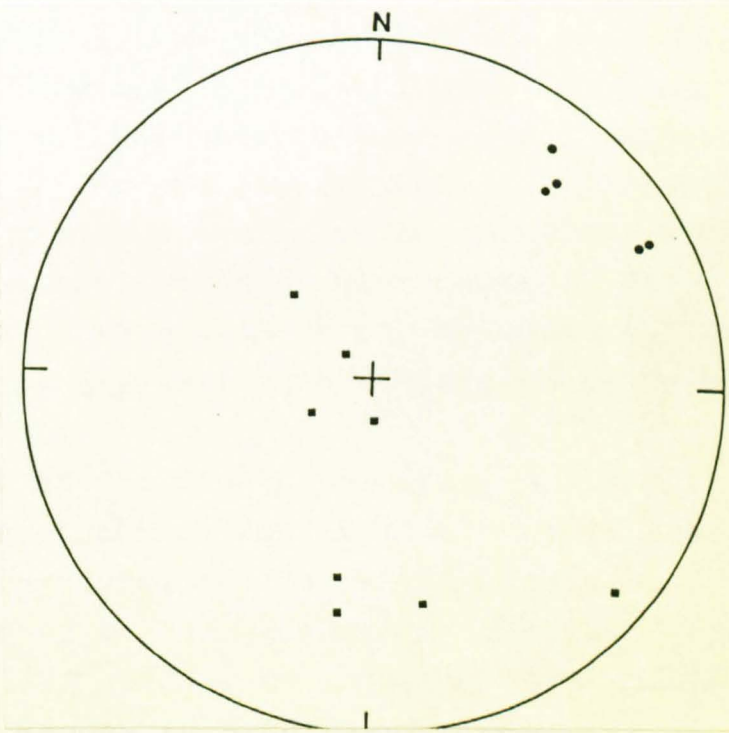

B

Figure 2.C.30. A. a series of small box folds on Tarskavaig Beach which affect and postdate the minor folds shown in Figure 2.C.29.A. and a stereogram (B) showing the orientations of these box folds and kink bands, ● = Fold Axes and ■ = Poles to Kink Bands

Eishort Anticline.

Within the Ord Window (Figure 2.C.20.) the Ord Syncline is exposed in a series of fault bounded blocks. The Ord Syncline prior to faulting was of comparable size to the Eishort Anticline and lay beneath it. Many large minor folds can be seen or mapped within the Window and they have limb lengths of several tens of metres. A typical fold profile is shown in Figure 2.C.31. from a minor fold on the west side of Sgiath bheinn an Uird. The fold axis of the Ord Syncline can be obtained from Figure 2.C.24. which shows poles to bedding for all the rock types within the Window. Between the Ord Thrust and the Western Fault (Figure 2.C.20.), the axial plane of that portion of the Ord Syncline is nearly vertical but within the fault blocks to the east it has a variable orientation but generally dips to the east. As described previously the asymmetry of the minor folds on Sgiath bheinn an Uird, Meall Da-bheinn and bheinn Chrossavaig suggests that the hinge of a major syncline lies beneath the present structural level. These minor folds are exposed between the many northwest -southeast trending faults which cross the Window. These faults are marked by wide zones of fault breccia often up to 100 metres thick and as shown in Figure 2.C.25., they may have been compartmental in origin.

To the west of the Ord Thrust (Figure 2.C.20.) the axial trace of the Eishort Anticline is folded into a broad open synform, the Tarskavaig Synform, which plunges gently to the southwest. The trace of this Tarskavaig Synform may be followed from within the Tarskavaig Nappes to Sron Daraich where it is truncated by the Ord Thrust. The orientation of bedding within the Kinloch Formation affected by the Tarskavaig Synform is shown in figure 2.C.32.. No minor folds related to the Synform are seen in the northern part of the Tarskavaig Nappe or in the Torridonian rocks

Figure 2.C.31. A photograph (looking north) of the minor fold within the Pipe Rock Member related to the Ord Syncline. This fold is exposed on the west side of Sgaith bheinn an Uird.

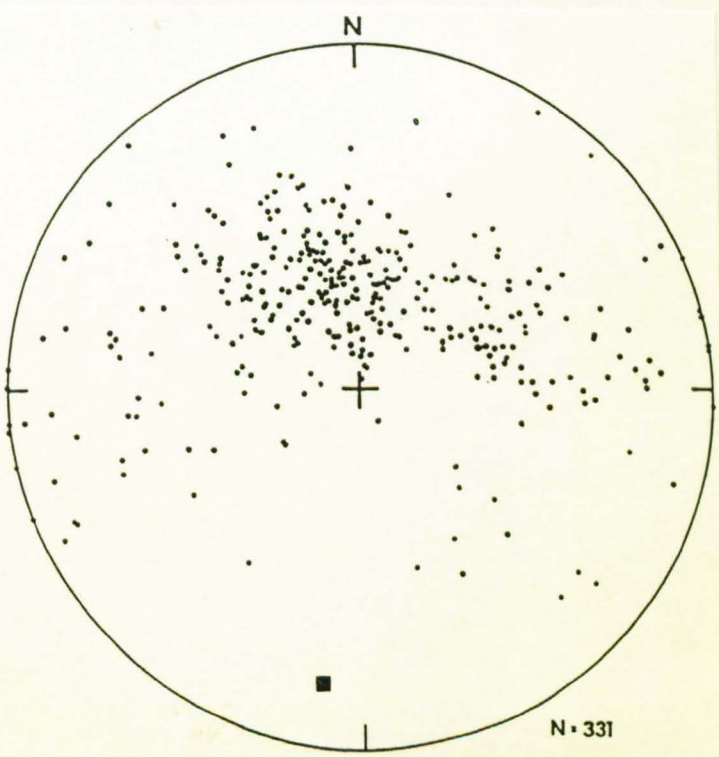

Figure 2.C.32. A stereogram of poles to bedding from the Kinloch Formation around Tokavaig. The beds are affected by the Tarskavaig Synform. ■ = Fold Axis.

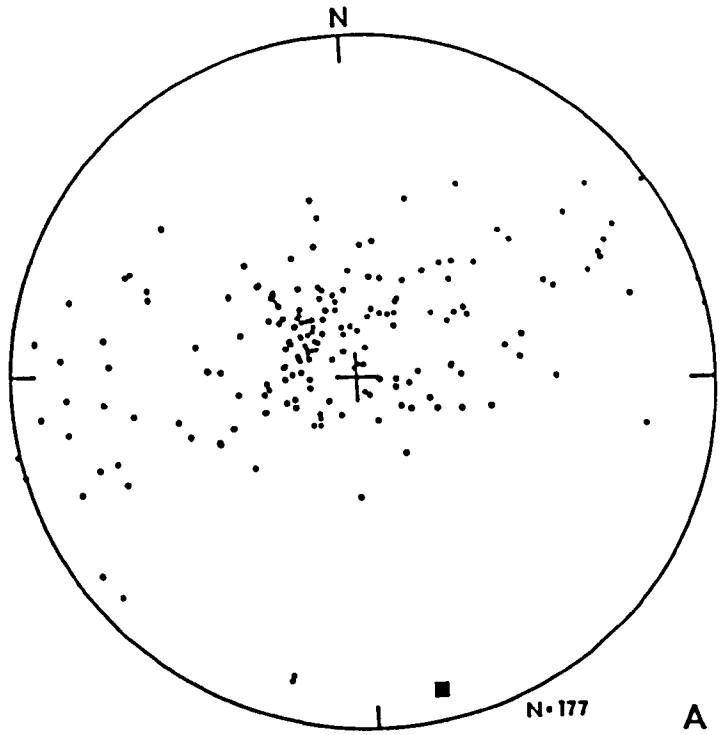

Figure 2.C.33. Poles to the mylonitic fabric from within the Tarskavaig Nappe (A). The fabric is folded around the Tarskavaig Synform as is the grain shape lineation (B).

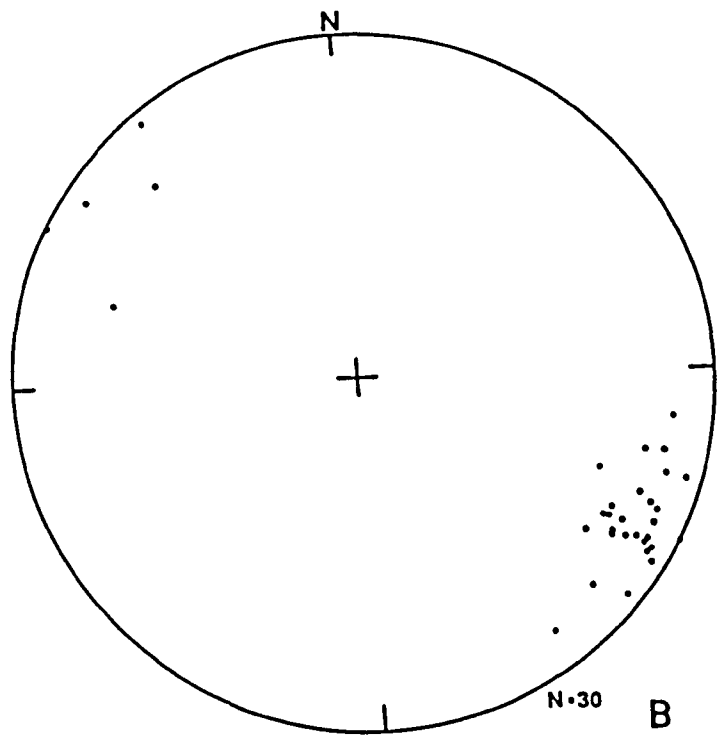

Figure 2.C.33. Poles to the mylonitic fabric from within the Tarskavaig Nappe. A, the fabric is folded around the Tarskavaig Synform (■= Fold Axis) as is the grain shape lineation (B). Unrotated lineations are shown in B.

beneath, but within the latter some of the kink bands may have been generated during this period of folding.

Within the Tarskavaig Nappe the Tarskavaig Synform folds the mylonitic grain shape fabric and the Tarskavaig Thrust beneath and thus must postdate the emplacement of the Tarskavaig Nappes.

The Tarskavaig Nappe (s.s.), at the northern end of its outcrop around Acnacloich, consists of a thin sliver of green mylonitic Lewisian Gneiss overlain by a cover of arkosic sandstone. This suggests that the overall structure of the Tarskavaig Nappe is the correct way up and this is confirmed by the few sedimentary structures preserved in the coarse beds of the arkosic sandstones where the mylonitic fabric is weak.

The strong mylonitic grain shape fabric seen within the Tarskavaig Nappe is parallel to the bedding with a strong grain shape lineation. The lineation has been folded by the Tarskavaig Synform and when the fabric is restored to the horizontal, the lineation plunges gently to the east southeast (see Figure 2.C.33.).

Section 2D Cleavages and Fabrics Within the Kishorn Nappe

To the south of Loch na Dal no cleavages or fabrics can be seen within the Kishorn Nappe. The relative ages and distributions of the cleavages within the Nappe to the north of this cleavage front will now be described together with related minor structures. Several cleavages have been recorded and their relative ages determined, these ages differ from those of Kanungo (1956), Johnson (1955a) and Coward and Whalley (1979) and possible correlations with their work will be discussed later.

The earliest cleavage seen on the Kyle of Lochalsh

and Sleat is a strong grain shape fabric which is restricted to the overturned limb of the Lochalsh Syncline. The fabric does not occupy the whole of the overturned limb and becomes more clearly defined eastwards. The fabric dips gently to the east-southeast with a strong down dip mineral or grain shape lineation. Within the sandstones of the Sleat Group the fabric is parallel to bedding and when most strongly developed, it forms a linear,rather than planar fabric. Within the overlying Lewisian Gneiss it replaces earlier structures and fabrics often leaving augens of less deformed material. In the most highly deformed Lewisian rocks, sheath folds (Cobbold and Quinquis 1980) are present but not common. As described previously on Sleat, some folds of bedding within the Epidotic Grit have fold axes which are parallel to this grain shape fabric. Figure 2.D.1. shows the strong linear fabric on a bedding surface of Epidotic Grit and Figure 2.D.2. shows the mylonitic fabric affecting quartzofeldspathic Lewisian material. Relatively undeformed Lewisian material is shown in Figure 2.D.3.. Amphibolitic material is present within the Lewisian rocks of Lochalsh but it is the quartzofeldspathic material and its derivatives which dominate the area.

From localities within the Sleat Group of the northern and central areas the orientation of the lineations is shown in Figure 2.D.4.. Data from the mylonitised Lewisian rocks of Carn a Bhealaich Mhoir are shown in Figure 2.D.5..

Thin sections from sandstones of the Sleat Group indicate that the bedding parallel fabric is defined by the preferred orientation of grain long axes. In thin section the grains of quartz and feldspar are elliptical and their long axes lie at a small angle to the trace of the fabric, as shown in Figure 2.D.6.. In general, the strength of the bedding parallel fabric

Figure 2.D.1. A bedding surface from within the Epidotic Grits on Skye, showing the strong lineation related to the bedding parallel fabric.

Figure 2.D.2. Highly mylonitised Lewisian Gneiss from Carn na Bhealaich Mhoir showing the strong fabric defined by flattened quartz grains and phylosilicates.

Figure 2.D.3. A photograph of relatively unmylonitised Lewisian Gneiss from Carn na Bhealaich Mhoir.

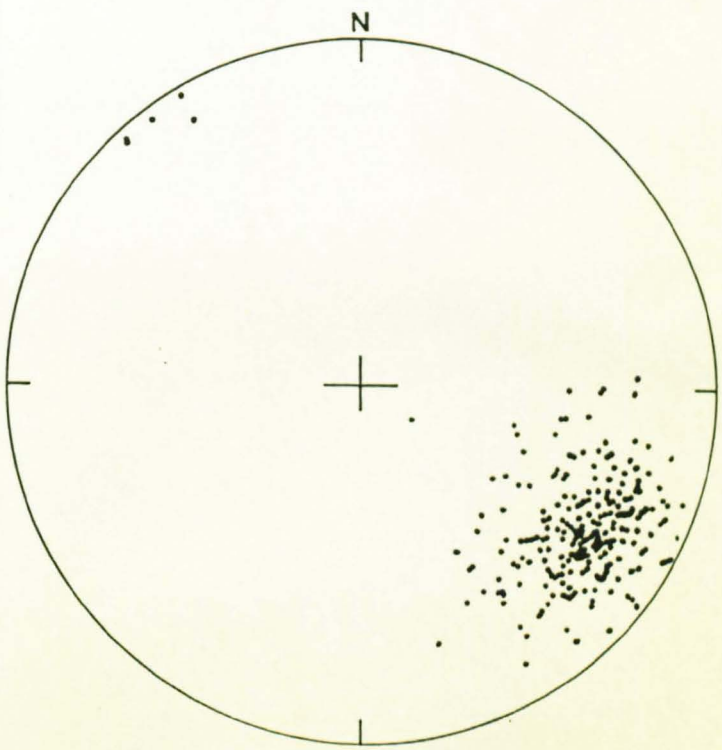

Figure 2.D.4 A stereogram showing the orientation of the grain shape lineation related to the bedding parallel fabric within the sandstones of the Sleat Group.

Table 2.D.1

Kanungo (1956)	Barber (1969)	Coward and Whalley (1979)	Present Work
S_4 Bedding Fissility & Thrust Cleavage	Development of the Lochalsh Syncline and the Mylonites	Development of the Lochalsh Syncline, Slickensides and Bedding parallel Fabric/ Mylonites	Bedding parallel fabric, Axial Planar Cleavage & Slickensides- Lochalsh Syncline
S_2 Axial Planar Cleavage S_3 Fracture Cleavage	Asymmetrical Folding	D_2 Folding of Slickensides and Associated Cleavage	Transverse Cleavage, Folding of Slickensides
	?	D_3 Second Bedding Parallel Fabric ?	?
	Monoclinal Folding and Kinking	D_4 Kink Bands and Gash Arrays	Kinks Bands and Gash Arrays

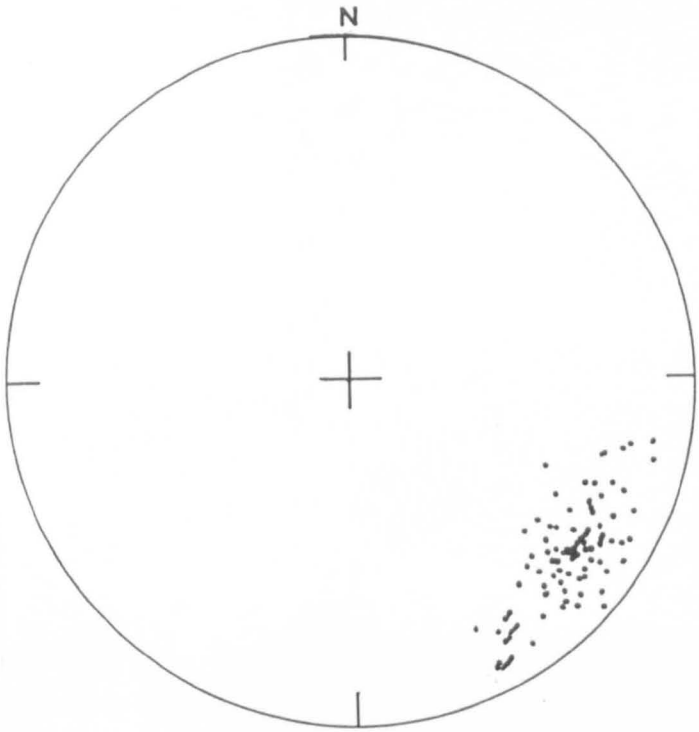

Figure 2.D.5. A stereogram showing the orientation of the grain shape lineation related to the bedding parallel fabric within the mylonitic Lewisian Gneiss of Carn na Bhealaich Mhoir.

Figure 2.D.6. A photomicrograph showing the bedding parallel fabric in a sample of sandstone from the Sleat Group (NG 77852375).

increases to the east, in thin section, this is marked by an increase in the proportion of white mica and a reduction in the grain size of the quartz and feldspar. There is a preferred orientation of the white mica flakes which tend to lie at a small angle to the trace of the fabric.

In the weakly deformed Lewisian rocks of Carn a Bhealaich Mhoir (Figure 2.A.1.) quartz rich areas may be seen surrounded by a mixture of quartz, feldspar and white mica. The rock is coarse grained (4-10mm), almost pegmatitic in appearance. With increase in the degree of deformation the grain size of the quartz and feldspar is reduced. This is replaced by a fairly homogeneous matrix of white mica, chlorite and quartz. The quartz grains show a strong preferred orientation of long axes. The grains lie with their longest axes in the fabric plane.

On the western end of Lochalsh, in the hinge of the Lochalsh Syncline, on both limbs of the fold, two cleavages may be seen (Figure 2.D.7.). In the field they are both spaced, but in thin section the spacing is a function of grain size, where the true spacing is only one grain width. Figure 2.D.8. shows the orientation of both cleavages from within the area shown in the inset map. The stereogram shows two defined maxima and these correspond to a shallow and a steep cleavage. At many localities within this area only one cleavage is seen and in such cases it is not possible to distinguish which cleavage isspresent on the basis of orientation.

In the field an age relationship may be distinguished for these cleavages. The shallow cleavage can be seen to be older. In the hinge at Port Cam, between the strongly developed cleavage planes (shown in Figure 2.D.9.), a shallowly dipping, weakly developed earlier

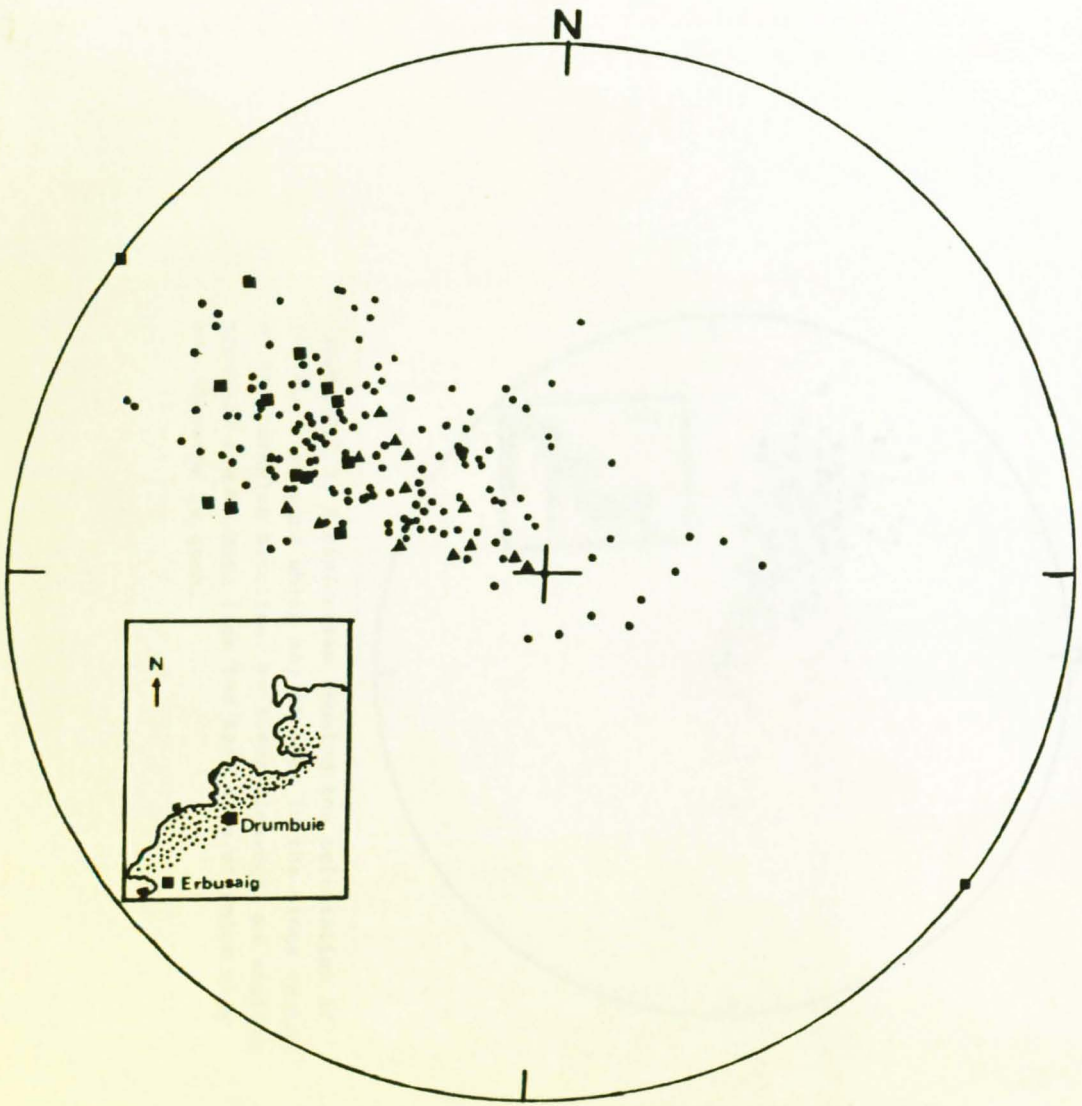

Figure 2.D.8. A stereogram showing the orientation of the two cleavages which may be seen in the hinge region of the Lochalsh Syncline. ■= steep cleavage, ▲= shallow cleavage and ●= data from the same area at which only one cleavage is seen.

Figure 2.D.7. A photograph, looking north, at the two cleavages seen in the hinge region of the Lochalsh Syncline around Drumbuie by Kyle.

Figure 2.D.9. A photograph, looking south, at the transverse cleavage in the hinge of the minor fold exposed at Port Cam.

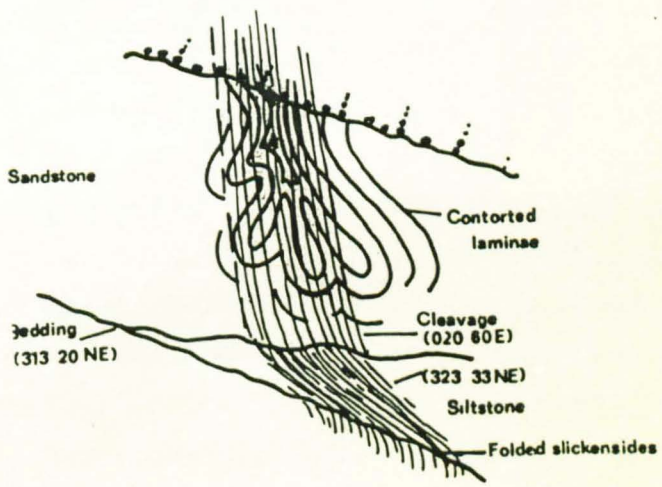

Figure 2.D.10. A field sketch showing the refraction of the transverse cleavage as it passes from sandstones into siltstones. In the sandstones, the transverse cleavage dips to the east (020 60E) and in the siltstones it dips to the northeast (323 22NE). The transverse cleavage is axial planar to minor folds of slickensides. (NG 75982101).

cleavage may be seen. This weak cleavage lies at an angle to the bedding. At several localities including NG 77403216 the shallower cleavage appears to be kinked into parallelism with the steeper cleavage suggesting that the shallow cleavage is older.

The second cleavage is more stfongly developed to the south and at the southern end of the northern zone only one cleavage is visible. One discordant cleavage is seen in the central zone and this is probable due to the different structural levels seen in the two areas.

In the central zone the axial trace of the Lochalsh Syncline is exposed in rocks of the Sleat Group whereas in the northern area the axial trace lies within the Applecross Formation. In the latter case the hinge is much tighter and as a result an axial planar cleavage has developed. This portion of the fold is not seen in the central area due to erosion.

On Skye, on the normal limb of the Lochalsh Syncline, one spaced cleavage is seen which is steeper than bedding. As shown in Figure 2.C.16., on Beinne na Greine, this cleavage postdates the minor folds of bedding which are related to the Lochalsh Syncline. Therefore, this cleavage must postdate the Lochalsh Syncline.

On the overturned limb of the Lochalsh Syncline in the northern and central areas there is a cleavage which is often spaced but generally penetrative and this is most clearly seen in shale beds. This cleavage is steeper than bedding, on the overturned limb of the fold and must therefore postdate the inversion. It is suggested that the cleavage described in the paragraph above, the second of the two cleavages seen in the hinge of the Lochalsh Syncline around Drumbuie,

and the cleavage which is steeper than the bedding on the overturned limb of the Lochalsh Syncline, are one and the same cleavage. This cleavage will be termed the transverse cleavage.

There is a discrepancy in the orientation of the transverse cleavage; in the west it is steeply dipping, whereas in the east it has a more shallow dip. This discrepancy is thought to be due to cleavage refraction. In the west the cleavage is seen principally in sandstones. In the east it is seen mainly in shaly beds. At NG 75982101 a massive bed of sandstone may be seen which fines into a shaly top. The cleavage in the shaly portion dips at a much shallower angle almost parallel to the transverse cleavage in the east, whereas, the cleavage in the sandy portion is steeply dipping. A field sketch of the cleavage refraction is shown in Figure 2.D.10..

Figure 2.D.11. shows bedding cleavage intersection lineations for the whole of the northern and central areas. The intersections define a great circle suggesting that the transverse cleavage is not axial planar to the Lochalsh Syncline. Since this cleavage is not folded and dips more steeply than the bedding on the overturned limb it must postdate the major fold. This is similar to the relationship of folding and cleavage seen in minor folds on Beinne na Greine and to the north of Loch na Dal which is shown in Figure 2.C.16.. The great circle distribution of intersections and the age relationship of the transverse cleavage to the Lochalsh Synoline suggests that the cleavage cuts accross the fold obliquely to the fold axis, hence the name transverse cleavage.

The steeper of the two cleavages seen around Drumbuie (Figure 2.A.1.) has been assigned to the transverse cleavage. The more shallowly dipping cleavage is thought to be parallel to the axial plane of the Lochalsh

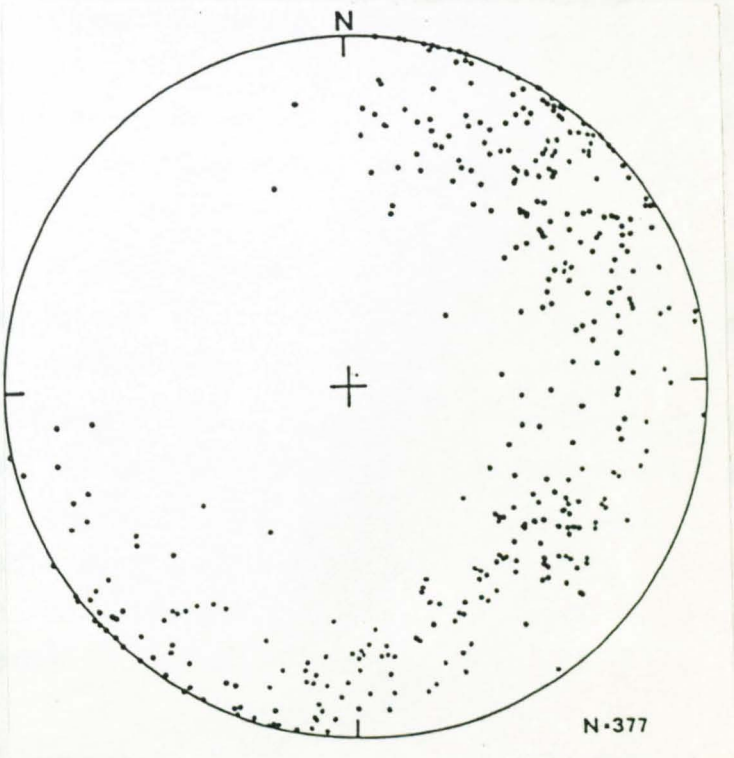

Figure 2.D.11. A stereogram showing bedding cleavage intersection lineations from the northern and central areas of the Kishorn Nappe.

Figure 2.D.12. A phtograph, looking east, at the bedding parallel fabric on Carn an t-Seachrain. The bedding parallel fabric can be seen in the sandy laminae. The transverse cleavage is seen as a spaced cleavage in the silty matrix.

Syncline. From Figure 2.D.8. it has the correct orientation and it is very similar in orientation to the axial planar cleavage seen in the minor fold at Plockton NG 79903421 shown in Figure 2.C.5..

Within the Kishorn Nappe we may distinguish three cleavages, these are, the bedding parallel fabric, the axial planar cleavage and the transverse cleavage. The bedding parallel fabric is seen throughout a large portion of the overturned limb of the Lochalsh Syncline. The axial planar cleavage is only seen close to the axial trace of the Lochalsh Syncline to the north of Kyle. The transverse cleavage is seen throughout the area on both Skye and the Kyle of Lochalsh.

The bedding parallel fabric is older than the transverse cleavage and this is most clearly seen around Carn an t-Seachrain (Figure 2.C.8.) as shown in Figure 2.D.12.. The coarse detrital grains of quartz and feldspar lie with long axes parallel to the bedding parallel fabric but they are slightly modified by the transverse cleavage which is seen in the surrounding shale.

There is no clear evidence of the age relationship of the shallow early cleavage, seen in the hinge zone of the main Lochalsh Syncline, to the bedding parallel fabric. However, it has been shown in the previous section that both predate the transverse cleavage and therefore may be of the same age and may be related to the development of the Lochalsh Syncline.

The transverse cleavage the orientation of which is shown in Figure 2.D.13., affects bedding parallel quartz veins which are of two types, the most common of these are composed of massive white quartz and pink feldspar. They are rarely slickensided and occur as planar veins with irregular surfaces within shale beds. Often there are several veins of 1-10 cm thickness

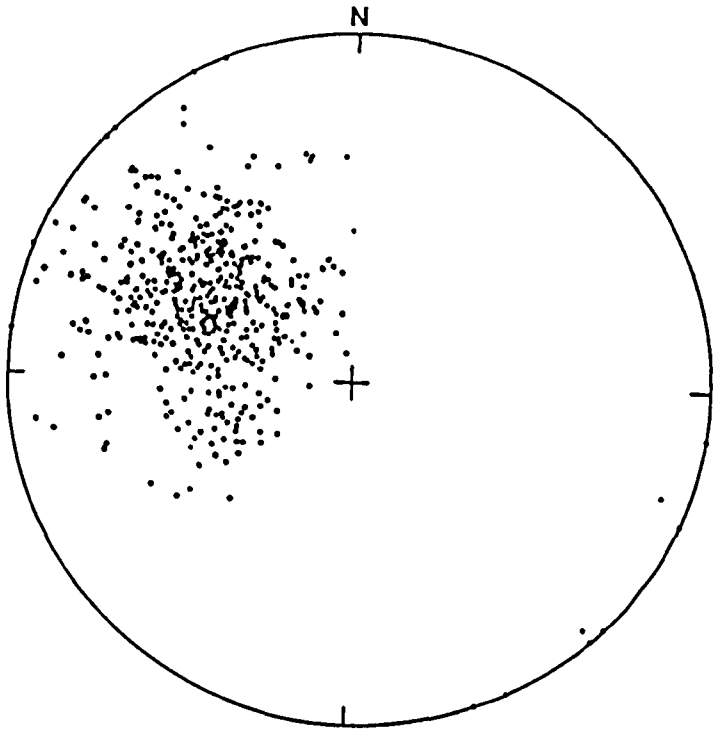

Figure 2.D.13. A stereogram showing the orientation of the transverse cleavage in the northern and central areas of the Kishorn Nappe.

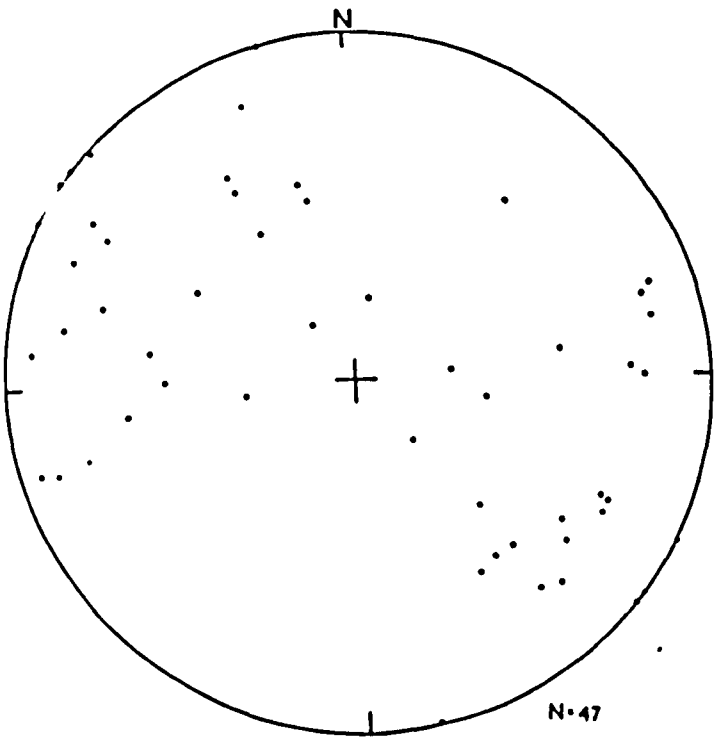

Figure 2.D.14. A stereogram showing the orientations of the slickensides in the northern and central areas of the Kishorn Nappe.

within a single bed which may be up to 2 metres thick. At several localities on Ben Aslak these veins are affected by the transverse cleavage and must therefore predate it. The second type of veins consist of sheets of quartz fibres and are considered to be slickensides. These sheets are 1-2 mm thick and 5-10 sheets are usually present on each bedding surface. The slickensides are parallel to bedding and are seen on both limbs of the Lochalsh Syncline. As shown in Figure 2. D.14. the orientation of the fibres define a great circle about the fold axis of the Lochalsh Syncline as defined by the bedding. The movement sense determined from the slickensides is consistent with flexural slip on the bedding surfaces (Ramsay 1967). The slickensides are folded and the transverse cleavage is axial planar to these folds. The folds of slickensides may be seen on both Lochalsh and Skye but are more commonly developed on Skye. The folds occur on both limbs of the Lochalsh Syncline and have a consistent asymmetry unrelated to the Lochalsh Syncline. The constant asymmetry of the folds is shown in Figure 2.D.15., an example from northern Sleat. This suggests that the transverse cleavage postdates the Lochalsh Syncline since it folds slickensides related to the development of the fold.

The axial planar cleavage and the transverse cleavage cannot be distinguished in thin section. In sandstones both cleavages are marked by the preferred orientation of quartz and feldspar grains. The quartz grains tend to be more elongate than the feldspar and both lie within their long axes at a small angle to the trace of the cleavage. Coward and Whalley (1979) have described these cleavages as pressure solution cleavages marked by the alternation of quartz rich and quartz poor lamellae. There is no clear evidence of pressure solution in the quartz rich areas. The quartz poor lamellae consist almost entirely of white mica, which has a strong preferred orientation of flakes

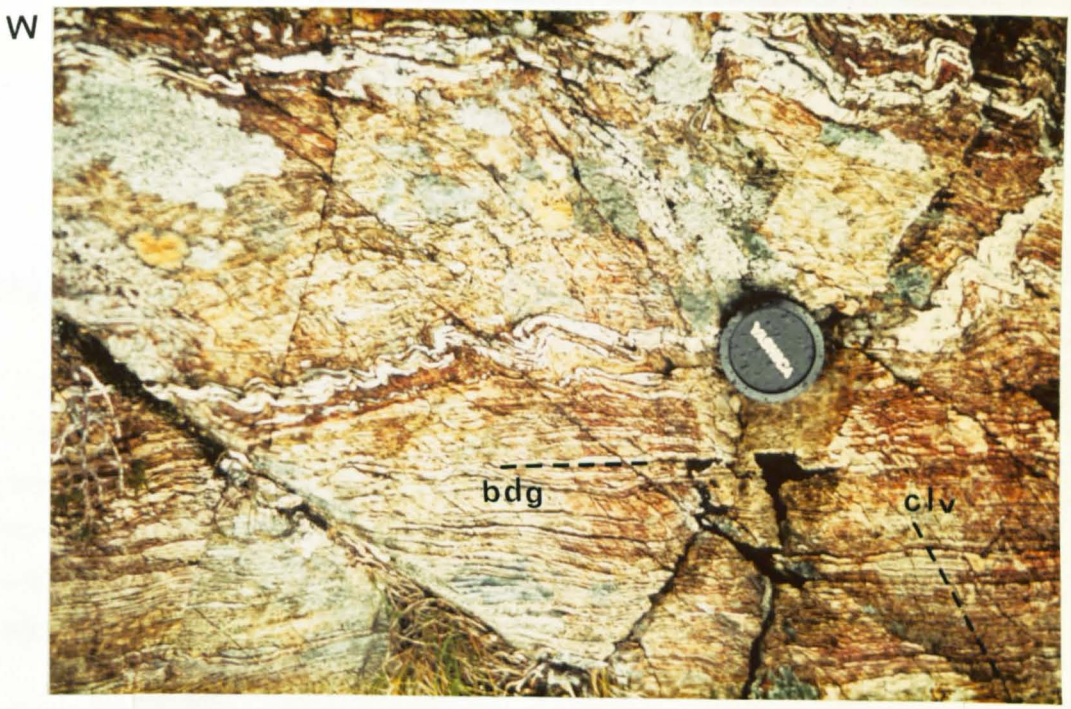

Figure 2.D.15. The bedding parallel slickensides shown in the photograph are related to the Lochalsh Syncline. The transverse cleavage is axial planar to the minor folds and dips to the east. The asymmetry of the folds is constant on both limbs of the Lochalsh Syncline.

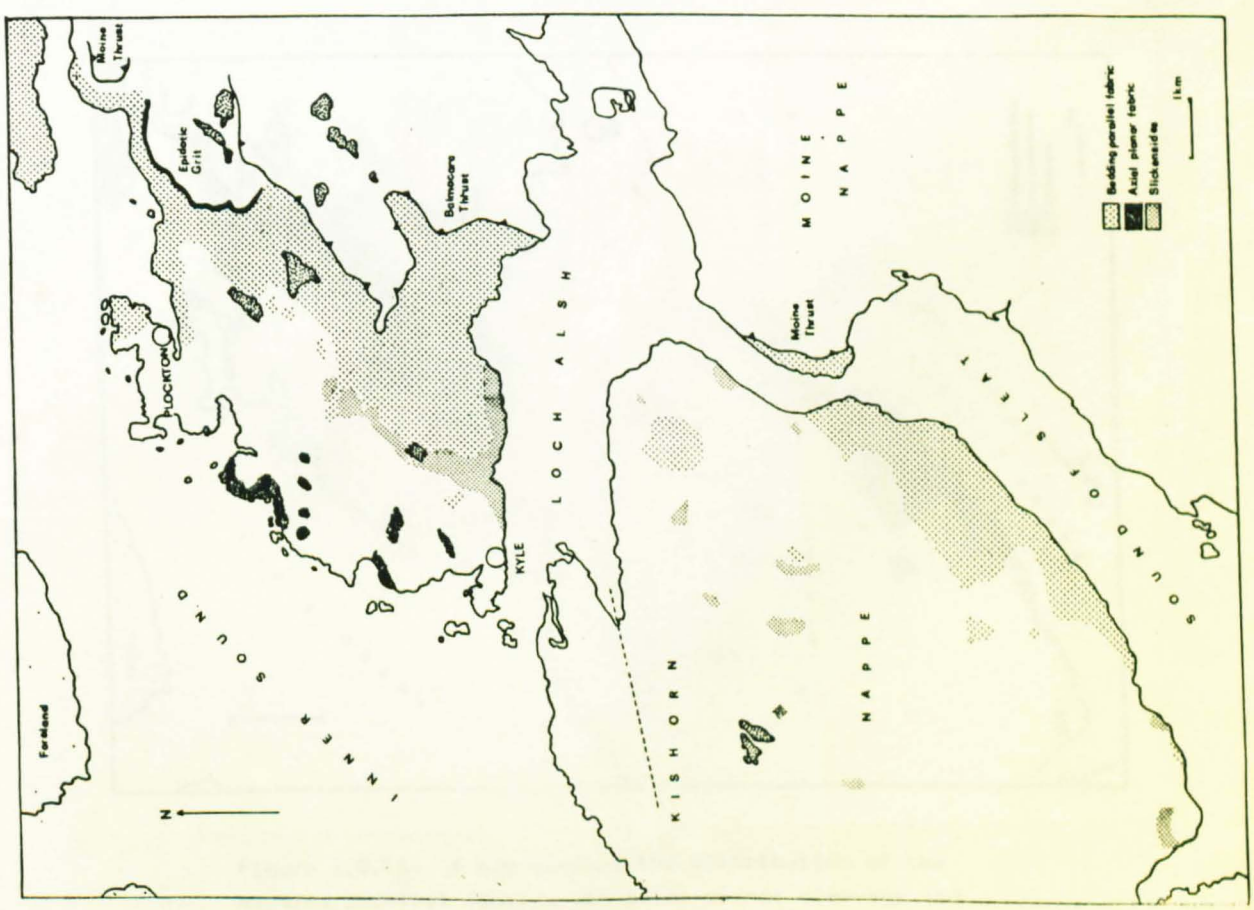

Figure 2.D.16. A map showing the distribution of the bedding parallel fabric, the axial planar cleavage and the slickensides in the northern and central areas of the Kishorn Nappe.

parallel to the trace of the cleavage.

Relationships of the Cleavages to the Lochalsh Syncline

From data presented in this chapter, the Lochalsh Syncline has a fold axis which plunges at 10 degrees to 045 degrees. Fold axes with similar orientations have been observed for minor folds of bedding within the northern and central areas. The axial plane dips gently to the east-southeast.

The orientation of slickensides are normal to the fold axis of the Lochalsh Syncline and it is thought that they were produced during the development of the recumbent fold. This is in agreement with the observations of Coward and Whalley (1979).

It has been shown that the slickensides, the bedding parallel fabric and the axial planar cleavage predate the transverse cleavage. No evidence can be seen in the field to establish an age relationship for the minor structures which predate the transverse cleavage and they are taken to be broadly synchronous. The distribution of the bedding parallel fabric, the axial planar cleavage and the slickensides is shown in Figure 2.D.16.. The distribution of the transverse cleavage is shown in Figure 2.D.17.. The bedding parallel fabric, the slickensides and the axial planar cleavage are never seen in the same outcrop and only occasionally are slickensides seen at the same locality as the bedding parallel fabric. Thus these minor structures tend to occur in mutually exclusive areas of the Kishorn Nappe. This is clearly seen in Figure 2.D.16. where the localities with particular minor structures, tend to form broad zones the boundaries of which are parallel to the strike of the bedding. Working westwards from the higher

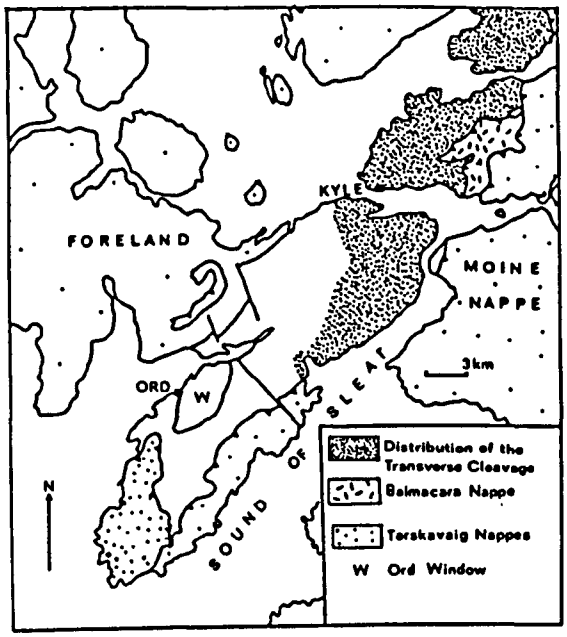

Figure 2.D.17. A map showing the distribution of the transverse cleavage in the northern and central areas of the Kishorn Nappe.

thrusts these zones contain; bedding parallel fabric, slickensides and the axial planar cleavage. There is a slight overlap of each zone but there is a general antithesis between the bedding parallel fabric and the slickensides. The overlap zone between the bedding parallel fabric and the slickensides is sinuous and where the bedding parallel fabric extends more to the west, the slickensides are absent.

The mutually exclusive zones shown in Figure 2.D.16. suggest that the bedding parallel fabric, the slickensides and the axial planar cleavage may be related structures. Since the slickensides may be related to the development of the Lochalsh Syncline, then it is possible that the bedding parallel fabric and the axial planar cleavage are also related to the Syncline. Possibly the bedding parallel fabric records some kind of extension on the outer arc of the Lochalsh Syncline and the axial planar cleavage records the compression on the inner arc. The distribution of extension and compression suggests that the folding was accommodated by some form of tangential longitudinal strain (Ramsay 1967) and that the slickensides may represent the neutral surface of the fold.

The transverse cleavage is common throughout the eastern portion of the Lochalsh Syncline and it postdates the bedding parallel fabric, the slickensides and the axial planar cleavage. It clearly postdates the slickensides which were formed by the development of the Lochalsh Syncline and therefore it must postdate the development of the Lochalsh Syncline.

It would appear that a very simple pattern of cleavages exists within the Kishorn Nappe. An early phase of cleavage development related to the Lochalsh Syncline followed by the transverse cleavage. It has been

suggested, above, that this early phase of cleavage development approximates to tangential longitudinal strain, but in the east the bedding parallel fabric is so strongly developed that it is unlikely that it was developed by this process alone. This strong fabric is particularily well seen beneath the Balmacara Nappe at Ard Hill, where the bedding parallel grain shape fabric is indistinguishable from the isoclinally folded mylonitic fabric and banding described by Barber (1965).

Peach et al (1907) suggest that the cleavage seen on Sgurr na Coinnich is axial planar to the Lochalsh Syncline but it has been shown (Figure 2.C.16.) that this cleavage is the transverse cleavage which postdates the folding. The Survey also described the existence of a lineation which occurs in the eastern portion of the Nappe on Lochalsh and Sleat. This is equivalent to the bedding parallel fabric.

Kanungo (1956) recognised all of the cleavages described in this thesis but the sequence he suggested is different. Kanungo suggested that his S_2 and S_3 cleavages (S_1 = bedding) were equivalent in age, the S_2 cleavage being axial planar to the Lochalsh Syncline. The S_3 cleavage, being a spaced cleavage, was taken to be a fracture cleavage which occupied a circular section in the same strain ellipsoid. As described previously a definite age relationship can be established for these two cleavages and Kanungo's (1956) S_3 cleavage is later. The S_3 cleavage is considered to be the transverse cleavage of this thesis.

Kanungo (1956) described a "bedding fissility" and related lineation in the eastern portion of the Kishorn Nappe on Lochalsh. He related this lineation to movements on structurally higher thrusts and suggested a similar origin for his S_4 or "thrust cleavage". The

S_4 thrust cleavage is always steeper than bedding on the inverted limb of the Lochalsh Syncline and Kanungo (1956) recognised that it must postdate the Lochalsh Syncline. He did not suggest an age relationship for the bedding fissility relative to the folding but implied that it must be late as it is related to the higher thrusts. Kanungo's S_4 cleavage has been correlated with the transverse cleavage and it has been shown that the bedding fissility or bedding parallel fabric predates the transverse cleavage. A comparison of Kanungo's (1956) deformation history with the sequence now proposed is given in table 2.D.1..

Coward and Whalley (1979) recorded several cleavages, an early bedding parallel fabric (D_1), overprinted by a later D_2 cleavage, and they suggested that the bedding parallel fabric is only of limited extent. Figure 2.D.16. shows that the bedding parallel fabric has a much wider extent. In the field no evidence was seen for their D_3 bedding parallel fabric and in thin section no comparable cleavage was seen. In general their structural sequence is similar to that proposed here and may be compared in table 2.D.1..

Section 2E Quartz Veins Within the Kishorn Nappe

Several types of quartz vein are seen within the Kishorn Nappe and these will now be described. In general quartz veins are more common in the northern and central areas. The vein types are

(i) Lacy veins
(ii) Syntectonic vein arrays
(iii) Gash arrays
(iv) Principal vein arrays

Lacy Veins

The lacy veins are generally less than 1mm wide and they totally penetrate the bed, Figure 2.E.1. shows a tracing of a lacy vein network. Veins of this kind tend to occur around Sgurr na Iolaire (Figure 2.C.20.) and are occasionally present on Lochalsh.

Syntectonic Vein Arrays

Around Kylerhea, complex vein networks are seen, Figure 2.E.2. shows a photograph of a bedding plane near Kylerhea (Figure 2.A.1.). The quartz veins penetrate the bed and occur in arrays which are irregular in shape, often several metres cross. The veins within these arrays are of two types: the first type is infilled with massive white quartz and the second type consists of fibrous quartz. The fibres in the vein lie at a high angle to the vein wall and are parallel to the grain shape lineation in the surrounding rocks. There are generally two orientations of veins, frequently branched, which appear to be broadly synchronous. The constituent veins are not orthogonal and their morphology is shown in Figure 2.E.2.. These arrays do not have the geometry of semi-brittle tension gash arrays (Ramsay 1967, Beach 1974, Ramsay 1980). The origin of this type of vein array is uncertain and from the orientation of the fibres in relation to the grain shape lineation of the bedding parallel fabric they are possibly syntectonic.

Gash Arrays

The third type of vein array occurs throughout the central and northern areas but they are more common in the northern area. Broadly they have the geometry

Figure 2.E.1. A tracing showing the morphology of a lacy vein array on Sgurr na Iolaire.

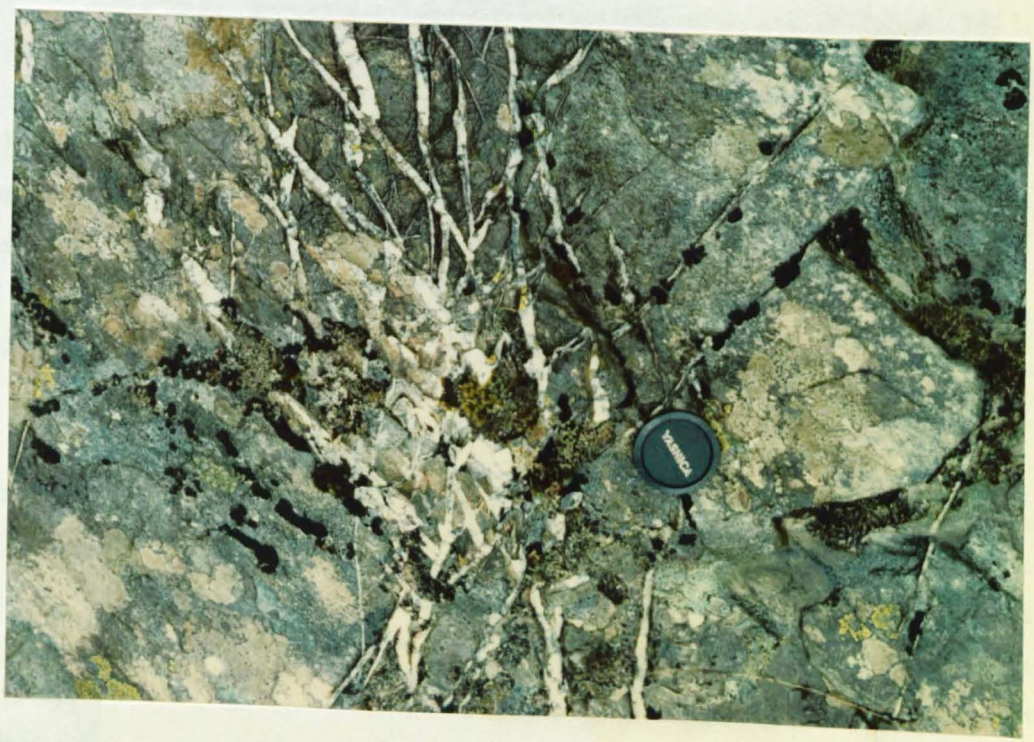

Figure 2.E.2. A photograph, looking northwest, of a bedding plane near Kylerhea showing the morphology of a syntectonic vein array.

of semi-brittle gash arrays and with only a few exceptions they all postdate the fabrics and cleavages. The arrays dip moderately to the northwest or southeast sometimes forming conjugate pairs. The intersection of the arrays is nearly horizontal, plunging gently to the northeast or southwest. The northwesterly dipping arrays have a sinistral sense of shear and the southeasterly dipping arrays have a dextral sense of shear suggesting that the principal compressive stress was vertical (Beach 1974). The veins of the arrays are regularily spaced and generally parallel. Often the veins are sigmoidal but the most common feature of these arrays is that the length of the vein down dip is very much greater than the width of the sigmoidal zone (see Figure 2.E.3.).

Principal Vein Arrays

Principal vein arrays (Beach 1974) are arrays of planar veins, often several metres in length and spaced at regular intervals. In general, two sets of veins are present forming an orthogonal network (see Figure 2.E.4.). These vein systems are extremely common on the Kyle of Lochlash where they appear to be of similar age to the gash arrays described above. The orientations of the two sets of veins in the principal vein arrays are fairly constant throughout Lochalsh

Kanungo (1956) recognised the presence of many different types of vein systems on the Kyle of Lochalsh. In general, it is possible to place all of these vein systems into one or other of the types described above. Often, he made several subdivisions of essentially the same vein system, which is thought to be unecessary.

With the exception of the syntectonic vein arrays, the vein systems within the Lochalsh Syncline tend to

Figure 2.E.3. A photograph, looking north, of the sigmoidal vein arrays which are common throughout the northern and central areas of the Kishorn Nappe. The photograph was taken on the road section between Kyle and Balmacara where these veins are clearly seen.

Figure 2.E.4. A photograph, looking south, showing the morphology of a principal vein array.

postdate the cleavages and fabrics seen. Slickensides have been described previously and they may be ascribed to the development of the Lochalsh Syncline. It has been shown that the transverse cleavage post-dates the development of the Lochalsh Syncline and therefore the vein systems which postdate the transverse cleavage,must also postdate the Lochalsh Syncline and are not a direct consequence of its development as described by Kanungo.(1956).

The syntectonic vein arrays are only developed where the bedding parallel fabric is strongly developed and it is thought that they represent areas of internal boudinage which developed where the bedding parallel fabric was unable to develop at a sufficient rate.

Section 2F The Structural Geology of the Balmacara Nappe

In this section the structural geology of the Balmacara Nappe will be described. Possible correlations between this and the other nappes within the Moine Thrust Zone will be discussed in the section which follows.

The Balmacara Nappe lies above the Balmacara Thrust which may be followed from Ard Hill northwards to Sgurr Beag (Figure 2.F.1.) and eventually to Letter Hill. The thrust plane is clearly exposed at Ard Hill, Balmacara Burn and Sgurr Beag (see Figure 2.F.1.). The Nappe consists almost entirely of mylonites, some derived from Lewisian rocks and some derived from the Sleat Group. The Balmacara Nappe lies between the Moine and Kishorn Nappes. Around Letter Hill it overlies the overturned Lewisian rocks of Carn na Bhealaich Mhoir, and southwards it overlies sandstones from the lower portion of the Sleat Group. The results of mapping of the Balmacara Nappe are shown in Figure 2.F.1..

At Letter Hill the Balmacara Nappe contains sandstones of the Sleat Group which are, in turn, overlain by Epidotic Grits and Lewisian rocks. All these rock types have a strong fabric which is parallel to bedding in the rocks of the Sleat Group. This inverted sequence suggests that the Balmacara Nappe contains rocks which are inverted. This is confirmed by the outcrops of Epidotic Grit seen within the outcrop of the Nappe. Near Loch na Doire Moire, Loch a Ghlinne Dhuirch and Loch na Smeoraich outcrops of Epidotic Grit may be seen. Their outcrops patterns suggest that they have been carried up in the hanging walls of small imbricates, thus uplifting inverted Epidotic Grits from beneath the Lewisian rocks. Thrust planes beneath the imbricate slices were not seen but it is thought that they have a common, sole thrust, which is

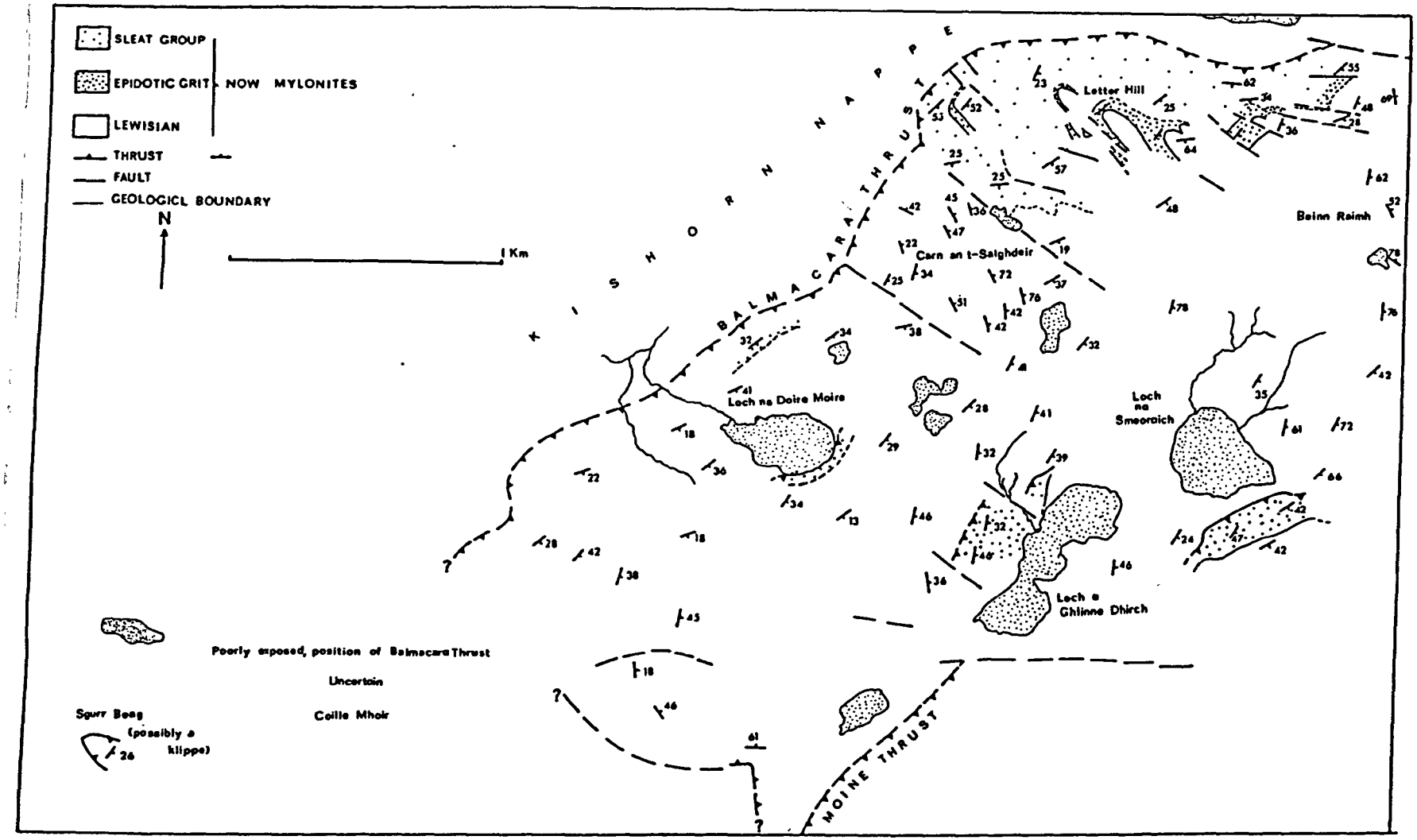

Figure 2.F.1. A map of the Balmacara Nappe showing the major rock types which are exposed within the Nappe. The diagram is based on recent mapping and much of the detail has been omitted for clarity.

the Balmacara Thrust.

The trace of the Balmacara Thrust has a highly sinuous path (Peach et al 1907). Mapping suggests that the thrust plane dips gently to the southeast. Around Coille Mhor (Figure 2.F.1.) it is very difficult to determine the position of the thrust plane. Barber (1965) makes a distinction between the thrust seen at Ard Hill and Balmacara Burn and the thrust seen at Sgurr Beag. From the dip on the thrust plane, approximately 30 degrees to the southeast, it seems unlikely that the trace of the plane will follow the course suggested by Peach et al (1907) across the broad, open valley to the north of Balmacara Square. It is possible, though not proven, that portions of the Balmacara Nappe seen on Coille Mhor and Sgurr Beag are klippes to the main outcrop of the Nappe.

Throughout the Balmacara Nappe all of the rock types present have a strong grain shape fabric. The fabric dips to the east-southeast and often has a strong down dip mineral or grain shape lineation (see Figure 2.F.2.). In the sandstones around Letter Hill this fabric is parallel to the bedding. To the south of Loch na Doire Moire sheath folds (Cobbold and Quinquis 1980) may be seen. These folds are almost isoclinal with highly thickened hinges. The limbs of the fold are parallel to the dominant fabric. The fold axes of this type of fold are gently plunging, either to the east-southeast or north-northeast. At some localities highly curved hinges are present which suggest that these folds are sheath like in form and broadly synchronous with the mylonitic fabric (Cobbold and Quinquis 1980). They are very similar in style to the isoclines beneath the Balmacara Nappe at Ard Hill (Barber 1965).

Folds may be seen within the Balmacara Nappe which fold

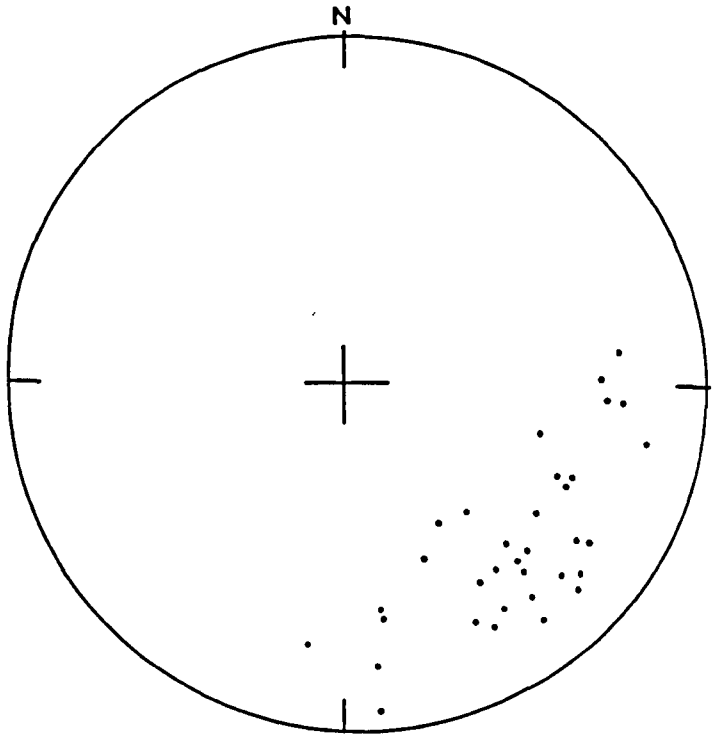

Figure 2.F.2. A stereogram showing the orientation of grain shape lineations from within the Balmacara Nappe.

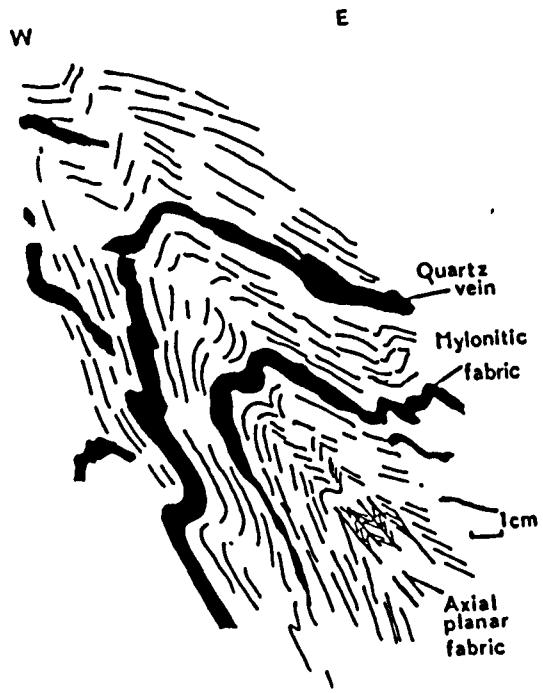

Figure 2.F.3. A tracing from a photograph (looking north) showing the constant asymmetry of the minor folds within the imbricates of Epidotic Grits. The folds are overturned to the west and postdate the mylonitic fabric.

the mylonitic fabric. Two types of fold are seen, those which have no related cleavage will be described later and those which develop their own cleavage will be described now. Asymmetrical folding is commonly seen within the imbricates of Epidotic Grit (see Figure 2.F.1.). Where these folds are seen they have a constant sense of asymmetry as shown in Figure 2.F.3.. The axial planes to these folds dip moderately or gently to the southeast and the fold axes plunge gently to the northeast. An axial planar cleavage is developed in the hinges of these folds which crenulates and replaces the mylonitic fabric. The orientation of this cleavage is similar within each of the imbricates and the asymmetry of the folds always indicates the presence of an antiform beneath the present erosion level but no large fold is seen. Folds of this kind are not seen beneath the position of the imbricate thrust.

The second type of folding to affect the mylonitic folding forms kink bands, chevron folds and box folds. This style of folding appears to postdate the asymmetrical folding described above as the axial planar cleavage is occasionally kinked. The kink bands and chevron folds range in size from several centimetres to several metres. However, large areas of fabric and banding exist where there is no evidence of folding such as at Carn an t-Saighdeir where the fabric does not dip to the southeast. It is possible that such areas are the internal part of large kink bands with dimensions of several tens of metres. The narrow kink bands affect the post mylonite cleavages and it would appear therefore, that the kinks and chevron folds are late in the deformation history of the Balmacara Nappe. The orientation of these structures is shown in Figure 2.F.4..

The deformation sequence proposed by Barber (1965)

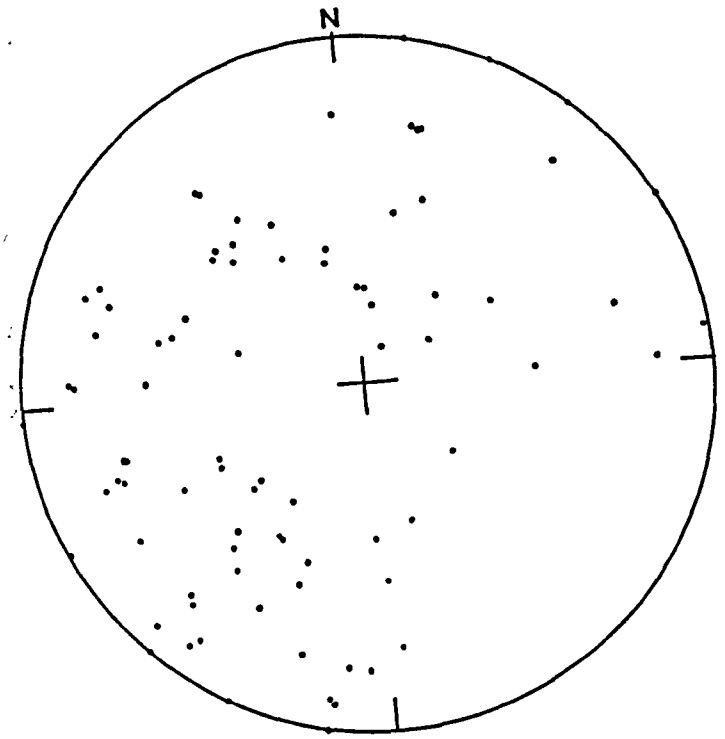

Figure 2.F.4. A stereogram showing the orientations of the kink bands which affect the mylonitic fabric of the Balmacara Nappe.

for the Balmacara Nappe and the adjacent portion of the Kishorn Nappe, which was given in section 28, is in broad agreement with the results presented in this thesis. However, there is evidence to suggest that the mylonitisation, isoclinal folding on east-southeast axes and recrystallization cannot be separated into three distinct events. Within the Balmacara Nappe folds of the mylonitic fabric can be seen which have an axial planar fabric which is parallel to the dominant mylonite fabric and the limbs of the fold. It is thought that these folds and fabrics are a consequence of continuous reworking during the development of the mylonite fabric in a system dominated by sheath folding (Cobbold and Quinquis 1980). The isoclines present beneath the Balmacara Nappe at Ard Hill are probably of the same origin. These areas represent the most intense development of the bedding parallel fabric.

It has been shown that the Balmacara Nappe contains rocks which are inverted. It is thought that the Nappe represents a portion of the overturned limb of the Lochalsh Syncline carried forward by the Balmacara Thrust, which forms the sole thrust to a series of imbricates within the Balmacara Nappe. The bedding parallel fabric in the Kishorn Nappe is thought to be equivalent to the mylonitic fabric which dominates the Balmacara Nappe.

Section 2G Structural History of the Kishorn and Balmacara Nappes

A sequence of deformations for the Kishorn and adjacent Nappes will now be described. Although they will be described as a series of discrete events, it is emphasized that this should not be taken to imply that the structures necessarily formed as a series of events. They may have formed as part of a continuous sequence.

The first period of folding to affect rocks of the Kishorn Nappe is indicated by the diverse orientation of bedding within the Applecross Formation, immediately beneath the Eriboll Sandstone , in the Ord Window. This suggests some folding of the Torridonian had occurred prior to the deposition of the Cambro-Ordovician sucession. As cross sections through the Ord Window cannot be restored with any degree of confidence this pre-Caledonian folding is considered to have fold wavelengths and amplitudes similar to those determined by Soper and Barber (1979).

A sequence of Caledonian structures will now be described principally for the Kishorn Nappe, but all the nappes at the southern end of the exposed Moine Thrust Zone will be discussed.

Based on the revision of the Ord Window presented in this chapter a thrust sequence for the southern portion of the Moine Thrust Zone may be proposed. Modern theories of thrust tectonics (Dahlstrom 1970, Elliott and Johnson 1980) suggest that the Moine Thrust, the structurally higher thrust, developed first.

It has been shown (Figure 2.C.7.) that near Fernaig the Moine Thrust appears to cut across structures in the Lochalsh Syncline. A similar situation is seen further north on Lochcarron and in the Coulin Forest (Johnson 1955a). The Lochalsh Syncline is the structurally highest fold in a train of recumbent folds beneath the Moine Thrust and it is possible that the Lochalsh Syncline formed as a footwall syncline to the developing Moine Thrust, eventually cut by the Thrust.

From the revision of the Ord Window it has been suggested that the Lochalsh Syncline, the Eishort Anticline and the Ord Syncline formed a fold train

beneath the Moine Thrust. It is not known whether these folds formed as a continuous fold train (Figure 2.G.1.) and represent a highly folded footwall to the Moine Thrust, or that the Eishort Anticline and Ord Syncline formed as an anticline-syncline pair related to a blind thrust (Figure 2.G.2.), presently unexposed. Both models require a detachment horizon at an unknown depth, perhaps within the Sleat Group, although Lewisian Gneisses of the basement have been decoupled in the Lochalsh Syncline.

These folds are thought to be the earliest Caledonian structures seen within the Kishorn Nappe. The Balmacara Nappe appears to represent the next thrust in a Foreland propagating sequence (Dahlstrom 1970). It has been shown that the Balmacara Nappe is a structurally lower portion of the overturned limb of the Lochalsh Syncline which has been thrust to the northwest over the rocks of Carn na Bhealaich Mhoir. The Balmacara Thrust cuts up section in the direction of transport and it carries inverted Epidotic Grit over Lewisian rocks (Figure 2.G.3.) which suggests that the Lochalsh Syncline was in existence, or developing, during the formation of the Balmacara Thrust. The Balmacara Thrust may be the sole thrust to a series of small imbricates of Epidotic Grit (Figure 2.F.1.).

The Tarskavaig Nappes were emplaced on to rocks of the Kinloch Formation (Figure 2.C.20.) and since they were folded by the Tarskavaig Synform during the development of the Ord Thrust they appear to represent a stack of imbricates (see Figure 11 of Cheeney and Matthews 1965) intermediate in age, between the higher Moine Thrust and the younger, lower, Ord Thrust beneath. This age relationship confirms the suggestion that the thrusts of Sleat developed in a foreland propagating sequence.

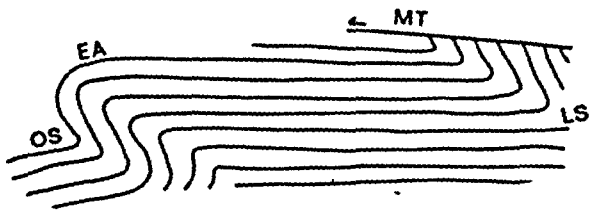

Figure 2.G.1. A schematic section which shows the Eishort Anticline (EA) and the Ord Syncline (OS) as a footwall fold train together with the Lochalsh Syncline (LS) beneath the Moine Thrust (MT).

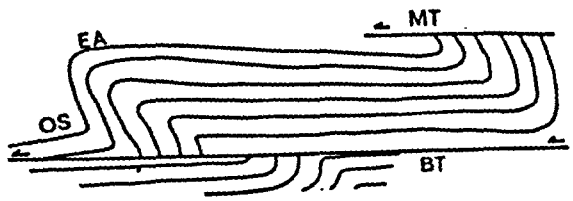

Figure 2.G.2. A schematic section which shows the Eishort Anticline and Ord Syncline as a fold pair related to a blind thrust (BT).

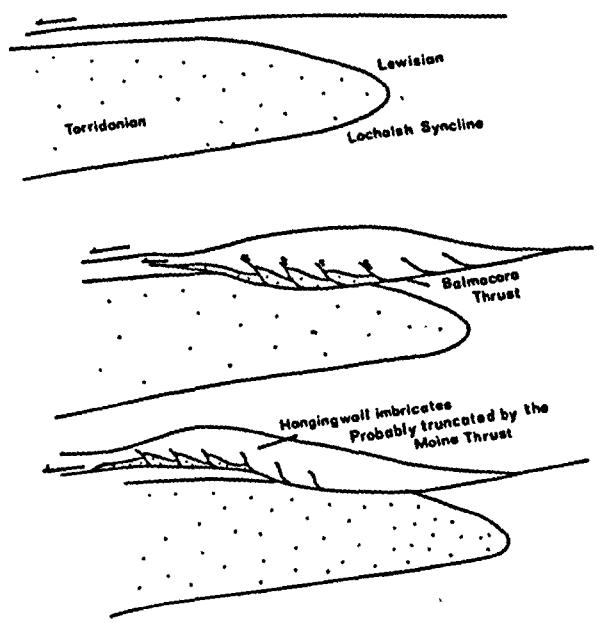

Figure 2.G.3. Schematic cross sections showing the development of the Balmacara Nappe.

The age of emplacement of the Tarskavaig Nappes relative to the Eishort Anticline and Ord Syncline is unknown, as the Tarskavaig Thrust must climb through the Applecross Formation and Cambro-Ordovician sequence above the present level of erosion.

The Balmacara Nappe occupies the same structural position as the Tarskavaig Nappe , immediately beneath the Moine Thrust (Figure 2.G.3.) and since both Nappes contain mylonites it is tempting to correlate them. However, it has been shown that the rocks of the Balmacara Nappe are inverted whereas the rocks of the Tarskavaig Nappe are the correct way up, relative to the now folded thrust plane. Therefore, these two Nappes cannot be the same structure and cannot be correlated.

Since the Tarskavaig Nappes are the correct way up and they must have travelled from the southeast (Peach et al 1907), their position within the stack of nappes exposed on Skye is a problem. The Tarskavaig group of nappes rest on the correct way up limb between the Lochalsh Syncline and the Eishort Anticline (see Figure 2.G.4.). To occupy their present position and be the correct way up the nappes cannot have come from the overturned limb of the Lochalsh Syncline. Therefore, they must have come from the hanging wall of the thrust, to which the Lochalsh Syncline is a footwall structure (see Figure 2.G.4.). It has been suggested above that this thrust was the Moine Thrust. However, the Tarskavaig Thrust may represent a portion of the thrust plane responsible for the recumbent folding within the Kishorn Nappe and this folding is unrelated to the present Moine Thrust. This is supported by the observations of Clough in Peach et al (1907) and Cheeney (1965) that the Tarskavaig Thrust is truncated by the Moine Thrust at Ard Thuirnish suggesting that the Moine Thrust

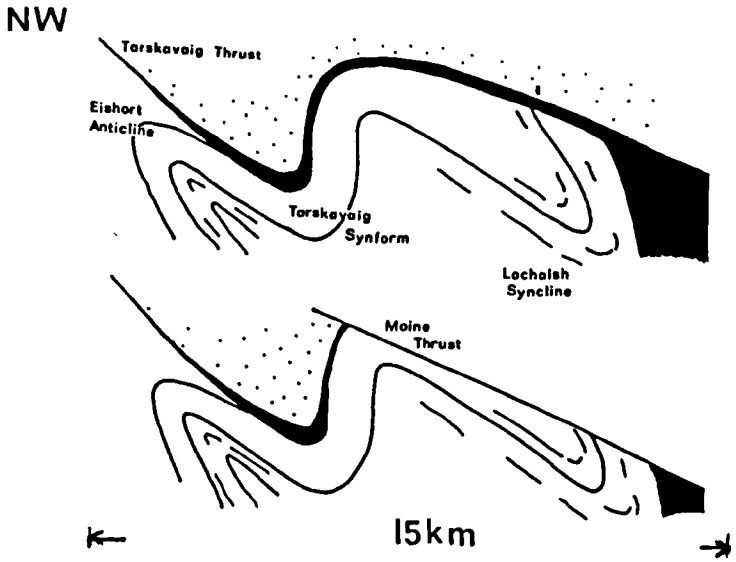

Figure 2.C.4. Schematic cross sections showing the development of the Tarskavaig Nappes.

presently exposed is a late structure. Truncation of the Tarskavaig Thrust is in conflict with the foreland propagating thrust sequence outlined above. It is possible that displacement of the Moine Thrust as presently exposed, continued throughout the development of the thrust zone beneath. Alternatively, the present Moine Thrust was the last fault surface to develop and the Tarskavaig Thrust initiated folding and thrusting in this region and was preserved on Skye by involvement with the recumbent folding of the Kishorn Nappe.

The Eishort Anticline is folded by the Tarskavaig Synform which is related to the Ord Thrust (Figure 2.C.26 .). The Ord Syncline is also affected by the Ord Thrust which appears to be the lowest thrust exposed on southern Sleat. The rocks of the Ord Window, once thought to have formed part of the Foreland (Bailey 1939) have been affected by both thrusting and normal faulting of comparable age. The rocks of the Ord Window are now considered to form part of the Kishorn Nappe and the structurally lowest fold, the Ord Syncline, is exposed in this structural outlier.

Since a foreland propagating sequence has been established for the higher Tarskavaig and Ord thrusts it is logical to suggest that the structurally lowest thrust in the area, the Kishorn Thrust (Peach et al 1907, Bailey 1939) was the last thrust to form. Therefore, the sequence of thrusts at the southern end of the Moine Thrust Zone is thought to be;

Moine Thrust
Tarskavaig Thrusts
Balmacara Thrust
Ord Thrust
Kishorn Thrust

As described above the relative age of the Moine Thrust is uncertain and it is possible that the Balmacara Thrust formed at a similar time to the Tarskavaig Thrust. The thrust sequence proposed is in conflict with all previous studies referenced in section 2B, which suggest that the nappes developed such that the highest thrusts were the last to form. Further, previous workers, in particular Johnson (1955a), Kanungo (1956) and Barber (1965) suggest that the thrusting was a late brittle event. It has been shown that the thrust at the southern end of the Moine Thrust Zone represent part of an almost continuous sequence of thrust development intimately associated with recumbent folding of the Torridonian and Cambro-Ordovician sucession.

The recumbent folds present on Sleat to the south of Loch na Dal were able to proceed without internal deformation as no cleavages or fabrics are seen in this area. Flexural slip processes are thought to be responsible for the development of these folds and this is supported by the presence of slickensides on bedding planes within the Torridonian sequence. The cores of the Eishort Anticline and the large angular folds on the normal limb of the Lochalsh Syncline (Figure 2.C.20.) are strongly folded. These folds are often chevron in style and they reflect the major structure. They are thought to have been necessary to permit shortening and thickening in the hinges of the larger folds without internal deformation.

To the north of Loch na Dal the presence of slickensides on the bedding surfaces indicate that flexural slip operated during the development of the Lochalsh Syncline. However, many "accommodation" structures are seen in this area which permitted the development of the Lochalsh

Syncline. These structures, such as minor folds, the out-of-syncline thrust and the cleavages of Lochalsh, operated to a greater or lesser extent within different parts of the fold producing a variety of fold profiles which are seen in Figures 2.C.7.,2.C.11.,2.C.12., 2.C.13. and 2.C.14..

The essential features of the Lochalsh Syncline will now be described. On the normal limb of the Lochalsh Syncline the bedding dips gently to the northwest. Before becoming overturned, the dip of the beds increases producing the broad open arcs of bedding seen at Port Cam, Erbusaig and Beinn Bheag. There is a small region in the hinge of the Syncline where the beds dip very gently to the north and then they become overturned. The inverted limb of the Lochalsh Syncline dips uniformly to the southeast, thus the Lochalsh Syncline tends to have long very straight limbs and a relatively very small hinge zone.

The distribution of the axial planar cleavage, the slickensides and the bedding parallel fabric (Figure 2.D.16.) suggest that the Lochalsh Syncline was able to develop by compression of the inner arc of the fold and extension on the outer arc. The former is recorded by the axial planar cleavage and the latter by the bedding parallel fabric.

Where folding could not be accommodated by internal deformation, an out of syncline thrust developed in the hinge of the Lochalsh Syncline and this is most clearly seen on Sleat (Figures 2.C.8. and 2.C.11.). Since the out of syncline thrust affects rocks which posses the bedding parallel fabric both internal deformation and thrusting may have been necessary to permit the development of the Lochalsh Syncline.

In other areas, minor folds such as those at Plockton (Figure 2.C.5.), Beinn na Greine (Figure 2.C.16.) and around Loch na Dal (Figures 2.C.17.and 2.C.18.) developed. These minor folds permitted shortening on the inner arc of the Lochalsh Syncline and allowed the major fold to develop. The persistance of different hinge structures along the strike of the fold may be controlled by the compartmental faults (see Figure 2.C.8.). Within each compartment each process was able to operate to a greater or lesser extent. The distribution of the axial planar cleavage, the slickensides and the bedding parallel fabric may indicate some form of tangential longitudinal strain in the Lochalsh Syncline. However, the strength of the bedding parallel fabric to the east of the area is probably too great to have been produced by tangential longitudinal strain alone. The sheath folds related to the bedding parallel fabric which may be seen at Ard Hill and within the Balmacara Nappe give some indication of the strength of this fabric and they suggest that some form of simple shear may have operated during the development of this fabric (Cobbold and Quinquis 1980). The east-southeast plunging folds in the central area (Figure 2.C.19.) are probably of a similar origin.

Tangential longitudinal strain develops due to the curvature of the layering (Ramsay 1967);thus it is unlikely that the large areas of bedding parallel fabric on the relatively straight overturned limb of the Lochalsh Syncline could have been produced by tangential longitudinal strain alone. It is thought that in addition, some components of simple shear related to the thrusting of the Zone is recorded by the bedding parallel fabric and the comparable mylonitic fabric in the Lewisian rocks of the Kishorn and Balmacara Nappes.

The transverse cleavage postdates the recumbent folding

within the Kishorn Nappe. The asymmetry of the related folds (Figure 2.D.15.) suggests that they lie on the common limb between a syncline above and an anticline beneath. Thus the transverse cleavage may have developed as a consequence of continued footwall folding related to the higher thrust (Kanungo 1956). Alternatively, the folds may form part of a developing anticline in the hanging wall of the thrust beneath. The former model is supported by the lack of cleavage in the western portion of the nappe. However, the latter model is favoured because it forms part of a foreland propagating sequence, but more convincingly, similar folds are seen in the hanging wall of the imbricates of Epidotic Grit seen within the Balmacara Nappe. These folds are only locally developed and may be related to the thrust beneath. They form part of the hanging wall anticline of the associated thrust.

It is emphasized that, even though the transverse cleavage of the Kishorn Nappe and the cleavages related to the asymmetrical folds in the imbricates of the Balmacara Nappe are similar in style and orientation, they should not be correlated and assigned a common deformation number. Within the Balmacara Nappe the development of these cleavages will be sequential due to the sequential development of the imbricates and within the stack of nappes as a whole, the transverse cleavage must be related to the development of a thrust later in the sequence.

The deformation within the Kishorn Nappe was brought to a close by the development of post-tectonic vein arrays (section 2E). In contrast, within the Balmacara and Tarskavaig Nappes,the deformation was closed by the extensive development of kink bands and box folds.

Chapter 3. Metamorphic Grade of the Kishorn Nappe

Section 3A Previous Work

The metamorphic grade of the rocks of the Kishorn Nappe is poorly defined as the Nappe appears to have undergone deformation at conditions below those recorded by conventional metamorphic mineral assemblages.

On Lochalsh Peach et al (1907) recorded granulitisation of quartz and the presence of epidote and chlorite within the basal conglomerate at Fernaig. Unfortunately they make no reference to the relative ages of the epidote or chlorite. Within sandstones of the Loch na Dal Formation on Lochalsh, Peach et al (1907) described brown mica associated with secondary sericite and they also suggest that the association of new sericite and chlorite is common throughout Lochalsh.

The observations of Peach et al (1907), that the Torridonian of the Foreland is red, whereas that of the Kishorn Nappe is green or grey, were taken by Bailey (1955) to indicate the presence of low grade metamorphism. Bailey (1955) also notes that within the Kishorn Nappe, the beds of the normal limb of the Lochalsh Syncline are red whereas those of the inverted limb are grey. This is not entirely true. On Beinn na Seamraig where beds of the normal limb are exposed, the Sleat Group are grey whereas the sandstones of the Torridon Group are red. This suggests that these two groups have undergone contrasting diagenetic histories rather than metamorphisms. Bailey (1955) described the Kishorn Nappe as non-metamorphic, but on the basis of thin sections and previous work he established on Lochalsh, a western limit for the presence of metamorphic biotite between Craig and Balmacara.

X-ray diffraction scans, θ/2θ, undertaken by Coward

and Whalley (1979) indicate that muscovite and chlorite are present and from measurements of the 10 Å peak, they suggest that no detectable non-metamorphic illite is present on the Kyle of Lochalsh.

To establish a temperature for the deformation related to the Lochalsh Syncline, specimens of the bedding parallel quartz veins and the fibrous slickensides were collected through Lochalsh and Skye. It was intended to use bubble thermometry on these specimens, but as initial thin sections showed, strong development of deformation microstructures within the veins and that many of the bubbles are attached to sub grain walls, bubble thermometry was not pursued.

Section 3B X-ray Diffraction Studies

To determine the general metamorphic grade of the Kishorn Nappe shales and slates were sampled throughout the area. Powdered specimens were prepared and analysed by X-ray diffraction (XRD) to determine the mineralogy of the phyllosilicates present. Shales and slates were chosen as these are most responsive to change in metamorphic conditions. An extensive thin section study of shales from the Kishorn Nappe was thought impractical, since clay minerals and the different polymorphs of white mica cannot be readily distinguished in thin section. The measurements were made using a Siemens Crystalloflex 4 generator attached to an iron tube which emitted Fe K-alpha radiation. Scans were made of 2θ values from 5-80 degrees using a chart recorder such that 1cm = 1 degree scanned. The traces obtained were classified into groups on the basis of peak morphology. The peaks of each group were determined using the Standards Index of Minerals (1981) and compared with 2θ scans of pure minerals available at the Department of Earth Sciences, University of Leeds (these were quartz, 2M1 muscovite,

chlorite, kaolinite, pyrophyllite and illite). Since quartz was found to be present in all specimens it was used to correct for alignment errors in the equipment. Characteristic traces of the groups are shown in Figure 3.B.1. and it is clear that the traces are distinct enough for phase identification. Some specimens from the North Wales Slate Belt were also analysed, where the mineralogy was previously known, as a check on the method.

All shales sampled from the Kishorn Nappe were grey, green or greenish grey, with the exception of the Fucoid Beds Member, where the shales were red or yellow. The results will be described group by group according to the characteristic trace obtained. Unless it is stated otherwise, the results refer to shales or slates from the Torridonian rocks of the Kishorn Nappe.

Group 1

The traces of this group show a broad ill defined peak between 7 and 22 degrees. No chlorite peaks were detected and the remaining peaks could be attributed to the presence of 2M1 and 2M2 muscovite. The principal peak of the 2M1 muscovite forms a small shoulder to the principal quartz peak at 33.90 degrees. The 2M2 muscovite peaks are much smaller than the 2M1 muscovite peaks and this may reflect the varying proportions of these two minerals. For group 1 the mineral assemblage is

Quartz + 2M1 and 2M2 Muscovite + Broad ill defined peak

This broad ill defined peak is thought to be due to the presence of poorly crystalline clay minerals and perhaps mica.

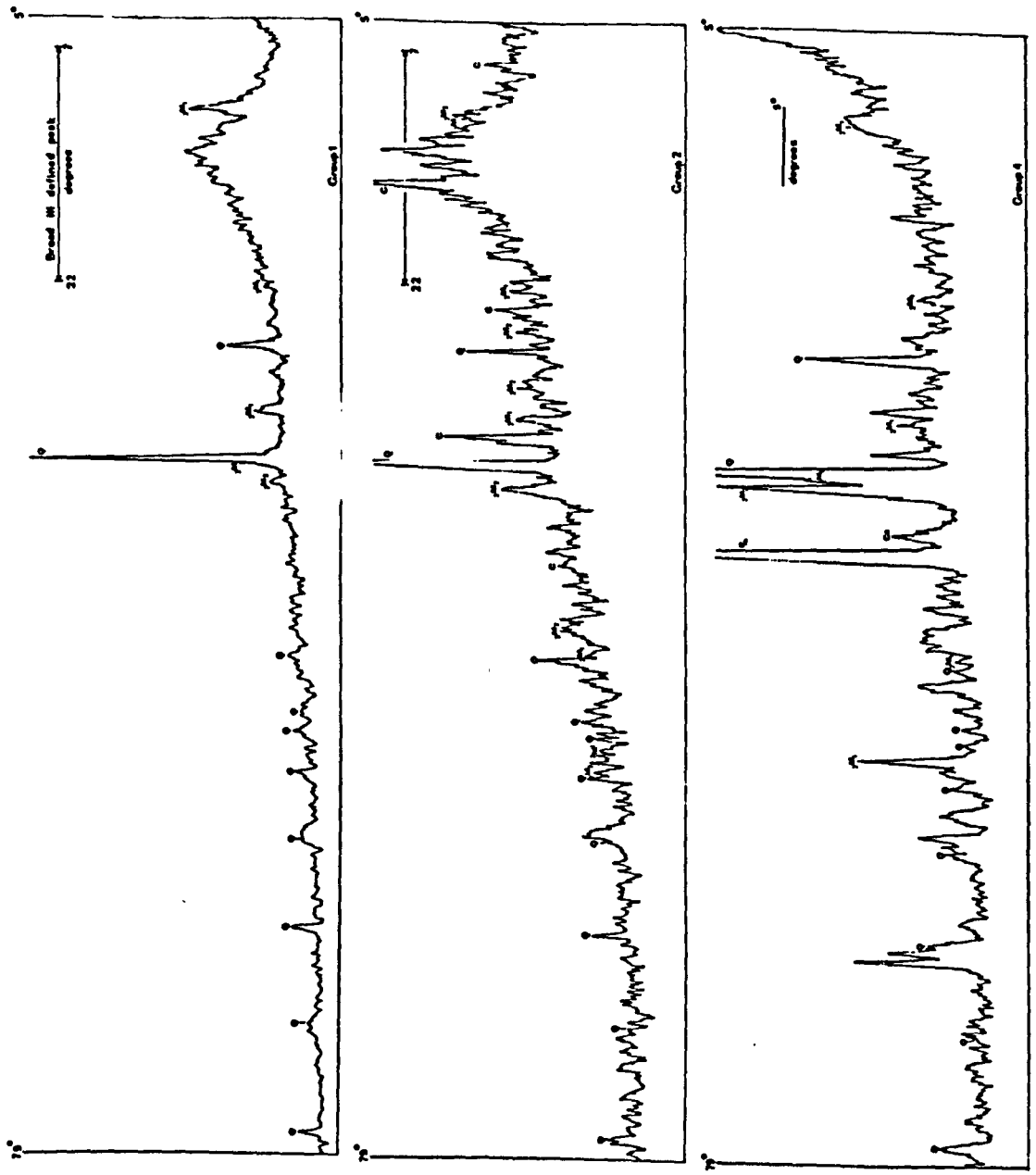

Figure 3.B.1 A series of characteristic traces obtained from the XRD study of shales from the Kishorn Nappe. Each trace is typical of a particular group and the peaks are labelled according to the convention

Q Quartz
2M1 2M1 Muscovite
2M2 2M2 Muscovite
Pm Pumpellyite
Py Pyrophyllite
C Chlorite
St Stilpnomelane
Ca Calcite

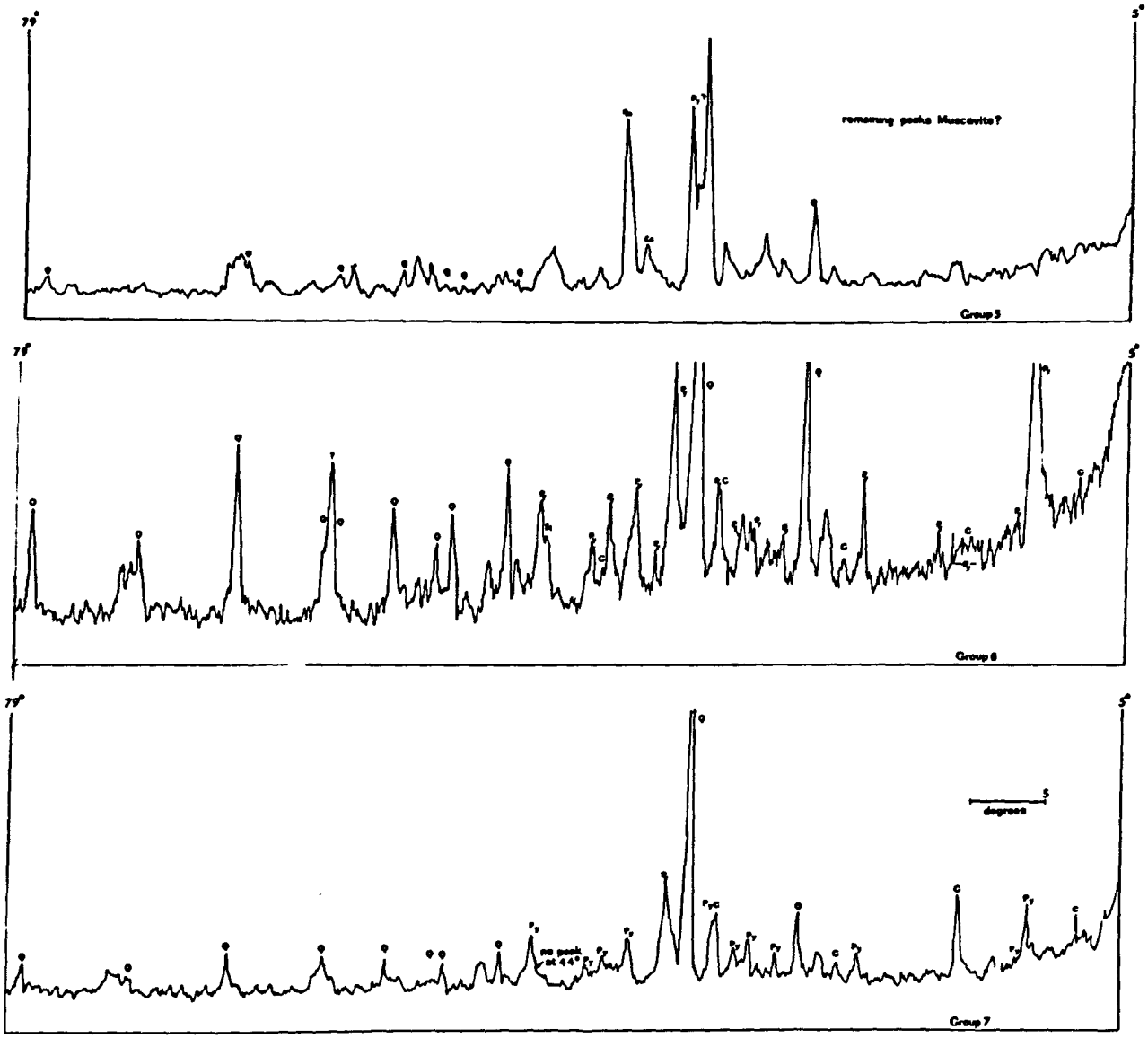
79°
5°
remaining peaks Muscovite?
Group 5
79°
5°
Group 6
79°
5°
5
degrees
Group 7

3B1

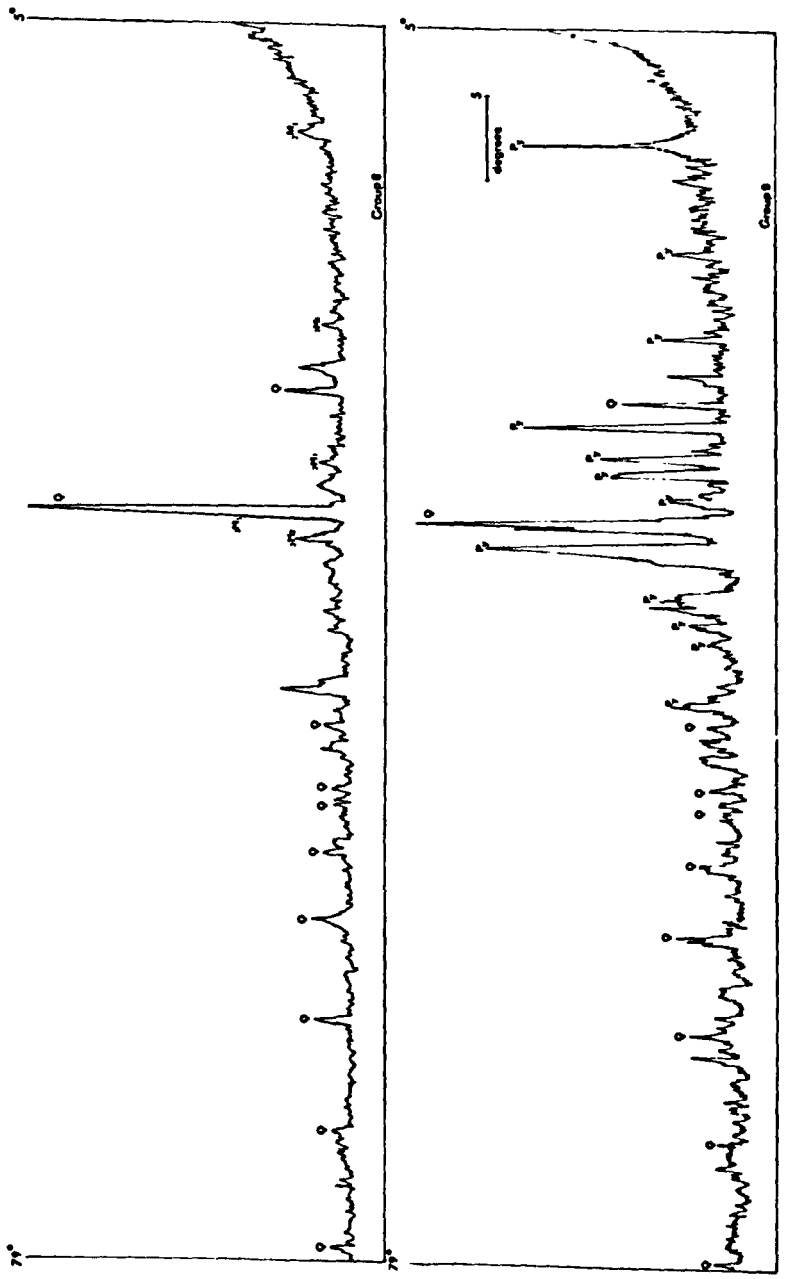

3B1

Group 2

The broad ill defined peak of 7 and 22 degrees is present in group 2 traces but in addition to 2M1 and 2M2 muscovite peaks chorite peaks are also present. The principal 2M1 muscovite peak forms a weak shoulder to the pincipal quartz peak, but in contrast to group 1 the 2M2 muscovite peaks are well defined. The mineral assemblage for group 2 is

Quartz + 2M1 and 2M2 Muscovite + Chlorite + Broad ill defined peak

All the traces were analysed without prejudice of rock type, locality or stratigraphical horizon. As a result all members of Group 3 were Norwegian specimens from the Mellene Nappe and these will be described later. The numbering of groups is consistent throughout this thesis to enable comparisons to be made.

Group 4

This group contains only one specimen which is a yellow brown shale taken from the Fucoid Beds Member and contains well preserved carbonaceous trace fossils. The trace contains quartz and both types of muscovite peaks, but two additional peaks are also present. A 37.20 degree peak was taken to be calcite and a 39.00 degree peak was taken to be pumpellyite. The 2M2 muscovite peaks are extremely well defined and in all cases the principal 2M2 peak is larger than the 2M1 peak. The mineral assemblage for group 4 is

Quartz + 2M1 and 2M2 Muscovite + Calcite + Pumpellyite

Group 5

This group which contained specimens from the Fucoid

Beds Member alone, was much more difficult to analyse and contained quartz, possibly pumpellyite, calcite and pyrophyllite but no chlorite. No clear muscovite peaks could be established or separated into 2M1 and 2M2. The mineral assemblage for group 5 is

Quartz + Pyrophyllite + Pumpellyite + Calcite + Mica Peaks

Group 6

This group contains well defined chlorite peaks in addition to quartz peaks. No muscovite peak could be indentified but pyrophyllite peaks are present. A further peak at 44.61 degrees is also present and this has been interpreted as Stilpnomelane. The mineral assemblage for group 6 is

Quartz + Chlorite + Pyrophyllite + Stilpnomelane

Group 7

This group shows identical peaks to group 6 but no peak is seen at 44.61 degrees and therefore the mineral assemblage for group 7 is

Quartz + Chlorite + Pyrophyllite

Group 8

Quartz 2M1 and 2M2 muscovite peaks are clearly seen in members of this group but poorly defined chlorite peaks are also present. No other peaks are present therefore the mineral assemblage of group 8 is

Quartz + Chlorite + 2M1 and 2M2 Muscovite

Group 9

This group has only one member and only quartz and pyrophyllite peaks are seen. The mineral assemblage for group 9 is

Quartz + Pyrophyllite

The group number has been plotted on a locality map as shown in Figure 3.B.2.. The distribution of the groups bears no relationship to any of the major structures or cleavages recorded within the Kishorn Nappe. Specimens which contain chlorite i.e. those of groups 2,7 and 8 are not restricted to the areas of cleavage development (cf Coward and Whalley 1979). Specimens of groups 1 and 2, which show the broad ill defined peaks, are not restricted to areas outside the cleavage front.(cf Coward and Whalley 1979). Therefore, it is thought that the mineral assemblages present in the rocks analysed are not related to the deformation history which they have suffered.

Since specimens from the Fucoid Beds Member tend to show traces which are unlike those of the Torridonian Shales, then it is possible that the different mineral assemblages obtained are a product of the bulk chemistry of the rock. The shales of the Fucoid Beds Member tend to be dolomitic (Peach et al 1907) and this is reflected in the traces which show calcium rich phases to be present. From the contrast between these two rock types it may be inferred that the different mineral assemblages seen within the Torridonian shales are due to differences in the bulk chemistry of the shales. This would account for the irrational distribution of the results seen in Figure 3.B.2..

From this study of the shaly units within the Kishorn

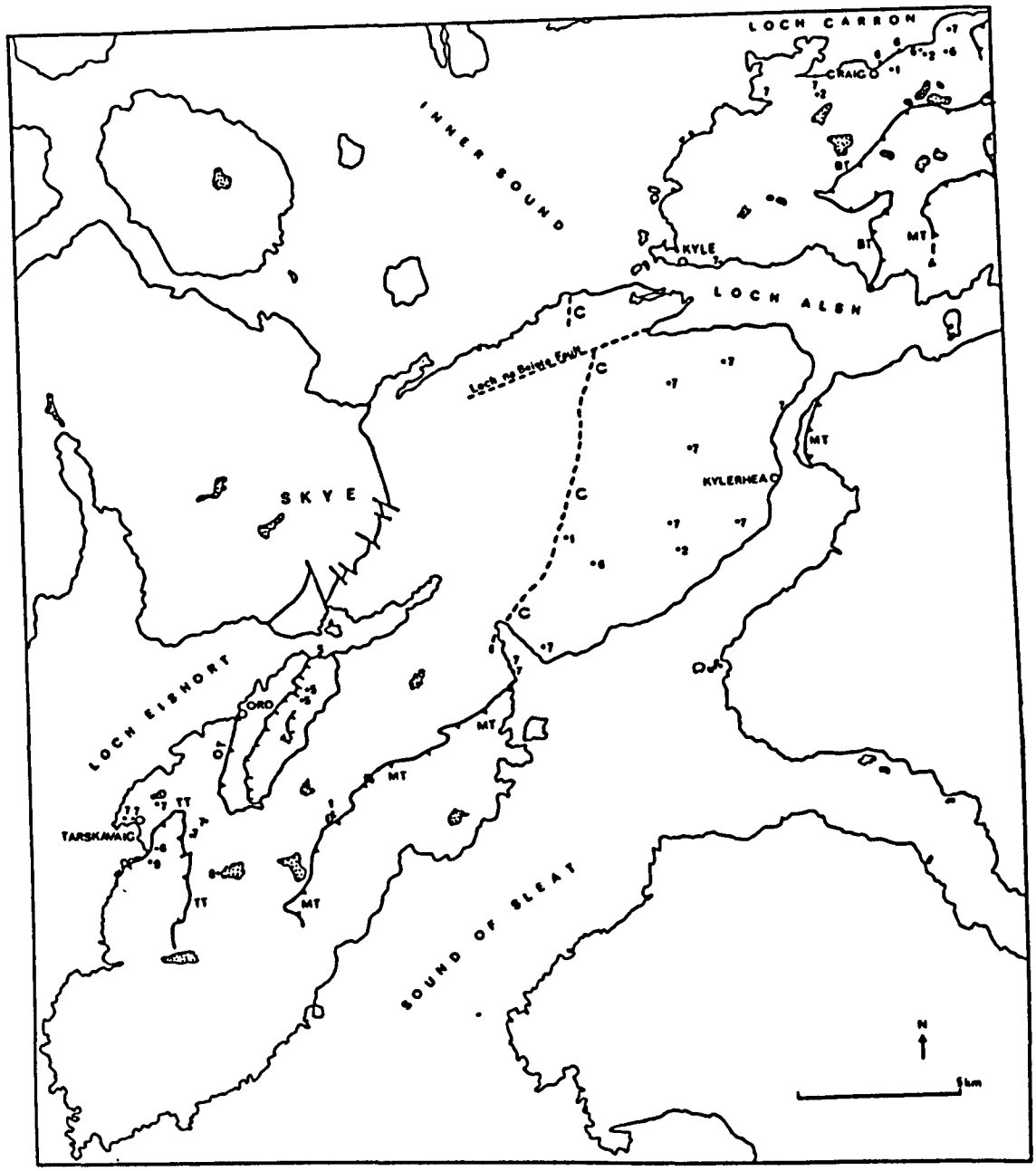

Figure 3.8.2 Locality map showing the position of of the sampling sites relative to the major structures of the Kishorn Nappe. The group number of a particular mineral assemblage marks the position of the sampling site MT= Moine Thrust. BT= Balmacara Thrust. OT= Ord Thrust. TT= Tarskavaig Thrust. C= Cleavage Front, within the Kishorn Nappe the Transverse Cleavage lies to the east of the front.

Nappe it may be concluded that the Kishorn Nappe underwent deformation at low greenschist facies metamorphism indicated by the presence of chlorite and 2M1 and 2M2 muscovite. The work of Bjørlykke (1965) and Englund (1973) suggests that there is a systematic change of muscovite polymorphs from the Foreland to the higher nappes in Norway. No systematic pattern of muscovite polymorphs was found and the Kishorn Nappe is not dominated by one particular muscovite polymorph. Therefore, it is thought that the mineral assemblages found within the Kishorn Nappe can only be related to metamorphic grade in the broadest sense and that the specific mineralogy of the rock is related to the bulk chemistry.

The above conclusion has important consequences in the fields of illite crystallinity (Kubler 1968) and the study of mica polymorphs (Siddans 1979). Both of these methods rely on the proportions of specific phases within a shale or slate and they have been calibrated to provide estimates of paleotemperature. Such studies have been frequently used on a regional scale and little regard has been given to the bulk chemistry of the rock. The results of the study presented here, suggest that within an apparently homogeneous series of shales, such of those of the Sleat Group, variations of chemistry exist and these may result in contrasting mineral assemblages suggesting different metamorphic conditions within a relatively small area. Therefore, any systematic regional study using illite crystallinity (Kubler 1968) should involve whole rock chemical analyses in order that similar chemistries may be compared. Such a study is beyond the scope of this project and therefore methods such as illite crystallinity were not used.

The mineral assemblages found in this study broadly

define the metamorphic grade of the Kishorn Nappe to be low greenschist facies. However, many of the mineral phases identified in the specimens analysed are often the products of weathering and these would lead to an underestimate of the metamorphic grade. In this study weathered material was rejected but its effects cannot be neglected. Through its complex geological history the Kishorn Nappe has been exposed to erosion and weathering at several times since its development (Peach et al 1907, Richey 1935) and it is possible that the products of weathering, if present, developed during one of these periods. For this reason several of the specimens studied using XRD were examined in thin section to determine whether the mineral phases identified by XRD are present in the deformation microstructure of the rock.

Section 3C Comparison of the XRD Results With the Mineralogy of Certain Specimens Seen in Thin Section

Of the specimens analysed using XRD, thin sections were available for groups 6 and 7. These were not chosen in any systematic manner. The samples collected for thin section study were taken to solve various structural problems. Consequently only two groups were studied but they reflect a wide range of tectonic situations. This comparison was made to determine whether the phases identified using XRD techniques make a significant contribution to the microstructure of the rock.

The specimen from group 6 (see Figure 3.B.1.) which were studied using both techniques is a sample from the conglomeratic portion of the Epidotic Grit (NG 84453363). The rock contains a strong fabric, the bedding parallel fabric. In thin section, this fabric is defined by

elongate quartz porphyroclasts which lie with their long axes at a small angle to the trace of the fabric. The matrix of the rock is composed of fine grained quartz and phyllosilicates. Two phyllosilicates may be distinguished in thin section, green pleochroic chlorite and white mica (possibly pyrophyllite). The chlorite dominates the matrix and the grains show a strong preferred orientation parallel to the fabric. The white mica tends to occur in small areas of the thin section. These areas are elongate parallel to the trace of the fabric and the flakes of white mica within them show a strong preferred orientation parallel to the trace of the fabric. No grains were seen that could be identified as stilpnomelane. However, it would appear that the main phases identified in this specimen using XRD make a significant contribution to the microstructure of the rock. This suggests that the phases identified are the products of the processes which produce the bedding parallel fabric and are not due to weathering. Many other thin sections were made of this horizon of the Epidotic Grit. These have exactly the same mineralogy and microstructure as that described here and this suggests that these results are applicable to the whole of the Epidotic Grit presently exposed on Lochalsh.

Several specimens from group 7 could be studied in thin section, these will be described in turn and the conclusions drawn later.

From the area to the north of the Kinloch Lodge Hotel (Figure 2.A.1.) a specimen of folded shale was collected. These folds are chevron like in style and are related to the Lochalsh Syncline (see chapter 2. section C). In thin section very thin layers of fine sand and shale may be seen. No grain shape fabric can be seen in the quartz and feldspar grains and the quartz shows only undulose extinction. In general, the shale

layers are too fine grained to be resolved using the optical microscope, but some large white micas (possibly pyrophyllite) may be seen in the matrix. In thin section, the folds are chevron like in style and numerous slip horizons may be seen which are parallel to the fine layering. Many limb thrusts can be seen which are similar to those described in much larger examples of chevron folding (Ramsay 1974). Both these thrusts and the dilation sites in the hinges of the folds are composed of penninite, a variety of chlorite.

Two specimens were collected from the highly folded Kinloch Formation on Tarskavaig beach (Figure 2.A.1.). Neither specimen shows any fabric in hand specimen. The fold which may be seen in thin section are chevron like in style and are identical to those which may be seen in the field (Figure 2.C.23.). They are related to the Eishort Anticline. Between the layers of fine sand and shale there are slip horizons marked by grains of chlorite. These horizons have staircase geometries (Rich 1934) which cross the sandy units by means of ramps. Both chlorites and white micas are common on these ramps and often the surface of the ramp is formed by a single phyllosilicate crystal. In the shale layers the phyllosilicates lie parallel to the bedding but they cannot be clearly resolved, both white mica (possibly pyrophyllite) and chlorite appears to be present. In one of the specimens from Tarskavaig Quarry (1431) there may be a weak cleavage associates with some of the folds, this cleavage is formed by crenulation of both the white mica and the chlorite grains.

The specimen shown in Figure 3.C.1. is from northern Sleat (NG 75512354) and it shows folded slickensides. These folds are related to the transverse cleavage and the affect the slickensides developed during the formation of the Lochalsh Syncline. Within the shaly portion of

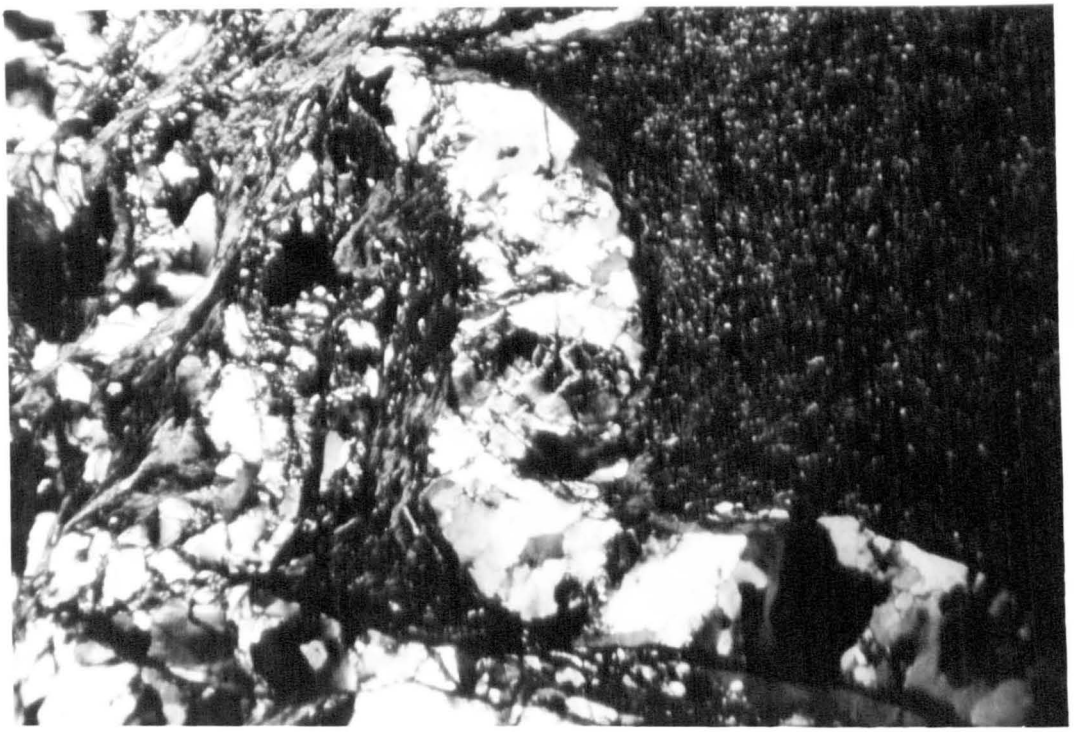

Figure 3.C.1. A photomicrograph of folded slickensides. The slickensides are related to the development of the Lochalsh Syncline. The folds are related to the transverse cleavage which postdates the recumbent folding within the Kishorn Nappe.

this specimen both white mica (possibly pyrophyllite) and pleochroic green chlorite may be seen. Fine grains of quartz are also present. In general, the phyllosilicates lie parallel to the bedding but where the transverse cleavage is strongly developed they are crenulated. In the field the transverse cleavage often appears to be spaced. However, it would appear from this thin section that the transverse cleavage may be a crenulation cleavage modified by diffusive mass transfer. The dilation sites in the hinges of the folds are filled with penninite and it appears that two types of chlorite are present in this specimen. Chlinochlore is developed in the shale whereas penninite is developed in the hinges of the folds.

From the above descriptions the mineral assemblage of quartz, chlorite and pyrophyllite appears to be a valid one for group 7. It would appear from the different tectonic situations studied that, the bedding parallel fabric, the Lochalsh Syncline, the Eishort Anticline and the transverse cleavage all developed under the low grade of greenschist facies metamorphism indicated by the XRD results.

Chapter 4. Strain Studies Within the Kishorn Nappe

In this chapter the results of several local studies will be presented. Each study provides information on the strain distributions which are related to the various minor structures studied and these distributions were used to suggest possible origins for the structures. There are no general conclusions drawn from these studies. Each section has its own conclusions related to the particular structure examined and these conclusions will be used later in the thesis to suggest possible mechanisms for the origin of recumbent folds of the Kishorn Nappe. The methods used will be described in each section.

Section 4A Strain Analysis in the Deformed Conglomerates of Lochalsh

Along the crags of Creag an Duilisg and Carn na Bhealaich Mhoir the Basal Conglomerates of the Sleat Group are exposed in outcrops of the Epidotic Grit. Kanungo (1956) measured the finite strain in these conglomerates using the arithmetic mean of pebble axial ratios. Since many advances have been made in the analysis of finite strain recorded by conglomerates, the conglomerates were remeasured and the strain determined by modern methods.

The thickness of the conglomerates is extremely variable; locally they may be absent. The conglomerates are strongly deformed and the dominant fabric, which dips gently to the southeast, appears to be equivalent to the bedding parallel fabric in the sandstones beneath. The clasts are matrix supported and on joint planes at a high angle to the cleavage they lie with their long axes parallel to, or very close to, the cleavage trace (Figure 4.A.1.). The shape of the pebbles on such planes tends to be elliptical with pointed, or tapered ends. These have been described as subellipses by Lisle (1980) who suggests that the shape arises where the clasts are less

ductile than the matrix during deformation. On the cleavage plane the clasts tend to be rounded (Figure 4.A.2.), and lie with their long axes parallel to an east-southeast lineation on the fabric surface.

Boudinage of the clasts is not common but does occur (Figure 4.A.2.). It takes the form of quartz filled veins often fibrous, which cut the clasts at a high angle to the PQ plane of the pebbles. Boudinage suggests that the clasts were less ductile than the matrix. The limited occurrence of boudinage may be due to the aspect ratio of the clasts falling below the critical length for boudinage to occur (Lloyd et al 1981), or that the clasts have been deformed in a ductile manner. Thin sections of quartz clasts from the conglomerate show deformation microstructures typical of ductile deformation with the marked development of subgrains and dynamic recrystallization along deformation bands and at grain boundaries, producing small strain free grains. Some recrystallization can be seen along planes normal to deformation of growth features, such as planar bubble arrays. Some clasts show evidence of pinch and swell and it is possible that many of the "clasts" measured are in fact relict boudins. The clasts tend to be quartz,though quartz and feldspar aggregates do occur and were derived from the Lewisian Gneiss.

The study was limited by the number of suitable localities and by the number of suitable faces at each locality (see Milton 1980 p68). Where possible a minimum of thirty clasts were measured on each face using a ruler graduated in millimetres, larger clasts were measured to reduce errors. On vertical or steep faces the orientation of the long axes was measured as pitch using a compass clinometer. Where surfaces had a shallow dip such as the cleavage plane, the bearing of the long axes was recorded and the pitch obtained from a stereographic construction. All data obtained

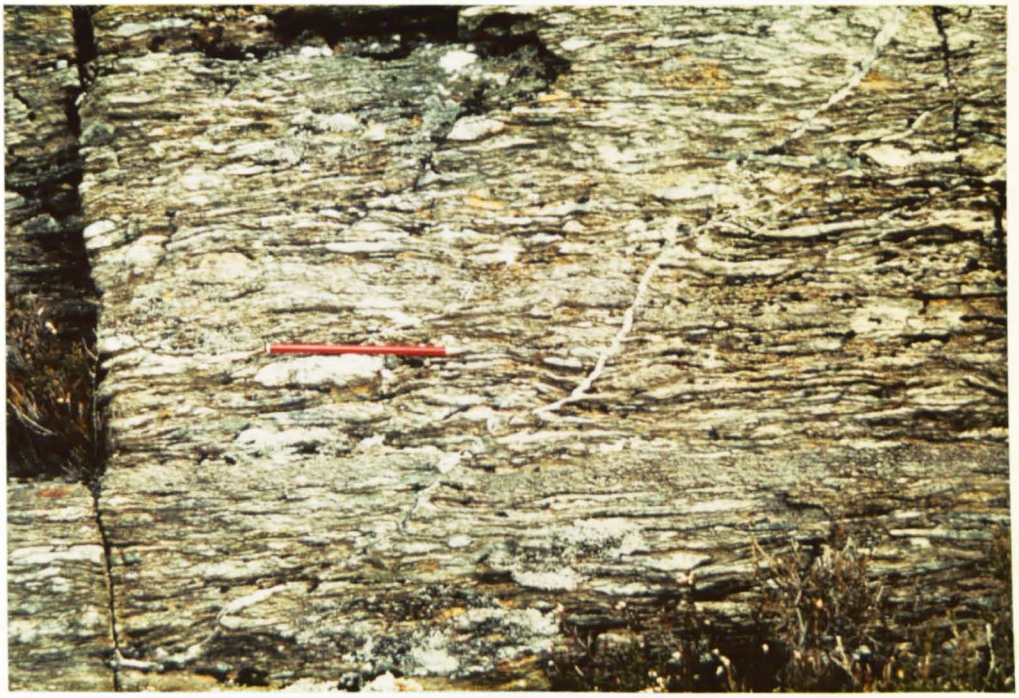

Figure 4.A.1. Photograph of the deformed basal conglomerate at NG 82643272. The photograph was taken looking to the southeast at a joint plane which lies at a high angle to the bedding parallel fabric.

Figure 4.A.2. A photograph of the deformed basal conglomerate at NG 82643272. The photograph shows the fabric plane and the quartz clasts are elongate parallel to the ESE lineation. The photograph was taken looking to the NNE.

was plotted on scattergrams of long axis (a) against short axis (b) and where a range of long axis orientation was found the results were plotted on a Rf/Ø diagram (Ramsay 1967, Dunnet 1969). The measurement of strain in deformed conglomerates has been reviewed by Milton (1980) and further review is unnecessary here. The main problem in the analysis of these conglomerates was that in planes normal to the cleavage the clasts tended to lie with their long axes parallel to the cleavage trace and therefore the methods of Ramsay (1967 p221), Dunnet (1969), Dunnet and Siddans (1971), Shimamoto and Ikeda (1975), Lisle (1977a) could not be used, as a range in long axis orientation is necessary. It cannot be assumed that the clasts were originally spherical,therefore valuable information has been lost. To obtain an estimate of the strain ratio on these surfaces the harmonic mean of pebble axial ratios (Lisle 1977b) and the method of extremes (Ramsay 1967, p210) were used.

At one locality (NG 82643272) some clasts stood proud of the weathered cleavage plane and all three axes could be measured, P, Q and R where P>Q>R. Twelve clasts were measured in this manner and the ratios of their long axes were plotted on a Flinn diagram and they defined a field similar to that described by Ramsay (1967 p210) Figure 4.A.3.. The method of strain analysis for such data suggested by Ramsay (op cit) is difficult to use and instead the results are plotted on a three axis diagram and the strain ratio determined using methods described by Owens (1974), see Figure 4.A.4.. The centre of the field was obtained by construction, giving little weight to point G. The centre of the field lies close to a plane strain path (Owens 1974) with no change in the length of the Y axis. Assuming no volume loss the strain ratio is 2.459 : 1.0 : 0.406 ($K=1$). The results for these clasts are presented in table 4.A.1. and the coordinates of the three axis diagram were

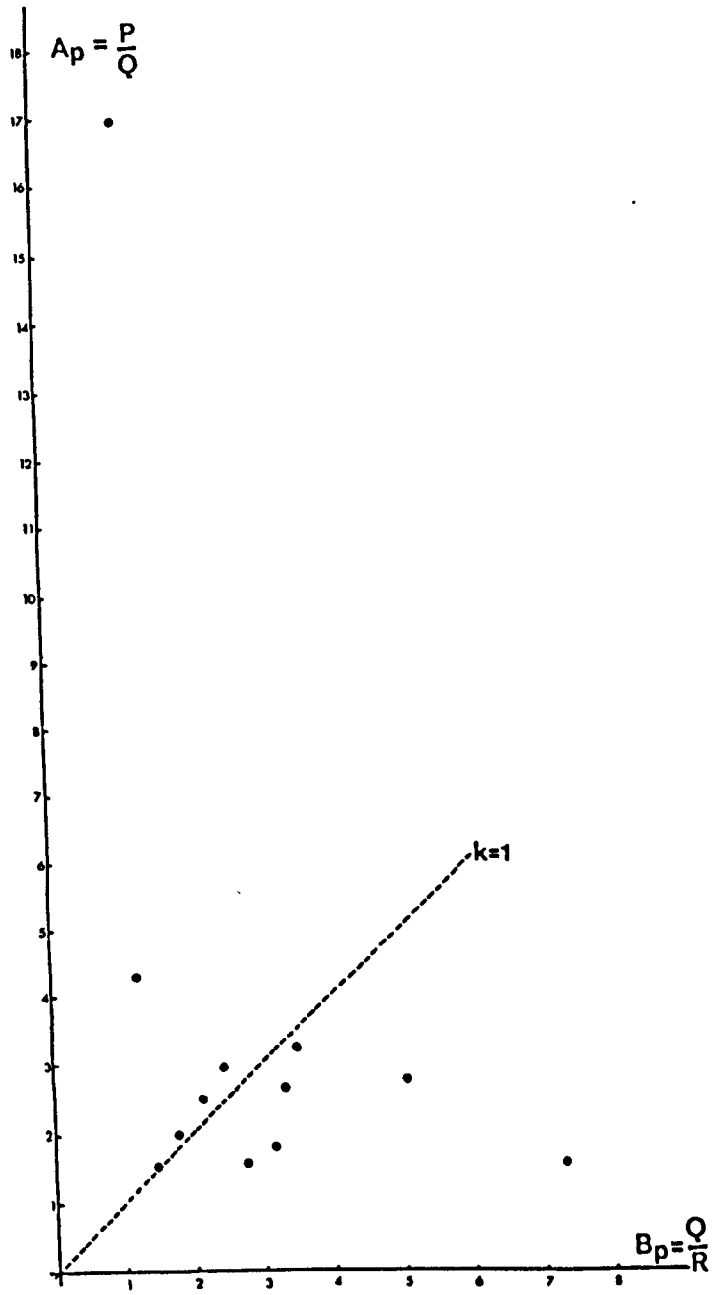

Figure 4.A.3. A Flinn plot of pebble axial ratios (Ap, Bp) obtained from the basal conglomerate at NG 82643272.

Table 4.A.1.

P	Q	R	K_p	P'	Q'	R'	ε_x	ε_y	ε_z
1.563	1	0.136	0.089	2.614	1.675	0.228	0.960	0.514	-1.474
16.830	1	0.833	79.150	6.980	0.346	0.415	1.943	-0.880	-1.603
2.470	1	0.470	1.307	2.349	0.951	0.448	0.854	-0.050	-0.804
1.964	1	0.559	1.224	1.903	0.969	0.542	0.644	-0.031	-0.612
1.545	1	0.364	0.311	1.873	1.212	0.441	0.627	0.192	-0.819
3.206	1	0.286	0.882	3.301	1.030	0.294	1.194	0.029	-1.224
2.918	1	0.411	1.338	2.746	0.941	0.387	1.010	-0.061	-0.949
2.643	1	0.302	0.709	2.850	1.079	0.325	1.048	0.076	-1.123
4.261	1	0.826	15.489	1.314	0.308	0.255	1.030	-0.420	-0.610
1.763	1	0.316	0.352	2.143	1.216	0.384	0.762	0.195	-0.957
1.512	1	0.683	1.103	1.496	0.989	0.676	0.403	-0.011	-0.392
2.732	1	0.196	0.424	3.362	1.230	0.242	1.213	0.207	-1.420

Table 4.A.2.

Locality	Orientation of Fabric	Orientation of Plane	N	Harmonic Mean	Method of Extremes Rs	Ri
NG 84223363	005 12	340 90	30	2.924	3.481	3.230
		180 110	25	3.236	3.346	2.510
		078 90	6	1.790	1.924	1.732
NG 83963361	016 20	280 90	42	2.662	2.774	2.410
		210 70	16	2.192	2.457	2.035
NG 84453363	032 28	287 90	41	3.114	3.928	3.238
		310 90	9	2.938	2.582	2.324
		000 72	4	3.111	4.689	2.772
NG 84313364	028 29	028 29	4	2.273	2.920	2.123
NG 84253364	033 26	313 90	5	2.691	3.120	2.197
NG 82643272	033 22	033 22	39	2.409	2.800	1.995
		213 72	12	1.712	2.171	1.913

Table 4.A.3

Locality	Orientation of plane	Inferred plane of strain ellipse	Harmonic Mean	ε_x	ε_y	ε_z
NG 84223363	340 90	-	2.924			
	180 110	YZ	3.236	-0.003	0.589	-0.585
	078 90	XZ	1.790			
NG 83963361	280 90	XZ	2.662	0.391	0.197	-0.588
	210 70	YZ	2.192			
NG 84453363	287 90	XZ	3.114			
	310 90	-	2.938	0.379	0.378	-0.757
	000 72	YZ	3.111			
NG 82643272	033 22	XY	2.409	0.765	-0.114	-0.652
	213 72	YZ	1.712			
NG 82643272 (thin sections)	-	-	-	1.095	-0.283	-0.812

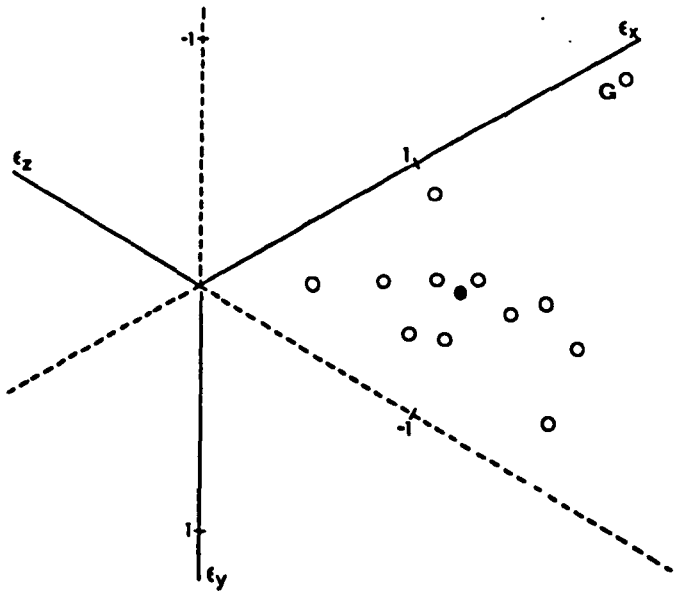

Figure 4.A.4. A three-axis diagram showing the pebble data from NG 82643272. The centre of the field (solid circle) was obtained by construction giving little weight to point G.

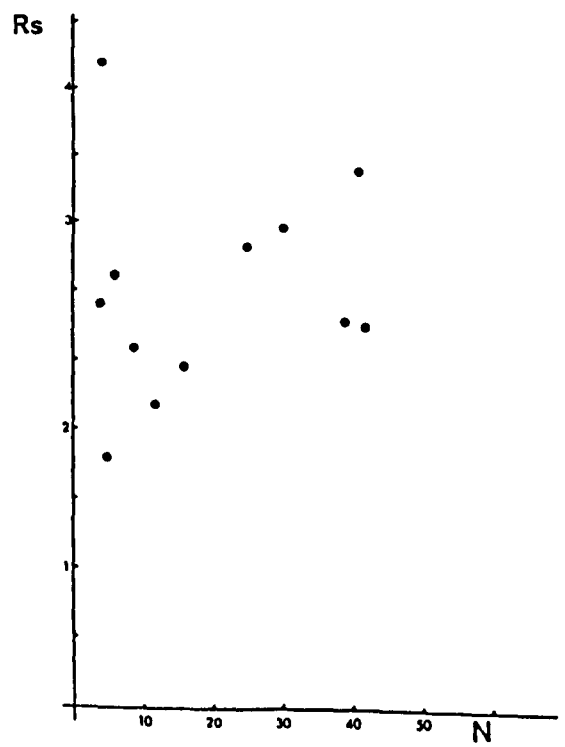

Figure 4.A.5. A graph of strain ratio (Rs), obtained from the method of extremes (Ramsay 1967), against the population of clasts measured on a particular face (N). The values of Rs are not biased by the sample size. The data shown is from all the planes which were measured in the field.

determined by using the equations

$$\varepsilon_x = \frac{2}{3} \ln Ap + \frac{-1}{3} \ln Bp$$

$$\varepsilon_y = \frac{-1}{3} \ln Ap + \frac{1}{3} \ln Bp$$

$$\varepsilon_z = \frac{-1}{3} \ln Ap + \frac{-2}{3} \ln Bp$$

where Ap = P/Q and Bp = Q/R. The axes were chosen to coincide with the inferred strain axes, X_t = lineation on the cleavage plane, Z_t = normal to the cleavage plane and Y_t = strike of the cleavage. The use of the method is justified in that the pebble axes are parallel to the axes of the coordinate system. Though only twelve clasts were measured, the result is probably valid as it is the centre of the group which is important and not the total distribution.

The results obtained from all surfaces are shown in table 4.A.2.. The method of extremes allows the calculation of the strain ratio (Rs) and the initial clast ratio (Ri) from the two extreme pebble axial ratios, Rf max and Rf min, by the equations

$$Rs = \sqrt{Rf\ max \times Rf\ min}$$

$$Ri = \sqrt{Rf\ max \div Rf\ min}$$

Due to the small sub population used when taking only two clasts from a population one might expect the method of extremes to be strongly dependent on the size of population. This however does not appear to be the case. In a graph of Rs against population (N) for the method of extremes, Figure 4.A.5., no correlation is apparent. Further, there is a close correlation between the harmonic mean and the Rs obtained from the method of extremes, suggesting that the results given by the method of extremes are valid see Figure 4.A.6.. Since it can

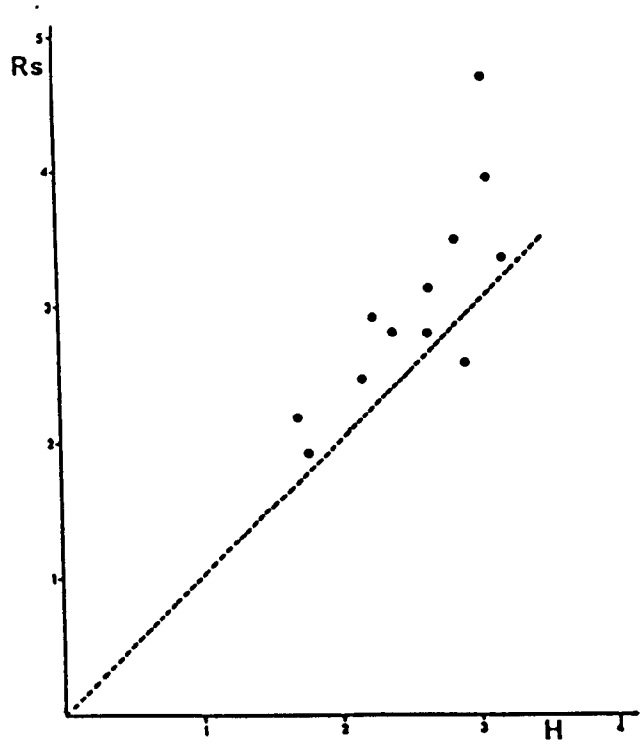

Figure 4.A.6. A graph of the strain ratio (Rs), obtained from the method of extremes, against the harmonic mean of pebble axial ratios (H). The data show a very close correlation though Rs tends to be greater than H.

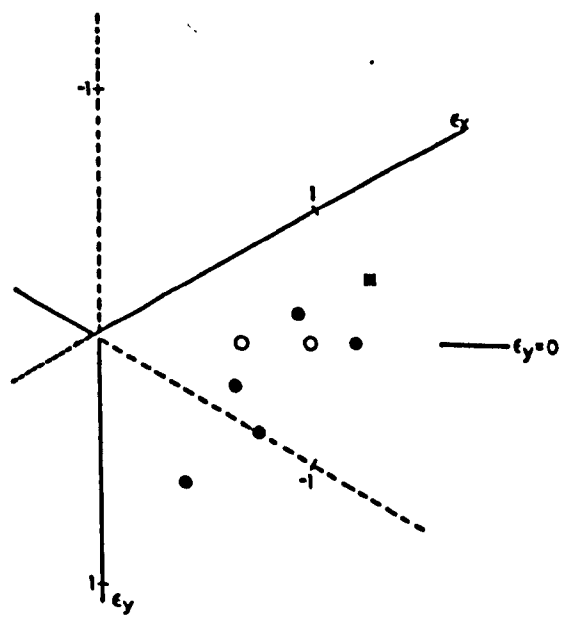

Figure 4.A.7. A three axis diagram showing the axial ratios of the strain ellipsoids obtained by the analysis of deformed pebbles in the basal conglomerate on Lochalsh. Open symbols = data from Kanungo (1956), closed symbols = data presented in this thesis, square = strain estimate from the matrix of the conglomerate at NG 82643272.

be shown that for moderate strain ratios the harmonic mean overestimates the strain ratio (Lisle 1977b), then it is probable that both are an overestimate of the true strain ratio. Values of the harmonic mean are given in table 4.A.3. and these were used as an estimate of the finite strain ratio.

The above comparison between the harmonic mean and the method of extremes was made to test the quality of the strain estimates obtained from the twelve clasts, which is essentially a method of extremes. It is possible that such a small population will produce a strain estimate with large errors,but it has been shown that the strain ratio obtained from the method of extremes is very similar to the harmonic mean. It is thought that the strain ratio obtained from the twelve clasts from NN 82643272 is a valid one.

Where more than one plane was measured at a locality the two dimensional data was combined by assuming that the planes used lay close to the principal planes of the finite strain ellipsoid. The results are shown in table 4.A.3. and the strain ellipsoids plotted on a three-axis diagram Figure 4.A.7.. A three-axis diagram was used where the axes of the strain ellipsoid are parallel to different tectonic axes. Owens (1974) has shown that on a three axis diagram coaxial deformation paths plot as straight lines with a simple relationship to the axes of the diagram. No simple path can be constructed for the determined ellipsoids and a more complex deformation path must be inferred.

At NG 82643272 an orientated sample of conglomerate matrix was taken and the ratios and orientations of the strain ellipses were determined on three mutually perpendicular sections. The Rf/Ø data for each thin section was obtained using the program ELLA FORTRAN

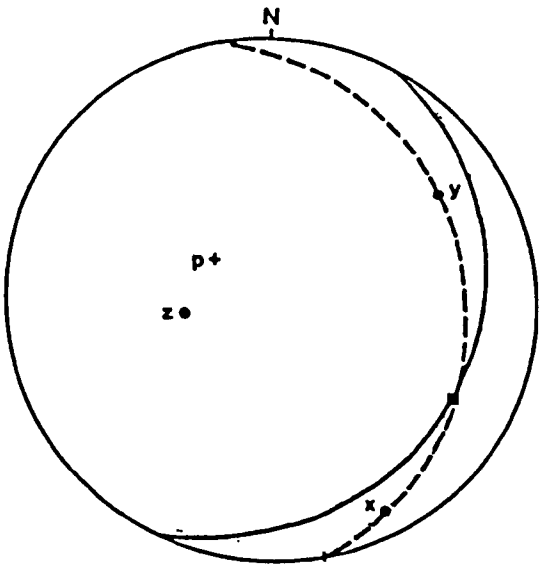

Figure 4.A.8. The orientation of the finite strain axes determined from three mutually perpendicular thin sections of the conglomerate matrix from NG 82643272. The X-Y plane of the finite strain ellipsoid is shown as a pecked great circle. The mineral lineation on the fabric surface is shown as a square, p = pole to bedding plane and fabric.

(see appendix 1.) and the results were analysed using the program THETA FORTRAN (Peach and Lisle 1979). THETA FORTRAN (op cit) was used rather than STRANE FORTRAN (Dunnet and Siddans1971) because the latter program requires, on the plane studied, a bedding trace and a cleavage trace which are distinct. Obviously this is not possible when the bedding parallel fabric is being studied. The results were combined into a strain ellipsoid using the program FITELI FORTRAN (Dayan 1981). The principal planes of the strain ellipsoids obtained from FITELI FORTRAN are very close to the orientation of the fabric plane and lineation seen in the rock (see Figure 4.A.8.). The results from this sample are shown in table 4.A.3. and may be compared with the data obtained from the conglomerate pebbles at the same locality. The strain ratio obtained from the porphyroclasts is greater than that obtained from pebbles. It would appear from this result that the conglomerate pebbles, because of their larger grain size are underestimating the strain ratio. However, in thin sections, the porphyroclasts are seen to be single crystals and it is possible that these grains were able to deform more easily than the polycrystalline pebbles. Also, feldspar is not commonly seen in thin section but it is often found in the pebbles and it may be that the less ductile feldspar is inhibiting the deformation of the larger clasts.

In an earlier part of this section it was suggested that the pebbles of the conglomerate were less ductile than the matrix but not truly rigid. This is confirmed in thin sections of the conglomerate matrix. The thin sections consist of porphyroclasts mainly of quartz, although some of feldspar and epidote may be seen and all of these are found in the matrix of chlorite, white mica and small strain free quartz grains. Chlorite (possibly clinochlore) and white mica define a strong fabric and on the fabric plane a strong lineation is

produced by fibrous growths of chlorite and the preferred orientation of quartz porphyroclasts. The chlorite and quartz grains are the dominant components of the matrix.

In all three sections the quartz porphyroclasts show the same deformation microstructures as the quartz pebble studied in thin section; these are undulose extinction, deformation bands, sub-grains and a recrystallization of small strain free grains. Deformation lamellae are rarely seen. The undulose extinction is due to the misorientation of deformation bands. The quartz porphyroclasts have a distinct core and mantle structure (White 1976) but occasionally recrystallization textures may be seen within grains along deformation bands . The matrix wraps around porphyroclasts and small strain shadows of fine grain quartz and white mica are seen,suggesting that the porphyroclasts are less ductile than the matrix. The common occurrence of deformation microstructures within the large quartz grains suggests that the clasts deformed in a ductile manner. There is a fluctuation in porphyroclast long axes in all of the three planes measured. Those porphyroclasts which have a greater axial ratio and are at a smaller angle to the fabric trace show a greater degree of recrystallization and in many cases these porphyroclasts are completely recrystallized. Such porphyroclasts have much smaller strain shadows and occasionally these may be absent. Variations of axial ratio and orientation within a population of strain markers have been attributed by Ramsay (1967) to the initial shape and orientation of non circular markers and this may well have had an effect in this case. The variable proportion of recrystallization seen in the porphyroclasts suggests that the orientation of the crystal axes in the original grain may be the important factor in controlling the amount of deformation a grain is able to endure and hence influence the final ratio. This illustrates the

dangers of using single crystals such as grains as strain markers.

The epidote grains are less ductile than both the matrix and the quartz grains. They are much more equi-dimensional than the quartz and they have marked strain shadows. The epidote porphyroclasts appear to be single crystals which deformed by a combination of fracture and rotation. However, some of the epidote grains appear to have deformed by the growth of new grains which are much smaller than the host. These new grains appear to have some preferred crystallographic orientation (on the basis of polarisation colour) but it is not known whether this is an effect of host grain control or the growth of a preferred orientation. Feldspar clasts are not common,but where present,they have two dominant microstructures. The first consists of homogeneous feldspar grains which are filled with small inclusions of white mica and the second consists of feldspars which are twinned in a polysynthetic manner.

From the presence of boudinage structures within the pebbles and the wrapping of the dominant fabric around both the pebbles and the porphyroclasts, it would appear that the quartz clasts were less ductile than the matrix during deformation. This being the case, the strain ratio determined from the pebbles will be an underestimate of the true strain ratio and this is illustrated in the variation of the strain ratio determined from the pebbles and the porphyroclasts at the same locality.

The strain ratio determined in thin section may also be an underestimate, as the quartz porphyroclasts were less ductile than the matrix; also there is a control on the final axial ratio of a porphyroclast by its initial crystallographic orientation and this may lead to a further underestimate of the strain ratio.

In deformed conglomerates such as these, where the pebble long axes are parallel to the dominant fabric, a combination of deformation mechanisms may have operated. Gay (1968) has shown how rigid body rotation of ellipsoidal paricles can produce an extremely rapid rotation of particle long axes into parallelism with the strain axes. In this position the orientation of the grain is relatively stable and in the case of these conglomerates, further deformation of the pebbles may have been achieved by shape change. At present it is not possible to seperate these two components from a population of deformed pebbles and this may lead to considerable inaccuracies in strain ratio when determined by conventional methods (Dunnet and Siddans 1971, Lisle 1977a, b).

Accepting that the results obtained are, at best, only a poor estimate of the true strain ratio it is still possible to draw conclusions as to possible strain paths which may be obtained from Figure 4.A.7.. In this case the strain path may be of greater importance since the origin of the bedding parallel fabric is uncertain. Possible strain paths will be discussed in detail later, in the light of other strain data from this area.

Section 4B Finite Strains Obtained from Thin Sections of Sandstones from Lochalsh

To determine the orientation and axial ratio of the finite strain ellipsoid (with axes X, Y, Z where $X > Y > Z$) at a number of localities around the village of Craig (Figure 4.B.1.), orientated specimens were collected from sandstones of the Sleat Group. The localities from which samples were collected are shown in Figure 4.B.1.. This

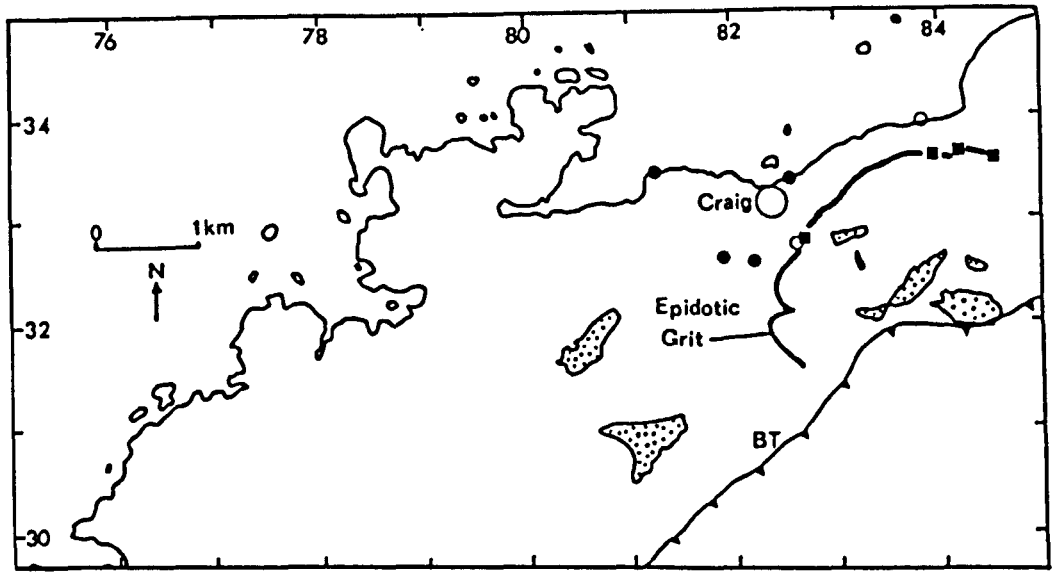

Figure 4.B.1. Position of the sampling sites around Craig (see Figure 2.A.1.). Solid symbols indicate successful analyses and the conglomerate sites are marked by squares.

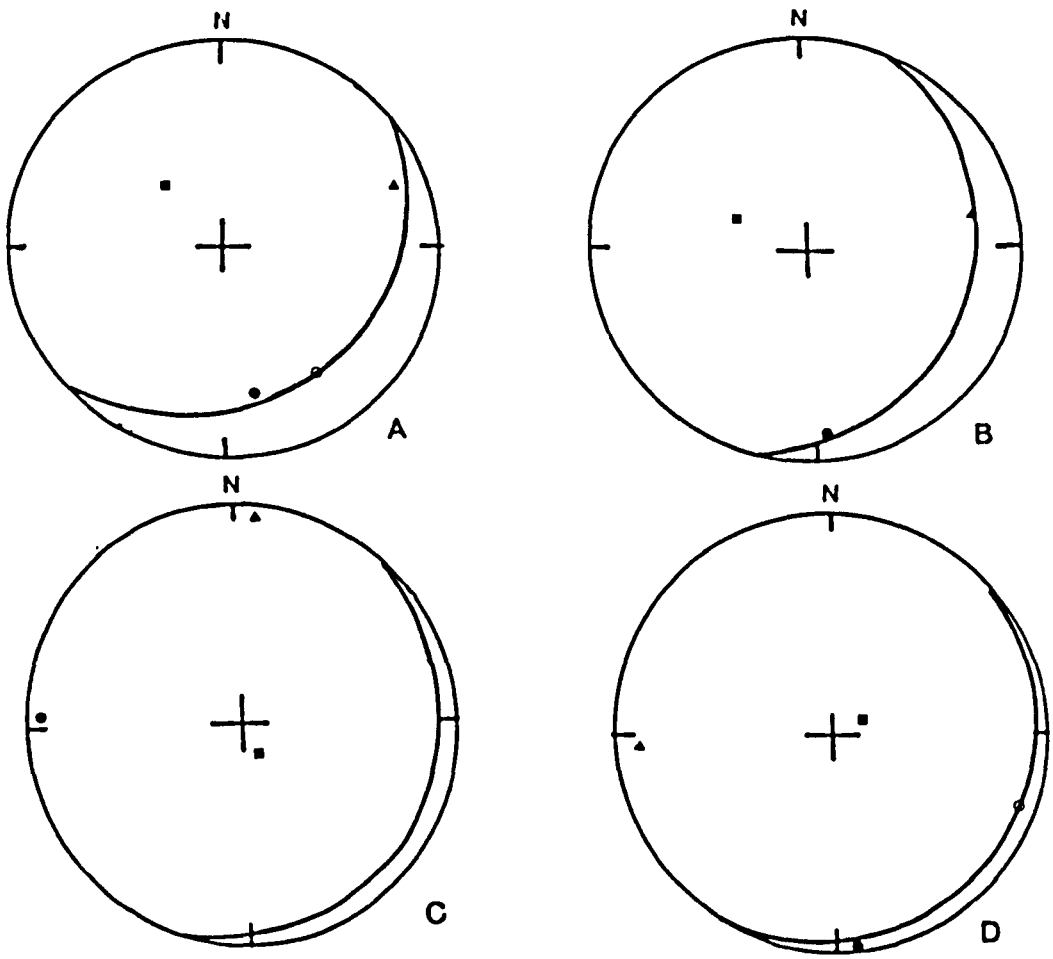

Figure 4.B.2. Orientation of the finite strain axes determined for samples of the Sleat Group from around Craig. ● = X, ▲= Y, ■= Z. The great circle marks the position of the bedding parallel fabric and O= grain shape lineation. A. NG 81303350 (1605). B. NG 82883264 (1594). C. NG 82473258 (1593). D. NG 82513330 (1608).

Table 4.8.1.

Locality	Orientation of Bedding	Orientation of Strain Axes X, Y, Z.			Axial Ratio (ass no vol ch)			K
NG 81303350	050 30(i)	30/169	17/070	58/321	1.166	1.120	0.766	0.170
NG 82883264	018 24(i)	14/175	23/079	62/294	1.520	1.071	0.614	0.629
NG 82473258	032 12(i)	09/274	07/007	78/148	1.290	1.100	0.704	0.357
NG 82513330	043 09(i)	04/174	14/266	77/068	1.377	0.958	0.758	1.537

i = inverted bedding

area was chosen for study as the results may be compared with those obtained from the conglomerates and in the field this area is dominated by the bedding parallel fabric. The transverse cleavage is occasionally present in shale beds but it is never seen in any of the sandstones.

From the orientated samples three mutually perpendicular thin sections were prepared. The Rf/Ø data for each of the thin sections was obtained using the program ELLA FORTRAN (appendix 1.) on tracings of the thin sections. On Rf/Ø diagrams (Dunnet 1969) the data show a strong preferred orientation and cluster about the trace of the bedding parallel fabric. The orientation and axial ratio of the strain ellipse for each of the thin sections was obtained using the program THETA FORTRAN (Peach and Lisle 1979).

The two dimensional results from the thin sections were combined into a finite strain ellipsoid using the program FITELI FORTRAN(Dayan 1981). The orientation of the strain ellipsoids are shown in Figure 4.B.2., together with the orientation of the bedding and any lineations that were seen in the field. The results are summarized in table 4.B.1.. In all the four cases available,the X and Y axes of the strain ellipsoid lie close to the bedding plane and the Z axes lie close to the pole to the bedding. The X axes plunge to the south or southeast (Figure 4.B.2.) close to the grain shape lineation seen in the field and this lineation may be related to the X axis of the finite strain ellipsoid.

Only four strain ellipsoids could be determined for this area around Craig despite the number of samples collected.(see Figure 4.B.1.). At NG 82583266 and NG 83763384 no strain estimates were possible due to the high degree of recrystallization seen in the rocks from these two localities.

All of the thin sections, from which a strain ratio was obtained, have similar deformation microstructures. The quartz porphyroclasts show core and mantle structures (White 1976). The mantle of the porphyroclasts is generally composed of small strain free quartz grains. The cores of the porphyroclasts show undulose extinction, deformation bands and some sub-grains. The sub-grains tend to have similar dimensions to the recrystallized strain free grains and these new grains may have developed by sub-grain rotation. These porphyroclasts tend to have axial ratios of approximately 2:1. Large areas of small strain free grains are common in the thin sections. These areas have axial ratios of approximately 10:1 and they may represent the highly recrystallized products of original quartz grains. The contrasting behaviour between these two types of porphyroclasts may be due to the original crystallographic orientation of the grains relative to the tectonic axes. Only the porphyroclasts with the smaller axial ratios could be measured and the results may seriously underestimate the strain ratio. The fabric in the matrix wraps around the quartz porphyroclasts which suggests that during deformation these were less ductile than the matrix. This will lead to an underestimate of the true strain ratio.

Feldspathic porphyroclasts were also measured and often these are fractured. The fractures are infilled by quartz fibres. Some strain shadows are present around the feldspar porphyroclasts and the shadows are composed of fine grained quartz and white mica. Strain shadows are present around the quartz porphyroclasts but often they are difficult to see due to the core and mantle structure. The feldspars often contain inclusions of white mica and appear to have undergone a reaction which produces white mica. The matrix is compsed of fine grained quartz, chlorite and white mica, other minerals

are present but these are limited in number.

It is thought that the feldspars underestimate the true strain ratio as during deformation they were more rigid than the matrix and the quartz porphyroclasts.

There is a strong fabric in the matrix defined by the preferred orientation of the phyllosilicates. The proportion of matrix to porphyroclast varies between each section and it is thought that the strain ratios obtained from the porphyroclasts underestimate the true strain ratio.

The specimens for which no strain estimate could be obtained have a different microstructure. There is much less contrast between the grain size of the quartz porphyroclasts and the matrix (compare Figures 4.B.3. and 4.B.4.). The rocks consist almost entirely of small strain free grains of quartz and chlorite. The chlorite grains lie parallel to the trace of the bedding parallel fabric. Feldspar porphyroclasts are present, but show little evidence of deformation. In general, strain shadows are rare and the fabric is only occasionally affected by the porphyroclasts. The specimens appear to record strong recrystallization following intense deformation and this strong degree of recrystallization prevents accurate strain determinations.

Analysis of the Finite Strain Results From Around Craig

The results from this thin section study were plotted on a three-axis diagram (Owens 1974) together with those from the previous section. In one case, NG 82513330 , the position of the X and Y axes of the strain ellipsoid have been exchanged, compared with the rest of the results. Consequently this data point lies in the same segment of the diagram (Figure 4.B.5.) as that from NG 84223363. The results of this study conform with those of section 4A.

Figure 4.B.3. A photomicrograph of sandstone (Sleat Group) From NG 81303350 . From measurments of the quartz porphyroclasts in this specimen a successful strain determination could be made.

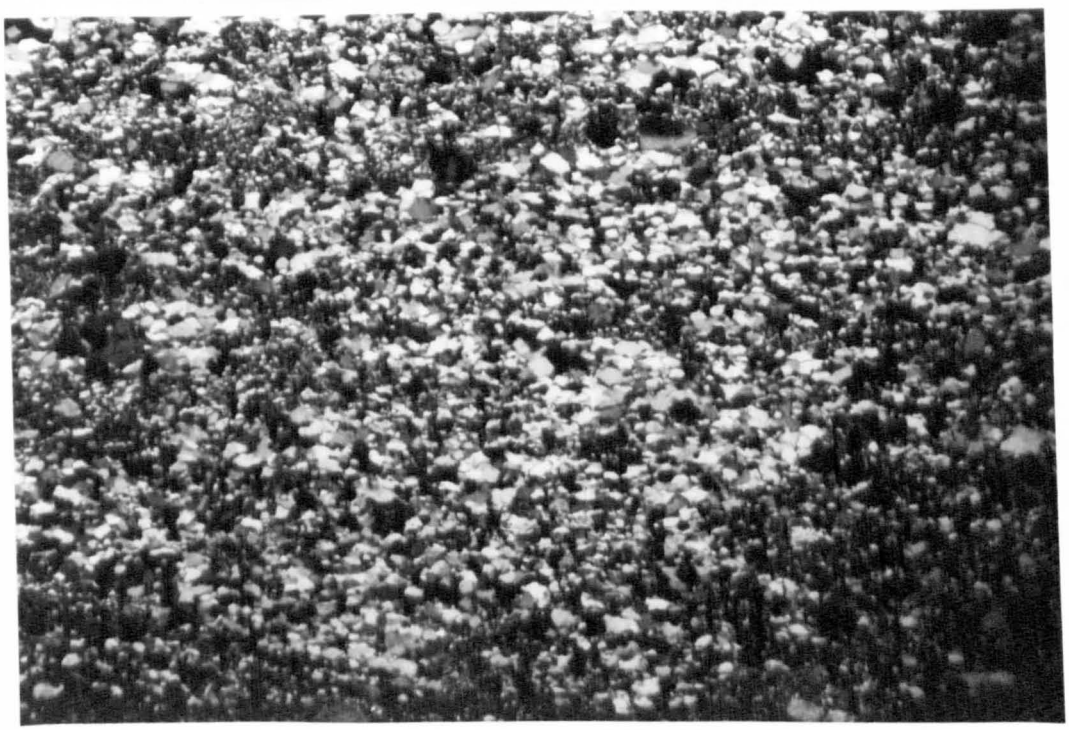

Figure 4.B.4. A photomicrograph of sandstone (Sleat Group) from NG 82583266 . Due to the strong degree of recrystallization in this specimen no strain estimate could be made.

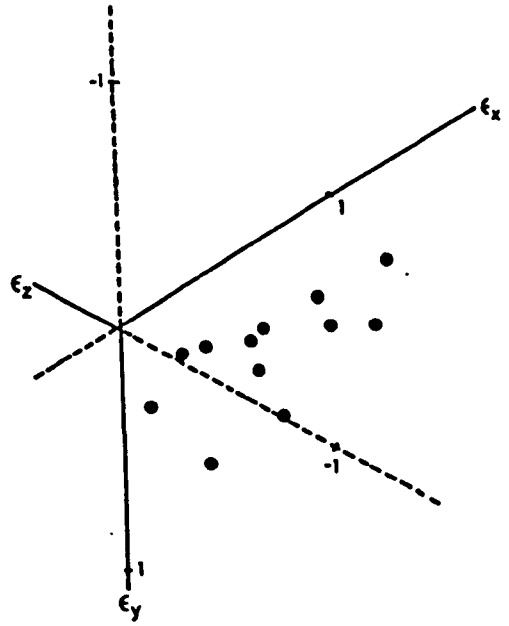

Figure 4.8.5. A 3-axis diagram showing the finite strain results from the deformed conglomerates (previous section) together with those from the samples of sandstone from around Craig.

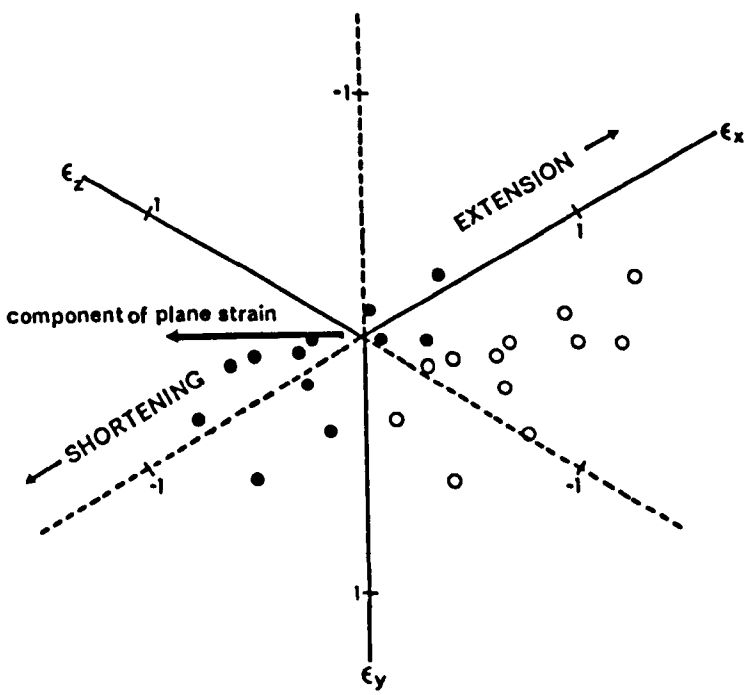

Figure 4.8.6. When a plane strain component of 1.978: 1.0:0.506 is removed from the data shown in Figure 4.8.5. (open circles) the results lie on or about the ϵ_x axis of the diagram (closed circles). This suggests that various components of extension and shortening parallel to the ESE lineation are present in these results. Clearly this is unrealistic in view of the strong extension lineation seen in the rock.

Owens (1974) has shown how finite strains represented on a three-axis diagram may be factorised into components of strain, providing that the deformation was coaxial. In such cases the deformation path bears a simple relationship to the axes of the diagram. An example of this kind of study is provided by Milton and Chapman (1979). The situation which they report, of a sedimentary fabric which is modified by plane strain deformation cannot be used for the results presented here. The array of points lies parallel to the X_t axis rather perpendicular to one of the axes. Several of the many possible alternatives will be given in the following paragraphs.

If we remove a plane strain deformation with no change of length in the Y_t direction a similar component may be removed from each of the results. The data then lie along the X_t axis Figure 4.B.6.. This suggests that some components of strain are present which involve uniaxial extension or shortening parallel to the X_t axis. From the diagram shown in Figure 4.B.5. it is not possible to suggest whether the uniaxial extension or the plane strain was first. The components of extension are large and such a variation,as seen in the diagram is unlikely in view of the strong lineation related to the bedding parallel fabric. This is perhaps, the simplest coaxial path which may be suggested for these results but geologically unlikely.

It is possible to infer the presence of components of extension or compression parallel to the strike of the bedding i.e. in the Y_t direction. This requires different amounts of plane strain deformation to produce the finite strain results obtained. A systematic pattern of plane strain is seen in Figure 4.B.7. this pattern

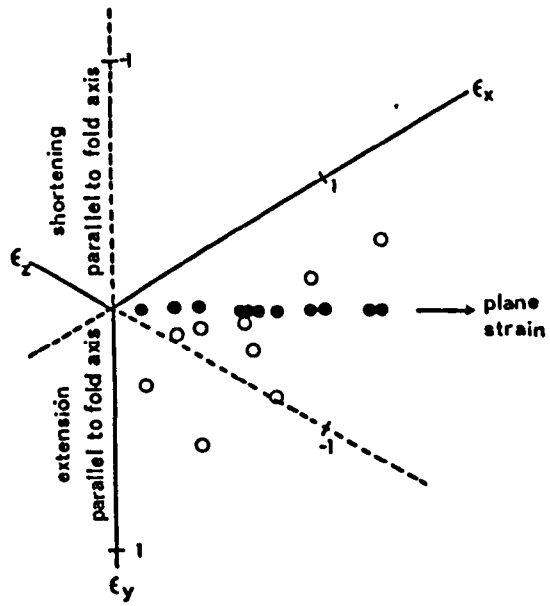

Figure 4.8.7. If we assume that the results of Figure 4.8.5. contain various components of plane strain, with no change in length parallel to the Y_t tectonic direction then, the finite state may be produced by components of uniaxial extension or shortening parallel to the fold axis.

bears no relationship to the location of the sampling sites in the field and may be coincidental.

Components of compaction strain may be included in the models above but these seem unlikely in sandstones, though sedimentary fabrics may be present which have similar geometrical consequences. These components may be included in the models above without changing the strain paths to any great extent.

It is clear from the preceding discussion that a large number of possible coaxial strain paths may be suggested for the finite strain results seen. Without more information regarding the position of one or two points on the strain path it is not possible to discriminate between any of the paths proposed. No unique coaxial path can be suggested for these results. However, it is thought that the second case given above is the most likely given the presence of the two points in a different segment to the main group in Figure 4.B.5.

Components of uniaxial or even triaxial volume change may be present in these results due to the reaction of the feldspars to white mica during deformation of these rocks. It is possible the range of results are due to errors in the strain estimation, but since these errors cannot be quantified they must be rejected and the range of strain values obtained considered to be real. Little information can be obtained from these results regarding the deformation path which the rocks have undergone and they provide little information on the origin of the bedding parallel fabric. The results do however provide information on the variation in axial ratio and orientation of the finite strain ellipsoids related to the bedding parallel fabric.

Section 4C Pipe Rock Strains of the Ord Syncline

In the Moine Thrust Zone of Northwest Scotland the Pipe Rock Member of the Cambro-Ordovician sequence has been used extensively to determine and map strain distributions (McLeish 1971, Wilkinson et al 1975, Coward and Kim 1981, Fischer and Coward 1982). The bioturbation tubes or "pipes" of the Pipe Rock Member are excellent strain markers, as there is little ductility contrast between them and the matrix.

The Pipe Rock Member of the Ord Window appears to be undeformed. On the bedding plane, the one centimetre diameter pipes are circular in cross section and the conical trumpet pipes are often elliptical, but show no preferred orientation of long axes (Figure 4.C.1.). In sections normal to the bedding plane, the pipes are perpendicular to the bedding (Figure 4.C.2.). This lack of strain was noted by Clough (in Peach et al 1907). No attempt has been made in this project to analyse the finite strain of the Pipe Rock Member throughout the Ord Window, as any strain, if present, is extremely low. Also, at many localities, the exact position of the site relative to the major structure is uncertain.

On the west side of Sgiath bheinn an Uird (NG 64151415) a large hinge is exposed, which represents a congruous minor fold on the overturned limb of the Ord Syncline (see chapter 2.). The portion of the hinge presently exposed is within the Pipe Rock Member and a detailed study was undertaken to analyse the finite strain around this hinge in order to determine the possible fold mechanism.

The dip of the bedding in the hinge varies between 23 degrees northwest (correct way up) and 76 degrees southeast (overturned). Figure 2.C31. shows a photograph of the hinge and a stereogram of poles to bedding is shown in Figure 4.C.4.

Figure 4.C.1. A photograph of part of the bedding surface from the minor fold on the west side of Sgiath bheinn an Uird (NG 64151415). In the photograph the bedding is almost vertical.

Figure 4.C.2. A photograph taken normal to the bedding surface showing that the pipes are still perpendicular to the bedding and have suffered no deformation.

bedding around the fold. Orientated photographs of the bedding surface were taken around the fold at several dip values. The long axis, short axis, ratio and orientation of the pipe cross sections were determined using the program ELLA FORTRAN (appendix 1.). Scattergrams of ellipse long axis (a) against short axis (b) were drawn for each photograph. The results cluster symmetrically about a line, with a slope equivalent to the harmonic mean of the ellipse ratios (Lisle 1977b). The harmonic means are given in table 4.C.1. and they are close to 1.0.

Rf/Ø diagrams (Ramsay 1967 p211, Dunnet 1969) were plotted for each of the photographs and these are shown in Figure 4.C.5.. All diagrams show Rf values of less than 3.0 and a complete range of Ø values between 0 degrees and 180 degrees. Tests on the program THETA FORTRAN (Peach and Lisle 1979), which is based on the "theta curve" method of Lisle (1977a), suggest that strains as low as 1.1 may be studied successfully by this method. The method depends on the grouping and statistical analysis of Ø values. To test the suitability of the data for use with the program THETA FORTRAN, histograms of Ø values were drawn and these are shown in Figure 4.C.6.. Only two of the histograms showed a systematic variation in Ø values, 216^{o} 90^{o} and 197^{o} 95^{o}. When analysed by THETA FORTRAN these two populations showed that a small finite strain was present (see table 4.C.1.) Rs = 1.395 for dip value 216^{o} 90^{o} and 1.122 for dip value 197^{o} 95^{o}. In contrast the remaining four populations showed no improvement on "unstraining" and gave strain ratios of approximately 1.0.

Contrary to suggestions made previously Potts (1982) a small finite strain is present in this minor fold. It is considered to be significant that this strain occurs on the steep overturned limb of the fold. The

Table 4.C.1.

Dip Value	N	H	Vector mean phi (pitch)	Rs
207 30	34	1.33	11.39	1.026
203 44	67	1.34	13.18	1.087
204 80	18	1.14	10.88	1.038
202 85	50	1.40	06.64	1.001
216 90	48	1.50	02.17	1.395
197 95	105	1.27	12.18	1.122

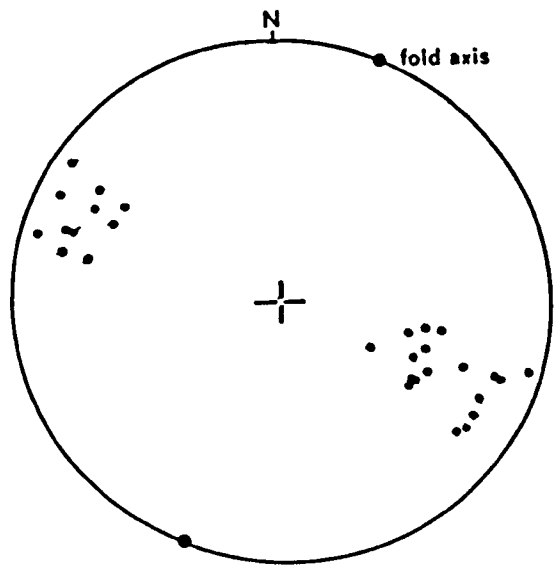

Figure 4.C.4. A stereogram of poles to bedding from the minor fold at NG 64151415.

Table 4.C.2

Sample	Orientation of bedding	Orientation of strain axes X,Y,Z	Axial Ratio (no vol. ch.)	K
1555	193 52	06/137 74/246 14/044	1.28 1.01 0.77	0.870
1556	202 62	29/054 58/283 14/170	1.05 1.04 0.91	0.093
1557	203 80	46/300 22/196 38/085	1.11 1.03 0.87	0.393
1559	250 59	62/207 18/333 20/070	1.21 0.95 0.87	2.771

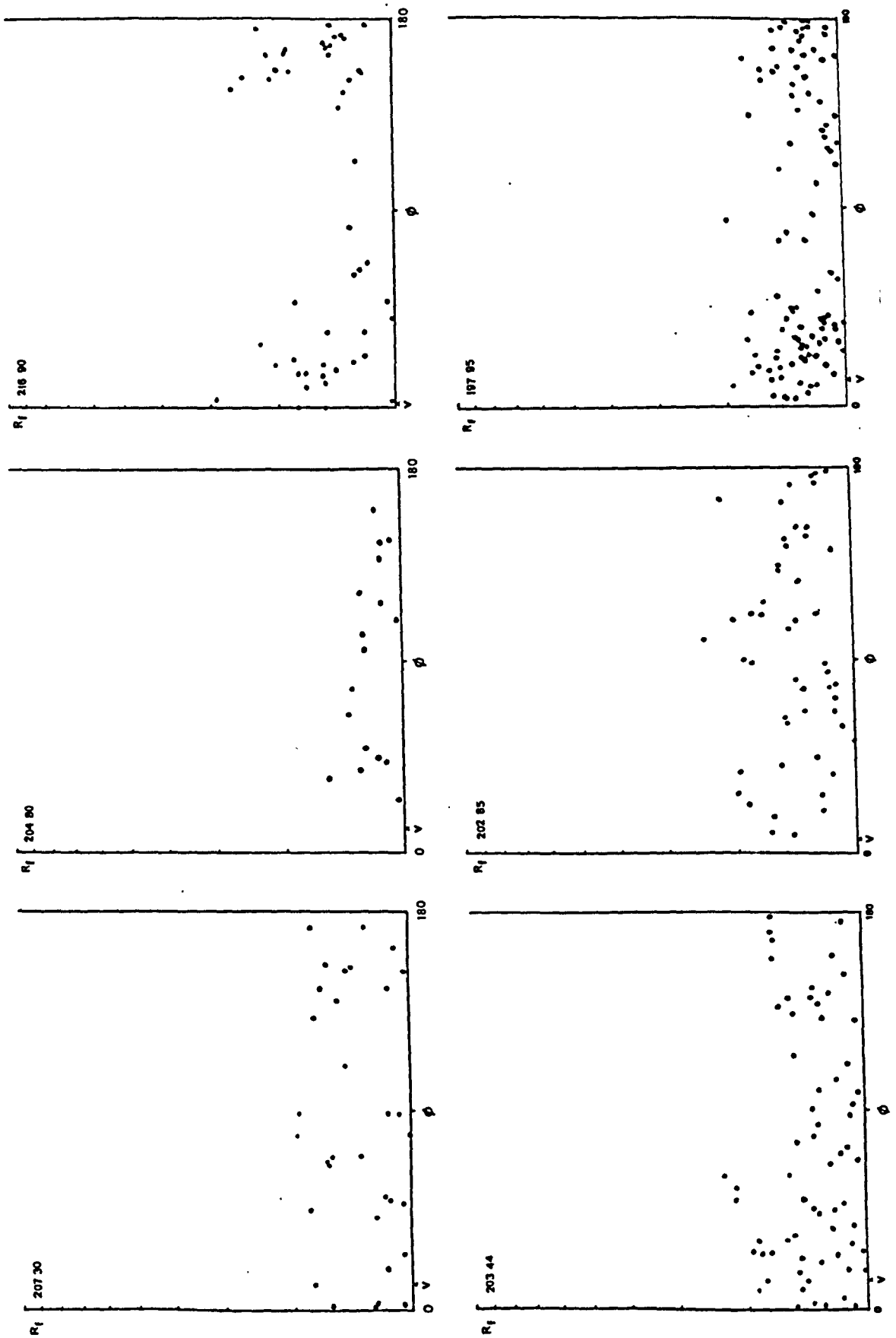

Figure 4.C.5. A series of Rf/Ø diagrams for the various dip values given in table 3.C.1. The vector mean phi (V) is given as a pitch from the strike direction.

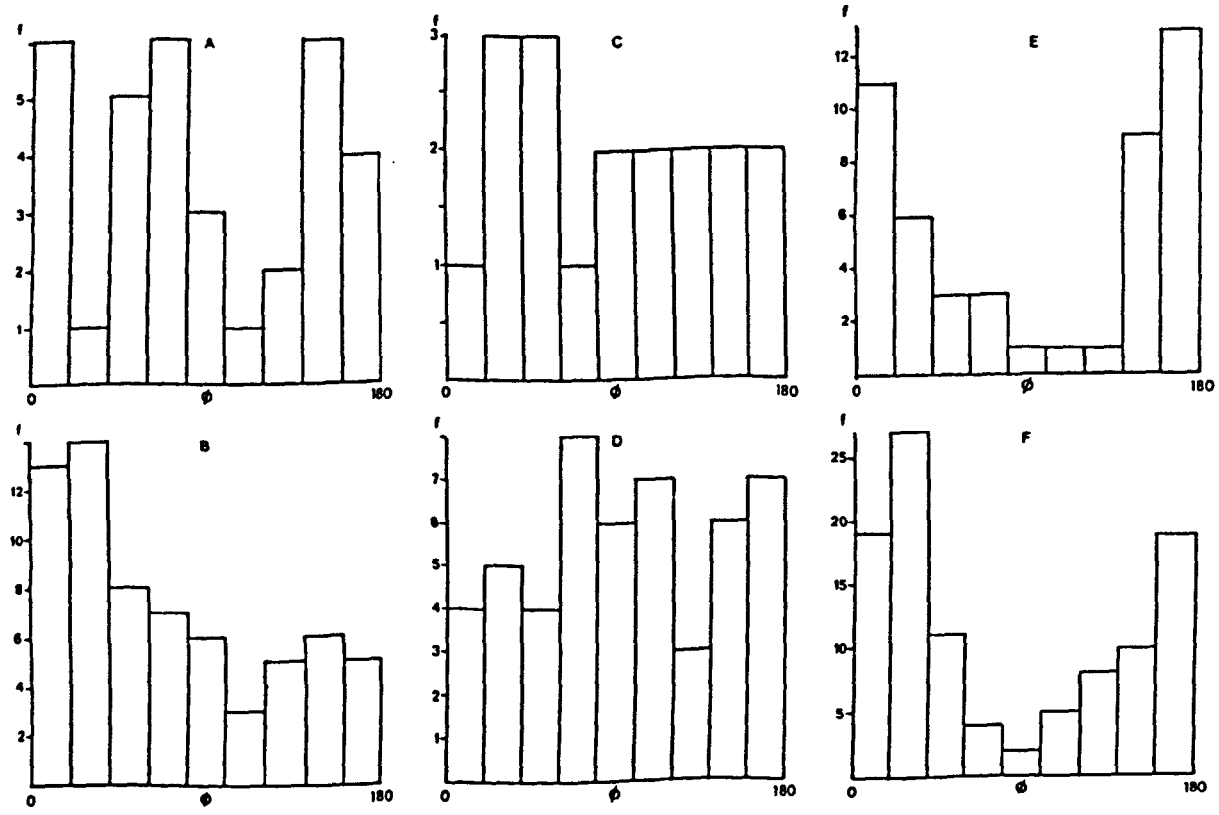

Figure 4.C.6. Aseries of histograms of ϕ values for the dip values given in table 3.C.1. A. 207 30, B. 203 44, C. 204 80, D. 202 85, E. 216 90, F. 197 95. The class interval is 20^{o}.

orientations of the long axes of the strain ellipses are parallel to the fold axis and the general trend of the Moine Thrust Zone. Two possibilities exist for the origin of this finite strain;

1. The strain is a consequence of the curvature of the fold.

2. The strain records a small amount of layer parallel shortening (Coward and Kim 1981).

It is unfortunate that no other folds could be sampled for comparison but no comparable outcrops exist. However, the possible origins of this strain will now be discussed in terms of simple geometrical models.

The asymmetry of strain in folds is a common feature and it has been noted in many natural examples from the Moine Thrust Zone by Fischer and Coward 1982. However, in this case it is only the steeper portion of the fold which is affected and there is no strain recorded at dip values of 202^{o} 85^{o} and 204^{o} 80^{o}. Further, folds seen elsewhere in the Thrust Zone within the Pipe Rock Member appear to be dominated by flexural flow processes (Coward and Potts in press a, Fischer and Coward 1982) which are not seen in this case as the pipes are perpendicular to the bedding. Therefore, some form of model which includes a component of tangential longitudinal strain must be suggested. Donath and Parker (1964) and Ramsay (1967) have proposed geometrical models for folds from which it is possible to calculate the strains in any given situation of tangential longitudinal strain.

As described earlier the strain ratios around the fold are extremely small. However, these may still be modelled in terms of layer parallel shortening with or without tangental longitudinal strain.

The layer parallel shortening may be considered as homogeneous or heterogeneous over the fold segment studied. Strains arising from tangential longitudinal strain show much more variation. The portion of the fold studied may lie above or below the finite neutral surface and the change in curvature of the bedding around the fold will affect the ratio at a particular point (Ramsay 1967). If there is no change in length parallel to the fold axis i.e. a situation of plane strain in the line of section, then the change in strain ratio on the bedding surface may be studied with relative ease.

Qualitatively, the change in strain ratio on the bedding surface can be obtained from the diagrams in Figure 4.C.7.; each possible combination of strains will produce a characteristic type of curve. Layer parallel shortening, if homogeneous, will produce a constant increase in the strain ratio along the potential fold surface. Folding by tangential longitudinal strain will increase or decrease the strain ratio. If the fold segment under study lies on the inner arc of the fold then the strain ratio will be increased due to compression. If the fold segment lies in the outer arc of the fold,then the strain ratio will be reduced. The change in curvature of the fold will control the actual ratio at a point on the fold and the shape of the curves in Figure 4.C.7..

Homogeneous layer parallel shortening followed by tangential longitudinal strain developed by a symmetrical fold will produce symmetrical curves as shown in Figure 4.C.7.. Asymmetrical curves may be produced by a combination of homogeneous layer parallel shortening and asymmetrical folding, heterogeneous layer parallel and symmetrical folding, and asymmetrical folding. The curve obtained for the fold at Sgiath bheinn an Uird is shown in Figure 4.C.8.. The curve is

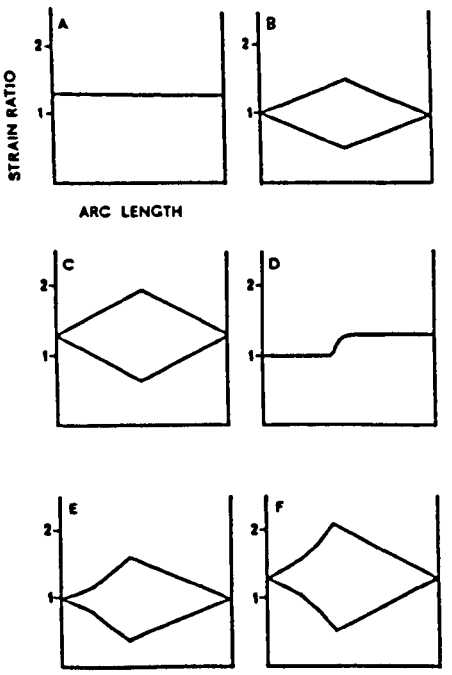

Figure 4.C.7. A series of schematic curves of strain ratio against arc length between two inflection points. The natural curves are probably curved, however, the diagrams give an indication of the contrast between the different types of curve. A. Homogeneous layer parallel shortening, B. Symmetrical folding by tangential longitudinal strain, C. Case A. followed by case B., D. Heterogeneous layer parallel shortening following Fischer and Coward (1982), E. Asymmetrical folding by tangential longitudial strain, F. Case A followed by case E.

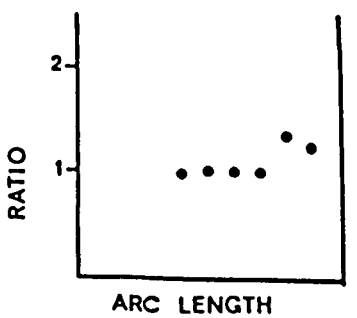

Figure 4.C.8. Results from the minor fold at NG 64151415 The arc length was measured from the most western part of the fold.

asymmetrical and there is no strain gradient on the normal limb over a large change in dip. There is little or no strain on the normal limb of the fold.

For the strain distribution seen in the fold at Sgiath bheinn an Uird only one model is possible and this is heterogeneous layer parallel shortening. There is no strain or strain gradient on the normal limb of the fold. Any tangental longitudinal strain, unless it affects only one limb of the fold, must affect all curved portions of the fold. Homogeneous layer parallel shortening cannot be cancelled by opposite and equal components of tangential longitudinal strain to produce a finite strain ratio of 1.0, as tangential longitudinal strain will produce a strain gradient on the curved portion of the fold. A strain gradient could not cancel the effects of homogeneous layer parallel shortening and small residual strains would be present. It is unlikely, that the results of such an imposition of strains would be cancelled so perfectly, so frequently, throughout the Ord Window. Heterogeneous layer parallel shortening combined with asymmetrical strains developed from the folding could produce a strain ratio 1.0 but the coincidence seems too great.

If the fold is considered to be a large anisotropic single layer i.e. the fold wavelength is controlled by a layer which is composed of many tens of beds then the model of Ramsay (1967) could be used. However, the position of the bedding surface studied relative to the neutral surface of a fold is not known and this makes the modelling of the strain impossible.

It would appear that the folds of the Ord Window are so large that the r/t ratio of the layer involved in the folding never falls below 20 see Figure 4.C.9.. This is the critical ratio at which geologically

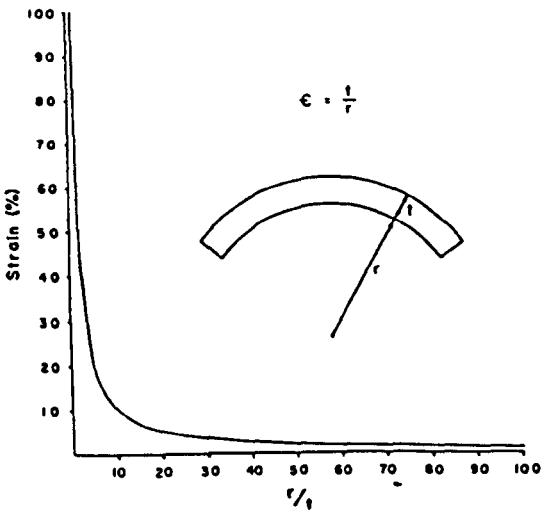

Figure 5. Effect of radius to thickness ratio (r/t) on strain (ε) in flexural-slip folding. From Donath (1963a).

Figure 4.C.9. Figure 5. of Donath and Parker (1964) showing the calculation of finite strain in an ideal flexural slip fold.

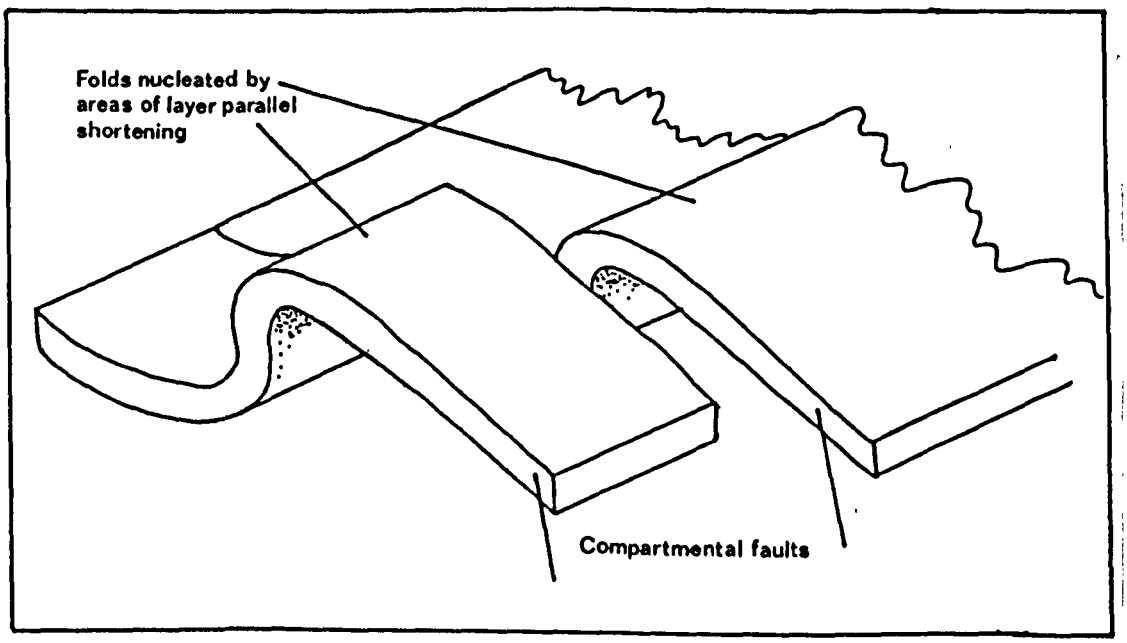

Figure 4.C.10. A diagram showing how compartmental faults permit the growth of two different folds in adjacent blocks. The faults suffer a large amount of movement but relatively little displacement occurs between the blocks.

significant strains develop(Donath and Parker 1964). The fold studied at Sgiath bhienn an Uird is thought to have one of the smallest radii of curvature for any of the folds seen or mapped in the Window. However, even in this case the strain due to the radius of curvature of the bedding is too small to be significant. Therefore, it would appear that the folds of the Ord Syncline have developed without significant strains. The only strains recorded are thought to be due to the initiation of folding by layer parallel shortening. This study suggests that most of the bedding planes must have been zones of slip during folding. Many of the bedding surfaces in the quartzites of the Ord Window are strongly polished and this may indicate that the surfaces were active during folding. However, no quartz fibres or slickensides have been found on bedding surfaces in the Ord Window.

Coward and Potts (in press a)have emphasised the importance of layer parallel shortening in the nucleation of folds and thrusts within the Moine Thrust Zone and Fischer and Coward (1982) have presented strain data from a fold at Ben Heiliam which supports this model. The restricted distribution of the strain in the fold at Sgiath bheinn an Uird overturned limb suggests that it may be a result of layer parallel shortening which nucleated the fold. Certainly the magnitude and orientation of the strain ellipse is consistent with layer parallel shortening. Several hinges are seen, or may be mapped throughout the Ord Window between compartmental faults (Dahlstrom 1970). These faults are marked by thick zones of breccia often up to several metres, which suggests that they have suffered considerable amounts of movement, yet they often show little or no displacement (see Figure 2.C.20). It is suggested that such compartmental faults are essential to the development of these recumbent folds. If the folds initiate as a result of stick on a moving

thrust surface or, as a consequence of propagation of the thrust (Coward and Potts in pressa)then it is not necessary for each fold to initiate at the same point. Thus the numerous hinges mapped within the Window may be positioned, not by a dominant wavelength, such as those predicted in the models of Biot (1964, 1965) or Ramberg (1965), but by the occurrence of stick recorded by the layer parallel shortening. The compartmental faults must then develop to permit propagation and amplification of two adjacent folds (see Figure 4.C.10.). In the Ord Window ductile deformation appears to have been inhibited as compared to Assynt or Eriboll and as a result brittle compartmental faults were developed with thick zones of breccia.The traces of these faults within the rocks of the Ord Window are shown in Figure 2.C.20.

Strain Obtained From Thin Sections From Around the Minor Fold at Sgiath bheinn an Uird

At three dip values around the fold at Sgiath bheinn an Uird orientated samples of quartzite were taken. For each specimen three perpendicular sections were prepared. Tracings were made of these sections and ELLA FORTRAN was used to determine the axial ratio and orientation of the grains present. Scattergrams of ellipse long axis against short axis and Rf/Ø diagrams were drawn for each thin section, and the harmonic mean lies at the centre of the clusters on the scattergrams. There is no preferred orientation of grain long axes on the Rf/Ø diagrams and no preferred orientation may be seen in histograms of Ø values (see Figure 4.C.11.). The data from each plane was analysed by use of the program THETA FORTRAN (Peach and Lisle 1979) and the results combined into three dimensional ellipsoids using the program FITELI FORTRAN (Dayan 1981). The results are shown in Figure 4.C.12. and given in table 4.C.2..

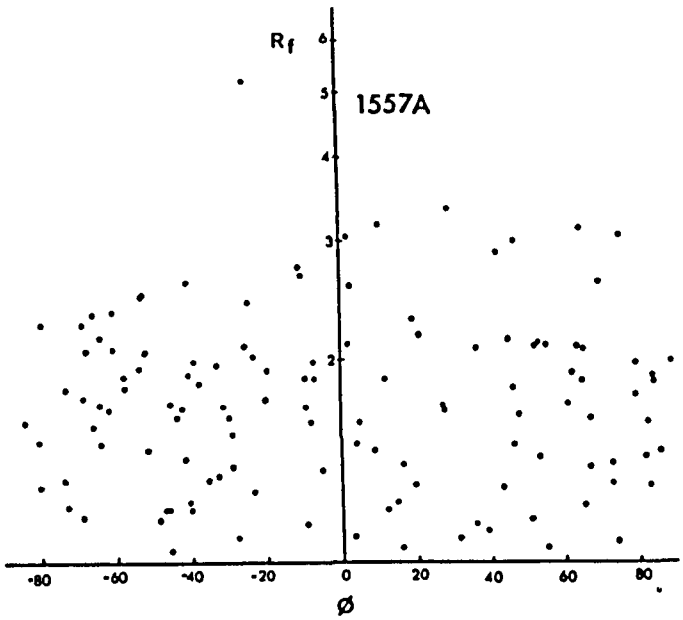

Figure 4.C.11. A typical Rf/Ø diagram obtained from thin sections of the Pipe Rock Member around the fold at NG 64151415. The diagram shows the wide range of Ø values common in these rocks.

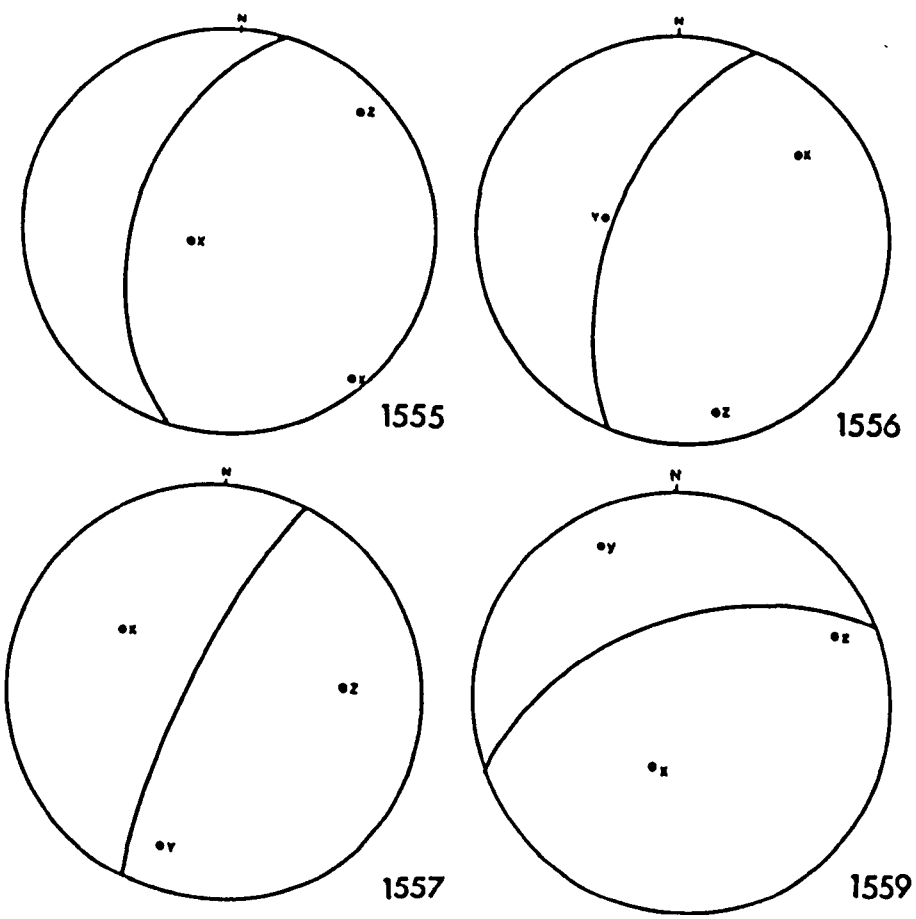

Figure 4.C.12. Stereograms showing the orientation of the finite strain axes given in table 4.C.2. The great circle marks the position of the bedding.

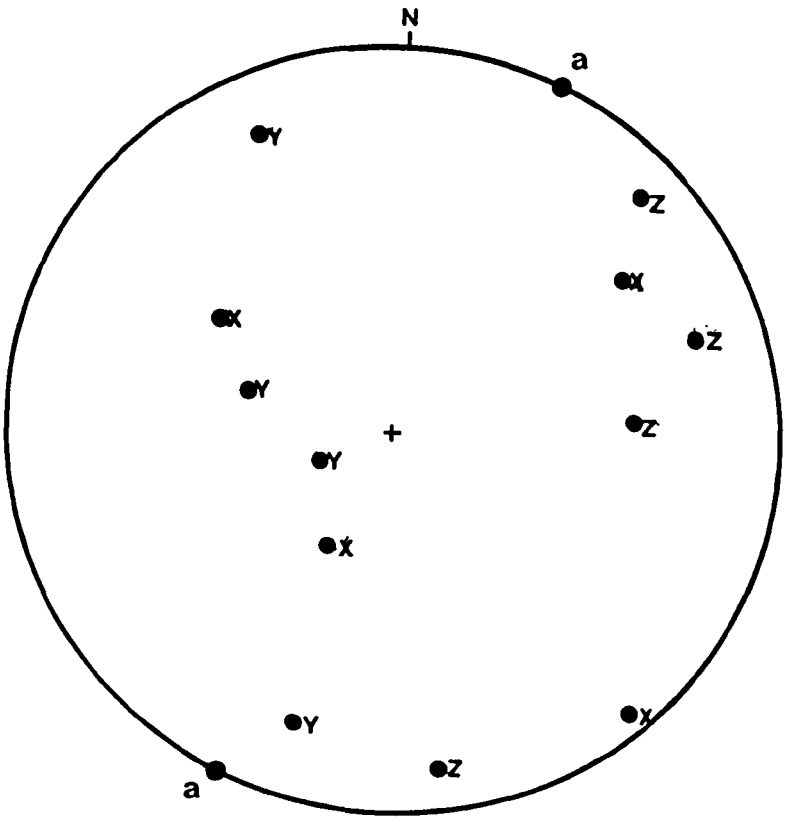

Figure 4.C.13. A stereogram summarizing the results from table 4.C.2. The fold axis is marked (a).

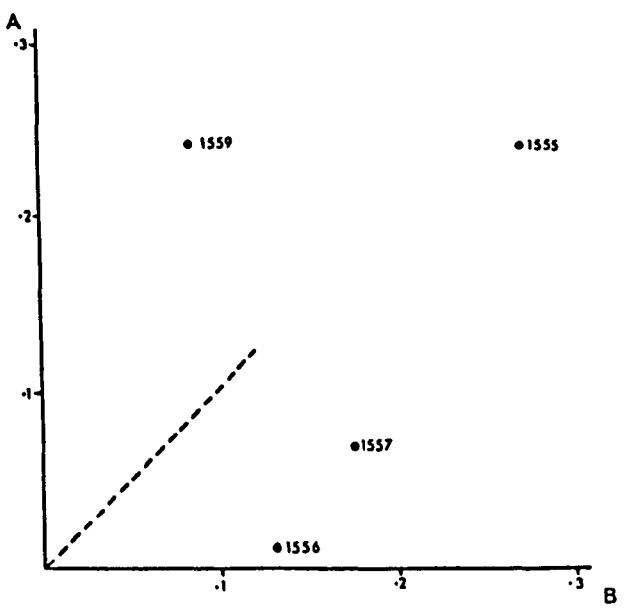

Figure 4.C.14 A Flinn plot of the finite strain ellipsoids from around the minor fold studied. Note, the extreemly small axial ratios.

The orientation of the strain ellipsoids obtained around the fold are shown in Figure 4.C.12.. Rarely do any of the axes bear any relationship to the bedding. Layer parallel shortening would cause the X and Y axes of the strain ellispoid to lie in a plane normal to the bedding and the Z axis to lie in the plane of the bedding parallel to thrust transport direction. A combination of layer parallel shortening and tangential longitudinal strain would produce ellipsoids with axes which are parallel to or perpendicular to the bedding. The close association expected between the bedding, and the strain axes for these combinations of strain is not seen in the fold at Sgiath bheinn an Uird.

When the orientation of the strain axes are compared to the geometry of the fold (Figure 4.C.13.), no relationsip can be seen. The strain ellipsoids are very nearly spherical as seen in table 4.C.2. and Figure 4.C.14. and thus, the orientation of the ellipsoid axes and their relationship to the fold, if any exists, may be obscured. The two dimensional strain results indicate extremely small strain ratios, if any strain is present. In this case, the results produced by FITELI FORTRAN (Dayan 1981) are thought to be spurious and the strain ellipsoid is almost spherical.

Microstructures Within the Quartzites of the Ord Window

It is possible that the small finite strains recorded by both the pipes and the grains around the minor fold of Sgiath bheinn an Uird are a consequence of a complex strain path which results in little or no finite strain. It has already been stated that this is unlikely but this point will be considered further. Such a complex strain path would produce grains with deformation microstructures incompatible with the amount of strain indicated by their shapes. As yet such a relationship

has not been calibrated but may be assessed on a purely qualitative grounds.

All three thin sections from each of the specimens taken from around the fold show similar deformation microstructures in similar proportions. Two contrasting areas may be seen within the sections. In phyllosilicate rich areas the quartz grains (approximately 90% of the rock) show the following deformation microstructures. Approximately 83% of the grains show undulose extinction, deformation bands are seen in around 17% of the grains and only 5% of the grains show any evidence of dynamic recrystallization. Subgrains are rarely seen. Two other microstructures are seen, a few quartz overgrowths are present which show some suggestion of grain boundary adjustments. Areas of quartz are present which appear to be a single grain in optical continuity, but the "grain" has a distinct grain boundary down its centre. This appears to represent the development of two new grains by the development of a single grain boundary. This method of grain shape change has important consequences in Rf/Ø studies as axial ratios are effectively doubled with little change in orientation.

In the phyllosilicate poor areas of the thin sections the grain boundaries of the quartz grains are straight and they tend to meet at angles of approximately 120 degrees; this has been described as a quartz foam texture by Roermund et al (1979) and may indicate grain boundary adjustments after deformation. These adjustments may have removed evidence of more intense deformation, for example sub-grains. However, this seems unlikely, since such microstructures are rarely seen elsewhere in the thin sections, where the adjustments were prevented by the phyllosilicates. The contrast between the mica rich and mica poor areas is shown in Figure 4.C.15. The strain estimates are

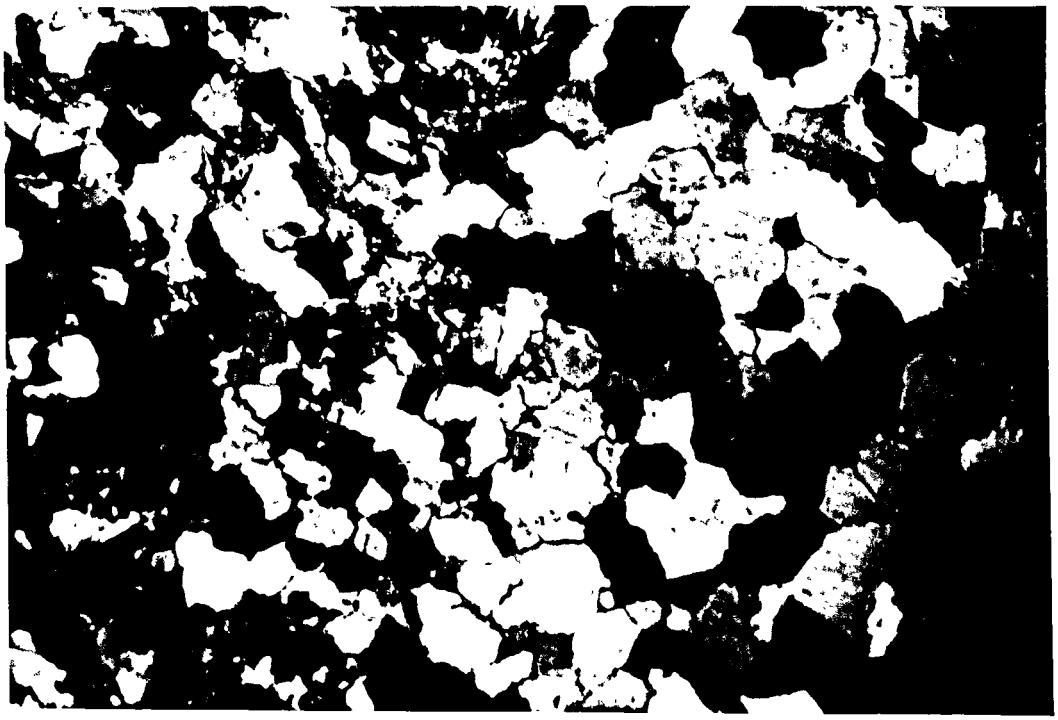

Figure 4.C.15. A photomicrograph showing the contrasting microstructures between the phyllosilicate rich and phyllosilicate poor areas of the Pipe Rock Member in the Ord Window (1557A).

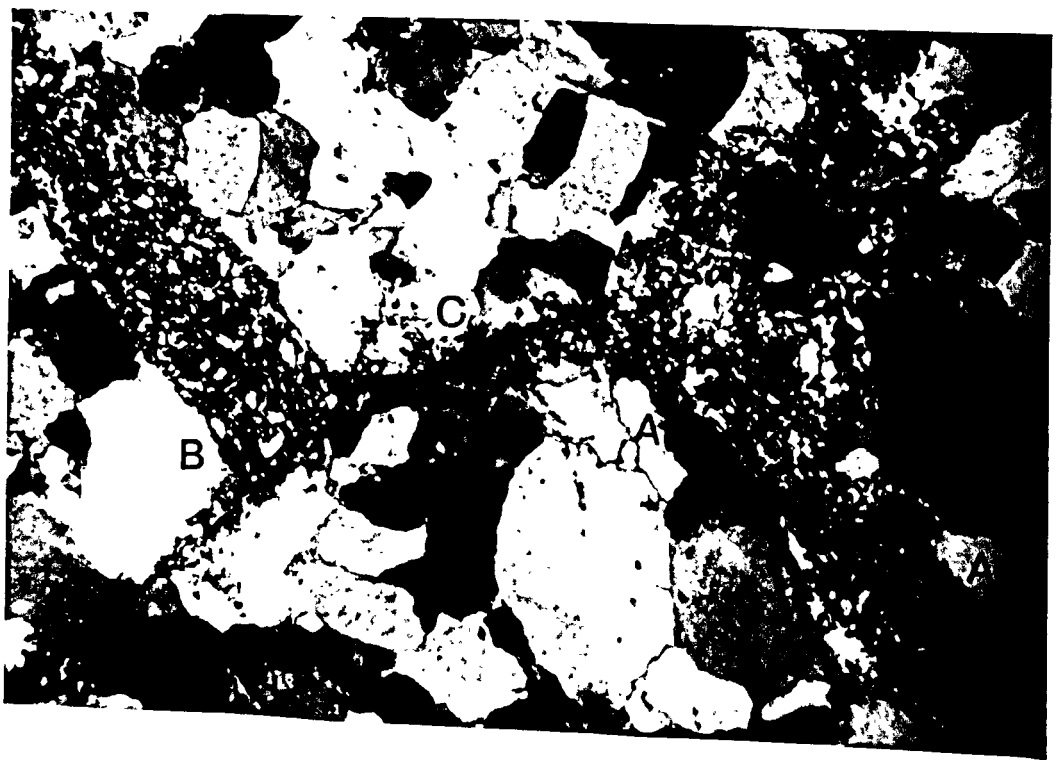

Figure 4.C.16. A photomicrograph of the cataclastic bands which affect the quartzites (s1) of the Ord Window. See text for further details. (1559A).

based on measurements from the mica rich areas of the thin sections and they are thought to be realistic. Since 90% of the grains in the thin sections are quartz there will be little ductility contrast present (Gay 1968a,b) and the strain estimates obtained will be reasonably accurate.

The common occurrence of undulose extinction, together with the limited development of deformation bands and subgrains suggests that the rocks have undergone little or no deformation and that the low finite strain reflects a lack of deformation rather than the end product of a complex strain path.

A further sample of quartzite was taken some distance from the fold. This specimen shows the strong development of a particular microstructure which may be seen in the specimens described above, but is not common. The microstructure is shown in Figure 4.C.16.. The structure is composed of bands up to 0.4mm wide with almost parallel sides. In general displacements across the bands are difficult to see, but in Figure 4.C.16. it is thought that grain A has been displaced by band B and band B has been displaced by band C. The bands appear to have undergone shear displacements. The quartz grains within the bands are fine grained and angular. Within a particular band a wide range of grain sizes may be seen but the grains are always much finer than those of the host. It is thought that these bands represent some form of cataclastic deformation involving the fracturing of grains. Often the bands thin and pass into discrete fracture surfaces with a single clean fracture surface. In contrast, the bands may widen and develop a median zone of fibrous or needle like quartz grains. The long axes of these grains lie at a high angle to the band boundary and appear to have grown on a free surface, see Figure 4.C.17.. It is thought that these areas represent dilation sites produced by displacements of the bands.

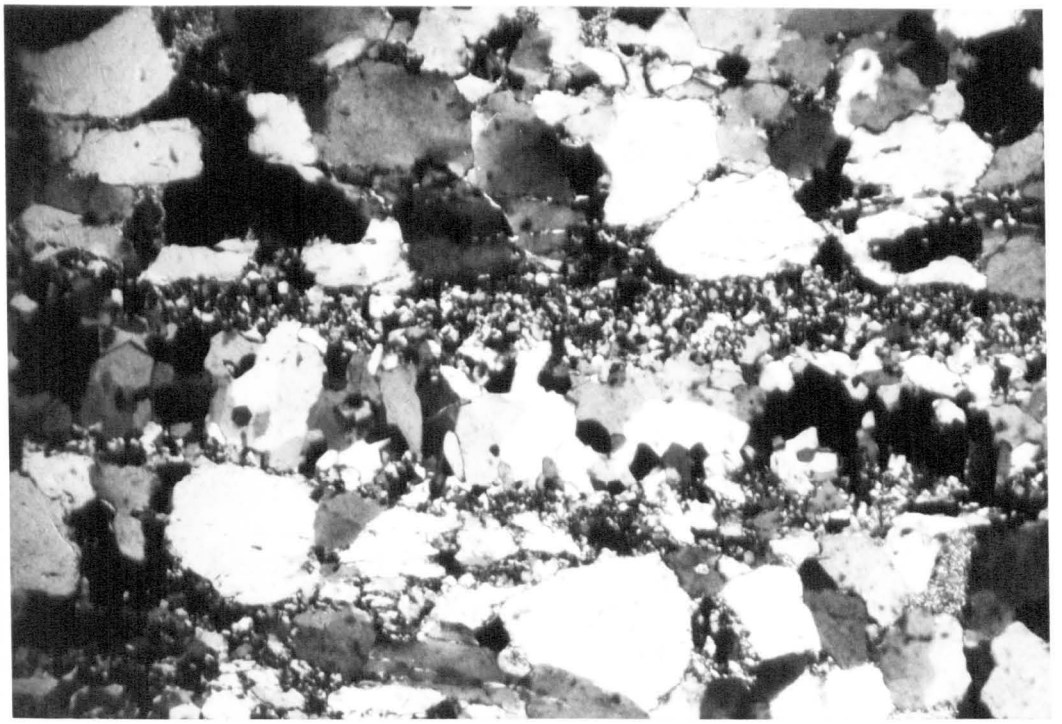

Figure 4.C.17. A photomicrograph showing a cataclastic band with well developed fibrous quartz grains at the centre of the band. (1559B).

It is possible that these structures represent some form of vein deformed by cataclastic deformation but this is unlikely,given the association of the bands with the fracture surfaces.

These cataclastic bands are common to all of the thin sections of quartzite studied from the Ord Window. The presence of cataclastic deformation is consistent with the large zones of breccia developed by the compartmental faults and the limited development of intracrystalline deformation microstructures. It is possible that these cataclastic bands allowed small displacements which were necessary for the continued development of the folds and that they represent an important deformation mechanism in the quartzites of the Ord Window. This may account for the low strains recorded by the pipes and the grains within the Pipe Rock Member.

Section 4D Finite Strains Related to the Minor Folds at Plockton and Port Cam

The occurrence of minor folds related to the Lochalsh Syncline is extremely limited and in the northern area these minor folds are of two types. To determine the distribution of strain in these contrasting fold profiles, samples were collected at various values of dip around the hinges of the minor folds at Plockton (NG 79903421) and Port Cam (NG 76853130). The results of these studies will now be described.

Results From the Minor Fold Near Plockton

At Plockton, the sampling was restricted in both number and the size of specimens to preserve the outcrop. The position of the samples around the fold is shown in Figure 4.D.1.. The orientation of the bedding and the results are given in table 4.D.1..

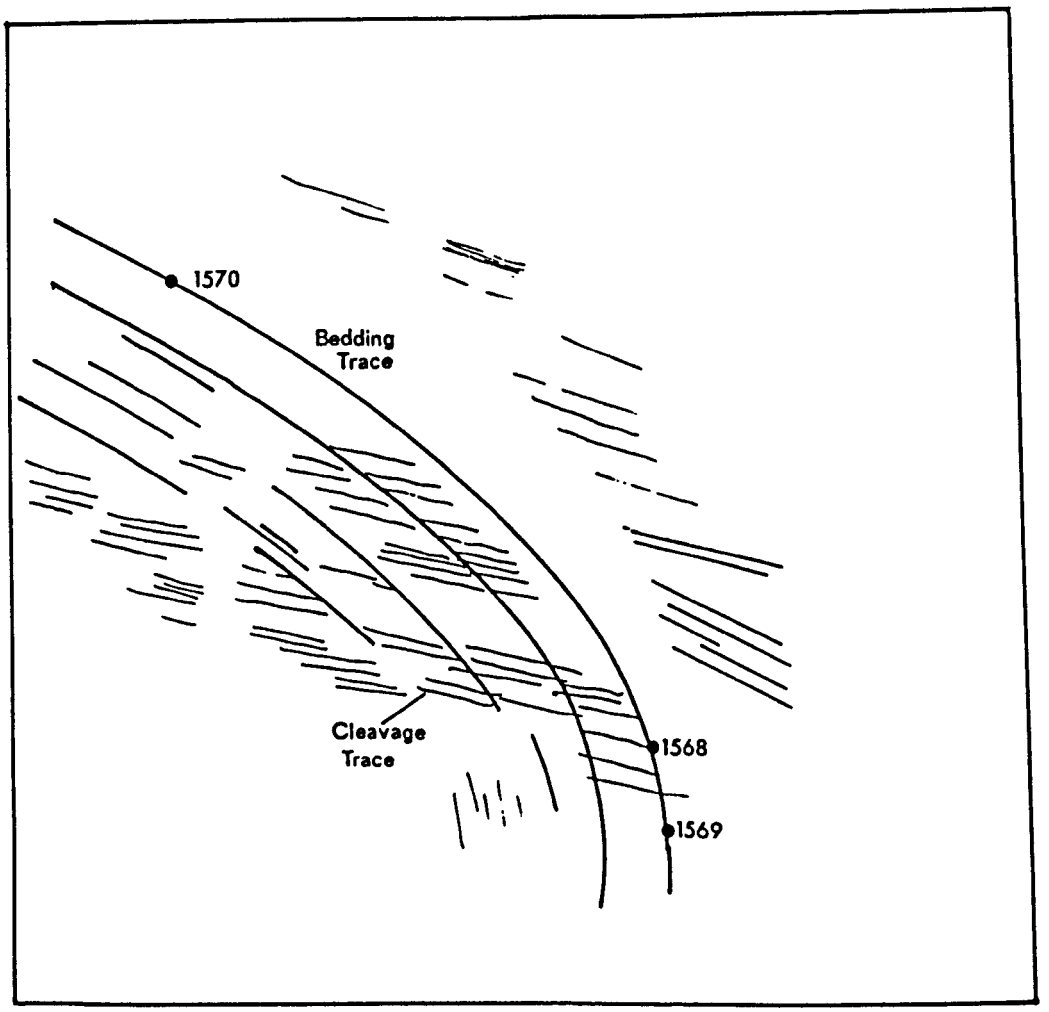

Figure 4.D.1. A sketch of the minor fold at NG 79905421 which is related to the Lochalsh Syncline. The position of the samples are shown together with the trace of the axial planar cleavage, which dips to the east.

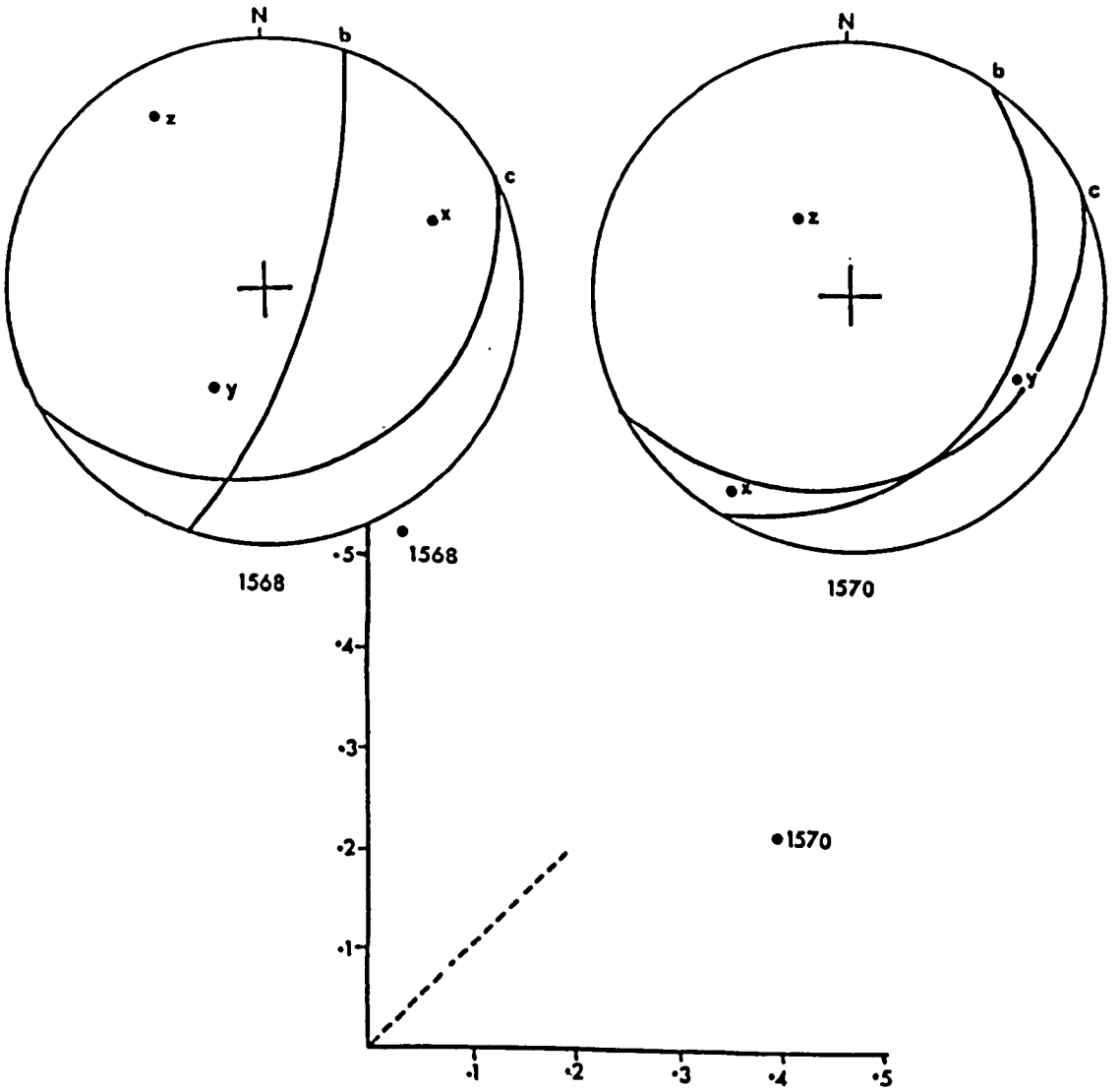

Figure 4.D.2. Stereograms showing the orientation of the finite strain axes and a Flinn plot showing the axial ratios of the finite strain ellipsoids for the specimens 1568 and 1570. b=bedding, c= axial planar cleavage.

Table 4.D.1.

Specimen	Orientation of bedding	Orientation of Strain Axes X, Y, Z.			Axial Ratio (ass no vol ch)			K
1568	015 76(i)	30/069	54/209	20/328	1.443	0.862	0.804	7.505
1570	033 34(i)	11/213	29/117	59/325	1.315	1.062	0.716	0.542

i = inverted bedding

For the specimens 1568 and 1570 three mutually perpendicular thin sections were prepared. However, due to problems of preparation only one thin section could be made from specimen 1569 and this was cut perpendicular to the cleavage and perpendicular to the fold axis. Tracings were made of each thin section and the axial ratios and orientations of the grains were obtained using the program ELLA FORTRAN. The strain ratio for each thin section was obtained using the program THETA FORTRAN (Peach and Lisle 1979). Despite the presence of the axial planar cleavage, this method was thought to be the most applicable, since undeformed sandstones from the Applecross Formation show a complete range of Ø values between 0 and 180 degrees. The two dimensional results from specimens 1568 and 1570 were combined into a strain ellipsoid using FITELI FORTRAN (Dayan 1981). No ellipsoid could be obtained for specimen 1569. The orientation of the ellipsoid axes are shown in Figure 4.D.2. and the axial ratios are shown on a Flinn plot (Flinn 1956, Ramsay 1967). For the specimen 1570 the X and Y axes of the strain ellipsoid lie on the cleavage plane and the Z axis of the strain ellipsoid lies at a small angle to the pole to the plane of the axial planar cleavage. In specimen 1568 the orientation of the strain ellipsoid is very similar but the X and Y axes do not lie on the cleavage plane. It is not known whether this discrepancy is real, or due to measurement errors and since these errors cannot be quantified, it is not possible to discriminate between the two. The errors in orientation will be ascribed entirely to measurement errors. On the basis of their orientation, the two strain ellipsoids appear to record finite strains due principally to the axial planar cleavage.

To determine the contribution made by the axial planar cleavage to the fold profile seen in Figure 4.D.1. the bedding around the fold was restored to its pre-strained

position using the techniques described by Ramsay (1967 p 129) for the restoration of planar features. In this case it is assumed that a portion of the fold development, entirely predates the cleavage and the results of the restoration will indicate how much of the fold development is due to tightening of the structure by the axial planar cleavage.

A comparable exercise was undertaken using the strain ratio determined for the single section cut from the specimen 1569. The section was cut perpendicular to the axial planar cleavage and in the constructions used, it was assumed to lie in the XZ plane of the finite strain ellipsoid. If this assumption is valid, then the bedding may be restored to its pre-strained position. Since only one plane has been used to obtain the strain ratio this particular result may be subject to large errors.

Figure 4.D.3. shows the finite strain axes and the present orientation of the bedding. Each stereogram shows the orientation of the restored bedding. It is clear that the finite strains due to the axial planar cleavage do not alter the orientations of the bedding to any great extent. A range of dip values were sampled and consequently the bedding makes a range of angles with the axes of the finite strain ellipsoids. Thus, the small angular changes seen during restoration are not due to the position of the bedding relative to the finite strain axes but due to the low strains related to the axial planar cleavage.

It may be concluded that the axial planar cleavage makes only a small contribution to the fold profile of the minor fold at Plockton. The orientation of the bedding around the fold owes little to the effect of the axial planar cleavage and a large component of flexural slip must be suggested for the development of

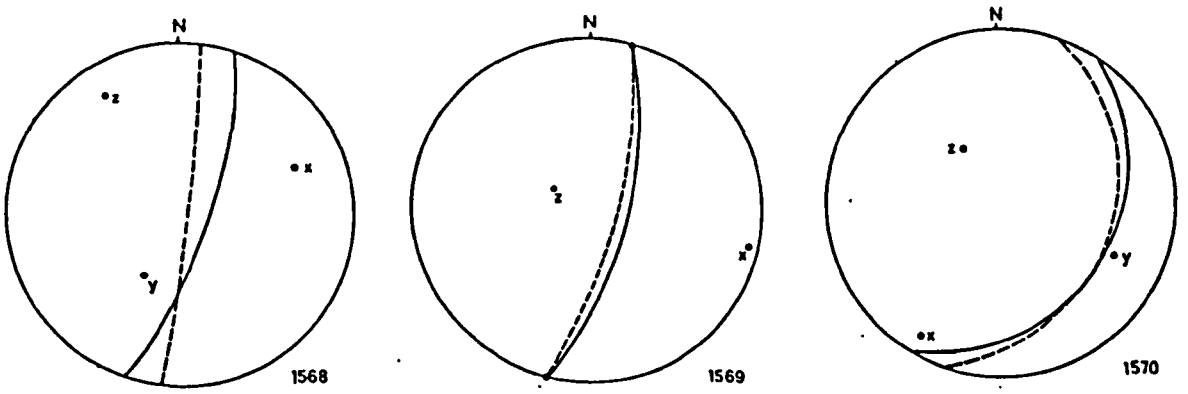

Figure 4.D.4. Stereograms showing the finite strain axes and the bedding around the minor fold at NG 79903421. The pecked great circle shows the position of the bedding after the removal of the finite strain determined from thin sections.

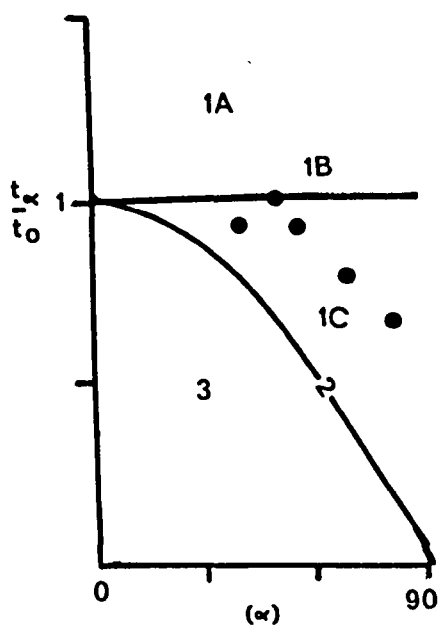

Figure 4.D.4. Measurements of tα/to against α from the fold at NG 79903421. Following Ramsay (1967 p359). The fold is of Class 1C.

the minor fold.

There are many sources of errors in this analysis. Errors in the original strain estimates, which cannot be quantified, will be passed into the subsequent calculations. Errors in the measurement of orientations will also increase the magnitude of the total errors. The method of restoration assumes that folding is followed by the axial planar cleavage and this is probably the largest source of error in the calculations. It is more likely that both processes operated together throughout most of the folds' development and that the contribution made to the reorientation of the bedding by the axial planar cleavage is much greater than that determined here. Without knowledge of the relative rates of the two processes it is not possible to quantify the contributions made by each process.

From the results presented here it is suggested that the minor fold at Plockton developed by flexural slip folding. The strains developed by the axial planar cleavage were necessary to relieve some of the congestion in the core of the fold and permit the folding to continue. The main contribution to the development of the fold was made by flexural slip processes and this is supported by measurements of bed thickness around the fold which are shown in Figure 4.D.4.. These measurements suggest that the fold at Plockton is a class 1C fold (Ramsay 1967) and this may be taken to indicate that flexural slip processes operated together with homogeneous flattening.

The sequence of flexural slip folding followed by homogeneous irrotational strain generates folds known as flattened parallel folds (Ramsay 1962). Such an origin for the folds at Plockton seems unlikely since a range of strain ellipsoids were obtained indicating heterogeneous rather than homogeneous strain. These

variations may be due to components of flexural flow or tangential longitudinal strain folding, but the small variations in bed thickness around the fold suggests that flexural slip folding was the dominant process.

To test this suggestion of flattened flexural folding, an orientated specimen was taken of a small parasitic minor fold. Several of these folds may be seen and these are related to the minor fold at Plockton. The fold profile is shown in Figure 4.D.5. and measurements of layer thickness and dip around the fold are shown in Figure 4.D.6.. The isogon pattern shown in Figure 4.D.5. is weakly convergent, typical of a 1C type of fold (Ramsay 1967). Flattened parallel folds show isogon patterns of type 1C which suggests that this fold may have been developed in this manner. However, it is clear from Figure 4.D.6. that the fold studied does not conform to a flattened parallel fold. The results obtained do not relate to any particular line on the graph (cf Ramsay 1962) and they tend to form two groups which indicate different amounts of strain for the limbs and the hinge of the fold. The stippled area in Figure 4.D.6. shows the range of strain values obtained from a thin section of the fold. The strain values were obtained using THETA FORTRAN. None of the data points lie within this region and therefore the model proposed of a parallel fold which has been flattened by homogeneous strain must be rejected.

The strains developed by the axial planar cleavage are heterogeneous and this may account for the two groups of data points seen in Figure 4.D.6.. In the thin section of the small fold the quartz and feldspar grains lie with their long axes close to the trace of the axial planar cleavage. There is a variation in axial ratios throughout the thin section but in general, the axial ratios tend to be larger towards the inner arc of the fold. This is reflected in the two strain values shown

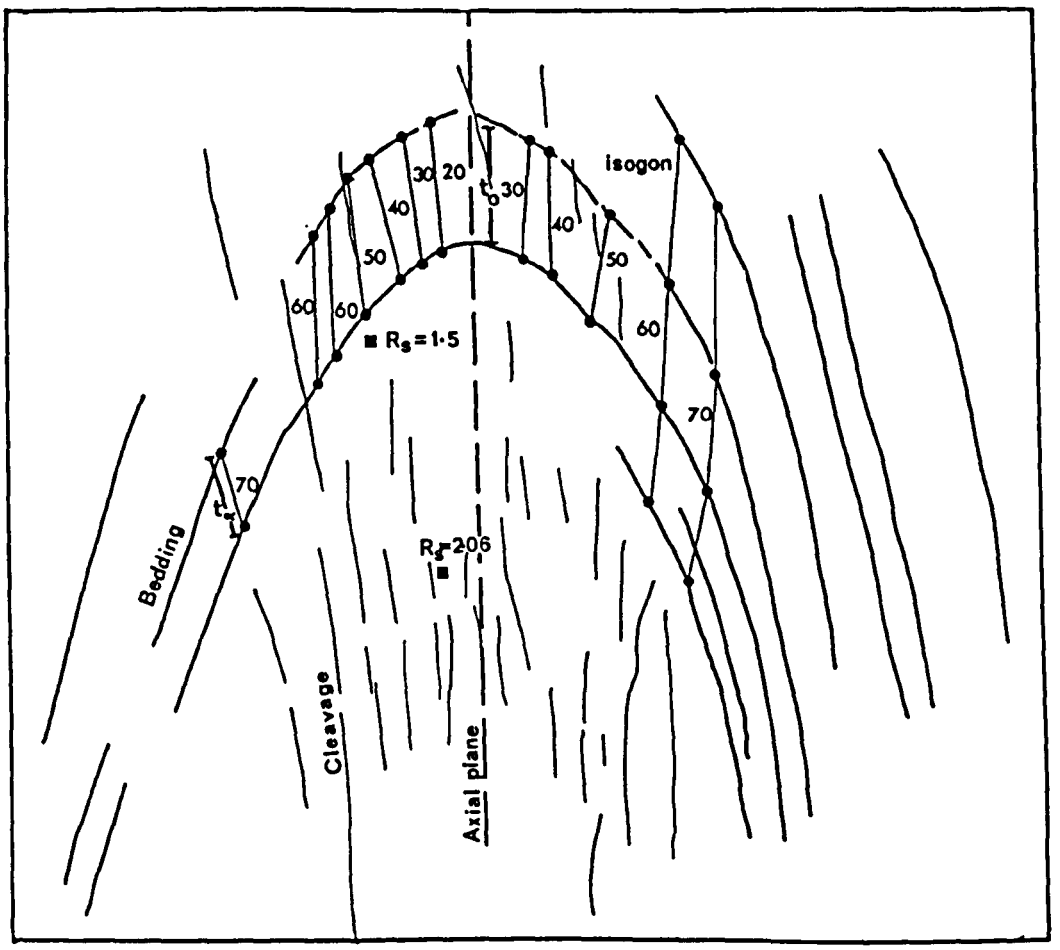

Figure 4.D.5. Profile of a minor fold related to the fold in Figure 4.D.1.. The limb length is approximately 15cms.

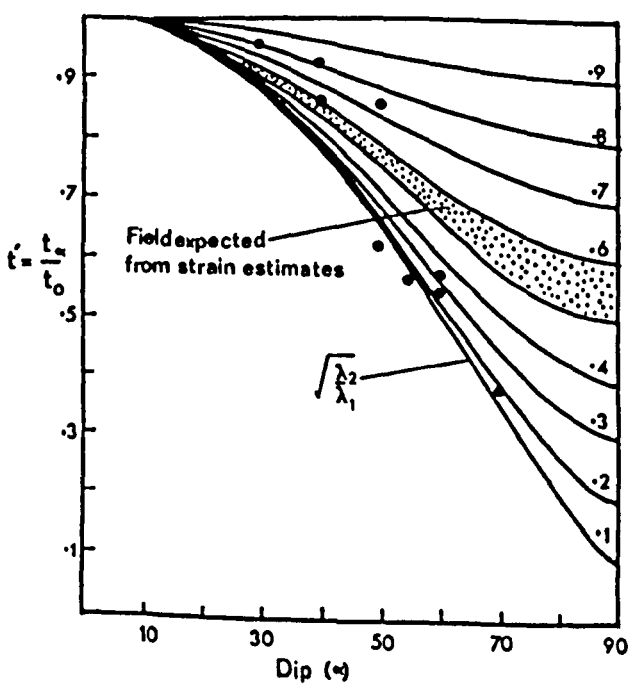

Figure 4.D.6. The results from Figure 4.D.5. plotted on a graph of tα/to vs.α . The curves of equal applied shortening are after Ramsay (1967). The stippled area marks the range of strains obtained from thin sections of the fold

in Figure 4.D.5.. There are always problems of strain heterogenity in grain shape studies but the variations described here appear to be systematic throughout the section. The distribution of strain in the minor fold suggests that the strain ratio increases towards the inner arc of the fold.

The minor folds seen near Plockton appear to have been developed by flexural slip folding and the development of the axial planar cleavage was necessary to permit the folding to continue. The strains related to the axial planar cleavage increase towards the inner arc of the fold suggesting that this cleavage may have developed to relieve congestion in the core of the fold.

Results From the Minor Fold at Port Cam

Several orientated samples were collected around the fold at Port Cam. From two of these samples thin sections were prepared. The sections were cut perpendicular to the cleavage and the axis of the fold. Tracings were made of the thin sections, and the axial ratios and orientations of the grains were obtained by using the program ELLA FORTRAN. Strain ratios were obtained using THETA FORTRAN (Peach and Lisle 1979).

As described in section 2C, two cleavages may be seen at this locality,these are the transverse cleavage and the axial planar cleavage. Figure 4.D.7. shows the orientation of the transverse cleavage. The axial planar cleavage has a much more shallow dip. The orientation of the long axis of the strain ellipse for each of the thin sections is shown in Figure 4.D.7.. These lie close to the trace of the transverse cleavage on the section planes. The long axes of the strain ellipses lie at a high angle to the bedding and at a small angle to the transverse cleavage. It is thought

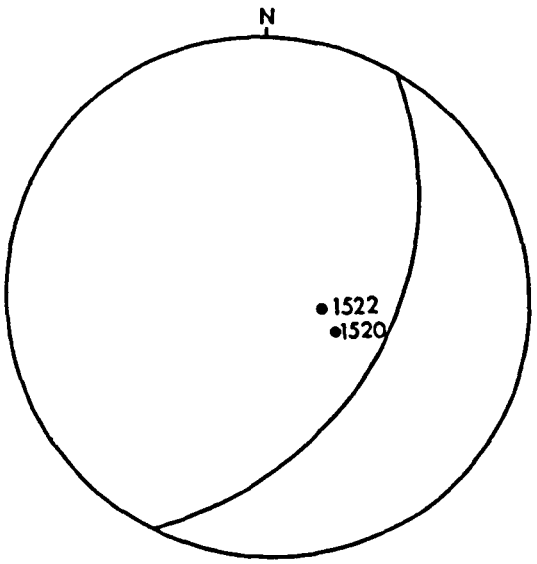

Figure 4.D.7. Stereogram showing the orientation of the transverse cleavage at Port Cam and the orientation of the long axes of the strain ellipses cut normal to the cleavage and the fold axis.

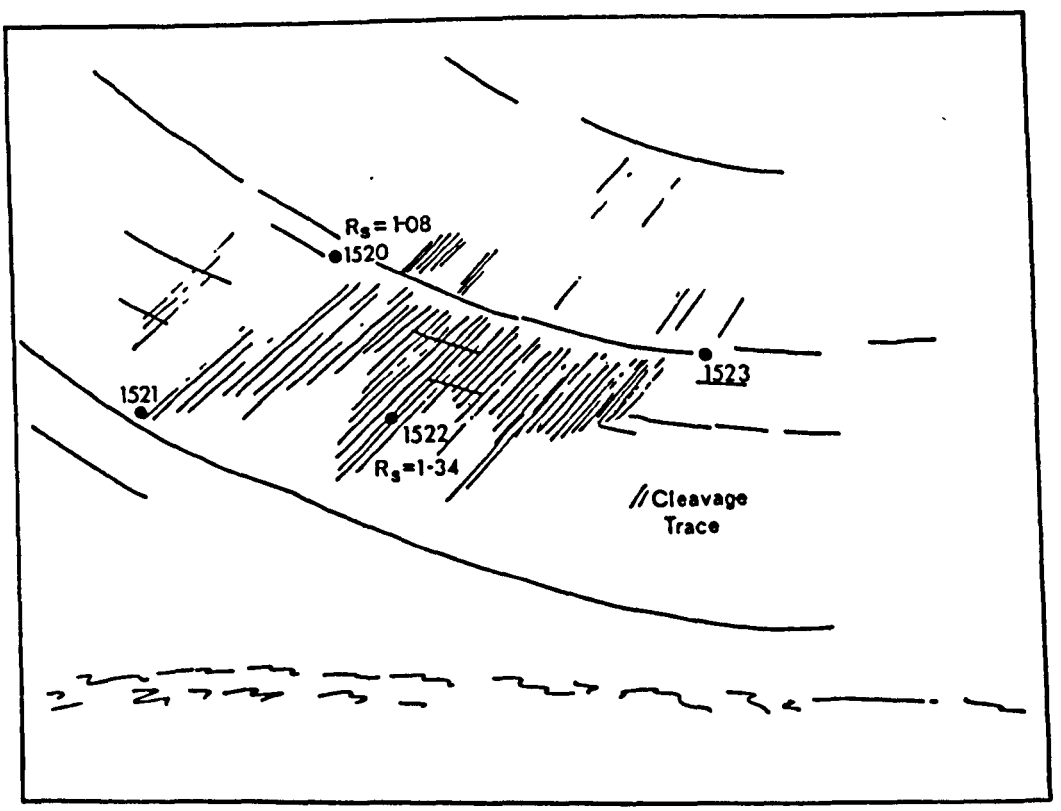

Figure 4.D.8. Sketch showing the fold profile at Port Cam and the position of samples collected from the fold.

that the finite strain in the thin section planes is dominated by the transverse cleavage. A contribution from the axial planar cleavage may be present, but no contribution could be resolved. The position and axial ratio of the strain determinations are shown in Figure 4.D.8.. These determinations may be compared with the models of Donath and Parker (1964) and Ramsay (1967) and such comparisons will now be discussed.

The model of Donath and Parker (1964) for the strains developed during flexural slip folding,assumes that the outer arc of the fold suffers extension and the inner surface remains unstrained. This may be modified so that the outer arc of the fold remains unstrained and the inner arc of the fold is shortened. The magnitude of the strains developed in these two cases is almost identical, obviously a range of possible cases exist with the above as end members.

At Port Cam the particular bed studied was 1.41 metres thick and the radius of curvature is thought to lie within the range 6.0 to 6.3 metres. Following the model of Donath and Parker (1964) these dimensions suggest an extension of 22% to 24% on the outer arc of the bed. Due to the extension in this model the strain ellipse should lie parallel to the bedding throughout the bed. However, it has been shown that the strain ellipses lie at a high angle to the bedding and this orientation is incompatible with the model suggested. In view of the orientations of the strain ellipses a situation of no strain on the outer arc of the fold may be more applicable, but as shown in Figure 4.D.8. the lowest strain was recorded on the inner arc, and it must be concluded that the model of Donath and Parker (1964) is inapplicable to the fold at Port Cam.

The model of Ramsay (1967) for the strain distribution

in a tangential longitudinal strain fold is more realistic. If we apply this model to the fold at Port Cam problems immediately arise. The point with the lowest strain lies on the upper surface of the bed and this must form the finite neutral surface of the fold. Therefore, the remainder of the bed must have suffered extension producing a range of strain ellipses with their long axes parallel to the bedding. Since the strain ellipse obtained from within the bed lies at a high angle to the bedding this model cannot be applied successfully.

In view of the close association between the long axes of the strain ellipses and the traces of the transverse cleavage on the planes sectioned, it is thought that the strains recorded around the fold at Port Cam are related to the transverse cleavage. Attempts to separate the component of strain related to the axial planar cleavage failed. Insufficient data is available to assess whether the folding and the axial planar cleavage make significant contributions to the finite strain recorded.

Chapter 5. Palaeomagnetic Studies In The Kishorn Nappe

Section 5A Review Of The Methods Used In This Palaeomagnetic Study

Palaeomagnetism is a method not commonly used in the study of geological structures. However, it is an extremely useful tool as palaeomagnetic directions can be considered as lineations and their behaviour during deformation studied accordingly. Palaeomagnetic studies on the Kishorn Nappe were undertaken for a number of reasons and these will now be described.

Ramsay (1969), in a discussion of strain and displacement in orogenic belts, described the importance of translation, strain and rotation in the development of natural structures. He concluded, that from geological data, translation is impossible to determine, strain may be determined with precision, and in bedded rocks, rotation may be approximated by restoring the bedding to the horizontal.

In favourable circumstances the large scale displacements or translations of major crustal blocks may be obtained from palaeomagnetic studies, for example the work of Grubbs and van der Voo (1976) and van der Voo and Channell (1980). However, it is doubtful that the displacement of nappes is of sufficient magnitude to be obtained from palaeomagnetic studies, even under the most favourable circumstances of translation direction. The crustal block or nappe must have a movement direction which, during translation, was oblique to the lines of latitude, as longitude is indeterminate in palaeomagnetic work. The higher the angle of the movement direction to the lines of palaeolatitude, the greater will be the accuracy of the method.

Palaeomagnetic directions are most useful in the study of

rotation. In bedded rocks palaeomagnetic studies provide a method of confirming the rotations indicated by the dip of the bedding and if remagnetization has occurred during the development of a structure then components of incremental rotation may be determined. For example, Creer (1962), Chamalaun (1964) and Chamalaun and Creer (1964) found that some of the sandstones of Pembrokeshire (South Wales) were remagnetized during the development of the folding. By restoring the palaeomagnetic directions around the fold it is possible to obtain an intermediate stage in the development of the fold. Since a variety of rocks are palaeomagnetically stable then it may be possible to estimate components of rotation, about axes of any orientation, in many of the structures developed in orogenic belts.

The use of lineations in the analysis of strain and rotation may be seen in a variety of examples such as Ramsay (1960, 1967) and Williams (1978). One of the advantages of lineations is their widespread distribution within an area studied and their contrasting behaviour around structures is extremely useful in the analysis of strain. The rocks of the Kishorn Nappe in common with other rocks of low metamorphic grade rarely have a visible lineation. Palaeomagnetic directions provide a lineation whose relationship to the structures may be studied. However, the palaeomagnetic directions may not act like true material lineations.

Torridonian magnetization directions were established on the Caledonian Foreland and it was the presence of these well defined directions which prompted the use of palaeomagnetism in this structural study. Two separate studies were undertaken. In the first of these, measurements were made to determine whether internal deformation was a significant process in the development

of the Eishort Anticline. Results in which the measured directions may be restored to a Torridonian position by application of the Graham Fold Test (Graham 1949) implies no strain. Results in which an angular correction is required for strain by the techniques described in Ramsay (1967) implies that internal deformation of the rock has occurred.

The second study was undertaken on the highly deformed basal conglomerates of the Sleat Group which are exposed in outcrops of the Epidotic Grit. The aim of this study was, using palaeomagnetic methods, to date the bedding parallel fabric which is strongly developed in these rocks. Samples of sandstone were also taken from Lochalsh to date both the bedding parallel fabric and the transverse cleavage. These attempts were unsuccessful. The basal conglomerates produced results which were unreliable and often unrepeatable in specimens of the same site. In contrast, the sandstones when deformed, have extremely weak magnetizations which could not be studied successfully with the equipment available. These results will not be presented in this thesis as no valid conclusions could be drawn.

The data from the study of the Eishort Anticline will be described in two stages: firstly, from a purely palaeomagnetic viewpoint and then how the results may be used in a structural analysis. The study will include a description of the remagnetization of the rocks by Tertiary thermal activity.

It must be emphasized at the outset that laboratory measurements provide a palaeomagnetic direction with coordinates of declination and inclination relative to the axes of the core. This direction may be corrected into geographical coordinates (an in situ direction) and then corrected for the dip of the bedding and the plunge

of the fold. The convention used in palaeomagnetism is that declination is measured in degrees to the east of north and inclination is measured in degrees from the horizontal, down being positive. Assuming that, at the time of magnetization the earth has a dipole field similar to the present field. Then, the palaeomagnetic direction may be used to determine a palaeomagnetic pole position relative to the sampling site. This palaeomagnetic pole position is in coordinates of latitude and longtitude. Geological evidence must be used to determine whether the in situ or the dip corrected palaeomagnetic direction is geologically the more significant.

Section 5B Practical Techniques

Conventional palaeomagnetic sampling using a portable rock drill proved unsuitable in this study. The time taken for sampling was too great and many of the critical areas were inaccessible carrying a rock drill.

At each site a minimum of three blocks were taken. A surface on each block was orientated, before removal, by means of a magnetic compass. Where possible the orientated surfaces were chosen to be as diverse as possible.

The blocks were drilled in the laboratory using a 2.54cm cylindrical drill and the cores obtained were sliced into lengths of 2.3 to 2.54 cms. using a diamond saw. The cores were sliced from the base upwards and any weathered material discarded. Each slice was numbered in the following manner, the block number, followed by a letter for the core and then a single digit recording the position of the slice within the core. The number (1) being the lowest in the core and by implication the least weathered. Generally three cores were drilled from each block so that for a site, a minimum of fifteen

measurements of the NRM could be made.

Assuming that the errors in orientating the surface of the block sampled are no greater than those in orientating a core drilled in the field, the main source of error in block sampling is in the assumption that the axis of the core is parallel to the pole of the orientated plane. In many cases this is not so. In this study the cores were accurately orientated by placing a pipe into the core hole and measuring the acute angles between the pipe and the directions of strike and dip. As shown in Figure 5.B.1. these measurements define two planes, the intersection of which is parallel to the core axis. The statistical precision (k) of the data for each site was improved by this method.

The cores were measured in a Digico fluxgate spinner magnetometer where the results are output as declination (D) and inclination (I) relative to the axes of the core. Facilities exist to reorientate this direction into geographical coordinates and where necessary this in situ direction may be corrected for the tilt of the bedding.

NRM's generally consist of several components; the measured NRM is the vector sum of these components. Thermal, and alternating field demagnetization techniques were used to isolate and characterise these components of magnetization. The general principles of demagnetization techniques may be obtained from McElhinny (1973) or Collinson et al (1967).

Thermal demagnetization was achieved by heating the specimens to successively higher temperatures and cooling in field free space. The earth's magnetic field was annulled by a system of Helmholtz coils. At the centre of the coils the field is close to zero and the

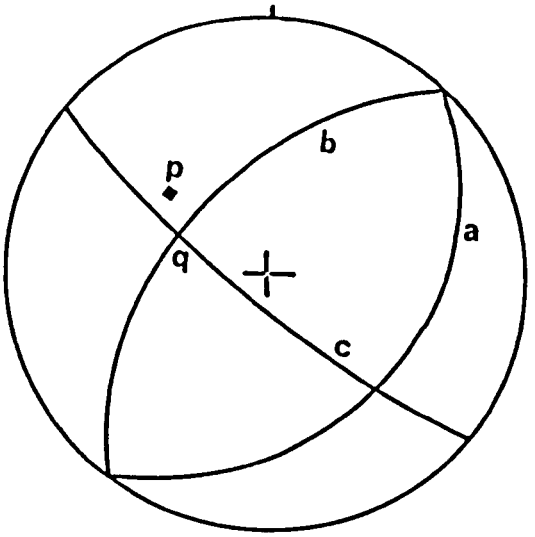

Figure 5.B.1. A stereogram showing the construction necessary to determine the orientation of a core drilled from a block sample. p=pole to the orientated plane a. Plane b includes the strike direction and the core. Plane c includes the dip direction and the core. Thus, the intersection of planes b and c is the true orientation of the core.

gradients extremely small. A furnace is situated at the centre of the coils and it is possible to reach temperatures up to a maximum of 700°C. Between each successive heating the specimens were remeasured in the magnetometer. The system used at Leeds University was described in detail by McClelland-Brown (1980).

Alternating field demagnetization was achieved by rotating the specimen in a two axis tumbler at the centre of a system of Helmholtz coils. An alternating field is applied to the tumbling specimen by means of a large coil. The field produced by this coil is increased to a peak, held for three seconds, and then decreased smoothly. Application of successively higher fields results in the progressive demagnetization of the specimen. A detailed description of the method used at Leeds University is given in Duff (1978).

The measurements obtained from thermal and alternating field demagnetization techniques were analysed using the following FORTRAN programs; DVEC1 (Foss 1981), ZPLOT (Turnell 1982), THPLOT (Turnell 1982), PREP (Turnell 1982) and XEQA10 (Clark pers com). These programs are essentially graphical routines for the rapid processing of data. The prgram DVEC1 FORTRAN uses the laws of vector addition to obtain the components of magnetization removed during successive cleaning steps. In this way, the methods of demagnetization described above were used to isolate and characterise the components of remanent magnetization present in the specimens and the results will be discussed, first in terms of these components and then the contribution which these components make to the NRM's measured.

Section 5C Palaeomagnetic Study Of The Sites Around The Eishort Anticline

In the field, the rocks of the Eishort Anticline show no

evidence of internal deformation. No cleavage or fabric is seen which may be related to this fold. In thin sections of the sandstones taken from around this fold few deformation microstructures are seen. However, in some of the siltstones and fine sandstones exposed in Tarskavaig Bay some evidence of internal deformation associated with the chevron folding may be seen (see chapter 3. section C). To determine the strain distribution and possible mechanisms of formation of the Eishort Anticline samples were collected for a palaeomagnetic study. The geometry of the Eishort Anticline is described in chapter 2. (section C). The fold lies in the southern area of the Kishorn Nappe and it involves rocks of the Kinloch Formation, the Applecross Formation and the Eriboll Sandstone. Samples were collected from both the Kinloch and the Applecross Formations. In this area the two formations may be transitional; they are certainly conformable and only the highest portions of the Kinloch Formation were sampled.

Palaeomagnetic directions in the Torridonian sequence were first described by Irving and Runcorn (1957) and later, these were refined by Stewart and Irving (1974). Recently, McClelland (1976) has presented a detailed study of the magneto-stratigraphy of the Applecross Formation on the hills of Mullach an Raithain and Spidean a Choire Leith. Possible origins of the magnetizations in the Torridonian sandstones were studied by Irving (1957), Stewart and Irving (1974) and McClelland (1976).

Irving and Runcorn (1957) obtained a series of directions which are given in Table 5.C.1.. Using thermal and alternating field demagnetization Stewart and Irving (1974) were able to refine these results. Both studies were on samples taken from the Caledonian Foreland where the Torridonian rests unconformably on the Lewisian

Table 5.C.1.

Rock unit	Polarity	D	I	N (R)	κ	α_{95}
Torridon Group	N	294	-28	28(25.14)	9	9
Torridon Group	R	129	51	53(49.45)	15	5
Stoer Group	N	307	34	13(12.70)	40	7

Table 5.C.2

Stoer Group

Locality	Cleaned/ Uncleaned	N	R	D	I
Stoer Bay	500° C	16	15.11	315	+27
Stoer Bay	NRM	16	14.88	319	+24
Achiltibuie	500° C	16	15.47	307	+33
Achiltibuie	NRM	16	16.15	310	+37
Enard Bay	500° C	2	1.98	292	+49
Enard Bay	NRM	2	1.99	291	+57
Rubha Reidh	500° C	3	2.67	305	+42
Rubha Reidh	NRM	3	2.71	302	+50

Torridon Group (basal)

Enard Bay	500° C	6	5.79	132	+75
Enard Bay	NRM	6	5.85	106	+83
Achiltibuie	500° C	3	2.75	097	+38
Achiltibuie	NRM	3	2.77	095	+45
Rubha Reidh	500° C	2	1.95	091	+49
Rubha Reidh	NRM	2	1.97	096	+56

Table 5.C.3.

Rock unit	Polarity	D	I	N (R)	κ	α_{95}	Treatment
Basal Torridon Group	R	099	73	11(10.42)	17	11	NRM
Basal Torridon Group	R	106	61	11(9.95)	10	16	500°C
Stoer Group	N	316	28	20(18.66)	14	9	NRM
Stoer Group	N	313	29	20(18.95)	18	8	500°C

Gneiss. The bedding is gently folded by very open folds which are thought to be of Caledonian age (Peach et al 1907). The results presented here represent the first attempt to study the palaeomagnetism of rocks within the Moine Thrust Zone.

Stewart and Irving (1974) presented a series of mean directions following the method described by McElhinny (1967). Individual measurements were combined into site means. These site means were combined to give locality mean directions and these in turn are combined to give formation mean directions. The locality means obtained by Stewart and Irving (1974) are given in Table 5.C.2.. The original results of Irving and Runcorn (1957) are very close to those of Stewart and Irving (1974) the latter having the benefit of demagnetization techniques. The formation means obtained from these pieces of work are given in Table 5.C.3..

Using alternating field demagnetization techniques McClelland (1976) was able to identify, after cleaning, both normal and reverse sites within the Applecross Formation and obtain the following formation means;

Reversed	D = 108.0	I = 51.4
Normal	D = 311.5	I = -29.2

which are very similar to those of Irving and Runcorn (1957) and Stewart and Irving (1974).

The results of Irving and Runcorn (1957), Stewart and Irving (1974) and McClelland (1976) are shown in Figure 5.C.1.. The directions obtained in this study from the Applecross Formation around the Eishort Anticline will be compared with these results.

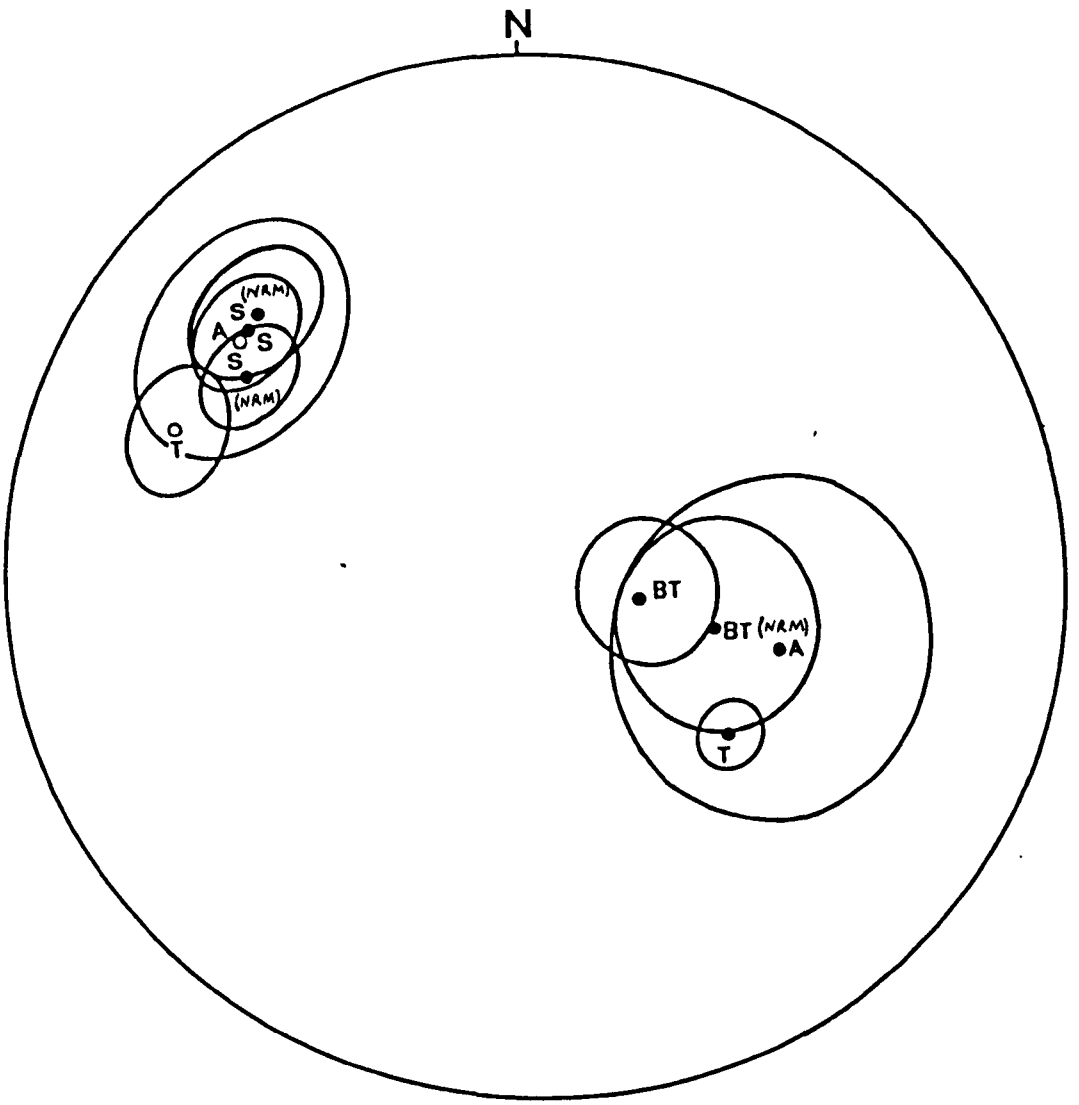

Figure 5.C.1. Stereogram showing the formation mean directions obtained by previous workers from the Torridonian of the Foreland. S-Stoer Group (Stewart and Irving, 1974 and Irving and Runcorn 1957) T-Torridon Group (Irving and Runcorn) BT-Basal Torridon Group (Stewart and Irving) A-Applecross Formation (McClelland 1976).

Sites Around The Eishort Anticline Which Show Only Torridonian Components

The sites sampled around the Eishort Anticline are shown in Figures 5.C.2. and 5.C.3.. Sites 1,22,21,20,19,18 and 17 lie on the common, correct way up limb, between the Lochalsh Syncline and the Eishort Anticline (Figure 5.C.2.). Sites 7,8,11,12,13,14,32 and 33 lie in the hinge of the Eishort Anticline (Figure 5.C.3.). Site 15 is from within the Ord Window. The NRM's of sites 7,9,11 and 14 were extremely low, less than 1.0 emu/cc.10^{-6} and no consistent direction could be obtained for these sites using the Digico spinner magnetometer. No further palaeomagnetic work was attempted on these four sites.

The sites around the Eishort Anticline may be divided into three groups on their behaviour during demagnetization by both thermal and alternating field techniques. The behaviour of the samples will be described in terms of demagnetization curves and ranges of blocking temperature and coercivity. A demagnetization curve is a graph of normalised intensity of magnetization against peak temperature or peak demagnetizing field. At each step the intensity of the magnetization remaining is normalised by the intensity of the NRM

$$M_n = M/M_o$$

A rapid decline of the curve shows that a large proportion of the NRM has been removed over those demagnetizing steps. A more gradual decline shows that little or none of the magnetization has been removed. The presence of multi-component magnetizations distorts the shapes of the curves. Demagnetization curves indicate the ranges over which significant portions of the magnetization are removed, thus

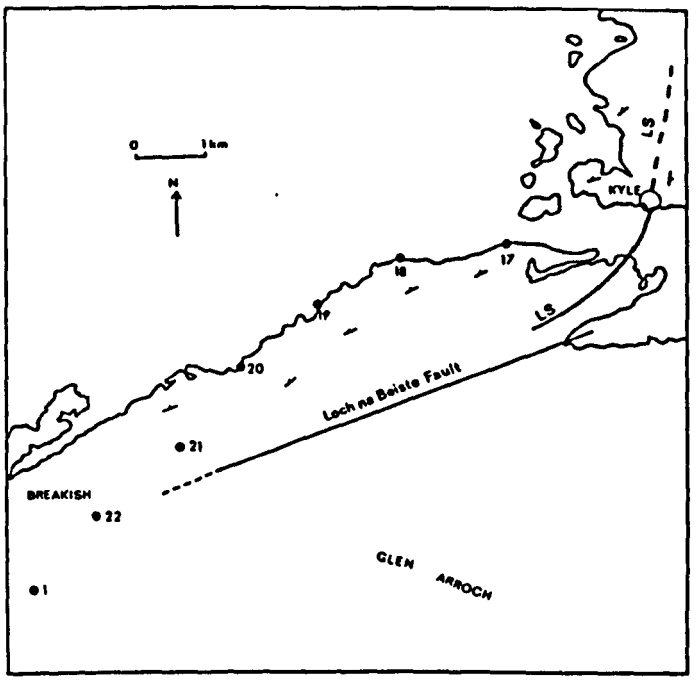

Figure 5.C.2. Map of northern Sleat showing the position of sampling sites on the correct way up limb between the Lochalsh Syncline and the Eishort Anticline. LS - Axial trace of the Lochalsh Syncline.

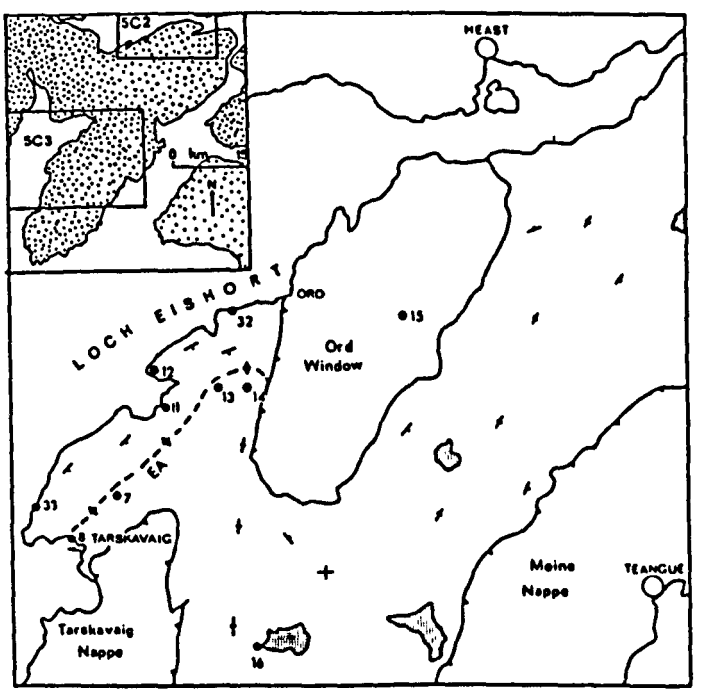

Figure 5.C.3. Map of southern Sleat showing the position of the sampling sites around the Eishort Anticline (EA). The inset map shows the relative position of the two areas.

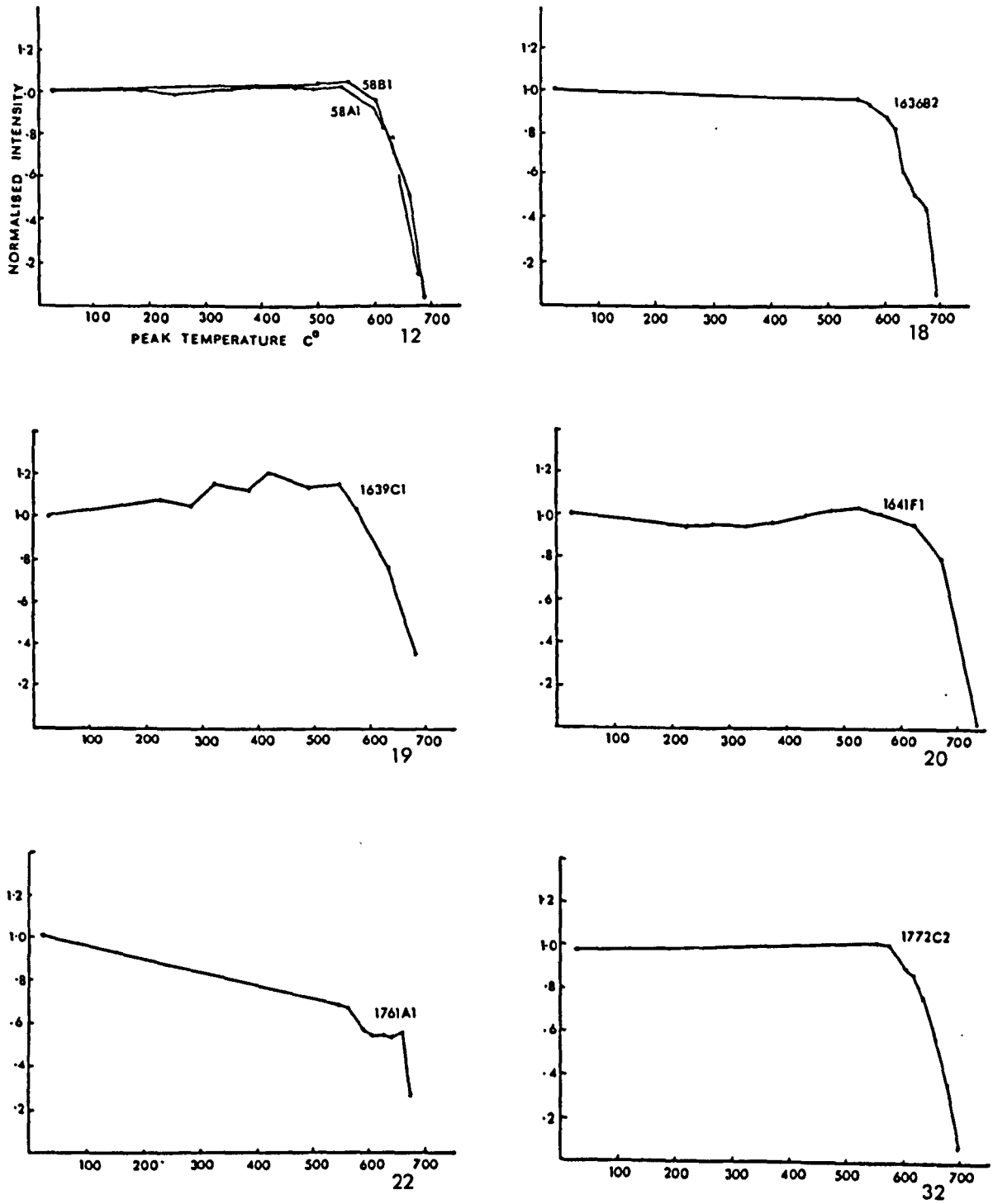

Figure 5.C.4. Series of demagnetization curves which are typical of sites 12-32 during thermal demagnetization. The curves are plots of normalized intensity (Mn) against peak furnace temperature at each step. The furnace temperature is given in degrees centigrade. These axes will be used throughout this chapter but will not be labelled again.

indicating the presence of grains with those particular blocking temperatures or coercivities.

Figure 5.C.4. shows some of the demagnetization curves obtained from specimens of the sites 12,18.19,20, 22 and 32 during progressive stepwise thermal demagnetization. They are typical of the results from this group of sites and many results have not been included. At low blocking temperatures the curves are flat which suggests that little or none of the magnetization has been removed over that particular range of blocking temperatures. At approximately 550°C the curves begin to decay. Initially, this decay is gradual which suggests that only a small portion of the NRM is removed in each step. Within the range 650 to 700°C the decay is extremely rapid which shows that a large proportion of the magnetization has been removed in that step. Many blocking temperatures were seen above the Curie point of haematite.

Progressive stepwise thermal demagnetization shows that sites of this group have extremely limited ranges of blocking temperature. Generally, these are in the range 550 to 695°C but blocking temperatures within the range 650 to 685°C dominate the NRM. During thermal demagnetization the direction of magnetization remains stationary (see Figure 5.C.5.). At low blocking temperatures, this because little or no magnetization is removed. At higher blocking temperatures where significant amounts of the NRM are removed the directions still remain stationary and this suggests that the NRM is composed of only one component of magnetization.

Figure 5.C.6. shows the demagnetization curves of several specimens from the above mentioned sites

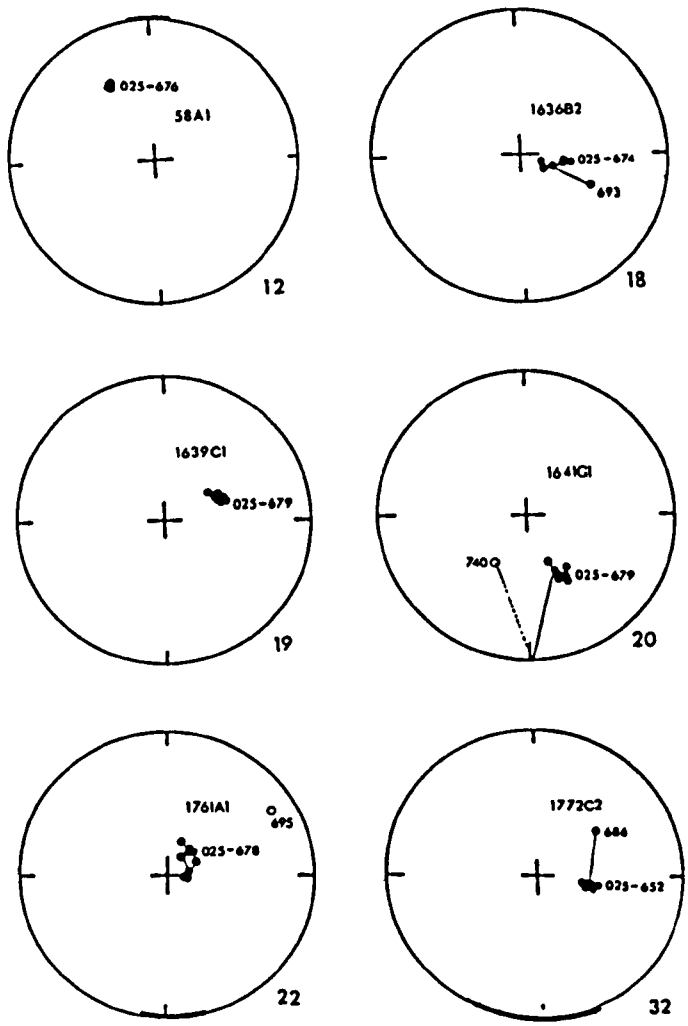

Figure 5.C.5. The orientations of the directions of magnetization (dip corrected) during thermal demagnetization of some of the sites around the Eishort Anticline. The results shown are typical of these sites and the samples chosen correspond with those of Figure 5.C.4.. Where possible each step of the demagnetization is labelled in degrees centigrade. Closed symbols indicate positive inclinations which plot in the lower hemisphere of the stereogram.

around the Eishort Anticline, during progressive alternating field demagnetization. The curves show little or no decrease in the intensity of magnetization up to a peak field of 200 mT (which is the greatest field attainable with the equipment available at Leeds University). The specimens are unaffected by this method of demagnetization at the fields applied and in general are thought to have coercivities greater than 200 mT. During alternating field demagnetization the directions remain stationary since little or none of the NRM has been removed (see Figure 5.C.7.).

Results from progressive demagnetization may be illustrated on orthogonal projections or Zijderfeld diagrams (Zijderfeld 1967). On this type of diagram the directions of magnetization, after each step, are projected on to two orthogonal planes (hence the two curves). The NRM direction lies at the periphery of the diagram and with progressive demagnetization the resultant direction moves towards the origin. Components of magnetization can be isolated from these curves as they form linear segments. Multi-component NRM's are indicated by two or more linear segments. If two components are removed together the results lie on a curved track.

Typical results obtained for these sites from around the Eishort Anticline are shown on Zijderfeld diagrams in Figure 5.C.8.. At low blocking temperatures, during thermal demagnetization the position of the magnetization does not change. At higher blocking temperatures (greater than 500^{o}C) the position of the results moves along a straight line to the origin of the diagram. This indicates that a single high blocking temperature component is present. In contrast, no such movement is seen during alternating field demagnetization and the position of the results on the diagram does not change. These diagrams illustrate clearly the contrasting

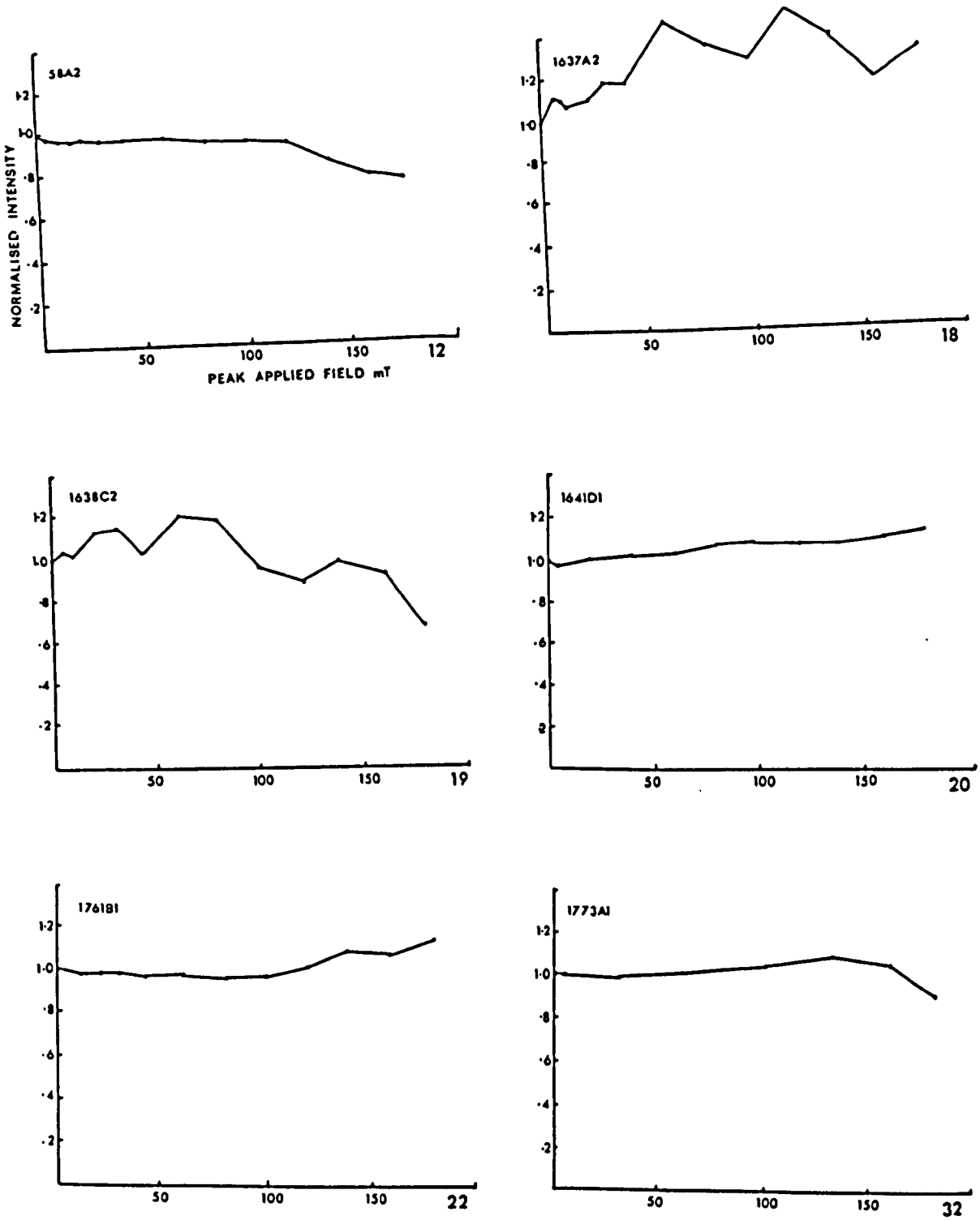

Figure 5.C.6. A series of demagnetization curves obtained from sites 12,18,19,20,22 and 32 from around the Eishort Anticline during alternating field demagnetization. The axes of normalised intensity against peak applied demagnetizing field will be used throughout this chapter. The peak field is given in milliTesla (mT) and will not be labelled again. The site number is given in the diagram.

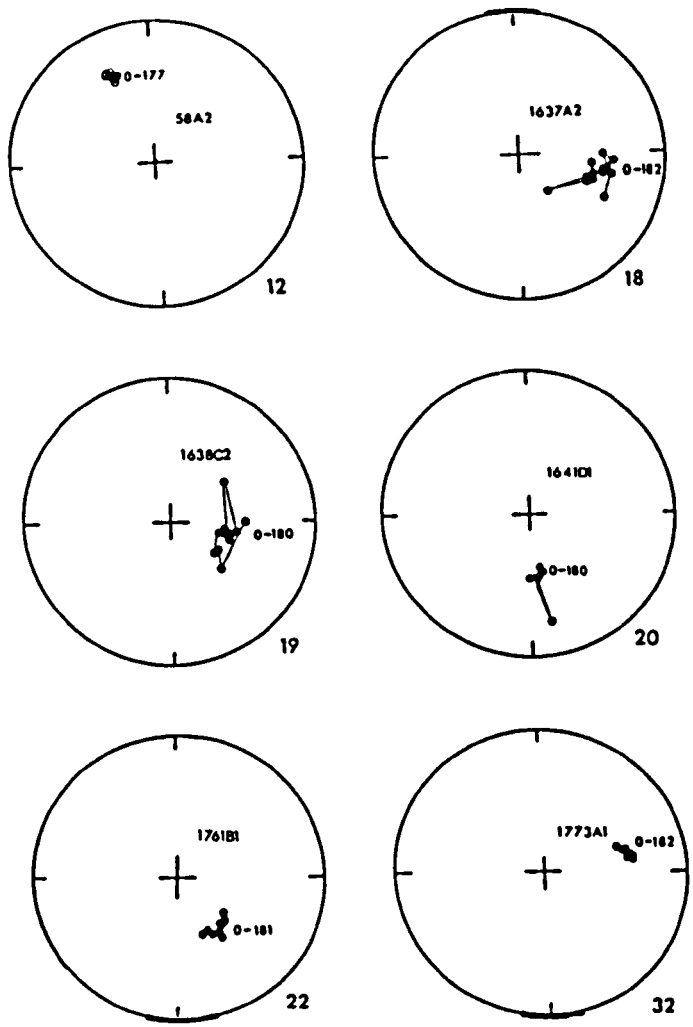

Figure 5.C.7. The orientation of the directions of magnetization (dip corrected) during alternating field demagnetization. These results are typical of these sites and the samples chosen correspond with those of Figure 5.C.6.. Where possible each step is labelled in mT corresponding to the peak applied demagnetization field.

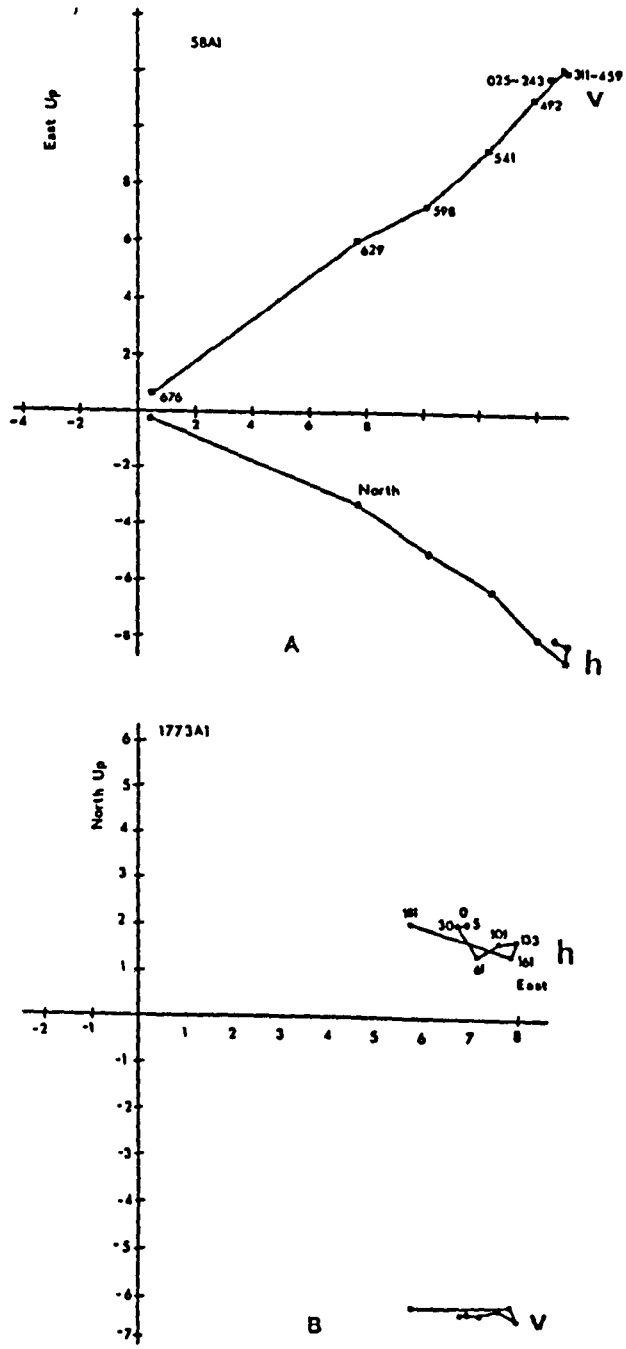

Figure 5.C.8.A. A Zijderfeld diagram(dip corrected) of specimen 58A1 during thermal demagnetization (see Figures 5.C.4. and 5.C.5. for corresponding information). Each step is labelled with the peak furnace temperature in degrees centigrade. This practice is followed throughout this chapter.

B. A Zijderfeld diagram (dip corrected) of specimen 1773A1 during alternating field demagnetization. (See Figures 5.C.6. and 5.C.7. for corresponding information). Each step is labelled with the peak applied demagnetization field in milliTesla. This practice is followed throughout this chapter.

behaviour of these specimens during thermal and alternating field demagnetization.

In Table 5.C.4. the grid reference, dip of the bedding, blocking temperature and peak alternating field results are given for the sites studied. The dip corrected directions are given for the components of magnetization islolated during cleaning together with relevant statistics (Fisher 1953). The direction results (dip corrected) are shown in Figure 5.C.5.. Several of the specimens studied deviate slightly from these results and these will now be described.

The thermal demagnetization curves of specimens 59A2, 59C1 and 59C2 are shown in Figure 5.C.9. together with the alternating field demagnetization curves of 59A1. They show a marked contrast to the rest of the samples from site 12 (compare Figures 5.C.9. and 5.C.5.). As shown in Figure 5.C.10. these specimens have NRM directions which are different from the rest of the site.

The demagnetization curves indicate the presence of grains with blocking temperatures of less than 570^{o}C and grains of low coercivity. Below 570^{o}C the directions of demagnetization remain almost stationary (see Figure 5.C.11.). Above this blocking temperature the directions move to a second distinct direction. This movement is thought to indicate the presence of two components of magnetization. A similar movement is recorded during alternating field demagnetization, but this is not as distinct (see Figure 5.C.11.).

When dip corrected, the high blocking temperature components correspond well with the rest of the site and they are thought to represent a comparable direction. The low blocking temperature component, when dip corrected, is almost anti-parallel to the remainder of

Table 5.C.4.

Site No.	Grid Reference	Dip of Bedding	Blocking Temperature Range °C	Coercivity Range mT	Orientation D	Orientation I	N	R	κ	α_{95}
12	NG 59751200	229 142	495 - 690	>100	332.1	-45.3	9	8.65	23.0	9.7
18	NG 72722645	235 27	554 -684	>180	100.4	72.6	11	10.67	30.5	7.6
19	NG 71472581	235 25	590 - 683	>160	092.4	65.5	8	7.43	12.3	14.1
20	NG 70412494	230 21	624 - 679	0-5>180	175.1	59.8	11	9.53	6.8	16.2
21	NG 69502378	230 36	593 - 683	>180	137.1	78.1	9	8.78	35.7	7.8
22	NG 68232282	238 20	560 - 683	>180	078.5	77.2	7	6.45	10.9	16.0
32	NG 60701290	278 159	620 - 683	>160	122.5	47.9	5	4.44	7.1	23.5

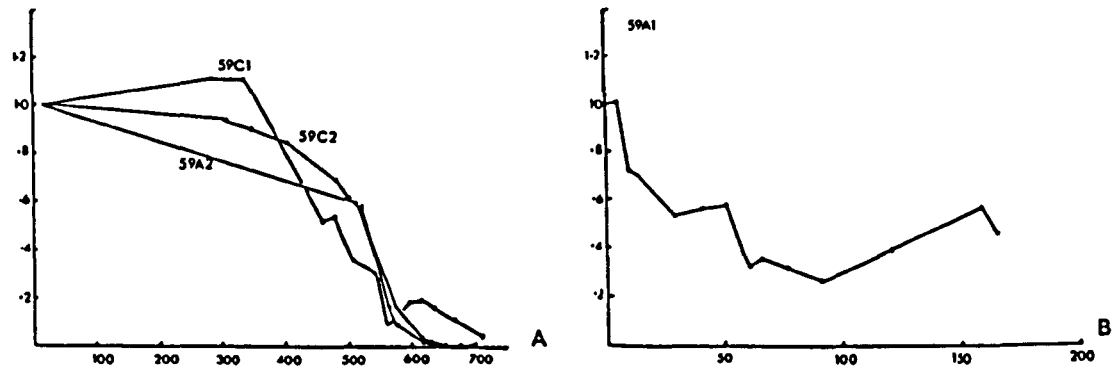

Figure 5.C.9.A. Thermal demagnetization curves of specimens 59A2, 59C1 and 59C2 from site 12. B. Demagnetization curve obtained from specimen 59A1 during alternating field demagnetization.

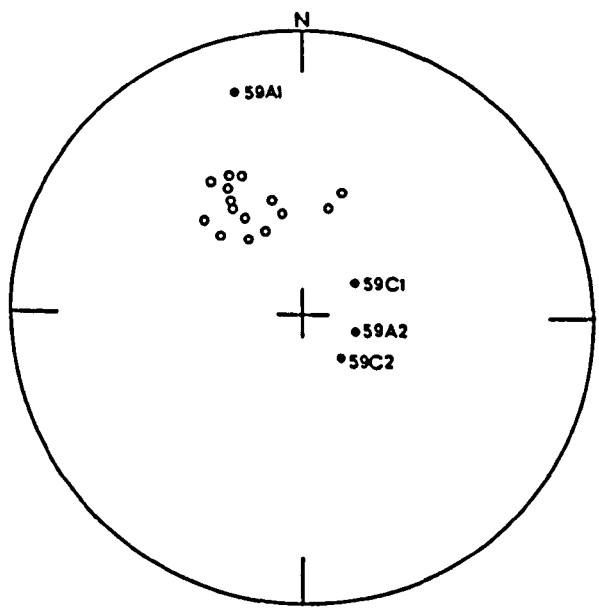

Figure 5.C.10. The NRM directions (dip corrected) of site 12. The contrast between sample 59 and the rest of the group is clearly seen. The standard palaeomagnetic convention is followed and thus results from sample 59 tend to plot in the lower hemisphere.

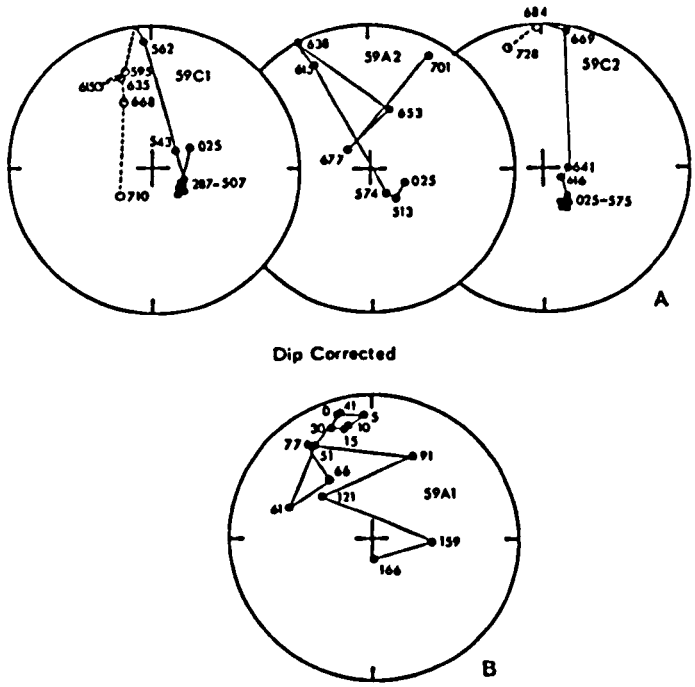

Figure 5.C.11. The orientation of the direction of magnetization (dip corrected) during both thermal (A) and alternating field demagnetization (B) of specimens 59A2, 59C1, 59C2 and 59A1. See Figure 5.C.9..

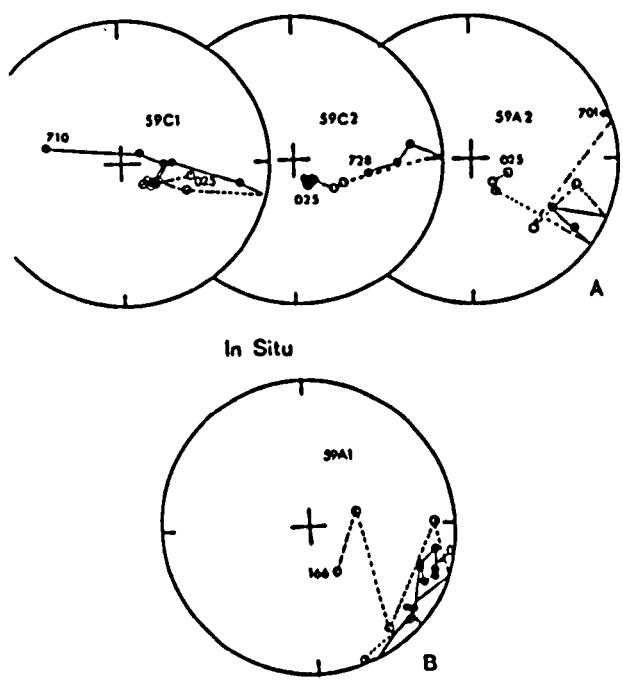

Figure 5.C.12. The In Situ orientation of the direction of magnetization during thermal (A) and alternating field (B) demagnetization. See Figure 5.C.11. and 5.C.9.

of the site and may represent an opposite polarity of the same field. However, when in situ (Figure 5.C.12.) the low blocking temperature component is parallel to reversed Tertiary directions which will be discussed later. Details of the low blocking temperature component are given in Table 5.C.5..

Viscous Remanent Magnetizations (VRM) are low blocking temperature, and often low coercivity, magnetizations present in rocks where the direction of magnetization is parallel to the earth's present field. A VRM arises from the thermal fluctuation of the grains and the physical theory was described by Neel (1955). A VRM is seen in three specimens from site 21. The remaining sites in this group show no evidence of a VRM.

In site 21 the demagnetization curves for the samples 1764 and 1765 are very similar to the rest of the group (Figure 5.C.13.) and show a restricted range of blocking temperatures between 550 and 690^{o}C. However, in specimens 1763A1,1963A2 and 1763B2 demagnetization occurs at much lower blocking temperatures. Removed vector analysis (Foss 1981) was used to isolate this low blocking temperature component and it was found to be, when in situ, parallel to the earth's present field (Figure 5.C.14.). The result is most marked in specimen 1763A2 where the NRM is parallel to the earth's present field. In this case the NRM is dominated by a VRM of low blocking temperature and high coercivity. The ranges of this VRM are given in Table 5.C.5. together with relevant orientation data.

In the remainder of the specimens from this site the NRM is composed of the high blocking temperature component described earlier. On specimens from site 21 alternating field demagnetization techniques are ineffective. As shown in Figure 5.C.15. the direction of magnetization remains stationary and the demagnetization curves show no decrease over the entire procedure.

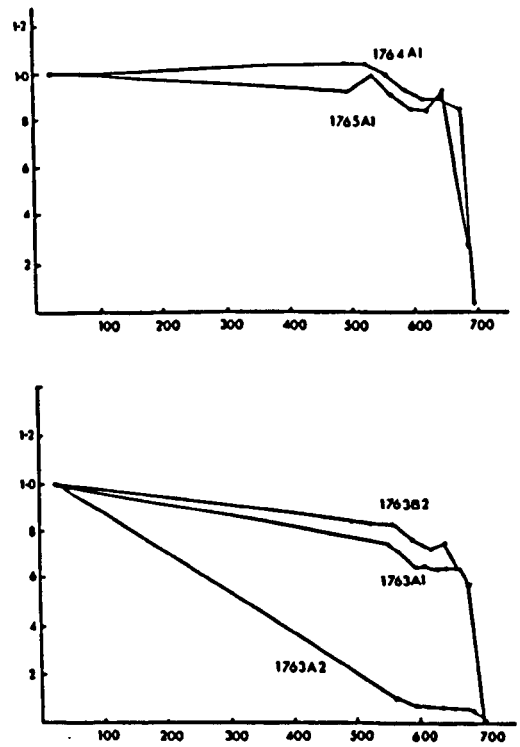

Figure 5.C.13. Thermal demagnetization curves of specimens form site 21. The curves of specimens 1764 and 1765 correspond with the rest of the group and contrast with those of specimen 1763.

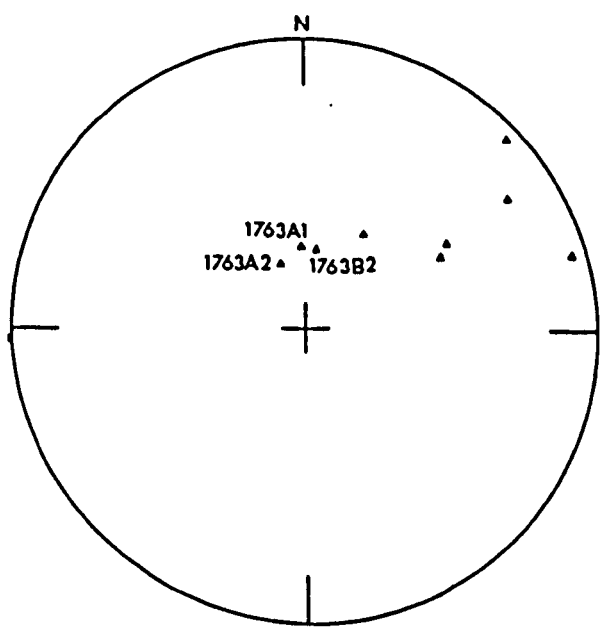

Figure 5.C.14. The In Situ orientation of the removed vectors from site 21 which were isolated during the first step of thermal demagnetization.

The specimens 1772B2, 1772D1 and 1774D1, unlike the rest of site 32, plot in the northeast negative quadrant (dip corrected, see Figure 5.C.16). During thermal demagnetization of these specimens the resultant direction tends to remain in the same quadrant (see Figure 5.C.17.). The thermal demagnetization curves of these particular specimens cannot be distinguished from the rest of site 32 and indicate a comparable range of blocking temperatures. The lack of movement of the resultant direction during thermal demagnetization of these specimens suggests that only one component of magnetization is present in these three specimens. The two polarities present in this group of sites cannot be combined in any way using the laws of vector addition to produce a resultant direction which lies in the northeast negative quadrant and therefore, a single component of unknown origin must be present in the specimens 1772B2, 1772D1 and 1774D1 of site 32. Both the in situ and the dip corrected orientations of this component have no known geological significance and they are given in Table 5.C.5..

The behaviour of specimens from site 22 during both thermal and alternating field demagnetization is similar to the rest of the sites in this group. Thermal demagnetization indicates the presence of a single high blocking temperature component and in general, alternating field demagnetization is ineffective. Two of the specimens from this site, 1761A2 and 1760B2 show contrasting results during thermal demagnetization. The demagnetization curves for these two specimens are indistinguishable from the rest of the site (see Figures 5.C.4. and 5.C.18.). Using removed vector analysis (Foss 1981) it was not possible to isolate any directions which, in situ or dip corrected, could be related to the geological history of the rocks and therefore these two results were dicarded from subsequent analyses.

Table 5.C.5.

Site No.	Grid Reference	Dip of Bedding	Blocking Temperature Range °C	Coercivity Range mT	Orientation D	Orientation I	Orientation Dip Corrected		N	R	κ	α_{95}
12	NG 59751200	229 142	287 - 641	5 - 166	111.1	-65.7	103.9	70.4	3	2.93	27.2	15.5
21	NG 69502378	230 36	<500		346.9	52.3	338.5	28.2	3	2.98	136.9	6.9
22	NG 68232282	238 20	<495 - 677		Not Applicable		Not Applicable		2	-	-	-
32	NG 60701290	278 159	552 - 674		103.9	70.4	080.1	-28.8	3	2.90	19.7	23.4

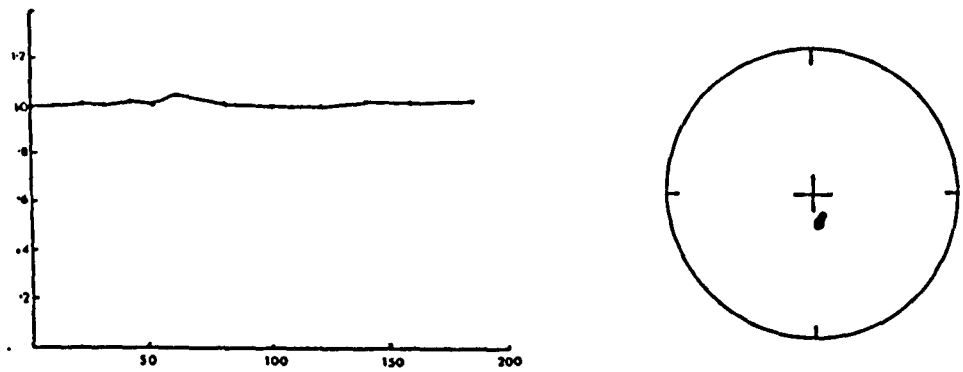

Figure 5.C.15. Typical results obtained during alternating field demagnetization of specimens from site 21. The dip corrected orientation is shown in the stereogram. The results are similar to those shown in Figures 5.C.6. and 5.C.7. from the rest of the sites in this group.

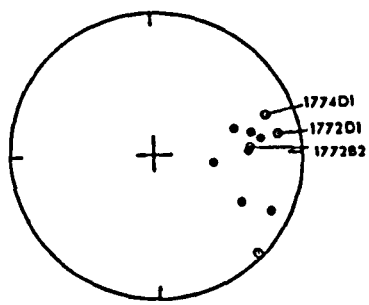

Figure 5.C.16. The NRM directions of specimens from site 32 (dip corrected). Three specimens plot in the northeast negative quadrant.

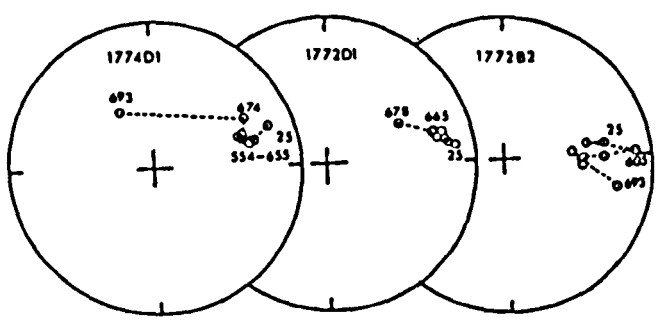

Figure 5.C.17. The orientations of the directions of magnetization (dip corrected) during thermal demagnetization of specimens 1774D1, 1772D1 and 1772B2.

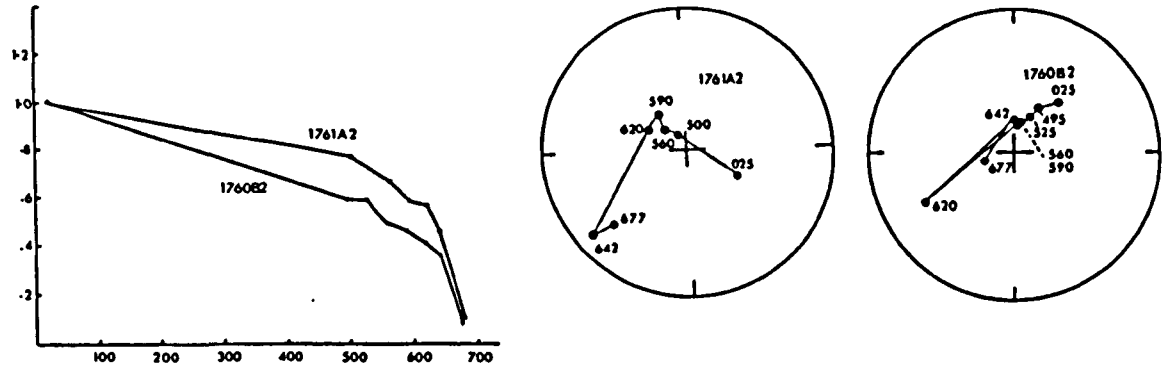

Figure 5.C.18. Thermal demagnetization curves of the specimens 1761A2 and 176082 from site 22, together with the orientation of the magnetization directions (dip corrected) of these specimens.

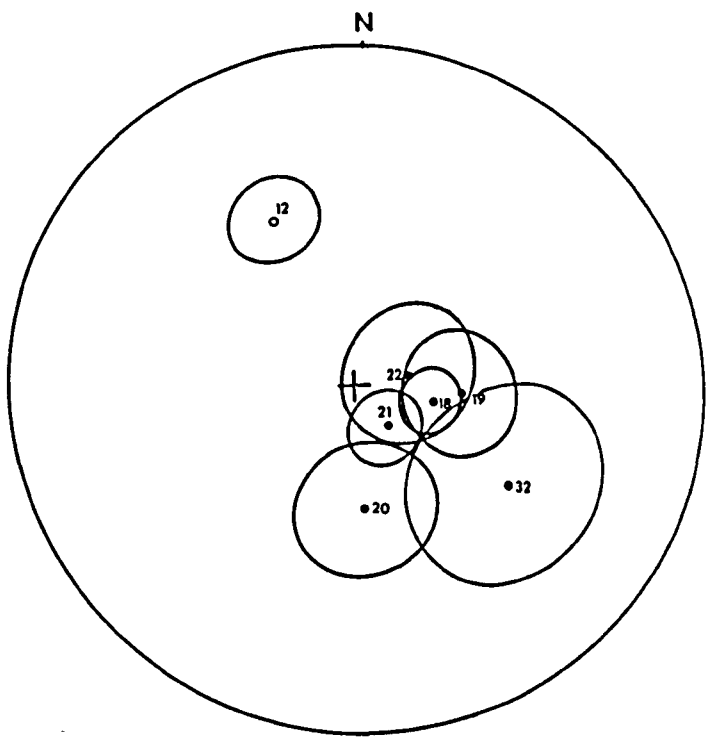

Figure 5.C.19. The site mean directions (dip corrected) of the high blocking temperature component isolated by thermal demagnetization of sites 12,18,19,20,21,22 and 32. Only thermal demagnetization results are presented as, in general, alternating field demagnetization is ineffective on these specimens.

Summary Of The Palaeomagnetic Results For The Sites Which Carry Only A Torridonian Remenance

In Table 5.C.4. the dip corrected values are given for the high blocking temperature component isolated during the thermal demagnetization of sites 12,18,19, 20,21,22 and 32. The in situ directions of this component have no geological significance and no direction is common to them all. With the exception of site 21 (which possesses a VRM) none of the in situ directions are parallel to the earth's present field.

The Eishort Anticline has a fold axis which is almost horizontal and therefore, it is only necessary to untilt the bedding by rotation about the strike direction. When the results are corrected for dip, the high blocking temperature component of magnetization lies in the northwest negative or southeast positive quadrants of the stereogram as shown in Figure 5.C.19.. These directions are parallel to or at a very small angle to the NRM directions. Therefore, it may be concluded that, in general, the NRM measured in these sites is composed of a single high blocking temperature component which lies in the northwest negative or southeast positive quadrants. The exceptions to this situation have been described.

This high blocking temperature component is parallel to the directions obtained for the Applecross Formation on the Foreland by previous workers. Following the convention of Irving and Runcorn (1957) both normal and reversed polarities are present. At each site, only one polarity is present though, an opposite polarity may be seen in some of the specimens from site 12.

In general, the blocking temperature ranges of these sites lie above the Curie point of magnetite, which is around 575^{o}C. This suggests that the dominant mineral

which carries the NRM's measured in these rocks is haematite which in this case, has blocking temperatures up to 695°C. The alternating field demagnetization equipment used in this study is incapable of demagnetizing the majority of natural haematite grains and since alternating field demagnetization is ineffective it would appear that the principal remanence carrier is haematite.

The low blocking temperature components isolated in sites 12 and 21 may be carried by magnetite. This is indicated by the low blocking temperature and in particular, the low coercivity nature of these remanences. The rapid fall in the demagnetization curves around 570°C also suggests that magnetite is present in these specimens. The high blocking temperature component (above 570°C) is carried by haematite.

In sites 12,18,19,20,21,22 and 32 it is possible to isolate, during progressive thermal and alternating field demagnetization, a high blocking temperature and high coercivity component. The blocking temperature range of this component is extremely limited (550 to 695°C) and within this range most of the NRM is carried by a series of grains with blocking temperatures of approximately 670°C. The coercivity of the grains is such that demagnetization rarely occurs below 200 mT.

When these components are corrected for the dip of the bedding they are restored to primary Torridonian magnetization directions similar to those obtained on the Foreland by Irving and Runcorn (1957), Stewart and Irving (1974) and McClelland (1976). The mean directions obtained from this study are shown in Figure 5.C.20. together with those of the previous workers. From this study the following mean directions and palaeomagnetic pole positions have been established for the Applecross Formation;

Reversed D= 122.1 I= 69.9 N= 6 k= 21.3 R= 5.76

Normal D= 344.2 I=-45.6 (One site only)

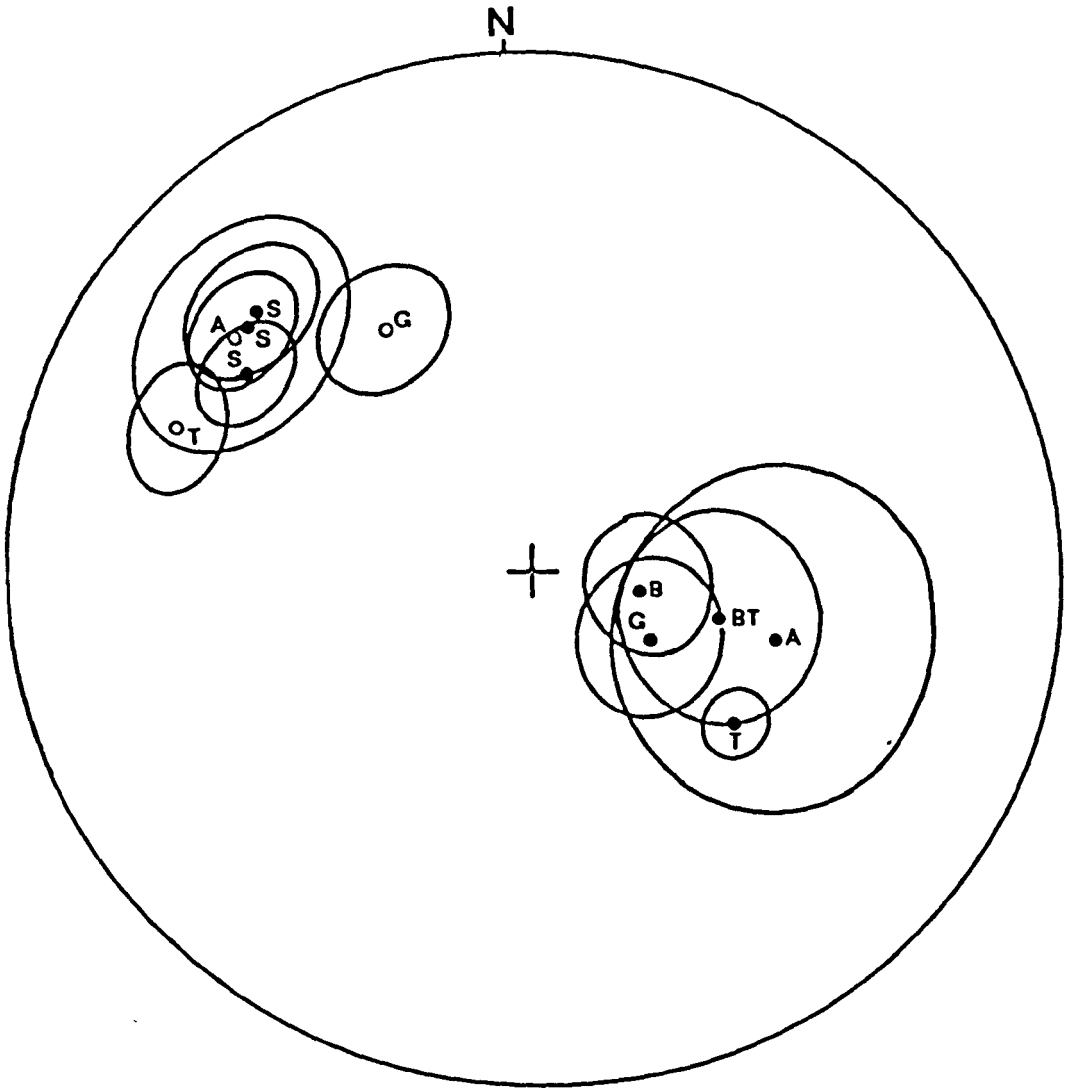

Figure 5.C.20. The formation of mean directions obtained in this study (G) are compared with those obtained from the Foreland (see Figure 2.C.1. for the notation used).

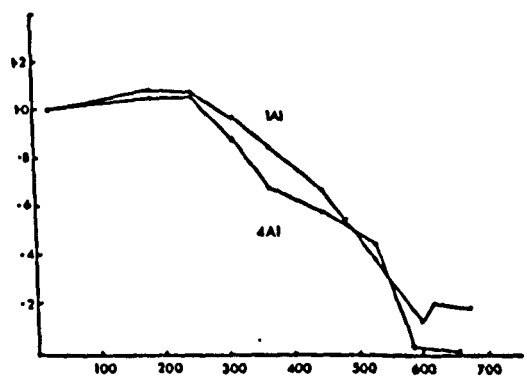

Figure 5.C.21. Typical thermal demagnetization curves of specimens from site 1.

Palaeomagnetic pole position for the Applecross Formation

(Reversed)

Lat = 30.4 Long = 29.6 (dp= 13.7, dm= 16.00)

(Normal)

Lat = 4.7 Long =188.0 (dp= 7.81 , dm = 12.31)

Since the principal remanence carrier has been shown to be haematite the NRM is thought to be of chemical origin which formed during the diagenetic growth of the haematite cement. The magnetite which is thought to be present in sites 12 and 21 is possibly of detrital origin.

Sites Around The Eishort Anticline Which Show A Tertiary Overprint

Sites 1,13,15 and 33 have contrasting demagnetization behaviour to the sites described above. Slightly different demagnetization curves are obtained for each of these four sites and each site will be discussed in turn and the results summarised later.

Site 1 The demagnetization curves produced during the thermal demagnetization of site 1 are shown in Figure 5.C.21.. The curves decline over the entire demagnetization proceedure falling most rapidly in the range 500 to 550°C and between 550 and 600°C the curves show a distinct minimum. Frequently, the curves rise only slightly after the minimum. The minimum in the curves suggests that two components of magnetization are present. The directions of magnetization during thermal demagnetization move along great circle paths (see Figure 5.C.22.). It is possible to extract the two components of the NRM by methods of vector analysis (Foss 1981). The presence of two components is clearly seen in the Zijderfeld diagram shown in Figure 5.C.23.. The removal of magnetizations throughout the proceadure shows that a wide range of blocking temperatures are present between 200 and 700 degrees centigrade.

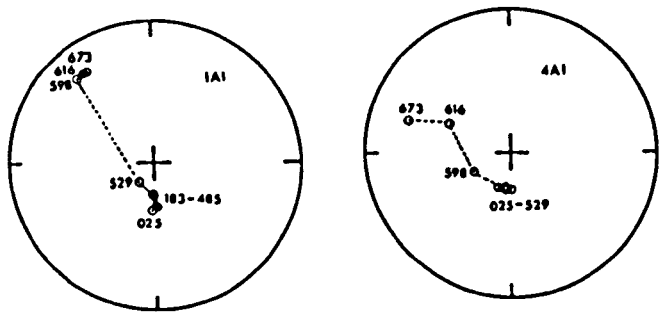

Figure 5.C.22. The directions of magnetization (In Situ) of specimens 1A1 and 4A1 from site 1, during thermal demagnetization. These results are typical of this site though, other members, during demagnetization, move towards a high blocking temperature component with a southeast positive direction.

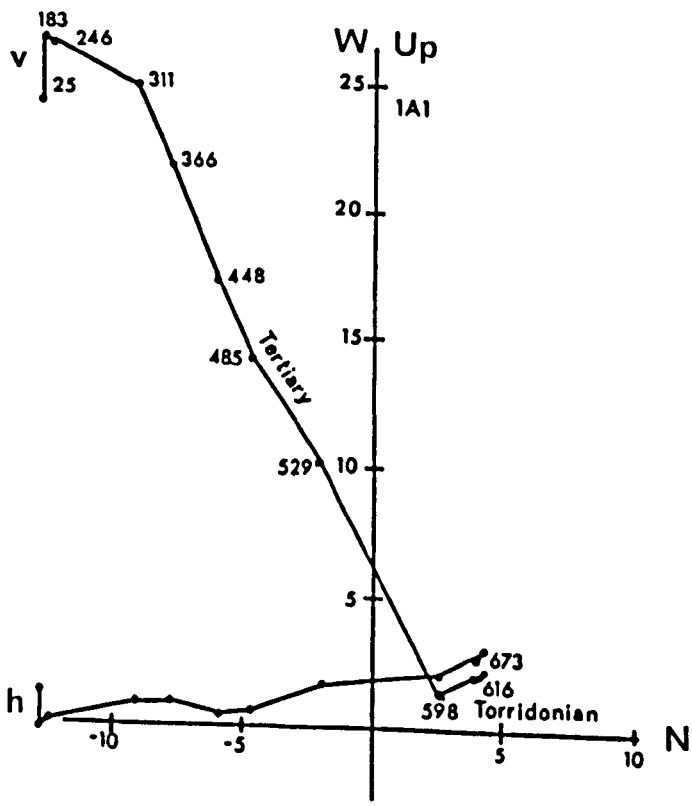

Figure 5.C.23. A Zijderfeld diagram (In Situ) of specimen 1A1 showing the presence of two components of magnetization. The age of the components is indicated on the diagram.

The demagnetization curves for alternating field demagnetization show no corresponding minima. The curves decay rapidly at low field, with a much more gentle decay at higher fields. A small amount of the NRM remains above peak fields of 180 mT. As shown in Figure 5.C.24. during alternating field demagnetization the directions move along a great circle path. The clear separation of two components was not achieved by alternating field demagnetization.

The remanence must be carried, at least above 575°C by haematite. However, it is not certain which mineral or minerals are responsible for the low blocking temperatures and low coercivities seen in these specimens. Since alternating field techniques are effective in removing significant proportions of the NRM and the results lie below the Curie point of magnetite, then it is possible that the mineral is magnetite. Further discussion of this problem will be given later in this chapter.

Thermal demagnetization on specimens from site 1 suggests that two components of magnetization are present. The low blocking temperature component has blocking temperatures up to approximately 600°C. The high blocking temperature component has blocking temperatures in the range 600 to 680°C. These two components cannot be resolved using alternating field demagnetization.

Site 13 The thermal demagnetization curves of site 13 are shown in Figure 5.C.25.. They show a gradual decline up to 500°C and a rapid decline between 500 and 600°C. A small proportion of the NRM remains above 600°C. The curves show a wide range of blocking temperatures, dominated by grains within the range 550 to 600°C.

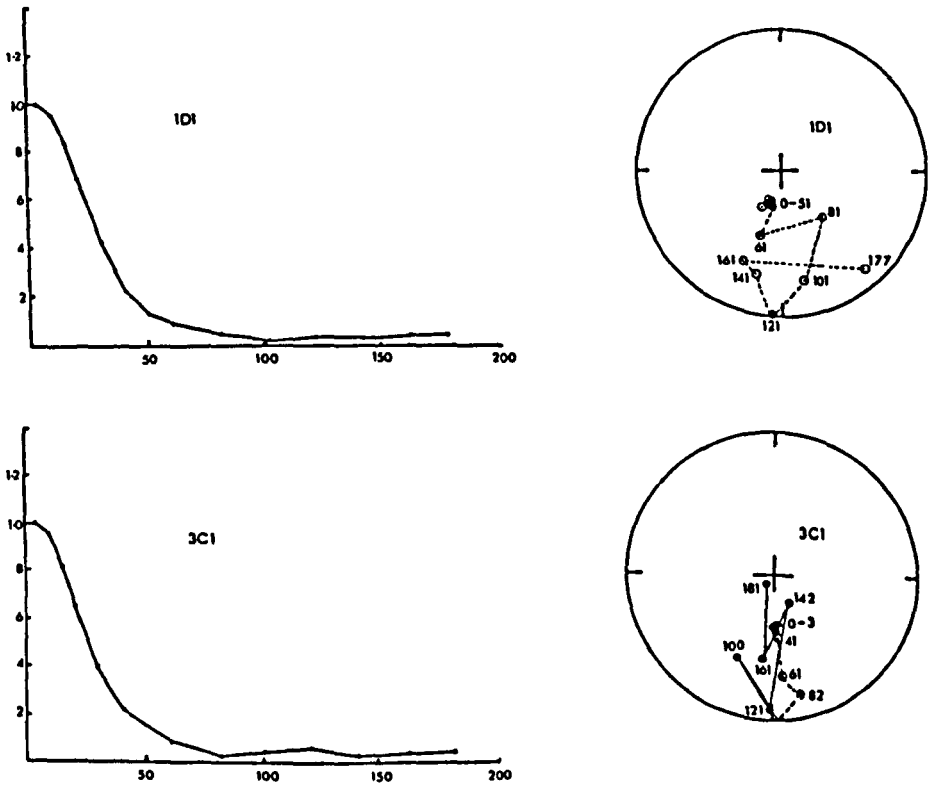

Figure 5.C.24. Demagnetization curves and the directions of magnetization (In Situ) obtained during alternating field demagnetzation of specimens from site 1.

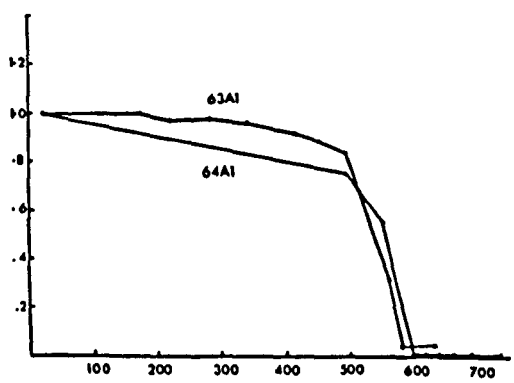

Figure 5.C.25. Typical demagnetization curves obtained during thermal demagnetization of specimens from site 13.

During thermal demagnetization the directions tend to move along great circle paths (see Figure 5.C.26.). Specimens 64A1 and 65B1 show movement between two well defined directions but the remainder of the specimens from this site show a gradual but continuous movement. In specimens 64A1 and 64B1 the low blocking temperature components fall in the southern upper hemisphere of the stereogram and have blocking temperatures up to 574°C. This upper limit coincides with the rapid fall in the demagnetization curves. Thus, it would appear that a well defined low blocking temperature component exists below 574°C. Above this blocking temperature the directions move northwards, A clearly defined direction is reached by specimen 65B1 but the remaining specimens do not reach a clearly defined end point. The low blocking temperature component is clearly seen on the Zijderfeld diagrams shown in Figure 5.C.26. but no common high blocking temperature component can be found.

During alternating field demagnetization the intensity of the NRM shows a rapid decline up to fields of 50mT. Above this point a more gradual decline is seen (see Figure 5.C.27.). The curves show a wide range of coercivities with many grains of very low coercivity. There is no clear separation of the NRM into two components and the directions of magnetization remain close to the NRM throughout the whole proceedure. The Zijderfeld diagrams obtained during alternating field demagnetization show only one component of magnetization to be present and the high blocking temperature component is thought to be spurious.

Site 15 The curves of thermal demagnetization for site 15 show a gradual decline up to 500°C and a much more rapid decline up to 700°C. Many of the curves show an increase in intensity during cleaning (Figure 5.C.28.). The curves show a wide range of blocking temperatures

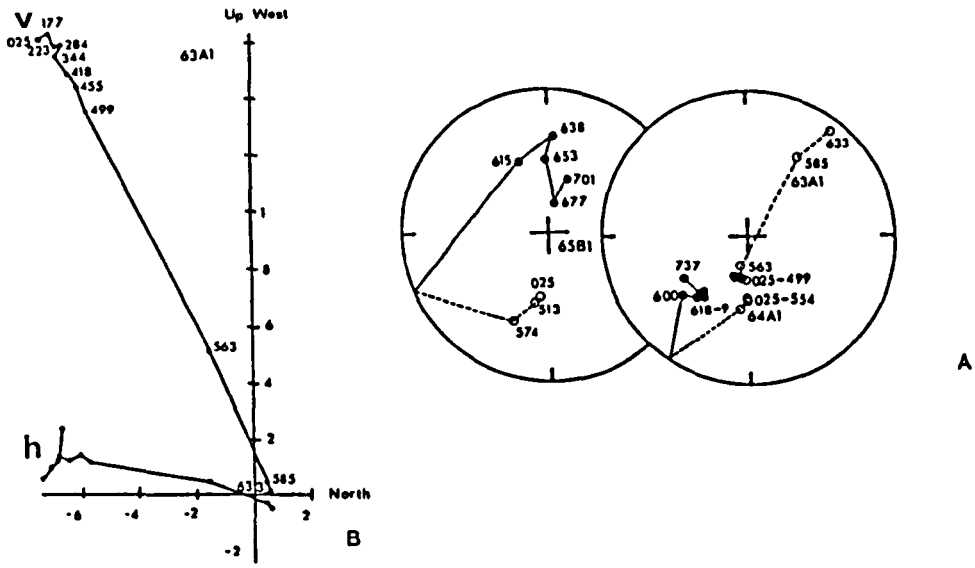

Figure 5.C.26. A. In Situ directions of magnetization obtained from several specimens from site 13 during thermal demagnetization. B. A Zijderfeld diagram (In Situ) of the thermal demagnetization of specimen 63A1. The behaviour is typical of this site and indicates a single component of magnetization.

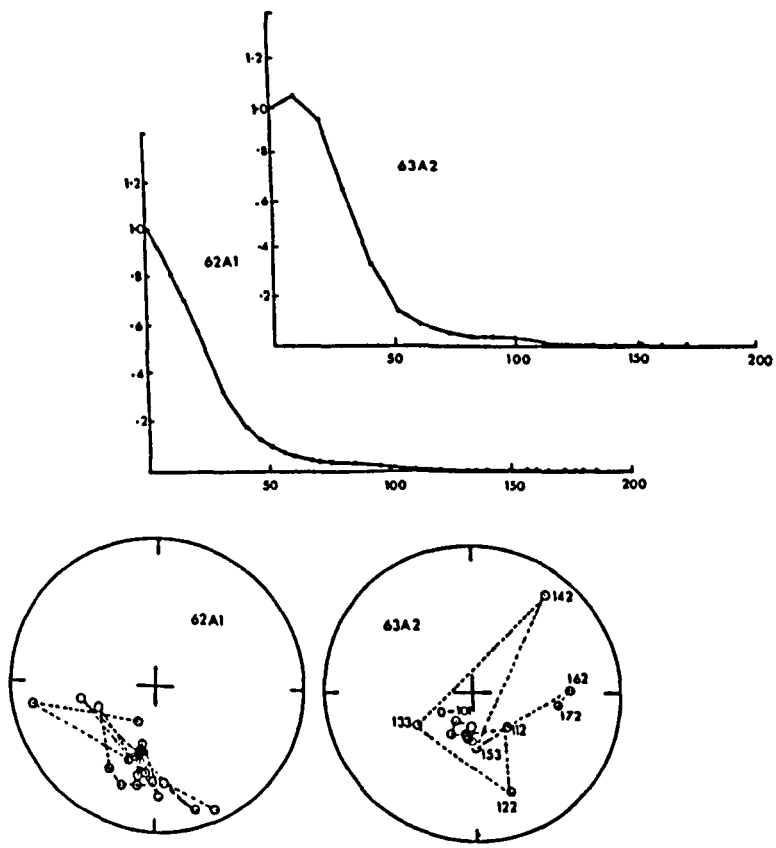

Figure 5.C.27. The demagnetization curves and corresponding directions of magnetization obtained during alternating field demagnetization. These results are typical of site 13.

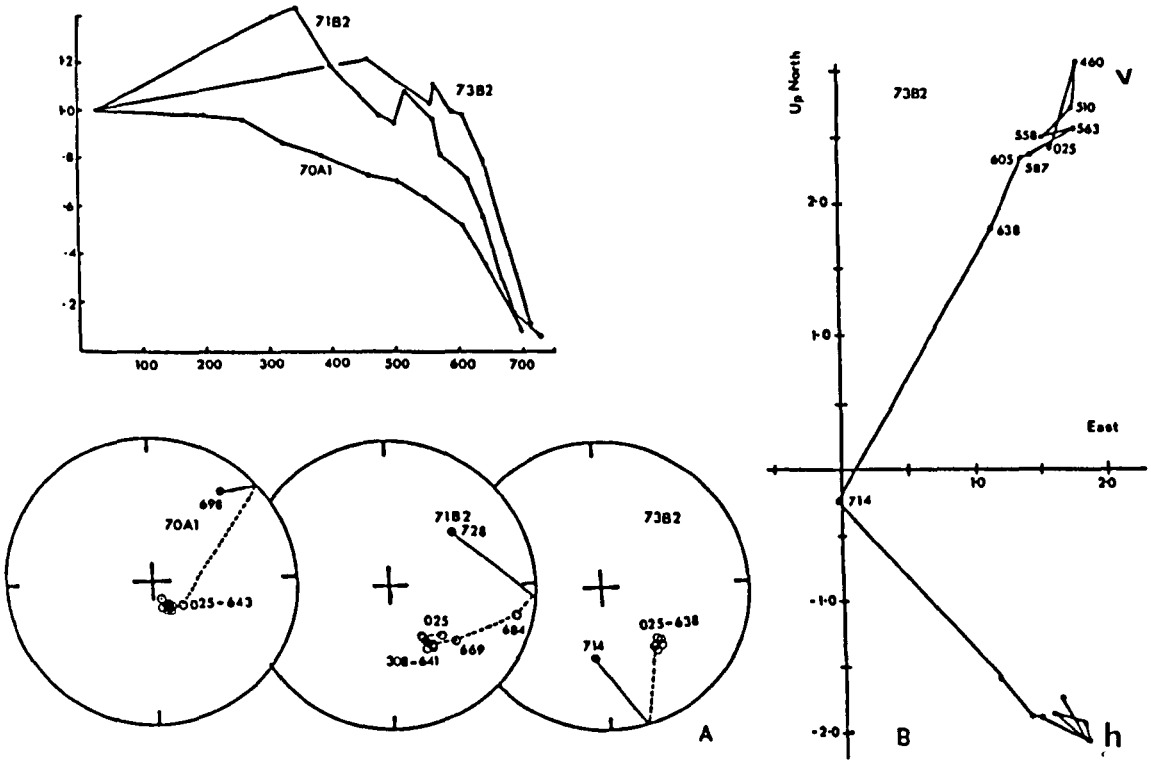

Figure 5.C.28. A. Typical demagnetization curves and directions of magnetization (In Situ) from the thermal demagnetization of specimens from site 15. The slight increase in intensity during the early stages of demagnetization is typical of this site. B. A Zijderfeld diagram showing the thermal demagnetization of specimen 7382 from site 15. The early movement away from the origin is due to the small increase in intensity during demagnetization.

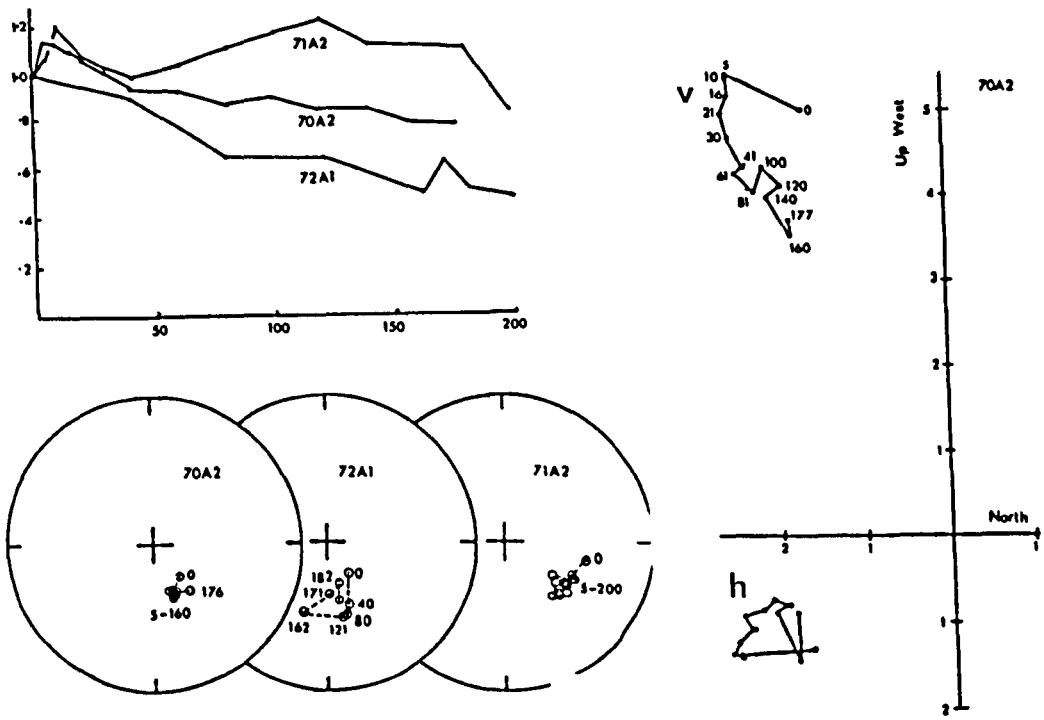

Figure 5.C.29. The results of alternating field demagnetization on specimens from site 15. The directions of magnetization shown, and the Zijderfeld diagram are both In Situ.

up to a maximum of approximately 700°C.

During thermal demagnetization the directions remain stationary. Where a consistent trend is present during demagnetization the directions tend to decrease in inclination. Above 675°C the directions move rapidly towards the northeast positive and negative quadrants (in situ) but no consistent direction is found. It is thought that these directions are random, generated by stray fields during demagnetization.

The majority of demagnetization curves from alternating field demagnetization (Figure 5.C.29.) show a slight increase in the intensity of magnetization below 20 mT. A gradual decline is seen throughout the cleaning proceadure and at 200 mT a large proportion of the NRM remains this indicates the presence of grains with very high coercivities.

During alternating field demagnetization the directions remain around the NRM with only a small amount of movement (Figure 5.C.29.). The results indicate the presence of some grains which can be cleaned using alternating field demagnetization but the majority of the grains cannot.

Site 33 During thermal demagnetization of specimens from site 33 a series of curves were obtained. These curves decline slowly up to blocking temperatures of around 500°C (Figure 5.C.30.). A more rapid decline is seen up to blocking temperatures of 625°C. Specimen 1775 shows a more gradual decline than the other specimens and definite minima are seen in the curves of sample 1777.

The directions remain almost stationary during cleaning. This may be due to only a small proportion of the NRM being removed in each step. However, little movement

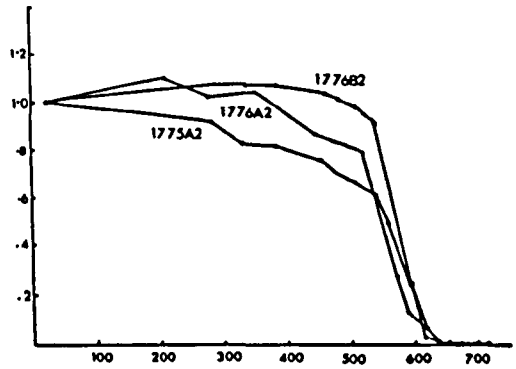

Figure 5.C.30. Thermal demagnetization curves typical of specimens from site 33.

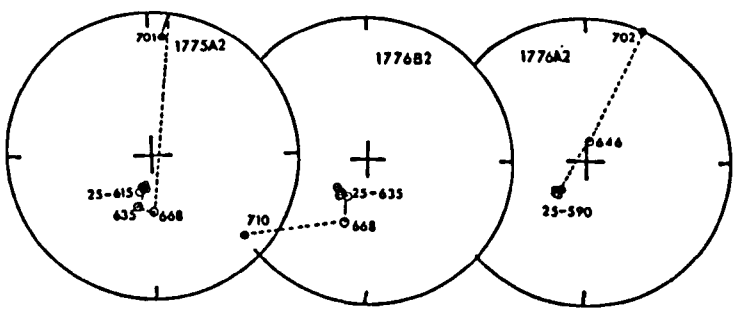

Figure 5.C.31. The directions of magnetization (In Situ) obtained during thermal demagnetization of specimens from site 33.

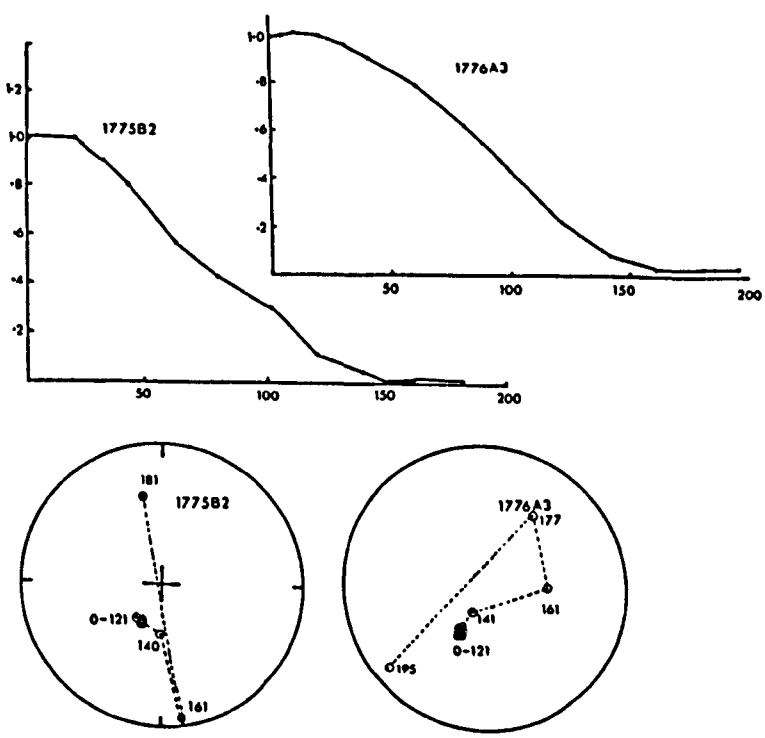

Figure 5.C.32. The results of alternating field demagnetization on specimens from site 33. The directions of magnetization are In Situ.

of the magnetization direction occurs during the steep portion of the curves and in many cases, during cleaning, between 625 and 675^{o}C,a common direction remains. Above the haematite Curie point the directions of magnetization become random. No direction could be found for the range 625 to 675, in situ or dip corrected, which had any geological significance.(Figure 5.C.31.).

The demagnetization curves from alternating field demagnetization are shown in Figure 5.C.32.. The curves show a gradual decline up to 140 mT and a much more gradual decline up to 200 mT. The directions remain stationary until 200 mT when they become random (see Figure 5.C.32.). Only one component of magnetization is present in this site as indicated by the Zijderfeld diagrams shown in Figure 5.C.33..

In the preceading discussion all the directions shown have been in situ directions. With the exception of site 1, the directions during demagnetization remain close to the NRM until they become random at high blocking temperatures or high applied fields. Site 1 shows a clear movement towards a second high blocking temperature and high coercivity component. The ranges of blocking temperature and coercivity for the components present in these sites are shown in Table 5.C.6. together with relevant statistics (Fisher 1953).

Sites 13,15 and 33 are composed of a single component which has a southerly declination and a steep, negative inclination. These directions have more geological significance in situ, than dip corrected and are interpreted as reversed Tertiary directions following the results of Wilson et al (1981) (see Figure 5.C.34.).

Site 1 shows a low blocking temperature and low

Table 5.C.6.

Site No.	Grid Reference	Dip of Bedding	Blocking Temperature Range °C	Coercivity Range mT	Orientation D	Orientation I	N	R	κ	α_{95}
1	NG 674220	175 08	311 - 690	20 - >180	184.5	-62.2	15	14.91	150.4	2.9
13	NG 605118	060 26	223 - 605	5 - >180	186.6	-57.3	5	4.96	91.8	6.5
15	NG 63201275	245 61	202 - 677	>100	146.6	-55.7	9	8.44	14.2	12.4
33	NG 57871017	258 168	287 - 684	30 - >180	206.4	-68.1	11	10.93	163.9	10.9
					Dip Corrected					
1	NG 674220	175 08	598 - 697	>180	300.6	-38.7	4	3.26	4.0	35.0
					146.0	40.1	3	2.85	13.6	21.9

Table 5.C.7.

Site No.	Grid Reference	Dip of Bedding	Blocking Temperature Range °C	Coercivity Range mT	Orientation D	Orientation I	Orientation (Dip corrected)		N	R	κ	α_{95}
8	NG 58260973	356 24	177 - 599	5-180	034.6	52.8	050.7	35.0	10	9.89	84.5	4.8
17	NG 74362662	228 40	226 - 571	3-182	110.1	41.5	061.0	68.9	5	4.81	21.9	13.4

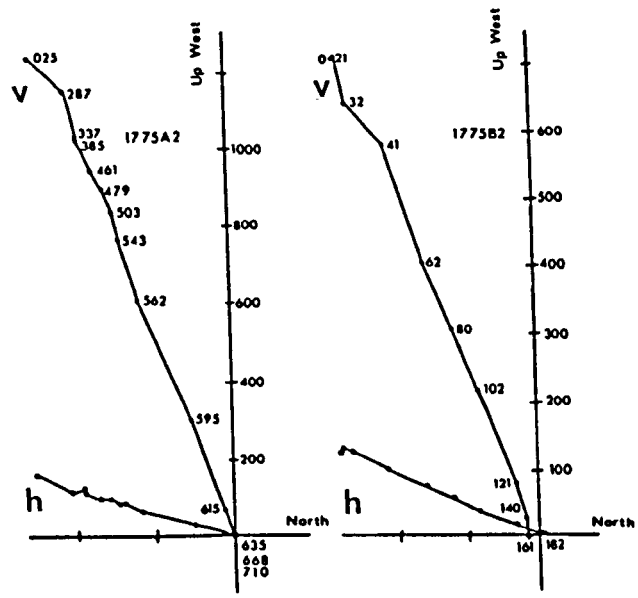

Figure 5.C.33. Zijderfeld diagrams showing the behaviour of specimens from site 33 during demagnetization. Specimen 1775A2 shows the results of thermal demagnetization and specimen 1775B2 shows the results of alternating field demagnetization.

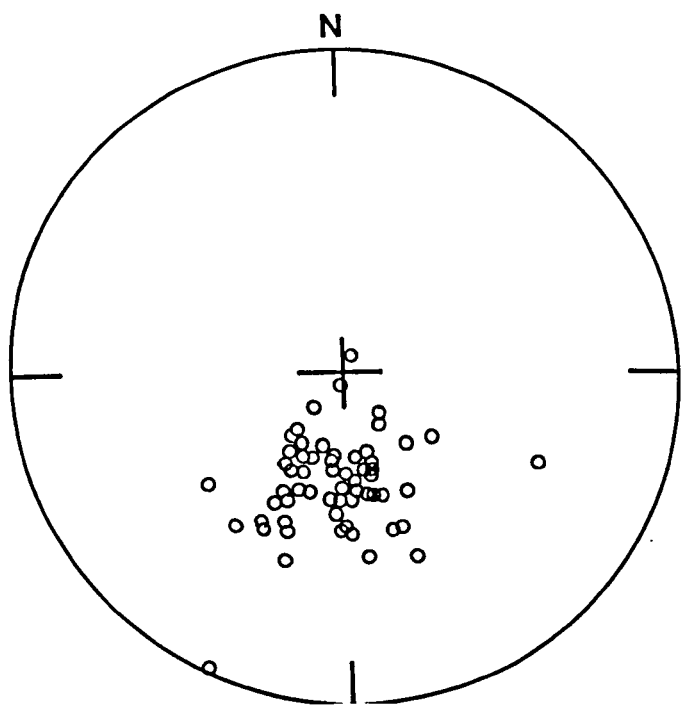

Figure 5.C.34. Reversed Tertiary magnetization directions obtained from the Vaternish Dyke Swarm of Northern Skye (Figure 2. of Wilson et al of 1974, Geophys. J.R. astr.Soc. 37, 23-30.). The directions are comparable to those obtained by Wilson et al 1981 for the Sleat Dyke Swarm.

coercivity component which when in situ corresponds closely to a reversed Tertiary direction (Figure 5.C.34.). However, the high blocking temperature component bears no relationship to the Tertiary directions and when dip corrected corresponds closely to the Torridonian directions obtained by previous workers (Irving and Runcorn 1957, Stewart and Irving 1974, McClelland 1976). Both normal and reversed Torridonian polarities are present within this site and often within a single core.

The demagnetization of specimens 59A1, 59A2, 59C1 and 59C2 from site 12 show a behaviour very similar to site 1. The demagnetization curves for these specimens (Figure 5.C.9.) are very similar to those of site 1 (Figure 5.C.21.). The in situ orientation of this low blocking temperature component from site 12 is very similar to the orientation of the reversed Tertiary magnetization found in site 1. Therefore, since the demagnetization curves are almost identical it is thought that, within these specimens from site 12, a low blocking temperature Tertiary component is present. (See page 208).

From this study the following mean Tertiary magnetization direction and pole position was obtained;

Lat =-76.6 Long = -0.7 (dp= 13.9 dm= 17.9)

D= 178.4 I= -62.6 N= 4 κ= 37.8 R= 3.92

The Nature Of This Tertiary Overprint

Sites 1,13,15,33 and some of the cores of site 12 record a Tertiary overprint (see Figure 5.C.35.) which, in the case of sites 1 and 12 has only partially reset the magnetization. The nature of this remagnetization will be discussed in relation to all of the sites so far

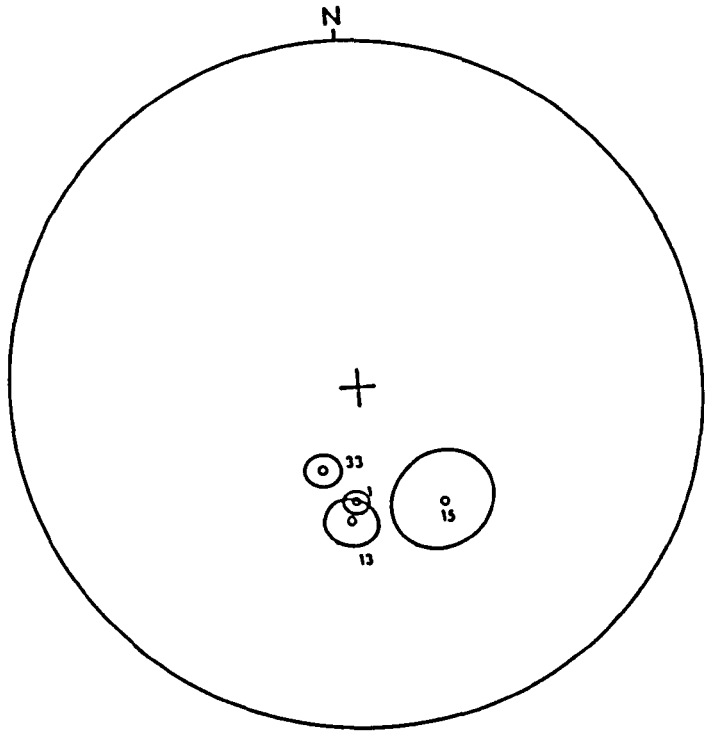

Figure 5.C.35. The site mean directions (In Situ) of the low blocking temperature component isolated during thermal demagnetization of sites 1,13,15 and 33.

described around the Eishort Anticline.

Figure 5.C.36. shows the position of the sites around the Eishort Anticline and the outcrop of Tertiary igneous rocks on Skye. It is clear from this diagram that the sites which posses a Tertiary overprint bear no relationship to the main outcrop of Tertiary igneous rocks on Skye. Often, the sites which contain only Torridonian components lie closer to the main outcrop of igneous rocks than those with a Tertiary component. The distribution of the sites with a Tertiary overprint cannot be related to the effects of a large thermal aureole alone, since a more rational pattern of overprinting would be seen.

Sleat is affected by dyke swarms of Tertiary age which are related to the igneous centre and it is possible that the dykes are responsible for the Tertiary overprint. Only reversed Tertiary directions were obtained in this study and Wilson et al (1981) report that in general, the Tertiary dykes of Sleat tend to be of reversed polarity. Thus, the sporadic nature of the overprint may be accounted for by the irregular distribution of the dykes. However, during sampling, outcrops with Tertiary dykes were actively avoided, and therefore, a hidden dyke must be inferred for each of the sites with an overprint and this seems unlikely. More significantly, site 32 shows no evidence of a Tertiary component. This site was collected from within the baked margin of a large dyke.

The ranges of blocking temperature for the sites sampled around the Eishort Anticline are given in Tables 5.C.4. and 5.C.6.. These ranges are summarised is Figure 5.C.37.. Those sites which do not posses the Tertiary component have minimum blocking temperatures of approximately 550^{o}C. Those sites which record the Tertiary overprint have minimum blocking temperatures

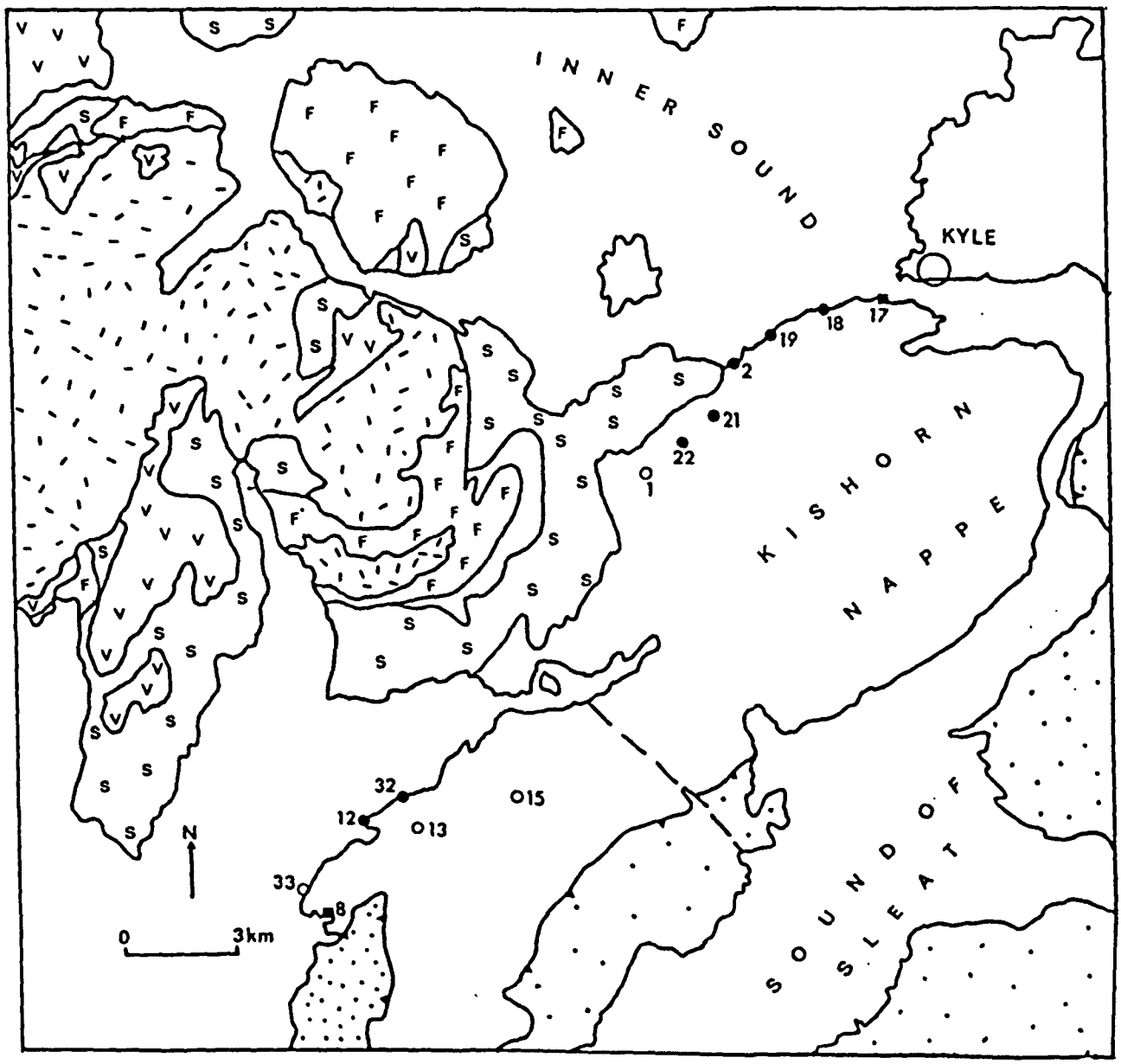

Figure 5.C.36. A map showing the position of the sites studied around the Eishort Anticline together with the outcrop of Foreland rocks (F), Tertiary volcanic rocks (V), post Caledonian sediments (S) and Tertiary plutonic rocks (cross hatch). Open symbols denote the presence of the Tertiary overprint. ■sites to be discussed.

below this value. Therefore, it would appear that the Tertiary thermal overprinting is recorded only when the sites contain suitable blocking temperatures. Thus, the sporadic distribution of the overprint is related to the sporadic distribution of suitable sites. This is confirmed by the results from sites 12 and 32. As described above site 32 was sampled from within the baked margin of a large dyke. No low blocking temperature grains are present in this site and the Tertiary event is not recorded. In the specimens 59A1, 59A2, 59C1 and 59C2 from site 12 the Tertiary overprint can be seen. These samples have suitable low blocking temperature grains in contrast to the remainder of the specimens from this site. These two examples illustrate clearly the petrological control on the overprinting behaviour of these rocks. It is thought that the main igneous centre on Skye was the heat source for this Tertiary event.

Above 575^{o}C the remanence must be carried by haematite but it is uncertain what mineral or minerals carry the remanence below 575^{o}C. It may be haematite or magnetite. Curie point determinations and XRD have been used in attempts to determine the mineralogy of the low blocking temperature grains. These studies have not produced satisfactory results and all of the following suggestions must be considered as possible explanations for the presence or absence of the low blocking temperature grains.

Stewart and Irving (1974) suggested that detrital specular haematite or specularite is the principal magnetic phase in the Torridonian rocks. Further, they suggest that the finely divided red pigment makes little or no contribution to the NRM. Studies of other red bed sequences suggest that in certain circumstances it is the red pigment which is the principal magnetic phase (Collinson 1966, Park 1970). If haematite is the

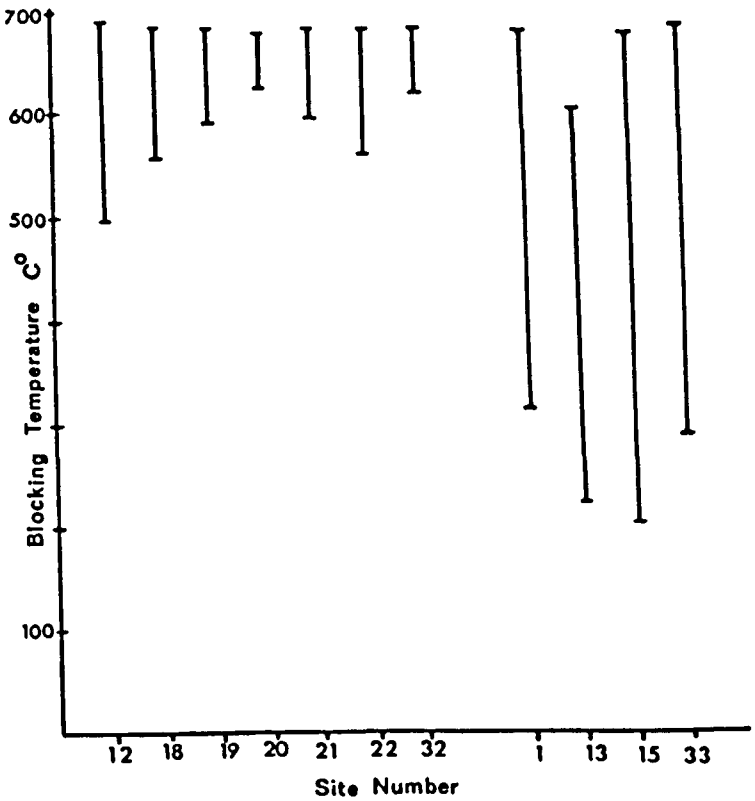

Figure 5.C.37. The ranges of blocking temperature indicated by thermal demagnetization for the sites around the Eishort Anticline (excluding site 8 and 17). Two groups of sites are shown; 12-32 which posses a Torridonian component alone and 1-33 which possess a Tertiary overprint. The lower limit of the Torridonian sites is indicated by the first fall of intensity during demagnetization. The lower limit for the sites which possess a Tertiary component is the lowest blocking temperature at which the demagnetization procedure commenced and lower blocking temperatures are possible.

only magnetic mineral present in these rocks then three possibilities exist for the different ranges of blocking temperature which may be seen in the two types of site.

(a) Different ranges of blocking temperature were produced by different diagenetic histories.

(b) The low blocking temperatures are due to the presence of detrital specularite and the high blocking temperatures are due to diagenetic haematite.

(c) Detrital grains of haematite are the only significant magnetic mineral present in these rocks and contrasting ranges of grain size produces the two types of site. Smaller grains tending to produce lower blocking temperatures (McElhinny 1973).

If the rocks contain both haematite and magnetite then a fourth possibility exists.

(d) The low blocking temperatures are due to the presence of detrital magnetite and the high blocking temperatures are due to detrital specularite or diagenetic haematite.

Polished specimens were prepared from all of the sites studied. In reflected light these showed two types of haematite to be present, detrital specularite and interstitial red pigment which coats the quartz and feldspar grains. The specularite grains are well rounded and often occur in thin bands typical of detrital grains. Occasionally, fine grains of haematite may be seen in the grains of quartz or feldspar but these are not common.

The only significant difference which can be seen, using the optical microscope, between the two types of site is that the sites which show only the Torridonian component contain coarser speculite grains (0.1 to 0.2 mm diameter). In the sites in which the Tertiary component is present the specularite grains are generally 0.01mm in diameter. This suggests that case (c) is the most probable.

As seen in Figure 5.C.37. there is an overlap in the range of blocking temperatures in the two types of site studied. Tertiary components can be recorded up to blocking temperatures of 680°C. This is similar to the range of blocking temperatures in the sites in which Torridonian components are present alone. The simplest explanation of this situation is that the low blocking temperature component is carried principally by magnetite of detrital origin. The high blocking temperature component is carried by diagenetic haematite. During the Tertiary thermal event some of the magnetite was oxidized to haematite and produced a slightly higher range of blocking temperatures. Magnetite was only seen in specimens from site 21 and this may be responsible for the VRM recorded in this site. The apparent absence of magnetite in the remainder of the specimens does not invalidate the conclusions given above, as magnetite grains which are palaeomagnetically useful are too small to be resolved by optical microscopy. Magnetite is thought to be present in all of the sites which record the Tertiary overprint. This is indicated by the ability to clean these sites using alternating field techniques, and the rapid decline in the demagnetization curves around 575°C. Therefore, the Tertiary thermal overprint is only recorded in sites which contain detrital magnetite grains.

Sites 8 and 17 Which Record A Stable Component Of Unknown Origin

The samples for site 8 were collected from Tarskavaig Beach on the normal limb of the Eishort Anticline. Both fine sandstones or siltstones and coarse feldspathic grits were sampled. The thermal demagnetization curves for both types of rock are the same (see Figure 5.C.39.) which shows that the NRM is carried by a similar population of grains with similar physical properties in the two rock types. Typically, the curves fall slightly up to blocking temperatures of 500°C. Above this temperature the curves fall rapidly to leave only a small remanence above 600°C. This suggests a wide range of blocking temperatures with a large proportion of the grains having blocking temperatures in the range 500 to 600°C. The thermal demagnetization curves for site 8 are shown in Figure 5.C.39. and the directions of magnetization during cleaning are shown in Figure 5.C.40.. During demagnetization the directions remain stationary until they become dispersed at very high blocking temperatures. Few directions survive above the magnetite Curie point of 575°C and magnetite is thought to be the principal magnetic mineral.

The curves of alternating field demagnetization show a rapid decline below 40 mT and a more gradual decline at higher fields (Figure 5.C.41.). During demagnetization the directions remain stationary while large proportions of the NRM are removed. This suggests only one component is present in these rocks and this is confirmed by the Zijderfeld diagrams shown in Figure 5.C.42..

A small VRM may be present at this site. During thermal demagnetization a common vector is removed from all of the specimens during the early stages of cleaning. This is most clearly seen in specimen 33A1. During the first step (25 to 177°C) a vector is removed which is parallel to the earth's present field. This VRM is

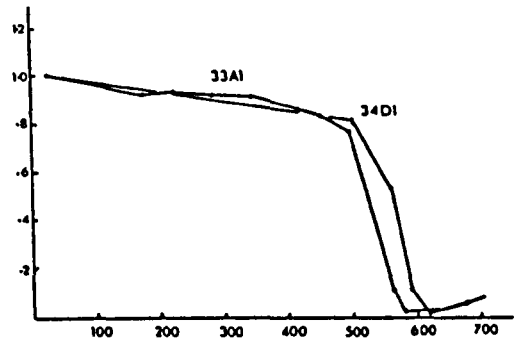

Figure 5.C.39. Thermal demagnetization curves of two specimens from site 8. Similar types of curve are produced by both rock types which were sampled from this site.

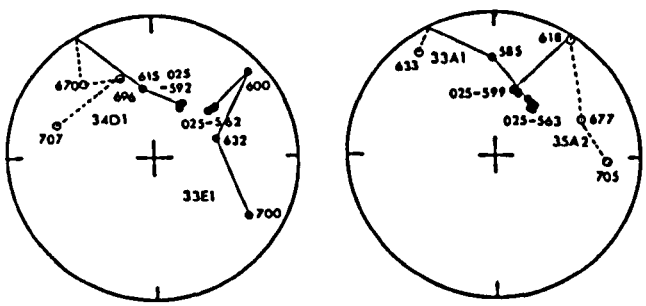

Figure 5.C.40. In Situ magnetization directions of specimens from site 8.

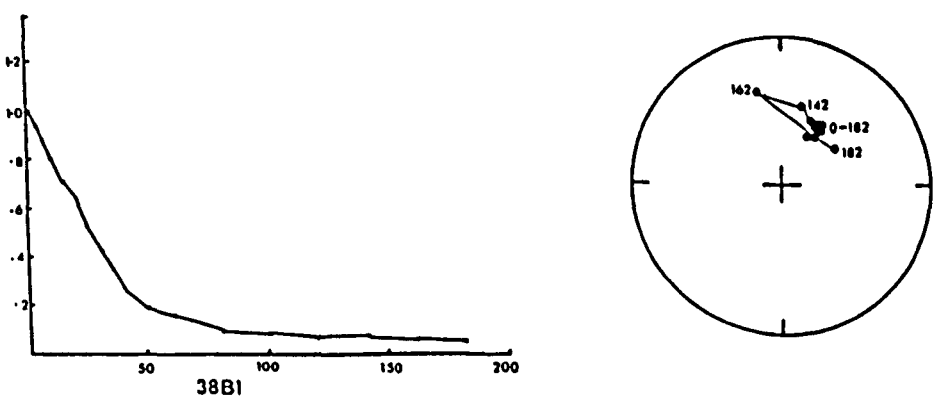

Figure 5.C.41. A typical example of the demagnetization behaviour of specimens from site 8 during alternating field demagnetization. The directions shown are In Situ.

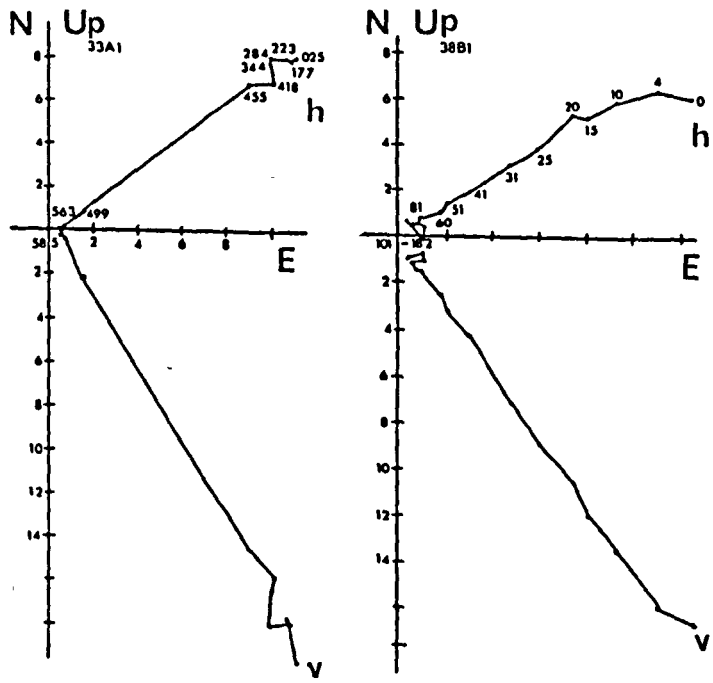

Figure 5.C.42. Zijderfeld diagrams showing the behaviour of specimens from site 8 during thermal (33A1) and alternating field (38B1) demagnetization. One stable component is present in this site.

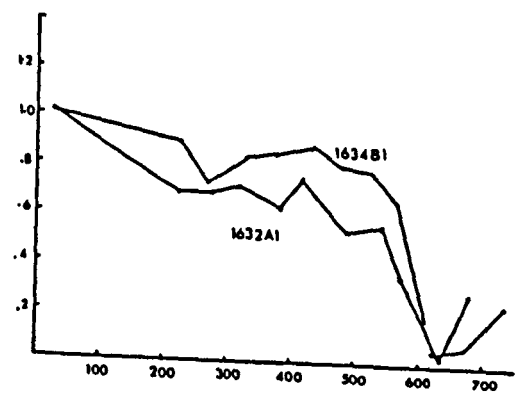

Figure 5.C.43. Thermal demagnetization curves of two specimens from site 17.

extremely small and the NRM is dominated by a single component with a wide range of blocking temperatures and coercivities. The ranges are given in Table 5.C.7.. This component, whether in situ or dip corrected, plots in the northeast positive quadrant.

The in situ directions of this component cannot be related to the Tertiary palaeomagnetic directions established in this thesis or recorded by Wilson et al (1981). The dip corrected directions cannot be related to any of the Torridonian directions isolated in this thesis.

Site 17 is located near Kyleakin on northern Sleat. At this locality the transverse cleavage is strongly developed. The demagnetization curves of specimens from this site are shown in Figure 5.C.43.. The erratic nature of these curves is due to the low intensity of these specimens (less than 1.0 emu/cc.10^{-6}). This intensity is close to the limits of the magnetometer used. Small measurement errors will result in dramatic effects.

Generally, the curves of thermal demagnetization show a moderate decline to around 500^{o}C. This is followed by a rapid decline up to blocking temperatures of 570^{o}C. On two of the curves a minimum is seen at 250^{o}C. Due to the low intensity of these specimens it is not certain whether this feature is significant. Since no magnetization remains above 575^{o}C magnetite is thought to be the principal magnetic mineral.

The demagnetization curves produced during alternating field demagnetization are shown in Figure 5.C.44.. A rapid decline is seen up to 40 mT. Above this point the decline is more gradual.

Below approximately 570^{o}C the directions of magnetization

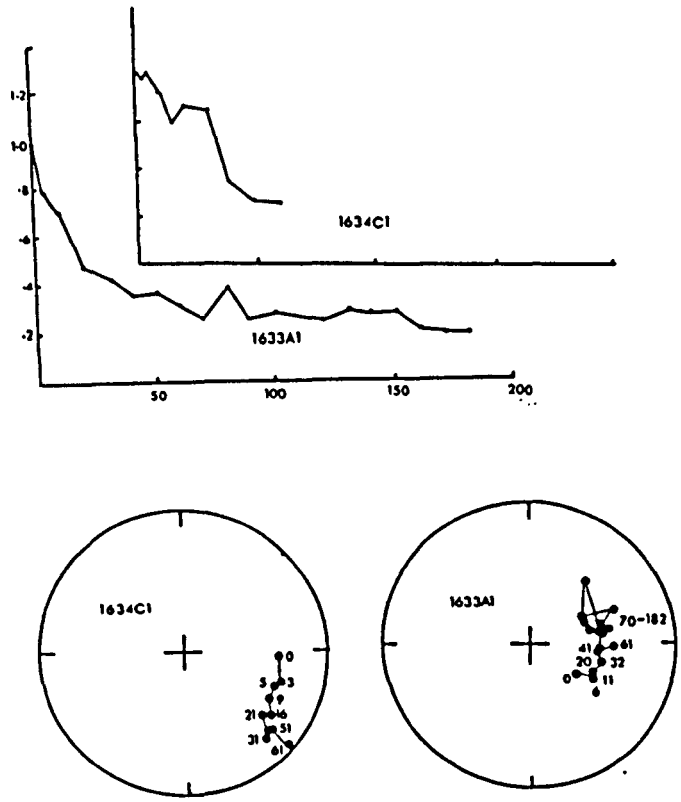

Figure 5.C.44. The results of alternating field demagnetization on specimens from site 17. The directions of magnetization are In Situ.

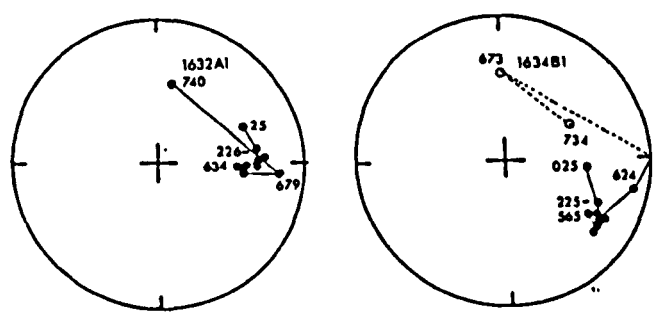

Figure 5.C.45. The orientation of the magnetization directions during the thermal demagnetization of specimens from site 17. The directions of magnetizat are In Situ.

plot close to the direction of the NRM. Above 575°C the directions become dispersed and no common direction is seen.(Figure 5.C.45.). Similar results are seen during alternating field demagnetization and only one component of magnetization is thought to be present in site 17.

The component of magnetization lies in the northeast positive quadrant and cannot be related to the geological history of the rocks. The directions, whether in situ or dip corrected, have no geological significance. The blocking temperature and coercivity ranges for this site are different to the remainder of the sites in the Applecross Formation. It is thought that site 17 may contain a CRM produced by the development of the transverse cleavage. However, this direction is presently unknown in the lower Palaeozoic.

It is thought to be significant that this northeast positive direction is common only to the two sites which show microstructural evidence of Caledonian deformation. This is the only common feature of these sites which come from different structural positions and are separated by 20 Km. Site 17 clearly shows the development of the transverse cleavage and site 8 shows some evidence of deformation in thin section. See chapter 3. section C.

To establish the possible age of this magnetization many sites were sampled on the overturned limb of the Lochalsh Syncline. However, none of these proved suitable,and until confirmed by future work, this north-east positive direction must be treated with caution.

Section 5D Summary and Conclusions

From the results presented in this chapter it is clear that within the rocks of the Eishort Anticline a

Torridonian magnetization is preserved. Some of the sites have been partially or totally remagnetized by a Tertiary thermochemical overprint which is related to the Tertiary igneous complex on Skye. In one of these sites Torridonian directions are still preserved. In the preceading discussion the directions of magnetization have been described as "in situ" or "dip corrected" directions. The high blocking temperature components which have been ascribed to the Torridonian only have geological significance when dip corrected. This result has important structural consequences. The process of dip correction involves rotation of the bedding about the strike direction, no correction was necessary for the plunge of the fold since the fold axis of the Eishort Anticline is horizontal.

Both limbs of the Eishort Anticline were sampled. In general, the normal limb dips gently or very gently to the northwest. The inverted limb dips gently to the southeast and is almost completely inverted. It was not necessary to correct any of the high blocking temperature components for internal deformation. Even sites 12 and 32 which are on the inverted limb of the fold did not require any correction for internal deformation. All Torridonian directions were restored to comparable directions obtained on the Foreland and therefore, it may be concluded that the rocks of the Eishort Anticline suffered no internal deformation during the development of the fold. Since no internal deformation is recorded in these rocks then it must be suggested that the dominant folding mechanism was flexural slip with movement on the bedding surfaces.

The absence of deformation microstructures in the sandstones around the Eishort Anticline may be taken to indicate that deformation was achieved by grain boundary sliding. However, such a process, which involves

rotation of the grains will affect the palaeomagnetic direction. Since the Torridonian directions are unaffected then deformation by grain boundary sliding can be rejected. Evidence of Caledonian deformation is seen in two sites and these record a magnetization direction which is distinct from the rest of the sites but is presently unknown in the lower Palaeozoic. This direction may have been produced by deformation and recrystallization during the development of the fold.

Chapter 6 Studies of The Anisotropy of Magnetic Susceptibility Within the Kishorn Nappe

Magnetic susceptibility relates the induced magnetization (J) to the applied field (H)

$$J = kH$$

In anisotropic rocks and minerals k is a second order tensor which can be approximated by an ellipsoid, the ellipsoid of magnetic susceptibility, with principal axes k_{max}, k_{int}, and k_{min}. The anisotropy of magnetic susceptibility in natural rocks arises from the anisotropy of the minerals and grains which are present in the rock. A useful review of magnetic anisotropy in natural rocks is given by Bathal (1971), and a mathematical analysis of how individual grain anisotropies contribute to the anisotropy of the rock was presented by Owens (1974b).

In this study measurements were made using a Digico Complete Results Anisotropy Delineator (CRAD). The anisotropy of susceptibility is field dependent and Bathal (1971) provides a review of the contrasting behaviour of different minerals at high and low applied magnetic fields. The CRAD operates at fields of 7 Oe. At this low field, in rocks containing ferromagnetic and paramagnetic minerals k is linearly dependent on the field. The magnetic minerals of the rocks were determined using the palaeomagnetic results described in chapter 5., XRD studies and Curie point determinations. This was supplemented by thin section studies to determine the distribution and possible orientations of the minerals concerned.

At the fields used in the CRAD the anisotropy of susceptibility of individual magnetite grains is dependent on the shape of the ellipsoidal grains. The principal axes of magnetic susceptibility are parallel to

the dimensional axes of the grains. Thus, the anisotropy of the rock is produced by the preferred dimensional orientation of the ellipsoidal magnetite grains.

The susceptibility anisotropy of haematite grains is of magnetocrystalline origin, an effect which is minimal in magnetite grains at low fields. In haematite the axes of maximum and intermediate susceptibility lie in the basal plane of the crystal and the minimum axis is parallel to the c-axis. Thus, in rocks containing haematite the anisotropy arises from the preferred orientation of haematite basal planes.

In paramagnetic minerals the anisotropy is of magnetocrystalline origin and produces an anisotropy in the rock due to the preferred crystallographic orientation of the grains. In the rocks studied chlorite is thought to be the principal paramagnetic mineral and thus the anisotropy of the rocks arises from the preferred orientation of chlorites parallel to the cleavage in the rock. Useful reviews of magnetic anisotropy are given by Bathal (1971) and Owens and Bamford (1976) who provide a comprehensive range of references.

The CRAD system may suffer from instrumental errors which depend on the mean susceptibility of the rock. These problems arise principally from the shape of the core. The effects of instrumental errors was reviewed by Urrutia-Fuchugauchi (1980). Recently, Addison (1981) has modified the CRAD system and suggests that the dependence of the system on the shape of the sample has been removed. For this reason the measurements of magnetic anisotropy were made in the Department of Physics at the University of Newcastle-Upon-Tyne where a modified CRAD system is available. This problem will not be reviewed here as it is not central to the geological nature of this thesis.

Relationship Of Magnetic Susceptibility to Rock Fabric and Finite Strain

Graham (1954) described how the anisotropy of magnetic susceptibility could be used to determine the orientation of weak rock fabrics. He found that in undeformed sediments the magnetic fabric is oblate and the minimum axis of susceptibility lies normal to the bedding. In folded ferruginous sandstones he found that the maximum susceptibility was normal to the bedding and the minimum susceptibility is normal to the fold axis. In schists, he found that the minimum axis of susceptibility lies normal to the foliation and the axis of maximum susceptibility is parallel to the lineation on the foliation plane. Thus, magnetic anisotropy provides a method of determining the orientation of weak fabrics in deformed rocks. Later, Graham (1966) suggested that in some deformed rocks there is a correlation between the magnetic anisotropy and the degree of deformation. Since this observation several attempts have been made to quantify the relationship between magnetic anisotropy and strain. Of these attempts, the most successful have been Kneen (1976), Wood et al (1976), Rathore (1979, 1980), Kligfield, Owens and Lowrie (1979) and Kligfield, Pfiffner and Lowrie (1982).

Wood et al (1976) showed a quantitative correlation between the strain determined from reduction spots and the magnetic anisotropy in selected types throughout North Wales. Rathore (1979) presented results from the Welsh slates and found that the ellipsoid of magnetic susceptibility was oblate and the axis of minimum susceptibility was normal to the cleavage while the axis of maximum susceptibility was parallel to the extension lineation seen in the rock. He was able to correlate magnetic anisotropy with the strain determined

using the "March model" (March 1932) on measuremants of grain preferred orientation from X-ray goniometry (Oertel 1970). Rathore (1979) on the basis of these results proposed the relationship

$$(k_f/k_i) = (l_f/l_i)^a$$

where i=1,2,3 are the orthogonal principal axes and where k_f and k_i are the final and initial susceptibilities along a given principal axis i, and lf and li are the final and initial axial dimensions of the strain ellipsoid. Though reduction spot data was available at the localities measured, Rathore (1979) chose to use the March model (March 1932) to determine the strain. Siddans (1976) has expressed doubts regarding the validity of measuring strain using X-ray goniometry , but Oertel (1978) suggests that this is an accurate determination of the strain in a rock. Rathore (1980) suggested that the relationship given in the equation above may infact be universal for all rock types, where the exponent = 0.145.

The studies of Kligfield, Pfiffner and Lowrie (1979), Kligfield, Owens and Lowrie (1981) and Kligfield, Pfiffner and Lowrie (1982) show a correlation between magnetic anisotropy and the strain determined from reduction spots and oolites. These results are more acceptable since the strain was determined from conventional strain markers. In the case of the reduction spots the correlation of the magnetic anisotropy with the strain path, determined by Graham (1978), is remarkably close. This suggests that the correlation between the magnetic anisotropy and the strain may be realistic. To achieve their correlation Kligfield et al (1981) and Kligfield et al (1982) used a graph of $Mi = (ki-\bar{k}/\bar{k})$ where $\bar{k} = (kmax + kint + kmin)/3$ (i=1,2,3) against Ei, the principal logarithmic strain and this form of diagram will be used in this thesis.

Coward and Whalley (1979) in a study of cleavage development on Lochalsh found no correlation between the degree of anisotropy and the strain. They suggest that magnetic anisotropy could be used as a method of mapping the distribution of deformation mechanisms as each mechanism made an important and often contrasting contribution to the magnetic anisotropy. These results confirm the theoretical work of Owens (1974b) who suggested that individual grain anisotropy, the initial and final preferred orientation of grains, and the strain response model (which can take account of the different deformation mechanisms) were important in the production of a given magnetic anisotropy. Recently, the effect of deformation mechanisms on the magnetic anisotropy of weakly deformed rocks has been studied by Borradaile and Tarling (1981).

Magnetic anisotropy measurements were made on the Kishorn Nappe for three reasons.

(a) It was hoped to determine the orientation and distribution of weak rock fabrics in areas of low strain following the work of Graham (1954).

(b) Following the results of Rathore (1979,1980) and Kligfield et al (1981),it was hoped to establish a relationship between the strain and the magnetic anisotropy for the rocks of the Kishorn Nappe and to use this to provide an estimate of the finite strain throughout the area studied.

(c) The measurements were used to determine the influence of deformation mechanisms seen in thin section on the magnetic anisotropy and to determine the distribution

of these mechanisms using magnetic anisotropy.

The results from sites at which palaeomagnetic work has been undertaken can be compared with magnetic anisotropy results to determine any influence which the magnetic anisotropy may have on the remanent direction

Section 6A Practical Techniques

As described in chapter 5. conventional palaeomagnetic sampling using a portable rock drill proved unsuitable in this study. At sites where palaeomagnetic studies were undertaken several of the cores drilled were used for magnetic anisotropy. At the sites where magnetic anisotropy was studied alone, one or two blocks were taken. A surface on each block was orientated, before removal, by means of a magnetic compass. The blocks were drilled in the laboratory using a 2.54 cm. cylindrical drill and the cores obtained were sliced into lengths of 2.3cm using a diamond saw. The cores were sliced from base upwards and any weathered material was discarded. Each slice was numbered in the following manner, the block number, followed by a letter for the core and then a single digit recording the position of the slice within the core. The number (1) being the lowest in the core and by implication the least weathered. Sufficient cores were drilled from each block to allow approximately seven measurements of the anisotropy to be made. The results from sites at which several blocks were taken are not affected by the orientations of the cores and therefore it is thought that the results obtained truely reflect the anisotropy of magnetic susceptibility in these rocks (Addison 1981). The scatter of axes at a given site rarely differed for the different number of blocks sampled. For this reason it is thought that little precision was lost where only one block was taken.

The measurements of the anisotropy of magnetic suseeptibility were made on a Digico Complete Results Anisotropy Delineator. Measurements were made on the equipment in the Department of Physics at the University of Newcastle-Upon-Tyne and their permission is gratefully acknowledged. This piece of equipment was used as the coil configuration has been modified by Addison (1980). The results are output in terms of declination and inclination relative to the core and these were corrected to in situ directions. The orientation of the core relative to the orientated surface was obtained using the method described in chapter 5..

The orientation of the susceptibility ellipsoids will be presented on equal area stereographic projections. All directions were made to fall in the lower hemisphere. The following symbols convention will be used throughout this thesis, circle - maximum principal susceptibility, triangle - intermediate principal susceptibility and square - minimum principal susceptibility. This convention may differ from other workers and caution should be exercised when comparing data. The orientation of bedding and cleavage are plotted as great circles on the stereopgraphic projections. the shape of the ellipsoids of susceptibility will be illustrated on a series of Flinn plots (Flinn 1962 , Ramsay 1967) where

$$A_m = \ln(k_1/k_2) \qquad B_m = \ln(k_2/k_3)$$

Due to the nature of the measurements of the principal susceptibilities the ratios given above are strongly dependent on the mean susceptibility of the rocks. As a result, the position of the data relative to the origin of the Flinn plot is dependent on the mean susceptibility and therefore the Flinn plot may only be used to compare the shape of the ellipsoids of susceptibility. An additional parameter is necessary to describe the degree of anisotropy of the specimen. Such parameters have

been summarised by Hrouda (1981) and these are

k_1/k_3	Nagata
$100(k_1 - k_3)/k_1$	Graham
$(k - k_3)/k_2$	Rees
$(k - k_3)/k_m$	Owens
$\exp(2((n_1-n)^2+(n_2-n)^2+(n_3-n)^2))$	Jelinek

The last parameter is very similar to the value Hs given by Coward and Whalley (1979) which is

$$H_s = \frac{2}{3}\left((k_1'-k_2')^2 + (k_2'-k_3')^2 + (k_3'-k_1')^2 \right)^{\frac{1}{2}}$$

To describe the degree of anisotropy correctly, the parameter must be independent of both the mean susceptibility of the specimen and of the shape of the ellipsoid. With the exception of the parameters proposed by Jelinek (1981) and Coward and Whalley (1979) all the above parameters have been rejected as they do not conform to both of these requirements. In the study of deformed rocks we require a parameter which reflects the amount of mechanical work done to arrive at the anisotropic state and thus ellipsoids of different shape which have undergone the same total amount of shape change have the same value. Hossack (1968) suggested that the parameter E_s could be used in the measurement of the total amount of work done to arrive at a finite strain state. Coward and Whalley (1979) adjusted his equation to facilitate its use in the study of magnetic anisotropy. However, the equation they present is normalised by the bulk susceptibility which is the value of the susceptibility measured along the axis of the core. This value provides the CRAD with the necessary information to scale the susceptiblity ellipsoids. When this value is used to normalise the principal axes of susceptibility it is somewhat arbitrary as it depends on the orientation

of the ellipsoid of susceptibility relative to the core. It is suggested that the mean susceptibility or the susceptibility of an equal spherical volume should be used to normalise the axes and thus provide a relationship which is independant of the mean susceptibility. It is difficult to decide whether the mean susceptibility or the susceptibility of an equal spherical volume is the most geologically realistic. If we consider deformation without volume change then the latter is most realistic. However, in the case of magnetic susceptibility the numerical value of both normalising factors is identical and thus the parameter Hs is given by the equation

$$Hs = \frac{2}{3}\left(\left(k_1' - k_2'\right)^2 + \left(k_2' - k_3'\right)^2 + \left(k_3' - k_1'\right)^2\right)^{\frac{1}{2}}$$

where $k_i' = \ln\left(k_i/\bar{k}\right)$ and $\bar{k}$ is given by $(k_1+k_2+k_3)/3$ or $(k_1 \cdot k_2 \cdot k_3)^{\frac{1}{3}}$ depending entirely on preference. In this thesis the mean susceptibility has been used as the normalising factor.

The results of the study will be described in three sections, the southern area, the northern area and the central area. These areas are shown in chapter 2. and correspond to different structural levels. This sequence was chosen as it follows the deformation sequence from low strain to the bedding parallel fabric which is occasionally overprinted by the transverse cleavage.

Section 6B Magnetic Anisotropy Results From The Southern Area of The Kishorn Nappe

The anisotropy of magnetic susceptibility was measured at twelve localities which are shown in Figure 6.B.1. to determine whether a fabric could be found which can be related to the Eishort Anticline. The Eishort Anticline

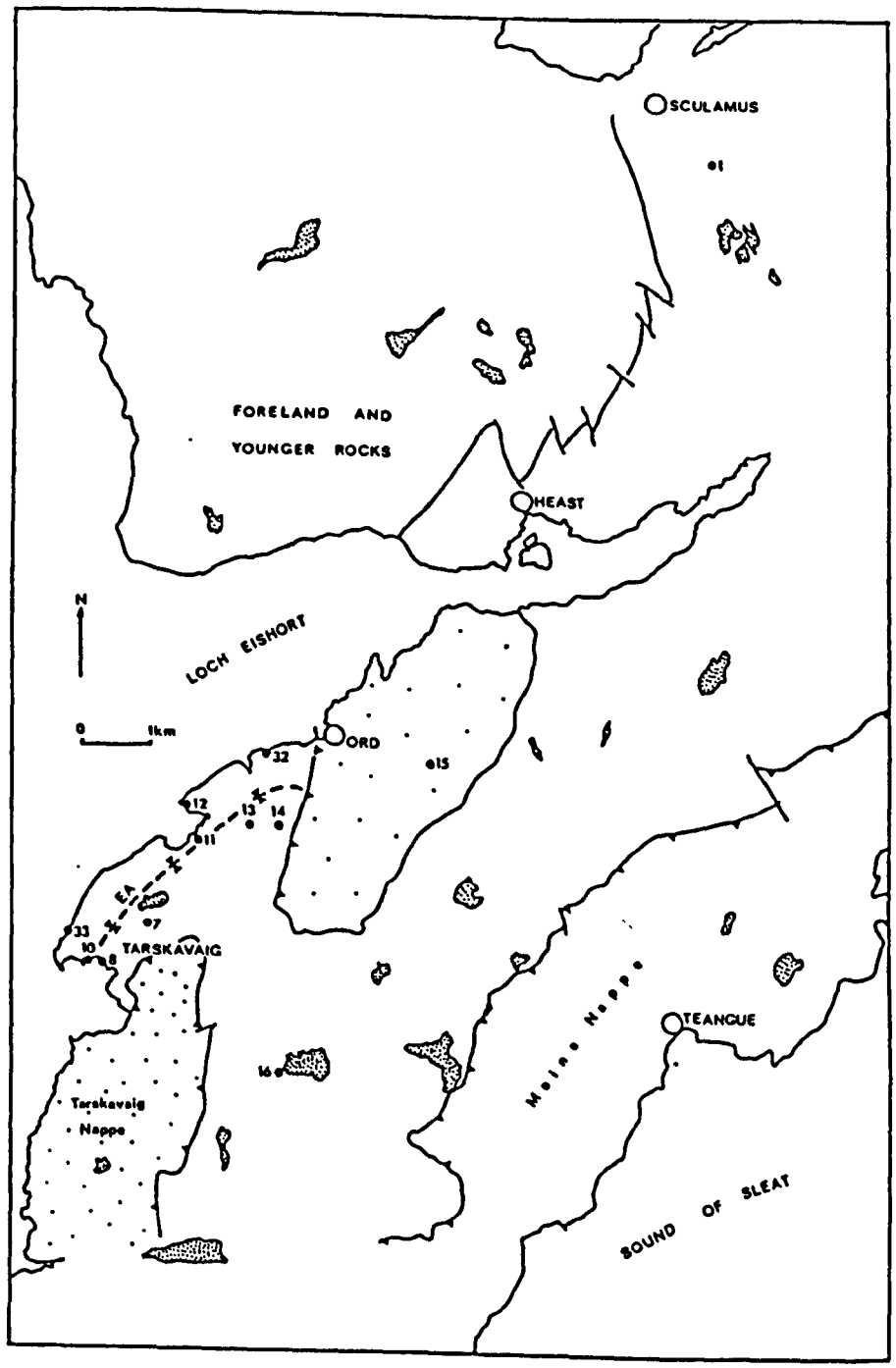

Figure 6.8.1. A simplified geological map showing the distribution of sites around the Eishort Anticline. EA = the axial trace of the Eishort Anticline.

is the lowest fold within the Kishorn Nappe and it is exposed between the villages of Ord and Tarskavaig. The geometry of the fold has been described in chapter 2.. Site 1, is from the common, correct way up limb, between the Eishort Anticline and the Lochalsh Syncline and it represents the site least involved in any of the recumbent folding. With the exception of sites 15 and 16 the remaining sites were collected around Tarskavaig and Ord. The sites are from both limbs of the Eishort Anticline and in particular from the hinge of the Anticline on Tarskavaig beach. Site 15 was collected from within the Ord Window and site 16 was collected on the steep limb of a large angular fold on the correct way up limb of the Eishort Anticline. No cleavages were seen in any of these sites and in thin section only the siltstones of sites seven and eight (near Tarskavaig) showed any evidence of deformation (see chapter 3. section C). The majority of these sites were sampled from the Applecross Formation. However, some samples were taken from sandstones and siltstones in the upper parts of the Kinloch Formation. The grid reference and dominant rock type of each of these sites is given in Table 6.B.1..

Figure 6.B.2. shows the orientation of the axes of susceptibility for the sites around the Eishort Anticline. There is a large scatter in the orientation of a particular axis at any one site. It is thought that this reflects the weakness of any fabric which may be present and is not due to measurement error. Results will be presented later from sites which have a strong fabric and these sites show less scatter in the orientation of the principal axes of susceptibility. The scatter in the deformed sites is thought to be due to measurement errors as a similar amount of scatter is produced during repeat measurements of a single specimen. The common result for the sites around the Eishort Anticline is that the axes of maximum and

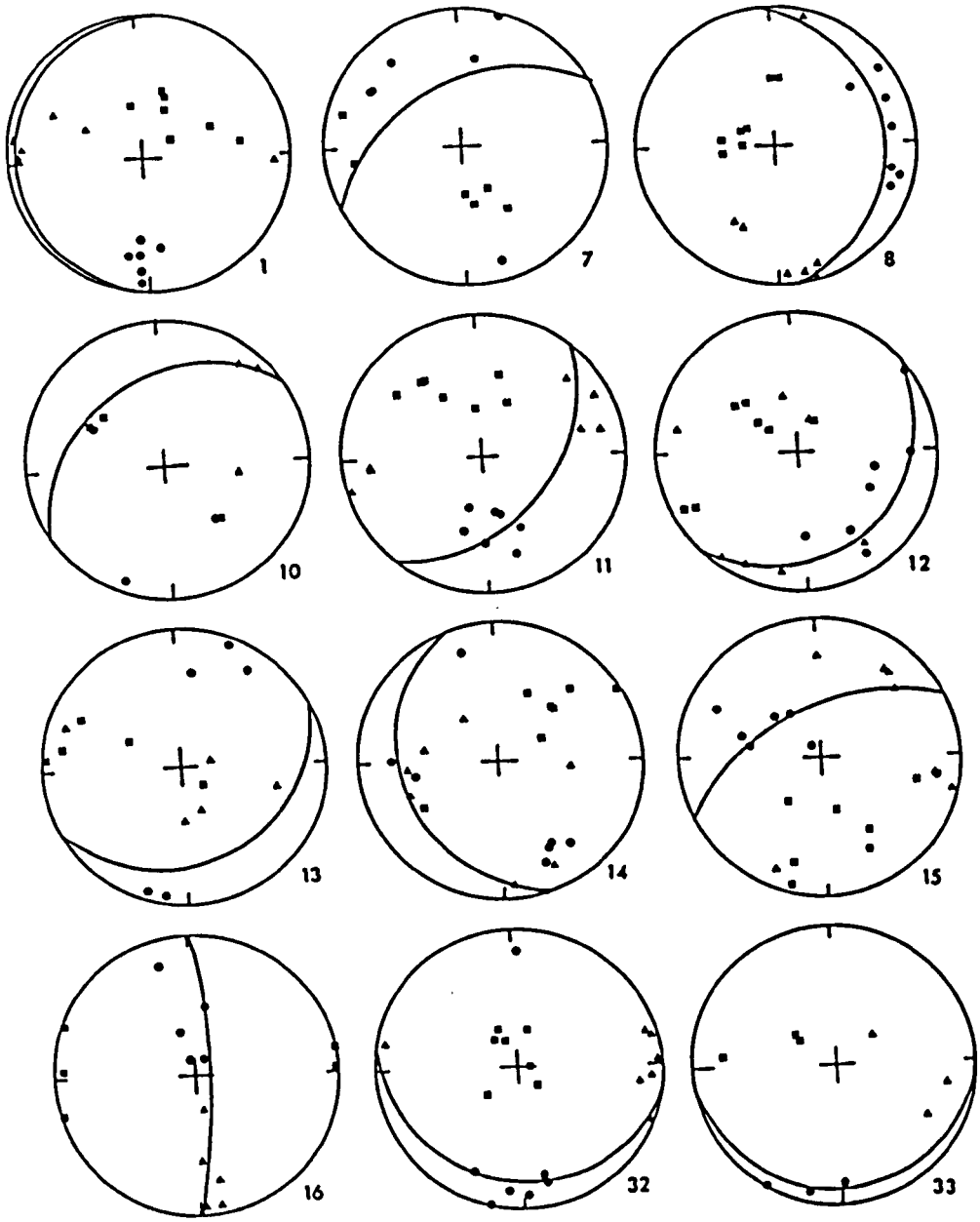

Figure 6.8.2. Stereograms showing the orientations of the axes of magnetic susceptibility for the sites around the Eishort Aiticline. The projection is lower hemisphere, equal area and the grear circle marks the position of the bedding. The axes convention used is given in the text. ◆ = pole to bedding.

Table 6.8.1.

Site No.	Grid Reference	Orientation of Bedding	Rock Type	Mean Hs
1	NG 67402200	175 08	Sandstone	0.022
7	NG 59001030	241 52	Siltstone	0.035
8	NG 58330973	356 24	Sandstone	0.014
			Siltstone	0.049
10	NG 58080985	236 40	Siltstone	0.053
11	NG 59551150	226 134	Sandstone	0.038
12	NG 59751200	229 142	Sandstone	0.019
13	NG 60501180	060 26	Sandstone	0.017
14	NG 60881178	160 32	Sandstone	0.015
15	NG 63201275	245 61	Sandstone	0.029
16	NG 61100820	359 98	Siltstone	0.054
32	NG 60701290	278 159	Sandstone	0.028
33	NG 57871017	258 168	Sandstone	0.039

intermediate susceptibility lie in the bedding plane and the axes of minimum susceptibility lie around the pole to the bedding. This result is independent of the dip of the bedding or the position of the site within the Eishort Anticline.

There are varying degrees of scatter but these cannot be related to the dip of the bedding or the position of the site within the Eishort Anticline.

The mean susceptibility of all of these sites is very similar and the anisotropy of the results may be compared on the Flinn plot. Figure 6.B.3. shows the combined results from sites 7, 10 and 15. At these sites fine sandstones, siltstones and shales were sampled. The ellipsoids determined for these sites are strongly oblate and the degree of anisotropy is not related to the dip of the bedding.

The results from sites 1,11,12,13, 14 and 15 are shown in Figure 6.B.4.. There is a much wider range in ellipsoid shape and in general, the degree of anisotropy is much less than the sites of Figure 6.B.3.. All of the latter sites were sampled from the Applecross Formation and the range in ellipsoid shape reflects small variations in the almost spherical ellipsoids of susceptibility.

The results from site 8, (Figure 6.B.5.) are plotted seperately as both siltstones and feldspathic sandstones were sampled from this site. As shown in Table 6.B.1. the Hs values of the shales are much greater than those of the sandstones. The feldspathic sandstones or grits show a range in ellipsoid shape and have a much lower degree of anisotropy. This site shows the contrasting behaviour of the two rock types to the same conditions. A similar contrast is seen between the sites shown in Figures 6.B.3. and 6.B.4.. In these sites, the shales

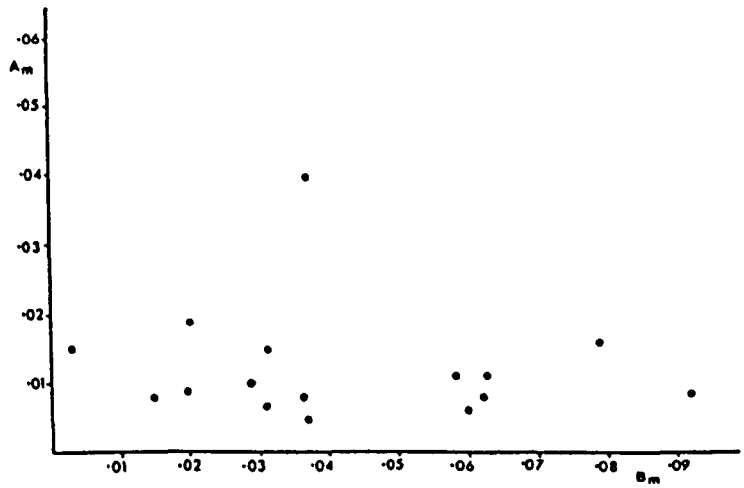

Figure 6.B.3. A Flinn plot showing the shape of the susceptibility ellipsoids from sites 7, 10 and 15.

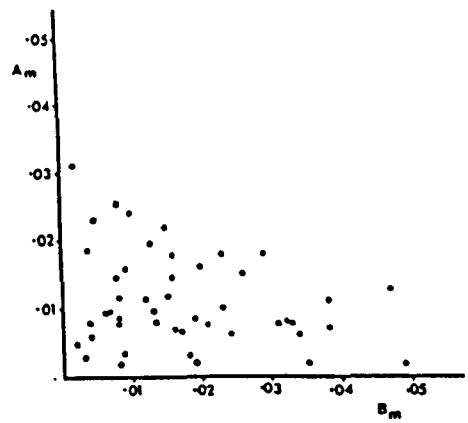

Figure 6.B.4. A Flinn plot showing the shape of the susceptibility ellipsoids from sites 1, 11, 12, 13,14 and 15.

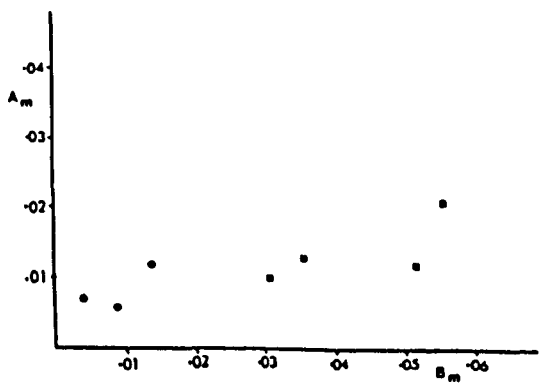

Figure 6.B.5. A Flinn plot of data from site 8. At this site two rock types were studied, coarse feldspathic grits (●) and fine sandstones and siltstones (■).

have higher Hs values and tend to be more anisotropic.

The anisotropy of magnetic susceptibility measured at these sites around the Eishort Anticline show no magnetic fabric which may be related to the Anticline or the Tarskavaig Synform. The axes of maximum and intermediate susceptibility lie in the bedding plane and it is thought that this could represent a depositional fabric or a compactional fabric. The differing degrees of anisotropy shown by the siltstones and the sandstones may be a reflection of the differing amounts of compaction which the rocks have suffered. The siltstones with a high percentage of phyllosilicates were able to compact to a greater extent and produce more anisotropic ellipsoids of susceptibility and consequently greater Hs values. It is unlikely that sandstones were able to compact to the same extent and therefore the magnetic fabric recorded in these rocks is thought to be depositional or slightly compactional in origin. Thus, the only rock fabric reflected by the magnetic anisotropy in these sites around the Eishort Anticline is a depositional and/or compactional fabric.

Related to this study of the Eishort Anticline a small fold of approximately 1 metre limb length was sampled. The fold is exposed on Tarskavaig beach and it was possible to sample several different dip values around the fold. The fold is chevron like in style and the bedding surfaces have a thin layer of green chlorite. Often the chlorite forms slickensides which are normal to the fold axis. Relative to the thickness of the bed,the radius of curvature of the fold is small,and this should enhance any strains that may be present due to the folding (Donath and Parker 1964). Figure 6.8.6. shows the orientation of the axes of susceptibility from the samples around the fold and Figure 6.8.7. shows the shape of the susceptibility ellipsoids on a Flinn plot. In general, the axes of maximum and

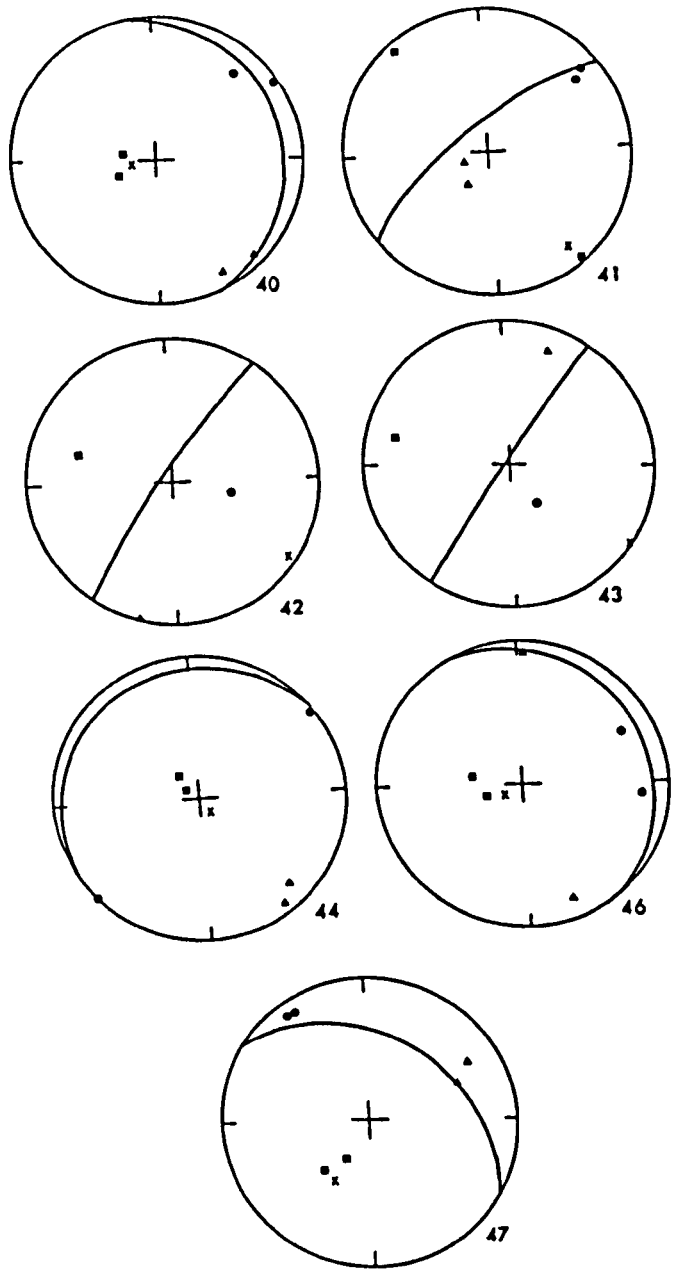

Figuer 6.8.6. Stereograms showing the orientations of the axes of magnetic susceptibility for various positions around a minor fold on Tarskavaig beach. X= pole to bedding.

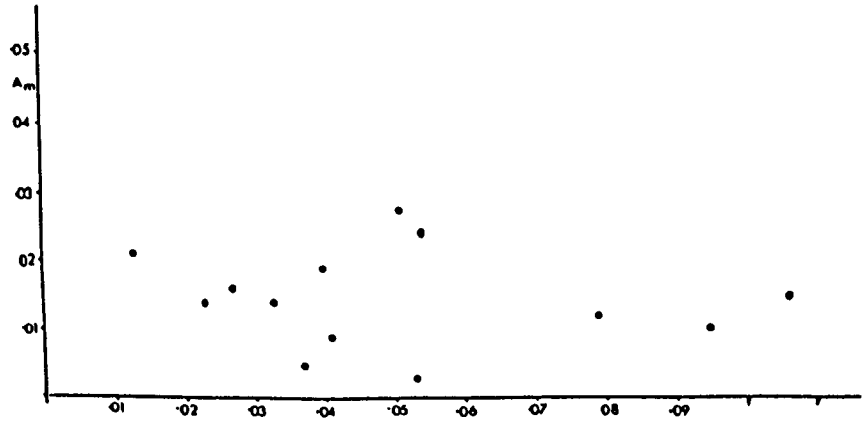

Figure 6.8.7. A Flinn plot showing the shape of the ellipsoids of magnetic susceptibility around the minor fold from Tarskavaig beach. (Site 9).

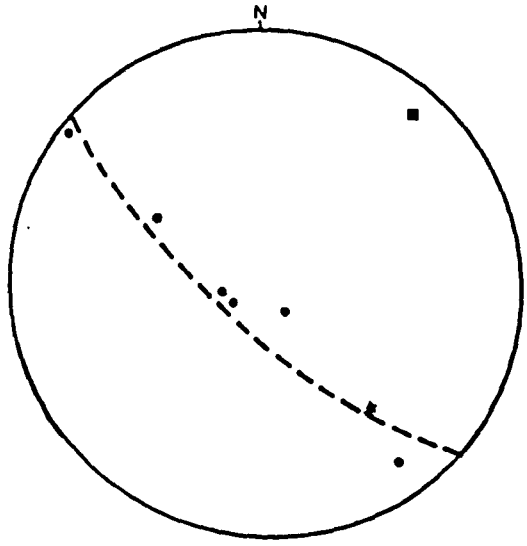

Figure 6.B.8. Poles to bedding from around the minor fold studied on Tarskavaig beach, ■= fold axis.

intermediate susceptibility lie very close to the bedding plane. However, in two cases, samples 42 and 43 , the axes have a similar orientation relative to the bedding but the angular difference between the axes and the bedding is much greater than in the rest of the samples. This does not appear to be related to the dip of the bedding since sample 41 which has a similar dip, has axes of susceptibility which lie very close to the bedding. This discrepancy in the orientation of the axes for the samples 42 and 43 may be due to measurement error. It is doubtful that these two results represent any tectonic fabric since the inferred cleavage plane, which should include the axes of maximum and intermediate susceptibility cannot be related to the geometry of the fold which is shown in Figure 6.8.8.. The cleavage would cut across both limbs of the fold at a very high angle. With the exception of the samples 42 and 43 the axes of maximum susceptibility lie in the northeast quadrant. This strong preferred orientation in the axes of maximum susceptibility may be due to sedimentary or tectonic processes. The preferred orientation may reflect a current direction but this is thought unlikely. Alternatively, this may reflect a tectonic fabric which may be one of two types, either there is extension parallel to the fold axis or there is a compaction fabric which has been modified by shortening parallel to the axial planar fold and this has produced a strong lineation parallel to the fold axis. This is an apparent extension lineation and may have been produced following the method described by Ramsay and Wood (1973). Such a fabric was recorded by Kligfield et al (1981) in a study of the magnetic anisotropy of Permian mudstones which were described by Graham (1978).

The shape of the anisotropy ellipsoids around the minor fold on Tarskavaig beach tends to be oblate (Figure

6.B.7. with only one prolate ellipsoid recorded. The samples collected are siltstones or fine sandstones and the oblate shape of the ellipsoids appears to reflect a depositional fabric of oblate phyllosilicate grains and/or a compaction fabric as described previously. It is considered that some tectonic modification of this fabric must have occurred to produce the strong preferred orientation in the axes of maximum susceptibility for such oblate ellipsoids. In oblate ellipsoids, the axes of maximum and intermediate susceptibility will be very similar and some feature of the rock fabric must be present to produce a strong preferred orientation in the axes of maximum susceptibility.

It would appear, that a compactional fabric has been modified by some form of tangential longitudinal strain or layer parallel shortening during the development of the fold. This produced a strong preferred orientation in the axes of maximum susceptibility. Borradaile and Tarling (1981) have shown that in low grade rocks the axes of maximum susceptibility often lie parallel to the bedding cleavage intersection lineation. This situation is similar to the fold studied on Tarskavaig beach. However, no cleavage can be seen in thin sections from this area (chapter 3. section C).

The lack of any tectonic fabric which may be related to the Eishort Anticline and the associated minor folds suggests that they developed by flexural slip processes which involved little or no deformation of the layers. No strong magnetic fabric was found in any of the sandstones from around the Eishort Anticline and this is taken to indicate a lack of internal deformation. In the shales and the siltstones a strong compactional fabric may be present. In the minor folds a weak tectonic fabric may be present but it is not possible to determine the nature of this fabric. It may be due to some

component of shortening producing an axial planar cleavage or alternatively, it may be a small accomodation strain related to the development of the chevron style folds.

Section 6C Magnetic Anisotropy Results From The Northern Area Of The Kishorn Nappe

Figure 6.C.1. shows the position of the sites within the northern area of the Kishorn Nappe from which samples were taken for the measurement of the anisotropy of magnetic susceptibility. In general, medium grained sandstones of both the Sleat Group and the Applecross Formation were collected,though around Carn na Bhealaich Mhoir samples of the basal conglomerate were also taken. Near Strome Castle on Lochcarron samples of Lewisian Gneiss were also collected. Lochcarron (Figure 6.C.1.) consists entirely of the overturned limb of the Lochalsh Syncline (Peach et al 1907, Johnson 1955a). On Lochalsh and northern Skye both limbs of the fold may be seen. The bedding on the overturned limb of the Lochalsh Syncline dips gently to the east and the bedding parallel fabric is often seen. However, at some localities no fabric could be seen and samples were taken to determine whether the bedding parallel fabric is present throughout the northern area. The transverse cleavage is seen on both limbs of the Lochalsh Syncline. On the normal limb of the Syncline the cleavage is seen mainly in sandstones of the Applecross Formation. Further east, on the inverted limb,the cleavage is only seen in shaly units. The samples were collected to assess whether the transverse cleavage has an affect on the bedding parallel fabric seen in the sandstones.

In general, the bedding parallel fabric tends to be stronger in the east of the area (see Figure 2.D.10.). Samples were collected to determine whether this is associated with an

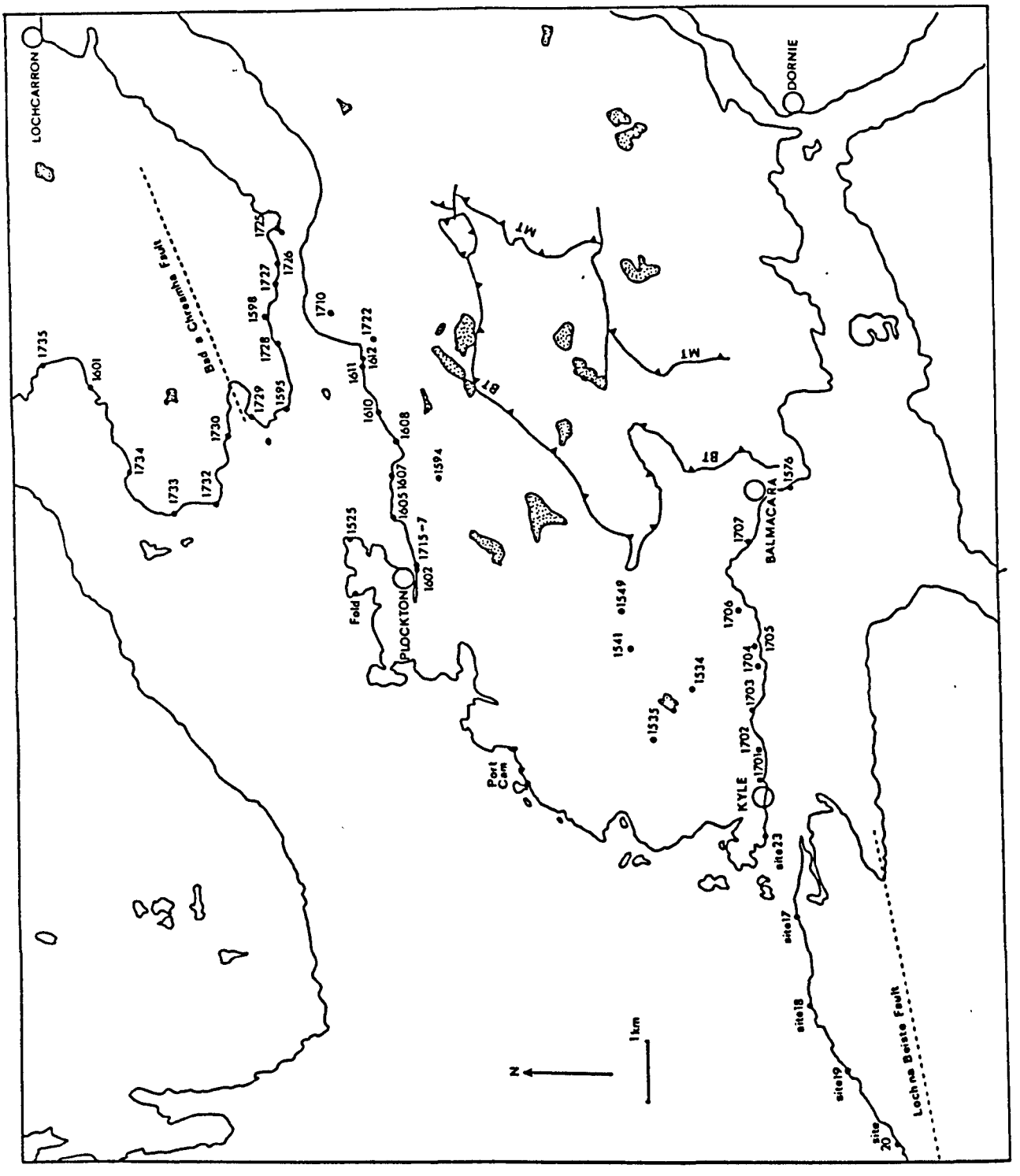

Figure 6.C.1. Sites from the northern area of the Kishorn Nappe which were studied using magnetic anisotropy. The sites to the east of Kyle lie on the overturned limb of the Lochalsh Syncline and the sites west of Kyle lie on the correct way up limb of the fold.

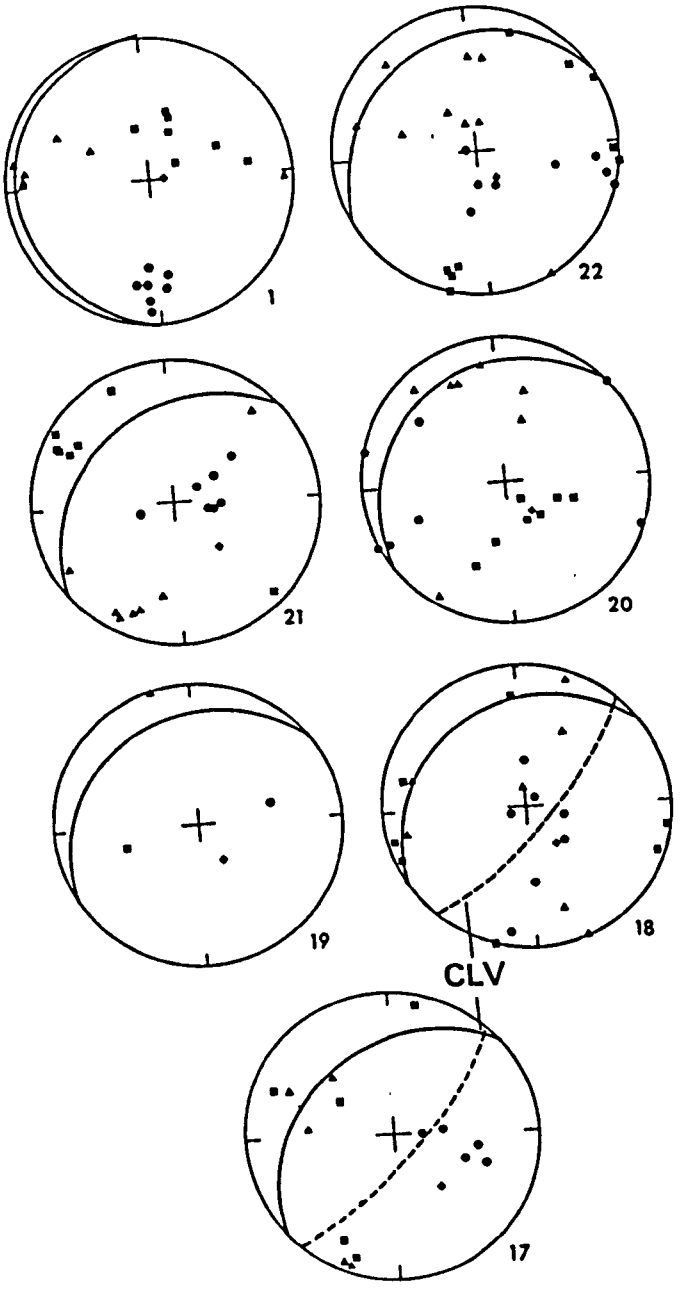

Figure 6.C.2. Stereograms showing the axes of magnetic susceptibility for the sites studied, between Broadford and Kyle, on the correct way up limb of the Lochalsh Syncline. ◆= pole to bedding.

increase in the anisotropy of magnetic susceptibility. Any variation in the anisotropy of magnetic susceptibility towards the east could reflect changes in the cleavage forming process and variations in the finite strain. A comparable study was made by Coward and Whalley (1979) who sampled a section between Kyle and Balmacara (see Figure 6.C.1.).

The results from the normal limb of the Lochalsh Syncline in the northern area are shown in Figures 6.C.2. and 6.C.3.. In some respects, they are similar to those of the sandstones around the Eishort Anticline. The degree of anisotropy is similar and there is a wide range in the shape of the susceptibility ellipsoids (Figure 6.C.3.). However, there is a large amount of variation in the orientation of the principal axes of susceptibility both within and between sites. In the sites around the Eishort Anticline there is a tendency for the minimum axes of susceptibility to lie at a small angle to the pole to the bedding. However, in the sites between Broadford and Kyleakin the axes have almost a random orientation and this is thought to indicate the early stages in the development of the transverse cleavage, but no clear relationship is seen between the orientation of the axes and the cleavage plane. Only at site 23 on the normal limb of the Lochalsh Syncline is there a clear grouping of the axes within a particular site.

At site 23 on the Plock of Kyle the transverse cleavage is clearly seen. Figure 6.C.4. shows the orientation of the susceptibility ellipsoids between the Plock of Kyle and Ard Hill. The orientation of the anisotropy of susceptibility at site 23 is difficult to explain as the axes of maximum susceptibility fall about the pole to the bedding. The axes of intermediate and minimum susceptibility lie in the plane of the bedding.

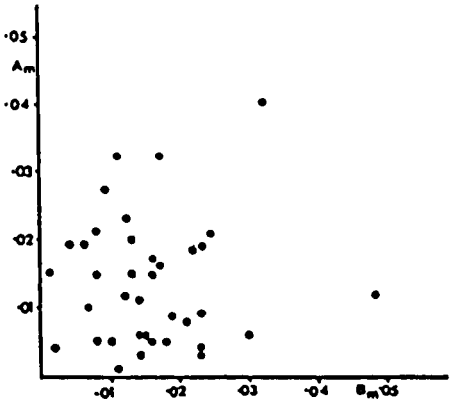

Figure 6.C.3. A Flinn plot showing the shape of the susceptibility ellipsoids on the normal limb of the Lochalsh Syncline between Broadford and Kyle.

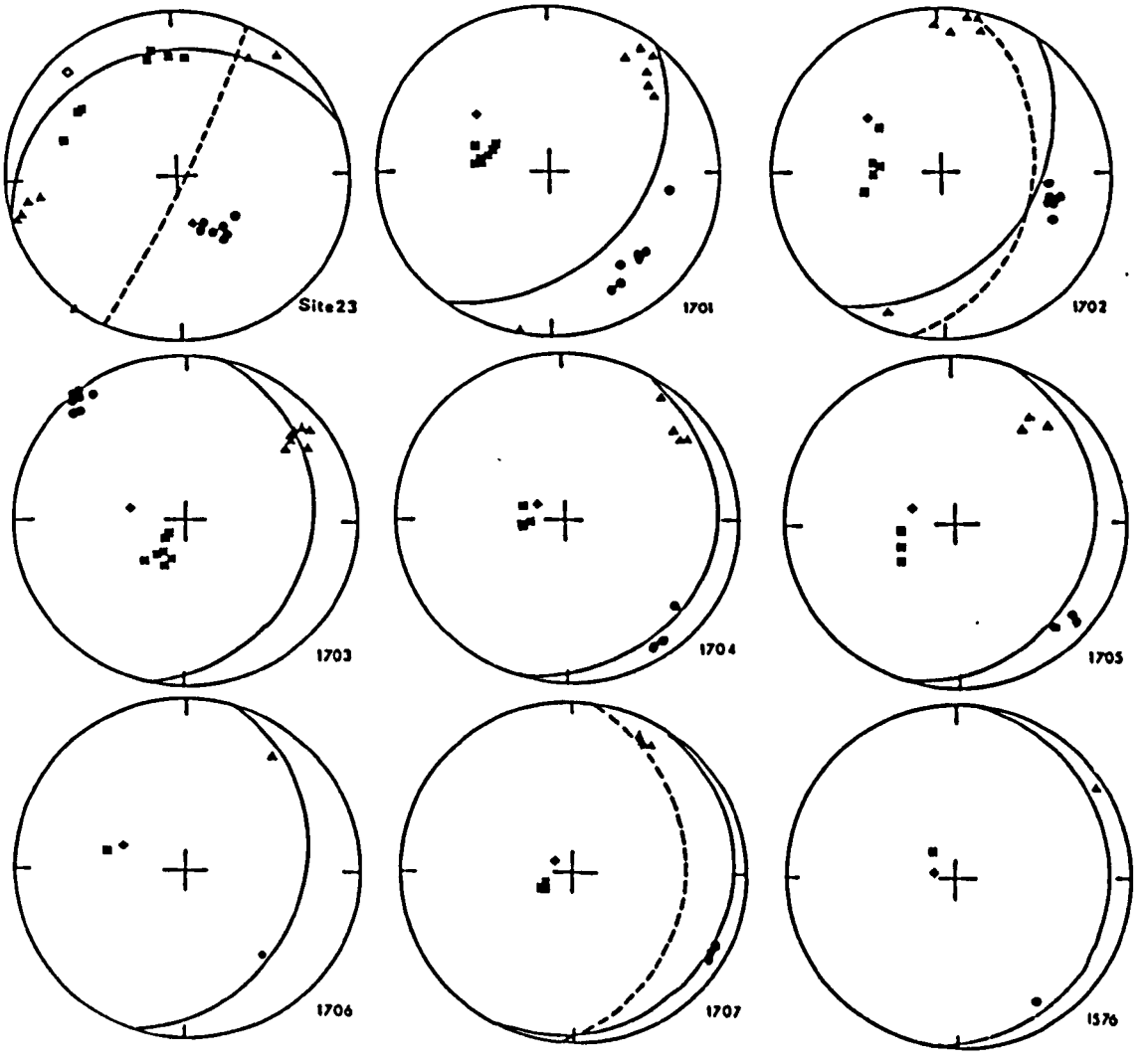

Figure 6.C.4. Stereograms showing the orientations of the ellipsoids of susceptibility between Kyle and Balmacara. Site 23 lies on the correct way up limb of the Lochalsh Syncline. The remaining localities lie on the inverted limb of the fold. ◆= pole to plane and the pecked great circle marks the position of the transverse cleavage.

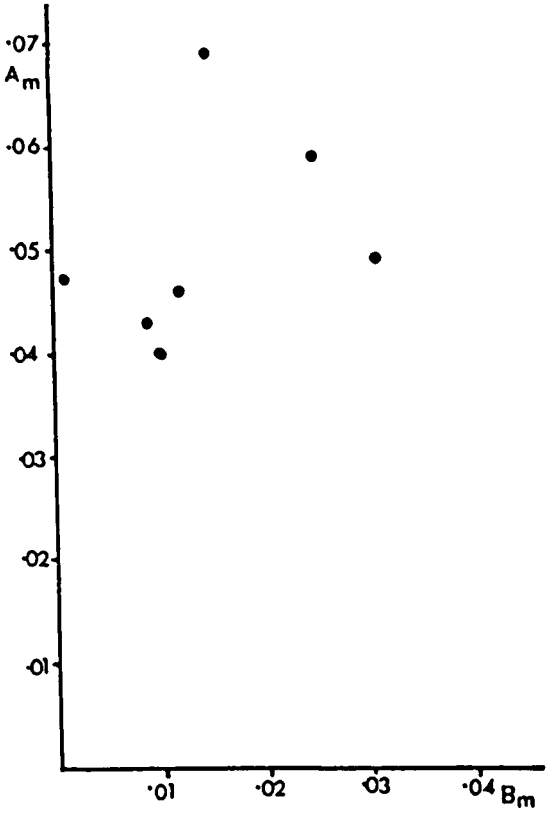

Figure 6.C.5. A Flinn plot showing the shape of the ellipsoids of susceptibility for site 23 on the correct way up limb of the Lochalsh Syncline.

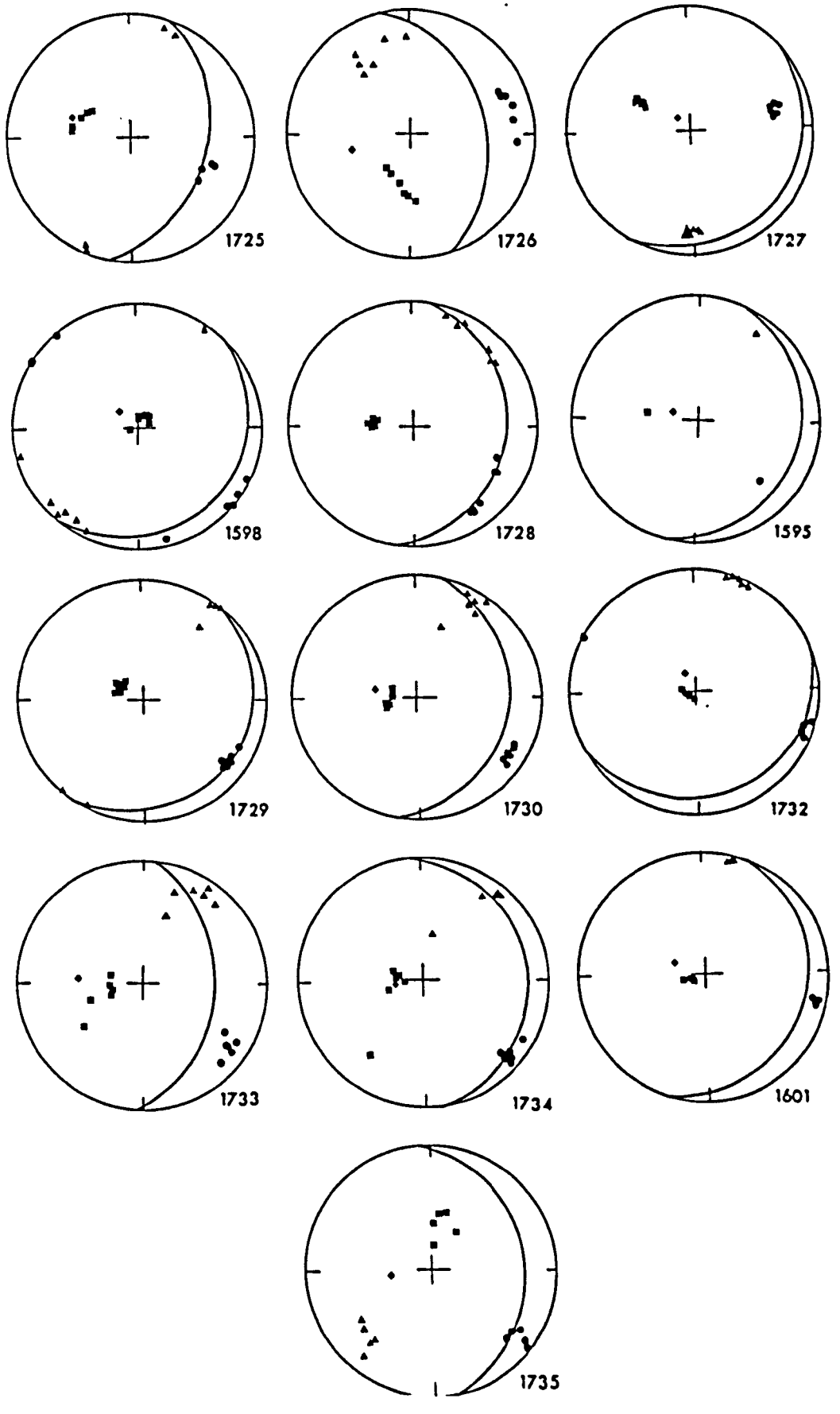

Figure 6.C.6. Stereograms showing the axes of susceptibility obtained for the sites from Lochcarron. All the sites lie on the inverted limb of the Lochalsh Syncline.

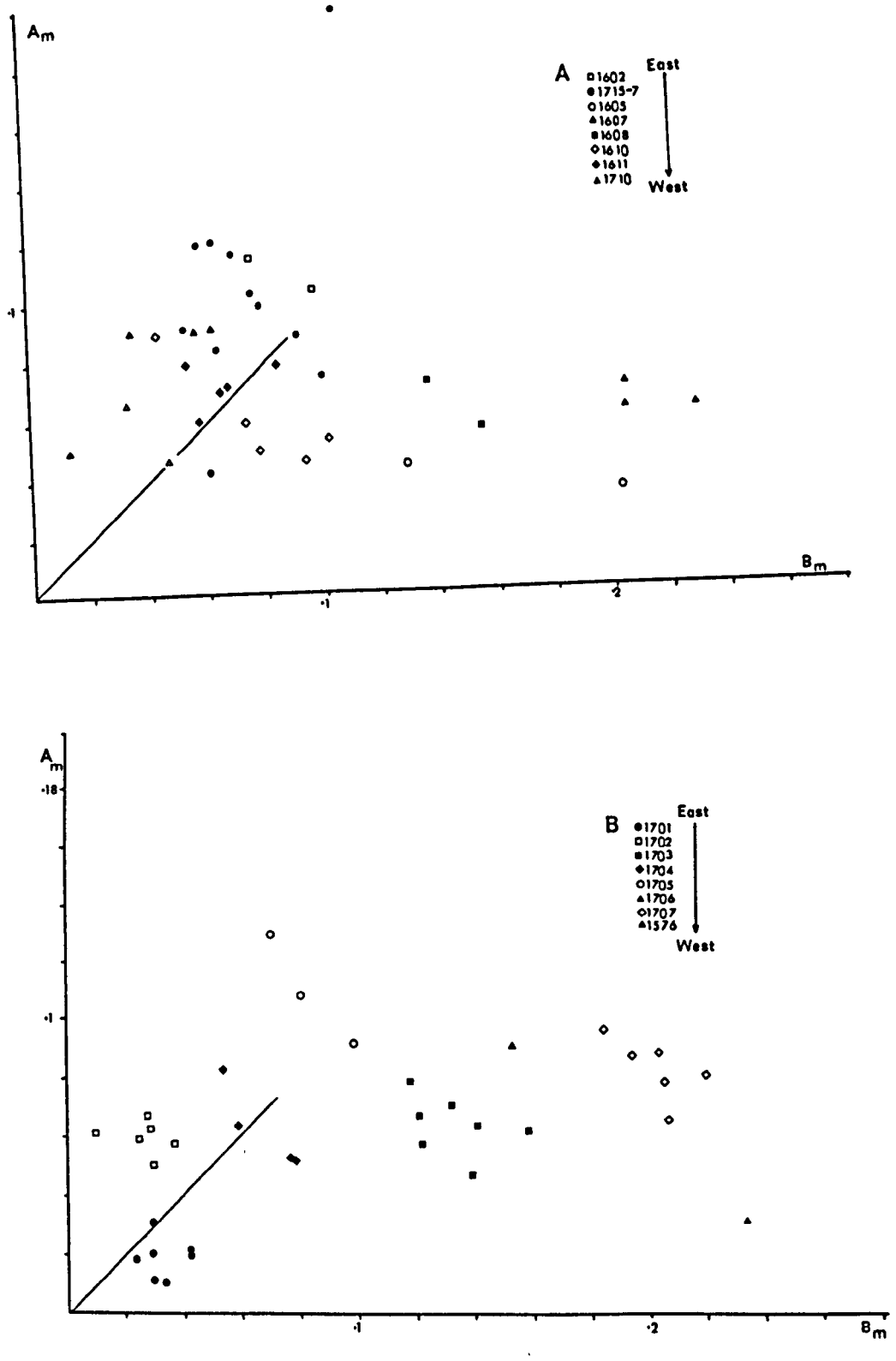

Figure 2.C.8. Cont. Magnetic Flinn Plots showing the ellipsoids of magnetic susceptibility for two areas of the inverted limb of the Lochalsh Syncline in the northern area of the Kishorn Nappe. A. Plockton to Craig, B. Kyle to Balmacara (see Figure 6.C.1. for the position of the sampling sites.). No rational pattern of ellipsoid shape can be seen in these or comparable diagrams for the inverted limb of the Lochalsh Syncline in the northern area of the Kishorn Nappe.

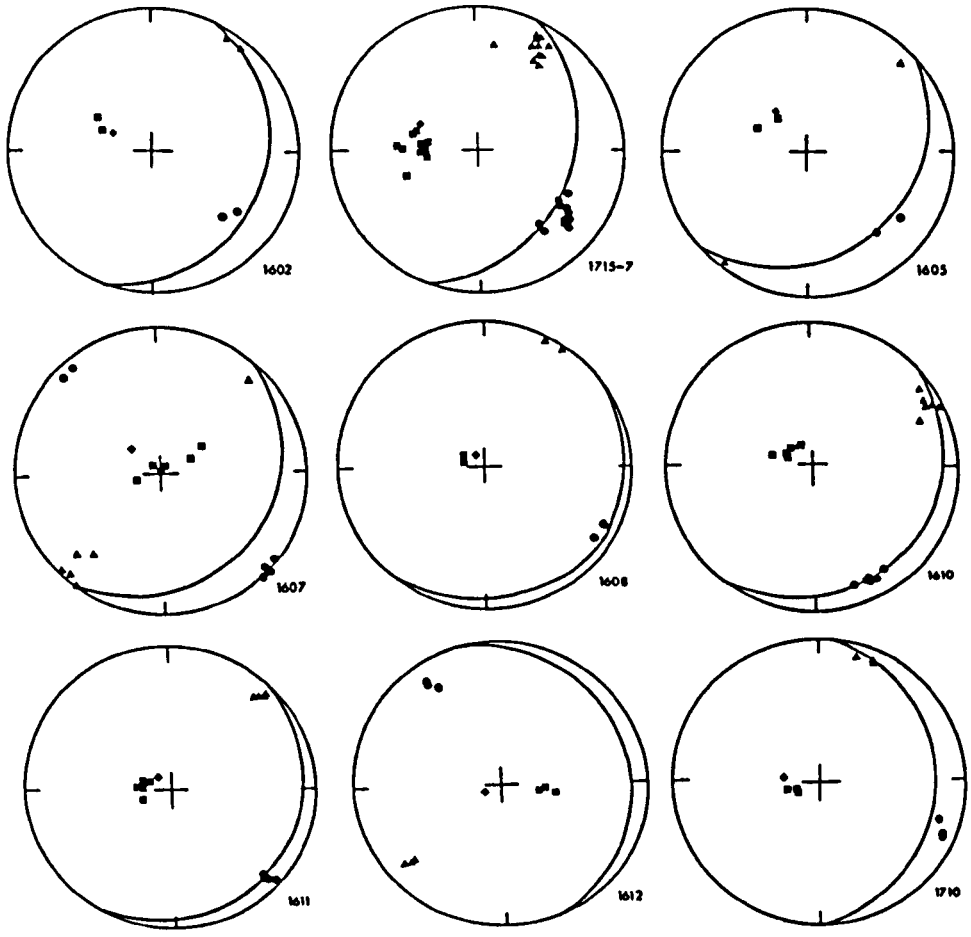

Figuer 6.C.7. Stereograms showing the axes of magnetic susceptibility for the north coast of Lochalsh between Plockton and Fernaig.

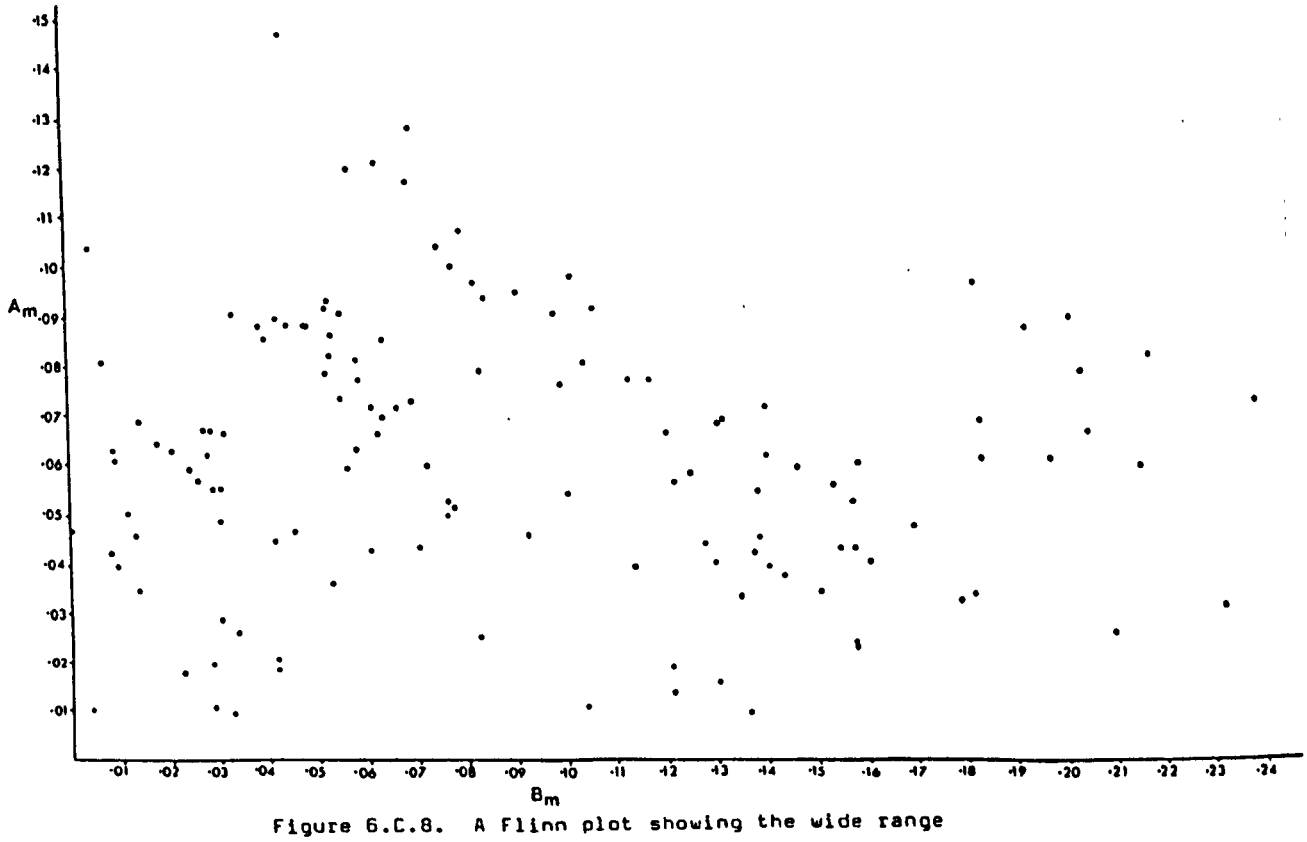

Figure 6.C.8. A Flinn plot showing the wide range in shapes of the ellipsoids of susceptibility on the inverted limb of the Lochalsh Syncline. This data is from the northern area and no systematic pattern can be found when smaller proportions of the data is studied.

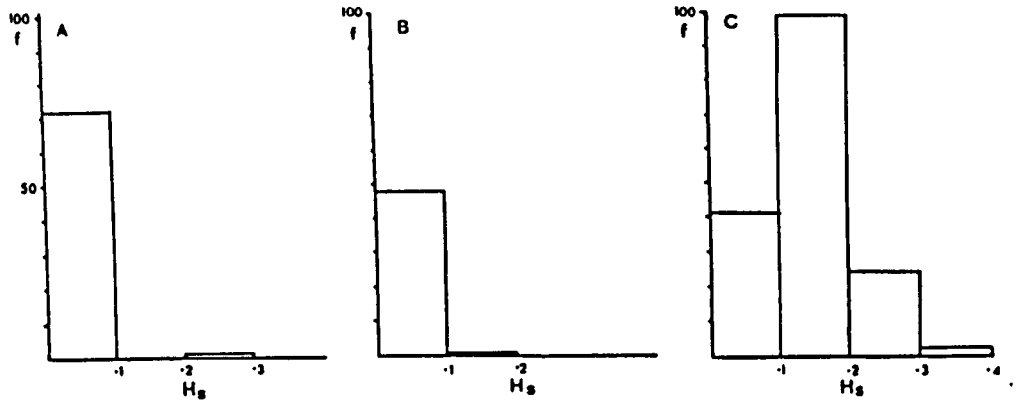

Figure 6.C.9. Histograms of Hs values from (A) around the Eishort Anticline, (B) the normal limb of the Lochalsh Syncline in the northern area and (C) the overturned limb of the Lochalsh Syncline in the northern area.

These axes tend to form two groups on the bedding plane which bear no relationship to any structures seen in the field. The axes of maximum susceptibility lie close to the transverse cleavage plane but is seems unlikely that there is a relationship between the two as the axes of intermediate susceptibility do not show any relationship to the cleavage plane.

Figure 6.C.5. shows the axial ratios of the susceptibility ellipsoids for site 23 on a Flinn plot. The ellipsoids are strongly prolate and this accounts for the strong preferred orientation in the axes of maximum susceptibility. The magnetic fabric at this site remains unexplained. Borradaile and Tarling (1981) suggest that in areas of low deformation, with the development of a spaced cleavage, the axes of maximum susceptibility lie parallel to the bedding - cleavage intersection lineation, but this is not the case at this locality.

Figures 6.C.4.,6.C.6. and 6.C.7. show the orientation of the susceptibility ellipsoids determined for the samples collected throughout the overturned limb of the Lochalsh Syncline in the northern area. There is relatively little scatter in the orientation of the axes at a site and there is no exchange of axes in any of the samples. This is thought to indicate a strongly developed fabric. The axes of maximum and intermediate susceptibility lie close to the bedding plane and the axes of minimum susceptibility lie around the pole to the bedding. In general, the axes of maximum susceptibility plunge gently to the east or southeast and frequently they lie on the bedding plane. Where a lineation is seen in the field the axes of maximum susceptibility lie very close to the lineation. The variation in the orientation of the axes of maximum susceptibility are consistent with the variation in the orientation of the east-southeast lineation. On the

basis of its orientation the anisotropy of magnetic susceptibility appears to be dominated by the bedding parallel fabric. There is no evidence that the transverse cleavage affects the magnetic fabric in any of these sites.

Though, in general, the shape of the susceptibility ellipsoids are consistent at a particular site there is no dominant shape of ellipsoids associated with the bedding parallel fabric. Both oblate and prolate ellipsoids of susceptibility are recorded (see Figure 6.C.10.

The histograms of Hs values shown in Figure 6.C.9. compare the results from around the Eishort Anticline with those from the northern area. The greater degree of anisotropy shown in the sites of the overturned limb suggests that the magnetic fabric associated with the bedding parallel fabric is of tectonic origin. The results show clearly the contrast between the two limbs of the Lochalsh Syncline.

Irrespective of whether a fabric can be seen in the field, it would appear that the bedding parallel fabric is common throughout the sandstones on the inverted limb of the Lochalsh Syncline in the northern area. The transverse cleavage is the dominant fabric in the shale beds. From the magnetic anisotropy measurements it would appear that the sandstones record only a portion of the deformation history suffered by this limb of the fold. The variation in the shape of the susceptibility ellipsoid, in this area, cannot be related to any structure which can be seen in the field. The variation in shape is similar on Lochcarron and Lochalsh and is shown in Figure 6.C.10.. Dominantly oblate zones alternate with dominantly prolate zones across the whole of the northern area. There is no dominant change in the shape of the susceptiblility ellipsoids towards the east.

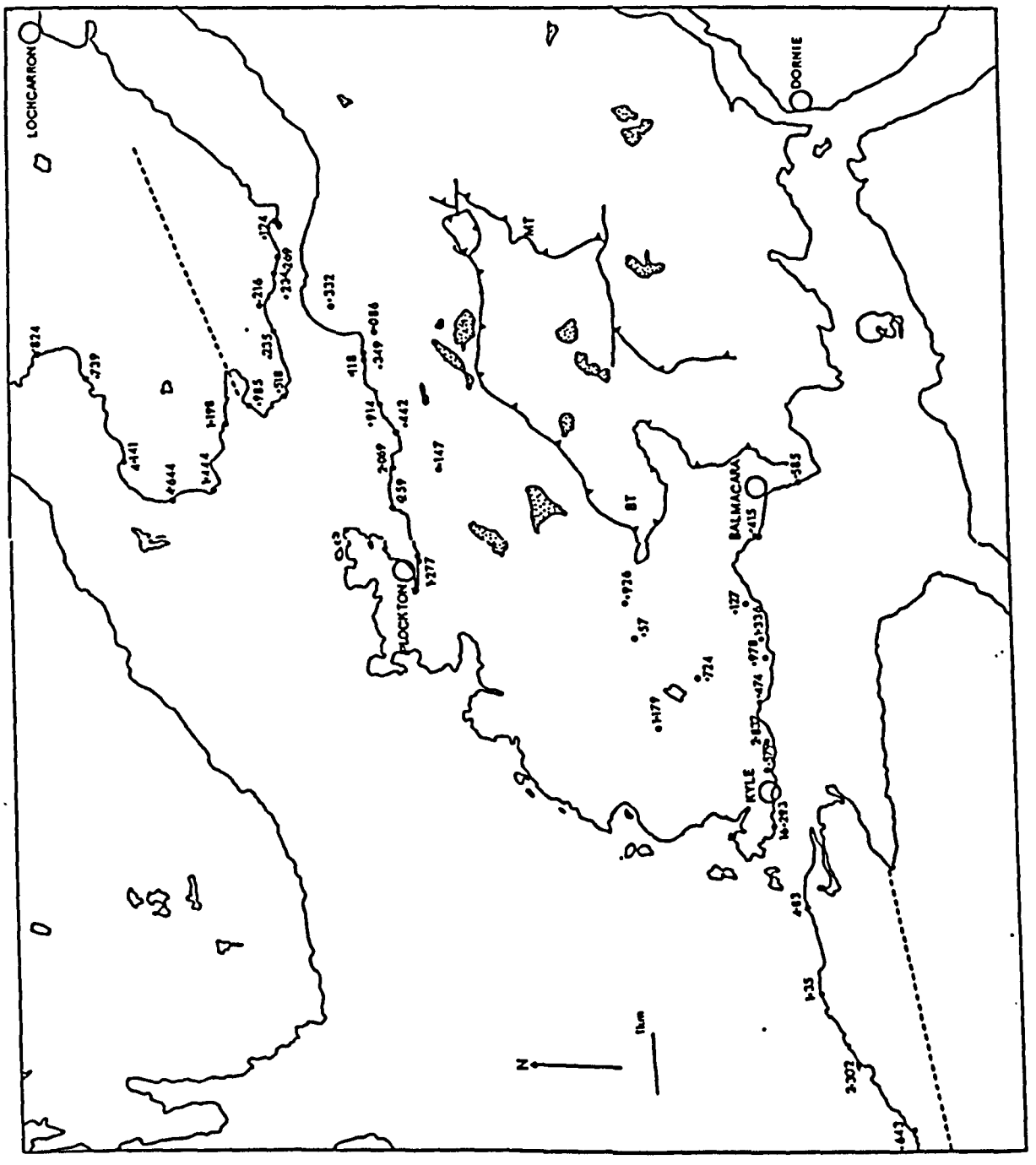

Figure 6.C.10. A map showing the values of Km throughout the northern area of the Kishorn Nappe (see Figure 6.B.1. for the locality numbers).

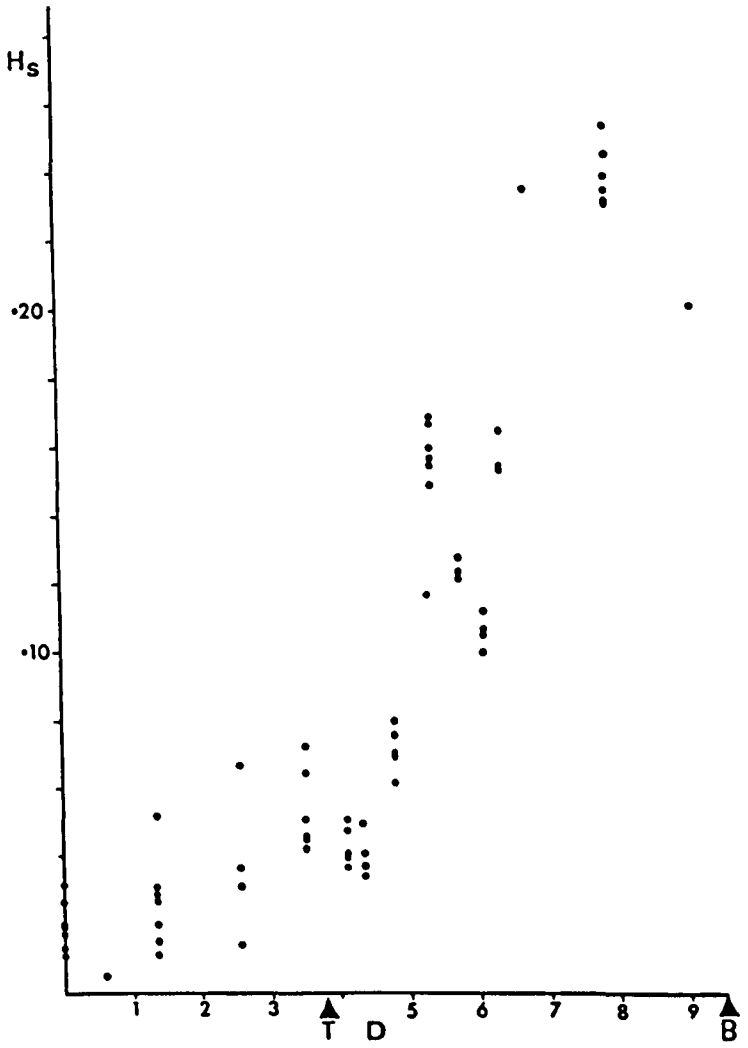

Figure 6.C.11. A profile of Hs against distance (D) along the section between site 20 and Balmacara (see Figure 6.C.1.). The rectangular co-ordinate system used makes an angle of 30° to true north and is parallel to the regional strike direction. The distance is measured in this system from site 20. T = axial trace of the Lochalsh Syncline and B = the position of the Balmacara Thrust.

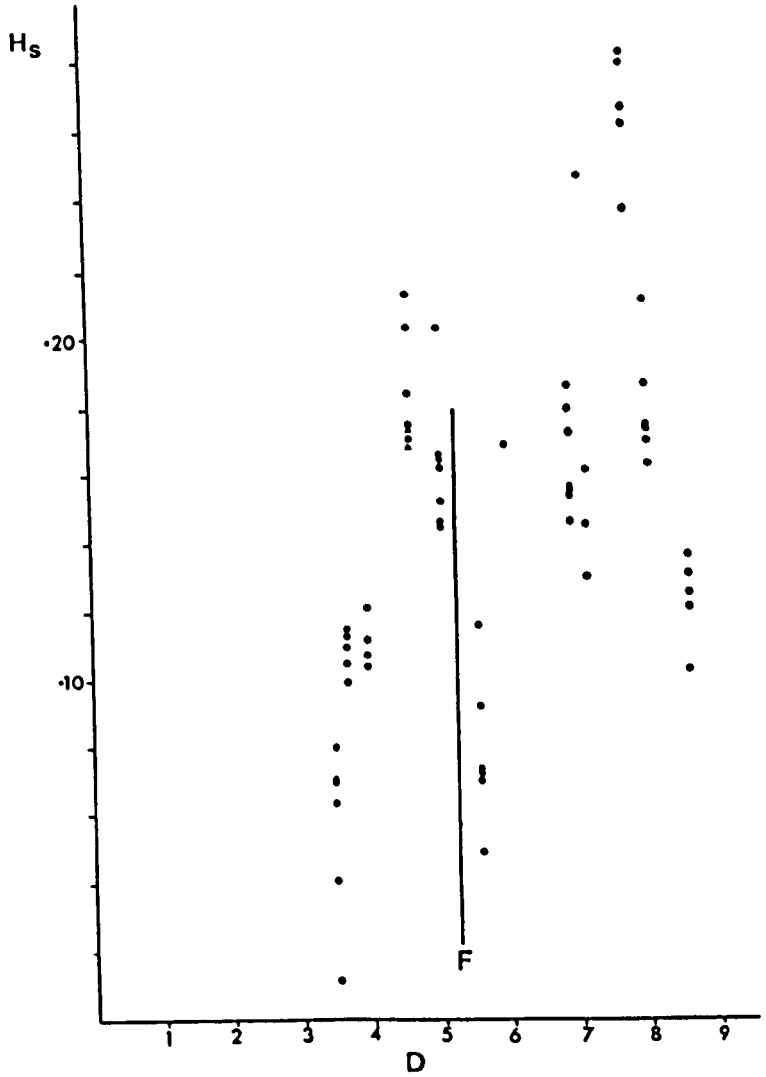

Figure 6.C.12. A profile of Hs against distance (D) across Lochcarron (see Figure 6.C.11. for details of the co-ordinate system used). F = the position of the Bad a Chreamha Fault.

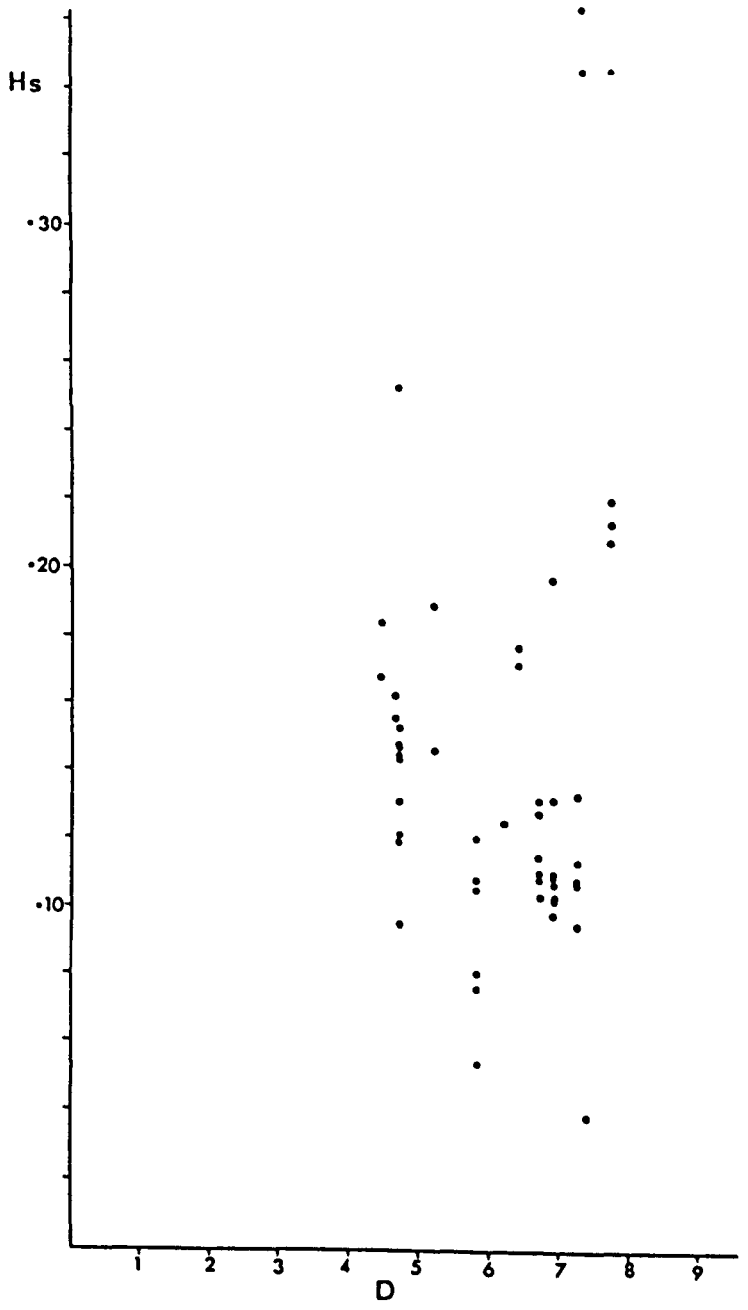

Figure 6.C.13. A profile of Hs against distance (D) along the north coast of Lochalsh between Plockton and Fernaig (see Figure 6.C.11. for details of the co-ordinate system used).

To determine variations in the degree of anisotropy on the inverted limb of the Lochalsh Syncline a series of profiles of Hs values were constructed. Initially, these profiles were constructed with rectilinear Cartesian coordinates parallel to the lines of the national grid. However, it was found that a more rational result was obtained when the Cartesian coordinates were taken to be parallel to, or perpendicular to, the strike of the bedding. Only these results will be presented in this thesis. The strike direction was taken to be 030. In general, there is an increase in the degree of anisotropy to the east of the area as shown by the Hs values. The three profiles for the northern area are shown in Figures 6.C.11., 6.C.12. and 6.C.13.. The increase may be clearly seen and it is almost linear. The profile seen in Figure 6.C.11. is constructed from samples collected along the same section as that of Coward and Whalley (1979) who suggest that no clear trend can be seen in their results. However, if as in this thesis, only the sandstones are considered a gradual increase in the degree of anisotropy, towards the east, can be seen in their results.

The results from Lochcarron presented in this thesis show a gradual increase in the values of Hs towards the east until the Lewisian Gneiss is encountered. Due to the change in rock type the anisotropy increases rapidly. Within the profile shown in Figure 6.C.12. there is a marked decrease in the value of Hs between the two specimens 1730 and 1729. If these results are compared to the location of the sites in Figure 6.C.1. they correspond to two areas. One of the areas lies to the north of Loch Reraig and one to the south. Within each sub-group the values of Hs increase towards the east. The rapid decline is probably due to a large fault which passes through Loch Reraig and to the north of Bad a Chreamha. This illustrates the problems which arise when correlating results on a regional scale without the necessary structural controls.

The results from the specimens along the north coast of Lochalsh do not show such a clear pattern as those described previously. In general, the degree of anisotropy is much greater than that seen in the undeformed portion of the Lochalsh Syncline and increases slightly to the east.

Comparison Of The Results Obtained In This Study With Those Of Coward And Whalley

The results from the samples which were collected between Broadford and Balmacara may be compared with those of Coward and Whalley (1979). Both the variation in the orientation and the shape of the susceptibility ellipsoids, found in this study, are consistent with the results of Coward and Whalley (1979). In the case of the sandstones the results of both studies show an increase in the degree of anisotropy towards the east (compare Figure 6.C.11. with Figure 10 of Coward and Whalley 1979). In both studies a decrease in the degree of anisotropy is seen close to the Balmacara Thrust at Ard Hill. Coward and Whalley suggest that this decrease is due to a change in the deformation mechanisms close to the thrust plane. They suggest that the decrease is due to a greater proportion of grain boundary sliding. Though, this is a possible explanation, others should be considered. The presence of sheath folds in these rocks suggest that the fabric seen is the final structure which may have bee reworked several times during a complex deformation history. During each phase of reworking the magnetic anisotropy of the old fabric may have been destroyed before a new one developed and the results record this period of transition. Alternatively, the decrease in anisotropy may be due to recrystallisation and annealing of the microstructure, a process which may have been less common in the less deformed rocks.

Magnetic Anisotropy Results From The Basal Conglomerates Of The Sleat Group

The basal conglomerates of the Sleat Group are exposed on Carn a Bhealaich Mhoir and these show the bedding parallel fabric. Frequently this fabric is associated with a mineral lineation in the phyllosilicate matrix and on the surface of the pebbles. The strain determined for these conglomerates was obtained from the pebbles and from thin sections and these are given in chapter 4..

Figure 6.C.14. shows the orientation of the susceptibility ellipsoids together with the finite strain axes determined for each of the sites. The most common feature of this diagram is the orientation of the axes of minimum susceptibility. These axes lie around the pole to the bedding and the scatter is relatively small. The axes of maximum and intermediate susceptibility lie in the plane of the bedding but there is considerable scatter of axes both within and between sites. Within a site the axes of maximum and intermediate susceptibility tend to form mutually exclusive groups (NG 82643275) the exchange of axes between these groups is common and when this becomes extreme the axes are spread throughout the bedding plane(NG 84453363)The orientation of the axes appears to reflect the strength of the bedding parallel fabric but the magnetic fabric does not reflect the strong lineation seen in the field. There is a correspondence in the orientation of the axes of minimum susceptibility and the Z axis of the finite strain ellipsoid butthere is no correlation between the orientation of the X and Y axes with the axes of maximum and intermediate susceptibility. This is due largely to the oblate shape of the susceptibility ellipsoids and the large amount of scatter.

The Hs values for these results are shown in Figure 6.C.14.. Clearly the anisotropy of these sites is

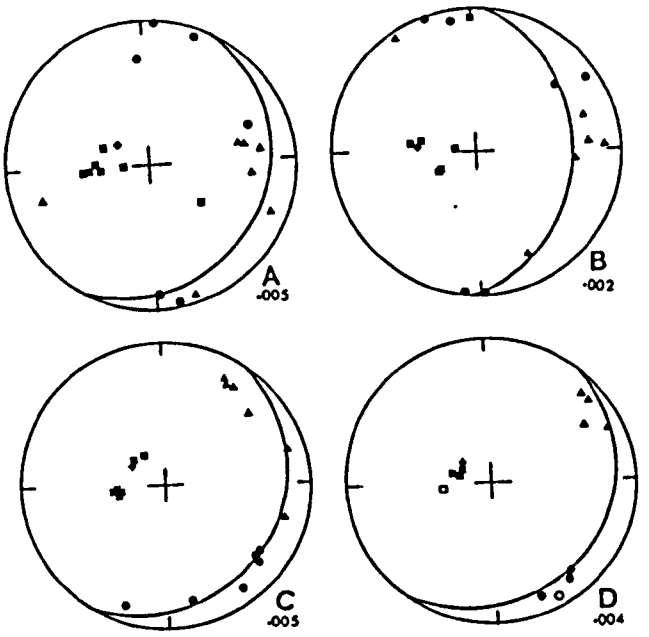

Figure 6.C.14. Stereograms of the axes of magnetic susceptibility determined for the conglomerate sites studied on Lochalsh. A. NG 84453363, B. NG 84813203, C. NG 82643273, D. NG 83963361.

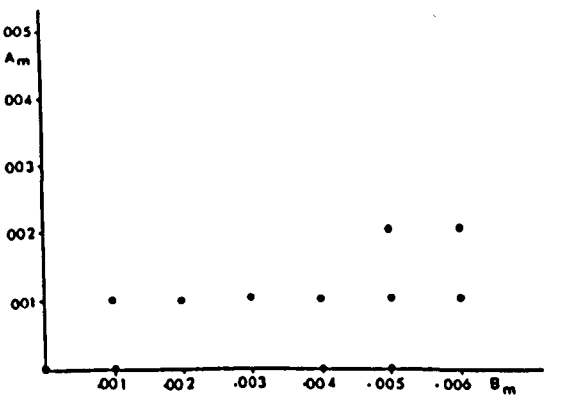

Figure 6.C.15 A Flinn plot showing the shape of the susceptibility ellipsoids obtained for the conglomerate sites studied in this thesis. The susceptibility ellipsoids are almost spherical in shape and this is reflected in the graduation of the axes.

extremely low despite the strong fabric and the high strains present in the rocks. Figure 6.C.15. shows the axial ratios of the susceptibility ellipsoids on a Flinn plot with the exception of one measurement the ellipsoids are entirely oblate in shape.

In thin sections of the basal conglomerate many large magnetite grains may be seen. These grains tend to be euhedral and they are strung out along the cleavage plane. It is probably this planar distribution which produces the oblate fabric (Owens 1974b). Some grains of magnetite have been deformed but the majority appear to have grown after the development of the bedding parallel fabric. It is possible that the relative proportions of deformed and undeformed magnetite grains controls the preferred orientation in the axes of maximum and intermediate susceptibility. When deformed, the magnetite grains show a shape fabric which is related to the bedding parallel fabric and its east-southeast lineation. A large proportion of deformed magnetite grains may produce a marked preferred orientation in the axes of maximum susceptibility parallel to the lineation.

The marked strains recorded by the pebbles of the conglomerates are not reflected in the anisotropy of these results. In this case the anisotropy of magnetic susceptibility may be attributed to the magnetite grains which, due to their high susceptibility will dominate the fabric. In general the magnetite grains postdate the development of the bedding parallel fabric and as a result the anisotropy of the fabric is relatively weak. This may explain the results described previously for the sites at the eastern margin of the

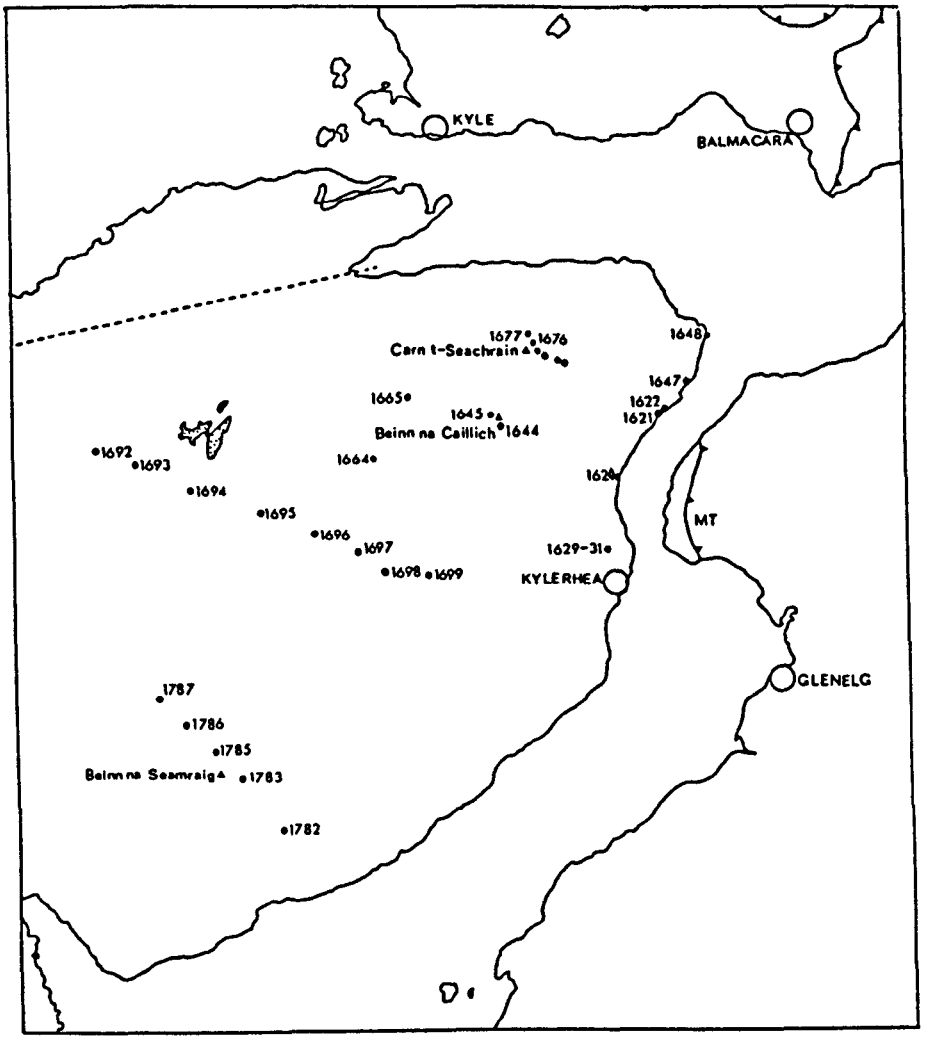

Figure 6.D.1. A simplified map for the sites of the central area of the Kishorn Nappe which were studied using magnetic anisotropy.

northern area where there is a decrease in the degree of anisotropy.

Section 6D Magnetic Anisotropy Results From The Central Area

The results of the study on northern Sleat, will now be discussed. The localities from which the samples were taken are shown in Figure 6.D.1.. In this area medium grained sandstones of both the Sleat Group and the Applecross Formation were collected. These results will be discussed as a series of transects, running east-west across the hinge of the Lochalsh Syncline. In the central area both limbs of the Lochalsh Syncline are exposed. On the overturned limb the beds posses the bedding parallel fabric. Both limbs of the Lochalsh Syncline are affected by the transverse cleavage and the studies provide information regarding the overprinting of the bedding parallel fabric by the transverse cleavage.

Figure 6.D.2. shows the orientation of the susceptibility ellipsoids and Figure 6.D.3. shows the axial ratios of the ellipsoids on a series of Flinn plots. The values of Hs for the particular sites are also shown in Figure 6.D.3.. The sites were collected along a transect between 1692 and site 32. The line of the transect is parallel to the section shown in Figure 2.C.11.. The sites will be described in sequence, working eastwards from specimen 1692.

The orientation of the axes determined for specimen 1692 show considerable scatter. The axes form three mutually exclusive groups but there is no strong preferred orientation in any of the axes. As shown in Figure 6.D.3. there is a wide range in ellipsoid shape and the ellipsoids are very nearly spherical. It is probably this low degree of anisotropy which produces the large scatter in the orientation of the axes. None of the axes appear to have any relationship to the

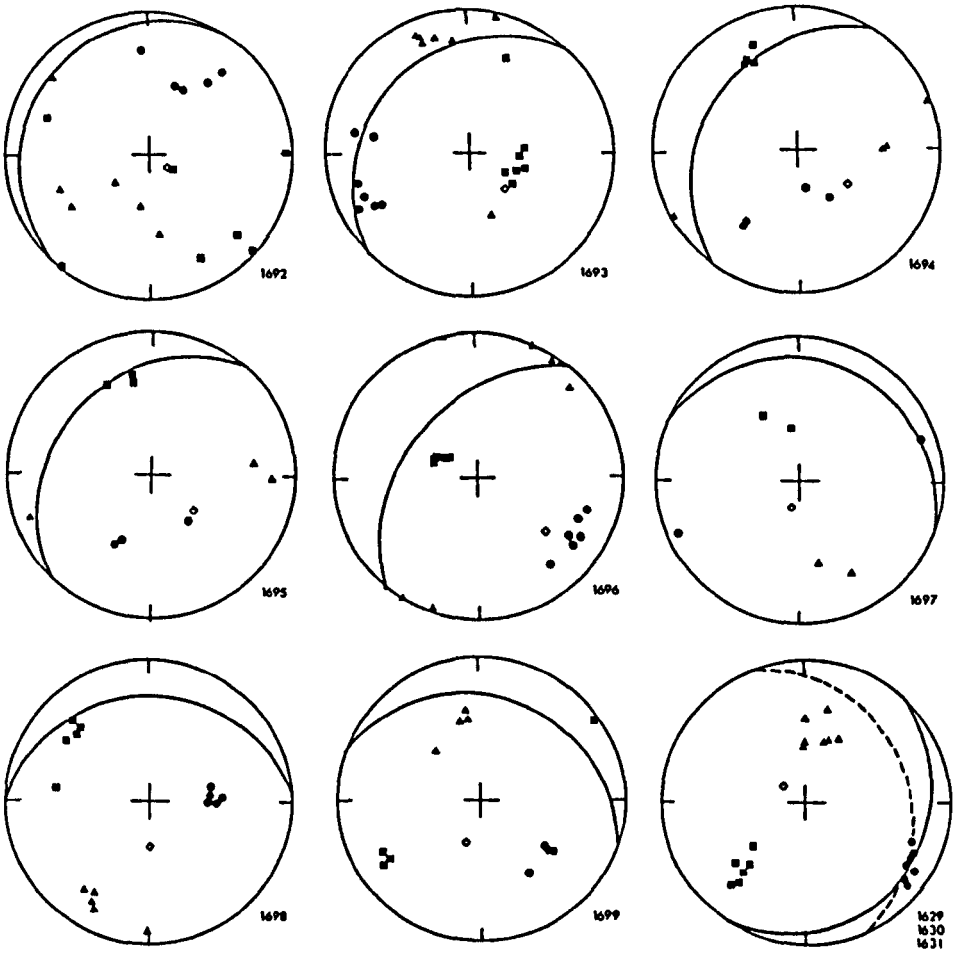

Figure 6.D.2. Stereograms showing the orientations of the axes of magnetic susceptibility for the samples collected on a transect through the hinge of the Lochalsh Syncline between 1692 and 1629-31, see Figure 6.D.1..
◆ = pole to bedding.

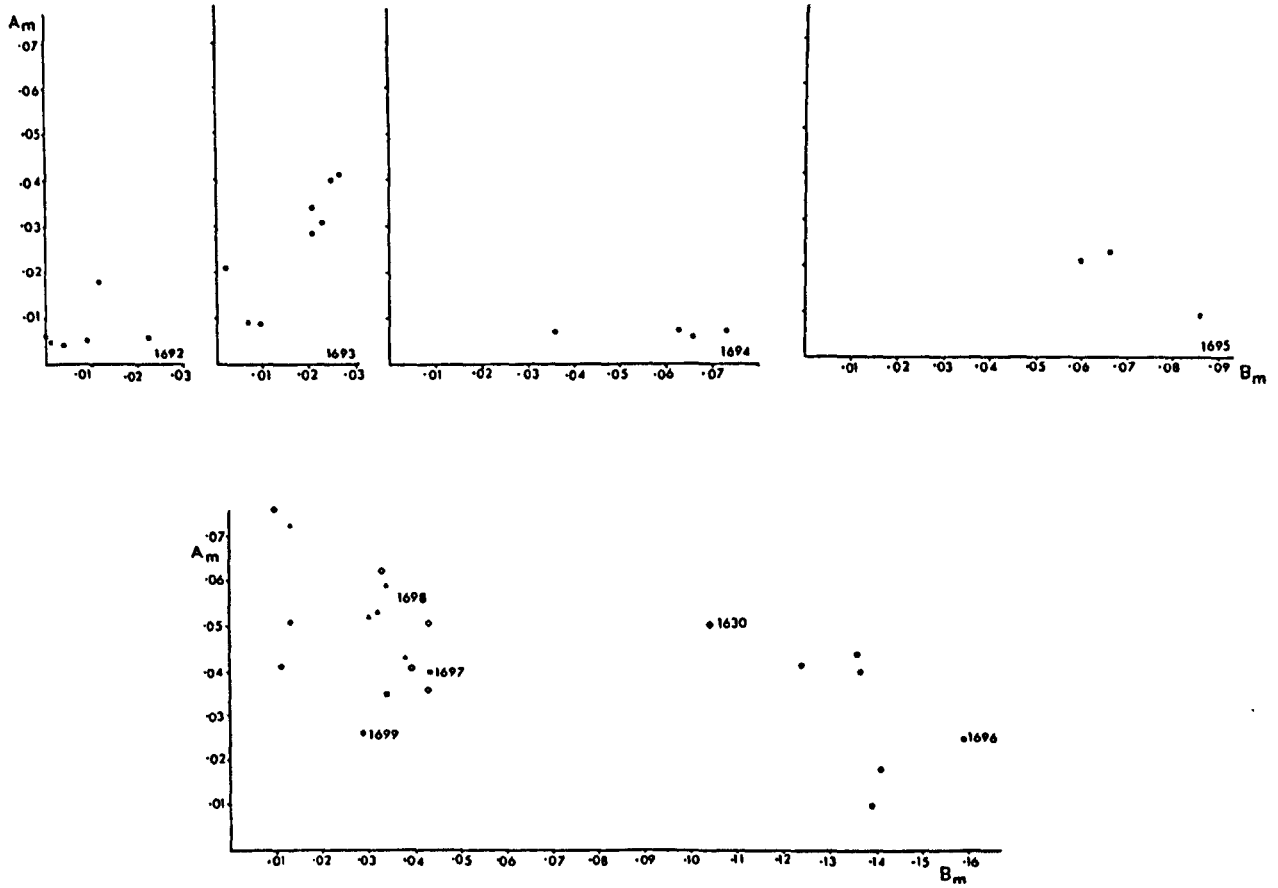

Figure 6.D.3. A series of Flinn plots showing the shapes of the susceptibility ellipsoids obtained from the transect between 1692 and 1629-31, see Figure 6.D.1..

bedding.

In specimen 1693 the orientation of the axes of magnetic susceptibility suggest a depositional or compactional fabric at this site. The axes of maximum and intermediate susceptibility lie in the plane of the bedding and the axes of minimum susceptibility lie close to the pole to the bedding. The ellipsoids tend to be prolate in shape and this may explain the exchange of axes seen in one of the measurements. In a prolate ellipsoid the minor axes will have similar lengths and their positions may be exchanged. The degree of anisotropy at this site is relatively low. The prolate fabric may represent a depositional fabric with the axes of maximum susceptibility defining a palaeocurrent direction. Alternatively, the results may indicate the modification of a sedimentary fabric by a weak tectonic fabric.

The specimens 1694 to 1698 have a distribution of axes which is common to them all but is independent of the bedding. At any site there is a strong preferred orientation in the axes of minimum susceptibility. These tend to plunge moderately or steeply to the north-west. The axes of maximum and intermediate susceptibility lie on a great circle and show a great deal of scatter in this plane, but generally they tend to form two mutually exclusive groups. The axes of maximum susceptibility tend to plot in the southeast quadrant. The planar distribution of the major axes suggests that a fabric may be present which is independent of the dip of the bedding. This fabric dips to the southeast and the axes of maximum susceptibility often lie at the point of greatest dip. The intersections of the planes of intermediate and maximum susceptibility with the bedding plane plunge gently to the northeast or southwest.

As seen in Figure 6.D.3. there is a dominant change in the shape of the susceptibility ellipsoids towards the

east. In the west, the ellipsoids are oblate in shape and as the degree of anisotropy increases the ellipsoids become prolate in shape. Accompanying this trend there is a general decrease in the degree of scatter in the axes of maximum susceptibility. With the increase in strength of the fabric towards the east the axes of maximum susceptibility tend to plot in the northeast quadrant.

In specimen 1699 the susceptibility ellipsoids tend to be prolate in shape and the axes of maximum susceptibility plunge to the southeast but are not related to the bedding. They bear only a slight relationship to the rest of the results from the correct way up limb. The axes of maximum and intermediate susceptibility define a plane which dips to the northeast.

At Kylerhea (site 31) specimens were collected from the overturned limb of the Lochalsh Syncline. Here, the ellipsoids plot around the K=1 line(Figure 6.D.3.).but tend to be prolate in shape. In the field, the bedding parallel fabric is dominantly linear and this appears to be reflected by the magnetic anisotropy. The axes of maximum susceptibility plot about the grain shape lineation.

Specimens 1692 to 1699 show the effect of the transverse cleavage on the correct way up limb of the Lochalsh Syncline. Eastwards, along the section the strength of the transverse cleavage increases and this is reflected in the increase of the Hs values. The transverse cleavage tends to change its orientation in the west it dips to the southeast and in the east the cleavage dips gently to the northeast. The magnetic fabric recorded at site 1692 is thought to reflect the initiation of the transverse cleavage in a similar manner to the results obtained, between Broadford and Kyleakin. Specimen 1693 appears to indicate a depositional and/or compactional fabric as the axes of maximum and

intermediate susceptibility lie in the plane of the bedding. The ellipsoids are prolate in shape and the axes of maximum susceptibility lie close to the intersections of the bedding and the magnetic fabric as shown in Figure 6.D.2.. It is thought that this fabric is truly transitional between a sedimentary fabric and the development of the transverse cleavage. This result casts doubts on the interpretation for site 1692.

In the samples 1694 to 1698 the change in the orientation of the axes of maximum and intermediate susceptibility appear to reflect the change in the orientation of the transverse cleavage towards the east. In sample 1699 it is inferred from the magnetic anisotropy that this cleavage dips to the northeast. The fabric seen at Kylerhea is considered to be the bedding parallel fabric. However, the orientations of the axes of susceptibility are very similar to those of specimen 1699. At Kylerhea the transverse cleavage may be seen and it dips to the northeast. The bedding-cleavage intersection lineation is parallel to the grain shape lineation and hence, the axes of maximum susceptibility. The magnetic fabric seen at Kylerhea is thought to be a composite, consisting of the bedding parallel fabric and the transverse cleavage. The axes of intermediate susceptibility have been drawn out of the bedding plane and into the cleavage plane while the axes of maximum susceptibility remain parallel to the east-southeast lineation.

To the north of this section a large segment of the hinge of the Lochalsh Syncline is exposed and samples were collected to determine the extent of the overprinting. The samples were collected throughout the area of Beinn na Caillich and Carn an t-Seachrain. This enabled both limbs of the Lochalsh Syncline to be studied including the area exposed beneath the out of syncline thrust near the shore of Kyle Rhea. Three types of results were

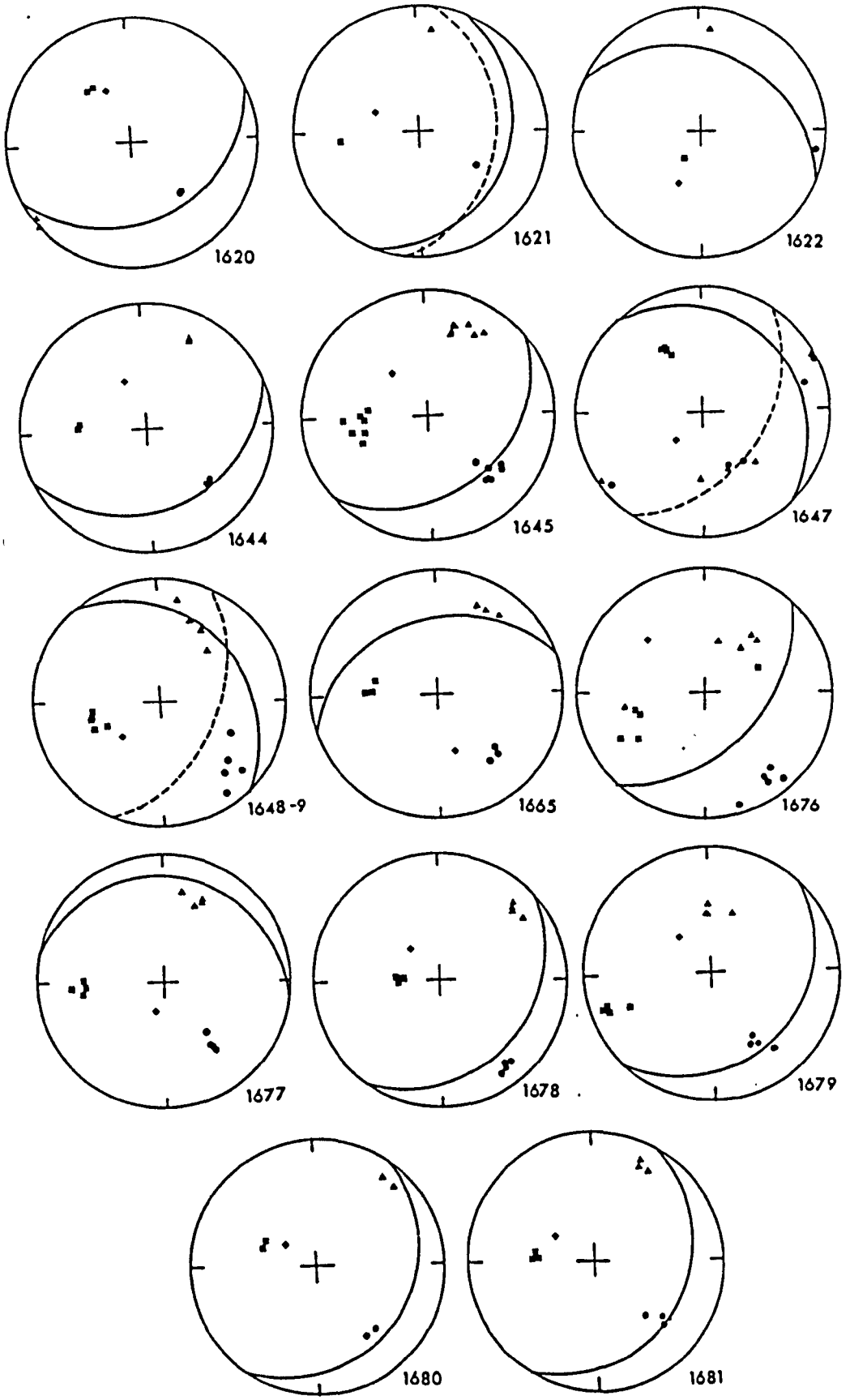

Figure 6.D.4. Stereograms showing the orientations of the axes of magnetic susceptibility for the sites collected around Beinn na Caillic and Carn an t-Seachrain.

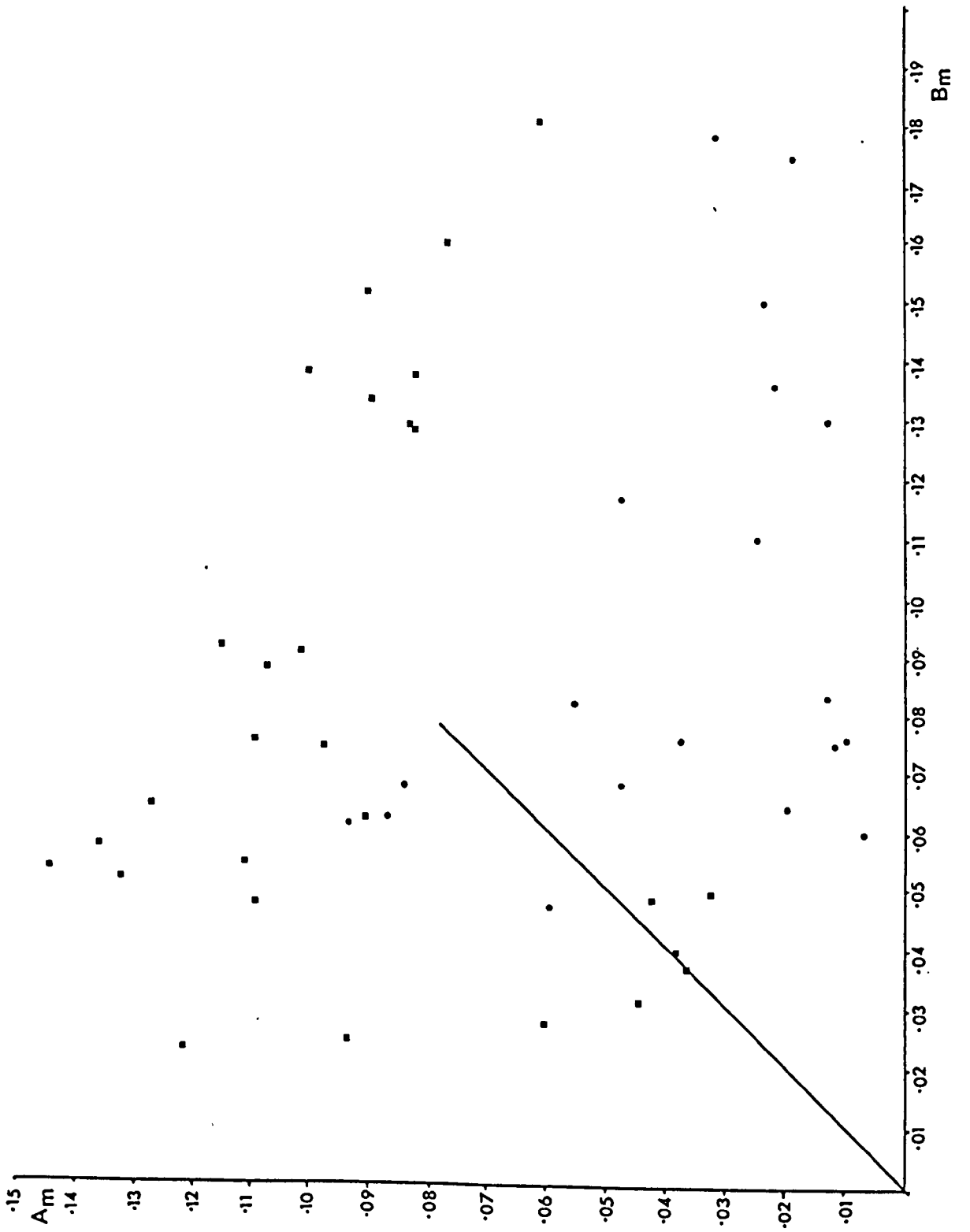

Figure 6.0.5. A Flinn plot showing the shapes of the suscepbility ellipsoids from both limbs of the Lochalsh Syncline around Beinn na Caillic and Carn an t-Seachrain. ■ = inverted limb.

obtained for this group of samples. The localities from which these were taken are shown in Figure 6. D.1..

The specimens given in Table 6.D.1. all come from the overturned limb of the Lochalsh Syncline. The bedding dips gently to the east or southeast at 20 to 30 degrees. In each case the axes of maximum and intermediate susceptibility lie close to the bedding plane and the axes of minimum susceptibility lie close to the pole to the bedding. There is relatively little scatter in the orientation of the ellipsoid axes and these are shown in Figure 6.D.4.. In the field, at some of these sites, a strong grain shape lineation may be seen and where present the axes of maximum susceptibility lie close to the lineation. Only some of these sites posses the bedding parallel fabric but the magnetic anisotropy suggest that it is present in all of these sites on the overturned limb of the Lochalsh Syncline. As shown in Figure 6.D.5. there is a wide range in the shape of the susceptibility ellipsoids. However, a strong prolate tendancy can be seen in these results.

Specimen 1647 records the presence of the transverse cleavage. In Figure 6.D.4. the axes of maximum and intermediate susceptibility lie on a great circle which dips to the southeast, very close to the plane of the transverse cleavage. The axes of minimum susceptibility lie close to the pole to the cleavage plane and show relatively little scatter. As shown in Figure 6.D.6. the ellipsoids of susceptibility determined for specimen 1647 are oblate in shape.

This result is from the overturned limb of the Lochalsh Syncdine in an area where the transverse cleavage is particularily strong and it is thought to indicate the overprinting of the bedding parallel fabric by the transverse cleavage. During this superimposition the axes of intermediate susceptibility rotate from the bedding

Table 6.D.1

Specimen number/Locality Number	Orientation of Inverted Bedding
1629-31	039 17
1620	066 37
1621	025 30
1644	069 34
1645	052 37
1676	043 53
1678	048 28
1679	050 29
1680	037 26

plane into the plane of the transverse cleavage. These results, in contrast to the northern area, indicate the overprinting of the bedding parallel fabric by the transverse cleavage with the sandstones. However, this rarely occurs and the magnetic fabric on the overturned limb of the Lochalsh Sycnline is dominated by the bedding parallel fabric.

The remaining sites from northern Sleat show a common orientation for the axes of magnetic susceptibility. The orientation of the axes is shown in Figure 6.D.5. and the sites all come from the correct way up limb of the Lochalsh Syncline. There is a varying degree of scatter in the orientation of the axes at each site but this is not related to any particular characteristic of the site. In these sites (1648, 1649, 1665 and 1677) the transverse cleavage may be seen. The susceptibility ellipsoids determined for these specimens tend to be oblate in shape. These results are thought to reflect the development of the transverse cleavage on the correct way up limb of the Lochalsh Syncline. Some of these sites come from the area of the normal limb exposed beneath the out of syncline thrust and they show a fabric which is similar to the remainder of this limb.

The values of Hs from both limbs of the Lochalsh Syncline in this area are shown in Figure 6.D.7.. The anisotropy of magnetic susceptibility is much greater on the overturned limb of the fold and this reflects the strength of the bedding parallel fabric.

The samples 1676 to 1679 were collected close to the hinge of the Lochalsh Syncline on Carn an t-Seachrain and no cleavage or fabric was recorded in these samples other than the bedding parallel fabric or the transverse cleavage. No axial planar fabric could be seen and the zone seen on Lochalsh must have been lost to erosion.

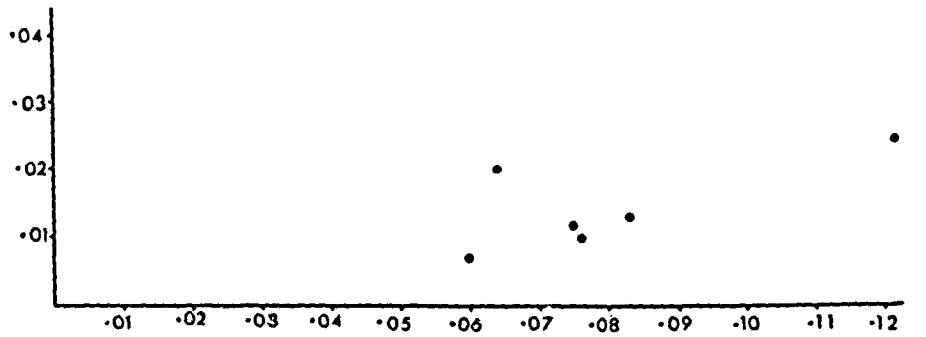

Figure 6.D.6. A Flinn plot showing the shapes of the susceptibility ellipsoids for specimen 1647.

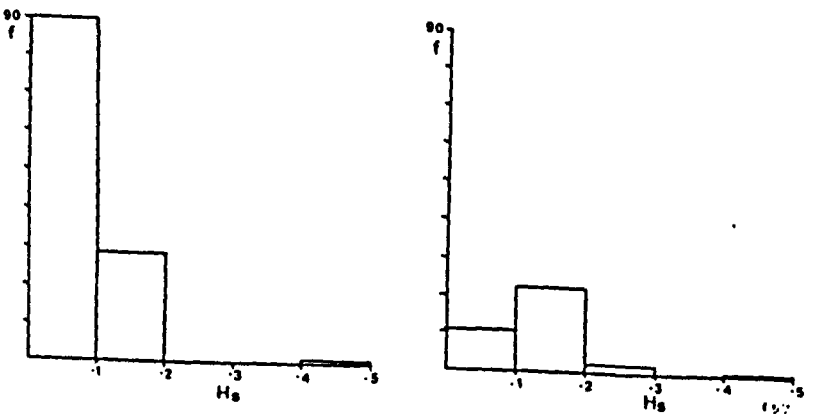

Figure 6.D.7. Histograms of Hs values from the cnetral area of the Kishorn Nappe. A. correct way up limb, B. inverted limb of the Lochalsh Syncline.

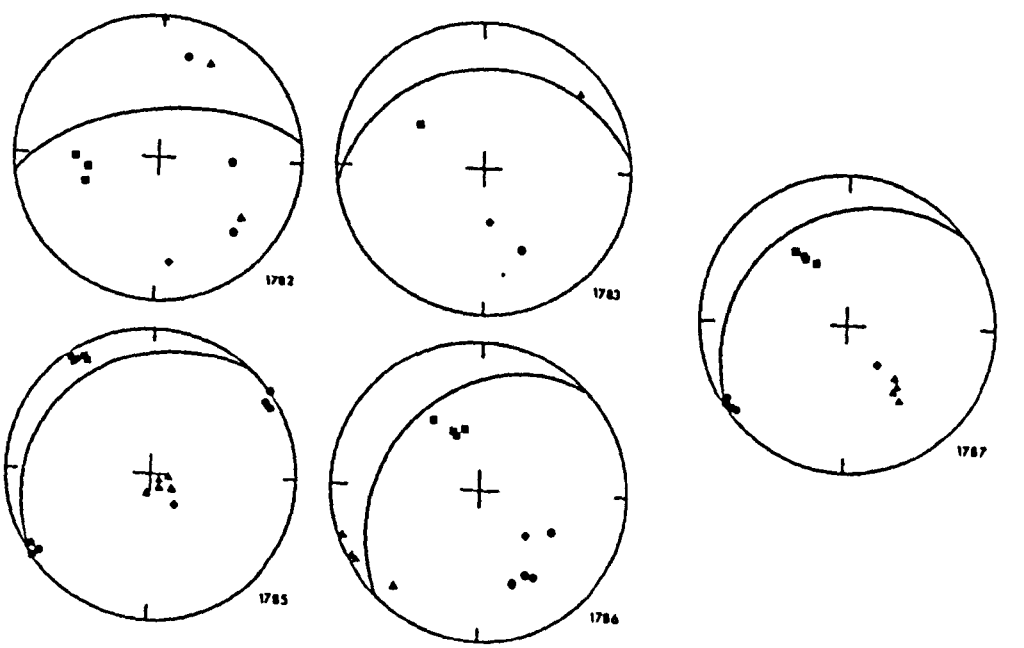

Figure 6.D.8. Stereograms showing the orientations of the axes of magnetic susceptibility for the samples collected around Beinn na Seamraig. ◆= pole to bedding.

Results Of The Transect Across Beinn na Seamraig

A series of samples were collected on a northwest-southeast transect across Beinn na Seamraig. The localities are shown in Figure 6.D.1. These samples were collected to determine the influence of the transverse cleavage on this portion of the normal limb of the Lochalsh Syncline. The transverse cleavage is often seen in shales and is usually spaced. The cleavage is rarely seen in the sandstones which in thin section rarely show any evidence of internal deformation.

The most common feature seen in Figure 6.D.8 . is the orientation of the axes of minimum susceptibility, they plunge to the west or northwest. The axes of maximum and intermediate susceptibility show varying degrees of scatter between the sample sites. The axes of maximum and intermediate susceptibility do not show a strong relationship to the bedding. In general, at a particular site, only one of these axes lies close to the bedding plane. In specimen 1782 the axes of maximum and intermediate susceptibility lie on a great circle which dips gently to the east. The orientation of the axes show a complete scatter in this plane which may define a cleavage. In the remainder of the samples the axes of maximum and intermediate susceptibility form two well defined groups which lie on a great circle which dips to the southeast. It would appear that the fine sandstones of Beinn na Seamraig are affected by the transverse cleavage.

There appears to be a consistent change in the shape of the susceptibility ellipsoids. To the east, the ellipsoids of susceptibility become increasingly oblate in shape from an initial, strongly prolate, shape. Throughout the transect the degree of anisotropy remains fairly constant (see Figure 6.D.9 .). The change in shape of the

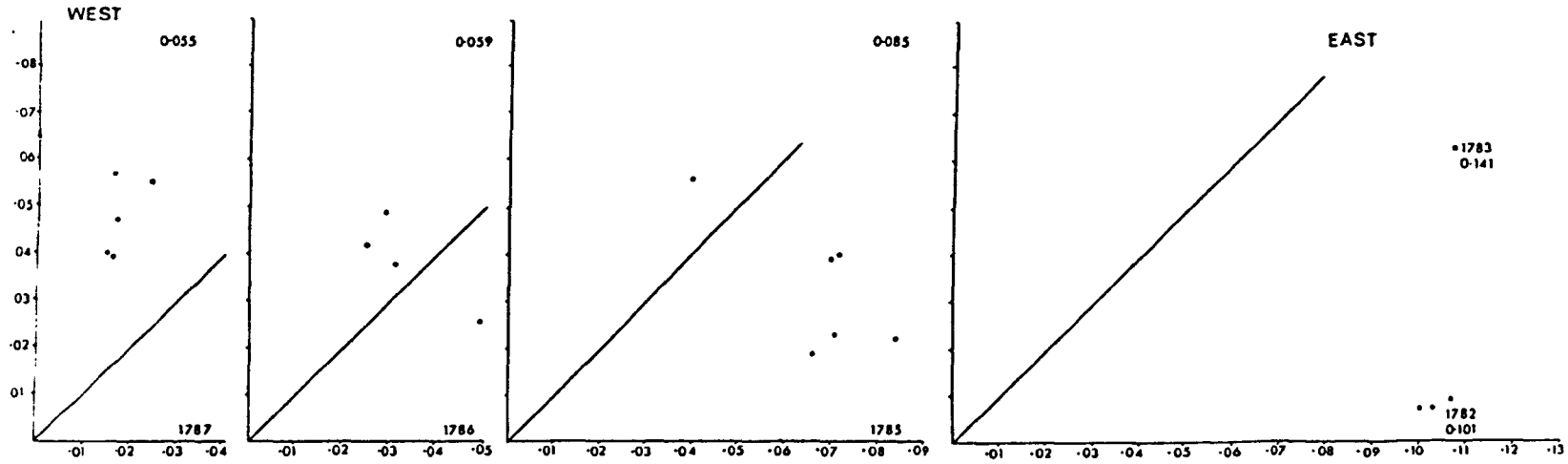

Figure 6.D.9. A series of Flinn plots showing the change in the shape of the susceptibility ellipsoids, to the east, across Beinn na Seamraig. The Hs values for these samples are given in the diagrams.

susceptibility ellipsoids may be interpreted in terms of the overprinting of an oblate sedimentary fabric by the transverse cleavage. It has been shown previously, that the strength of the transverse cleavage increases to the east. Thus in the west (specimen 1787) a prolate fabric is produced by overprinting of a sedimentary and/or compactional fabric by the transverse cleavage. To the east, the increasing strength of the transverse cleavage produces more oblate ellipsoids.

In conclusion, the sites from the normal limb of the Lochalsh Syncline record only the transverse cleavage and this appears to have been the first deformation event which they have suffered. In contrast, the overturned limb of the Lochalsh Syncline has suffered both the bedding parallel fabric and the transverse cleavage. Ther is a marked contrast in the degree of anisotropy between the two limbs and this is reflected in Figure 6.C.9. and 6.D.7.

The measurments of magnetic anisotropy show that the bedding parallel fabric is present throughout the overturned limb of the Lochalsh Syncline. Though some evidence can be seen on northern Sleat for the overprinting of the bedding parallel fabric by the transverse cleavage in general, the sandstones record only the bedding parallel fabric. On the overturned limb there is awide variation in the shape of the susceptibility ellipsoids. However, the principal axes of magnetic anisotropy have a constant orientation throughout this limb and a constant orientation in relation to the bedding. The variation in the shape of the susceptibility ellipsoids may be related to variations in the shape of the strain ellipsoids associated with the bedding parallel fabric. Sometimes, in the field, the bedding parallel fabric has a strong lineation and somtimes it is a planar fabric. Thus, there will be variations in the shape of the

the magnetic ellipsoids which may be related to this variation. However, the variations seen both throughout the overturned limb of the Lochalsh Syncline and within a particular site may be due to the nature of the grains responsible for the magnetic anisotropy.

Curie point determinations and XRD studies suggest that within the Sleat Group, the principal phases responsible for the magnetic anisotropy of the sandstones are paramagnetic, probably phyllosilicates. In thin sections the phyllosilicates, mainly chlorite and white mica,lie with a strong crystallographic preferred orientation parallel to the trace of the dominant cleavage or fabric. Thus, the magnetic anisotropy of the rock arise from the preferred orientation of the paramagnetic grains parallel to the cleavage.

In the sandstones of the Applecross Formation both paramagnetic minerals and haematite could be identified. Again, a problem arose during attempts to determine whether magnetite is present in these rocks, see chapter 5. In polished sections of undeformed sandstones of the Applecross Formation two types of haematite can be seen. The large detrital grains are slightly elliptical in cross section with a wide range in the orientation of the grain long axes. The matrix of red pigment cannot be resolved using the optical microscope. The weak anisotropy of the rocks around the Eishort Anticline is thought to be due to an almost random distribution of haematite basal planes, since the magnetic anisotropy of haematite is of magneto-crysalline origin.

In deformed portions of the Applecross Formation there is a marked increases in the proportion of phyllosilicates. The white mica and chlorite lie parallel to the trace of the cleavage or fabric and within the zones of mica growth new grains of haematite can be seen. Thus, in

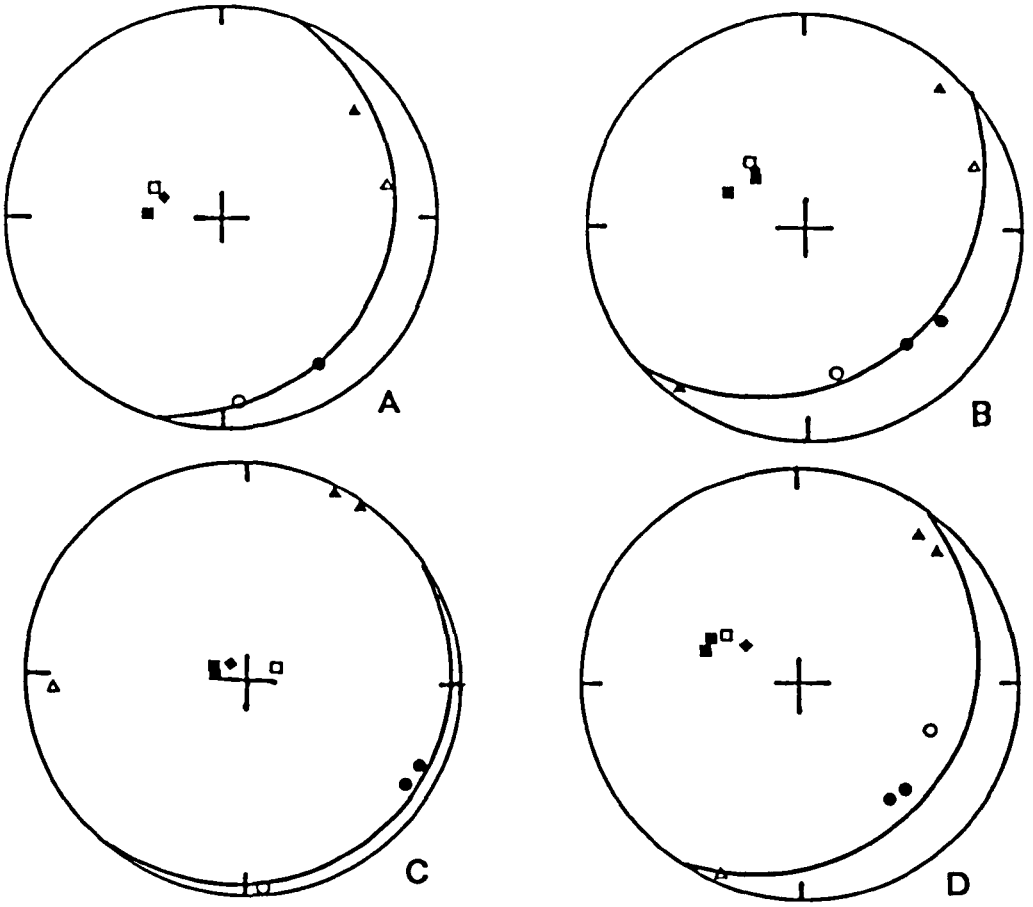

Figuer 6.E.1. Stereograms showing the corresponding axes of magnetic susceptibility and finite strain in the four specimens used for the calibration of the sandstones of the Sleat Group. The axes of magnetic susceptibility are shown as solid symbols and ● = maximum susceptibility, ▲ = intermediate susceptibility, ■ = minimum susceptibility. A. NG 81883264 (1594), B. NG 81313350 (1605), C. NG 82513330 (1608), D. NG 77852375 (1680).

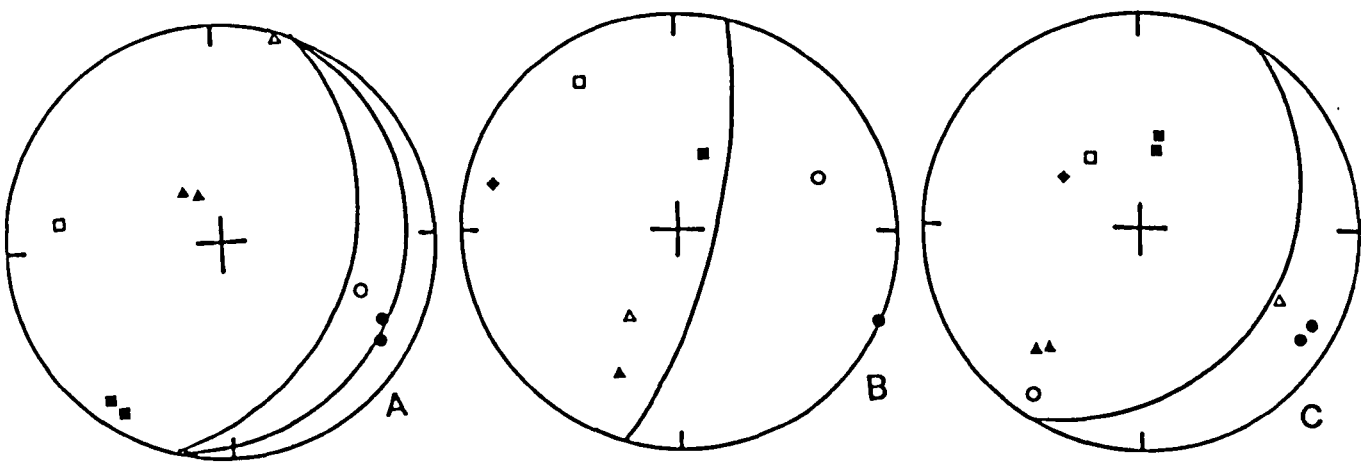

Figure 6.E.2. Stereograms showing corresponding axes of magnetic susceptibility and finite strain in the three specimens used for the calibration of the sandstones of the Applecross Formation. (See Figure 6.E.1. for the notation). A. NG 77203145 (1519), B. NG 700903421 (1568), C. NG 79903421 (1570).

deformed portion of the Applecross Formation the magnetic anisotropy is thought to be due to the preferred orientation of phyllosilicate grains and haematite basal planes parallel to the grain shape fabric.

Due to the platy nature of both phyllosilcate and haematite grains the individual grain anisotropies tend to be oblate in shape. The preferred orientation of such grains will tend to produce oblate anisotropy ellipsoids (Owens 1974b). The variation in the shape of the susceptbility ellipsoids, particularily within a site may be due the proportions of phyllosilicate grains or haematite grains within the rock which will, unless their distribution is strongly linear, produce oblate ellipsoids.

Section 6E The Calibration of Magnetic Aniotropy for Finite Strain.

To calibrate the magnetic anisotropy for finite strain the orientation of the axes of magnetic susceptibility and finite strain were compared on stereograms to determine whether there is a close relationship between the two types of axes. The comparison of axes in the specimens used to calibrate specimens of the Sleat Group are shown in Figure 6.E.1.. Clearly, there is a close association between the two types of axes in all of the specimens used except for NG 82513330. The discrepancy in this specimen is thought to be due to the oblate shape of the susceptibility ellipsoid and the prolate shape of the strain ellisoid.

The association of similar axes is not as clear in the specimens used to calibrate the sandstones of the Applecross Formation (Figure 6.E.2.). In each case this can be accounted for by the exchange of similar axes

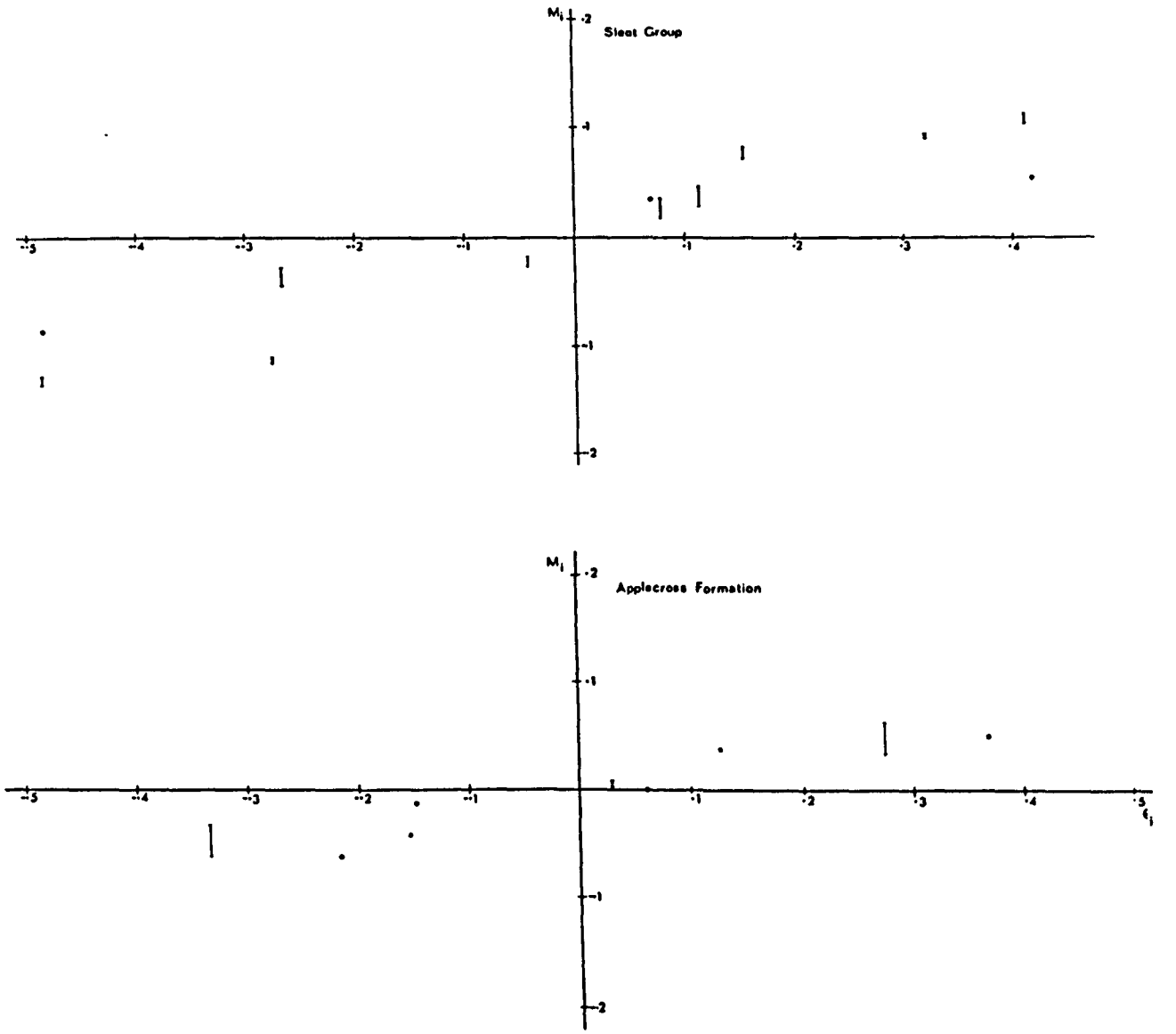

Figure 6.E.3. Calibration graphs following Kligfield et al (1981). The strain determination was obtained from the study of thin sections. The bars indicate the maximum and minimum values of Mi for each of the specimens. The Sleat Group and the Applecross Formation both required their own calibration curve.

in prolate or oblate ellipsoids. Where this variation has a significant effect on the magnitude of the axes, the correlation was madeusing the axes which corresponded most closely in terms of orientation.

The calibration graphs (after Kligfield et al 1981) for the Sleat Group and the Applecross Formation , obtained in this study, are shown in Figure 6.E.3. . Two curves were obtained one for each of the formations , Thus, a universal relationship of the type proposed by Rathore(1980) does not exist and calibrations must be made for each of the rock types studied within an area. The linear relationship described by Kligfield et al (1981) for the Permian mudstones which they studied is apparent in Figure 6.E.3. However different calibration curves were obtained for the Kishorn Nappe and these are;

$$\varepsilon_i = 3.10\ M_i \qquad \text{Sleat Group}$$

$$\varepsilon_i = 5.40\ M_i \qquad \text{Applecross Formation}$$

The value of the slope obtained for each calibration was a visual best fit line. Statistical methods such as least squares were not used as, in agreement with Kligfield et al (1981), it is thought that particularly errors, in strain estimation cannot be adequately quantified for such a rigorous analysis. The relatively small number of samples used to calibrate the results will introuce errors. Many specimens were rejected for strain analysis as they have suffered from recrystallization and original grains could not be recognised. In these cases no estimate was possible and illustrates the care which must be taken when attempting studies of this kind.

The different curves may arise from the different sources of the magnetic anisotropy. In this case the contribution to the magnetic anisotropy by haematite in the sandstones

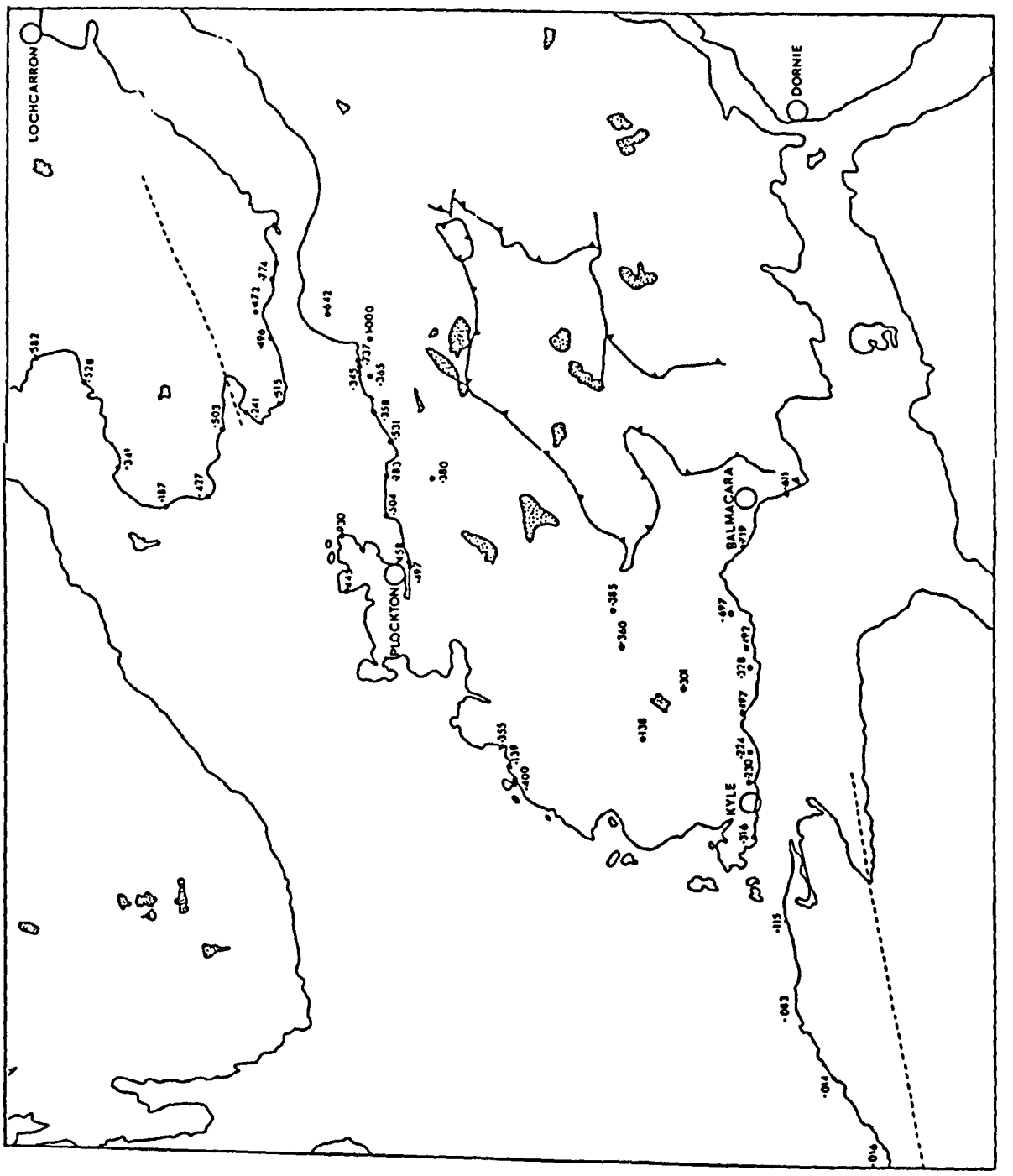

Figure 6.E.4. A map of the northern area of the Kishorn Nappe showing values of Es which were obtained from the calibrated magnetic anisotropy results. Thus, maps of strain distributions may be drawn using magnetic anisotropy which has been calibrated for finite strain.

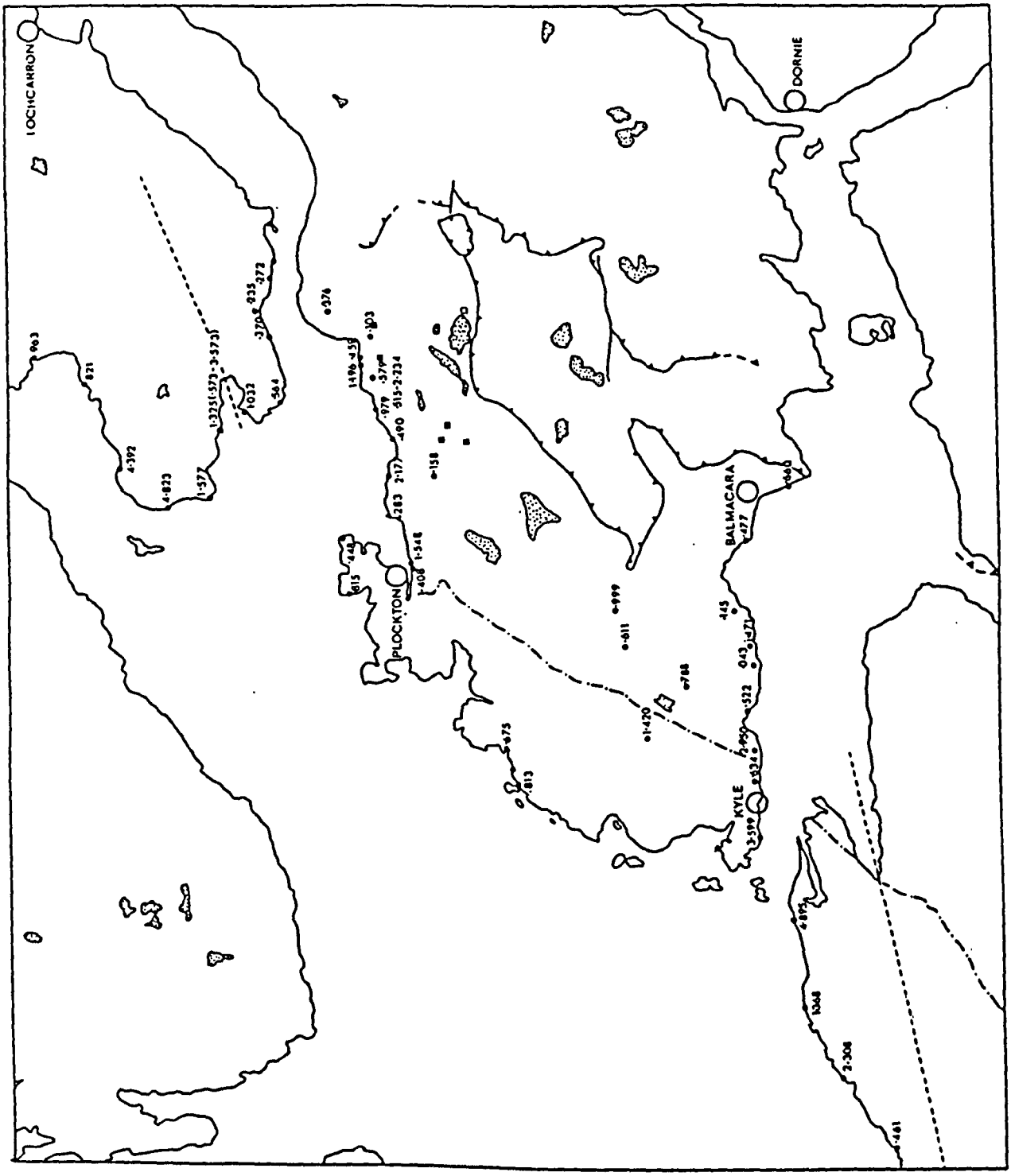

Figure 6.E.5. A map of the northern area of the Kishorn Nappe showing values of K which were obtained from the calibrated magnetic anisotropy results. The mean K value for each site is given, since a range in K values is generally seen in each specimen. Where the range is large the extreme values are given in brackets.

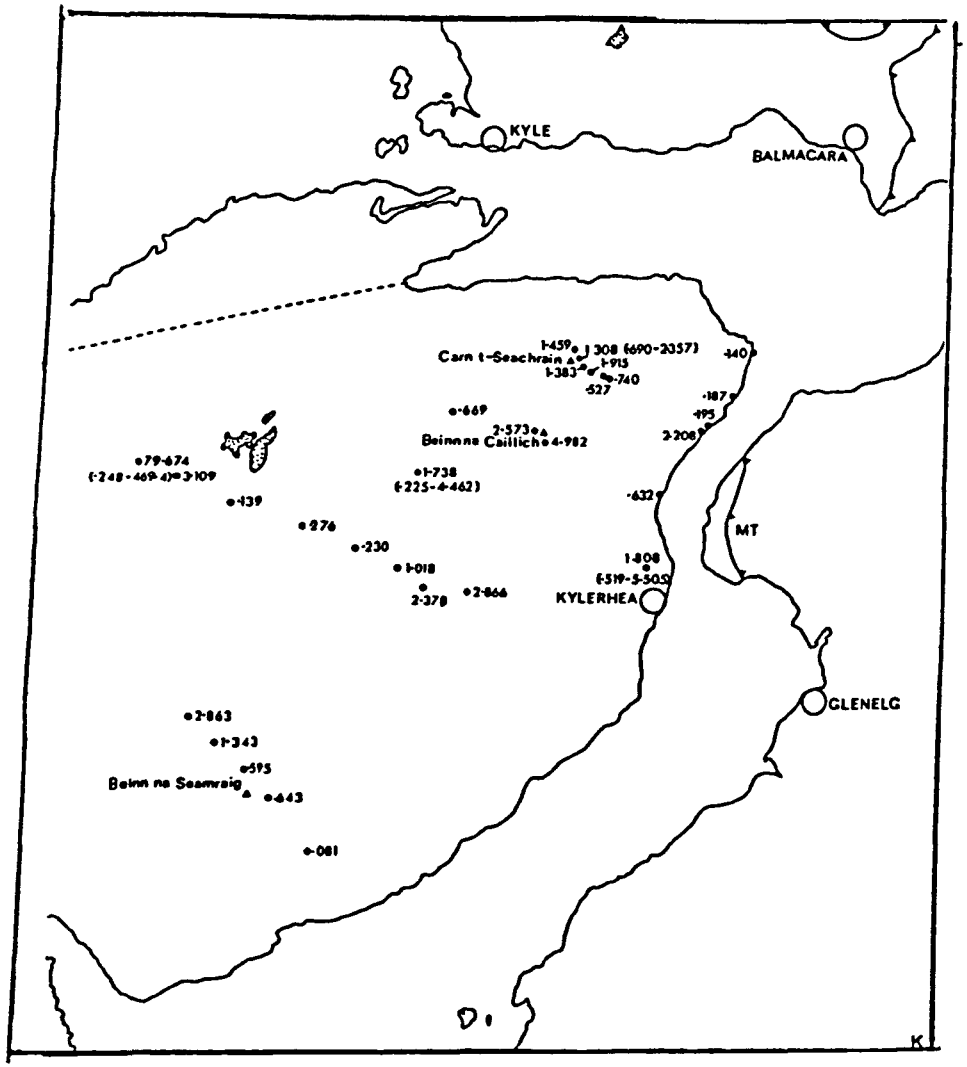

Figure 6.E.7. A map of the central area of the Kishorn Nappe showing values of K which were obtained from the calibrated magnetic anisotropy results. The mean K value for each site is given , since a range in K values is generally seen in each specimen. Where the range is large the extreme values are given in brackets.

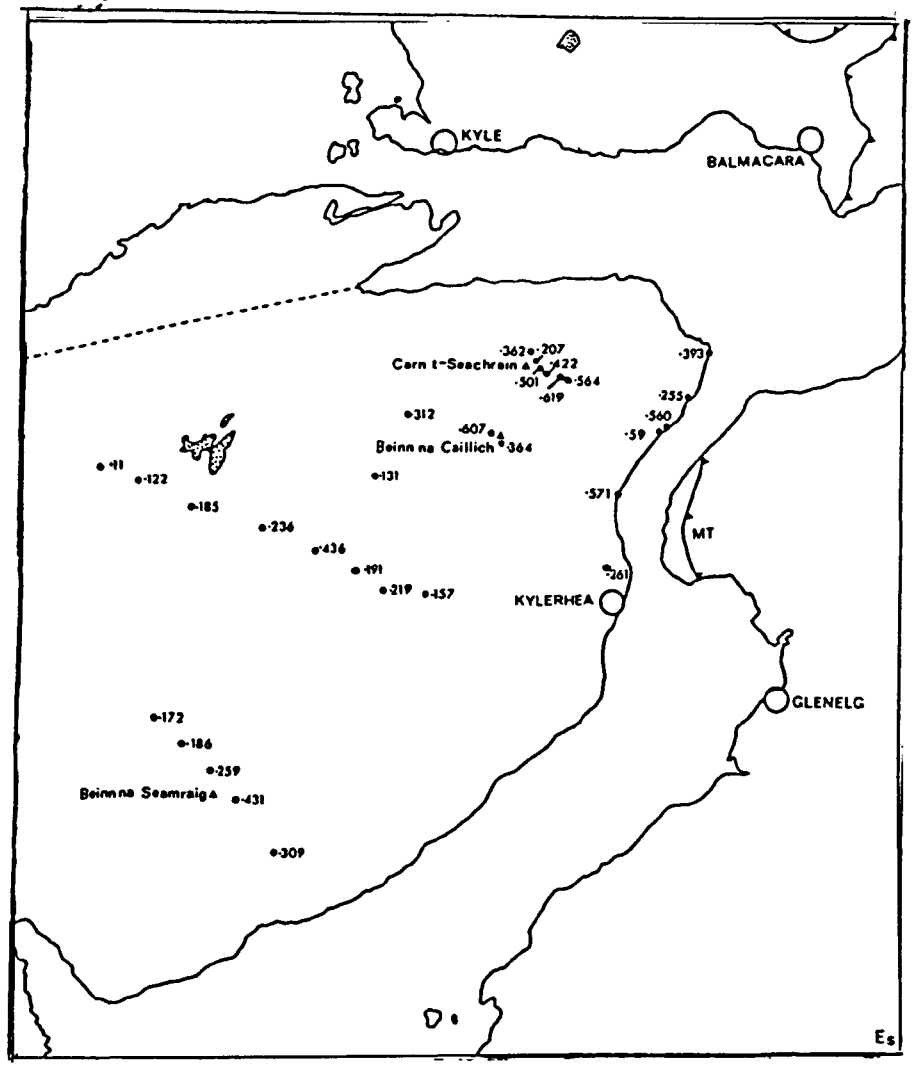

Figure 6.E.6. A map of the central area of the Kishorn Nappe showing values of Es which were obtained from the calibrated magnetic anisotorpy results.

of the Applecross Formation may result in the different calibrations for the two rock types.

Clearly, having made a successful calibration it is possible to construct maps of the strain distribution using the measurments of magnetic anisotropy. Four such maps are shown in Figures 6,E.4., 6.E.5, 6.E.6. and 6.E.7. and they show variations in Es and K throughout the northern and central areas of the Kishorn Nappe. It is also possible to recalculate the profiles of H_s into profiles of E_s.

The variations of K throughout the Nappe are comparable to those described for the magnetic anisotropy and will not be discussed here. The contrast in the anisotropy between the two limbs of the Lochalsh Syncline reflects the higher strains on the overturned limb of the fold, in common with many recumbent folds. There is a general increase in Es towards the east on the overturned limb of the Lochalsh Syncline. This increase can be seen in Figure 6.E.4 and Figure 6.E.6. and obtained from the recalculation of Figures 6.C.11., 6.C.12. and 6.C.13. Most simply this may be interpretated as an in increase in the degree of deformation towards the thrust plane above. However, as this increase in strain is due to the bedding parallel fabric problems immediately arise in explaining a strain gradient in which the axes bear a constant relationship to the bedding. A deatailed analysis of these results is given in chapter 8.

Chapter 7 The Mellene Nappe of Southern Norway

This chapter describes a study of the geology and strain within the Mellene Nappe of southern central Norway. The aim of this study was to provide a comparison with the Kishorn Nappe of northwest Scotland. The Mellene Nappe was chosen on the advice of Dr. J. Hossack (City of London Polytechnic) as it met the with the following requirements;

(a) It has an established stratigraphy
(b) The regional geology is reasonably well understood
(c) It has a low metamorphic grade
(d) There are suitable strain markers.

The regional geology of the area will be described first, followed by an account of previous work on the Mellene Nappe. The results from the present study will be described in the remaining sections of the chapter. The conclusions which may be drawn from this study and the comparisons which may be made with the Kishorn Nappe will be discussed in chapter 8.

Section 7A Regional Geology and Previous Work

The area studied lies to the north of the Lake Mellsenn and it forms part of a broad ridge between the Etnedal and eastern Slidre valleys, 12 Km to the north of Fagernes (Oppland)(Figures 7.A.1. and 7.A.2.). Figure 7.A.2. shows the main thrusts and nappes in the area (after Hossack et al 1981). The Mellene Nappe is the lowest of the Valdres Group of Nappes and is dominated by a large recumbent fold termed the Skarvemellen Anticline(Nickelsen 1967).

Between the Foreland Gneisses of the Baltic Shield and the Jotun Thrust a series of nappes are exposed. The basic geology of the area was originally described by

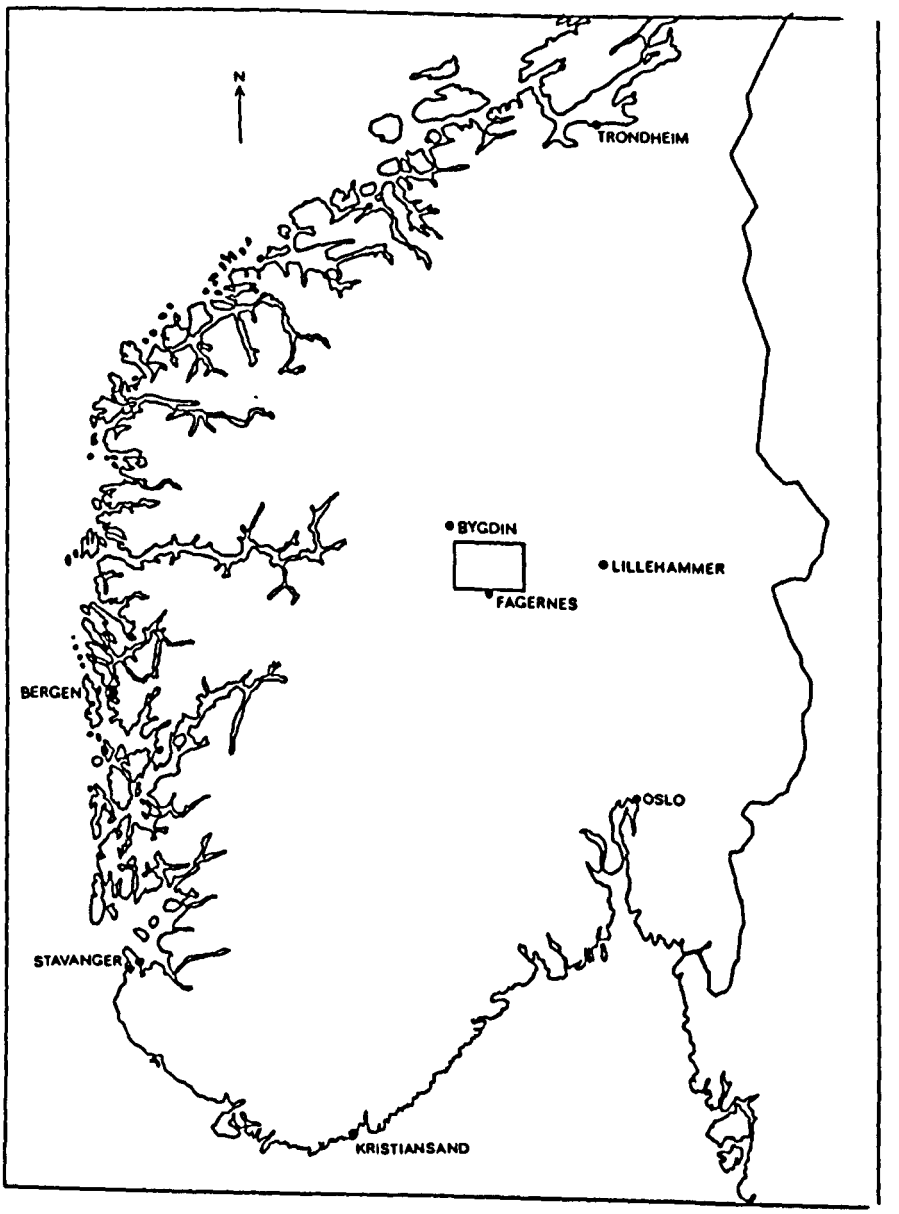

Figure 7.A.1. An outline map of southern Norway. The area studied is enclosed in the rectangle between Fagernes and Bygdin.

Bjorlykke (1905) and later by Goldschmidt (1919a,b). Recently Hossack et al (1981) and Nickelsen et al (1981) have produced a synthesis of the structural geology and stratigraphy of southern central Norway. This interpretation will be summarised here as it provides a framework into which this thesis work may be placed. The Foreland Gneisses are overlain by a thin autochthonous cover of Cambrian shales, see Figure 7.A.3.. Two large duplexes, the Aurdal and Synnfjell duplexes, of late pre-Cambrian to Ordovician sediments, are thrust to the southeast over the foreland (Hossack et al 1981). The Aurdal and Synnfjell duplexes contain many thrusts which repeat a stratigraphic sequence which is essentially the correct way up.

The Valdres Group of Nappes form the roof to the higher, Synnfjell duplex. The Valdres Nappes contain pre-Cambrian basement rocks and their late pre-Cambrian to Ordovician cover. The rocks of the Valdres Nappes are intensly folded and thrust and many of the nappes contain strata which are inverted.

Between the Valdres Nappes and the Synnfjell duplex the Strondafjord and Gausdal Formations are locally present (Figures 7.A.2. and 7.A.3.). These are a series of thrust bounded turbidites which are thought to represent a flysch like sequence related to early movements of the higher nappes. The highest nappe in the region is the Jotun Nappe which contains pre-Cambrian gneisses.

A full description of the geology and stratigraphy in this area may be obtained from Hossack et al (in press) and Nickelsen et al (in press) which are papers , based on their work, presented at the Uppsala Caledonide Symposium 1981(Hossack et al 1981, Nickelsen et al 1981). Extensive reference lists may be obtained from these papers.

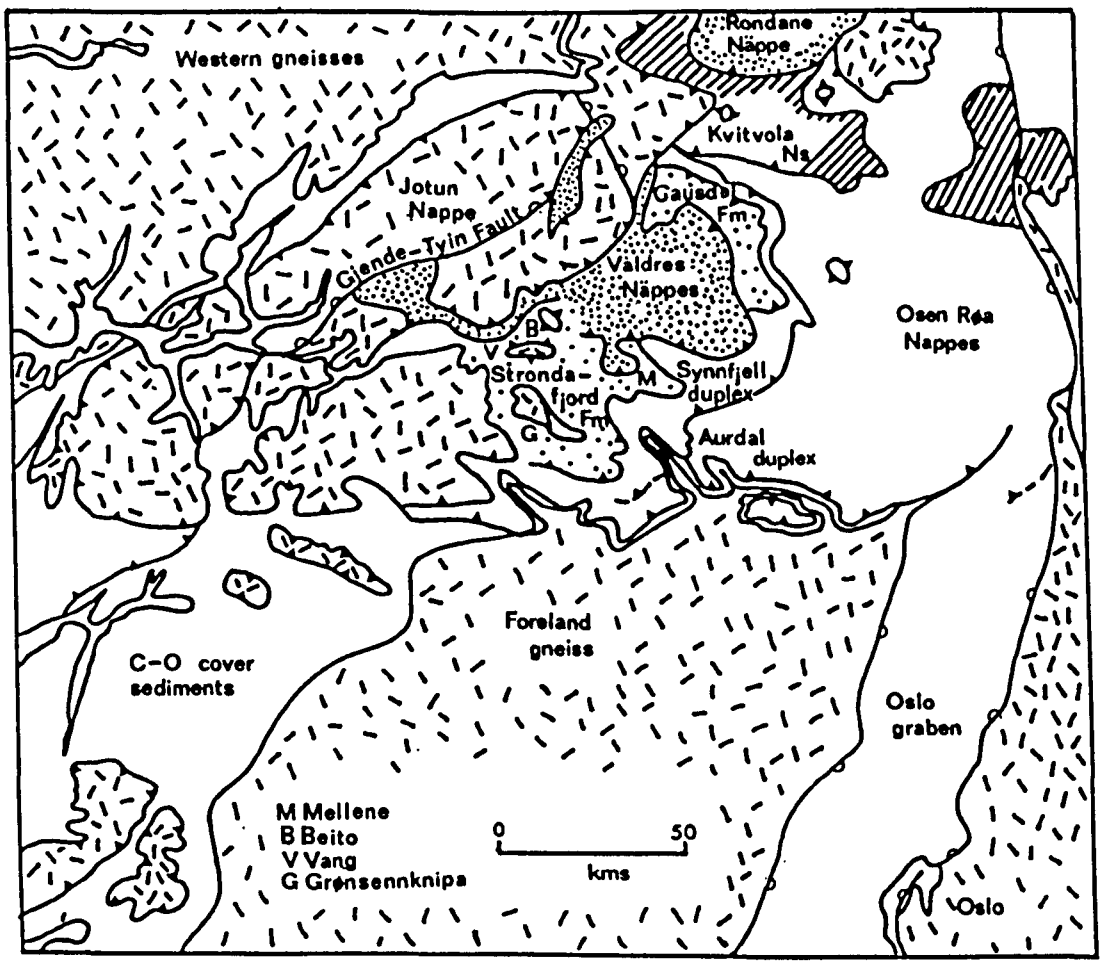

Figure 7.A.2. Geological map of southern Norway showing the major nappe units (after Hossack et al 1981, in press).

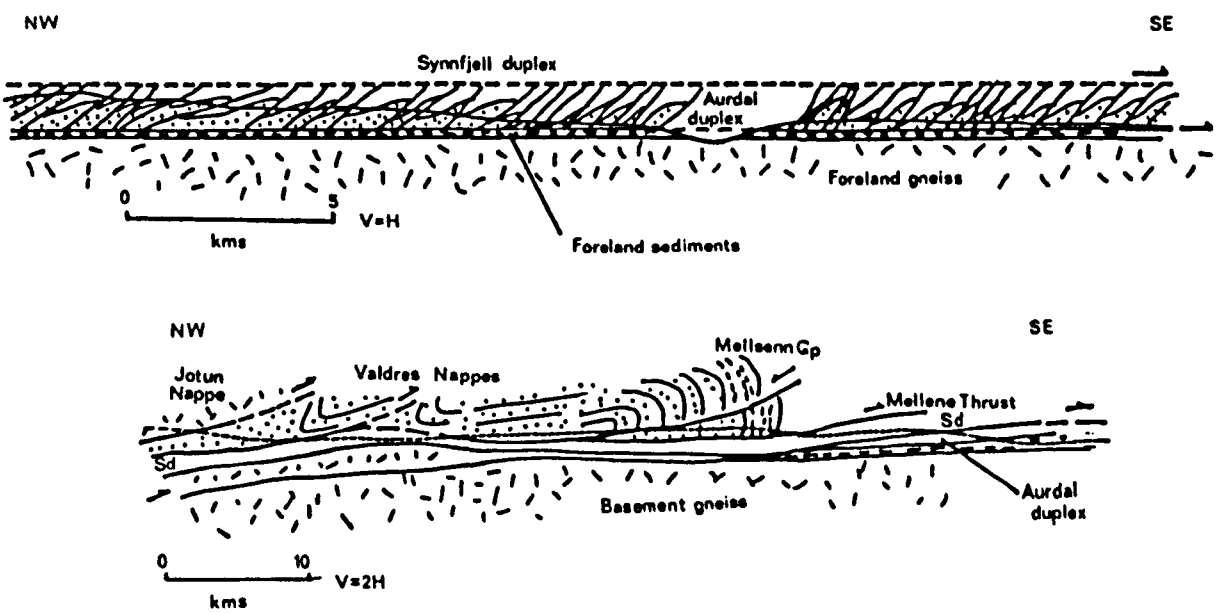

Figure 7.A.3. Geological cross sections throught the major nappe units between the Baltic Shield and the Jotun Nappe. Sd = Synnfjell duplex (after Hossack et al 1981, in press).

Previous Work

The Mellene region of southern central Norway contains the type section for the Valdres Sparagmite and the Mellsenn Group (Strand 1938,1951 and 1954). The relative ages of these two groups is crucial in the interpretation of the structure and stratigraphy of the rocks beneath the Jotun Nappe. On the basis of his mapping around Mellene, Strand (1954,1960,1962 and 1964) came to the conclusion that the Valdres Sparagmite was Upper Ordovician or Lower Silurian in age as it was underlain, conformably, by the fossiliferous Mellsenn Group in which Middle Ordovician graptolites had been found (Bjorlykke 1905). On this basis,the Valdres Sparagmite was thought to represent the normal stratigraphic sequence above the Phyllite Formation (Strand 1961) and the Mellsenn Group. However, this view was challanged by Kulling (1961), who proposed that the Valdres Sparagmite was Eocambrian in age based on a comparison between the stratigraphy of Mellene and a stratigraphy which he had established in Sweden.

The age of the Valdres Sparagmite at Mellene was resolved by the work of Loeschke (1967a,b) and Nickelsen (1967). Nickelsen and Loeschke worked in the same area over a similar period of time and their complimentary work was published in the same year.

Bjorlykke (1905) proposed the presence of a recumbent fold in the Mellene region and this was confirmed by the mapping of Nickelsen (1967), who used bedding - cleavage relationships, the sense of minor folds and the orientation of bedding to confirm his observations of way up from sedimentary structures. He was able to show clear evidence that the sequence at Mellene was in fact overturned and that it formed the southeastern limb of a large recumbent anticline, the Skarvemellen

Table 7.A.1

Rock Unit	Thickness metres	Stratigraphic age
Mellsenn Slate*	30	
Mellsenn Blue Quartz*	60	Cambrian to
Mellsenn Roofing Slate*	60	mid-Ordovician
Mellsenn Quartzite*	50	
Transitional Beds*	60	
Conglomerate 3 (Tillite)	0.5-3	
Valdres Sparagmite (Rundemellen type)	250	
Conglomerate 2	2	
Valdres Sparagmite (Rundemellen type)	400	Eocambrian
Conglomerate 1	30	
Valdres Sparagmite (Rognslifjell type)	1350	
Valdres Sparagmite (Rabalsmellen type)	1000	

The Valdres Sparagmite was not subdivided during mapping

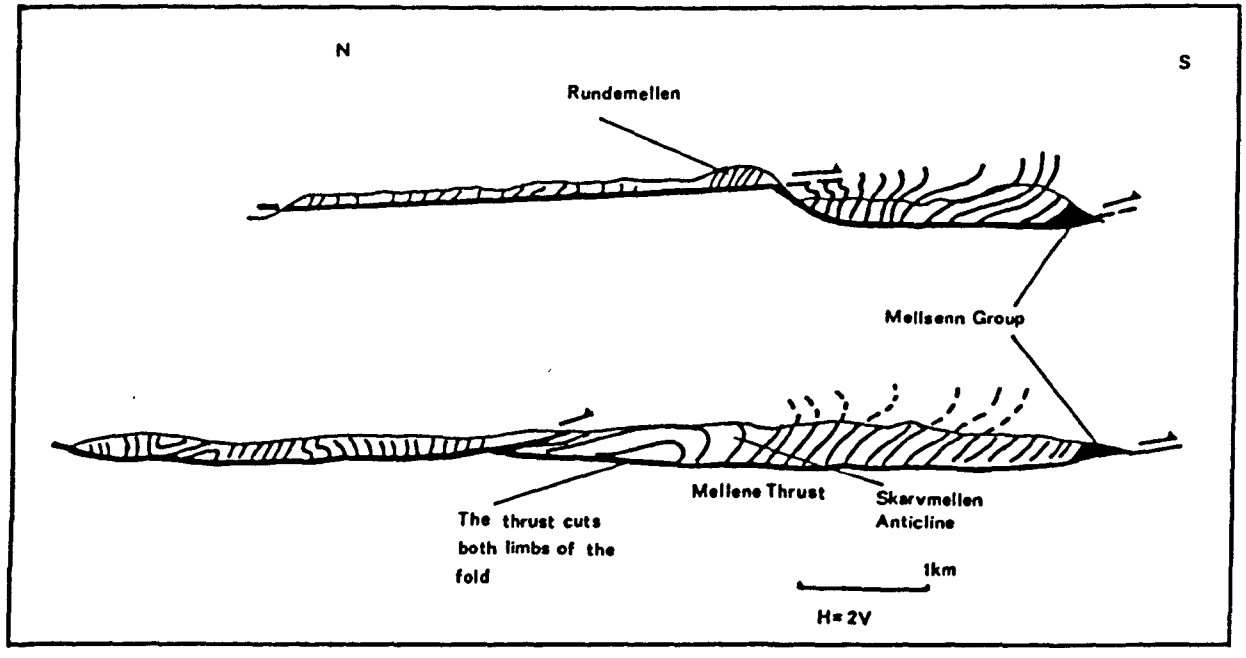

Figure 7.A.4. Geological cross sections through the Mellene Nappe showing the Skarvemellen Anticline (after Nickelsen 1967). In the lower section the Mellene Thrust cuts across both limbs of the fold.

Anticline, see Figure 7. A.4.. This shows the Mellsenn Group to be younger than the Valdres Sparagmite. This was supported by the work of Loeschke (1967a,b) who provided a revised stratigraphy for the Valdres Sparagmite and the Mellsenn Group which is given in table 7.A.1. together with stratigraphical thicknesses.

Nickelsen (1967) suggested that the rocks of the Mellene region form the Mellene Nappe, part of the Valdres Group of nappes, and that the Mellene Nappe was in tectonic contact with the Phyllite Formation (now Strondafjord Formation,Nickelsen et al 1974) this work was correlated with structures seen in the Grønsennknipa (Loeschke and Nickelsen 1968) and Dokkvatn regions (Nickelsen 1974) and thus, the stratigraphy and structure within the Valdres Group of nappes was revised.

Within the Skarvemellen Anticline, Nickelsen (1967) was able to recognise a slaty cleavage (S_1) which dipped moderately to the northeast and was affected by a weak second crenulation cleavage (S_2). The slaty cleavage was shown to be axial planar to parasitic minor folds and it had the correct sense on both limbs of the major fold to be considered axial planar to the major fold (it will be shown later, that this is not the case). Several lineations were also recognised, these were, bedding-cleavage intersections, intersections of the S_1 and S_2 cleavages, minor fold axes and extension lineations on the slaty cleavage plane (S_1).

Section 7B The Structural Geology of the Mellene Nappe

The Skarvemellen Anticline was mapped on a scale of 1:5000. Six rock types were mapped within the Mellene Nappe and these are shown in table 7.A.1. with the

thickness determined for each of the formations. The results of the mapping are shown in Figure 7.B.1..

In this study the Valdres Sparagmite was not sub-divided into the Rundemellen and the Rognslifjell types, unlike Loeschke (1967a,b), as the boundary between the types is difficult to define and may be transitional. Generally the Sparagmite is well bedded with good planar bedding surfaces. Beds tend to be of constant thickness, usually in excess of 1 metre. Many conglomeratic bands are present. When undeformed the clasts of the conglomerate are generally well rounded and typically consist of quartz and quartzite, though more exotic clasts are also present. Loeschke (1967a,b) provides a full description of the Valdres Sparagmite seen in the Mellene area.

The boundaries of the formations within the Cambro-Ordovician sequence are generally well defined because of the contrasting rock types which are present in the different formations and these are shown in table 7.A.1..

The Mellsenn Group outcrops in a broad arc which can be followed from Bergo in the west to the lake Mellsenn in the east. The boundaries of the formations within the group are usually clear and dip to the north (Figure 7.B.1.). The Mellsenn Group is underlain by the Valdres Sparagmite. The boundary is transitional, consisting of interbedded shales and sandstones. Sandstones may be either Sparagmite or Mellsenn Quartzite. Way up evidence seen in both the Valdres Sparagmite and sandstones of the Mellsenn Group confirms the work of Nickelsen (1967) and Loeschke (1967a,b), who suggest that the southern scarp of Skarvemellen forms the overturned limb of a large recumbent anticline. The overturned limb of the Skarvemellen Anticline dominates the area mapped. The bedding on the top of the

SEE BACK POCKET FOR MAP

Figure 7.B.1. Geological map of the Mellene Nappe. The area was mapped on a scale of 1:5000 and much of the detail has been omitted for clarity.

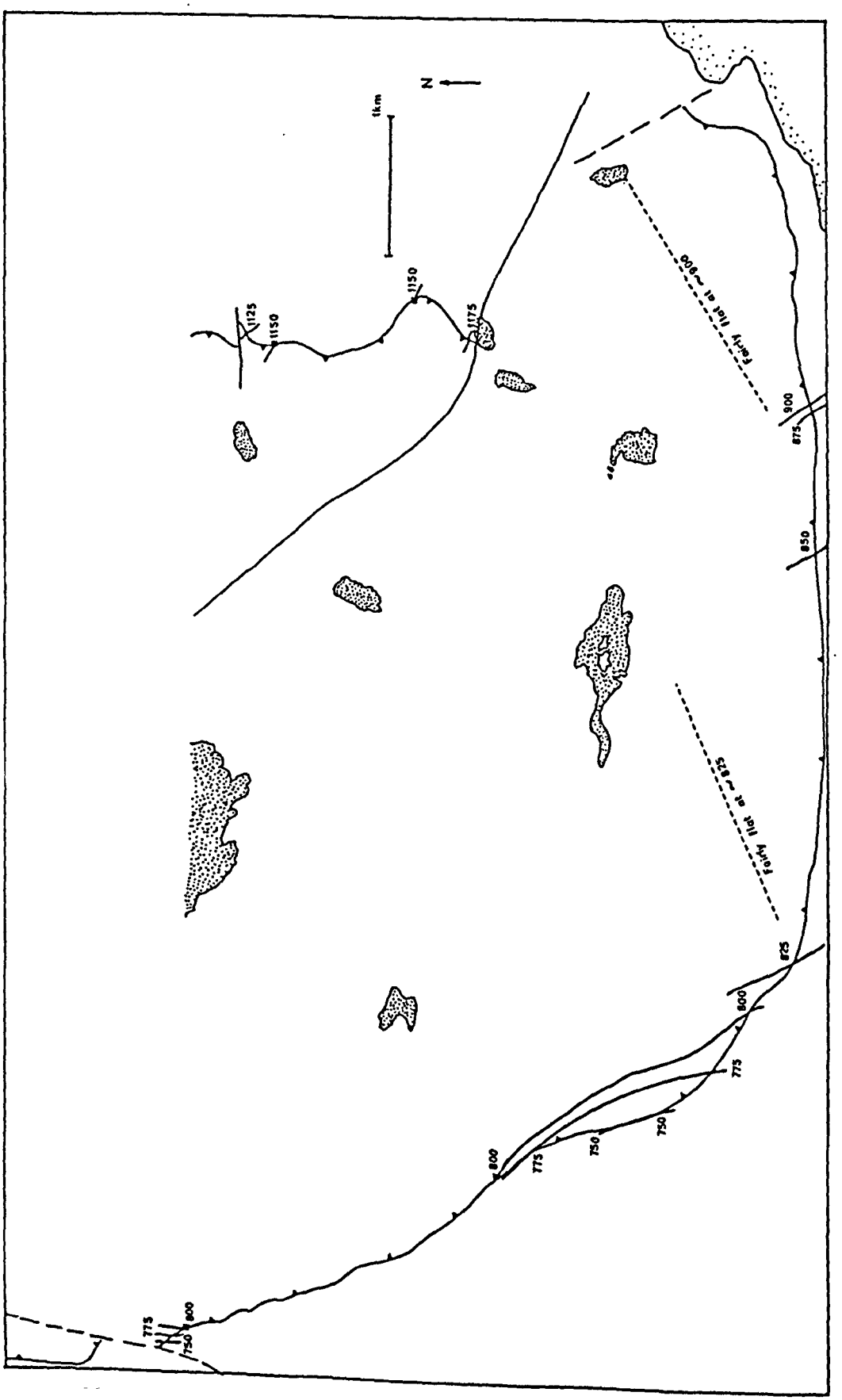

Figure 7.B.2. A map showing the contours constructed for the Mellene Thrust.

Skarvemellen is nearly vertical and it youngs to the south. Beneath, the dip of the bedding gradually decreases to around 20 degrees but is overturned. The axial trace of the Anticline outcrops within the Valdres Sparagmite and was mapped by Nickelsen (1967). The trace trends west-northwest - east-southeast and may be followed from the east of Moane, to the north of Rognslifjell to Melletjednet near Rundemellen. Only a few outcrops of the correct way up limb were seen during mapping, due to extremely poor exposure and this problem was described by Nickelsen (1967).

The underlying Mellene Thrust is never seen but it is marked by an abrupt change in slope and the thrust plane forms the saeter to the south and east of Mellsenn. The thrust plane is flat lying and may be mapped from Moane to Rabbalsvatnet. Figure 7.B.2. shows contours constructed for the thrust plane. The Mellene Thrust certainly cuts across the beds of the overturned limb of the Skarvemellen Anticline and between Bergo and Lake Mellsenn the Thrust is overlain by the Mellsenn Group. To the north it is overlain by the Valdres Sparagmite. Due to the limited outcrop of the upright limb of the Skarvemellen Anticline nowhere could outcrops be found to determine whether or not the thrust plane cuts across the beds of this limb. In the absence of evidence to the contrary and in view of the accurate mapping of Nickelsen (1967) confirmed in this work, the Mellene Thrust Plane is considered to cut across both limbs of the Skarvemellen Anticline (see Figure 7.A.4., after Nickelsen 1967).

On the southwest side of Rundemellen there is evidence of a large fault (Figure 7.B.1.) which may be followed northwards, from Rundemellen to Onyanagen, it occupies a large linear valley. To the southeast of Rundemellen it forms a scarp on the northeast ends of Storekalvemellin and Vesle Kalvemellin. Nickelsen (1967)

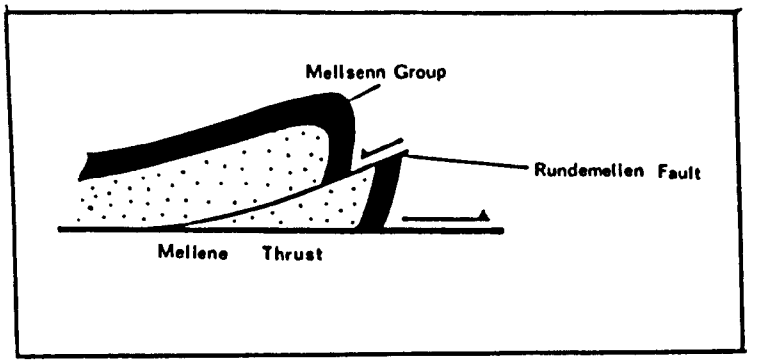

Figure 7.8.3. Hossack et al (1981) consicered the Rundemellen Fault to be a listric normal, downthrown to the north. This is in contrast to the previous work of Nickelsen (1967) who suggested that the fault was a thrust which climbed from the Mellene Thrust (see Figure 4.A.4.).

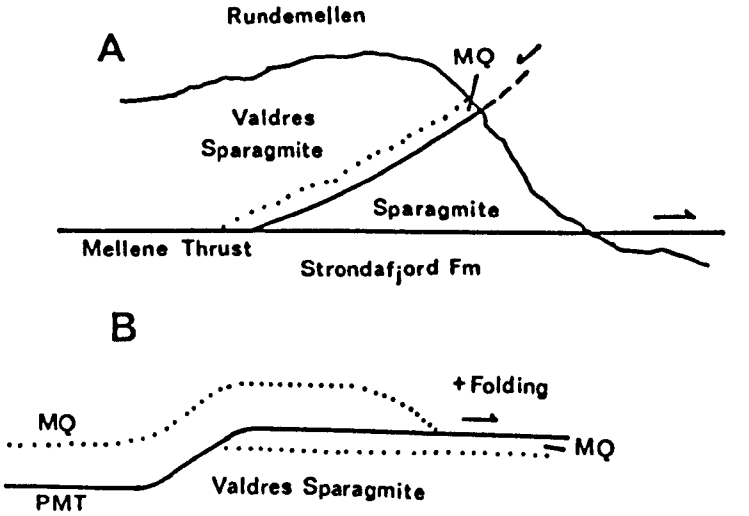

Figure 7.8.4. A. A sketched section (north-south) through Rundemellen showing the position of the Mellene Thrust and the Mellsenn Quartzite. The lower boundary of the quartzite must be tectonic and two possibilities may exist. A. A listric normal, downthrown to the north, which postdates the Skarvemellen Anticline. This fault is not equivalent to the Rundemellen Fault which trends almost parallel to the section. B. Thrusting of the Valdres Sparagmite over the Mellsenn Quartzite (on the pre-Mellene Thrust) prior to the development of the Skarvemellen Anticline and Mellene Thrust.

and Loeschke (1967a,b) considered this fault to be an imbricate thrust which rose from the Mellene Thrust. However, Hossack (pers com) has suggested that this fault is a listric normal fault which is downthrown to the north, see Figure 7.B.3.. The fault trace is parallel to the movement direction of the thrust zone (Hossack et al 1981) and parallel to other large faults which have been described as lateral ramps by Hossack (1980). It is suggested here that this fault, the Rundemellen Fault is a lateral ramp.

On the southeast face of Rundemellen (Figure 7.B.1.) the Mellsenn Quartzite crops out, it is overlain and underlain by Valdres Sparagmite. The upper boundary is conformable with the Valdres Sparagmite and therefore, the lower surface must be tectonic. There are two alternatives: the fault is a thrust which was active before the development of the Skarvemellen Anticline and it placed Valdres Sparagmite above the Mellsenn uartzite (see Figure 7.B.4.) and this was then folded. Alternatively the fault is a listric normal fault, which postdates the fold and shallows into the Mellene Thrust; it carries a portion of the Mellsenn Group to the northwest over the Valdres Sparagmite.(see Figure 7.B.4.).

To the east and northeast of Rundemellen the Mellene Thrust forms a shelf on the hillside; above the thrust plane the bedding is clearly seen. From Moane to Rundemellen the Mellene Thrust is underlain by sandstones and phyllitic slates of the Strondafjord Formation (Nickelsen et al 1981) but to the north of Rundemellen,small pieces of the Mellsenn Group and Valdres Sparagmite may be found. Loeschke (1967a) suggests that they form a single sequence of the Mellsenn Group, but they appear to be imbricated on a scale of a few tens of metres and none of the rock types seen are distinct enough to be ascribed to any particular horizon. It is suggested that to the east

of the Rundemellen Fault the footwall of the Mellene Thrust is composed of the Strondafjord Formation and imbricated rocks of the Mellsenn Group and Valdres Sparagmite, with a cross section similar to that shown in Figure 7.B.5.. To the west of the Rundemellen Fault the footwall is composed entirely of the Strondafjord Formation suggesting a profile similar to that shown in Figure 7.B.5.. The contrasting profiles are seen to either side of the Rundemellen Fault and this fault forms the lateral ramp between the two types of section (see Figure 7.B.5.).

Cross sections through the area are shown in Figure 7.B.6.. From field maps, contours were constructed for the Mellene Thrust and these were used in the construction of these sections. As the beds in the field appear to have a constant thickness, the sections were constructed using the Busk method (Ragan 1970), though the bed lengths obtained in this case are different for each of the formations. The Busk method itself will generate an excess of bed length in the upper part of the section. This will in part, contribute to the excess of bed lengths seen. However, in this case, the excess arises because the sections were drawn following those of Nickelsen (1967) (see Figure 7.A.4.)in which both limbs of the fold are cut by the thrust.

During mapping the orientation of bedding, cleavage, fold axes, mineral and intersection lineations were recorded. Stereograms of poles to bedding define a great circle which indicates a fold axis which plunges gently to the east or west (Figure 7.B.7.). The contoured plots shown here were obtained by use of the FORTRAN program GODP FORTRAN (Cooper and Nuttall 1979). Minor folds, generally seen within the Mellsenn Roofing Slate and the Mellsenn Slate, are shown in Figure 7.B.8. and lie extremely close to the fold axis defined by poles to bedding. Throughout the area mapped, these

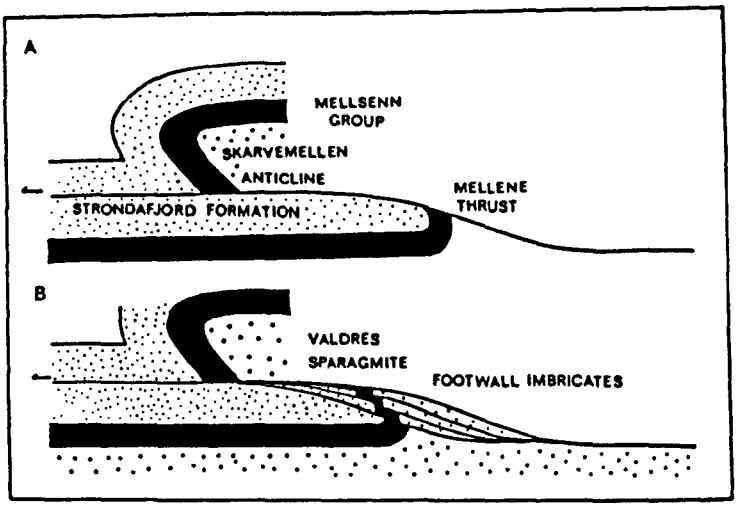

Figure 7.8.5. A schematic cross section through the Mellene Nappe to the west of the Rundemellen Fault. B. A schematic cross section through the Mellene Nappe to the east of the Rundemellen Fault. In this section the footwall of the Mellene Thrust is composed of both the Strondafjord Formation and imbricated Mellsen Group and Valdres Sparagmite.

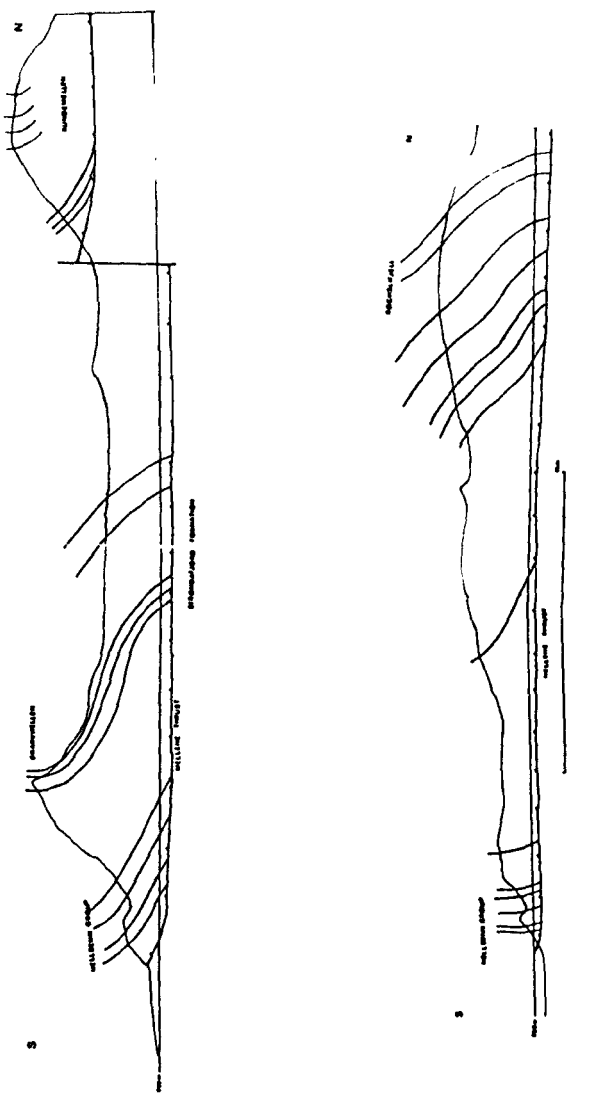

Figure 7.B.6. Geological cross sections through the Mellene Nappe based on the mapping shown in Figure 7.B.1.. The section lies as shown in Figure 7.B.1..

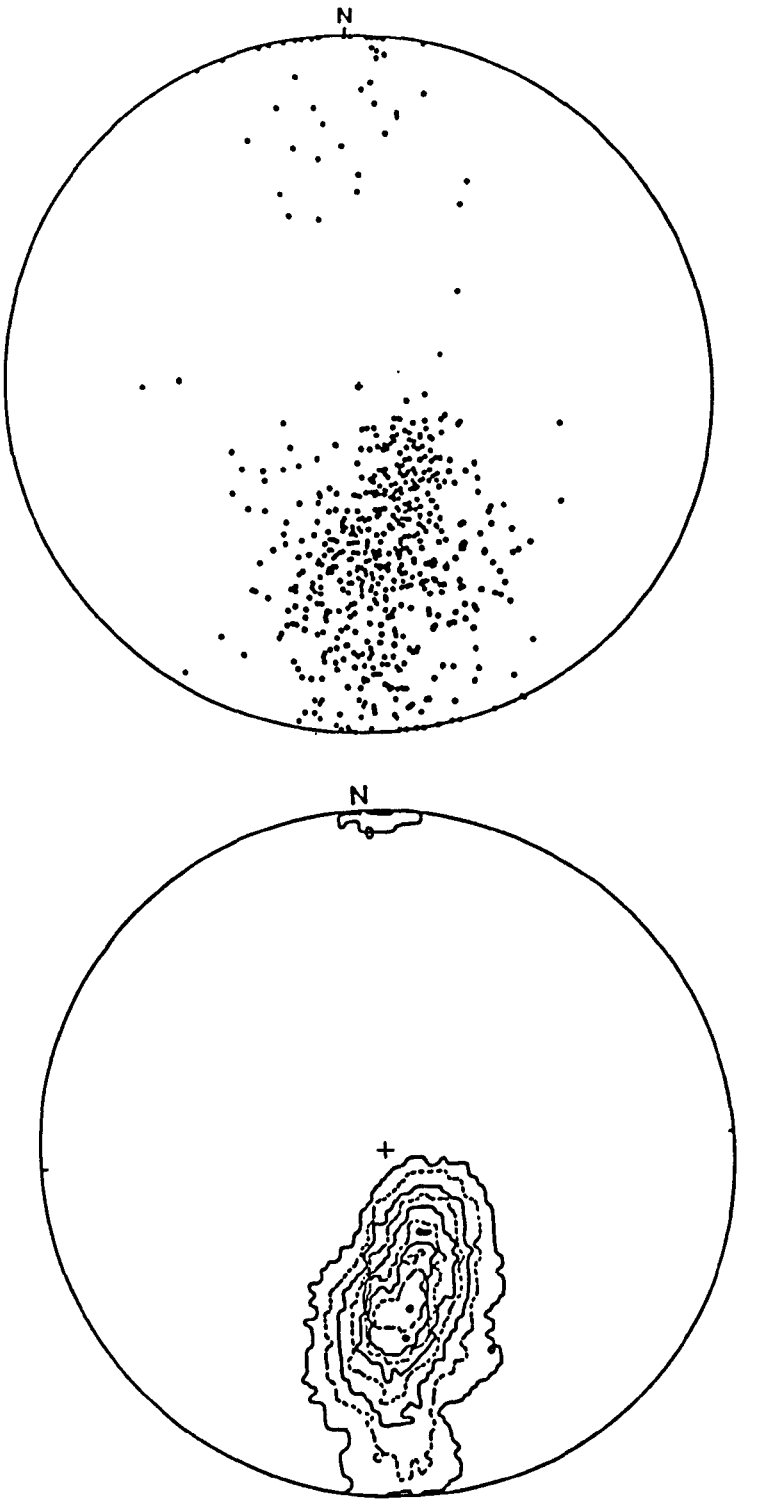

Figure 7.B.7. A stereogram of poles to bedding. The contoured plot was obtained using GODPP FORTRAN (Cooper and Nuttall 1979).

minor folds plunge both to the east and west and suggest that the major fold may be non-cylindrical with several shallow culminations and depressions. The minor folds were seen on the overturned limb of the Skarvemellen Anticline and posessed the correct asymmetry to be parasitic folds.

Two cleavages were recognised and their distribution mapped in the field. The first cleavage is a bedding parallel grain shape fabric, where the grains are prolate and tend to lie with their long axes in the plane of the bedding. The long axes of the grains define a grain shape lineation on the surface of the bedding parallel fabric, the orientation of which is shown in Figure 7.B.9. and these lineations define a similar field to the fold axes shown above. This suggests that during the development of the bedding parallel fabric there was extension parallel to the fold axis of the Skarvemellen Anticline.

The orientation and distribution of grain shape lineations is shown in Figure 7.B.10., together with the minor fold axes described above. The presence of quartz fibres in boudin necks of conglomerate pebbles, which are parallel to the grain shape lineation, suggest that the lineation is a true extension lineation. At many localities the bedding parallel fabric appears planar rather than linear. The bedding parallel fabric occurs throughout the sandstones of both the Mellsenn Group and the Valdres Sparagmite. Though few outcrops of the correct way up limb of the Skarvemellen Anticline were seen, the bedding parallel fabric does not appear to be present on this limb. The bedding parallel fabric is more strongly developed on the most overturned portion of the inverted limb around Langetjednet, Svartetjednet and Skarretjednet.

At the scale of an outcrop the second cleavage appears

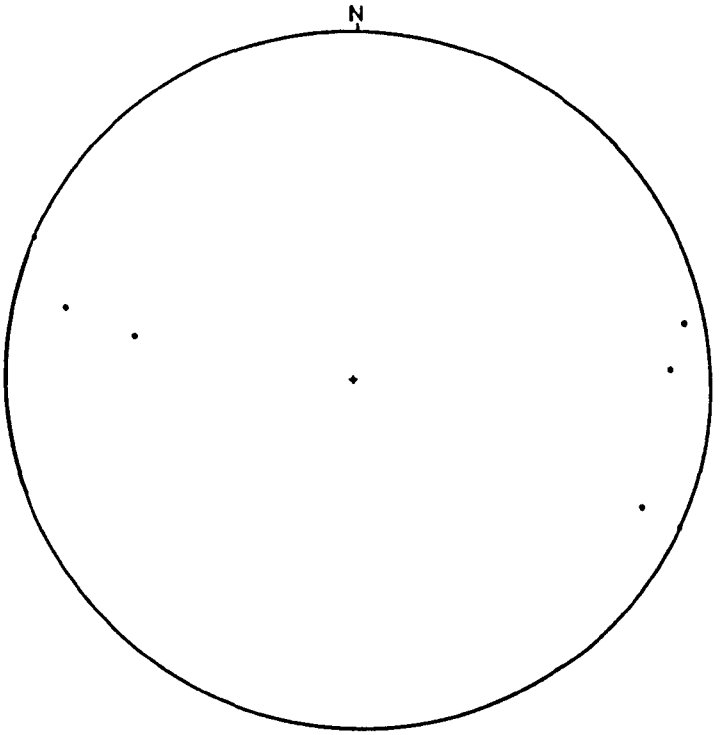

Figure 7.8.8. Stereogram of minor fold axes from the Mellene Nappe.

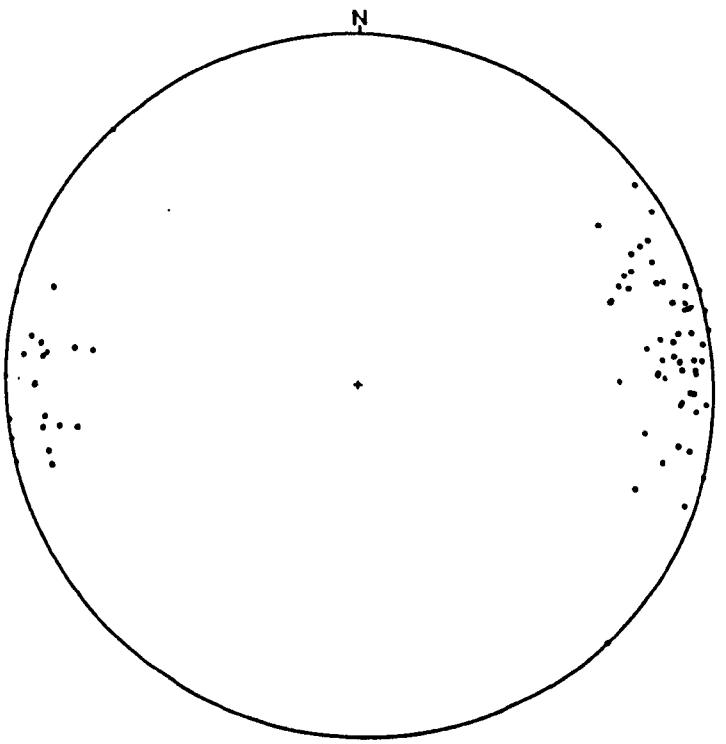

Figure 7.8.9. Stereogram of grain shape lineations from the Mellene Nappe.

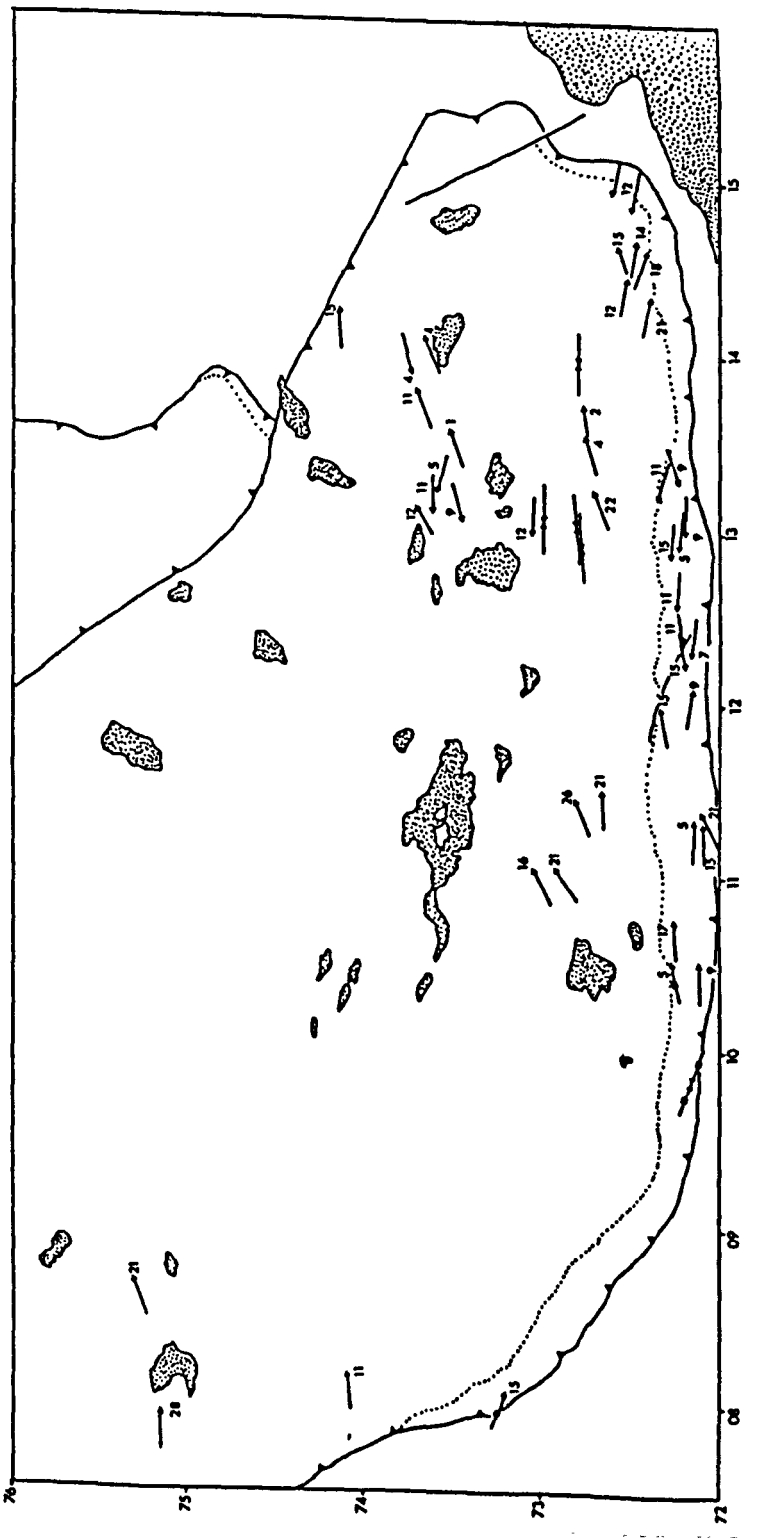

Figure 7.B.10. A map showing the distribution and orientation of minor fold axes (—■→) and grain shape lineations (——→) from within the Mellene Nappe.

to be axial planar to the major and minor folds. In the Mellsenn Slate and the Mellsenn Roofing Slate this cleavage is strongly developed. The cleavage is oblique to the bedding and is shown in Figure 7.B.11.. The cleavage is penetrative and in thin section it is produced by the preferred orientation of white mica and chlorite. Generally the phyllosilicates are very fine grained but some large white micas are present parallel to the fabric which may result from the secondary growth of the new mica. Small quartz grains are present which lie with their long axes parallel to the cleavage trace. The phyllosilicate fabric wraps around the quartz grains.

The cleavage dips gently to the northeast as shown in Figure 7.B.12. and it always dips less steeply than the bedding on the overturned limb of the Skarvemellen Anticline. Close to the axial trace of the Skarvemellen Anticline (as shown by Nickelsen 1967), in particular aroun Rognslifjell, the fine sandy and silty untis of the Valdres Sparagmite posses a cleavage which is generally a grain shape fabric but occasionally it appears to be spaced. This cleavage dips gently to the northeast and is thought to be equivalent to the penetrative cleavage seen in the slaty units of the Mellsenn Group. Around Rognslifjell there are numerous conglomerate beds and bands, often the pebbles of the conglomerate lie with their long axes close to the trace of the northeast dipping cleavage. However, at many outcrops the pebbles of the conglomerate lie with their axes parallel to the trace of the bedding parallel fabric, while the surrounding matrix on nearby shaly units the dominant cleavage dips to the northeast. This suggests that the bedding parallel fabric was the earliest cleavage and the northeast dipping cleavage was the second.

In the ground between Rognslifjell and the outcrop of

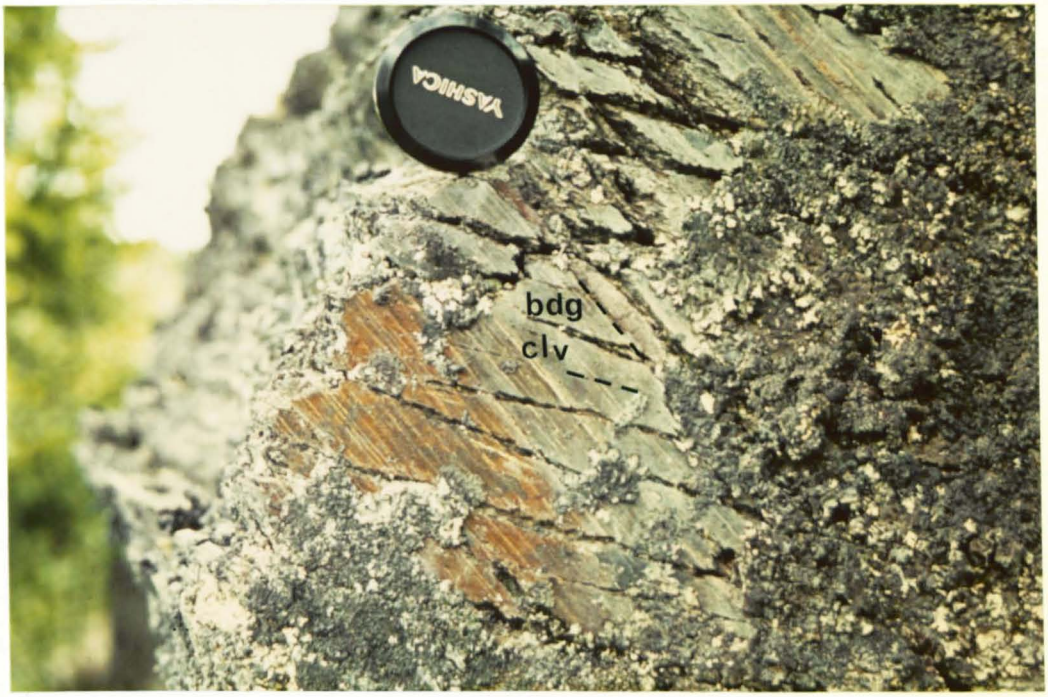

Figure 7.B.11. Photograph, looking to the west, showing the orientation of the axial planar cleavage in relation to the bedding on the inverted limb of the Skarvemellen Anticline at Valdres Skiferbrud.

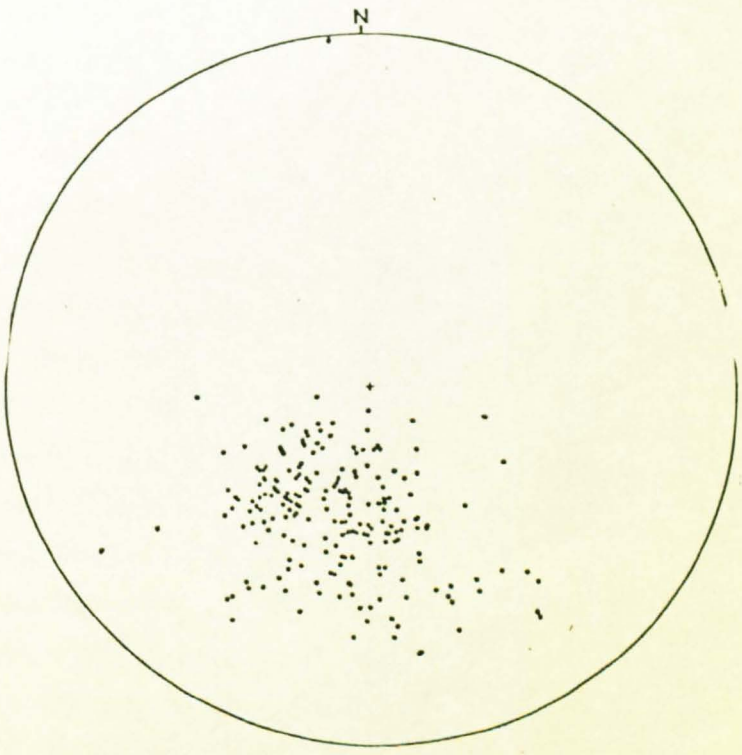

Figure 7.B.12. A stereogram of poles to the axial planar cleavage of the Skarvemellen Anticline.

the Mellsenn Group, shaly beds within the Valdres Sparagmite and the Transitional Beds show the north-east dipping cleavage. The sandstone beds on either side of these shale units usually, possess only the bedding parallel fabric suggesting that the northeast dipping cleavage was the second to form.

The northeast dipping cleavage is axial planar to the minor folds which are parasitic to the Skarvemellen Anticline. On the overturned limb of the Anticline the cleavage always dips less steeply than the bedding and Nickelsen (1967) reports that it dips more steeply than the bedding on the correct way up limb. These two pieces of evidence suggest that the northeast dipping cleavage is axial planar to the Skarvemellen Anticline as proposed by Nickelsen (1967). However, Figure 7.B.13. shows bedding - cleavage intersection lineations which have been measured in the field and constructed on a stereonet from bedding and cleavage values. The intersections define a great circle which dips gently to the northeast, close to that of the axial planar cleavage. In a cylindrical fold the bedding - cleavage intersection lineations should all lie parallel to the major fold axis. Clearly the intersections shown in Figure 7. B.13. are not parallel to the major fold axis as defined by the bedding and the orientation of the minor fold aaxes. Since the intersections all lie close to the cleavage plane then the cleavage must cut across the fold structure. This suggests that the cleavage is not related to the fold. However, the cleavage has the correct sense on both limbs of the Skarvemellen Anticline to be axial planar, which suggests that there is a relationship between the two structures. Therefore, it is thought that the Skarvemellen Anticline is an example of a transected fold

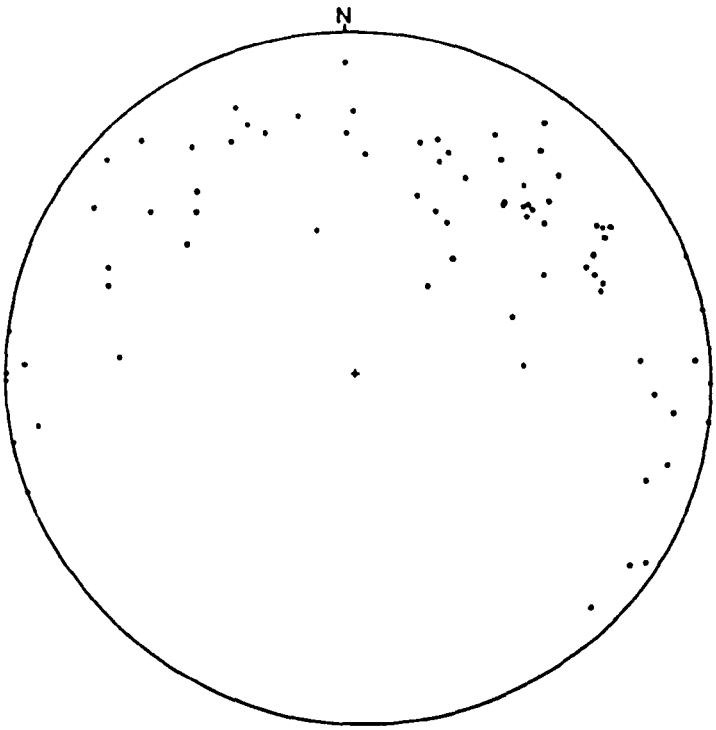

Figure 7.8.13. Bedding-cleavage intersection lineations from the Mellene Nappe. The lineations form a great circle which lies close to the plane of the axial planar cleavage (see Figure 7.8.12.).

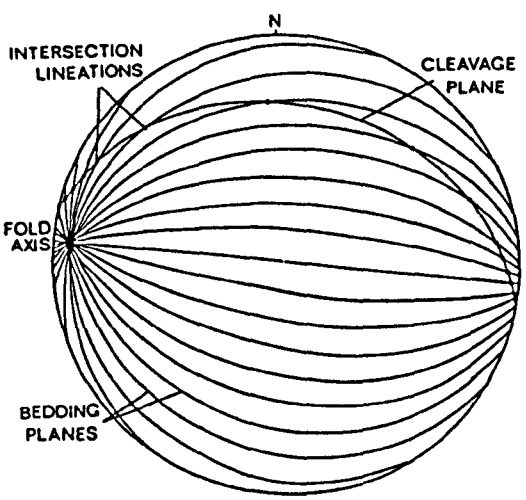

Figure 7.8.14. A stereogram which shows the orientation of the bedding-cleavage intersection lineations which are produced when a cleavage is not truely axial planar to the related fold.

(Powell 1974,Borradaile 1978) i.e. the cleavage is related to the fold but is not truely axial planar. The northeast dipping cleavage will be described as the axial planar cleavage in the remainder of the thesis, since it is synchronous with the fold and lies close to the axial plane. It should be remembered that this cleavage is not truely axial planar and this provides constraints on the fold development. A distinction is made between the axial planar cleavage and the Skarvemellen Anticline which transects the fold, and the transverse cleavage seen in the Lochalsh area of northwest Scotland. The transverse cleavage post-dates the development of the fold and dips more steeply than the bedding on both limbs of the fold. Though a clear relationship exists between the bedding parallel fabric and the axial planar cleavage they are probably both related to the development of the Skarvemellen Anticline.(See Figure 7.B.14.).

On the cleavage plane of the axial planar cleavage within the Mellsenn Slate and the Mellsenn Roofing Slate there is often a crenulation lineation. This takes the form of minute wrinkles of the fabric, often less than 1mm in wavelength and amplitude. At certain localities and extension lineation may be seen on the cleavage surface which is parallel to the fold axis of the Skarvemellen Anticline. However, as seen in Figure 7.B.15. the orientation of the crenulation lineation is very similar to that of the extension lineation and often it is difficult to distinguish between them. In thin section, the crenulation lineation is caused by the development of a conjugate pair of reversed kinks (Cobbold et al 1971). Crenulation of the axial planar cleavage was weak throughout the area mapped. The crenulation lineation is equivalent to the L_2 lineation of Nickelsen (1967) who reports, that, further north around Heggeberg it develops into a S_2

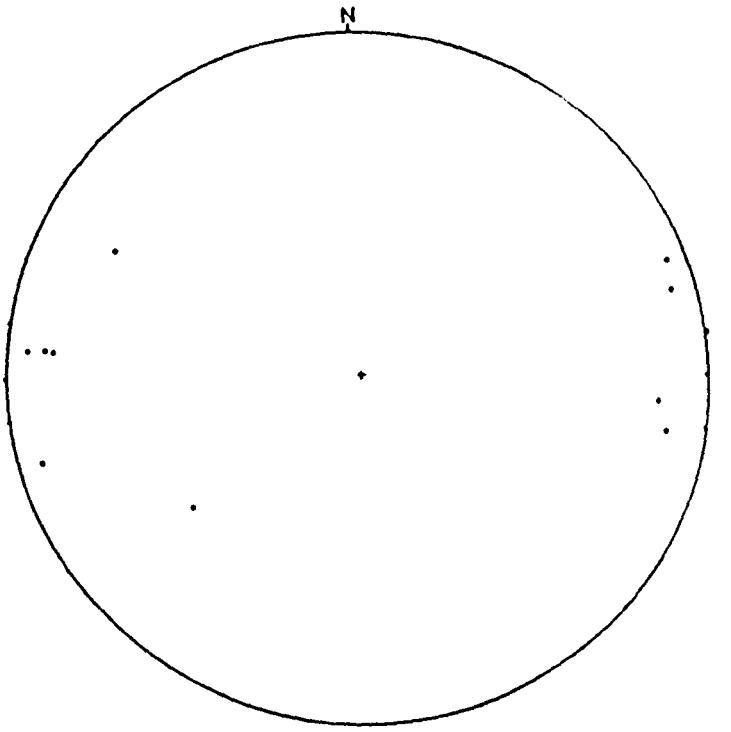

Figure 7.8.15. A stereogram of the crenulation lineations from the Mellene Nappe. The crenulation lineations affect the axial planar cleavage within the slates of the Mellsenn Group.

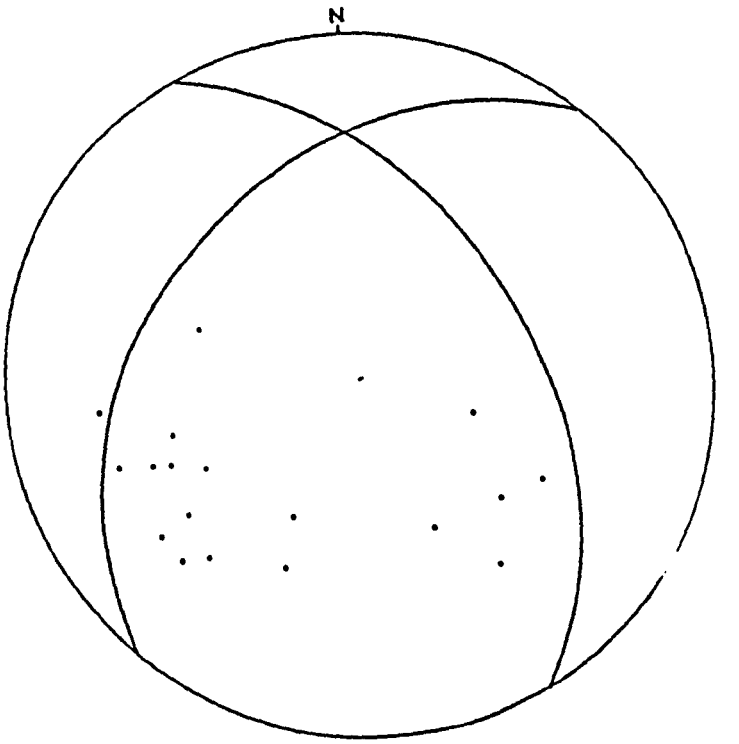

Figure 7.8.16. Poles to shear bands and shear fractures from within the slates of the Mellsenn Group. The two great circles show the mean orientation of the two sets of bands. Rarely do both sets occur within the same outcrop.

crenulation cleavage which postdates the axial planar cleavage.

The structures described above are similar,in relative age and orientation,to those described by Nickelsen (1967). Nickelsen recognised the lineation on the bedding surface due to the bedding parallel fabric but failed to recognise the presence of the fabric. A comparison of cleavages and lineations found in this study,with those of Nickelsen, is given in table 7.B.1.. Nickelsen (op cit) recognised the distribution of the bedding cleavage intersection lineations on a stereonet and ascribed it to the non-cylindrical nature of the folds within the Mellene Nappe, in particular the Skarvemellen Anticline. The non-cylindrical hinge of the Skarvemellen Anticline curves slightly in the 12 Km from Heggeberg to Mellsenn. The non-cylindrical nature of the fold, which is not disputed, will contribute to the distribution of bedding cleavage intersection lineations seen, but within the area mapped, on the basis of fold axes, the Skarvemellen Anticline is too cylindrical to produce the pattern seen. As described above, this pattern is attributed to the transected nature of the fold.

Within the slates of the Mellsenn Group a further structure may be seen. The axial planar fabric is often disrupted by the development of shear bands (Platt and Vissers 1980, Cobbold et al 1971). The shear bands dip to the west-northwest or east-northeast and at any particular locality one orientation is dominant. The shear bands are generally spaced a few centimetres apart and their displacement of the fabric suggests that movement on the shear band was down dip with the upper portion forming the hanging wall. The displacement on a shear band is typically a few millimetres. Often the centre of the shear band

is replaced by a discrete fracture plane with a similar movement sense . The fracture planes may be clean or infilled with fibrous material and the orientation of these fibres confirms that the upper surface is downthrown. In thin sections, these veins appear to be syncronous with a series of fabric parallel veins. Both types of veins contain fine grained quartz and calcite. The quartz grains have undulose extinction and deformation bands. The calcite is twinned, frequently two lamellae are seen which may be curved. The veins are affected by the crenulation described previously and must therefore have developed in the period between the axial planar cleavage and the crenulations. Figure 7.B.16. shows the orientations of shear bands, fractures and veins. These structures appear to represent an attempt by the slates of the Mellsenn Group to extend parallel to the major fold axis and this extension took the form of shear bands and related structures due to the anisotropic nature of the rocks.

Summary of Structures Within the Mellene Nappe

The structures of the Mellene Nappe will now be summarised. Above the Mellene Thrust, which dips gently to the northwest are a series of late pre-Cambrian and Cambro-Ordovician sediments which form the Mellene Nappe. These sediments are folded into a large recumbent fold, the Skarvemellen Anticline. The fold axis of the Anticline is very nearly horizontal and the hinge is curved, swinging from a northwesterly direction at Heggeberg (Nickelsen 1967) to and east-west direction around Mellsenn and a northeasterly direction around Rabbalsvann. Within the area mapped at Mellsenn the variation in azimuth is much smaller, between west-northwest and east-northeast. Several minor fold axes may be seen which are parallel to the major fold axis and these folds are parasitic to the

major fold and they posess a cleavage which appears to be axial planar. The axial plane of the Skarvemellen Anticline dips gently to the northeast.

Associated with the development of the Skarvemellen Anticline are two fabrics or cleavages. An early bedding parallel fabric which is overprinted by the later axial planar cleavage. The bedding parallel fabric is often planar but generally it is linear and the prolate grains tend to lie with their long axes in the plane of the bedding. This extension or grain shape lineation is parallel to the major fold axis and it suggests, that during the development of the Skarvemellen Anticline there was extension parallel to the fold axis. This fabric may be restricted to the inverted limb of the Anticline and it is most strongly developed on the more overturned portions of the limb. The second cleavage, termed the axial planar cleavage, is not truely axial planar. The bedding-cleavage intersection lineations fall on a great circle which is parallel to the mean cleavage plane which suggests that the cleavage postdates the fold. However, the cleavage has the correct sense on both limbs of the fold to be related to the fold and thus the Skarvemellen Anticline is an example of a transected fold as the synchronous cleavage is not axial planar to the fold.

Postdating the axial planar cleavage in the slates of the Mellsenn Group are a series of shear bands, fractures and veins which dip gently to the northwest or northeast and these appear to be extensional structures which were active between the axial planar cleavage and a phase of crenulation development. They reflect an attempt by the Skarvemellen Anticline to extend parallel to the fold axis, the high mechanical anisotropy in the slates causing shear bands and related structures to form.

Within the area mapped a large lateral ramp is

Table 7.B.1.

Present study	Nickelsen (1967)
Bedding	Bedding So
Bedding Parallel Fabric (and associated lineation)	L_1 extension lineation
Axial Planar Cleavage (and intersection lineations)	Slaty cleavage S_1 and L_1 intersection lineation
Crenulation lineation	Slip cleavage S_2, L_2 lineation

Table 7.C.1.

Locality	Rock Type	Charcteristic trace (figure 7.C.2.)
NN 12527373	Valdres Sparagmite	3
NN 11497392	Valdres Sparagmite	3
NN 12387427	Valdres Sparagmite	3
NN 14257232	Mellsenn Slate	7
NN 09207229	Mellsenn Roofing Slate	7
NN 09987212	Mellsenn Slate	7
NN 09157226	Mellsenn Slate	7
NN 12337220	Mellsenn Roofing Slate	7
NN 11677221	Mellsenn Roofing Slate	7
NN 10987206	Mellsenn Slate	7
NN 12047209	Mellsenn Slate	7
NN 13477224	Mellsenn Slate	7
NN 14237234	Mellsenn Roofing Slate	7
NN 12817190	Strondafjord Formation	7
NN 13787480	Transitional Beds	8

present, the Rundemellen Fault. The ramp is parallel to the thrust transport direction of 130 degrees (Hossack et al 1981) and has displaced the hinge of the Skarvemellen Anticline. The fault plane does not appear to persist downwards, beyond the Mellene Thrust. To the northeast of the Rundemellen Fault around Rennsennvann there is an area of poorly exposed folds and thrusts which are much smaller in scale than the Skarvemellen Anticline (Nickelsen 1967) and they appear to represent a series of folds and thrusts similar in style to those described by Coward and Potts (in press) in the Kempie Bay region of northwest Scotland.

Section 7C Metamorphic Grade of the Mellene Nappe

There have been no detailed studies of metamorphic grade within the Mellene Nappe. The work of Bjørlykke (1965) and Englund (1973) suggests that the presence of 1M muscovite indicates a lack of metamorphism in the Oslo region. Towards the thrust complex the 1M muscovite is replaced by 2M muscovite and the development of stilpnomelane and they took this to indicate the presence of low grade metamorphism affecting the Sparagmite and Cambro-Ordovician sediments of southern Norway. Bryhni and Brastad (1980) noted that these results do not form part of a systematic study and they suggest that the use of illite crystallinity or vitrinite reflectance is necessary to confirm this result. Hossack et al (1981) report a syntectonic temperature of over 300 ^{o}C from within the Synnfjell duplex from Conodont Alteration Index (A. Harris unpublished data). and a temperature of 220 ^{o}C from bubble thermometry in quartz fibres from the Synnfjell duplex and the Valdres Nappes (C. Morley unpublished data). These temperatures suggest low grade greenschist facies metamorphism above and below the Mellene Nappe.

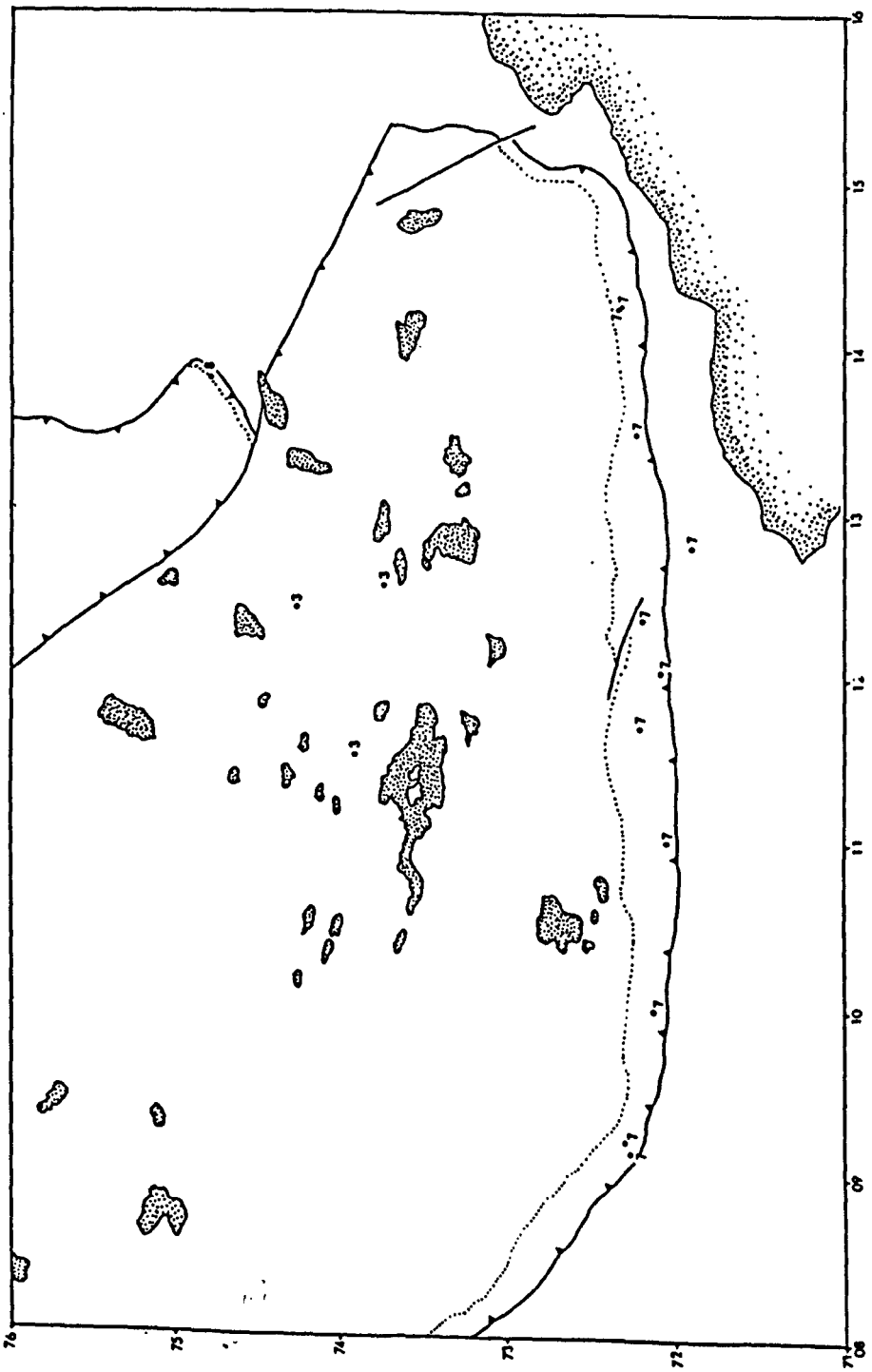

Figure 7.C.1. Map showing the distribution of sites from which shales and slates were sampled for analysis by XRD. The locality is marked by the group number of the mineral assemblage (see Figure 7.C.2. and 3.C.1.).

Table . . .1.

Locality	Rock Type	Charcteristic trace (figure 7.4.2.)
NN 12527373	Valdres Sparagmite	4
NN 11497392	Valdres Sparagmite	4
NN 12387427	Valdres Sparagmite	3
NN 14257232	Mellsenn Slate	7
NN 09207229	Mellsenn Roofing Slate	7
NN 09987212	Mellsenn Slate	7
NN 09157226	Mellsenn Slate	7
NN 12337220	Mellsenn Roofing Slate	7
NN 11677221	Mellsenn Roofing Slate	7
NN 10987206	Mellsenn Slate	7
NN 12047209	Mellsenn Slate	7
NN 13477224	Mellsenn Slate	7
NN 14237234	Mellsenn Roofing Slate	7
NN 12817190	Strondafjord Formation	7
NN 13787480	Transitional Beds	6

To determine the metamorphic grade of the Mellene Nappe; specimens of shale and slate were taken at several localities within the Nappe. Shales and slates were chosen as they tend to record the metamorphic grade more accurately than sandstones. Further, the metamorphic changes at low grades are more accurately known in shales and slates.

Powdered specimens were prepared and analysed by X-ray diffraction (XRD) using Fe-k_a radiation as described in chapter 3. XRD was used because it is the most rapid method of identifying fine grained phyllosilicates. The results were compared with those from northwest Scotland.

The localities from which the specimens were taken are shown in Figure 7.C.1. and the grid references are given in table 7.C.1.. In hand specimens no individual grains can be seen in the samples collected. Specimens from the Valdres Sparagmite are maroon to red in colour, lustreous, with a penetrative cleavage. The shales of the Transition Beds are red or green and these Beds were sampled as they posess a moderately strong penetrarive cleavage. The Mellsenn Roofing Slate is generally deep purple, though some green beds and horizons are present. The Mellsenn Roofing Slate has a strong penetrative cleavage which is the axial planar cleavage. In the Mellsenn Slate this cleavage is not as well developed. The Mellsenn Slate is generally dull grey in colour and around Skieferbrod dolomitic nodules are present. Both the Mellsenn Roofing Slate and the Mellsenn Slate show evidence of crenulations but the shales of the Vladres Sparagmite to not.

Three characteristic traces were obtained from XRD for all of the specimens analysed (see table 7.C.1.). The

first trace, Group 3 of Figure 7.C.2., shows many distinct peaks which may be attributed to the presence of quartz, 2M1 muscovite and 2M2 muscovite. No chlorite peaks were seen. A peak is present at 44.2 degrees which is thought to be due to haematite and this group were taken from within the Valdres Sparagmite and no specimen from the Sparagmite occurs in the other groups. The mineral assemblage is

Quartz + 2M1 Muscovite + 2M Muscovite

and the split quartz - 2M1 muscovite peak is a characteristic of this group. The specimens from the Mellsenn Slate and the Strondafjord Formation all have a trace of Group 7 Figure 7. C.2.. Only peaks which may be ascribed to quartz, chlorite or pyrophyllite are present and no muscovite peaks can be seen. There is no distinction between the various rock types and there is no distinction between the purple and green coloured portions of the Mellsenn Roofing Slate. The mineral assemblage of this group is

Quartz + Chlorite + Pyrophyllite

This is in agreement with thin sections of the Mellsenn Roofing Slate and Mellsenn Slate which show a strong cleavage which is often crenulated. The cleavage is formed by the preferred orientation of chlorite and white mica flakes. The white mica cannot be identified in thin section but the larger grains lack the mottled appearance typical of muscovite, presumably this is pyrophyllite. Both the chlorite and white mica are crenulated and it would appear that they were produced by low grade, prograde, metamorphic reactions during the development of the axial planar cleavage. Quartz is clearly seen in all thin sections.

Group 8. of table 7.C.1. has only one member a specimen

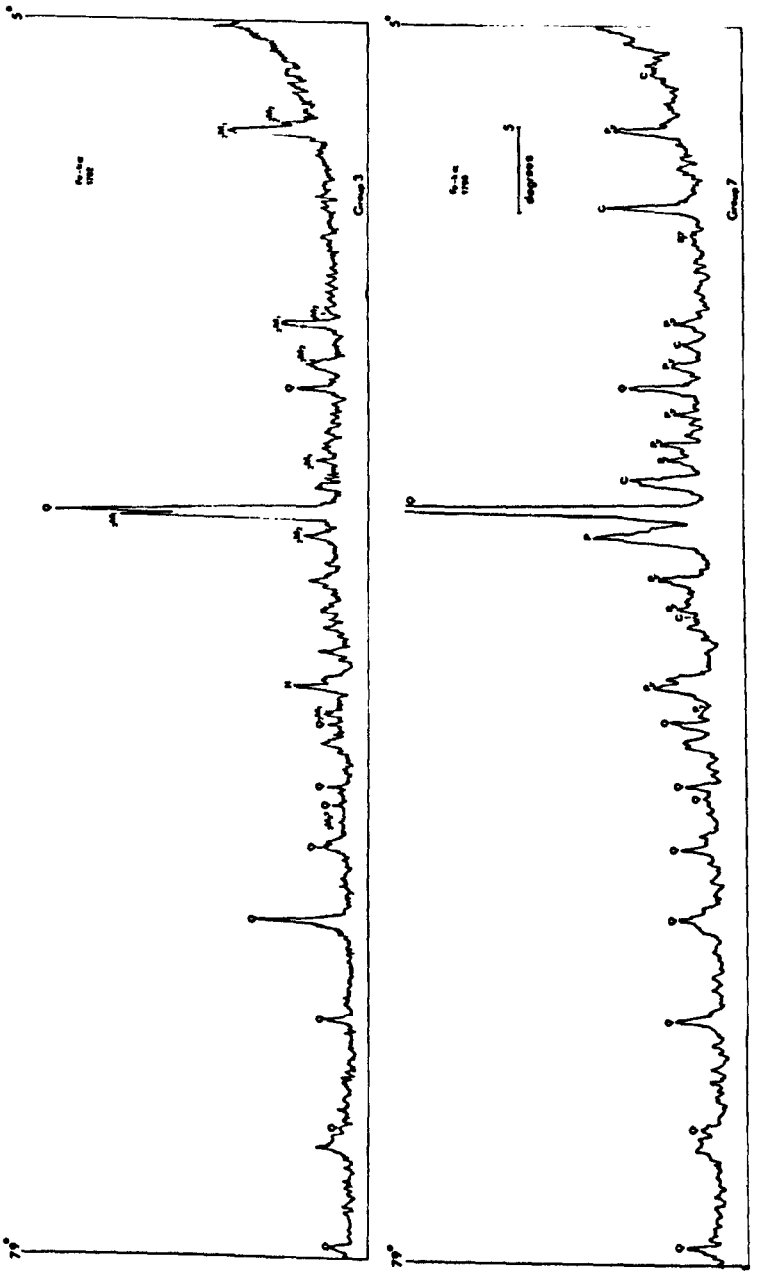

Figure 7.C.2. Traces characteristic of groups 3 and 7 from XRD analysis (see Figure 3.C.1. for notation).

from the Transitional Beds on Rundemellen. The trace is very similar to that of group 3 shown in Figure 7.C.2. but chlorite peaks are present, though not well developed. The mineral assemblage is

Quartz + 2M1 Muscovite + 2M2 Muscovite + Chlorite

No clay minerals were identified in any of the three groups (table 7.C.1.). It would appear, that the Mellene Nappe developed under low grade greenschist facies metamorphism which is indicated by the presence of chlorite and the lack of clay minerals. This is in agreement with the results of Bjørlykke (1965) and Englund (1973) and those reported in Hossack et al (1981). However, the main control on the mineral assemblage which may be seen in a specimen is the bulk rock chemistry. Distinct mineral assemblages were obtained for the Valdres Sparagmite, Transitional Beds and the Mellsenn Group and this must reflect difference in bulk rock chemistry. This control by rock type is more clearly seen in these results than in those from northwest Scotland. It must be emphasised that studies using XRD and the related techniques of illite crystallinity and mica polymorphs to determine temperature must be accompanied by whole rock chemical analyses so that similar compositions may be compared. Such work is beyond the scope of this project. Illite crystallinity was not studied because of the reservations expressed above.

Section 7D Strain Analysis Within the Deformed Conglomerates of the Valdres Sparagmite

To determine the finite strain within the Mellene Nappe the deformed conglomerate beds of the Valdres Sparagmite have been studied. The conglomerate beds and horizons are common throughout the outcrop of the Sparagmite and in particular at the boundary between Rognslifjell and

Rundemellen types (Loeschke 1967a,b). Nineteen sites have been studied and these are shown in Figure 7.D.1.. The site numbers correspond to those given in table 7.D.1.. The number of suitable sites was limited by the number of outcrops at which three planes could be measured. Ideally three mutually perpendicular planes should be studied but this was rarely possible. In general, the bedding surface and a joint plane were measured. These joint planes have a similar strike to the bedding and are perpendicular to the bedding surface. Where possible a third joint plane of diverse orientation was measured. It was also necessary to spread the sites as evenly as possible throughout the area studied and this limited the number of sites considerably. Milton (1980) has given an excellent review of strain measurements within deformed conglomerates. The problems of measurement, which he discussed at length, were encountered in this study. However, it was possible to sample a range of sites in which, qualitatively, the finite strain increased and this increase could be related to position in the fold and the associated cleavages.

Data of pebble axial ratio and orientation were measured directly in the field using the methods described in section 4B. These results were supplemented by data obtained form photographic slides which were taken where measurement was difficult or the grain size was too small for accurate measurement in the field. At some sites only photographs were taken and this was used to increase the number of sites sampled within the time available. Orientation marks were made on the surface photographed and the pebble axial ratio and orientation relative to these marks was obtained using the program ELLA FORTRAN on tracings made from the slides. When sampling, whether by direct measurement or by photographs, the orientations of bedding, cleavages and lineations were noted. Where possible only quartz

Table 7.0.1.

Site No.	Locality	Orientation of Fabric	Orientation of Plane	N	Strain ratio	Orientation of Long axis (Pitch)
1	NN 10897363	266 35 P (i)	061 58	37	3.163 H	14.0
			210 75	25	3.040 H	147.0
			000 00	15	1.670 L	98.0
2	NN 10807395	256 58 P (i)	088 32	42	2.580 H	170.0
			029 96	41	2.708 H	53.0
			256 58	20	1.158 L	129.4
3	NN 13807420	248 62 P (i)	018 39	27	3.120 H	25.0
			068 118	11	1.958 L	83.0
			128 90	10	3.636 H	120.0
4	NN 11947353	251 35 P (i)	002 90	27	2.658 H	30.0
			071 62	42	2.514 H	00.0
			251 35	21	1.144 L	169.0
5	NN 12327308	268 20 P (i)	088 20	31	2.393 H	00.0
			268 20	28	1.026 L	170.3
6	NN 13267358	269 38 P (i)	349 95	20	1.448 L	29.0
			069 50	31	3.045 H	00.0
			269 38	33	1.158 L	129.4
7	NN 14097369	246 30 P (i)	019 90	40	2.978 H	29.0
			053 60	38	2.937 H	00.0
			246 30	42	1.525 L	142.7
8	NN 13067331	260 24 P (i)	080 90	30	2.797 H	00.0
			018 75	23	2.395 H	22.0
			260 24	22	1.139 L	128.8
9	NN 12887295	265 26 P (i)	085 90	40	2.331 L	179.5
			265 26	42	1.797 L	171.9
			358 90	22	1.950 L	15.0
10	NN 13487275	264 71 B (i)	000 00	42	1.721 L	78.0
			078 110	42	2.356 L	179.5
			008 90	37	1.389 L	8.0
11	NN 14247256	270 50 B (i)	066 42	44	1.619 L	12.0
			272 55	36	1.598 L	171.1
			182 90	3	1.430 L	140.0
12	NN 14897317	248 10 P (i)	029 103	44	2.017 L	00.0
			060 90	36	2.380 L	179.7
			233 12	30	1.311 L	162.8
13	NN 12417382	317 20 D (i)	084 52	39	3.799 S	26.0
			010 82	42	1.399 S	17.0
			080 137	21	1.196 L	13.0
14	NN 08267408	284 32 D (i)	104 44	50	2.000 S	00.0
			091 120	8	1.404 L	24.0
			194 98	29	1.000 S	148.0
15	NN 08637530	308 38 D (i)	070 50	31	1.200 S	160.0
			154 90	11	1.000 S	32.0
16	NN 13337272	258 90 P (i)	078 90	71	2.052 L	170.4
			000 00	53	2.001 L	79.1
			159 65	40	1.031 L	93.0
17	NN 10447394	281 48 P (i)	136 75	34	1.593 L	165.4
			047 53	28	1.643 L	24.0
18	NN 12497380	255 52 P (i)	024 75	13	1.699 S	35.0
			083 32	34	1.000 S	12.0
19	NN 12817352	264 22 P (i)	078 90	43	2.498 L	2.0
			138 80	23	2.068 L	152.3
			264 22	22	1.028 L	8.0

P-Bedding Parallel Fabric D-Discordant Fabric B-Bedding (no fabrics)
H-Harmonic Mean L-Lisle Method (Lisle 1978) S-Strane (Dunnet and Siddans 1971)
(i) = Inverted Bedding

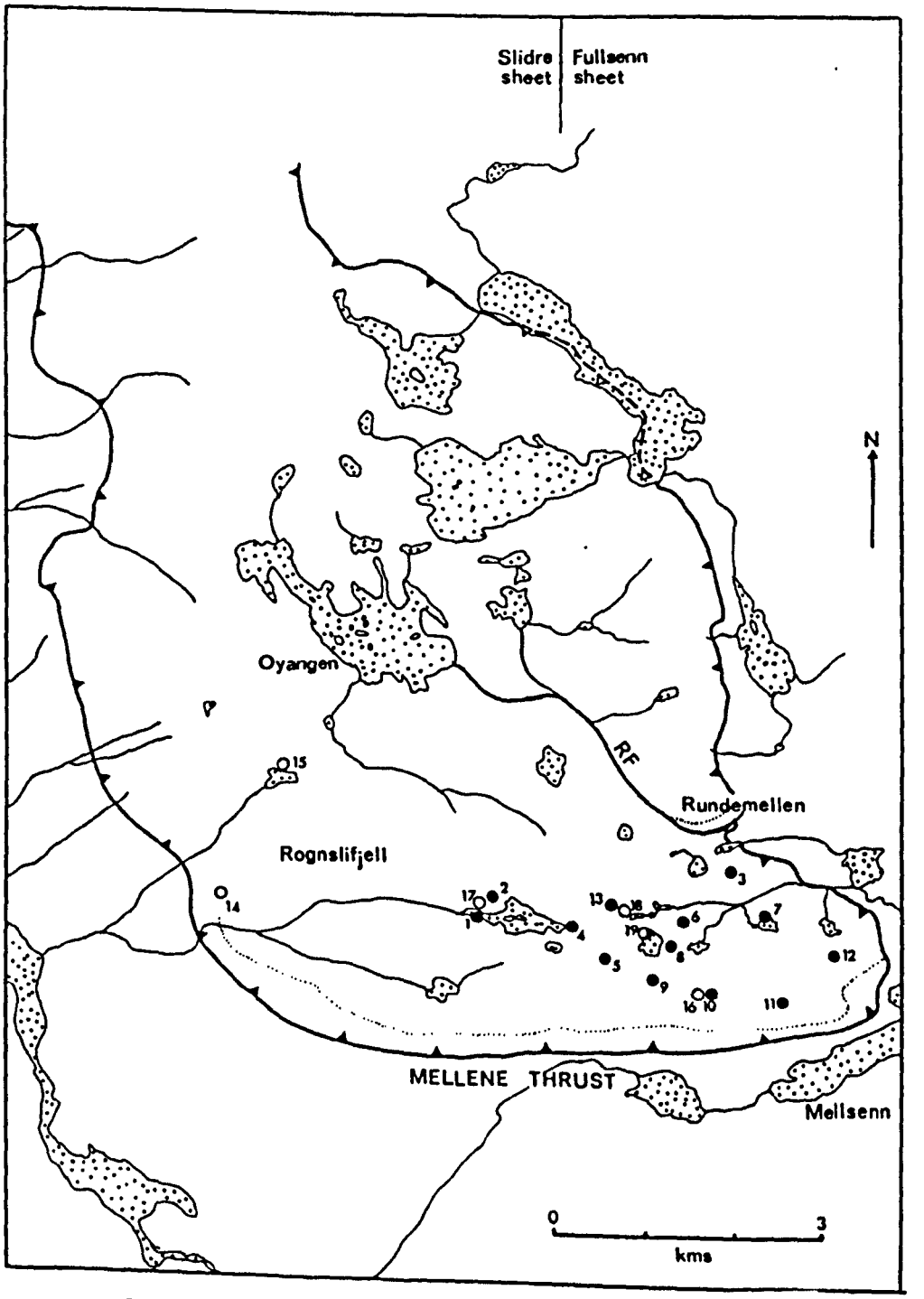

Figure 7.D.1. A map showing the distribution of conglomerate sites which are studied in this thesis. See Table 7.D.1. for details of the sampling localities.

and quartzite clasts were measured but at certain localities it was necessary to measure feldspar pebbles. Direct measurement is preferred as a method of sampling as it is easier to determine the lengths of the axes more accurately and a greater surface area may be studied. In this study, because of the low finite strain, it was often difficult to determine the orientation of pebble long axes on the bedding surface.

During analysis of the pebble data the sites were broken down into three groups. Each groups was analysed in a slightly different manner. Three estimates of the strain ratio were used and these will be described here.

In many of the sites, on planes at a high angle to the bedding the long axes of the pebbles lie parallel to the trace of the bedding parallel fabric and the methods of Dunnet (1969), Dunnet and Siddans (1971) and Lisle (1977a)could not be used. In these cases the harmonic mean was used as an estimate of the strain ratio (Lisle 1977b). It has been shown, that the harmonic mean is closer to the true strain ratio than the arithmetic or geometric means of pebble axial ratios (Lisle 1977b). The data from the bedding planes of these sites were analysed using the program THETA FORTRAN (Peach and Lisle 1979). This program was used because during its "unstraining process" the program tests for the most random fabric of Ø values and this point is used to calculate the strain ratio. Observations in the field suggest that this was the most suitable technique for determining the strain ratio as at low strains the fluctuation in pebble long axes is large due to the well rounded shape of undeformed pebbles. With increasing strength of the fabric the fluctuation in pebble long axes decreases rapidly.

The remainder of the sites studied show a fluctuation

in Ø values on all the planes measured. Where only the bedding parallel fabric is seen these sites were analysed using THETA FORTRAN (Peach and Lisle 1979). The program is based on the method of Lisle (1977a) and the criteria which it uses during unstraining were thought to be more valid than those of Dunnet (1969) and Dunnet and Siddans (1971).

In the sites where the axial planar fabric is present the results on the bedding surface were analysed by the use of THETA FORTRAN (Peach and Lisle 1979) and the results from the oblique planes were analysed using the program STRANE FORTRAN (Dunnet and Siddans 1971). The program STRANE FORTRAN "undeforms" the Rf/Ø data until a symmetrical distribution is obtained which is related to the trace of the bedding (Dunnet and Siddans 1971). This program provides the best estimate of the strain ratio due to the axial planar cleavage. The program STRANE FORTRAN (op cit) produces Ri/Ø data from the original Rf/Ø data on the basis of the strain ratio determined by the program. The Ri/Ø data may then be analysed by other methods and two sets of strain ratios obtained, in this case related to the bedding parallel fabric and the axial planar cleavage. However, in this study this was not possible because the strain ratio on the bedding surface could not be partitioned into components of strain related to the two fabrics. STRANE FORTRAN could not be used on the data from the bedding surface as the program requires a bedding trace and a cleavage trace which are distinct. Therefore, results from STRANE FORTRAN record the strain due to the axial planar cleavage whereas the results from THETA FORTRAN were used to record the strain due to both the axial planar cleavage and the bedding parallel fabric.

The sites which correspond to the groups above will now be described. Typical results will be presented

and their relationship to the cleavages discussed. The sites which show distinct patterns of Rf/Ø data which may be related to the cleavages seen in the field are extremely useful because their position on a Flinn diagram (Flinn 1962, Ramsay 1967) can be used to establish the strain path (Ramsay 1967). These points may be used as a control for those sites which the Rf/Ø data is less distinct or transitional between two types of sites.

The methods used in this study to analyse the data obtained from the conglomerates of the Valdres Sparagmite are based on several assumptions the most important of these being;

(a) Homogeneous pure shear deformation (Ramsay 1967)
(b) No ductility contrast between the pebbles and the matrix (Gay 1968a,b)

In this study the strain is considered to be homogeneous on the scale of an outcrop. However, components of simple shear deformation may have been recorded by the pebbles. Comparable programs to STRANE FORTRAN (Dunnet and Siddans 1971) and THETA FORTRAN (Peach and Lisle 1979) may be written, but they are clumsy and require knowledge of the orientation of both the shear plane and the shear direction. In natural situations these are rarely known and in cases where they are known,the strain ratio may be obtained more rapidly using alternative methods, for example Ramsay and Graham (1970). Therefore, in the absence of any alternative methods those cited above were used, but large errors in the strain ratio will be produced by these methods.

To reduce the effect of any ductility contrast which may exist between the pebbles of the conglomerate and the matrix, only quartz and quartzite clasts were

measured, whenever this was possible. Vein quartz and quartzite pebbles are generally more ductile than feldspar clasts (Milton 1980) and the latter will seriously underestimate the strain ratio. The quartz and quartzite pebbles may well underestimate the strain ratio and the influence of ductility contrast on the results obtained will be discussed later, as the matrix from site 7 was sampled for thin section study and the strain recorded by the pebbles and the matrix at this site may be compared.

Site eleven was chosen as in the field, it appeared to be the least deformed outcrop which could be studied and thus it provided information regarding initial fabrics and pebble axial ratios. No tectonic fabric could be seen at this outcrop. The pebbles are well rounded and in planes oblique to the bedding the pebbles lie with their long axes close to the bedding trace. This may represent an initial sedimentary fabric (Dunnet and Siddans 1971). However, as seen in Figure 7. D.2. there is a slight preferred orientation of pebble axes on the bedding surface and though this could be of sedimentary origin, the site may have suffered a small amount of deformation. Site eleven, on the basis of Rf/Ø diagrams appears to have one of the lowest finite strains in the conglomerates studied, this is indicated by the large range of Ø seen in the diagrams. The data from this site was analysed using THETA FORTRAN (peach and Lisle 1979).

Sites 9, 10, 12, 16, 17 and 19 have Rf/Ø diagrams which are similar. The Rf/Ø data for site 9 is shown in Figure 7.D.3. which is typical of the group. On the bedding surface there is a slight preferred orientation of pebble long axes. On the surfaces at a high angle to the bedding there is a fluctuation in long axes, but the points cluster about the bedding trace which is shown in the diagram. All sites in

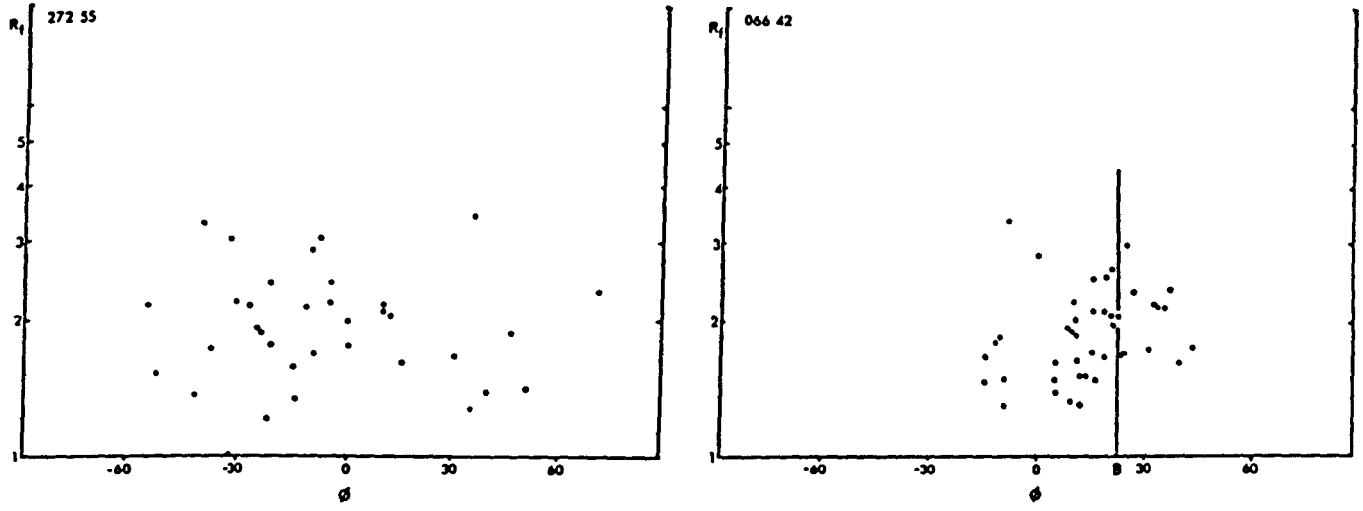

Figure 7.D.2. Rf/Ø diagrams from site 11. This site was chosen as, in the field, it appear to have been the least deformed of the sites studied.

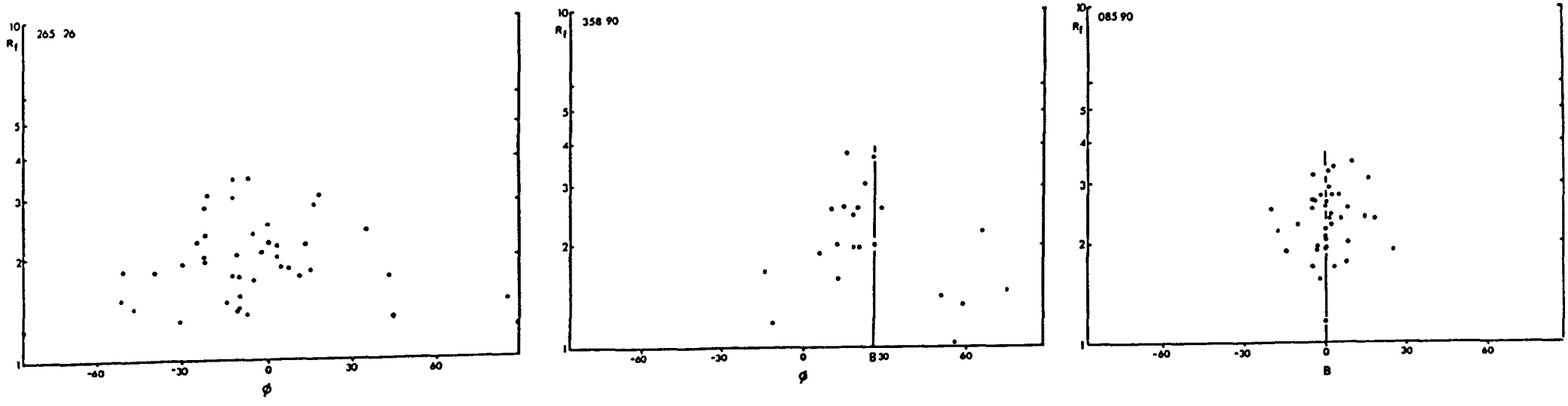

Figure 7.0.3. Rf/ϕ diagrams from site 9. The diagrams are typical of sites 9,10,12,16,17 and 19. There is a slight preferred orientation of grain long axes on the bedding surface and on planes at a high angle to the bedding the axes cluster around the bedding trace.

this group posess the bedding parallel fabric,which in the field, appears to be of tectonic origin. It is strongly developed in the conglomerate matrix and the pebbles have lost their well rounded shape; they tend to have pointed ends typical of deformed conglomerates (Lisle 1980).

Sites 1 to 8 record only the bedding parallel fabric. These sites appear to represent the most highly deformed of the sites which record only the bedding parallel fabric. There is a fluctuation in pebble long axes on the bedding planes, but this is restricted. Where a strong lineation is seen in the field, the lineation plots at the centre of the cluster seen on the corresponding Rf/Ø diagram (see Figure 7.D.4.). On planes oblique to the bedding the pebbles lie with their long axes parallel to the trace of the fabric. The data from each of the bedding planes was analysed using THETA FORTRAN. The harmonic mean of axial ratios was determined for each of the planes which were oblique to the bedding.

Sites 13, 14, 15 and 18 are distinct in recording the axial planar cleavage. In some sites in this area the bedding parallel fabric can be seen recorded in the pebbles but the surounding fine grained matrix appears to have the axial planar cleavage. At other sites, such as those mentioned above the clasts follow the orientation of the axial planar cleavage. Figure 7.D.5. shows the Rf/Ø data for site 13, which was the best example of this group. All surfaces sampled show a fluctuation in pebble long axes, the largest range of fluctuation being seen on the bedding surface. On the measurement planes, at a high angle to the bedding plane there is a strong preferred orientation of pebble long axes, but the data clusters about the cleavage trace rather than the bedding trace and this is in agreement with the examples given by Dunnet and Siddans (1971).

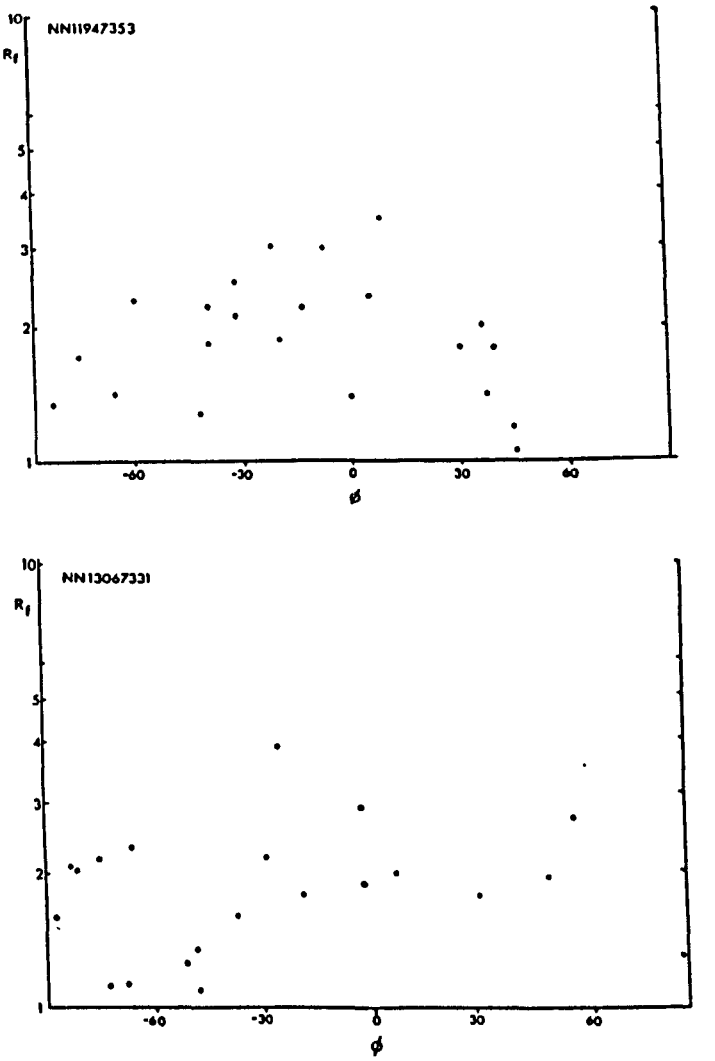

Figure 7.D.4. Rf/Ø diagrams from the bedding surfaces at sites 4 and 8.

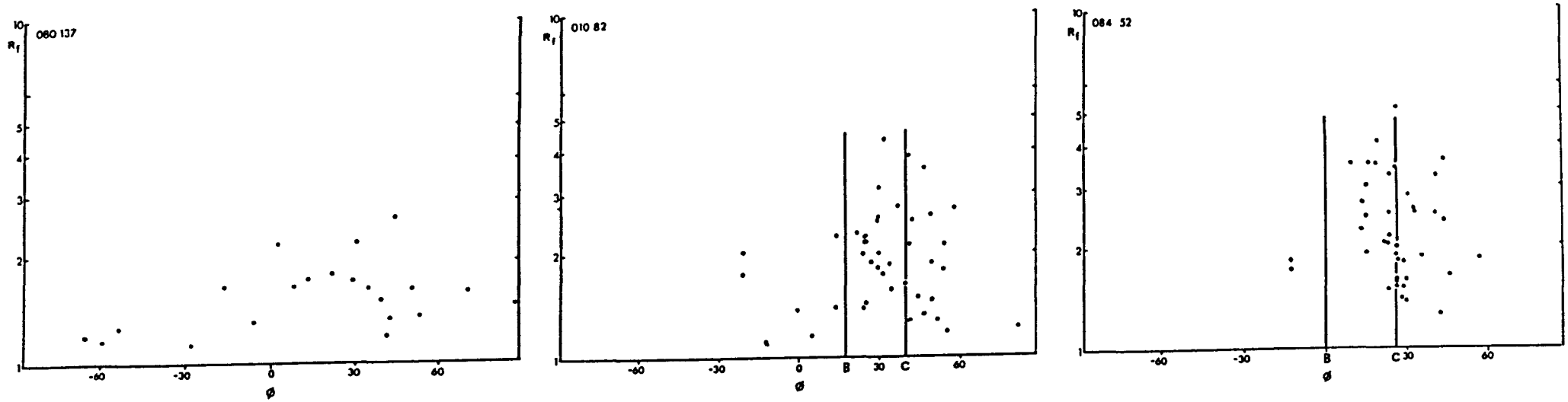

Figure 7.D.5. Rf/Ø diagrams for site 13. On planes at a high angle to the bedding the long axes cluster about the cleavage trace rather than the bedding trace.

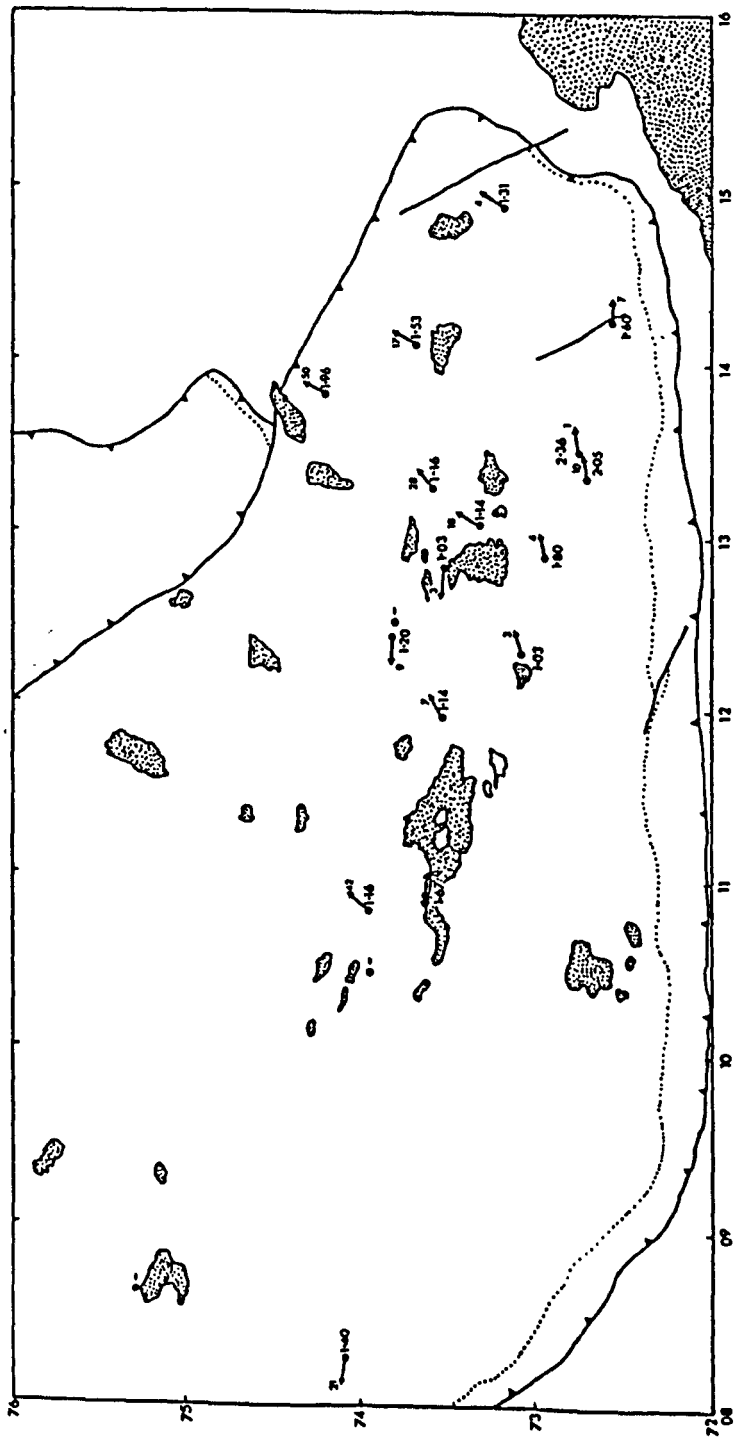

Figure 7.D.6. A map showing the orientation and ratio of the finite strain ellipse on the bedding surface at each of the sites studied. The arrow indicates the plunge direction of the long axis and the plunge is given in degrees.

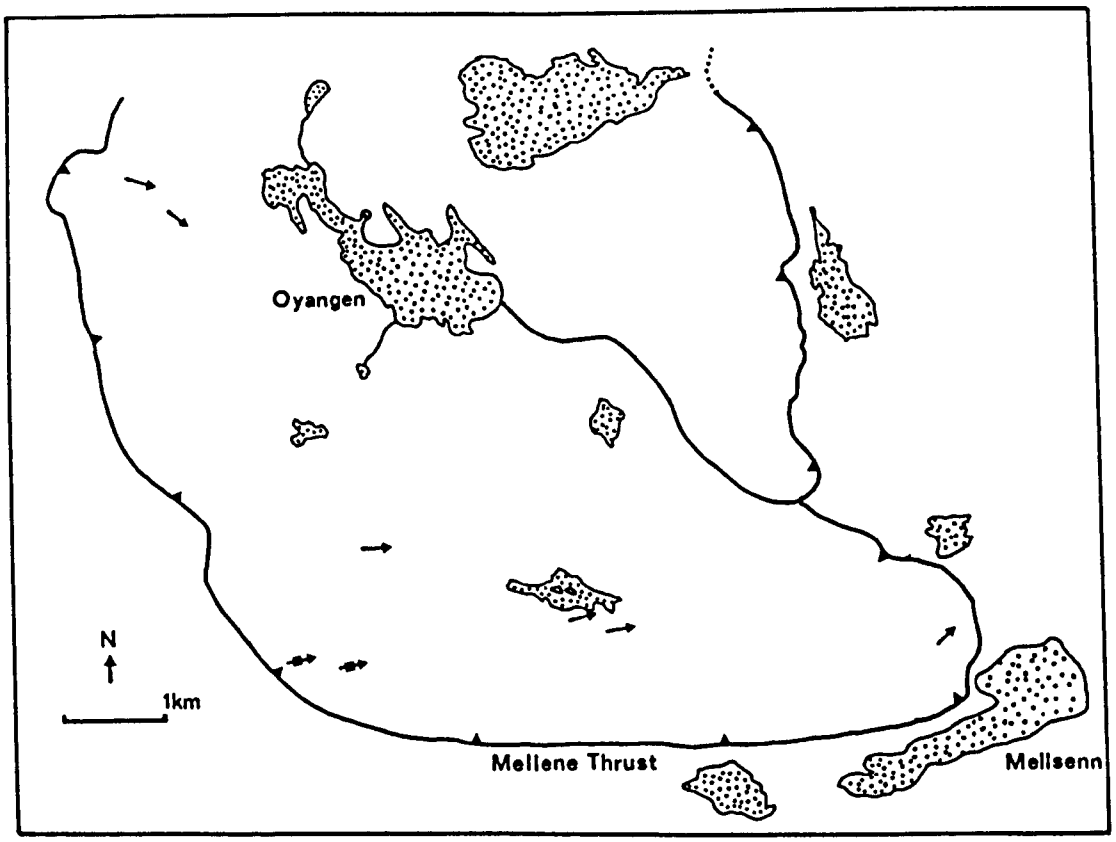

Figuer 7.D.7. A map showing the orientation of minor fold axes (⟷) and extension lineations (⟶) in the Mellene Nappe (after Nickelsen 1967).

Orientation and Ratio of the Strain Ellipse on the Bedding Surfaces

The orientations and ratios of the strain ellipses obtained on the bedding surfaces in this study are shown in Figure 7.D.6.. The patterns seen in this diagram may be related to the bedding parallel fabric. The bedding plane may be studied in this way since it represents the XY plane of the strain ellipsoid which is related to the bedding parallel fabric. The orientation of the long axis of the strain ellipse on the bedding plane indicates the orientation of the X axis of the strain ellispoid. Thus, variations in the orientation of the X axes of the strain ellipsoids may be studied.

The diagram, Figure 7.D.6. shows a strong relationship between the orientation of the long axes of the strain ellipses and the orientations of the minor fold axes. Figure 7. D.6. should be compared with Figure 7.B.10., which shows the results of the present study and Figure 7.D.7., after Nickelsen (1967). The results suggest that extension has occured parallel to the axis of the Skarvemellen Anticline. Ramsay and Wood (1973) have shown how an apparent extension direction may be produced by the superimposition of a tectonic fabric on a compaction fabric. However, in the field boudinage of the pebbles may be seen and the fibrous growth of quartz in the boudin necks indicates that the results in the Skarvemellen Anticline represent a true extension direction.

Though the orientations of long axes of the strain ellipses show such a good correlation with the minor fold axes, no systematic relationship between the strain ratio and the major structures could be found. There is no simple relationship between the strain ratio and the dip of the bedding at a site, or the

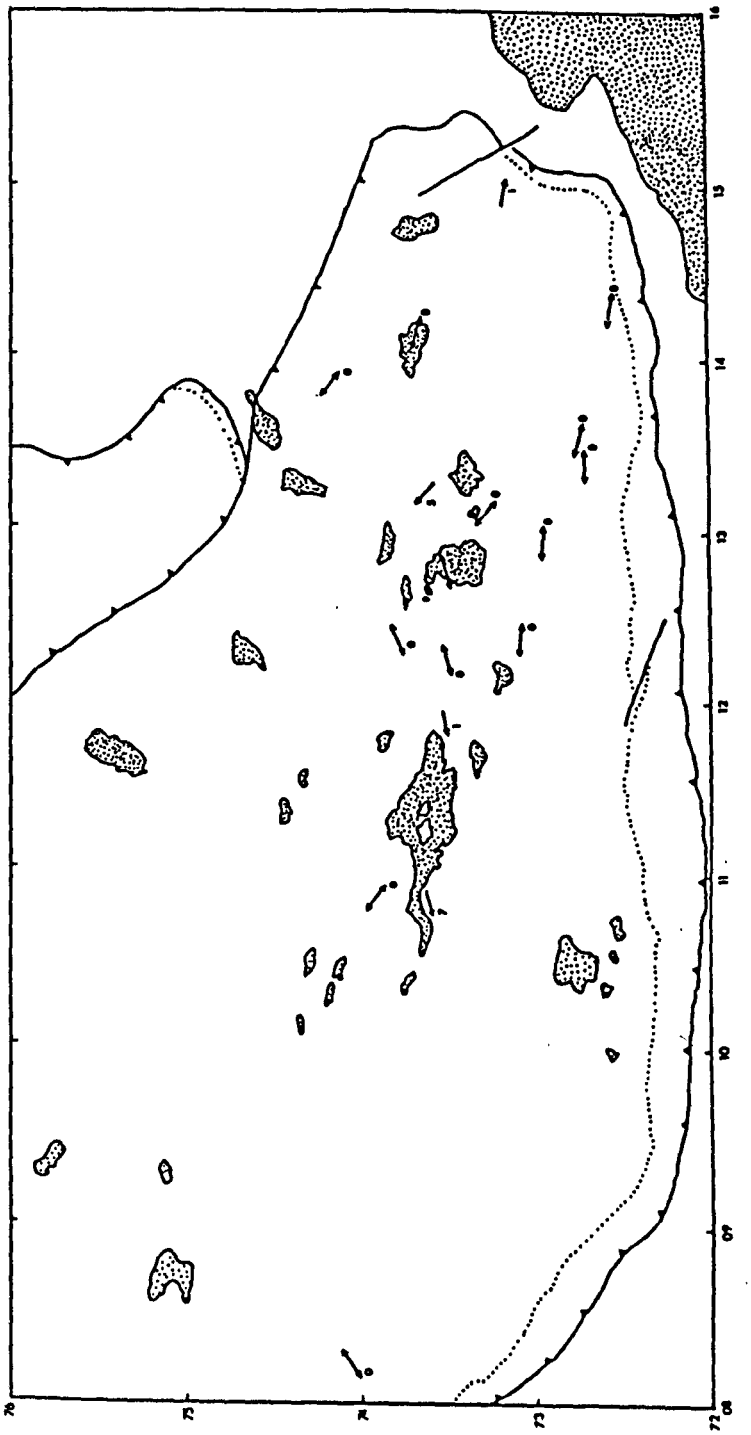

Figure 7.D.8. A map showing the orientation of the strain ellipse at each site after the bedding has been rotated to the horizontal and the correct way up. The tail of the arrow marks the position of the site.

height of a site above the Mellene Thrust. A complex relationship may exist between the strain ratio and the location of the site within the Skarvemellen Anticline and discussion of this type of distribution will be deferred until the axial ratios of the strain ellipsoids have been described.

Figure 7.D.8. shows the orientation of the strain ellipses on the bedding plane after the bedding has been rotated to the horizontal and is the correct way up. It is difficult to say, whether the orientations seen in Figure 7.D.8. are more or less systematic than those of Figure 7. D.6.. Since the orientations of ellipse long axes seen in Figure 7.D.6. show a strong relationship to the fold axes which are related to the Skarvemellen Anticline and the bedding at these sites has diverse orientations, it is thought that the distribution seen in Figure 7.D.6. is the significant one and that the bedding parallel fabric is a consequence of the folding process.

Three Dimensional Strain Results From the Deformed Conglomerates Within the Mellene Nappe

Measurements made of the two dimensional strain ratios were combined into three dimensional results using a computer program developed by W.H. Owens and J.S. Whalley (pers com). The program permits the combination of two dimensional data from three non-perpendicular planes. Their method is preferred over TRISEC FORTRAN (Milton 1980) which ,when tested, produced inaccurate and unreliable values for the strain ellipsoids. As the program of Owens and Whalley requires data from at least three planes,sites 5, 15, 17 and 18 had to be ignored as data was only available on two planes.

Three types of result were found on the basis of

Table 7.1.2.

Site No.	Axial ratio (Z.Y.X.)	A	B	K	E_1	E_2	E_3
1	0.344 : 1.000 : 1.538	0.430	1.067	0.430	0.643	0.212	-0.855
2	0.381 : 1.000 : 1.211	0.191	0.965	0.198	0.449	0.258	-0.707
3	0.403 : 1.000 : 1.957	0.671	0.909	0.738	0.746	0.081	-0.827
4	0.410 : 1.000 : 1.111	0.105	0.892	0.118	0.368	0.262	-0.630
5	0.578 : 1.000 : 1.643	0.497	1.730	0.287	0.514	0.017	-0.531
7	0.363 : 1.000 : 1.255	0.227	1.013	0.224	0.489	0.262	-0.752
8	0.413 : 1.000 : 1.152	0.141	0.884	0.159	0.389	0.248	-0.637
9	0.577 : 1.000 : 1.594	0.466	0.550	0.847	0.494	0.028	-0.522
10	0.728 : 1.000 : 1.758	0.564	0.317	1.779	0.482	-0.082	-0.399
11	0.763 : 1.000 : 1.398	0.335	0.270	1.241	0.313	-0.022	-0.292
12	0.563 : 1.000 : 1.286	0.252	0.574	0.439	0.359	0.107	-0.466
13	0.613 : 1.000 : 3.702	1.309	0.489	2.677	1.036	-0.273	-0.713
14	0.850 : 1.000 : 1.555	0.441	0.143	2.716	0.342	-0.099	-0.243
16	0.911 : 1.000 : 1.962	0.674	0.093	7.247	0.480	-0.194	-0.287
19	0.434 : 1.000 : 1.073	0.070	0.835	0.084	0.325	0.255	-0.580

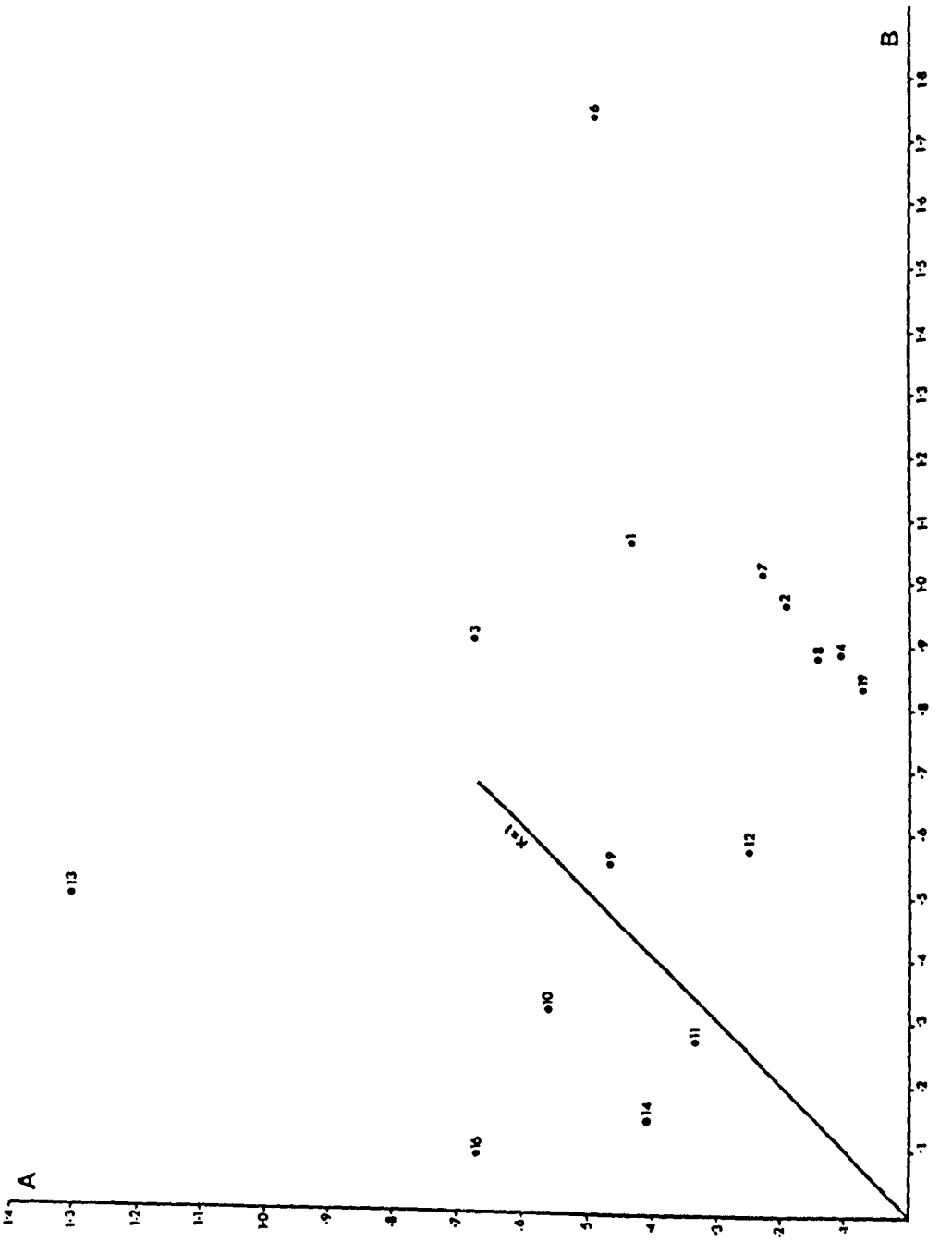

Figure 7.D.9. A Flinn plot of the finite strain ellipsoids from the conglomerate sites at which three planes were measured.

orientation and shape of the strain ellipsoid. The results which lie in the oblate field of the Flinn plot have a common orientation (Figure 7.D.9.). The X and Y axes of the strain ellipsoid lie close to the bedding plane and the Z axes lie close to the poles to the bedding (Figure 7.D.10.). In two cases the X and Y axes lie on the bedding plane when plotted on a stereogram. Where a grain shape lineation is seen in the field, the X axis of the strain ellipsoid lies close to the lineation, but rarely within 30 degrees of it. This angular discrepancy probably arises because the strain ellipsoids are oblate in shape and the XY plane the X and Y axes are very similar in length, as a result they are ill defined. These results appear to reflect the presence of the bedding parallel fabric which is dominantly planar even when a strong lineation can be seen on the bedding surface.

Three of the five prolate results (Figure 7. D.9.) have X axes which lie close to the fold axis of the Skarvemellen Anticline (Figure 7. D. 11.). The axes plunge both to the east and the west. In these sites, 10, 11 and 16, the Y and Z axes bear little relationship to the bedding and this is probably due to the prolate nature of the strain ellipsoid. In the YZ plane, the Y and the Z axes are ill defined as they are of similar length. Their position in the YZ plane is subject to errors inherited from the two dimensional data. The results in these sites reflect the presence of the bedding parallel fabric, but in this case it is strongly linear and the lineation is parallel to the fold axis of the Skarvemellen Anticline.

Sites 13 and 14 both possess the axial planar cleavage. In the field, the pebbles tend to lie in the cleavage plane rather than the bedding plane. As shown in Figure 7. D.12. the X and Y axes of the strain ellipsoid lie in the cleavage plane and the Z axes lie close to

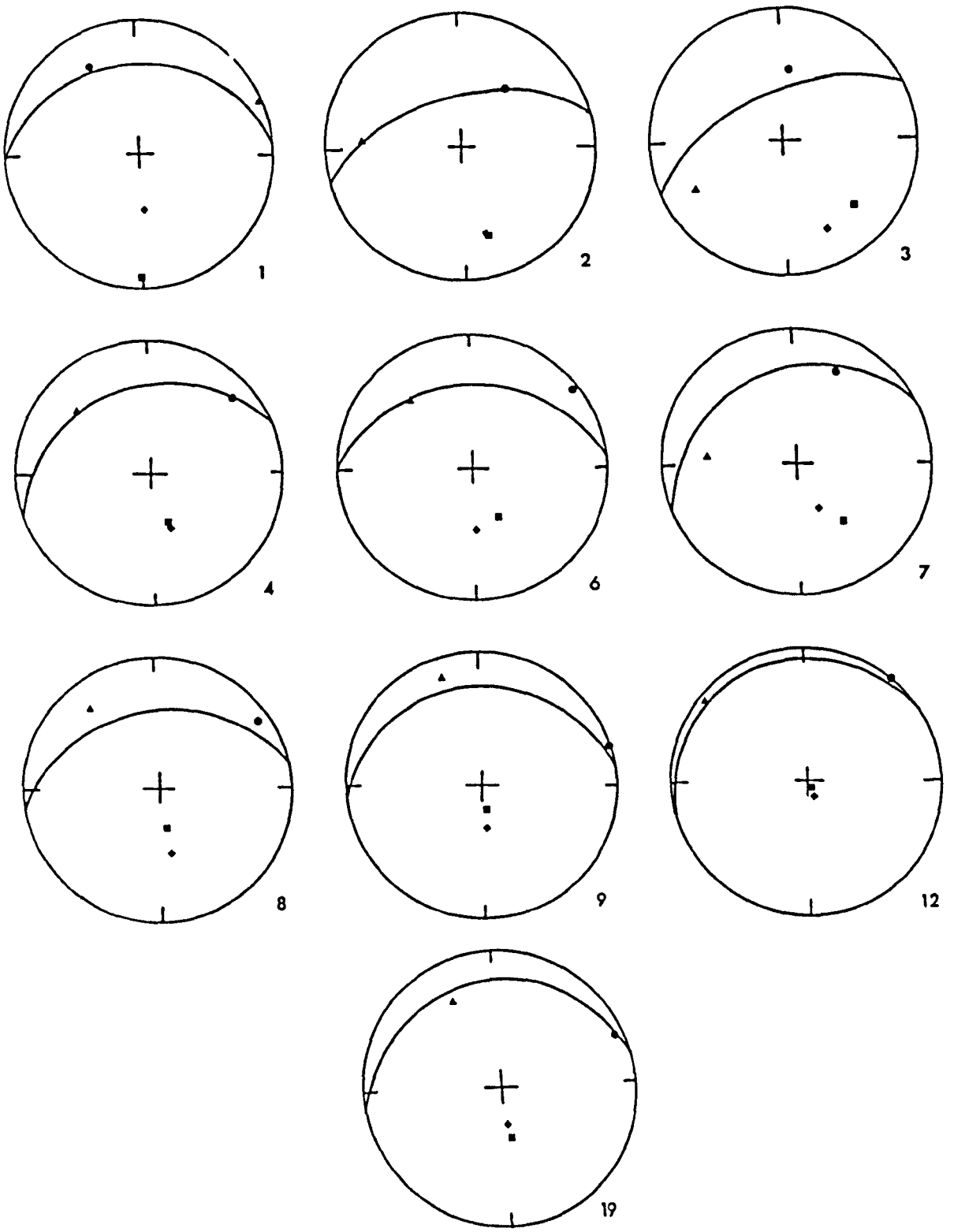

Figure 7.0.10. Stereograms showing the orientation of the axes of the finite strain ellipsoids determined for ten of the conglomerate sites studied. ● = X, ▲= Y and ■= Z. The great circle marks the position of the bedding and ◆= the pole to the bedding.

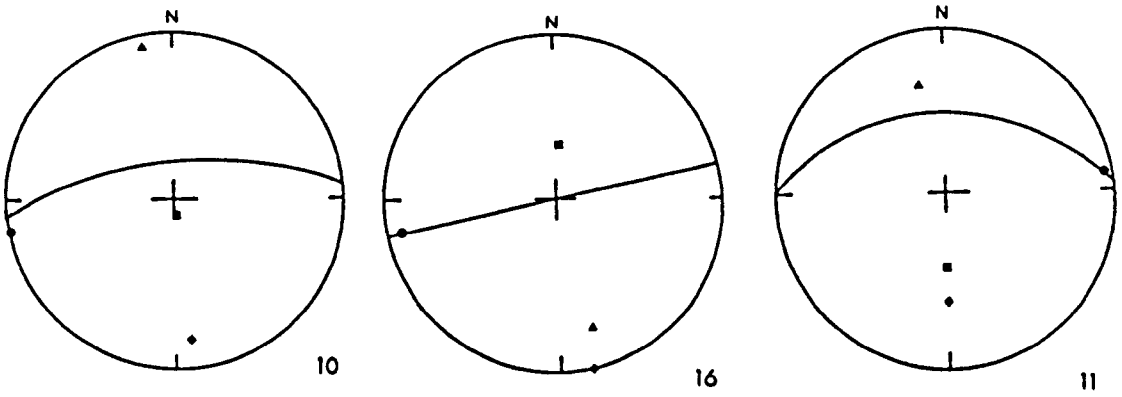

Figure 7.D.11. Stereograms showing the orientations for the axes of the finite strain ellipsoids determined for sites 10,16 and 11. At these sites the strain ellipsoids are prolate in shape and record the bedding parallel fabric (see Figure 7.D.10. for symbols).

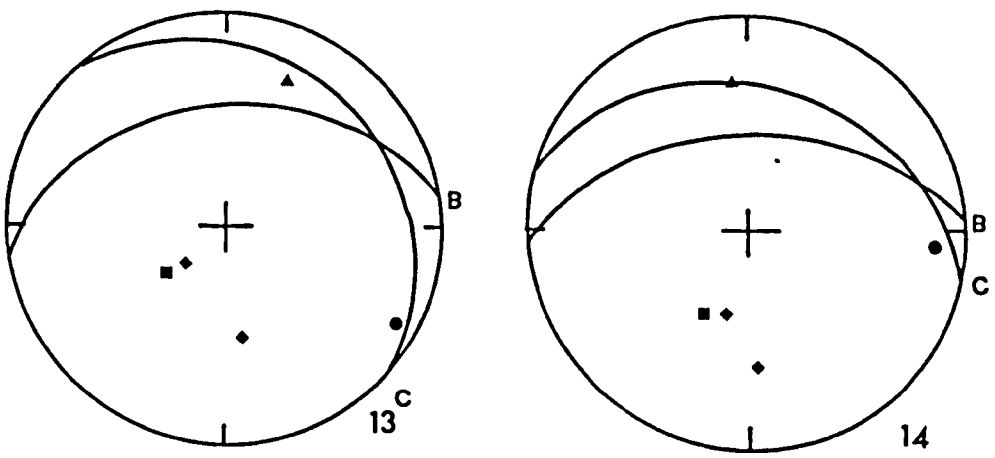

Figure 7.D.12. Stereograms for sites 13 and 14 showing the orientations of the axes of the finite strain ellipsoids. At these sites, the strain ellipsoids are related to the axial planar cleavage. B = bedding, C = cleavage and see Figure 7.D.10. for the remaining symbols.

the pole to the cleavage. The X axes bear no relationship to the orientation of the bedding and it would appear that if the bedding parallel fabric is present, it has been overprinted by the axial planar cleavage. The prolate shape of the finite strain ellipsoid is probably due to this overprinting as the X axes lie close to the bedding cleavage intersection lineations and this result represents apparent constriction, rather than true extension parallel to the X axes (Ramsay and Wood 1973).

On the Flinn plot shown in Figure 7.D.9. the sites have been labelled and since sites with different degrees of deformation have been sampled it is possible to construct a strain path (Ramsay 1967) for the deformation of the conglomerate sites around the Skarvemellen Anticline. See Figure 7.D.2. .

Qualitatively, site 11 has the least strain and it was sampled for this reason. Sites 10 and 16 were sampled on the top of Skarvemellen and show only slight evidence of deformation. With the exception of sites 13 and 14, the remaining localities for which a three dimensional result could be obtained all possess the bedding parallel fabric. In sites 9, 12 and 19 the bedding parallel fabric is less well developed. As described previously,there is a fluctuation in pebble long axes on all three planes which were measured at these sites. Sites 1,2,3,4,6,7 and 8 show no fluctuation of pebble long axes on planes at a high angle to the bedding surface and these sites represent those with the highest degree of strain recording the bedding parallel fabric.

Sites 13 and 14 posess the axial planar cleavage and represent the ends of the deformation path where the axial planar cleavage has begun to dominate the finite

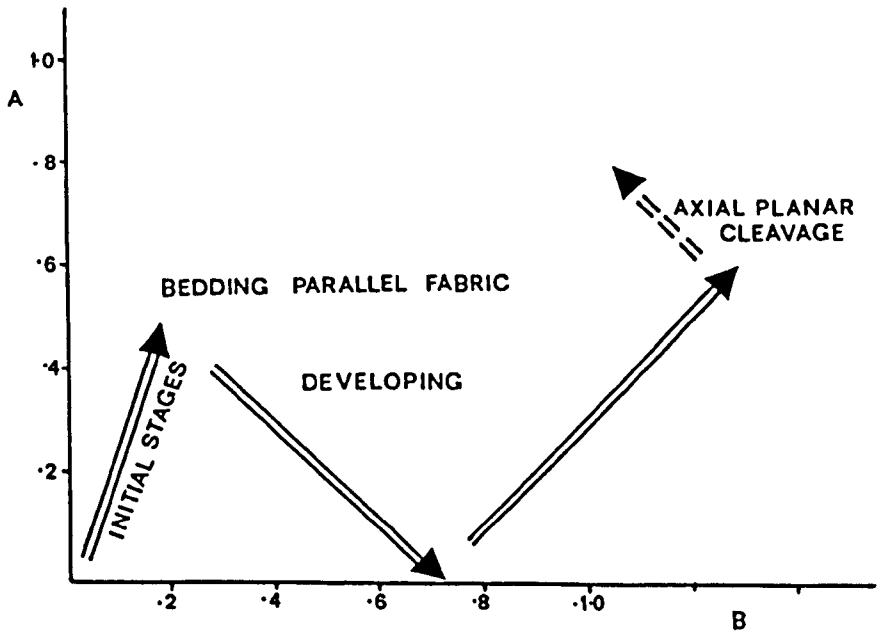

Figure 7.D.13. A Flinn plot showing a possible strain path for the rocks of the Skarvemellen Anticline. The bedding parallel fabric may be the result of a two stage process. The initial stages are characterised by prolate finite strain ellipsoids the X axes of which lie very close to the fold axis. During the second stage of development oblate finite strains are produced. While the X axes of the ellipsoids lie close to the fold axis, with higher strains they are progressively rotated towards the transport direction. The axial planar cleavage postdates the bedding parallel fabric and the finite strain ellipsoids are carried into the prolate field. This overprinting is similar to the path proposed by Ramsay and Wood (1973) for the superimposition of plane strain at a high angle to an earlier fabric.

strain. In the broadest sense, the strain path is shown in Figure 7.D.13.

Site 11 suggests a plane strain deformation in the early stages of the strain history, though, sites 10 and 16 suggest a strain path which results in a prolate finite strain. Development of the bedding parallel fabric produced oblate finite strain ellipsoids. The slope of the line joining these two groups is very close to -1 suggesting that some form of plane strain deformation operated (Ramsay and Wood 1973). Within the oblate group those sites which show the least evidence of deformation lie closer to the origin of the Flinn plot. These sites show a fluctuation in pebble orientation on all three planes studied,in contrast to the remainder of the oblate group. Sites 13 and 14 represent the end of the strain path marking the overprinting of the bedding parallel fabric by the axial planar cleavage.

Section 7E Finite Strains Determined From Thin Sections Taken From the Mellene Nappe

The conglomeratic portions of the Valdres Sparagmite occupy the core of the Skarvemellen Anticline. To determine the distribution of strain within the outer portion of the fold, within the Valdres Sparagmite, orientated samples were collected. Two specimens were collected from the Rogenslifjell type of Valdres Sparagmite (Loeschke 1967a,b), the remainder were collected from the Rundemellen type of Sparagmite. This sampling was necessary since the correct way up limb of the Skarvemellen Anticline could only be sampled in the Rogenslifjell type of Sparagmite at NN 12407480 and the results obtained may be compared with those obtained from NN 08637530 which was collected from the overturned limb at Fiskaloyse. Both specimens possess

the axial planar cleavage. NN 08637530 is a conglomerate locality (site 15) and it is possible to compare the strain determined from the pebbles with that of the matrix. A similar comparison may be made for the conglomerate site at NN 14097369 (site 7) which is part of a conglomerate band within the Rundemellen type of Sparagmite. To determine the distribution of strain on the outer most portion of the Skarvemellen Anticline,orientated specimens were taken from the Mellsenn Blue Quartz (see table 7.A.1.). This unit was chosen because,in the field, the bedding parallel fabric was seen in the Mellsenn Blue Quartz more often than in the Mellsenn Quartzite. Further, in the field, the Mellsenn Blue quartz appeared to be richer in feldspar than the Mellsenn Quartzite (this was subsequently confirmed using thin sections)and it was thought that the strain which it recorded could be related more closely to the quartzofeldspathic Valdres Sparagmite. A sample of Mellsenn Quartzite was taken as a comparison.

The localities where samples were taken for thin section study are shown in Figure 7.E.1. and the grid references and the results obtained are given in table 7.E.1.. From each of the specimens collected, three mutually perpendicular thin sections were prepared and the ratio and orientation of the grain long axes was determined for each thin section using the program ELLA FORTRAN on tracings of the thin sections. This data was analysed using the program THETA FORTRAN (Peach and Lisle 1979). This program was chosen as many of the specimens studied posess the bedding parallel fabric and in such cases the program STRANE FORTRAN (Dunnet and Siddans 1971) cannot be used. The program STRANE FORTRAN (op cit) requires a bedding trace and a cleavage trace which are distinct. Further, on a Rf/Ø diagram, the least deformed results show a wide spread of Ø values and this is the main criterion

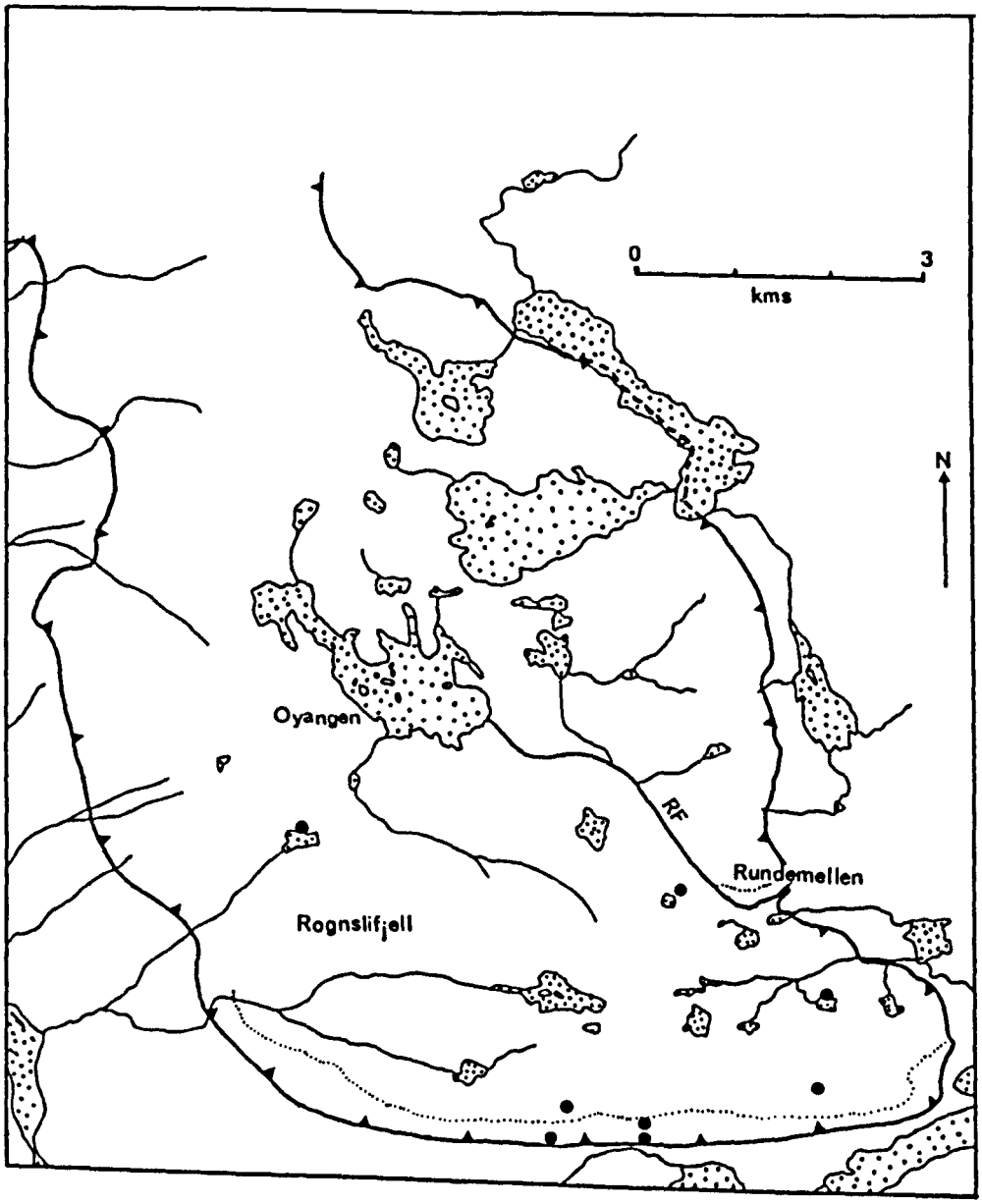

Figure 7.E.1. A map showing the relative position of the sampling sites within the Mellene Nappe for which strain estimates have been obtained using thin sections.

on which THETA FORTRAN is based. The two dimensional results were combined into a three dimensional strain ellipsoid by means of FITELI FORTRAN (Dayan 1981).

Three Dimensional Strain Results and Their Relationship to the Major Structure

The orientation of the strain axes obtained from the study of thin sections are shown in Figure 7.E.2. together with the bedding, cleavage and any lineations that were seen in the field. The orientation of the axes of the strain ellipsoids are summarised in Figure 7.E.3. together with a Flinn plot (Flinn 1962 , Ramsay 1967) of the axial ratios. For the specimens from the Rundemellen type of Sparagmite and the Mellsenn Group, the most common feature of these diagrams is that the X axes of the strain ellipsoids lie at a small angle to the strike of the bedding and parallel to the major fold axis of the Skarvemellen Anticline. In general, the Y axis of the strain ellipsoid lies in the plane of the bedding and the Z axis lies at a small angle to the pole to the bedding. Two exceptions were found, NN 11417212 and NN 12277226, where the Z axes lie in the bedding plane but this is probably due to switching of similar axes in highly prolate ellipsoids.

In view of the similar orientations of the strain ellipsoid axes seen in Figure 7.E.3. it would appear that all of these specimens record the presence of the bedding parallel fabric. In samples from the Mellsenn Group this fabric tends to be linear and in one case slightly flattened in the bedding. In the Rundemellen type of Valdres Sparagmite, the bedding parallel fabric is planar with a strong preferred orientation of the X axes of the strain ellipsoids.

In the specimens collected from the Rogenslifjell type of Valdres Sparagmite, which were collected from both

Table 7.E.1.

Locality	Orientation of Bedding	Orientation of Strain Axes X,Y,Z,	Axial Ratio (Ass.no.vol.ch.)			K
12407480$_1$	302 35	24/068 40/319 40/181	1.262	0.926	0.856	3.933
08637530$_1$	267 55(i)	04/077 35/339 36/181	1.135	1.006	0.876	0.878
12327226$_2$	270 48(i)	02/272 69/017 21/181	1.534	0.877	0.744	3.388
12277226$_4$	272 52(i)	04/087 64/188 24/353	1.382	0.914	0.792	2.901
11417212$_2$	288 62(i)	14/084 40/166 46/008	1.533	0.851	0.766	5.582
11667253$_3$	268 70(i)	04/075 60/339 29/166	1.199	1.017	0.820	0.752
14147269$_3$	250 40(i)	07/070 31/335 59/173	1.181	1.024	0.827	0.673
14097369$_3$	246 30(i)	06/233 16/330 64/127	1.186	1.166	0.723	0.035

i= inverted bedding. At NN12407480 the axial planar cleavage dips at 342 45 and at NN08637530 the axial planar cleavage dips at 308 38.

1 Rognslifjell Type 2 Mellsen Blue Qtz 3 Rundemellen Type 4 Mellsen Quartzite

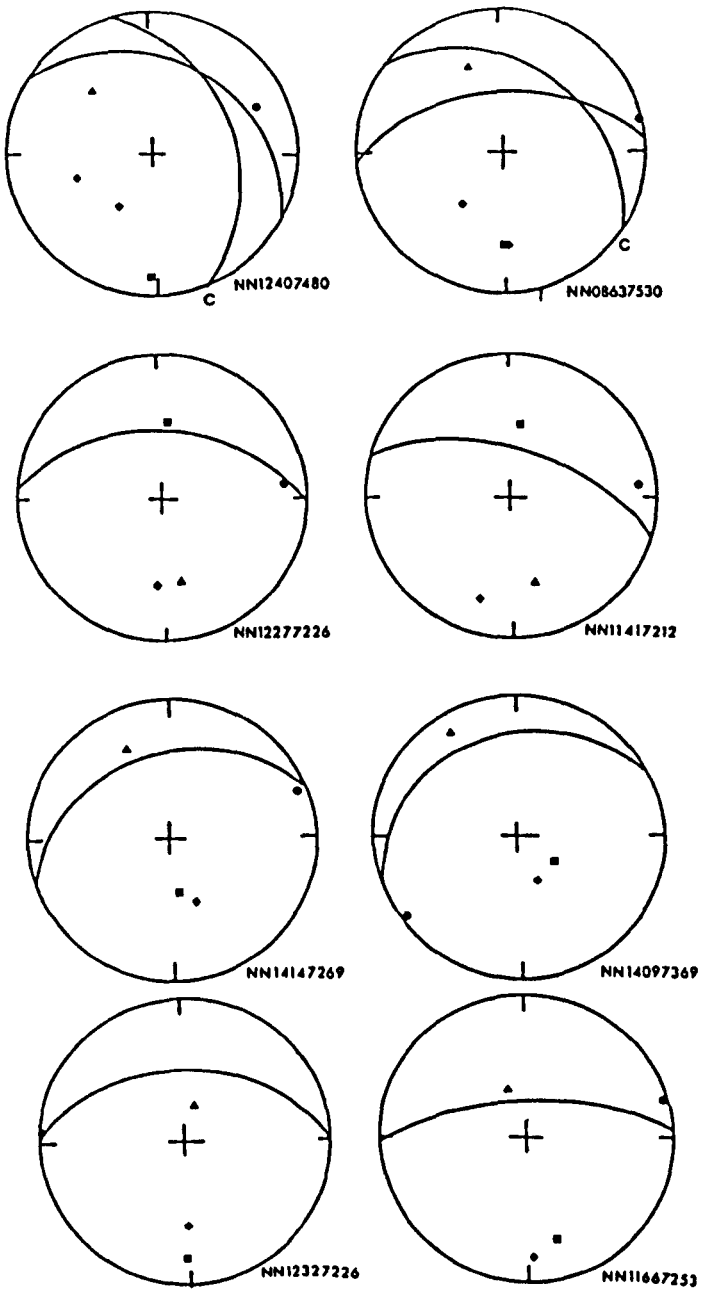

Figure 7.E.2. A series of stereograms showing the orientation of the finite strain axes (●=X, ▲=Y, ■=Z) relative to the bedding (a great circle) for the sites sampled throughout the Skarvemellen Anticline. The cleavage is also shown for the samples from NN 12407480 and NN 08637530.

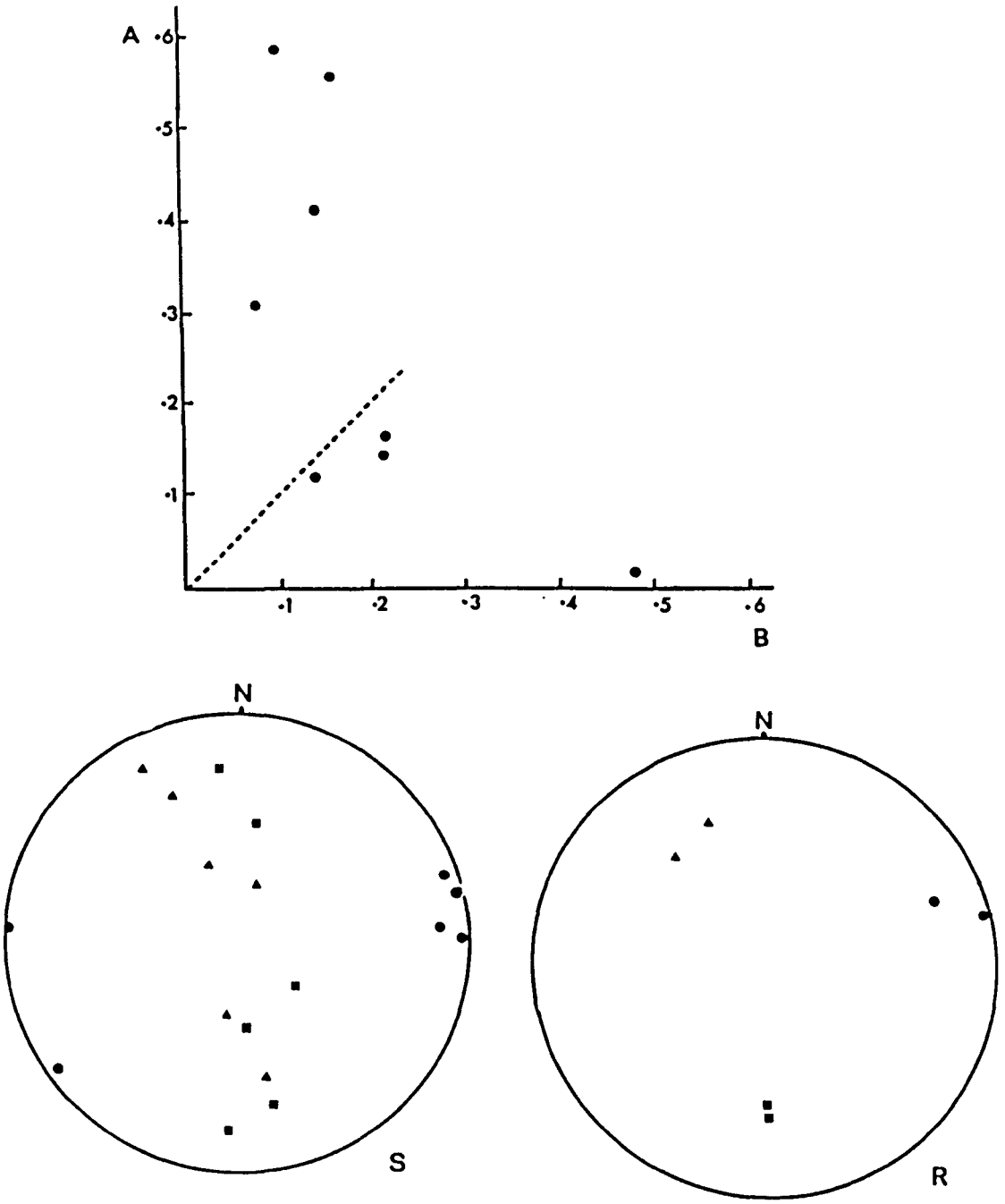

Figure 7.E.3. Stereograms showing the orientations of the finite strain axes determined from thin sections. R = Rognslifjell type of Sparagmite, S = Rundemellen type of Sparagmite and Mellsenn Group of sandstones. The axial ratios are shown on a Flinn plot.

limbs of the Skarvemellen Anticline, it is not possible to distinguish between the bedding parallel fabric and the axial planar cleavage. At both localities sampled, the bedding planes and the cleavage planes lie close together. For this reason it was not possible to use STRANE FORTRAN (Dunnet and Siddans 1971) to obtain separate strain values for the bedding parallel fabric and the axial planar cleavage.

On the Flinn plot shown in Figure 7.E.3. the results tend to group according to rock type; this is thought to reflect the position of the sampling site within the Skarvemellen Anticline as each of the rock types sampled occupies a slightly different position in the fold structure. No simple relationship could be found between the axial ratio of the strain ellipsoid obtained for a specimen and the dip of the bedding or the position of the site relative to the Mellene Thrust. The results suggest that the bedding parallel fabric is the dominant cleavage on the outer portion of the Skarvemellen Anticline and that the fabric has a strong extension lineation parallel to the fold axis. In the specimens from the Rogenslifjell type it is not possible to distinguish between the bedding parallel fabric, if present, and the axial planar cleavage due to the similar orientation of these two features at each locality. It is possible that the bedding parallel fabric is present on the correct way up limb of the Skarvemellen Anticline, though this is not proven.

The strain results from the thin section study described above fit well with those of the conglomerate data. The results tend to plot in the same broad field (compare Figures 7.E.3. and 7.D.9.) which suggests that the strain path described for the conglomerates is applicable to the results from the thin sections. In general, sampling localities and sites which are close together in the field or occupy a similar position within the

Skarvemellen Anticline lie close together on the Flinn plot and have axes with similar orientations. This suggests that the finite strain suffered by a particular locality is related to its position within the fold structure.

Deformation Microstructures and Their Relationship to the Cleavages Seen in Thin Section

The characteristic deformation microstructures of each of the rock types sampled will be described and their relationship to the cleavage and strain discussed. The strain recorded in the matrix of the conglomerates will be compared with the strains determined from the pebbles of the conglomerates.

The Rogenslifjell type of Valdres Sparagmite is extremely feldspathic, greater than 70% of the large detrital grains are feldspar; in the main these are microclines though some feldspars are present which have either perthitic textures or twin lamellae. The feldspar grains tend to be coarser (0.5 - 1cm diametre) than the quartz grains (0.2 - 0.5mm diametre). The quartz and feldspar porphyroclasts show a weak preferred orientation of grain long axes (see Figure 7.E.4.) which is related to the trace of the fabric on the section plane. Because of their large numbers it was necessary to measure feldspar grains in these samples.

The matrix of the Rogenslifjell type of Valdres Sparagmite is composed of very fine grained quartz (0.02mm diametre), white mica and chlorite. There is a strong crystallographic preferred orientation in the phyllosilicates parallel to the trace of the fabric, but this is ill defined as the matrix wraps around the porphyroclasts. This, and the common occurrence of strain shadows suggests that the porphyroclasts were

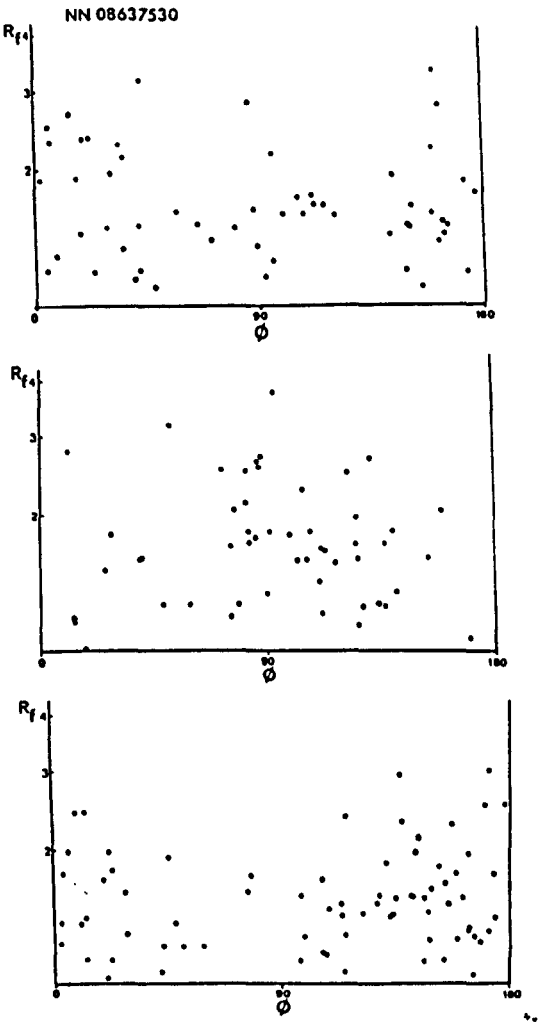

Figure 7.E.4. A series of Rf/Ø diagrams for the specimens of Rognslifjell type of sparagmite from NN 08637530. These show the possible effects of rigid body rotation. The grains tend to cluster to a greater or lesser extent but there is no increase in the maximum Rf values associated with the grains at the centre of the cluster.

less ductile than the matrix during deformation. The strains obtained from the measurements of the porphyroclasts will underestimate the true strain ratio.

The quartz porphyroclasts commonly show undulose extinction which is most strongly developed around indentations due to pressure solution by adjacent grains. Deformation bands (White 1976) are rarely seen indicating low degrees of deformation. In the quartz porphyroclasts the dominant deformation mechanism appears to have been pressure solution.

The shape of the feldspars appears to be unaffected by the deformation which they have suffered. The grains are very angular and rarely show undulose extinction. Fractures within the feldspars are commonly seen and these are infilled by quartz. The orientation of the fractures is usually at a high angle to the long axis of the grain and the cleavage trace. Fracturing of the feldspars and the common occurrence of strain shadows suggests that during deformation, the feldspars were less ductile than the matrix. This in turn suggests, that the preferred orientation of grain long axes (principally feldspars) is due to rigid body rotation of the grains (Gay 1968a,b). This is confirmed by the Rf/ϕ diagrams shown in Figure 7. E.4. which show a comparable range of axial ratios on all the planes studied and no increase in the axial ratio close to the cleavage trace. Such results may be analysed using the work of Gay (1968a,b) but the data must be obtained from the principal planes of the strain ellipsoid and this was not possible in this study as the cleavage planes in this type of Sparagmite are poorly defined. Many of the feldspars have very fine grained inclusions of white mica which may reach 30% of the host grain. This indicates that the feldspars may be undergoing chemical reaction during deformation.

The rocks of the Rogenslifjell type of Valdres Sparagmite appear to have undergone deformation by a combination of rigid body rotation and pressure solution of the grains. The strain estimates obtained for this rock type will seriously underestimate the strain ratio.

Rocks of the Rundemellen type of Valdres Sparagmite, the Mellsenn Blue Quartz and the Mellsenn Quartzite posses similar deformation microstructures. The proportion of feldspar in the Rundemellen type of Sparagmite and the Mellsenn Blue Quartz is very similar, generally around 25%. The proportion of feldspar in the Mellsenn Quartzite is generally less than 5%. During this strain study, where possible, only quartz grains were measured and these possess the following microstructures. Over 90% of the grains exhibit undulose extinction, 18% have deformation bands and 5% of the quartz grains show some evidence of recrystallization. Evidence of pressure solution is seen in 80% of the grains and in general, the deformation microstructures described above are concentrated around indentations due to pressure solution. Feldspar grains generally indent the quartz grains.

The quartz grains are strongly elliptical and show only a small range of $\emptyset$ values in two of the three sections taken from each of the specimens. The long axes of the grains lie at a small angle to the trace of the bedding and they define the bedding parallel fabric. The dominant deformation mechanism appears to have been pressure solution at the sides of the grains with deposition of material at the ends of the grains in the form of quartz overgrowths or mica beards. On thin sections which lie at a high angle to the extension lineation seen in the rock, indentation is more common than deposition.

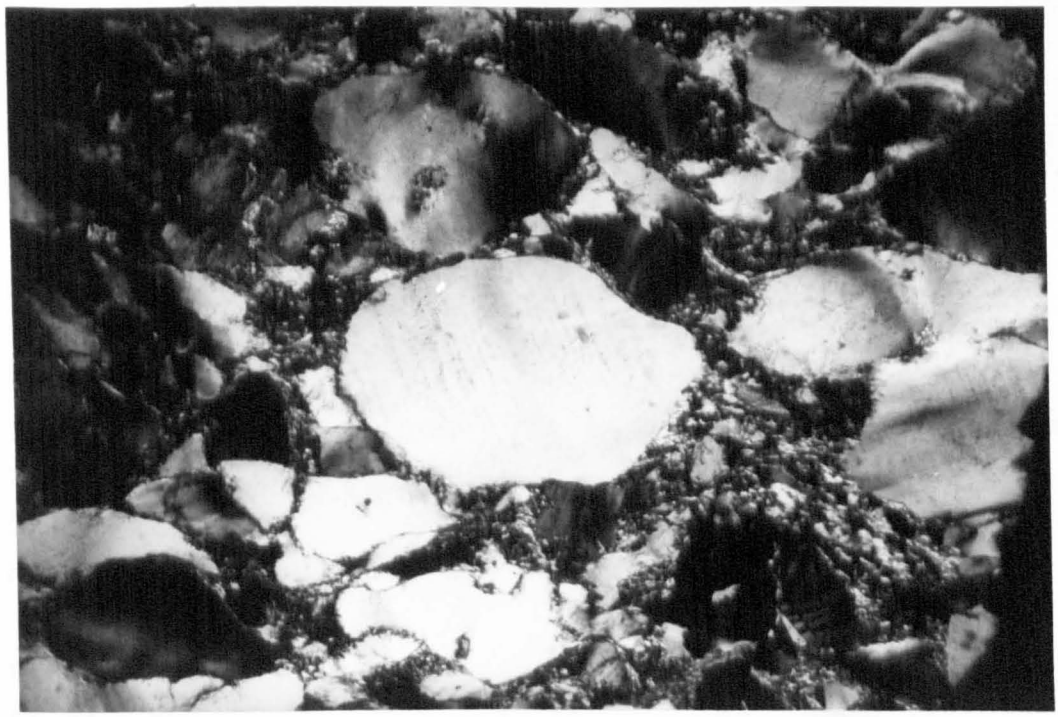

Figure 7.E.5. A photomicrograph of the Mellsenn Blue Quartz from NN 12327226. The grain at the centre of the photograph shows the planar arrays of inclusions which are common in these rocks.

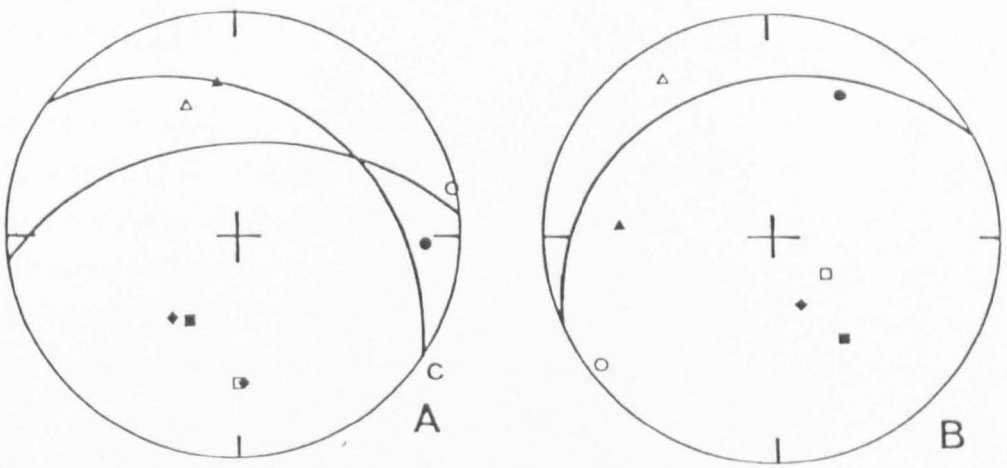

Figure 7.E.6. Stereograms showing the orientations of the strain axes determined at the same locality by two different methods. A. site 14 (NN 08267408) B. site 7 (NN 14097369). Open symbols indicate determinations from this sections and closed symbols indicate strain determinations from the pebbles. ● = X, ▲ = Y, ■ = Z and C = cleavage. ◆ = pole to bedding and ◇ = pole to cleavage.

A further microstructure may be seen in some of the quartz grains. These are planar arrays of inclusions which lie at a high angle to the long axes of the grains. Knipe and White (1979) suggest that this microstructure is developed by uniaxial extension parallel to the longest axis of the grain. The arrays of inclusions have a common orientation throughout the slide. This orientation appears to be independent of the crystallographic orientation of the host grain (Figure 7.E.5.). This suggests that the extension direction indicated by the X axes of the strain ellipsoids is a true extension direction.

In contrast to the Rogenslifjell type of Sparagmite, in the rock types under consideration, there is relatively little matrix. Where a matrix is present it is composed of white mica, quartz and perhaps chlorite. The feldspars are frequently fractured, and the fractures lie at a high angle to the extension direction in the specimen.

The sandstones of the Rundemellen type of Valdres Sparagmite and the Mellsenn Group appear to have undergone deformation by uniaxial extension of the grains and pressure solution. This extension appears to have occurred parallel to the fold axis of the Skarvemellen Anticline. Since mainly quartz grains were studied,and these are the dominant type of grain in these sandstones, then the strain estimates obtained are thought to be realistic. However, the common occurrence of pressure solution may introduce errors into the estimates (Lisle 1977a).

Comparison Between the Strain Recorded by the Pebbles and the Matrix

The axes of the strain ellipsoids obtained from measurement of the pebbles in conglomerates and the

grains in the matrix for site 14 (NN 08267408) are shown in Figure 7.E.6.. The X and Y axes determined from the measurements of the pebbles lie closer to the axial planar cleavage than those determined from measurements of the matrix. The strain ellipsoids have contrasting shapes. The strain ellipsoid determined from the pebbles is prolate in shape, whereas, the ellipsoid determined from thin section is oblate in shape. The close association of the axes suggests that the pebbles and the grains record the same fabric, which is the axial planar cleavage. Without information regarding the relative contributions made by the axial planar cleavage and the bedding parallel fabric to the finite strain ellipsoid, the origin of this variation in shape cannot be resolved. The contrast in shape, may reflect differences in pretectonic fabric between the pebbles and the matrix, or different deformation mechanisms in the pebbles and the matrix.

Only the Z axes of the strain ellipsoids determined for site 7 (NN 14097769) lie close together. This is not unreasonable, since both of the ellipsoids are strongly oblate in shape and in such cases only the Z axes of the ellipsoids will be well defined. The results of this site correspond well, both in terms of shape and orientation of the strain ellipsoids. The results appear to record the presence of the same fabric and this is the bedding parallel fabric.

In both cases the strain ellipsoids determined from the pebbles lie further from the origin of the Flinn plot. This may be taken to suggest that the pebbles have suffered a greater degree of deformation. Obviously this is unrealistic and alternative explanations must be discussed. It is possible that the matrix underestimates the amount of deformation suffered. The clasts measured were chosen so that they were mineralogically similar to the matrix and should have had

a similar ductility during deformation. At high strains the pebbles tend to have pointed ends, which is taken to indicate that they were less ductile than the matrix during deformation (Lisle 1980). It is strange that in such a situation the matrix underestimates the amount of deformation. It is possible that the matrix underestimates the amount of strain in a similar way to that described in section 4A but this is unlikely, as these rocks have not undergone a large amount of deformation and recrystallization. It is thought that the contrast between the pebbles and the matrix is due to a difference in pretectonic fabric. Dunnet and Siddans (1971) have suggested that bedding parallel fabrics are common in most clastic sedimentary rocks. It is suggested that a pretectonic fabric may have been present in many of the sites and samples studied, and that the pebbles of the conglomerate had a stronger fabric than those of the matrix. The methods of Lisle (1977a) which was used in this study takes no account of sedimentary fabrics and it is possible that it overestimates the strain due to the bedding parallel fabric. If the sedimentary fabric was stronger in the pebbles, then this would account for the overestimation of the amount of deformation suffered. This must explain why most of the conglomerate results lie further from the origin of the Flinn plot.

Section 7F Magnetic Anisotropy of the Mellene Nappe

To increase the number of strain estimates available around the Skarvemellen Anticline measurements were made of the anisotropy of magnetic susceptibility. These measurements were calibrated using the strain results obtained from the thin section study described earlier, following the method of Kligfield et al (1981).

Often in the field, localities were studied where no

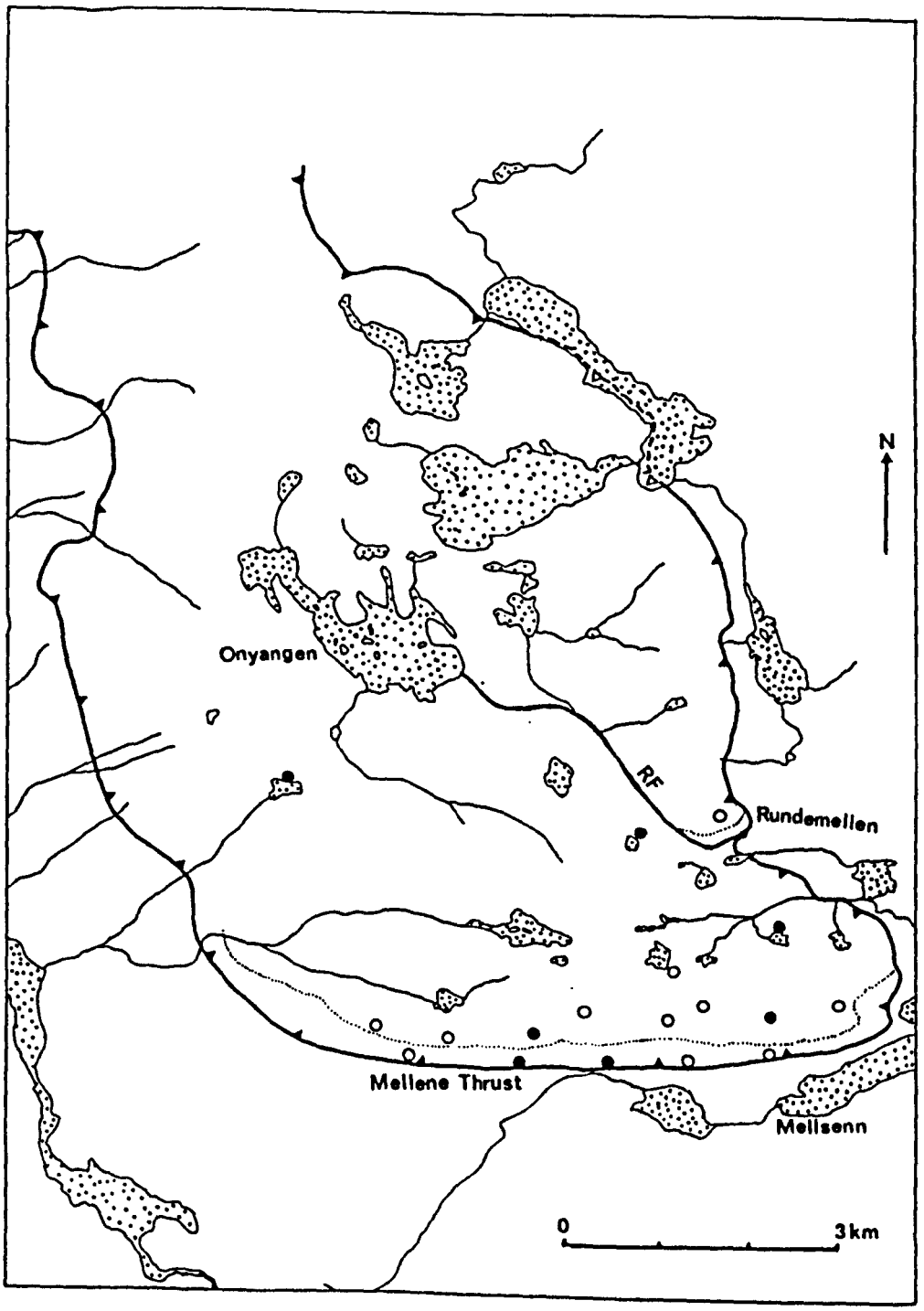

Figure 7.F.1. A map showing the relative positions of the sampling sites within the Mellene Nappe form which magnetic anisotropy measurements have been obtained. O = anisotropy measurements alone and ● = both magnetic anisotropy measurements and strain determination from thin sections.

cleavage or fabric could be seen and in such cases it is possible, using measurements of the anisotropy , to determine whether a weak fabric is present in the rock (Graham 1954). Thus, the area over which a fabric is weakly developed may be established. In addition to the strain estimation, the measurements of magnetic anisotropy on the samples from the Mellene Nappe were used to determine the extent of the bedding parallel fabric in the area studied.

For this study orientated specimens were collected from the Valdres Sparagmite and the Mellsenn Blue Quartz. the distribution of sampling sites is shown in Figure 7.F.1.. The methods of collection, orientation and measurement used were identical to those described in chapter 6.. Problems were encountered during measurement of the specimens from the Mellsenn Blue Quartz, due to the low mean susceptibilities of the samples from NN 11417212 and NN 13447225. The orientation of the ellipsoids of susceptibility determined for these specimens were compared with the results from NN 10067213, NN 12327226 and NN 14237233, which have higher mean susceptibilities. As shown in Figure 7.F.2. there is a close agreement between both sets of results and it is thought that the orientation of the susceptibility ellipsoids obtained for the Mellsenn Blue Quartz are correct. However, contrasting values for the principal axes of susceptibility were obtained during repeat measurements on the specimens from NN 11417212 and NN13447225 and these were not used in the strain estimations.

The magnetic anisotropy will now be described in relation to the structures which may be seen in the field and the finite strain axes determined in section 7E. Calibration of the strain and the magnetic anisotropy will be discussed later. None of the results

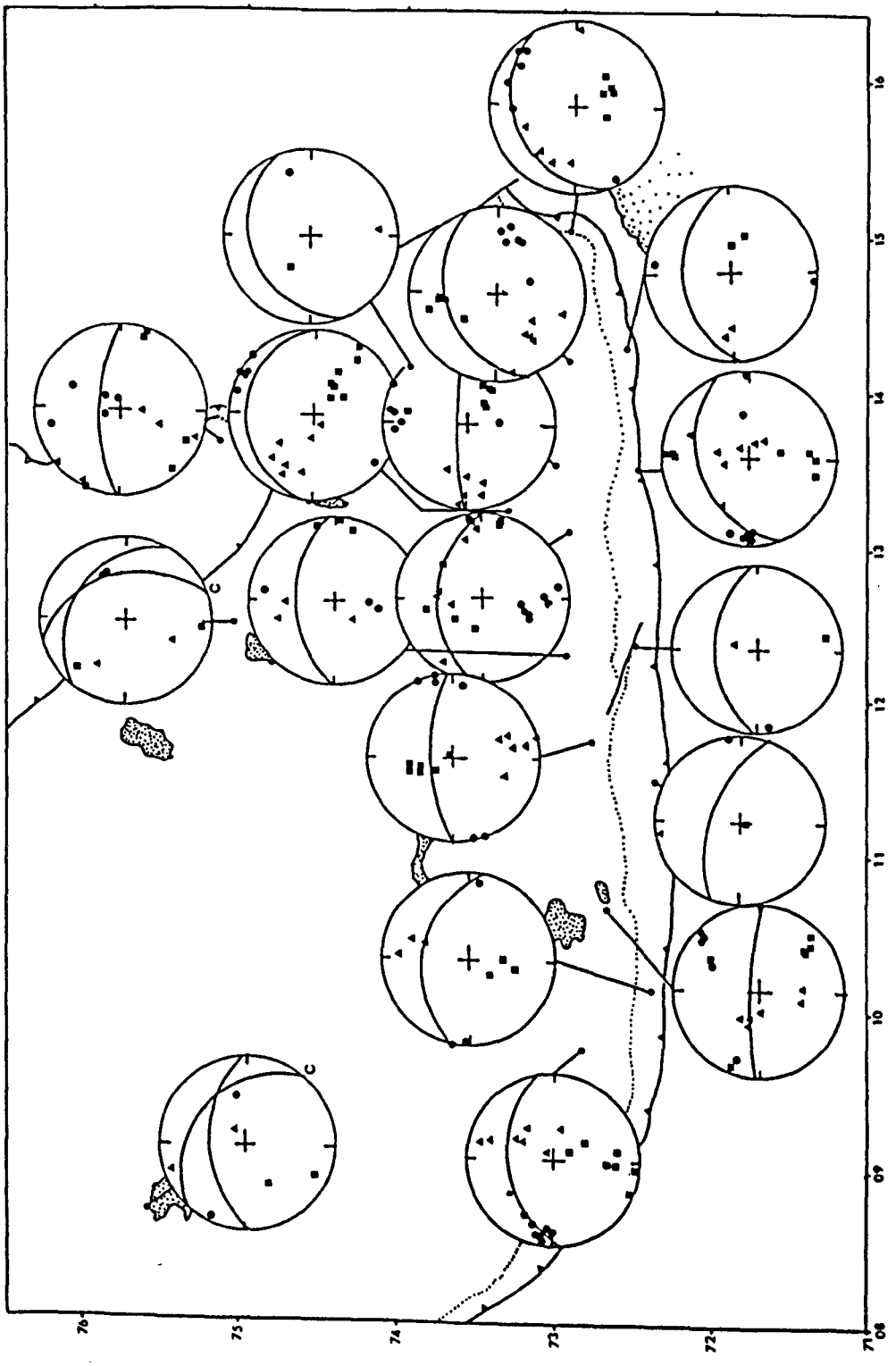

Figure 7.F.2. A map showing the distribution of sites within the Mellene Nappe from which magnetic anisotropy measurements have been obtained. The stereograms relate to the position of the sites and ● = maximum susceptibility, ▲ = intermediate susceptibility, ■ = minimum susceptibility and the great circle = bedding. C = cleavage.

obtained showed any correlation between the orientation of the sample core and the orientation of the susceptibility ellipsoid (see section 6A).

As in chapter 6. the orientation of the ellipsoid axes will be plotted on lower hemisphere equal area projections. The axial ratios of the principal axes of magnetic susceptibility will be plotted on a Flinn plot (Flinn 1962, Ramsay 1967), where $A_m = \ln (k_1 / k_2)$ and $B_m = \ln (k_2 / k_3)$.

Results From the Rognslifjell Type of Sparagmite

Two specimens from the Rognslifjell type of Valdres Sparagmite were measured. These specimens were also used in the thin section study. Both specimens posses the axial planar cleavage. Site NN 12407480 lies on the correct way up limb of the Skarvemellen Anticline and the site NN 08637530lies on the overturned limb of the fold. The results from NN 12407480 show a strong preferred orientation in the axes of maximum susceptibility (Figure 7.F.2.) and this reflects the prolate nature of the susceptibility ellipsoid. The axes of maximum susceptibility lie close to the cleavage plane and this suggests that there may have been an extension lineation on the cleavage plane. As shown in Figure 7.F.3. the axes of maximum susceptibility correspond well with the X axis of the strain ellipsoid. both the finite strain ellipsoid and the ellipsoid of magnetic susceptibility measured in this specimen are prolate in shape. These results suggest that a similar fabric is measured by the two methods.

In contrast, the axes of magnetic susceptibility obtained from the specimen from NN 08637530 show no preferred orientation (Figure 2.F.2.) and none of the axes correspond to the axes of the strain ellipsoid (Figure 7.F.3.). This result cannot be explained.

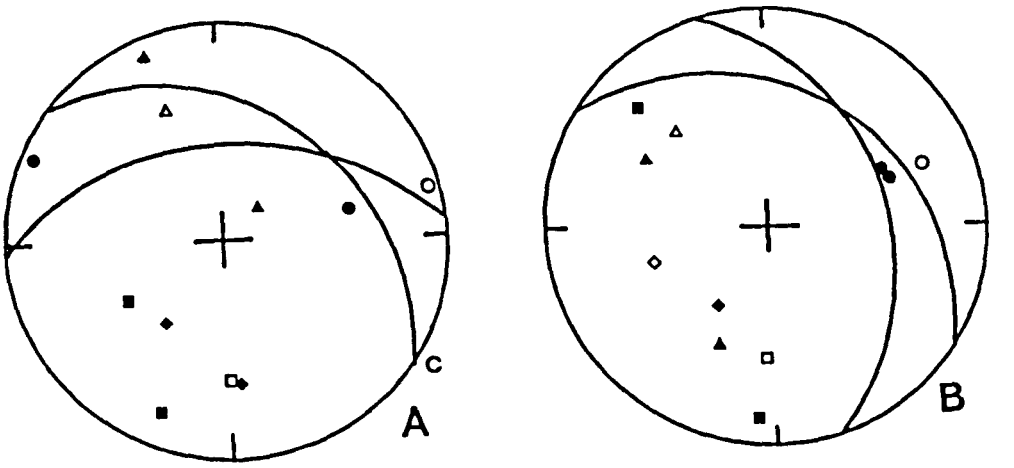

Figure 7.F.3. Stereograms (lower hemisphere projections) showing the orientation of both the principal axes of susceptibility (closed symbols) and the finite strain axes (open symbols). See Figure 7.F.2. for the symbols used. A. NN 08637530 B. NN 12407480.

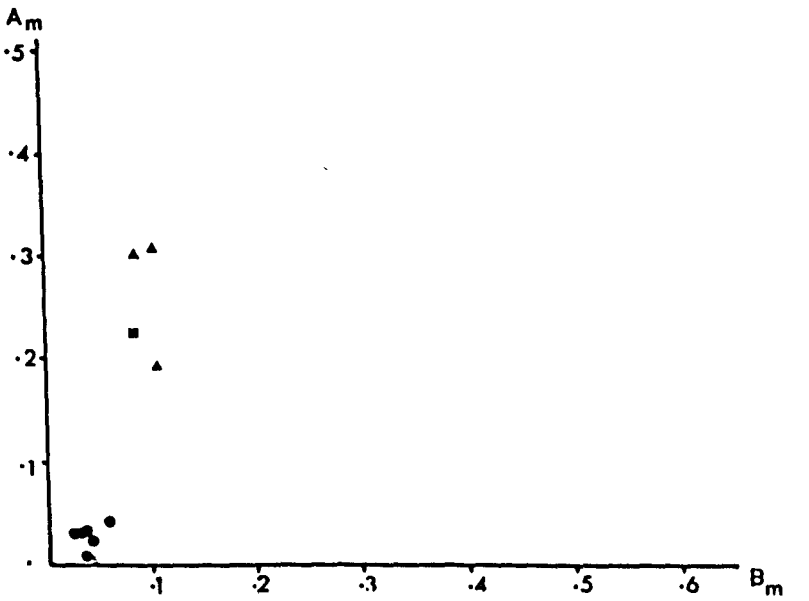

Figure 7.F.4. A Flinn plot showing the shape of the ellipsoids of magnetic susceptibility from NN 14907267 (●), NN 10067213 (▲) and NN 12327226 (■).

At this site a strong fabric is seen which is reflected by the strain results but the magnetic anisotropy does not show any evidence of this fabric.

None of the measurements of the magnetic anisotropy clearly relate to the axial planar cleavage. The results from NN 08637530 show no evidence of any fabric but a fabric is clearly present at NN 12407480. In this site the axes of maximum susceptibility lie close to the bedding-cleavage intersection lineation and the ellipsoid of susceptibility is prolate in shape. It is possible that this does not reflect a strong extension lineation related to the axial planar cleavage but an apparent extension direction caused by the superimposition of the axial planar cleavage on a compaction fabric or the bedding parallel fabric (Borradaile and Tarling 1981). This result suggests that the bedding parallel fabric may be present on the correct way up limb of the Skarvemellen Anticline though this is not proven.

Results From the Rundemellen Type of Sparagmite and the Mellsenn Blue Quartz

The results from these two rock types will be described together as they are similar. All the specimens studied come from the overturned limb of the Skarvemellen Anticline. In the field, the bedding parallel fabric is seen in some of these sites. In the specimens of the Valdres Sparagmite which were collected from the following localities NN 11667253, NN 09697258, NN 14907267, NN 13167307 and NN 10587243 and the specimens from the Mellsenn Blue Quartz at NN 10067213, NN 12327226, NN 13447225 and NN 11417212, the axes of maximum susceptibility have a common orientation. In each specimen the axes of maximum susceptibility lie close to the bedding plane at a small angle to the strike direction. Throughout the area studied the axes

may plunge either to the east or the west parallel to the fold axis of the Skarvemellen Anticline. Where a grain shape lineation is seen in the field (NN 14907267 and NN 12327226) the axes of maximum susceptibility lie at a small angle to the lineation.

In the specimens from NN 14907267, NN 10067213 and NN 12327226 the principal axes of susceptibility lie in three mutually exclusive groups (Figure 7.F.2.). The ellipsoids of magnetic susceptibility tend to be oblate in shape (Figure 7.F.4.) and the axes of minimum susceptibility lie close to the pole to the bedding. This suggests that a planar fabric is present which is parallel to the bedding with a well developed lineation.

The principal axes of magnetic anisotropy in the specimens from NN 11667253 and NN 11417212 form three mutually exclusive groups (Figure 7.F.2.). In contrast to those above the intermediate axes of susceptibility lie at a small angle to the pole to the bedding. The susceptibility ellipsoids obtained for the specimen from NN 11667253 tend to be prolate in shape (Figure 7.F.5.) and this may account for the exchange in the position of the minor axes. A prolate susceptibility ellipsoid is inferred for the specimen from NN 11417212 which is one of the weak specimens.

In each of the specimens from NN 13167307, NN 09697258 and NN 13447225 the axes of intermediate and minimum susceptibility are spread out in a plane, to which the axes of maximum susceptibility form the pole. No clear association exists between either of the minor axes and the bedding plane. A range of ellipsoid shapes were obtained for the specimens from NN 09697258 and NN 13167307, with a slight prolate tendency (Figure 7.F.6.). This tendency is confirmed by the orientation of the minor axes. In a prolate ellipsoid, where the

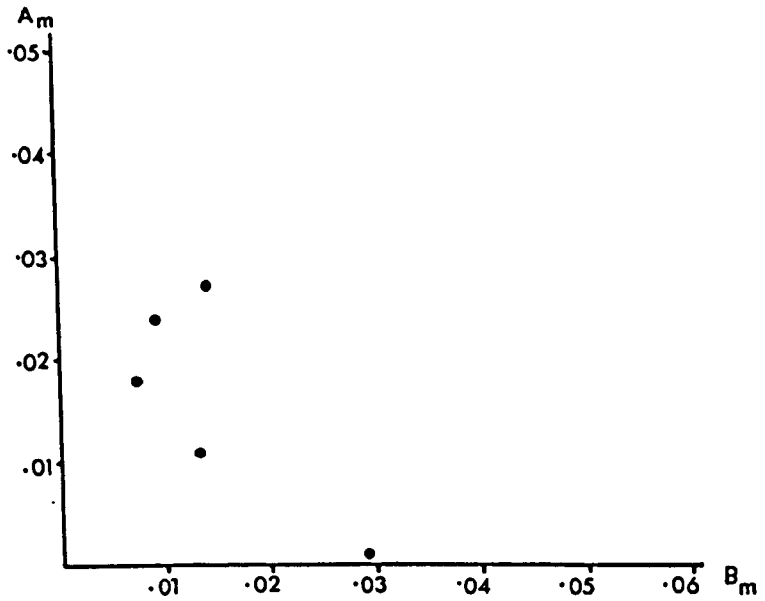

Figure 7.F.5. A Flinn plot showing the shape of the susceptibility ellipsoids from NN 11667253. Note, the axes in this diagram have a different scale to those of Figure 7.F.4..

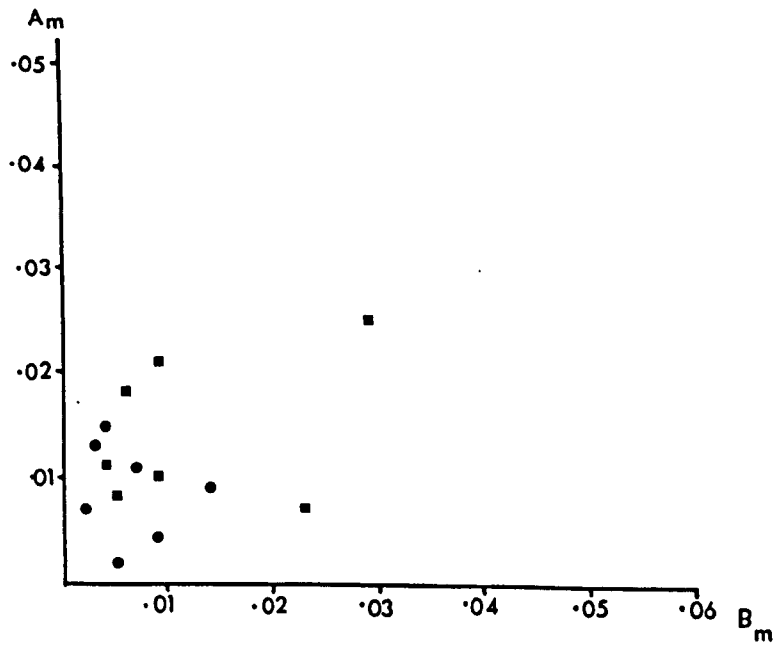

Figure 7.F.6. A Flinn plot showing the shape of the susceptibility ellipsoids from NN 09697258 and NN 13167307.

axes of intermediate and minimum susceptibility are almost equal, the position of the minor axes will be illdefined. A prolate ellipsoid is inferred for the specimen from NN 13447225.

In the field, the bedding parallel fabric is seen in only a few of these sites. The magnetic anisotropy appears to record the presence of the bedding parallel fabric and suggests that it is present in all of the specimens measured. The variation in the orientation of the minor axes corresponds to the shape of the susceptibility ellipsoid is comparable to the variation described by Kligfield et al (1977). The common orientation of the axes of maximum susceptibility indicate an extension lineation parallel to the fold axis of the Skarvemellen Anticline.

The corresponding axes of magnetic susceptibility and finite strain are shown in Figure 7.F.7. for three of the sites described above. For the specimen from NN 12327226 (Mellsenn Blue Quartz) there is a very close association between the axes which suggests that the magnetic fabric and the grain shape fabric both reflect the bedding parallel fabric. In the specimens from NN 11667253 (Valdres Sparagmite) and NN 11417212 (Mellsenn Blue Quartz) there is a close association between the axes of maximum susceptibility and the X axes of the finite strain ellipsoids. It is probably the variations in the shape obtained for the susceptibility ellipsoids which creates the poor correspondence between the minor axes measured by the two methods. The close correspondence of the X axes of the strain ellipsoid and the axes of maximum susceptibility suggests that the bedding parallel fabric is recorded by the magnetic anisotropy.

The presence of another form of "fabric" is indicated by the results from NN 13017268, NN 12227269, NN 13457279

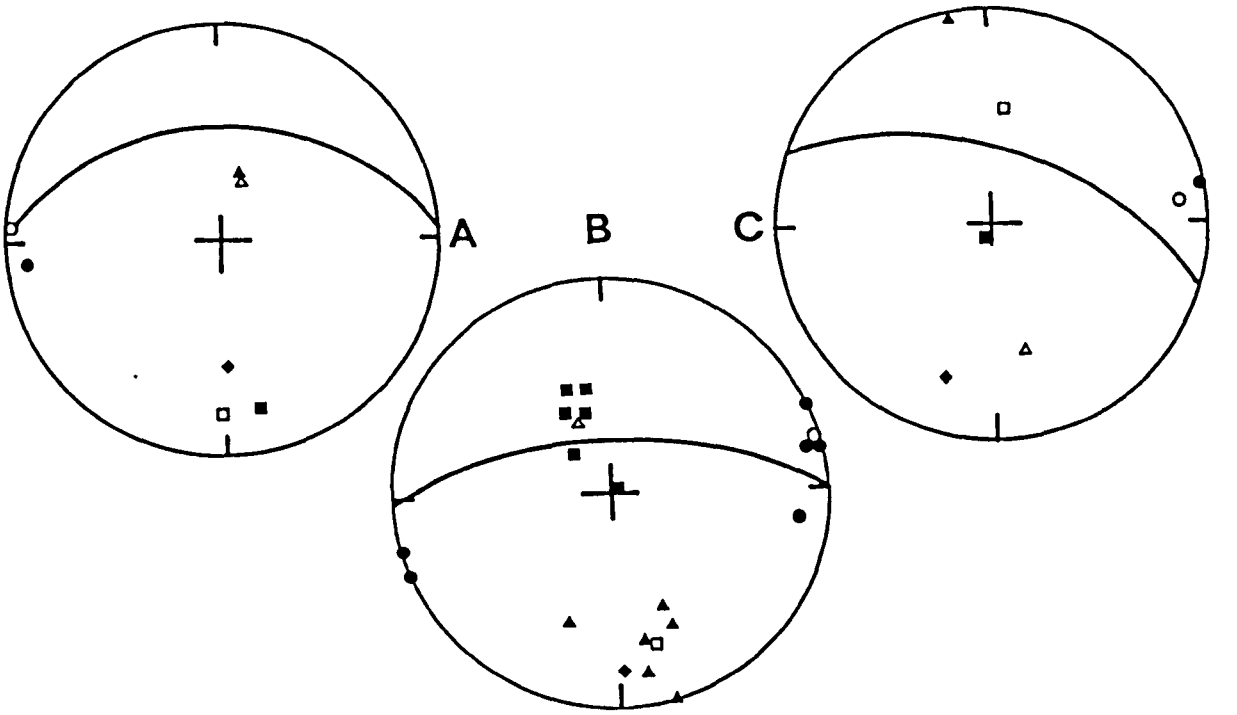

Figuer 7.F.7. Stereograms showing the corresponding axes of magnetic susceptibility and finite strain (lower hemisphere projections). The susceptibility ellipsoids are shown as closed symbols. See Figure 7.F.2. for the symbols used. A. NN 12327226, B. NN 11667253 and C. NN 11417212.

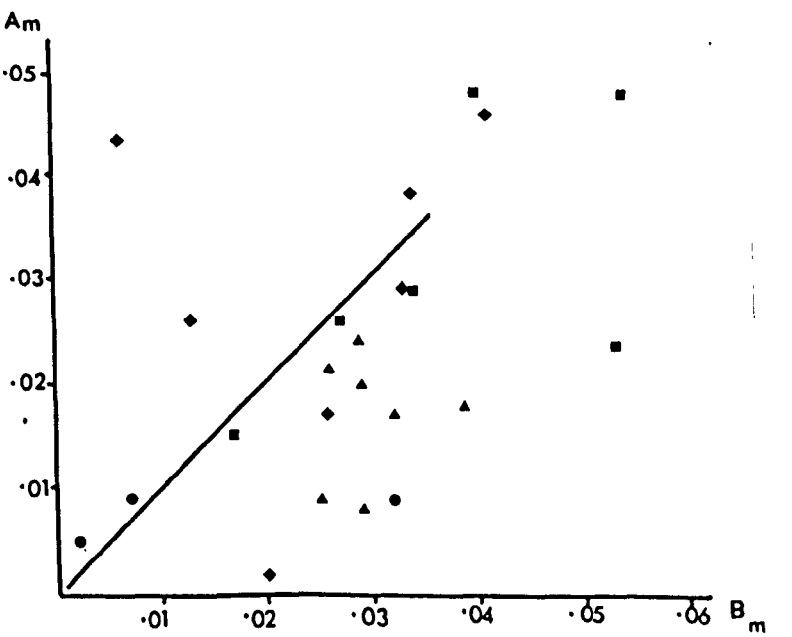

Figure 7.F.8. A Flinn plot showing the shape of the susceptibility ellipsoids from NN 13017268 (◆), NN 12227269 (●), NN 13457279 (▲) and NN 14147269 (■).

and NN 14147269 where samples of the Rundemellen type of Sparagmite were collected (Figure 7.F.1.). For each of the specimens, the axes of maximum susceptibility lie close together and at a small angle to the pole to the bedding. The axes of intermediate and minimum susceptibility lie close to the bedding plane. The ellipsoids tend to have oblate shapes (Figure 7.F.8.). In the field, no fabrics were seen at these sites and the orientation of the ellipsoids of susceptibility cannot be related to the bedding parallel fabric.

A similar result is seen in the specimen of Mellsenn Blue Quartz from NN 14237233. The axes of susceptibility have a similar orientation to those described in the paragraph above (Figure 7.F.1.). However, there is no clear correlation between the orientation of the susceptibility ellipsoids and the bedding. The axes of maximum susceptibility plunge very gently to the north or the south. The shape of the susceptiblity ellipsoid is oblate (Figure 7.F.9.). In the field, the bedding parallel fabric is seen at this locality, but the magnetic anisotropy cannot be related to this fabric. The orientation of the axes in this specimen and those described above are very similar, and it is possible that they reflect a flat lying fabric which is unrelated to the orientation of the bedding. The origin of this fabric is unknown. The localities at which it is recorded lie close together and close to Skarvemellen (Figure 7.F.1.).

The corresponding axes of magnetic susceptibility and finite strain are shown in Figure 7.F.10. for two of the sites described above. For the specimen from NN 14147269 there is a weak association between corresponding axes. Both types of axes lie close together on the stereogram but rarely do the same axes occur together. The axes of the finite strain ellipsoid clearly relate to the bedding parallel fabric and it is thought the the fabric recorded by the magnetic anisotropy

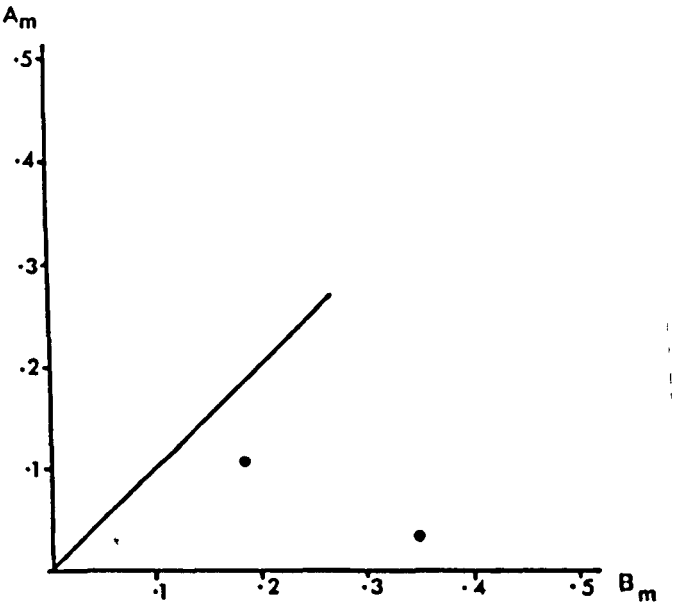

Figure 7.F.9. A Flinn plot showing the shape of the susceptibility ellipsoids from NN 14237233.

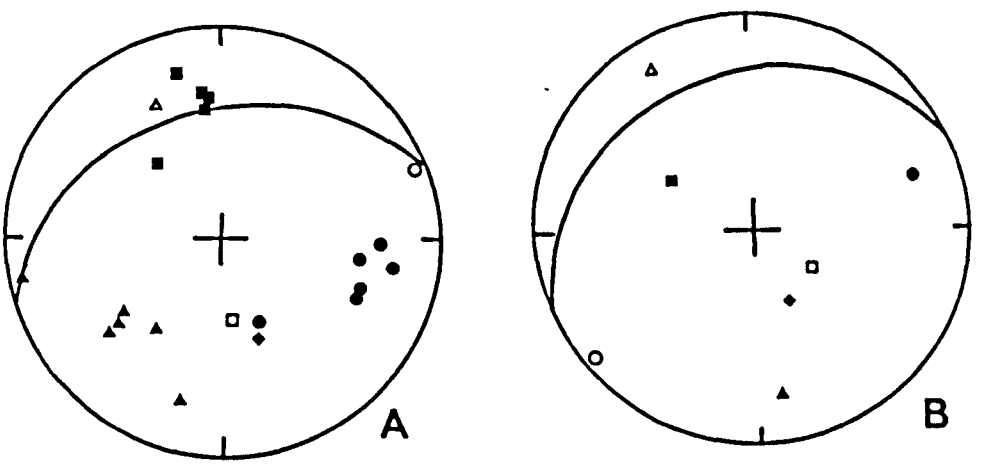

Figure 7.F.10. A stereogram showing the corresponding axes of magnetic susceptibility and finite strain (lower hemisphere projections). The susceptibility ellipsoids are shown as closed symbols. A. NN 14147269, B. NN 14097369.

has no geological significance and is of unknown origin. In the specimen from NN14097369 there is a close association between the axis of maximum susceptibility and X axis of the finite strain ellipsoid. However, there is a poor relationship between the minor axes. The variation in the orientation of the minor axes can be related to the shapes or the two ellipsoids, the finite strain ellipsoid is oblate in shape where as the susceptibility ellipsoid is prolate in shape. The axes of the finite strain ellipsoids correspond to the bedding parallel fabric and it is thought that the fabric recorded by the magnetic anisotropy at this site has no geological significance.

In general there is a close correspondence between the axes of magnetic susceptibility and finite strain but this not as clear as in the Kishorn Nappe. A calibration was attempted on these specimen from the Mellene Nappe following the method of Kligfield et al (1981). Where necessary (NN14147269, NN14097369 and NN12407480) allowence was made for the poor association of axes and the nearest axes were used. The calibration curves are shown in Figure 7.B.11. . Again separate curves were obtained for each of the rock types studied. The results from both type of Sparagmite are indistinguishable and they fall on the same straight line. There is only one specimen shown for the Mellsenn Blue Quartz as, in only on of the specimens the axes of magetic susceptib- could be measured accurately. The calibrations obtained in this study are

$$\varepsilon_i = 5.38\ M_i \qquad \text{Valdres Sparagmite}$$

$$\varepsilon_i = 2.30\ M_i \qquad \text{Mellsenn Blue Quartz.}$$

These calibrations must be treated with caution for two reasons. Firstly, in three of the cases, those

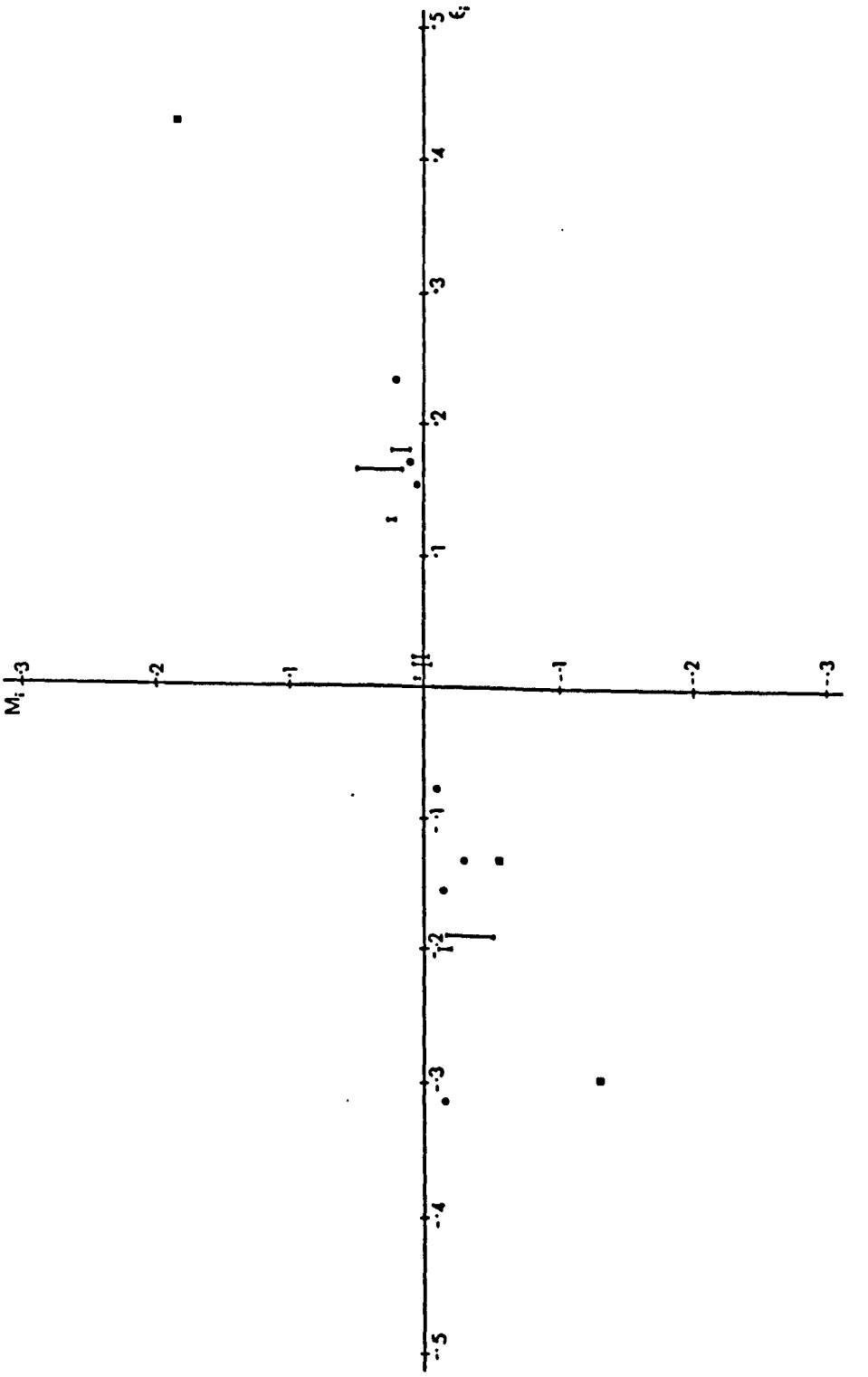

Figure 7.F.11. A correlation of the magnetic anisotropy with finite strain determined from thin sections. ● and bars indicate the Valdres Sparagmite and ■= data from the Mellsenn Blue quartz. The diagram was described by Kligfield et al (1981).

given above, there is a poor correspondence of axes and in particular in thespecimen from NN14147269 and NN14097369 the two methods record different fabric · Secondly, only one specimen could be used for the calibration of the Mellsenn Blue Quartz.

The finite stain data obtained from the calibration of the magnetic anisotropy are shown in Figure 7.F.12.. The calibrated results from the Mellsenn Blue Quartz are indistinguishable from those obtained independently. However,those from the Valdres Sparagmite lie close to the origin and are not of a similar magnitude. This is not due to the correlation and was passed from the strain measurments used in the calibration (see section 7.F.). The finite strain recorded within the Rundemellen type of Sparagmite appears to be less than that recorded in surrounding formations and by the conglomerate beds. It cannot be tested whether this refects a true low strain or not.

The calibrated results from the Mellsenn Blue Quartz confirm the strain path suggested for the bedding parallel fabric in Figure 7.D.13.. It can be clearly shown that the bedding parallel fabric predates the axial planar cleavage. The axial planar cleavage is not truly axial planar and in has been suggested that transected cleavages develop after the initiation of folding (Borradaile 1978). Thus, the axial planar cleavage may have developed during the tightening of Skarvemellen Anticline after its initial development during which the bedding parallel fabric was produced. The origin of the bedding parallel fabric will be discussed in chapter 8.

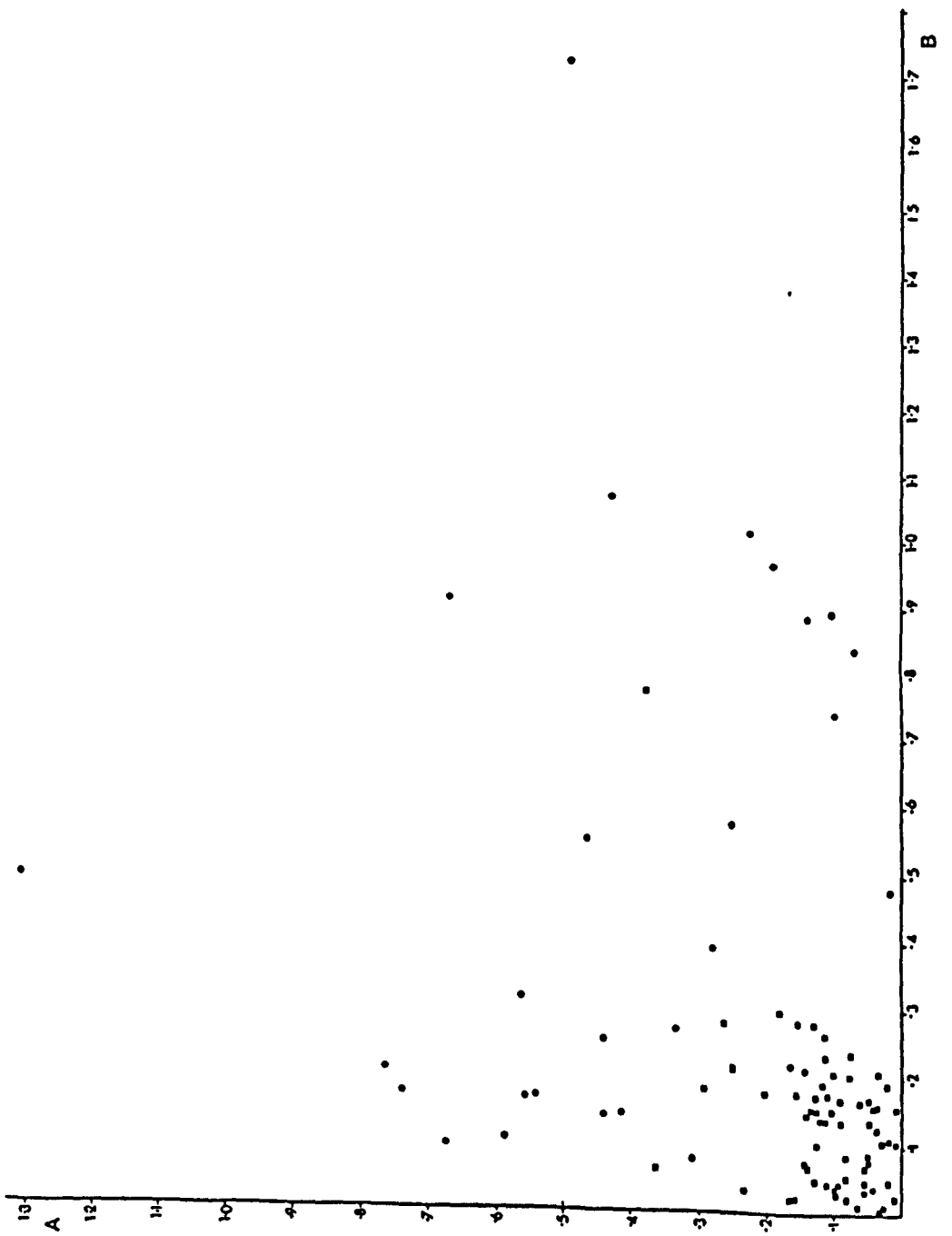

Figure 7.F.12. A Flinn plot showing the finite strain state on the overturned limb of the Skarvemellen Anticline. ■= data from the Valdres Sparagmite and ●= Data from the Mellsenn Group and the conglomerate beds of the Valdres Sparagmite.

Chapter 8 Analysis and Discussion of the Results Presented in This Thesis

In this chapter it is intended that the results of the various studies described in this thesis should be brought together and used to provide information on the possible mechanisms of folding which produce the recumbent folds of the Kishorn and Mellene Nappes. The origin of the following folds will be discussed, the Ord Syncline, the Eishort Anticline, the Lochalsh Syncline and the Skarvemellen Anticline. Each fold will be studied in turn and the models proposed will be compared with those of chapter 1. and a general model for the origin of recumbent fold nappes will be presented.

Section 8A The Ord Syncline

The Ord Syncline is the lowest of the recumbent folds in the Kishorn Nappe and it is exposed in a series of fault bounded blocks within the Ord Window (chapter 2.). In the field no cleavage or fabric may be seen which can be related to the folds of the Ord Syncline. Throughout the Ord Window the pipes of the Pipe Rock Member are perpendicular to the bedding which suggests that these rocks have suffered no bedding parallel shear strain. On the bedding surface the cross sections of the pipes are either circular or elliptical. Where the cross sections are elliptical there is a wide range in the pipe long axes. The results of a finite strain study around a single minor fold in the Pipe Rock Member of the Ord Window were presented in chapter 4. (section C). These results suggest the following;

(a) the general finite strain state of the Pipe Rock Member is extremely low. However, small finite strains do exists with ratios up to 1.3.

(b) These finite strains cannot be related to the growth of the minor fold and appear to record small amounts of layer parallel shortening which initiated that particular fold.

(c) Thin section study of the quartzite around this fold confirmed the low finite strain recorded by the pipes. The microstructures seen in thin section are entirely compatible with these small amounts of strain. This suggests that the low finite strain seen in these rocks is a true reflection of the deformation which they have suffered and not the consequence of a complex self-cancelling strain path.

The only possible fold mechanism which is consistent with this lack of strain is flexural slip with the movement on the bedding surfaces. Within the Ord Window no slickensides have been seen. However, the radius of curvature of even the smallest folds seen,is so large that geologically significant strains are not required to permit the folding to proceed and therefore a mechanism of flexural slip is inferred for the Ord Syncline.

The Kishorn Nappe is crossed by a series of northwest-southeast striking faults which are thought to be compartmental faults (Dahlstrom 1970). In the Ord Window these faults are marked by thick zones of breccia. The thickness of the breccia suggests that large amounts of movement have occurred on these faults. However, mapping of this area suggests that there is relatively little displacement on the faults. Compartmental faults are thought to be essential to

the development of the folds permitting different folds to develop with different rates, wavelengths and amplitudes in adjacent parts of the nappe. These variations in rates, wavelengths and ampliudes are thought to be due to differences in rheological behaviour between adjacent parts of the thrust sheet.

Section 8B The Eishort Anticline

The Eishort Anticline, which may be mapped around the villages of Tarskavaig and Tokavaig, has no cleavages or fabrics related to it. In the core of the fold, which is exposed around Tarskavaig, minor folds of chevron style are extremely common. Though accommodation structures may be seen in the hinges of these minor folds no cleavages or fabrics can be seen.

To validate the general observation of little or no finite strain in the rocks of the Eishort Anticline two strain studies were undertaken. The results of the palaeomagnetic study were presented in chapter 5.. Studies of the anisotropy of the magnetic susceptibility were described in chapter 6..

Within the Torridonian sandstones of the Eishort Anticline a high blocking temperature component may be isolated. This component is considered to be of Torridonian age and is a detrital remanent magnetization or a chemical remanent magnetization developed at the time of deposition. The component has no geological significance "in situ". Even when the beds are inverted and dip at less than 30 degrees no correction is necessary for internal deformation and the component may be restored to a Torridonian position by simple rotation about the strike. Therefore, a flexural slip model involving movement on the bedding surfaces is favoured in which the limbs of the Eishort Anticline reached their present positions by rigid body rotation.

The measurements of the anisotropy of magnetic susceptibility in the sites around the Eishort Anticline indicate only slight degrees of anisotropy. The ellipsoids of magnetic susceptibility are almost spherical in shape and tend to lie with their minimum axes at a small angle to the pole to the bedding. This is thought to indicate that, the only fabric present in these rocks is a weak sedimentary or compactional fabric. Similar results were obtained from both limbs of the fold. Therefore, it is thought that the Eishort Anticline was able to develop without internal deformation.

A similar result was found in the study of the magnetic anisotropy around one of the minor folds exposed in Tarskavaig Bay. In this fold only a weak sedimentary or compactional fabric could be measured. However, in one or two of the specimens a weak tectonic fabric may be present which is related to the folding but in general the magnetic susceptibility in these rocks is only weakly anisotropic.

The measurements of magnetic anisotropy made around the Eishort Anticline have been calibrated for finite strain (see chapter 6.). These calibrated results are shown in Figure 8.B.1. and they represent the finite strain of the rocks around the Eishort Anticline. These results indicate an extremely low strain consistent with the lack of cleavage, the lack of deformation microstructures and the results of the palaeomagnetic study.

Since the rocks around the Eishort Anticline have suffered no internal deformation during the development of the fold then the dominant folding mechanism is thought to be flexural slip with movement on the bedding surfaces. This is consistent with the numerous fine slickensides of chlorite which may be seen on the

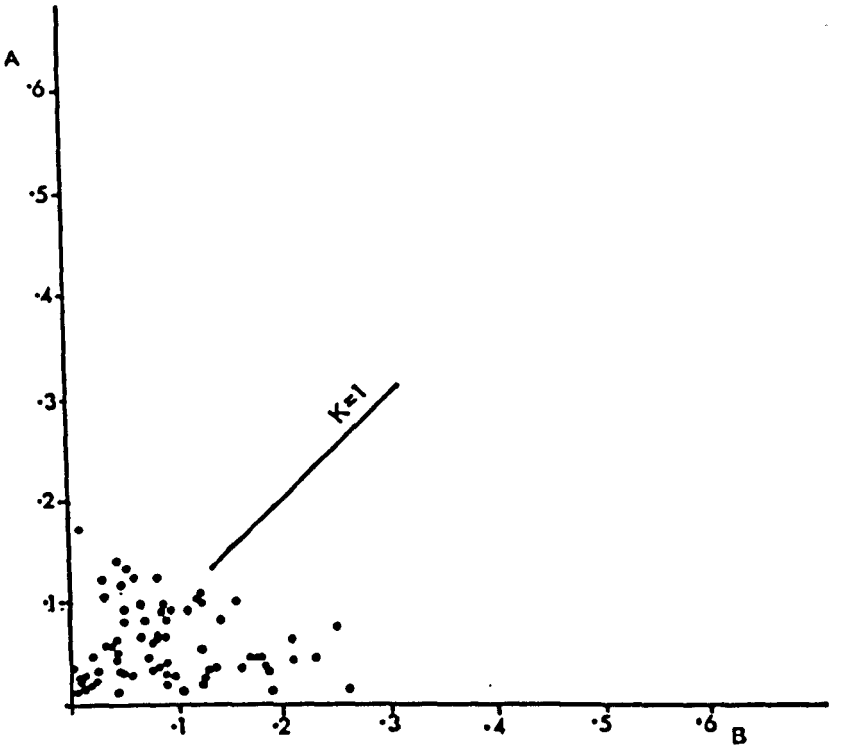

Figure B.B.1. A Flinn plot showing the finite strain state around the Eishort Anticline. The results are from the Applecross Formation and were obtained by calibration of the magnetic anisotropy measurements for finite strain. (See chapter 6.).

bedding surfaces of the Kinloch Formation around the Anticline. In thin section, the dominant deformation mechanism appears to have involved slip on the surfaces of the fine laminae (chapter 3. Section C). Thickening in the hinges of the minor folds appears to have been produced by folding on a much finer scale. Within the smallest folds seen thickening of the hinge has been achieved by the development of ramps across the fine laminae. On all scales the folds related to the Eishort Anticline are chevron in style and this is consistent with a flexural slip origin for the development of the Anticline. It is possible that the Eishort Anticline may be a large fold of chevron style. Minor folding rather than the development of a cleavage produced the necessary shortening in the hinge of the fold which permitted the folding to continue.

Section 8C The Lochalsh Syncline

The Lochalsh Syncline is the most difficult of the folds studied to analyse, since a variety of cleavages and minor structures are associated with it. The situation is further complicated by the presence of compartmental faults which permitted different processes to operate in different proportions between them. This results in changes in the fold profile along strike.

In contrast to the folds discussed previously there are a variety of finite strains associated with the development of the Lochalsh Syncline. Using the results of the grain shape studies presented in chapter 4. and the magnetic anisotropy, after calibration with the finite strain (chapter 6.), it is possible to construct maps and diagrams of the finite strain distribution related to the Lochalsh Syncline.

Where possible, the errors in these strain estimates have been assessed in previous chapters. All the finite

strain estimates used in this chapter are considered to have small errors associated with them and the variations seen are real and due to natural strain variations around geological structures.

Several methods have been developed for the analysis of regional finite strain data and these will be described briefly.

The contouring of strain parameters provides a simple method of analysing regional strain data and is of immediate visual impact. The distributions of the strains may be related to the major structure in the area and any possible correlations made. The contours may be used in subsequent analyses to increase the area over which strain estimates are available. Contouring has been used successfully by Hossack (1968), Chanman et al (1979). Milton and Williams (1981) and Fischer and Coward (1982) . However, contouring is often subjective especially when the data is not collected on a regular grid. Further, if only a limited amount of data is available the precise position and trend of contours is subject to large errors.

Finite strain trajectories are lines constructed on maps and diagrams which are parallel to the trace of the principal strain axes (Hossack 1968). These may be constructed in several ways. If it is assumed that the axes of the finite strain ellipsoid are parallel to the cleavage plane and the extension lineation on the cleavage plane, then maps showing the orientation of the cleavage and lineation may be used to determine the orientation of the finite strain trajectories. Sanderson et al (1980) showed how fabric maps can be used in regional tectonic studies in the Irish Caledonides.

From the orientation of strain axes determined from

deformed conglomerates it is possible to construct finite strain trajectories, and this method was used by Hossack (1978). The contours of strain values may be helpful when constructing the trends of finite strain trajectories.

The trajectories may be related to the major structures and possible correlations made. The method is most useful in areas where finite strain data is not available. In areas where this data is available it is often simpler to use contours of the strain parameters in conjunction with fabric maps. Cobbold (1979) has presented methods by which finite strain trajectories can be used to determine the pre-deformational shape of a body but these methods are not fully developed.

When a large amount of information on the three dimensional strain is available,and the axes of the strain ellipsoids bear a constant relationship to the regional structure then the position of the data on a Flinn plot (Flinn 1962 Ramsay 1967) or a three - axis diagram (Owens 1974) may be used to analyse the strain in terms of superimposed components. Successful studies of this kind include Ramsay and Wood (1973), Graham (1978), Coward and Potts (in press b) and Milton and Chapman (1979).

In general these methods require a knowledge of the strain path which the rocks have followed. In this method it is assumed that the position of a point on the diagram is related to the passage of the rocks along the inferred strain path.

Comparison of natural strain patterns with those obtained from geometrical models and occasionally analogue models may provide evidence for the origin of a particular structure. However, when the strain distribution is known at only a few points around a major structure such as the Lochalsh Syncline it is often difficult

to relate the finite strain seen to the models developed. Genenerally this arises because in the field, several structural levels may be sampled, whereas the geometrical models consider only one plane or level. In such cases it may be necessary to obtain strain values at intermediate points throughout the structure. These intermediate values may be obtained from contoured diagrams and maps. Alternatively, it is possible, using methods of strain integration, to obtain intermediate strain values which are compatible (Hossack 1978). The methods of strain integration have been described by Hossack (1978). Cobbold (1977, 1979, 1980) and Schwerdtner (1977) The methods of Cobbold (op cit) and Schwerdtner (1977) provide a means of obtaining the pre-deformational shape of a deformed body. However, their methods are not fully developed and in general they require more data than is available in this study.

The strain integration methods of Ramsay (1969) and Hossack (1978) are less complex, but they involve certain assumptions some of which, in natural situations, may not be valid. However, where necessary these methods were used.

To determine the possible mechanisms involved in the formation of the Lochalsh Syncline the following methods were used to analyse the finite strain data; position of the three-dimensional data on a Flinn plot, comparison of natural strain patterns with geometrical models and where necessary strain integration following the methods of Ramsay (1969) and Hossack (1978)

Distribution of Three- dimensional Data From the Lochalsh Syncline on a Flinn Plot

An analysis of the three-dimensional strain results from the conglomerates and sandstones of the Kishorn Nappe around the Lochalsh Syncline will now be

presented. If portions of this data are drawn on several Flinn plots conclusions regarding the possible deformation path of these rocks may be drawn.

Since the bedding parallel fabric is seen only on the overturned limb of the Lochalsh Syncline, two seperate strain paths must be suggested, one for each limb of the fold. On the correct way up limb of the fold there is considerable variation in the orientation of the ellipsoid axes. In chapter 6. this was attributed to low strains or the superimposition of different components of strain. On the inverted limb of the fold there is much less variation in the orientation of the ellipsoid axes and it is thought that these methods may be applied to the rocks of the Kishorn Nappe. The correct way up limb of the Lochalsh Syncline will be considered first.

Figure 8. B.1. shows the data from around the Eishort Anticline. The low strain indicated by these results has been confirmed by other methods. Since such a low strain is recorded in these rocks the results may be taken as the starting point of a deformation path (Ramsay 1967).

Data from two types of site on the correct way up limb of the Lochalsh Syncline are plotted in Figure 8.C.1. together with those from Figure 8.B.1.. The data from the two types of site plot in different fields of the Flinn diagram. Those with a weak cleavage tend to be prolate in shape whereas those with a strong cleavage tend to be oblate in shape. Both types of site show a finite strain which is greater than that of Figure 8.B.1.. It is possible that the prolate strain is produced by a compaction strain which is followed by the transverse cleavage. In these sites the transverse cleavage tends to be at a high angle to the bedding. This is similar to the path proposed by Ramsay

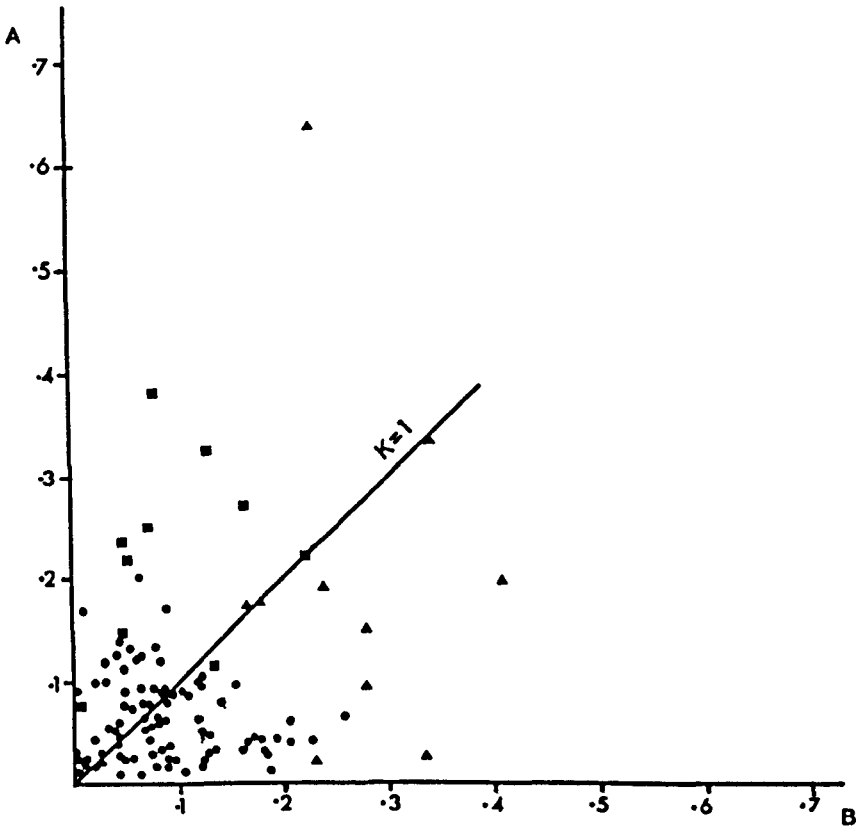

Figure 8.C.1. A Flinn plot of the finite strain results from the normal limb of the Lochalsh Syncline. ■denotes a site at which the transverse cleavage is weakly developed and ▲denotes a site where the transverse cleavage is strongly developed. (Calibrated magnetic anisotropy measurements). The data from Figure 8.B.1. is plotted as ●.

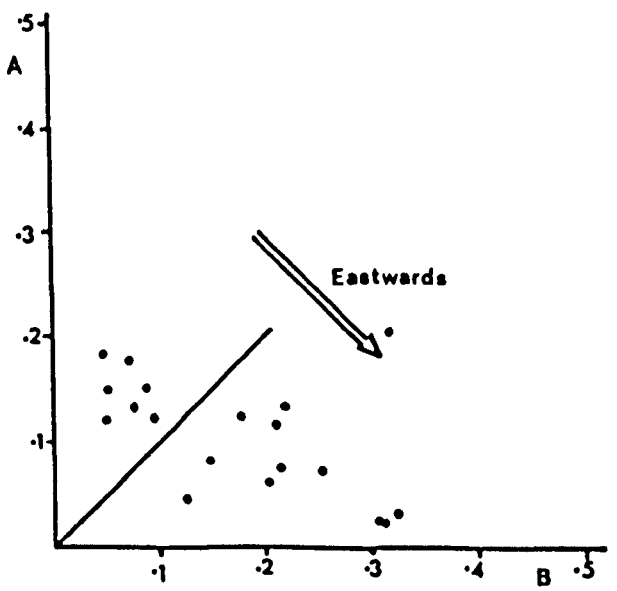

Figure 8.C.2. A Flinn plot showing the change in shape of the strain ellipsoids, eastwards, accross Beinn na Seamraig (Figure 2.A.1.). The transect lies on the normal limb of the Lochalsh Syncline and the transverse cleavage is stronger in the east (calibrated magnetic anisotropy measurements).

and Wood (1973) and Graham (1978) in deformed slates. With increased deformation the transverse cleavage dominates the rock and the strain becomes oblate in the finite state.

This pattern may be seen in the results of the transect across Beinn na Seamraig where only a weak cleavage is seen which tends to be stronger in the east. This cleavage is the transverse cleavage. Eastwards, the results tend to be more oblate in shape. Though not as well defined, the pattern appears to be similar to that of Figure 8.C.1. (see Figure 8.C.2.).

The studies of Ramsay and Wood (1973) and Graham (1978) were based on the deformation of slates. The significant compaction strains which they record are unlikely to be found in sandstones and therefore the initial oblate shape of the strain ellipsoid is due to a depositional fabric which may have been modified by a coaxial compaction strain. Certainly the magnitude of this component in the rocks of the Kishorn Nappe is consistent with this suggestion.

It would appear that a strain path may erected for the normal limb of the Lochalsh Syncline. This strain path is shown in Figure 8.C.3. and it is similar to the paths described by Ramsay and Wood (1973) and Graham (1978) for the imposition of plane strain tectonic deformations at a high angle to the bedding and previously, slightly, compacted sediments.

The possible strain paths for the inverted limb of the Lochalsh Syncline are more complex as strains due to

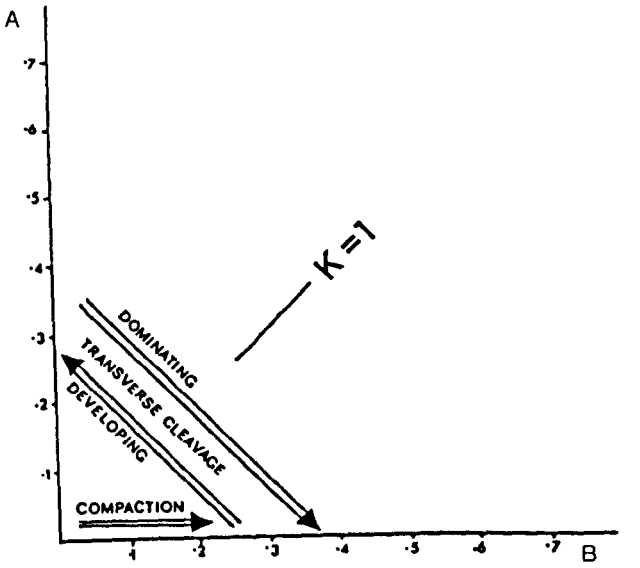

Figure 8.C.3. A proposed strain path for the development of the transverse cleavage on the correct way up limb of the Lochalsh Syncline.

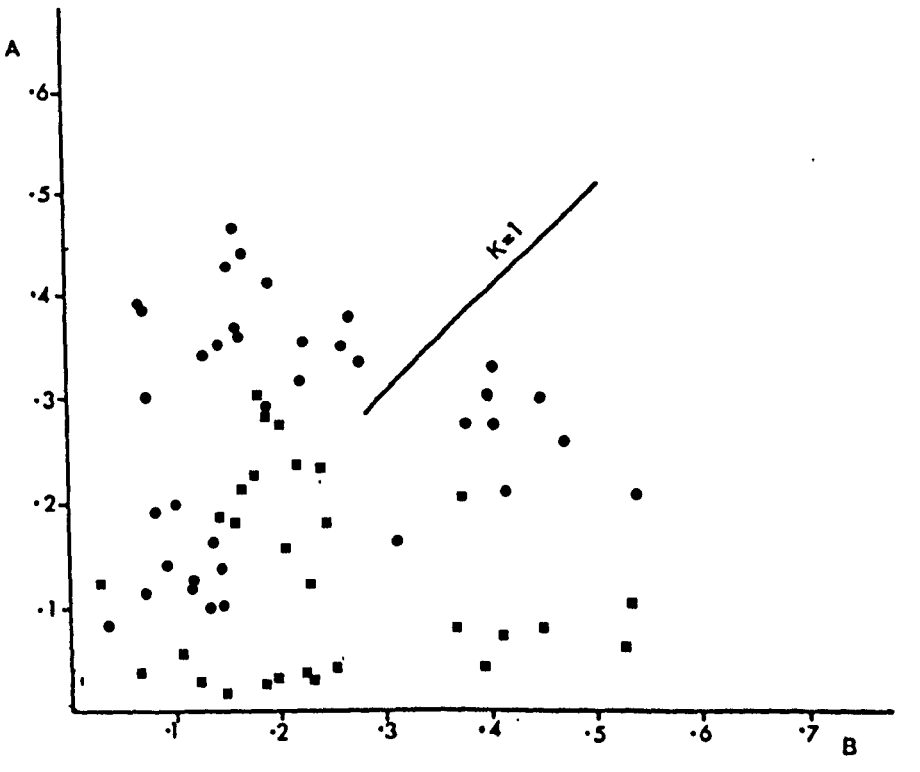

Figure 8.C.4. A Flinn plot of the finite strain ellipsoids determined for the central area of the Kishorn Nappe on northern Sleat. ▪ data from the normal limb, • data from the inverted limb (calibrated magnetic anisotropy measurements).

the transverse cleavage will have been superimposed on those arising from the bedding parallel fabric. To determine the nature of this overprinting samples were collected on northern Sleat around Sgurr na Coinnich where the transverse cleavage can be seen affecting the bedding parallel fabric in the sandstones of the Sleat Group. In contrast, to determine the strain path related to the bedding parallel fabric alone samples were collected on Lochalsh and Lochcarron. Coward and Whalley (1979) have shown how the shales in this area record the late stages of the deformation history and for this reason only sandstones were collected so that the bedding parallel fabric could be studied. In chapter 6. it was shown that the transverse cleavage does not appear to have any effect on the sandstones in this northern area.

The results shown in Figure 8.C.4. are from both limbs of the Lochalsh Syncline on northern Sleat around Sgurr na Coinnich. The ellipsoids determined for the normal limb lie close to the K=1 line or are oblate in shape. Those closest to the origin of the Flinn plot indicate only small strains and may be the products of a depositional fabric with or without compaction as no cleavages are seen at this site. At other localities on the normal limb of the Lochalsh Syncline the transverse cleavage may be seen. These sites show higher strains which may be related to the transverse cleavage and the results follow the deformation path proposed earlier. The data from the overturned limb tends to lie in the prolate field of the Flinn plot. However, a small group lies in the oblate field. The prolate finite strains on the overturned limb of the Lochalsh Syncline must represent the development of the bedding parallel fabric with its strong east-southeast lineation. In the field, the small group from the overturned limb which lie in the oblate field of the Flinn plot show evidence of the transverse cleavage in

the surrounding matrix and the nearby shale beds. It is possible that these oblate finite strains have been produced by the transverse cleavage overprinting an originally prolate ellipsoid produced by the bedding parallel fabric. In this area the transverse cleavage dips to the northeast and the bedding cleavage intersection lineation lies close to the east-southeast lineation of the bedding parallel fabric. If no change in length occurred parallel to this lineation during the development of the transverse cleavage it is possible to produce oblate finite strains.

Thus it is possible to suggest a deformation path for the inverted limb of the Lochalsh Syncline which involves the superimposition of the transverse cleavage on the bedding parallel fabric. However, as shown in Figure 8.C.5. the strain variation related to the bedding parallel fabric is extremely large and no simple path can be proposed for the bedding parallel fabric. Given the strains shown in Figure 8.C.5. the strains produced by the transverse cleavage may have negligable effect on the finite strain of the overturned limb.

The results shown in Figure 8.C.4. suggest that the bedding parallel fabric produces finite strain ellipsoids which are prolate in shape. However, if results from a much wider portion of the overturned limb are considered (Figure 8.C.5.) both prolate and oblate results are seen with a wide range in K values and axial ratios. The pattern produced cannot be related to variations in layer parallel shortening and shear strains within the nappe (cf Coward and Potts in press b) or variations in compaction and tectonic strains (cf Milton and Chapman 1979). Even when smaller areas of the nappe are considered no clear pattern can be seen for these results.

There is a marked spatial variation in the shape

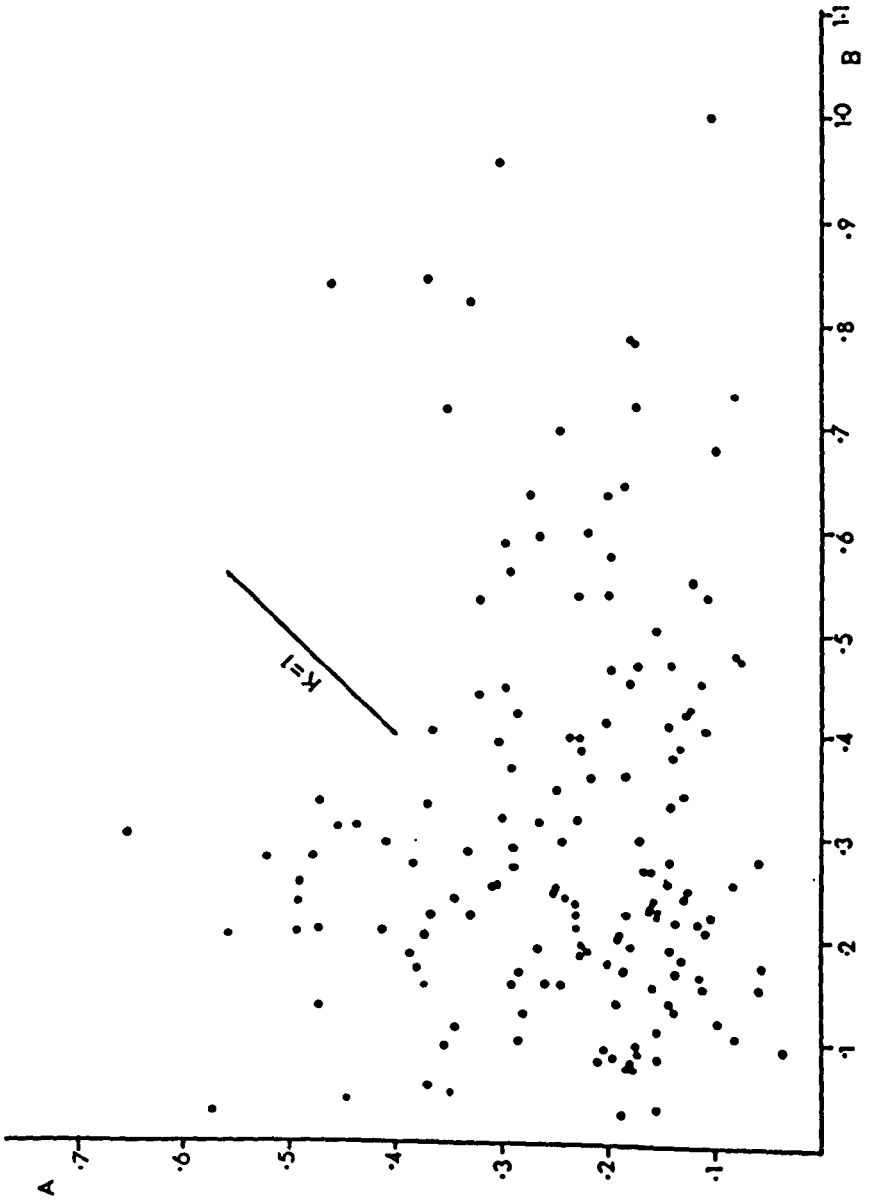

Figure 8.C.5. A Flinn plot showing the finite strain ellipsoids from the inverted limb of the Lochalsh Syncline in the northern and central areas of the Kishorn Nappe. (Calibrated magnetic anisortopy measurements).

of the strain ellipsoids throughout Lochcarron and Lochalsh. The shape of the finite strain ellipsoids(Figure 6.E.5.)shows a rational pattern of linear zones parallel to the strike of the bedding. It is possible to interpret these results in terms of a greater proportion of the transverse cleavage in the finite strain towards the east. The transverse cleavage producing an oblate strain ellipsoid when it begins to dominate the bedding parallel fabric. Such an overprinting was suggested for the results from northern Sleat (Figure 8.C.4.). However, the consistent orientation of the strain ellipsoids throughout Lochalsh and Lochcarron, suggest that this is unlikely and it is thought that, the variation in the finite strain on the overturned limb of the Lochalsh Syncline is due to the folding process.

Modelling of the Finite Strain Patterns Seen on the Overturned Limb of the Lochalsh Syncline

The strain distribution on the normal limb of the Lochalsh Syncline can be related to the transverse cleavage. The strain distribution on the overturned limb is more complex. The natural strain pattern will be compared with the following simple geometrical models of fold development.

(a) Flexural flow folding.
(b) Tangential longitudinal strain.
(c) Flexural slip folding.
(d) Folds related to a climbing shear zone, a special case of similar folding.
(e) Modified flexural slip folding.

Flexural Flow-Folding

The strain distribution related to flexural flow folding

has been described by Ramsay (1967). The shear strain is related to the dip of the bedding and increases to a maximum value on the limbs of the fold. This method of folding may be rejected since the cleavage produced is oblique to the bedding and cannot be related to the bedding parallel fabric. For similar reasons oblique flexural flow folding must also be rejected as a mechanism for the development of the Lochalsh Syncline. Furthermore, this mechansim of folding would affect both limbs of the fold and this is not seen in rocks of the Kishorn Nappe.

Tangential Longitudinal Strain

As described previously (Chapter 2.) tangential longitudinal strain may account for the distribution of the axial planar cleavage, the bedding parallel fabric and the slickensides within the Lochalsh Syncline. The strain distribution in tangential longitudinal strain folds has been described by Ramsay (1967). Within the fold profile there exists a neutral surface of little or no finite strain and this may correspond to the position of the slickensides. The main problem in applying this model to the Lochalsh Syncline is, that the strain arises from the curvature of the bedding but the bedding parallel fabric is seen on the overturned limb of the Lochalsh Syncline which is relatively straight. In the field, the bedding parallel fabric appears to be restricted to a portion of the overturned limb but the results from the magnetic anisotropy (Chapter 6.) suggests that the whole of the inverted limb is affected by the bedding parallel fabric. Since this limb is straight, then the bedding parallel fabric cannot have been generated by tangential longitudinal strain. However, the axial planar cleavage may have been produced by compression on the inner arc of the Lochalsh Syncline

in a similar manner to the cleavage on the inner arc of a tangential longitudinal strain fold.

Flexural Slip Folding

The presence of slickensides on many of the bedding surfaces suggest that flexural slip processes (not flexural flow folding) may have operated during the development of the Lochalsh Syncline. The angular profile of the Lochalsh Syncline shown in Figure 2.C.8. suggests that the fold may have developed by chevron processes (Ramsay 1967, 1974). This is supported by the presence of minor folds particularily around Loch na Dal, which have chevron styles. Cleavages and minor structures are often seen in the hinges of chevron folds which indicate small areas of rather intense deformation. Ramsay (1974) has shown how chevron folds may develop by flexural slip processes. In his model little or no strain is developed on the limbs of the folds and this cannot be reconciled with the strong bedding parallel fabric seen on the overturned limb of the Lochalsh Syncline. However, the axial planar cleavage in the hinge of the Lochalsh Syncline and the presence of slickensides is consistent with flexural slip folding or related chevron folding.

Fold Related to a Climbing Shear Zone

Barber (1965) proposed a model for the southern end of the Moine Thrust Zone in which the mylonitic fabric on the overturned limb of the Lochalsh Syncline and within the Balmacara Nappe was formed by the passage of a basement shear zone into the Torridonian cover of Lochalsh (Figure 2.B.5.). Subsequent thrusting produced the outcrop patterns seen. The Lochalsh Syncline, in this model, is essentially a drape fold over the basement shear zone and the fabric seen is produced by the

penetration of the overturned limb by the shear zone.

Ramsay (1980) proposed a similar model to that of Barber for the accommodation of basement shortening in overlying cover rocks. His model (Ramsay 1980 Figure 22 p98) produces recumbent folds and related thrust structures in the cover rocks. The geometrical consequences of this type of folding will be examined in detail and the relationship of the cleavage to the bedding studied.

Shear zones have strong strain gradients at their margins and the mylonitic fabric of the zone curves into the centre of the shear zone. Cross-cutting planar features will also curve as they pass through a shear zone and in this model the Lochalsh Syncline is produced by the curvature of the bedding within the shear zone, related to the strain gradient.

In this model it is considered coincidental that the mylonitic fabric in the Sleat Group is parallel to the bedding and that the bedding parallel fabric is a finite structure resulting from the rotation of the bedding and the fabric within the shear zone.

Coward (1980) has suggested that ductile shear zones may have ramp and flat geometries similar to thrusts. The model of Barber (1965) shows the bedding within the Torridonian sequence to be horizontal during the initiation of the Lochalsh Syncline. If the sub-Torridonian unconformity was nearly horizontal at this time then the shear zone must have developed as a ramp and cut the unconformity at 30 degrees or less. The mylonitic fabric of the Lewisian Gneiss in the Kishorn and Balmacara Nappes dips at approximately 30 degrees to the southeast and must therefore lie at a small angle to the shear zone boundary and by implication, at a small angle to the surface of the ramp. The shear zone has an overthrust sense of movement to the north-

west in common with the Moine Thrust Zone as a whole. Horizontal bedding will therefore lie at 150 degrees or greater, to the shear direction. For an ideal progressive simple shear zone with no tip strains, due to the propagation and the development of the zone, then the orientation of the fabric within the shear zone is given by the equation,

$$\tan 2\eta' = 2/\gamma \qquad (1)$$

The reorientation of a linear/planar feature by a shear zone is given by the equation,

$$\cot \alpha' = \cot \alpha + \gamma \qquad (2)$$

this equation may be used to calculate the orientation of the bedding within the shear zone where, $\alpha = 180^{o}$ - the ramp angle.

It has been noted that in the Lochalsh Syncline the mylonitic fabric must lie at a small angle to the shear zone boundary but for this to occur a shear strain of greater than 5.0 is required. For the fabric to lie within 5 degrees of the shear direction then a shear strain of greater than 10.0 is required (see Figure 8.C.6. curve A). Finite strains as high as these may occur within the Lewisian Gneiss where high shear strains are indicated by the presence of sheath folds (Cobbold 1980). However, on Lochalsh where the bedding parallel fabric is weakly developed the fabric dips at approximately 30 degrees and here, such high strains cannot be present. Furthermore, since this is an area of low strain, the fabric, if related to the shear zone would not dip at 30 degrees to the southeast.

If the bedding parallel fabric is considered to be a finite structure, formed by the rotation of both the

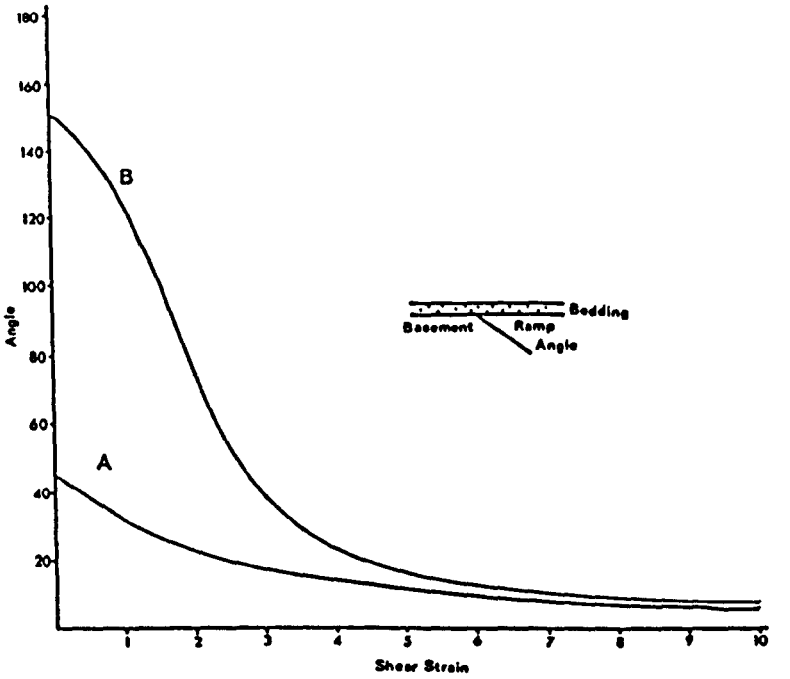

Figure 8.C.6. Curve A. The orientation of the developing fabric relative to the shear direction, in this case the surface of the ramp. Curve B. Orientation of the bedding relative to the shear direction, in this case the surface of the ramp. Curve B is the limiting value of a 30° ramp cutting horizontal bedding.

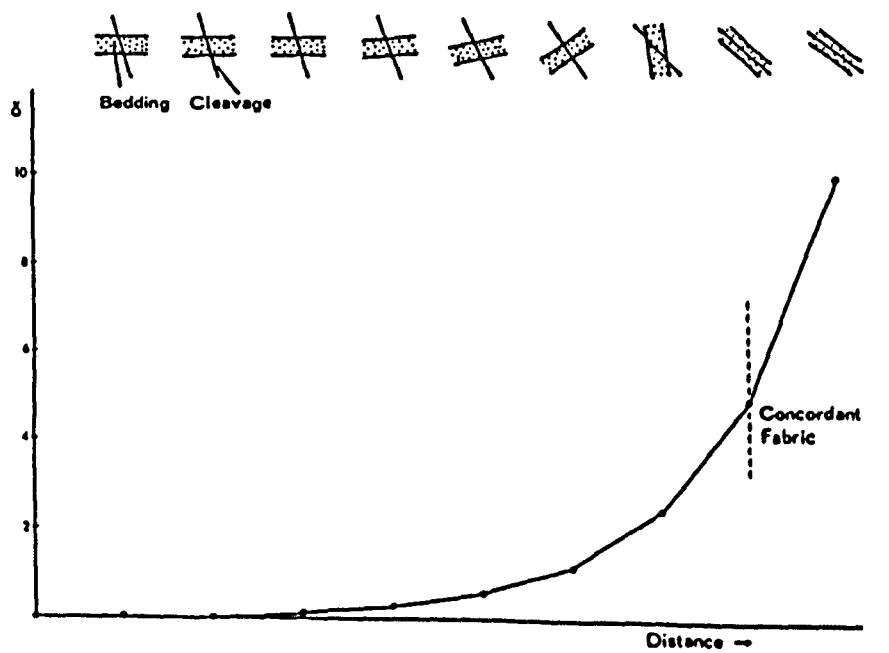

Figure 8.C.7. The reorientation of horizontal bedding by a sinistral shear zone which dips at 30°. γ = shear strain, Distance = distance into the centre of the shear zone. The diagram can refer to the development of a climbing shear zone with time.

bedding and the fabric into parallelism with the shear direction, then the shear strains required to produce the bedding parallel fabric may be obtained from Figure 8.C.6.. Curve B (Figure 8.C.6.) is the limiting value for horizontal bedding which is cut by a shear zone which dips at 30 degrees to the southeast. A shallower ramp angle will require strains greater than those given here and the orientation of the bedding will lie above curve B in Figure 8.C.6.. For the bedding and the fabric to lie within a few degrees of one another shear strains of greater than 5.0 are required. As described above strains as great as these are not seen where the bedding parallel fabric is weakly developed. Furthermore at low strains, the fabric and the bedding will be discordant in this model. The reorientation of horizontal bedding by a sinistral shear zone which dips at 30 degrees is shown, together with the orientation of the developing fabric in Figure 8.C.7.. As the diagram is drawn, it shows the finite state at the margins of a developing shear zone. However, the sequence shown in the upper part of the diagram may be considered as the path taken by a point at the centre of the zone. No cleavage pattern such as this can be seen on Lochalsh or northern Sleat. The bedding parallel fabric is parallel to the bedding even when it is only weakly developed.

In this model the bedding is a passive marker and will have a similar geometry (Ramsay 1980). The presence of flexural slip indicated by the slickensides, suggests that the bedding planes were active during deformation and this cannot be reconciled with the model. In view of the discrepancy between the cleavage patterns seen in the Kishorn Nappe and those generated by this model, the model of a climbing shear zone affecting previously horizontal bedding must be rejected for the origin of the Lochalsh Syncline.

Modified Flexural Slip Folding

From the preceding discussion it is clear that, for the bedding parallel fabric and the related mylonitic fabric in the Lewisian Gneiss to have been produced by a climbing shear zone the bedding could not have been horizontal before the development of the zone. This suggests that some folding was present before the development of the bedding parallel fabric. The relatively straight limbs of the Lochalsh Syncline indicate some form of angular fold profile.

The production of pre-shear folding may be attributed to the development of a kink band. Kink bands are common in the Moine Thrust Zone but they are generally late in the deformation history and postdate the development of strong fabrics. In general, the kink junction axis plunges to the southeast. However, folds with kink band geometry, such that the kink junction axis is parallel to the strike of the thrust zone may be seen at Kempie Bay. There the kinks are related to fore and back thrusts above a decollement horizon in the Fucoid Beds Member.

Elliott (1977) has shown the occurrence of folds with kink band geometries which may be related to the development of thrusts in the Canadian Rockies. It was suggested by Elliott (1977) that when a kink band ceases to grow the axial surfaces may fracture permitting the development of a thrust. However, such a sequence will not produce the overturned limb seen in the Lochalsh Syncline.

Simple shear has been proposed for the development of kink bands, but this origin has been rejected by Ramsay (1967). It is not suggested that the kink band develops by simple shear but when the kink band tends to lock up simple shear parallel to the boundaries takes over as the

dominant deformation mechanism.

If we consider a kink band with the geometry shown in Figure 8.C.8., and this kink band has developed on the decollement horizon at the point where thrust propagation has ceased then a geometrical model may be developed to determine the strain produced during the shearing of this kink band. Ramsay (1967,equation 7-54) has shown that the angles ν and β may be related by the equation

$$\beta + \nu/2 = 90^{o} \qquad (3)$$

At the point of lock up, or slow growth, the bedding within the kink band will dip at 60-80 degrees to the northwest. The value of β may be obtained from equation 3, given above, and will lie in the range 50-60 degrees. If homogeneous simple shear operates parallel to the kink band boundary the orientation of the layering within the band may be obtained from equation 2 where α is the orientation of the layering before simple shear and α' is the value after simple shear. The solutions to these equations are shown in Figure 8.C.9 . and these may be compared with the orientation of the fabric which is obtained from equation 1. It is clear from Figure 8.C.9 . that the bedding and the fabric will lie within a few degrees of each other from the initiation of the simple shear. The continuous development of simple shear affecting only one limb of the fold will generate the overturned limb.

This model fits well with the structure of the Lochalsh Syncline as, even at low strains, the fabric is parallel to the bedding, but the model suffers from several drawbacks. As the shear strain is homogeneous throughout the kink band then the strain related to the bedding parallel fabric must be homogeneous. As shown in Figure 8.C.5 . there is considerable variation in the finite

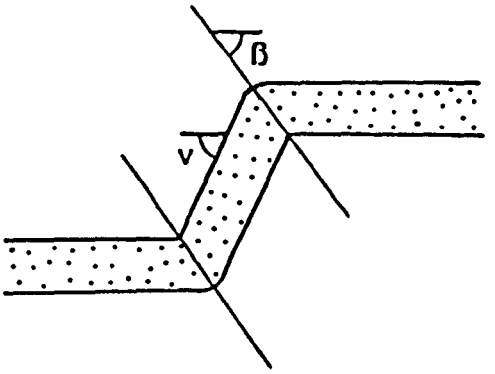

Figure 8.C.8. The geometry of a simple kink band (after Ramsay 1967) ß=dip of the kink band boundary, v=dip of the bedding within the kink band.

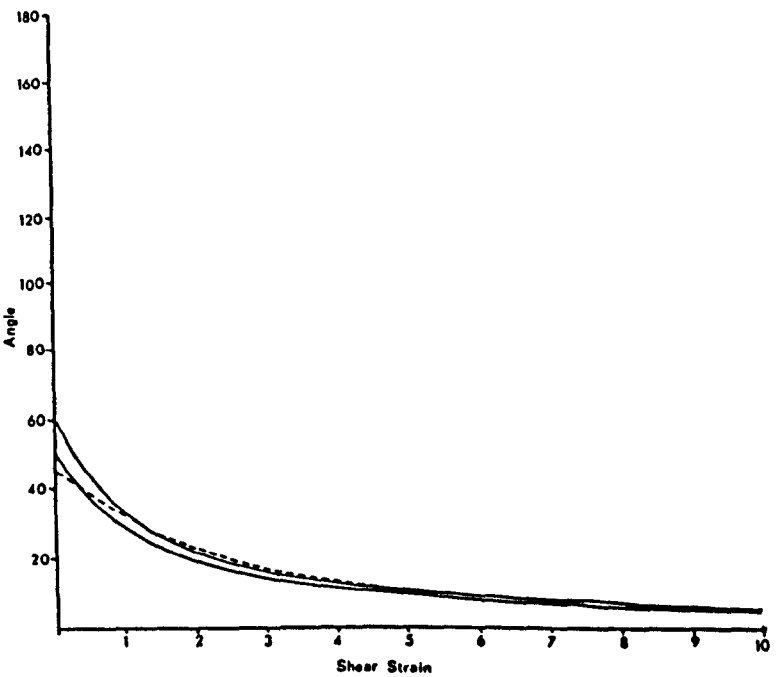

Figure 8.C.9. Orientation of the bedding (solid lines) and fabric (dashed line) relative to the boundary of the kink band which has been modified by simple shear.

strain ratios related to the bedding parallel fabric and this cannot be reconciled with the kink band model. Furthermore, the kink band will develop at a relatively high angle to the decollement horizon with a dip much greater than 30 degrees (Ramsay 1967). In this situation it is impossible to produce a ramp angle of less than 30 degrees and a fabric which dips at approximately 30 degrees and therefore this model must be rejected.

While the model described above cannot be reconciled with the overall structure of the Lochalsh Syncline it does illustrate the importance of the orientation of the bedding prior to the development of the shear zone. If we consider a situation with a ramp angle of 30 degrees or less, to produce the bedding parallel fabric the bedding must be overturned before the shear zone develops. The evidence for flexural slip related to the Lochalsh Syncline is extremely common. Therefore a second model is proposed in which a flexural slip fold develops ahead of the climbing shear zone. The geometrical consequences of this model will now be studied.

In a climbing shear zone ramp angles of 30 degrees or less are possible. At its initiation and at the margins of the zone the related fabric will lie at 45 degrees to the shear direction or the surface of the ramp. Given the range of possible ramp angles the fabric will dip between 45 and 75 degrees to the southeast when only weakly developed. In this orientation it is possible to produce the bedding parallel fabric, even at low strains, which is seen on the overturned limb just to the east of Kyle (see Chapter 6). To achieve this, the fold must be well developed and the shear zone must dip at 30 degrees to the southeast

Using the equations 1 and 2 it is possible to determine the shear strain expected from the reorientation of the bedding. From the finite strain ratio a value for the shear strain may be inferred for the overturned limb. However, since the orientation of the bedding before shearing is unknown, this situation cannot be modelled accurately. In Figure 8.C.10. the shear strain inferred from the finite strain ratio (X/Z) is plotted against the orientation of the bedding for some of the sites on the overturned limb of the Lochalsh Syncline. The results show an irrational pattern which cannot be related to increasing shear strains or to the simple modification of a fold profile by simple shear. The results showing dips of less than 30 degrees imply a ramp angle of less than 30 degrees. However, in this model the shear zone must dip at 30 degrees to produce the bedding parallel fabric in all of the beds throughout the overturned limb. This model is internally inconsistent and must be rejected.

It is possible to suggest a third model of flexural slip folding preceding the development of a shear zone. Lister and Williams (1979) have shown how, during simple shear deformation, the boundary conditions may be maintained while the layers undergo deformation by rotation and pure shear. They suggest that the situation shown in Figure 8.C.11. may be applicable to the deformation of thrust sheets and this model has been applied to the overturned limb of the Lochalsh Syncline.

using the relationship

$$\cot \alpha' = \cot \alpha + \gamma$$

and assuming that there is no change in the width of a shear zone. and that the layers are perpendicular to the shear direction it is possible to produce a simple model for the deformation within the layers. It is clear from Figure 8.C.11. that the fabric produced will be parallel

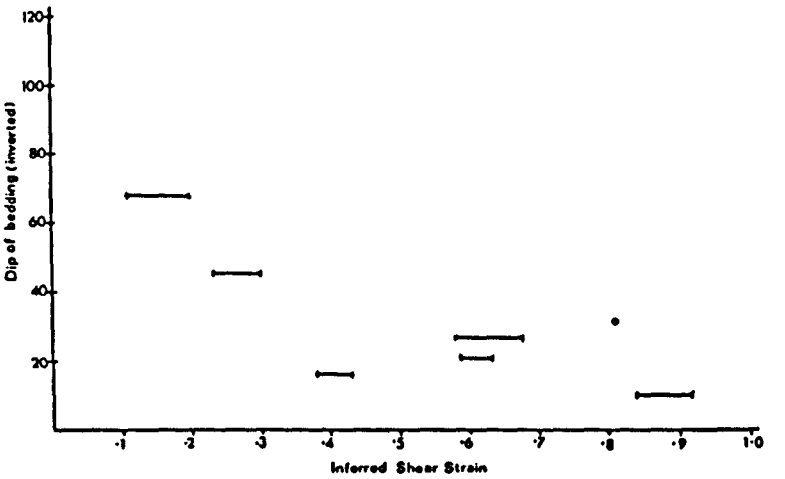

Figure8.C.10. Dip of the bedding on the overturned limb of the Lochalsh Syncline between Kyle and Balmacara plotted against the inferred shear strain. The shear strain was obtained from the strain ratio in a vertical plane parallel to the transport direction (X/Z). The range in shear strains lies between the maximum and minimum values of the strain ratio obtained from measurements of magnetic anisotropy.

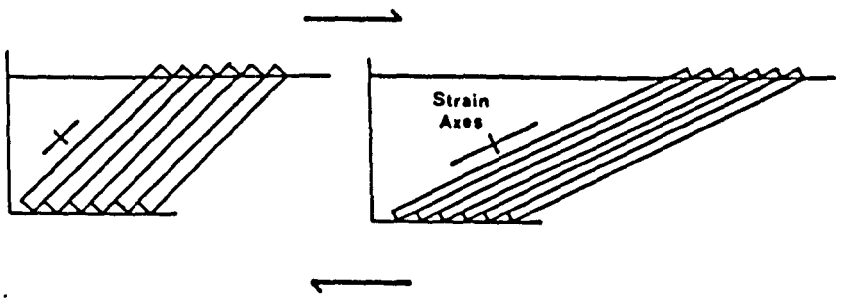

Figure 8.C.11. Bulk simple shear deformation achieved by rotation and pure shear (after Lister and Williams 1979). The rotation is permitted by slip on the surface of the layers.

to the layering. From Figure 8.C.12. the length of the layer before deformation is given by

$$l_o = \sqrt{(\cot \alpha)^2 + 1^2} \qquad (4)$$

The length of the layer after deformation is given by

$$l_1 = \sqrt{((\cot \alpha) + \gamma)^2 + 1^2} \qquad (5)$$

The change in the length of the layers is given by

$$\frac{l_1}{l_o} = \frac{\sqrt{(\cot \alpha')^2 + 1^2}}{\sqrt{(\cot \alpha)^2 + 1^2}} \qquad (6)$$

Using a modified version of equation 6 it is possible to relate the strain ratio, assuming plane strain deformation, to the final orientation of the bedding

$$\frac{l_1}{l_o} = \frac{\sqrt{(\cot \alpha')^2 + 1}}{\sqrt{((\cot \alpha') - \gamma)^2 + 1}} \qquad (7)$$

A graph of this equation is shown in Figure 8.C.13. for three values of applied shear strain. Three features of these curves are important firstly, for a homogeneous shear strain variation in the finite strain ratio is possible throughout the overturned limb. Secondly, there is a marked peak in the curves the position of which migrates towards the shear direction with increase in applied shear strain. The peak lies close to the position of the maximum angular shear strain. From equation 7 it can be seen that the strain ratio within the layers is related to the change in the orientation of the layer during simple shear. The greatest change in the orientation of the layers will occur close to the position of the maximum angular shear strain. This area moves towards the shear direction at progressively higher shear strains (Ramsay 1967) and

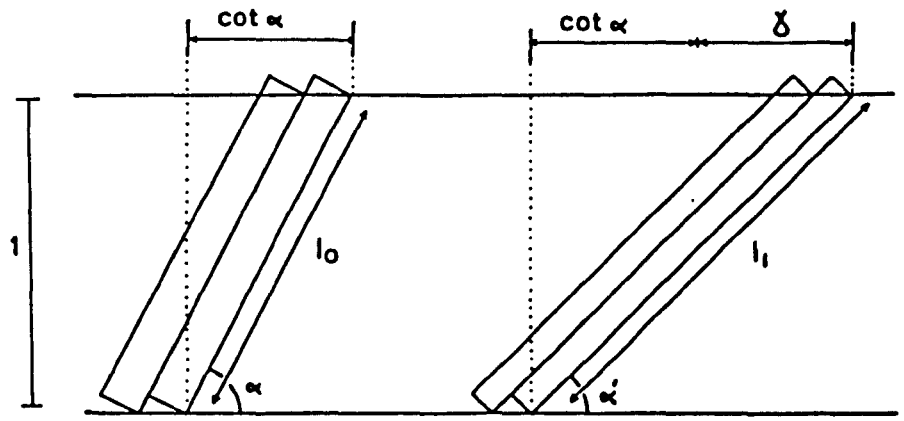

Figure 8.C.12. A simple geometrical model to determine the finite strain ratio within the layers undergoing rotation and pure shear deformation.

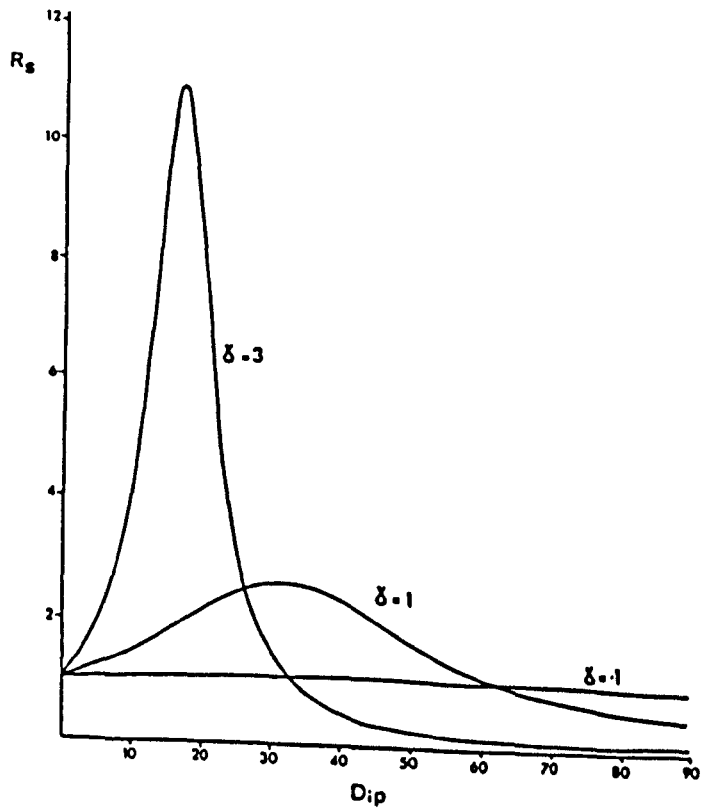

Figure 8.C.13. Graphical solutions of equation 7 for three values of applied shear strain (γ). Rs=finite strain ratio within the layers and dip=final dip of the bedding.

as a result the peaks in the curves move towards the shear direction.

Layers,which before shearing, lay at angles greater than 90 degrees to the shear direction will be initially shortened and this produces finite strain ratios of less than 1.0.

This model may be applied to the Lochalsh Syncline as the slickensides indicate that the bedding planes were active during the development of the fold. If we consider the layers in Figure 8.C.11. to be bedding on the overturned limb of the Lochalsh Syncline we may compare the strains produced in the model with those obtained from the natural example. In this case, we must assume that the two hinges above and below the limb do not migrate during the deformation and that the shear zone has a constant width throughout the deformation. This first assumption is probably valid since no evidence can be found in the field for hinge migration. The second assumption is, possibly valid as in the natural situation the overturned limb will be surrounded by the remainder of the thrust sheet. Changes in the width of the zone, which would develop during the rotation of a limb segment of constant length, could not be accommodated in the natural situation (see Figure 8.C.14.).

Figure 8.C.15. shows the strain ratio (X/Z) and the orientation of the bedding on the overturned limb of the Lochalsh Syncline. There is a peak in the values of the strain ratio at approximately 30 degrees. The fall in strain ratio at lower dip values cannot be explained by any of the previous models. However, the theoretical curves obtained from equation 7 for a horizontal shear zone fit with the natural data. Curves of different applied shear strain are found for each of the northwest-southeast sections studied. No common shear strain is obtained for the whole of the overturned limb. The

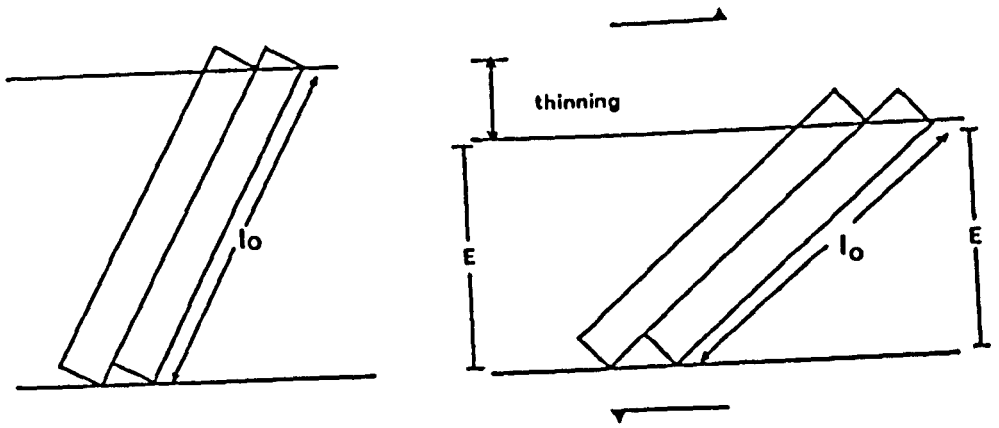

Figure 8.C.14. Rotation of a limb segment of constant length. This style of deformation can only occur if the material at the ends of the zone (E) thins during deformation. Clearly this is unreasonable for most geological situations.

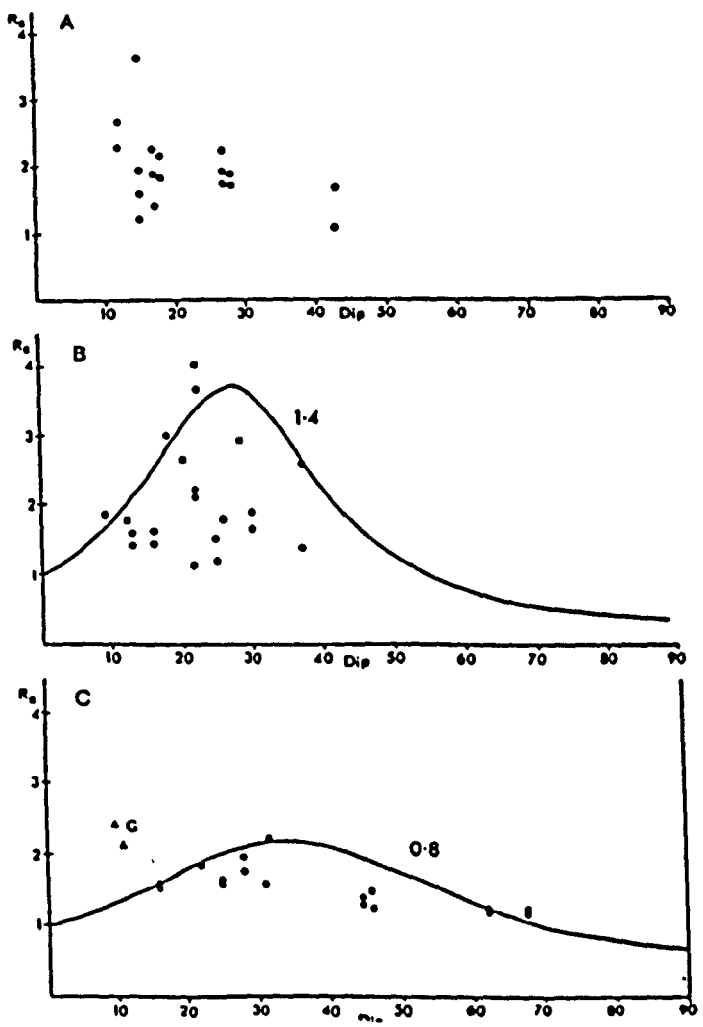

Caption shown overleaf (Figure 8.C.15.)

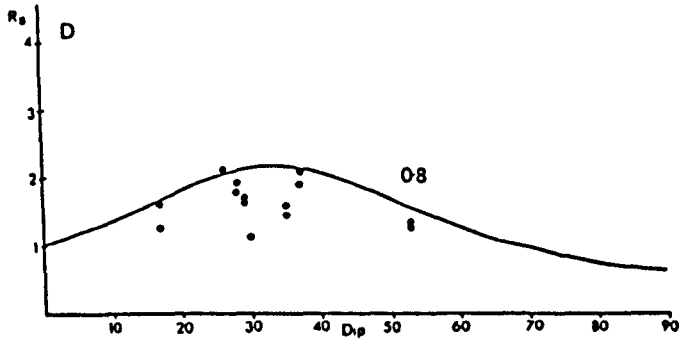

Figure 8.C.15. Finite strain ratios (X/Z) from the overturned limb of the Lochalsh Syncline plotted against the dip of the bedding (now inverted). A series of standard curves of applied shear strain were fitted to the natural data and the value of the shear strain obtained for each profile is given in each diagram. The areas shown are; A = Lochcarron B = Plockton to Duncraig C = Kyle to Balmacara D = Northern Sleat. ■= data from the conglomerates which were measured on Lochalsh (see chapter 4.) and ▲= areas close to Balmacara where the bedding has been replaced by a strong mylonitic fabric. Here, the model cannot be strictly applied as a new layering controls the deformation. Alternatively, these highly deformed rocks may represent the centre of the shear zone where the applied shear strain is much greater.

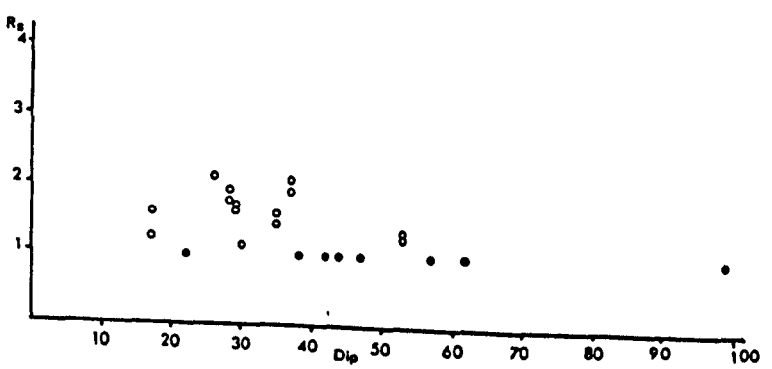

Figure 8.C.16. Removal of an applied shear strain of 0.8 from the data from northern Sleat. O = natural data (Figure 8.C.15.), ● = results after restoration. The normal limb dips at approximately 30° to the northwest thus, an interlimb angle of approximately 90° is indicated.

different shear strains obtained for the profiles suggests that different parts of the Kishorn Nappe have moved forward by differing amounts. This is in agreement with the results of Coward and Kim (1981) and Fischer and Coward (1982).

Though this model is rather simple it is thought to represent the processes which operated on the overturned limb of the Lochalsh Syncline during the development of the fold. Departures from this model may be explained in the following ways;

(a) Measurement errors and the incorrect choice in the orientation of the shear zone. The effects of measurement errors in natural strain data cannot be adequately assessed and this problem is largely unresolved. The incorrect choice in the orientation of the shear zone will displace the position of the natural data parallel to the horizontal axis in Fioures 8.C.13. and 8 C.15.. This situation can be easily recognised and adjusted accordingly.

(b) Imperfect slip on the bedding surfaces. This will introduce additional components of strain, the ratio and orientation of which will depend on the orientation of the layer and the applied shear strain during the period when slip was retarded. This may introduce changes in the strain ratio on the bedding surface leading to the production of prolate and oblate strain ellipsoids. These effects cannot be modelled in any systematic way but we must be aware that they could exist.

(c) Strain gradients in the shear zone. Natural strain gradients may result in profiles which depart from the theoretical curves. This is one possible explanation for the results labelled G in Figure 8.C.15.. This data comes from the easternmost outcrop of the Kishorn Nappe and may reflect higher shear strains at the centre of the climbing shear zone. This is particularily well seen at Ard Hill beneath the Balmacara Nappe where the bedding parallel fabric has been replaced by a strong mylonitic fabric and banding and related sheath folds. The curves suggest that the shear zone was horizontal during its development but departures of up to 10 degrees cannot be clearly recognised and it is thought that the shear zone dipped very gently to the east and the centre of the zone is exposed at Ard Hill, Sgurr Beag and Carn an Bhealaich Mhoir.

(d) Inherited or later strains. Inherited or later strains will change the ratio of the finite strain.If these are parallel or perpendicular to the bedding they may be easily modelled but when they are oblique knowledge of the strain path is necessary. This source of variation probably results in the non-K=1 strain ellipsoids obtained in the natural data.

The strain data from the overturned limb of the Lochalsh Syncline indicates that the fold was relatively well developed prior to the initiation of the shear zone. No strain ratios (X/Z) of less than 1.0 were found, which suggests that the bedding was overturned before the initiation of the shear zone. From the estimated shear strain (the best fit curve) the bedding may be restored to a pre-shear position using equation 2. One such

restoration is shown in Figure 8.C.16. and indicates the presence of a relatively angular fold profile with an interlimb angle of approximately 90 to 120 degrees

Though this model is relatively simple it does relate the development of the bedding parallel fabric to the overturning of the inverted limb. The major problem with the use of simple shear to explain the bedding parallel fabric is that the fabric produced will be oblique to the bedding. This model permits the development of the bedding parallel fabric with its strong east-southeast lineation, similar in orientation to the mylonites of thrust zone, during simple shear. This model of limb rotation is thought to reflect, if not describe the process which operated on the overturned limb of the Lochalsh Syncline during the development of the bedding parallel fabric. The model described is for homogeneous simple shear and may be refined by the introduction of progressive simple shear, but insufficient data is available from the Kishorn Nappe to verify the strain gradient. This is mainly due to the small range in vertical profiles available. Departures from the model are indicated by non-K=1 finite strain ellipsoids and may be ascribed to extensions parallel to the fold axis of the Lochalsh Syncline. These extensions cannot be modelled accurately without a large number of assumptions, the validity of which cannot be tested.

The model of limb rotation to generate the bedding parallel fabric on the overturned limb of the Lochalsh Syncline will be tested against field data presented in chapter 2..

It is clear from the analysis presented above that flexural slip processes must have preceeded the development of the shear zone. The common occurrence of slickensides indicate that flexural slip processes did operate during the development of the Lochalsh

Syncline. The Ord Syncline and the Eishort Anticline appear to have developed into recumbent folds by flexural slip alone. Therefore, a recumbent Lochalsh Syncline could have been present before the development of the shear zone.

If we consider the situation shown in Figure 8.C.17. as the limb of the fold overturns , material must be removed from the hinge of the fold. This problem exists whether the process of overturning is one of flexural slip or limb rotation by simple shear. In the Lochalsh Syncline this problem has been overcome by the development of the following structures:

(a) Minor folds of chevron style.
(b) Axial planar cleavage.
(c) Slickensides on the bedding surfaces.
(d) The out-of-syncline thrust.

As described previously, minor folding appears to have been the dominant process by which the Eishort Anticline overcame this problem in the core of the fold (see Figure 8.C.17.. Minor folds related to the Lochalsh Syncline are common only in the hinge region of the fold, such as on Beinne na Greine and around Loch na Dal. They probably developed to facilitate the growth of the Lochalsh Syncline. The folds could have been produced during the development of the flexural slip fold or during its modification when the bedding parallel fabric was produced. These minor folds tend to be more common where shaly units are present, such as around Loch na Dal.

In the Applecross Formation, where shale beds are rare, the axial planar cleavage appears to have been the dominant mechanism by which material was removed from the hinge of the fold (see Figure 8.C.17.). This is

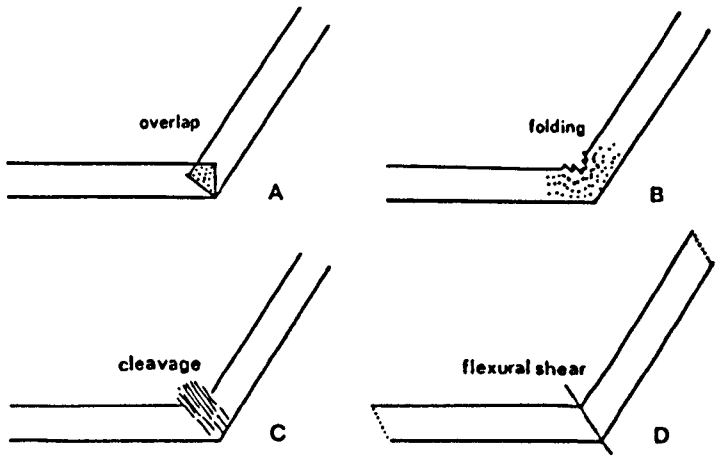

Figure 8.C.17. The development of any fold causes a space problem in the inner arc of the fold. A. the amount of overlap depends upon the orientation of the layering and in general this may be relieved by; B. folding, C. development of a axial planar cleavage, D. flexural shear by flexural flow of flexural slip.

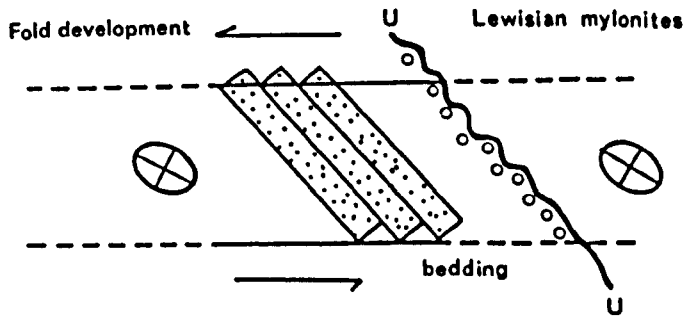

Figure 8.C.18. Rotation of the overturned limb of the Lochalsh Syncline must be accompanied by simple shear deformation at either end of the "zone". To the west, this may take the form of further fold development. To the east, beneath the unconformity (U), deformation may occur by the development of mylonites within the Lewisian Gneisses.

consistent with the results from the minor folds studied at Plockton (chapters 2.and 4.). The development of the axial planar cleavage in these minor folds can be related to heterogeneous flattening of the flexural slip folds. Shortening perpendicular to the axial plane of the fold increases towards the inner arc of the fold. The axial planar cleavage may have been produced by both the development of a chevron fold (Ramsay 1974) or rotation of the inverted limb during simple shear. It is not possible, from field evidence, to determine whether the axial planar cleavage developed as a response to one or both of the processes, since no age relationship can be established between the bedding parallel fabric and the axial planar cleavage.

The simplest method of removing material from the core of the fold is by flexural slip folding with movement on the bedding surfaces (see Figure 8.C.17.). Obviously this is reflected in the presence of slickensides on the bedding surfaces. The movement sense of the slickensides on the inverted limb of the Lochalsh Syncline is consistent with both flexural slip folding and rotation of the limb during simple shear. The movement sense on the overturned limb is the same for both processes and therefore the slickensides cannot be used to suggest whether one or other of the processes operated on the overturned limb of the Lochalsh Sycnline. On the normal limb of the Lochalsh Syncline movement sense of the slickensides is consistent with flexural slip folding..The large chevron folds seen on the normal limb of the Lochalsh Syncline on southern Sleat (Figures 2.C.20 and 2.C.22.) may have been initiated when this movement on the bedding planes was restricted or retarded, but this is largely speculation.

The out-of-syncline thrust appears to have developed in the massive sandstone units on Ben Aslak and Beinn na Caillich where minor folding was not possible. It

is thought that the thrust postdates the bedding parallel fabric since it carries rocks of the overturned limb, with a strong bedding parallel fabric, over the normal limb of the Syncline. Thus this structure appears to be related to the development of the fold during the growth of the bedding parallel fabric and may be a direct response to the tightening of the fold during the rotation of the overturned limb.

All of the four structures described above may have been produced by either chevron folding (Ramsay 1974) or the rotation of the overturned limb by simple shear. A clear age relationship can only be established for the out-of-syncline thrust and the bedding parallel fabric. However, there is no evidence to suggest that the process shown in Figure 8.C.11. could not have operated on the inverted limb of the Lochalsh Syncline and produced the bedding parallel fabric.

The fold profile shown in Figure 2.C.13. which is drawn through Beinn Bheag suggests that rotation of the overturned limb is a possible mechanism for the generation of the bedding parallel fabric. The slight curvature of the bedding on the most eastern portion of the normal limb, which is common in other areas of the fold and similar to the fold profiles at Erbusaig and Port Cam may represent a remanent portion of the flexural slip fold. There is a marked contrast between the two limbs of the fold. The sudden change in the orientation of the bedding across either the axial plane or the out-of-syncline thrust suggests that some process operated which modified the orientation of the overturned limb. Therefore it is thought that the bedding parallel fabric was generated by rotation of the overturned limb during simple shear.

The widespread development of mylonites within the Lewisian rocks of Kishorn and Balmacara Nappes may be

related to simple shear deformation which affected the overturned limb of the Lochalsh Syncline. As shown in Figure 8.C.18., during rotation of the overturned limb, deformation of the surrounding rocks must occur. The Lochalsh Syncline may propagate into the sediments above. Since the Lewisian rocks beneath have only a weak layering then the rotation of the limb must be associated with simple shear deformation and this produces the mylonites.

In the eastern and structurally highest portions of the Kishorn Nappe, bedding cannot be seen, and the bedding parallel fabric becomes indistinguishable from a strong mylonitic fabric and banding. This zone of intense fabric may be due to a continuation of the simple shear deformation which rotated the overturned limb and it marks the centre of the shear zone. Alternatively, the shear zone which developed in the Lewisian rocks may have propagated into the Torridonian succession. These two explanations of the intense fabric are virtually the same and cannot be distinguished on the basis of field evidence. This zone of very intense deformation and the centre of the shear zone marks the position where the thrust plane developed leading to the decapitation of the Lochalsh Syncline.

Section 8D The Skarvemellen Anticline

A strain path can be established for the rocks of the Skarvemellen Anticline and this was discussed in chapter 7.. The relationship of the finite strain to the Skarvemellen Anticline will now be discussed.

Contrary to the results of Milton and Williams (1981) there does not appear to be any relationship between the height of the site above the thrust plane and the intensity of the strain (see Figure 8.D.1). Therefore the strain distribution must be a consequence of the fold

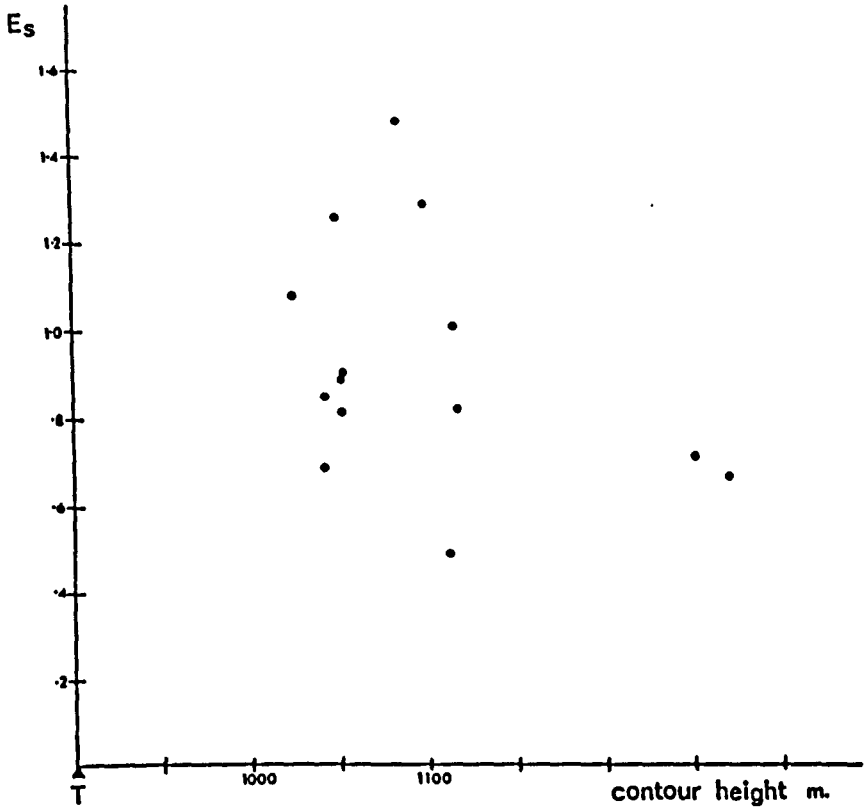

Figure 8.D.1. Graph of natural octahedral unit shear (Es) against the contour height of the site. T marks the approximate position of the thrust plane. Only conglomerate data is shown.

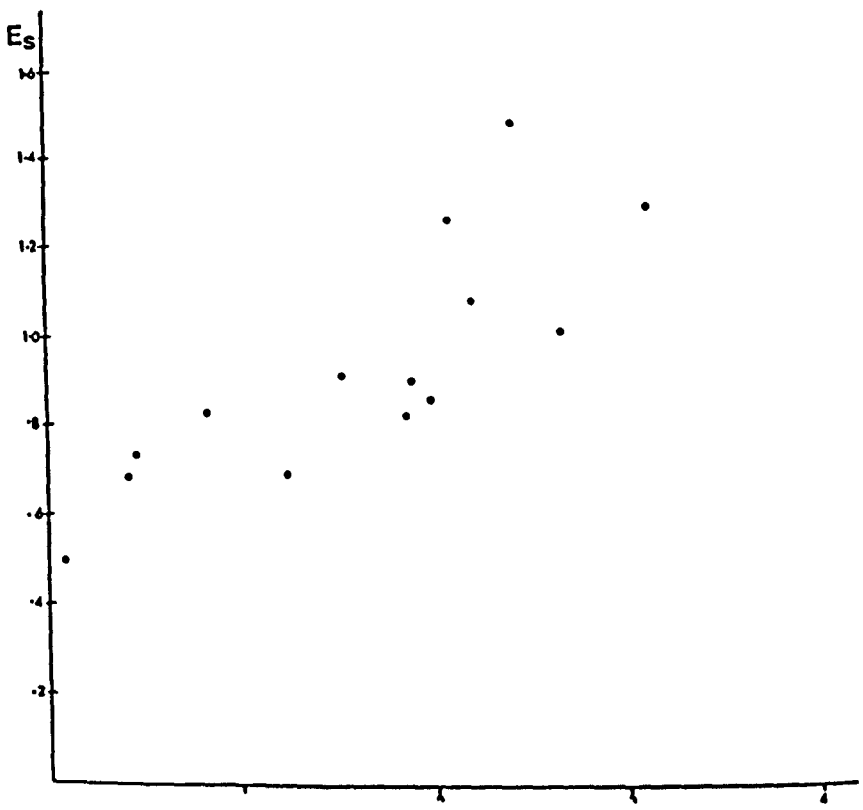

Figure 8.D.2. A graph of Es against distance (in Kilometres) of the site down the axial plane of the Skarvemellen Anticline from site 11. Only conglomerate data is shown.

development and will be studied accordingly.

From Figure 8.D.2. it is clear that a relationship exists between the amount of strain suffered at a particular site (Es) and the distance of the site down the axial plane of the fold. Furthermore, there appears to be a relationship between the amount of strain suffered and the perpendicular distance of the site from the axial plane of the fold. These graphs suggest that there is a relationship between the position of the site within the fold and the amount of strain which the site has suffered.

Figures 8.D.2. and 8.D.3. have been combined on a rectangular grid in a vertical plane which is orientated north-south perpendicular to the fold axis. A comparable diagram of axial ratios may be constructed and this is shown in Figure 8.D.5.. In the plane under consideration a clear relationship exists between the axial ratio of the strain ellipsoid (in this plane) and the position of the site within the fold. As shown in Figure 7.D.1. these sites are spread over several kilometres and it was thought that the strain suffered at a particular site may be related to its position along the fold axis. To determine whether this had any influence on the natural strain pattern a graph of Es against the position of the site along the fold axis was drawn and this is shown in Figure 8.D.6.. There does not appear to be any relationship as an irregular pattern is obtained with no common trend. Therefore, it is thought that the amount of strain suffered at a site is a consequence of the position of the site within the fold profile.

To determine the origin of the bedding parallel fabric on the inverted limb of the Skarvemellen Anticline graphs of dip against axial ratio were drawn (see Figure 8.D.7.). In this case both X/Z and Y/Z ratios

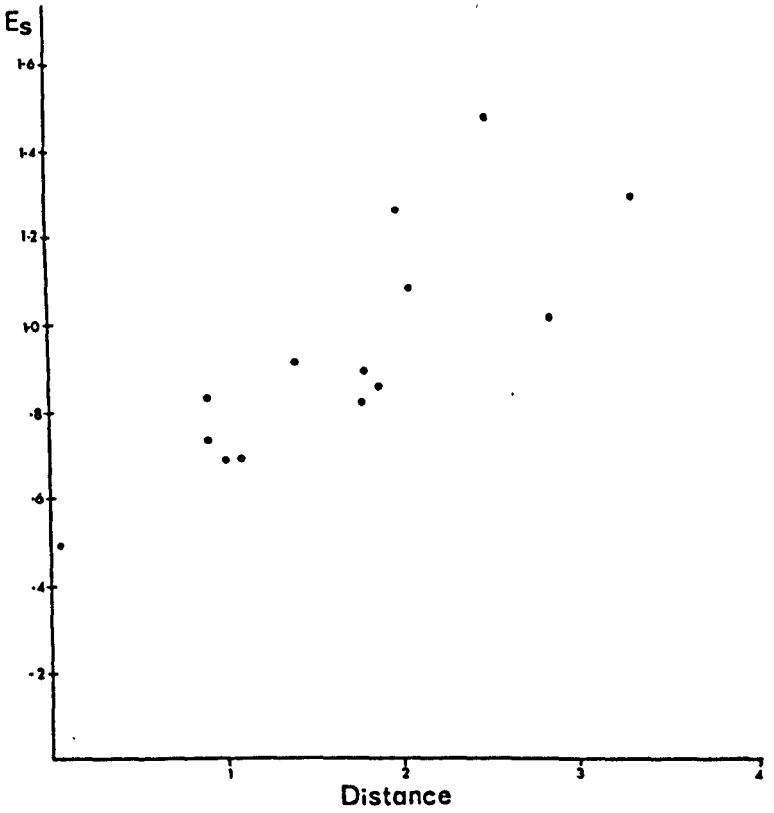

Figure 8.D.3. A graph of Es against the perpendicular distance (in kilometres) of the site towards the axial plane of the Skarvemellen Anticline from site 11.

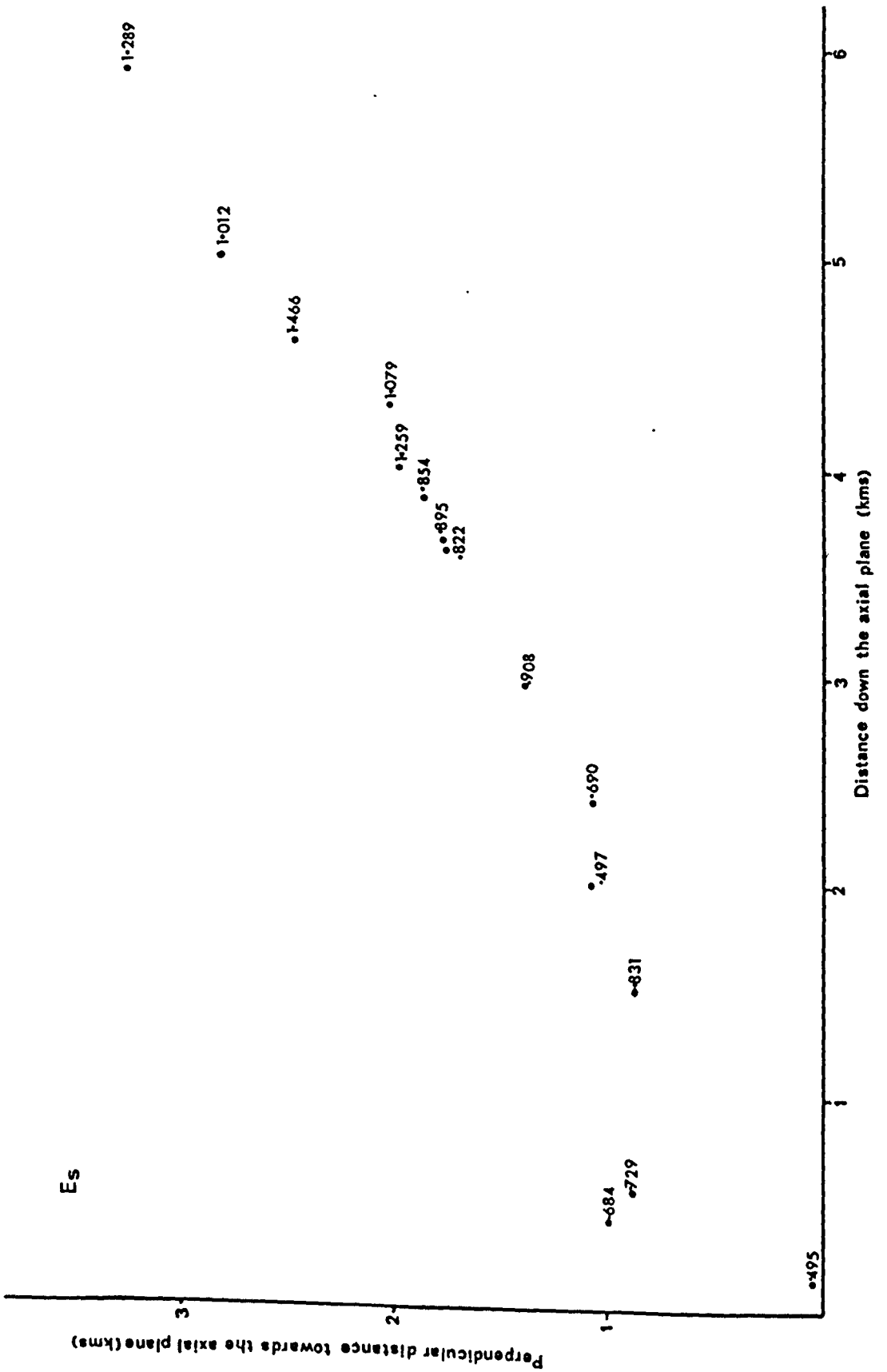

Figure 8.D.4. A combination of Figures 8.D.2. and 8.D.3. showing the relative position of the sites within the Skarvemellen Anticline and the associated values of Es. The horizontal axis of the diagram gives the distance of the site down the axial plane of th e fold from site 11. Sites 13 and 14 have been omitted as they possess the axial planar cleavage.

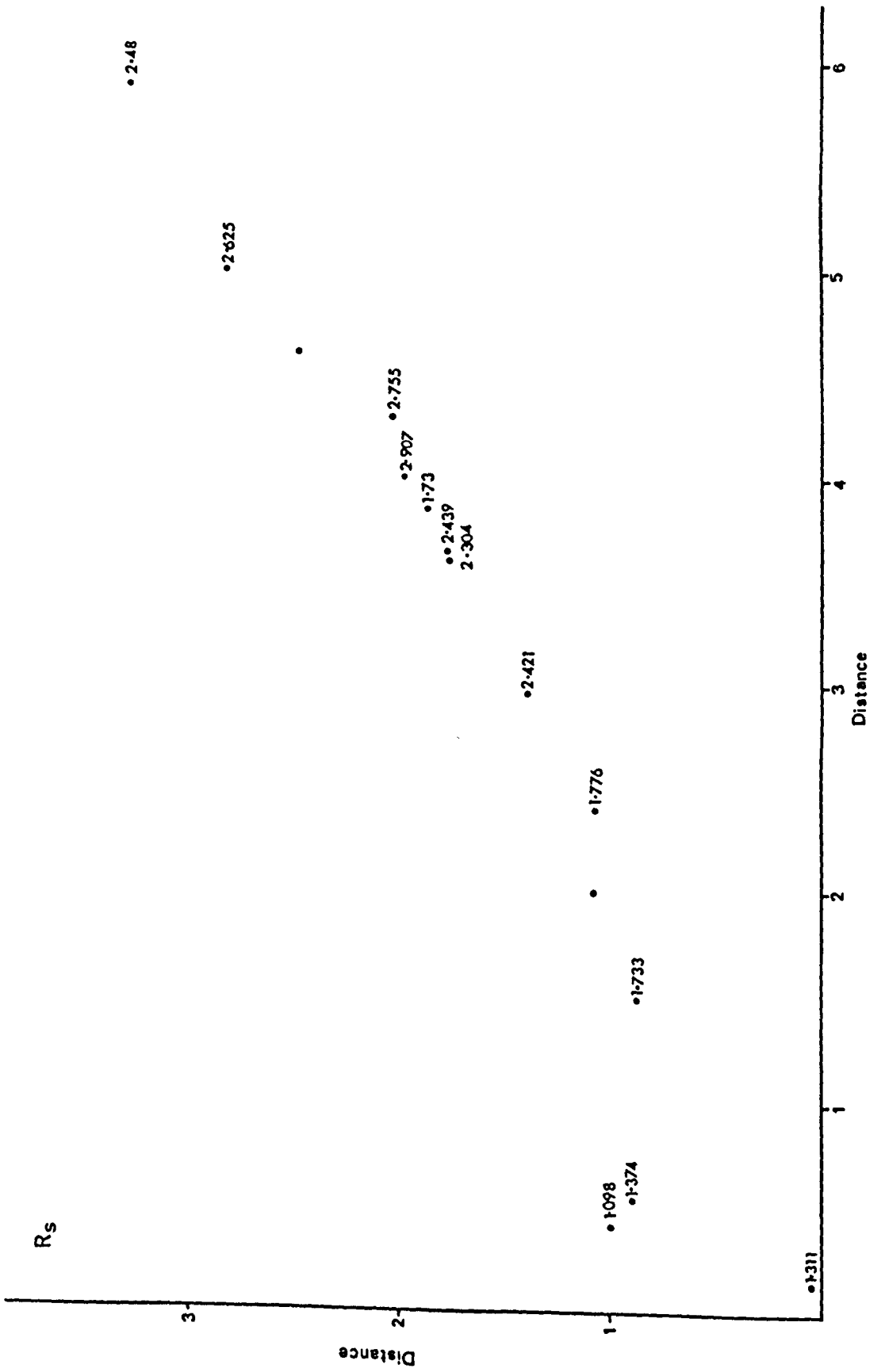

Figure 8.D.5. The relationship of the strain ratio to the position of the site within the fold profile. The horizontal axis of the diagram gives the distance of the site down the axial plane of the Skarvemellen Anticline from site 11.

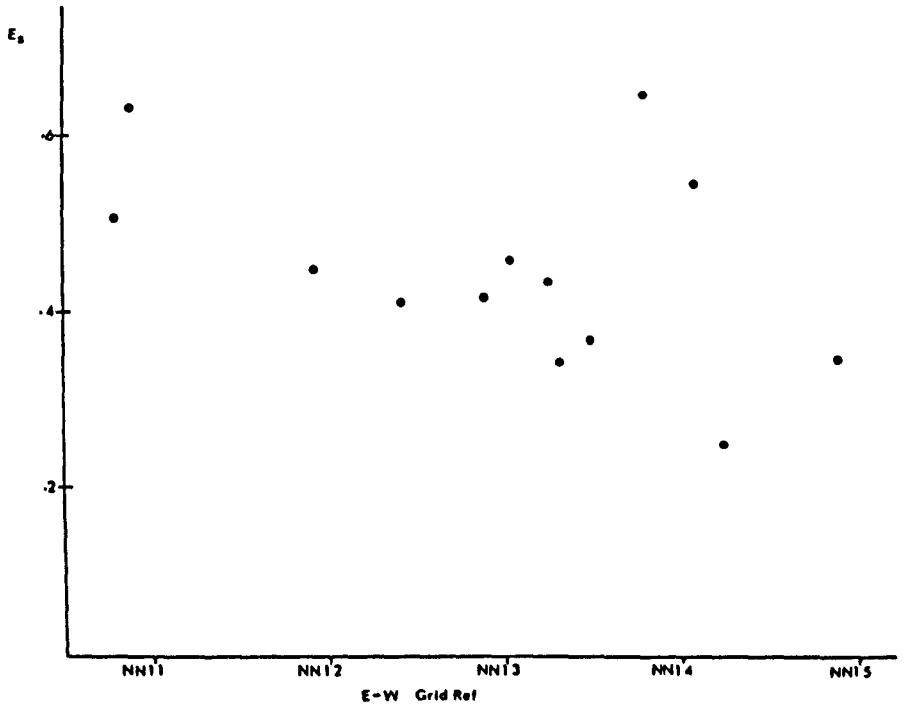

Figure 8.D.6. A graph of Es against the position of the site along the fold axis of the Skarvemellen Anticline. Only conglomerate data is plotted.

were used depending on the orientation of the X and Y axes of the strain ellipsoid within the bedding plane. The results show similar curves to those discussed for the Lochalsh Syncline. The approximate value of the applied shear strain may be obtained from the position of the peak. The results show strain ratios which are too great for the dip of the bedding. By varying the orientation of the shear direction between 0 and 30 degrees no theoretical curve could be found which would fit with the natural data.

Departures from the rotation model are discussed in the previous section. Slickensides are rarely seen in the Mellene Nappe and imperfect slip on the bedding planes may have produced the variations in the strain ratio, but it is unlikely that the bedding parallel fabric would have been developed parallel to the bedding. The most likely source of strain variation is thought to be inherited strains arising from extension parallel to the fold axis. It has been shown that there is considerable extension parallel to the fold axis of the Skarvemellen Anticline. Assuming constant volume deformation this extension would affect the strain ratio in the north-south section discussed here.

Two dimensional strain ratios orientated parallel to or perpendicular to the bedding can be easily incorporated into the model of limb rotation during simple shear (shown in Figure 8.C.11.). Since the two strain ratios are coaxial then the final axial ratio may be obtained by multiplication (Ramsay 1967). This operation is comutative and therefore applies to both inherited strains and later coaxial strains. In this instance later coaxial strains seem improbable and therefore the equation

$$\frac{l_1}{l_o} = \left(\frac{\sqrt{(\cot \alpha')^2 + 1^2}}{\sqrt{(\cot \alpha' - \gamma)^2 + 1^2}} \right)^2 \times R_s'$$

Where R_s' = inherited or later strain ratio.

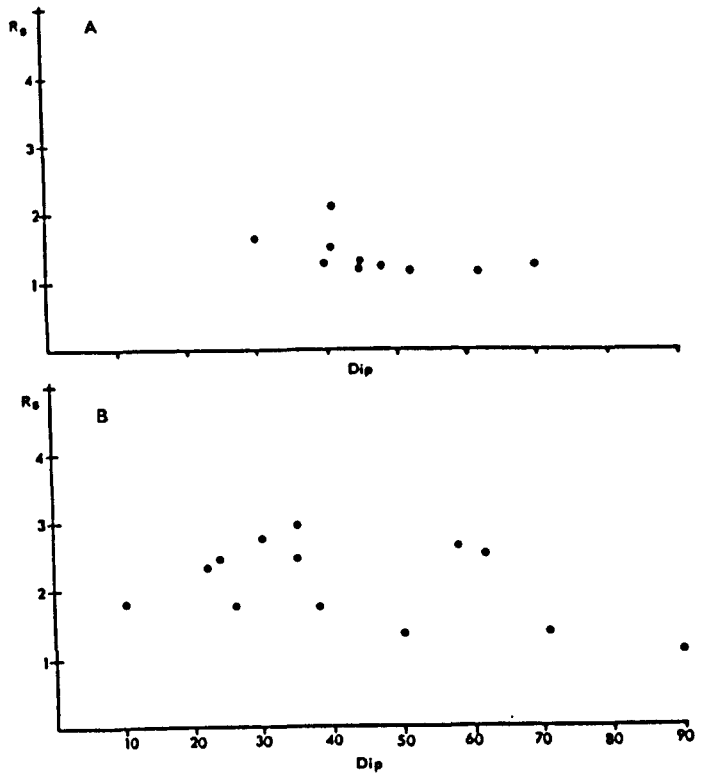

Figure 8.D.7. Graphs of the finite strain ratio in a north-south vertical plane against the dip of the bedding (now inverted). A. conglomerate data, B. data obtained from thin sections and magnetic anisotropy.

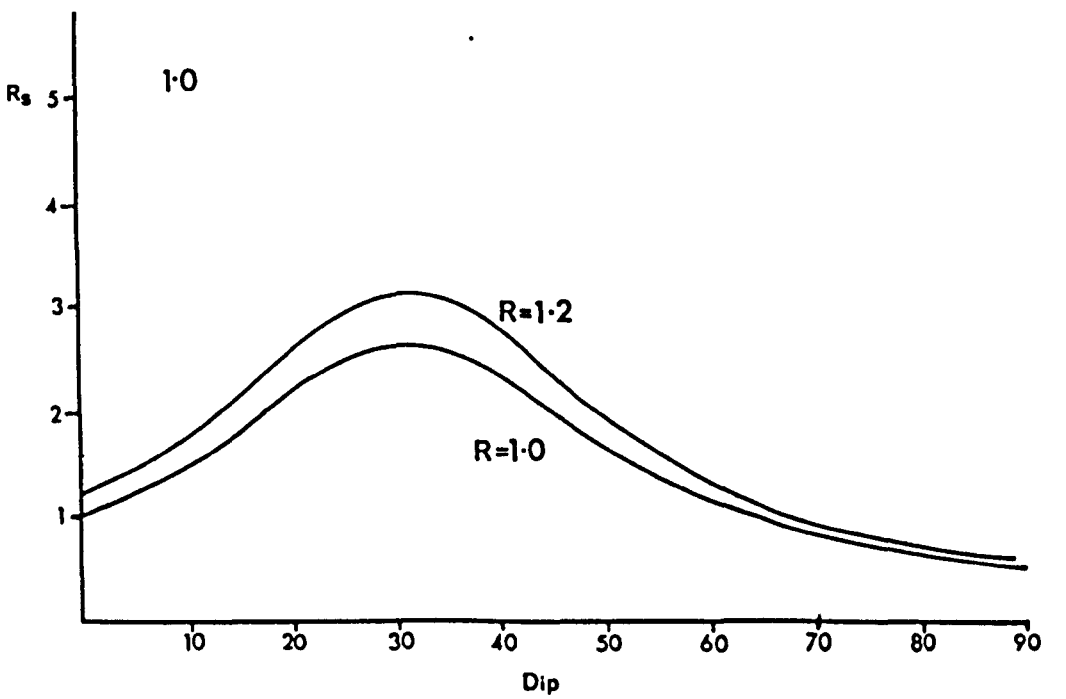

Figure 8.D.8. Theoretical curves of strain ratio against dip for limb rotation during simple shear following the model of Lister and Williams (1979). The applied shear strain (γ) = 1.0. The effect of an initial strain ratio (parallel to the bedding) of 1.2 is clearly seen.

may be used to determine the relationship of the finite strain ratio to the final orientation of the bedding. For various values of initial strain ratio and applied shear strain theoretical curves can be drawn. For each initial value and applied shear strain the curves are unique and two examples are shown in Figure 8.D.8...

Theoretical curves can be found which fit to the natural data, but it is thought unlikely that the model proposed truely reflects the processes which produce the bedding parallel fabric in the Skarvemellen Anticline. The value of the initial strain ratio obtained from the best fit curve cannot be related to the strain ellipsoids of the sites in the curve. The amount of extension parallel to the fold axis of the Anticline is extremely variable and possibly different in each of the sites studied. If it is this extension which controls the initial strain ratio then there will be considereable variation in this ratio and it seems unlikely that a common ratio can be obtained for each of the curves.

It is possible that extension parallel to the fold axis and limb rotation by simple shear operated together during the development of the Skarvemellen Anticline. Too many assumptions are necessary to model the situation accurately and it was not studied in any detail.

The peak in the curves of natural data shown in Figure 8.D.7. suggest that the process of limb rotation during simple shear may have operated during the development of the Skarvemellen Anticline. However, the axial ratios of the finite strain ellipsoids is related to the extension parallel to the fold axis of the Skarvemellen Anticline and this presents problems when modelling these results.

Extension parallel to the fold axis results from the growth of a non-cylindrical fold. Dubey and Cobbold (1977) have shown how a non-cylindrical fold develops by lateral propagation of the fold into unfolded strata. After the growth of the fold the length of the line A-A' (Figure 8.D.9) will be greater than in the unfolded state and extension parallel to the fold axis must have occurred. The amount of extension is related to the rates of amplification and propagation of the fold and variations in these rates with time. When the rate of amplification is very much greater than the rate of fold propagation the fold will be highly non-cylindrical with marked extension parallel to the fold axis. The rates of propagation and amplification are controlled by the material properties of the rocks and they may be related by these properties. Often in thrust zones, the lateral propagation of folds and thrusts is limited by some obstacle. Where this occurs consistently at the same position a lateral ramp is produced. Coward and Potts (in press a) have discussed the structures developed in an area of slightly oblique lateral ramps in the Assynt district. Using a series of propagation and amplification rates for a given fold mechanism, it should be possible to develop a model for the strain distribution in a non-cylindrical fold. This is beyond the scope of the present project. However, some conclusions may be drawn from the strain data obtained from the Skarvemellen Anticline.

Figure 8.D.10. shows the results of strain integrations which were performed on data from the Kishorn and Mellene Nappes. The profiles are drawn parallel to the fold axis. There is relatively little extension associated with the Lochalsh Syncline but there is considerable extension parallel to the fold axis of the Skarvemellen Anticline. This suggests that the propagation rate of the Lochalsh Syncline was able to keep pace with the

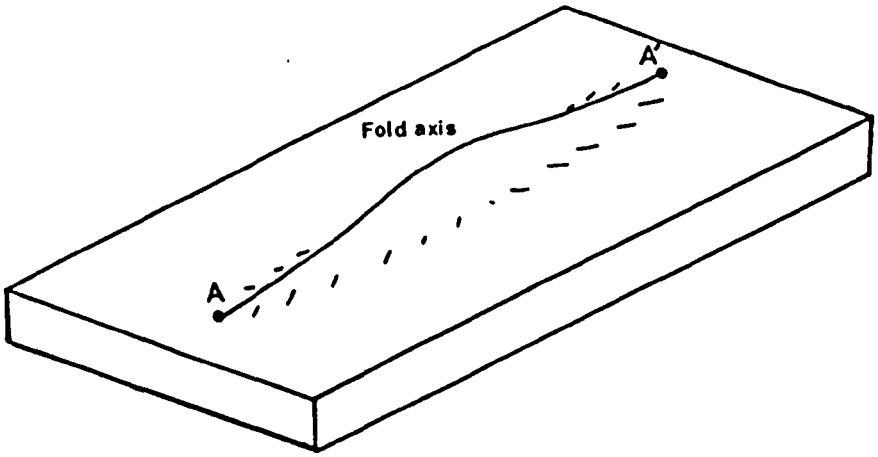

Figure 8.D.9. Development of a non-cylindrical fold in a sheet of unfolded strata. To permit amplification of the fold profile the fold complex must propagate laterally. Where this lateral propagation is inhibited a non-cylindrical fold results. To enable amplification of this fold the line A-A' must extend.

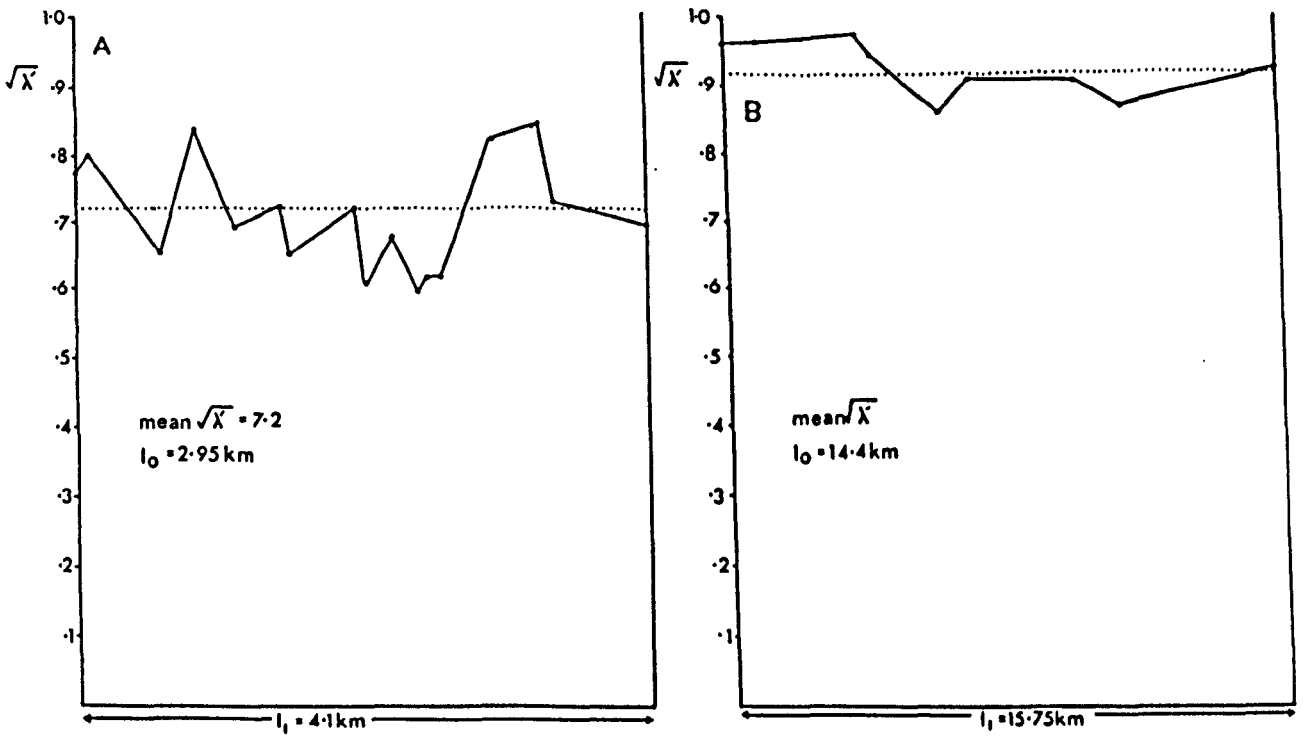

Figure 8.D.10. The results of strain integrations (Hossack 1978) parallel to the fold axes of the Skarvemellen Anticline (A) and the Lochalsh Syncline (B).

amplification of the fold. However, the propagation rate of the Skarvemellen Anticline could not keep pace with the amplification of the fold and as a result a highly non-cylindrical fold developed. This non-cylindrical nature was suggested by Nickelsen (1967) and was confirmed in this study. Many of the large valleys in southern central Norway marked the position of lateral ramps (Hossack et al 1981) and it is possible that the propagation of the Skarvemellen Anticline was prevented by two such lateral ramps.

The strong extension parallel to the fold axis of the Skarvemellen Anticline makes modelling of the strain distribution around the fold extremely difficult. Assumptions can be made regarding the growth of the fold and these assumptions change until the model is successful, but there is, at present, no way to test the validity of these assumptions. The strain ratio and the amount of strain suffered at a particular site appears to be related to the position of the site within the fold profile. However, it is possible that the position of the site along the fold axis of the anticline may also control the axial ratios of the finite strain ellipsoids, but insufficient data is available to test this.

The strain path discussed in chapter 7. suggests that two processes operated during the development of the bedding parallel fabric. An initial state of extension parallel to the fold axis, producing prolate finite strain ellipsoids and a second process,which generates oblate finite strain ellipsoids. It is possible that this second process is similar to the rotation of the overturned limb by simple shear as described in the previous section. This may contribute to the curves of natural data shown in Figure 8.D.7.

The model presented in the previous section for the rotation of the limb during simple shear assumes that the strike of the layers is perpendicular to the shear direction. If the layers are oblique to the shear direction the strain within the layers will depend not only on the initial and final orientation of the layers but also on the angle between the strike of the layering and the shear direction. It has been shown that the Skarvemellen Anticline is a non-cylindrical fold, and it is thought that the orientation of the bedding relative to the shear direction probably changed throughout the folds development,producing a highly complex strain pattern within the layers.

The pattern of natural strain data cannot be related to any of the fold mechanisms described by Ramsay (1967). The Valdres Sparagmite does not show any evidence of slickensides on the bedding surface. It is thought that the Eishort Anticline developed by flexural slip processes but there is no evidence of slickensides on the bedding surfaces of the Applecross Formation. These two rock types are very similar and it is thought possible that, in part, the Skarvemellen Anticline developed by flexural slip processes, but there is no direct evidence for this. The axial planar cleavage is an example of a transected cleavage and it is thought that it developed late in the development of the fold and may be a response to the tightening of the Skarvemellen Anticline during limb rotation.

There is no clear increase in the degree of deformation towards the thrust plane and in contrast to the Kishorn Nappe no strong mylonitic zone is present. Nickelsen (1967) suggested that the Mellene Thrust cuts across both limbs of the fold. This suggests that the Thrust is unrelated to the folding and it may account for the poor agreement between the intensity of

the deformation and the position of the thrust plane.

It is thought that the Skarvemellen Anticline developed by processes similar to that of the Lochalsh Syncline, in which flexural slip folding was followed by limb rotation and tightening of the fold. The development of the thrust plane may be unrelated to this particular fold. In the case of the Skarvemellen Anticline strong extension parallel to the fold axis has produced a complex strain pattern which cannot be modelled accurately. The finite strain results illustrate the importance of the fold's propagation rate on the final geometry and finite strain of the fold nappe.

Section 8E The Origin of Recumbent Fold Nappes

Having established the possible mechanisms for the recumbent folds studied a general analysis of the processes which operated during the development of the folds will be made. This analysis will be based, mainly, on the study of the Lochalsh Syncline.

The deformation histories proposed for the Kishorn and Mellene Nappes confirm the descriptive models of Heim (1922) and Willis (1891). It is clear that the folds develop first, grow and then form the nucleation site for the thrust plane. The overturned limb of both the Lochalsh Syncline and the Skarvemellen Anticline are strongly deformed. In the case of the Kishorn Nappe it can be shown that a portion of the fold's development predates the deformation of the overturned limb and a similar history can be inferred for the Mellene Nappe.

Willis (1891) differentiated between break thrusts and stretch thrusts and he illustrated how thrusting may occur at different stages during the development of the associated folds. From the contrast between

the deformation histories of the Kishorn and Mellene Nappes, established in this thesis, it is thought that the rock type involved controls the style of deformation and the relationship of the thrusting to the folding.

From the study of the finite strain distribution around the Lochalsh Syncline it is possible to define the processes which affected the overturned limbs of recumbent fold nappes. In previous published work these processes are illdefined and they were reviewed in chapter 1.. The model proposed for the development of the bedding parallel fabric on the overturned limb of the Lochalsh Syncline is one of limb rotation during simple shear. It is based on a suggestion by Lister and Williams (1979) and it is the only model which can explain the orientation and strain ratios related to the bedding parallel fabric. The thin zone of intense deformation close to the overlying thrust planes may be explained by a natural strain gradient. It is thought that this gradient marks the centre of a shear zone and when the fabric became so intense that the bedding was destroyed then, penetrative simple shear became the dominant deformation mechanism. This shear zone may develop as a natural consequence of the deformation within the thrust sheet or be due to the climb of the initial thrust or shear zone which gave rise to the development of the fold.(Coward and Potts in press a). These two processes cannot be distinguished by field evidence. The development of the shear zone in the overturned limb of the Lochalsh Syncline suggests that the dominant deformation mechanism on the overturned limb of recumbent fold nappes is simple shear.

Large finite strains associates with thrust faults have been described by many workers, for example Milton and Williams (1981), Ramsay (1981) and Fischer

and Coward (1982). It is suggested that these strains are due mainly to simple shear deformation. Elliott (1976a) discussed the role of folding in the development of thrust planes. He envisaged the folds as a method of producing deformed rock which permitted the development of thrust planes by ductile fracturing. In common with MacClintock and Argon (1966) he suggested that ductile fracturing develops by the coalesence of flaws. Lister and Williams (1979) suggest that at high strains, sliding on the fabric planes is a common mechanism of deformation within mylonite zones. It is suggested that the thrust plane related to the Lochalsh Syncline developed by sliding on the mylonite fabric and one particular plane became dominant. This is a case of ductile fracturing.

The model of Rich (1934) for the development of folds associated with thrusting, which was extended by Boyer and Elliott (1982) cannot be applied to recumbent fold nappes as overturned fold limbs are not produced by this type of model. The model proposed by Berger and Johnson (1980) for the production of overturned anticlines in the hanging walls of thrusts does not produce corresponding folds in the footwall of the thrust.

Coward and Potts (in press a) have shown that synclines generally occur in the footwalls of thrusts and they suggest that the development of the thrust is associated with these recumbent folds. They present a model involving stick on a thrust flat leading to the development of an anticline-syncline pair which is cut by a thrust plane in the common overturned limb of the fold pair. This generates an overturned asymmetric anticline in the hanging wall of the thrust and a syncline in the footwall. It was emphasised that the association of folds and thrusts is one of the common features of the Moine Thrust Zone and that rock type

controls only the observed fold mechanism.

The model of Coward and Potts (in press a) is almost identical to that proposed by Heim (1922) and Willis (1891).but their model provides a mechanism by which the fold is nucleated, namely "stick on the flat". The model must be extended as it can be shown that in the Kishorn Nappe several different processes acted at different times during the development of the recumbent fold nappe. It is necessary in a general model of recumbent folding to account for these changes in mechanism. Within the Kishorn Nappe four processes contributed to the development of this recumbent fold nappe.

(a) Following the model of Coward and Potts (in press a) propagation of the Moine Thrust (or Tarskavaig Thrust) was retarded within the Lewisian Gneiss.

(b) Partial development of the Lochalsh Syncline by flexural slip folding. The angular fold profile suggests that this stage was characterised by chevron folding (Ramsay 1974).

(c) Development of the bedding parallel fabric by rotation of the overturned limb during simple shear.

(d) Continued deformation of the overturned limb by simple shear leading to the development of a strong mylonitic fabric and ultimately, the production of a thrust plane by ductile fracturing.

It is not understood why the propagation of the thrust or shear zone ceased as no field evidence is available.

Some suggestions have been made by Coward and Potts (in press a) and the most probable of these is change in rock type within the Lewisian Gneiss.

Ramsay (1974) has shown how, after an initial threshold is overcome, chevron folding proceeds rapidly until interlimb angles of approximately 110 degrees are achieved. At this point the rate of fold growth declines. It is thought that chevron folding developed due to the highly anisotropic nature of the Sleat Group (Cobbold et al 1971) and that following the stick of the Moine Thrust the rocks preferred to fold rather than thicken homogeneously by layer parallel shortening. An initial buckle, produced by the sticking, overcame the initial threshold for chevron folding and as a result the Lochalsh Syncline was able to develop. At interlimb angles of approximately 110 degrees deformation of the Lochalsh Syncline appears to have changed from chevron folding to the development of the bedding parallel fabric. This process continued by intensification of the fabric until thrusting occurred. The main change in the dominant deformation mechanisms appears to have occurred when the process of chevron folding was slowing down.

Elliott (1976 b) showed how deformation of a thrust sheet may be related to its wedge shaped profile and that gravity is the main driving force. This suggests that a constraint is placed on the thrust sheet regarding the displacement rate required by the mountain belt. It is thought that when the propagation rate of the thrust plane decreases the rocks above must deform in order to maintain the displacement rate at the trailing edge of the thrust sheet. In the case of the Lochalsh Syncline initial low amplitude buckling was followed by chevron folding. When the rate of this folding decreased (Ramsay 1974) the deformation mechanism changed, so as to maintain the required displacement rate. Eventually

ductile deformation, mainly by simple shear, was replaced by thrusting on a clean cut thrust plane. Subsequent movements have produced the breccias seen on the fault planes particularily at Ard Hill.

Coward and Potts (in press a) have shown how different rock types within the Moine Thrust Zone develop folds by different mechanisms in response to a common process, that of stick on the flat. Using information obtained principally from the Moine Thrust Zone, the flow chart shown in Figure 8.E.1. was constructed to illustrate how the change in deformation mechanisms, associated with recumbent folding,are preceded by a decrease in the rate of the dominant process, and how these processes depend on the rock type.

The above analysis suggests that the ability of a thrust sheet to fold is an important control on the final geometry of the thrust belt. Douglas (1950) suggested that, "long thrusts are strong thrusts". Elliott (1976a) showed that a relationship exists between the outcrop length of a thrust and its maximum displacement, see Figure 8.E.2.. If we consider this in terms of the lateral propagation of the fold complex, a long thrust requires successful propagation of the initial fold, for example the Lochalsh Syncline and the overlying thrust plane. Limited propagation results in short thrusts with small displacements, for example the Mellene Nappe. Constraints on lateral propagation may be indicated by non-cylindrical folds and an extension lineation parallel to the fold axis. Thus areas of restricted propagation may result in many small nappes with small displacements on the underlying faults. In contrast, in areas where the fold complex has successfully propagated there will be a smaller number of larger nappes with large displacements on each fault. The two systems will produce the same total displacement and this will be constrained by the

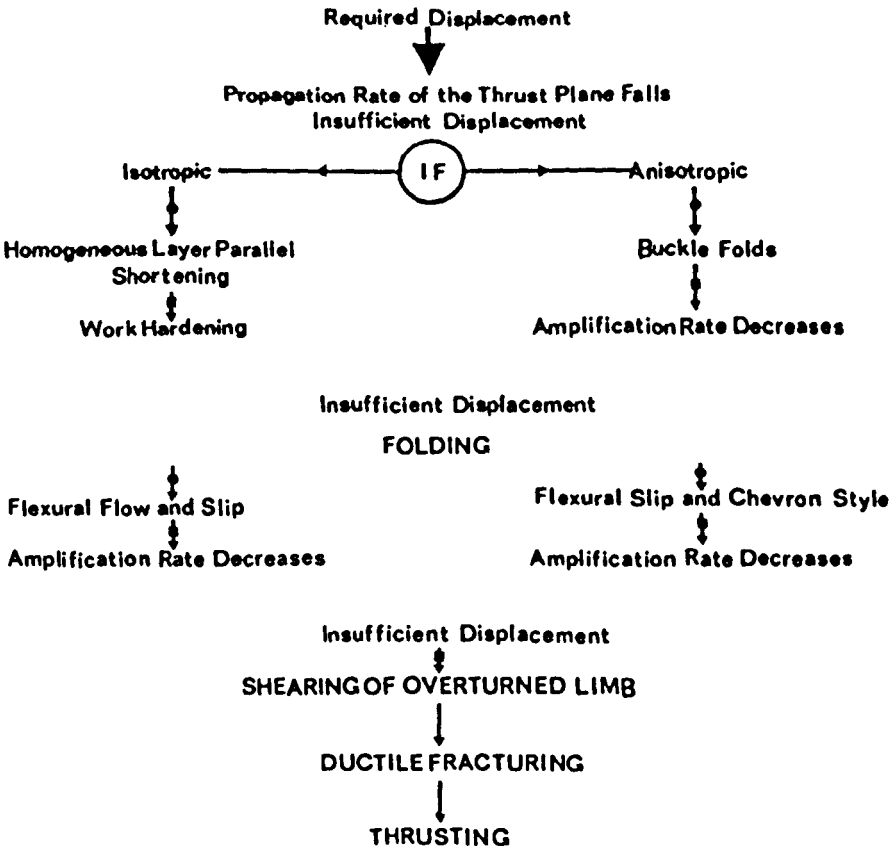

Figure 8.E.1. A flow chart which describes the development of recumbent fold nappes in rocks of the Moine Thrust Zone. The anisotropic case is based on this study of the Lochalsh Syncline where initial buckle folding (not seen) is replaced by chevron folding. When the rate of fold amplification declines then, simple shear deformation becomes dominant leading ultimately to the development of a thrust fault. The isotropic case describes the events in the folds of the Pipe Rock Member described by Fischer and Coward (1982) and Coward and Potts (in press a). The sequence of structures has been expanded to take into account the changes in deformation rate which may be inferred by analogy with the Lochalsh Syncline. ● = deformation mechanism, ■ = restraint on that deformation mechanism.

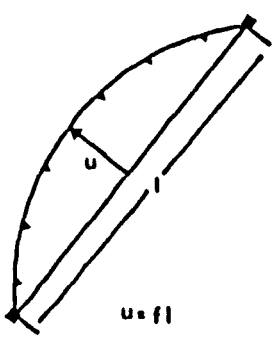

Figure 8.E.2. The maximum displacement of a thrust (u) is proportional to its map length (l). Elliott (1976a) has shown that f = 0.07.

geometry of the thrust belt as a whole.

Chapter 9 Conclusions

1. The Lochalsh Syncline forms the structurally highest fold in a series of folds within the Kishorn Nappe. The fold axis trends northeast-southwest and plunges at less than ten degrees to the northeast. Along the axis of the fold the profile changes across compartmental faults.

2. The Ord Window lies entirely within the Kishorn Nappe. The folding and thrusting associated with the Ord Window suggests that thrusts are intimately associated with the development of recumbent folds and that the thrusts formed as part of a Foreland propagating sequence.

3. Within the Kishorn Nappe three cleavages can be recognised. The axial planar cleavage is restricted to the hinge of the Lochalsh Syncline. The bedding parallel fabric is restricted to the overturned limb of the Loch Lochalsh Syncline. The transverse cleavage postdates the development of the Lochalsh Syncline, the axial planar cleavage and the bedding parallel fabric.

4.The Balmacara Nappe forms part of the overturned limb of the Lochalsh Syncline.

5. The Lochalsh Syncline developed as a footwall syncline to the Moine Thrust. The slickensides common on bedding indicate that a portion of the fold development was by flexural slip processes.

6. The absence of 1M muscovite and the presence of 2M muscovite polymorphs suggests that the Kishorn Nappe was developed under greenschist facies metamorphism.

7. Finite strain studies on Lochalsh indicate that the bedding parallel fabric may contain a component of extension parallel to the fold axis.

8. The finite strain around a minor fold related to the Ord Syncline indicates that the fold developed by flexural slip with movement on the bedding surfaces. Also that compartmental faults are important in the development of recumbent fold structures.

9. The minor folds in the core of the Lochalsh Syncline represent accommodation structures as does the axial planar cleavage. The out-of-syncline thrust repesents such a structure and developed as the fold tightened.

10. The Applecross Formation around the Eishort Anticline possess two components of magnetization, a syn-sedimentary Torridonian direction and a reversed Tertiary thermo-chemical overprint. This overprint is only present in sites which possesed the correct range of blocking temperatures.

11. The Torridonian component may be restored to its correct position by rigid body rotation of the bedding about the strike direction. No correction is necessary for finite strain and therefore it is thought that the Eishort Anticline developed by flexural slip processes with movement on the bedding surfaces.

12. The preservation of Torridonian directions during folding precludes grain boundary sliding as a significant deformation mechanism. In two sites a remagnetisation may have been produced by recrystallization.

13. Measurement of the anisotropy of magnetic susceptibility show that the Eishort Anticline developed without internal deformation.

14. The bedding parallel fabric is present throughout the overturned limb of the Lochalsh Syncline and the only non-sedimentary fabric developed on the correct way up limb of the fold is the transverse cleavage.

15. In general the axes of finite strain and magnetic susceptibility coincide. The measurments of magnetic anisotropy can be calibrated for finite strain and be used as a strain estimate. A separate calibration is required for each rock type studied.

16. The calibrated measurements show that, on the inverted limb of the Lochalsh Syncline the finite strain related to the bedding parallel fabric increases in intensity towards the east.

17. The Skarvemellen Anticline formed in the hanging wall of the Mellene Thrust. There are two cleavages related to the development of the fold. An early bedding parallel fabric which is marked by extension parallel to the axis of the fold. The second cleavage is not truly axial planar and the Skarvemellen Anticline may be a transected fold.

18. The presence of 2M muscovites and the absence of 1M muscovites indicates that the Mellene Nappe developed under greenschist facies metamorphism.

19. From measurment of the finite strain on the inverted limb of the Skarvemellen Anticline it is possible to propose a strain path which indicates the the development of the bedding parallel fabric is a two stage process. The strain related to the bedding parallel fabric are overprinted by those of the axial planar cleavage.

20. The proposed strain path is supported by measurements of the anisotropy of magnetic susceptibility, though, in this instance the calibration is poor.

21. A strain path may be proposed for the transverse cleavage which overprints a sedimentary fabric on the normal limb of the Lochalsh Syncline. Occasionally the transverse cleavage overprints the bedding parallel fabric.

22. The intensity of the strain suffered by a particular site within the Skarvemellen Anticline is related to the position of the site within the fold profile. The strain distribution may be modelled in terms of rotation and thinning of the layers during simple shear. However, a component of strain in present which records extension parallel to the axis of the fold.

23. The axial planar cleavage within the Skarvemellen Anticline possibly arose to relieve the space problem in the hinge of the fold.

24. Removal of the effects of the bedding parallel fabric from the Lochalsh Syncline indicates that before the development of the fabric the fold had an interlimb angle of 90^{o}-120^{o}. This is the point at which the rate of growth of chevron folds declines and it is thought that the transition from chevron folding to limb rotation is due to this decrease. Thus, each change in mechanism may be related to the decline of the current deformation mechanism. Elliott (1976a) suggested that deformation within a thrust belt is related to its wedge shaped profile.and this will place constraints on the displacement and displacement rate at the trailing edge of the thrust belt. Therefore a model may be suggested for the development of recumbent fold nappes. As the thrust plane propagates along the flat, displacement of the hanging wall may occur. If the thrust propagation rate is insufficient to maintain the displacement rate at the trailing edge of the thrust sheet the sheet must deform. When propagation is prevented (stick on the flat) the rocks fold, in this case recumbent folds are produced during a multistage process. The changes occur to maintain the displacement rate when the rate of the current process declines. The style of deformation in the early stages of fold development is controlled by the rock type. In general this leads to increased deformation of the inverted limb of the fold structure and ultimately to the failure of this limb by the development of a thrust.

25. The descriptive models of Heim (1922) and Willis (1891) are essentially correct and from the study of the Lochalsh Syncline it is possible to suggest that simple shear is the dominant style of deformation which produces the highly deformed inverted limbs of recumbent fold structures.

26. Where the development of a thrust is related to recumbent folding the outcrop length of the thrust plane will be controlled by the lateral propagation of the fold complex. When the folds were able to propagate with relative ease long thusts with large displacements are seen. Where this propagation is restricted shorter thrusts are produced and many more thrusts are necessary to produce the total displacement required by the thrust belt. The study of the Skarvemellen Anticline suggests that poor propagation of the fold complex results in highly non-cylindrical folds with marked extension parallel to the fold axis.

References

Addison, F.J., 1981. Problems of Sample Shape When Using a Digico Anisotropy Delineator. Geophy. J.R. ast. Soc., 65:277.

Bailey, E.B., 1939. Caledonian Tectonics and Metamorphism in Skye. Bulletin of the Geological Survey of Great Britain No. 2, 46-62.

1948. The Structural History of Scotland. International Geological Congress. Report of 18th Session, G.T. Brit, 1948, 230-254. Published 1950.

1955. Moine Tectonics and Metamorphism in Skye. Transactions of the Edinburgh Geological Society, 16:93-166.

Barber, A.J., 1965. History of the Moine Thrust Zo ?, Locharron and Lochalsh. Proc. Geol. Assoc., 76:215-242.

1969. Geology of the Country Around Dornie Wester Ross. Unpublished PhD Thesis, University of London (Imperial College).

Bathal, R.S., 1971. Magnetic Anisotropy in Rocks. Earth Science Rev., 7:227-253.

Beach, A., 1975. The Geometry of En-echelon Vein Arrays. Tectonophysics, 28:245-263.

Berger, P. and Johnson, A.M., 1980. First Order Analysis of Deformation of a Thrust Sheet Moving Over a Ramp. Tectonophysics, 70:T9-T24 .

Bertrand, M., 1884. Rapports de Structure des Alpes de Glaris et du Bassin Houiller du Nord. Bull. Soc. geol. France, ser. 3,12:318-330.

Biot, M.A., 1964. Theory of Internal Buckling of a Confined Multilayer Structure. Geol. Soc. Am Bull., 75:563-568.

Biot, M.A., 1965. Theory of Viscous Buckling and Gravity Instability of Multilayers With Large Deformations. Geol. Soc. Am Bull., 76:371-378.

Bjørlykke, K.O., 1905. Den centrale Norges fjeldsbygning: Valdres, Hemsedal, Laerdal. Nor. Geol. Unders., 39:461-542.

Bjørlykke, K., 1965. The Geochemistry and Mineralogy of Some Shales From the Oslo Region. Nor. Geol. Tidsskr. 45,435-56.

Black, G.P.and Welsh, W., 1961. The Torridonian Succession of the Isle of Rhum. Geological Magezine, 98:265-276.

Borradaile, G.J., 1978. Transected Folds: a Study Illustrated With Examples From Canada and Scotland. Geol. Soc. Am Bull., 89:481-493.

Borradaile, G.J. and Tarling, D.H., 1981. The Magnetic Anisotropy of Weakly Deformed Rocks. Tectonophysics, 77: 151-168.

Boyer, S.E. and Elliott, D., 1982. Thrust Systems. Bull. Am. Assoc. Petrol. Geol.,67.

Bryhni,I and Brastad, K, 1980. Caledonian Regional Meta -morphism in Norway. J. Geol. Soc. Lond., 137:251-259.

Bucher,W.H., 1933. The Deformation of the Earths Crust. Princeton University Press. Princeton.

Busk, H.G., 1929. Earth Flexures. Cambridge University Press, London.

Chamalaun, F.H., 1964. Origin of the Secondary Magnetiz -ation of the Old Red Sandstones of the Anglo-Welsh Cuvette. J. Geophys. Res., 69:4327-37.

Chamalaun, F.H. and Creer, K.M. 1964. Thermal demagnetization Studies of the Old Red Sandstones of the Anglo-Welsh Cuvette. J. Geophys. Res., 69:1607-16.

Chapman, T.J., Milton, N.J. and Williams, G.D., 1979. Shape Fabric Variations in Deformed Conglomerates of the Base of the Lakesfjord Nappe, Norway. J. geol. Soc. London, 136:683-689.

Cheeney, R.F., 1965. The Tectonic and Metamorphic History of the Moine Thrust Zone in Sleat Isle of Skye. Unpublished PhD Thesis University of London (Imperial College).

Cheeney, R.F. and Matthews, D.W., 1965. The Structural Evolution of the Tarskavaig and Moine Nappes in Skye. Scott. J. Geol. 1:256-281.

Cobbold, P.R., 1977. Compatibility Equations and the Integration of Finite Strains in Two Dimensions. Tectonophysics, 39:T1-T6.

1979. Removal of Finite Deformations Using Strain Trajectories. J. Struct. Geol., 1:67-72.

1980. Compatibility of Two-Dimensional Strains and Rotations along Strain Trajectories. J. Struct. Geol., 2:379-382.

Cobbold, J.W., Cosgrove, J.W. and Summers, J.M., 1971. Develpment of Internal Structures in Deformed Anisotropic Rocks. Tectonophysics, 12:23-53.

Cobbold, P.R. and Quinquis, H., 1980. Development of Sheath Folds in Shear Regimes. J. Struct. Geol. 2, 119-126.

Collett, L.W., 1972. The Structure of the Alps. Arnold & Co., London.

Collinson, D.W., 1966. Magnetic Properties of the Taiguati Formation. Geophys. J. Roy. Astron. Soc., 11:337-47.

Collinson, D.W., Creer, K.M. and Runcorn, S.K., 1967. Methods in Palaeomagnetism (Eds) Developments in Solid Earth Geophysics. No. 3. Elsevier, Amsterdam.

Cooper, M.A. and Nuttall, G., 1979. GODPP a Geological Plotting Package. Computer and Geosciences, 6:17-25.

Coward, M.P., 1980. Shear Zones in the Precambrian Crust of Southern Africa. J. Struct. Geol., 2:19-27.

Coward, M.P. and Kim, J.H., 1981. In McClay, K. R. and Price ,N.J. (Eds), Thrust and Nappe Tectonics. Geological Society of London Special Publication No. 9.

Coward, M.P. and Potts, G.J., in press. Fold Nappes, Examples From the Moine Thrust Zone. Geol. J. Special Issue "Basement and Cover Relationships" Related to Uppsala Caledonide Symposium 1981.

in press b. Complex Strain Patterns Developed at the Frontal and Lateral Tips to Shear Zones and Thrust Zones. J. Struct. Geol. Special Issue "Interpretation of Strain Patterns" Rennes 1982.

Coward, M.P. and Whalley, J.S., 1979. Texture and Fabric Studies Across the Kishorn Nappe, Near Kyle of Lochalsh, Western Scotland. J. Struct. Geol., 1:259-273.

Creer, K.M., 1962. The Natural Remanent Magnetizations of the Old Red Sandstones of the Anglo-Welsh Cuvette. J. Geophys. Res., 67:1357-69.

Dahlstrom, C.D.A., 1969. Balanced Cross Sections. Can. J. Earth Sci., 6:743-757.

1970. Structural Geology in the Eastern Margin of the Canadian Rocky Mountains. Bull. Can. Pet. Geol., 18:332-406.

Dayan, H., 1981. Deformation Studies of the Folded Mylonites of the Moine Thrust, Eriboll District, Northwest Scotland. Unpublished PhD Thesis University of Leeds.

Dodson, M.H. and McClelland-Brown E.A., 1980 Magnetic Blocking Temperatures of Single-Domain Grains During Slow Cooling. J. Geophys. Res., 85:2625-2637.

Donath,aF.A. and Parker, R.B., 1964. Folds and Folding Geol. Soc. Am. Bull., 75:45-62.

Douglas, R.J.W., 1950. Callum Creek, Langford Creek, and Gap Map Areas, Alberta. Geol. Surv. Can. Mem. 225: 124pp.

Dubey, A.K. and Cobbold, P.R., 1977. Non-cylindrical Flexural Slip Folds in Nature and Experiment. Tectonophysics, 38:223-239.

Duff, B., 1978.Palaeomagentic and Rock Magnetic Studies of Lower Palaeozoic Rocks on Jersey and the Adjacent Regions of the Armorican Massif. Unpublished PhD Thesis University of Leeds.

Dunnet, D., 1969. A Technique of Finite Strain Analysis Using Elliptical Particles. Tectonophysics, 7:117-136.

Dunnet, D. and Siddans, A.W.B., 1971. Non-Random Sedimentary Fabrics and Their Modification by Strain. Tectonophysics, 12:307-325.

Elliott, D. 1976. The Energy Balance and Deformation Mechanisms of Thrust Sheets. Philos. Trans. R. Soc. London, Ser. A, 283:289-312.

Elliott, D. 1976b. The Motions of Thrust Sheets. J.Geophys. Res., 81:949-963.

Elliott, D., 1977. Some Aspects of the Geometry and Mechanics of Thrust Belts. Part 1. 8th Annual Seminar Can. Soc. Petrol. Geol. Univ. Calgary.

Elliott, D. and Johnson, M.R.W., 1980. Stuctural Evolution in the Northern Part of the Moine Thrust Zone, Trans. R. Soc. Edinb., 71:69-96.

Englund, J.O., 1973. Geochemistry and Mineralogy of Pelitic Rocks From the Hedmark Group and Cambro-Ordovician Sequence, Southern Norway. Nor. geol. Unders. 286:1-60.

Fischer, M.W. and Coward, M.P., 1982. Strains and Folds Within Thrust Sheets: An Analysis of the Heilam Sheet, Northwest Scotland, Tectonophysics, 88:291-312.

Fisher, R.A., 1953. Dispersion on a Sphere. Proc. Roy. Soc. London, Ser. A, 217:295-305.

Fleuty, M.J., 1964. The Description of Folds. Proceedings of the Geological Association, 75:461-492.

Flinn, D., 1962. On Folding During Three-Dimensional Progressive Deformation. Geol. Soc. Lond. Quat. J., 118:385-433.

Foss, C.A., 1981. Graphical Methods for Rapid Vector Analysis of Demagnetization Data. Geophys. J.R. ast.Soc. 65:217-221.

Gay, N.C., 1968a. The Motion of Rigid Particles Embedded in a Viscous Fluid During Pure Shear Deformation of the Fluid. Tectonophysics, 5:81-88

1968b. Pure Shear and Simple Shear Deformation in Inhomogeneous Viscous Fluids. The Determination of the Total Finite Strain in a Rock From Objects Such as Deformed Pebbles. Tectonophysics, 5:295-302.

Goldschmidt, W.M., 1916a. Geologisch-Petrographische Studien im Hochegebirge des Suclichen Norwegens (IV). Ubersicht der Cruptirgestine im Kaledonischen Gebirge Zwischen Stavanger and Trondheim. Vid. Selsk. Skr. I, Math. Nat. Kl. No.2, 140pp.

1916b. Konglomeraterne Inden Hoif-jledskvartsen. Nor. Geol. Unders., 77:61pp.

Graham, J.W., 1949. The Stability and Significance of Magnetism in Sedimentary Rocks. J. Geophys. Res., 54: 131-67.

1954. Magnetic Susceptibility Anisotropy, on an Unexploited Petrofabric Element. Geol. Soc. Am. Bull. 65:1257-1258.

1966. Significance of Magnetic Anisotropy in Appalacian Sedimentary Rocks. In : Steinhart, J.S. and Smith, T.J. (Eds). The Earth Beneath the Continents, (p627-648) Geophys. Monogr. 10, Amer. geophys. Union, Washington D.C..

Graham, R.H., 1978. Quantitative Deformation Studies in the Permian Rocks of the Alpes - Marritimes. B.R.G.M. 219-238.

Hallam, A. and Swett, K., 1966. Trace Fossils From the Lower Cambrian Pipe Rock of the Northwest Highlands. Scott. J. Geol., 2:101-106.

Harris, L.D., 1970. Details of Thin Skinned Tectonics in Part of Valley and Ridge and Cumberland Plateau Provinces of the Southern Appalacians. In : Fischer,G.W., Pettijohn, F.J., Reed (Jr),J.C. and Weaver, K.N. (Eds). Studies of Appalacian Geology : Central and Southern. Interscience New York, pp161-173.

Harris, L.D., 1977. Characteristics of Thin Skinned Style of Deformation in the Southern Appalacians, and Potential Hydrocarbon Traps. U.S. Geol. Surv. Profess. Pap., 1018, 40pp.

Haug, E., 1900. Les Geosyclinaux et les Aires Continentales. Contributions a l'etude des Transgressions et des Regressions marine. Bull. Soc. Geol. Fr., Sev., 28:617-711.

Heim, A., 1878. Untersuchungen Uber den Mechanisms der Gebirgsbilding. Basel.

1922. Geologie der Schweiz Leipzig, 1919-1922.

Heritsch, F., 1929. The Nappe Theory in the Alps. Methuen & Co., London. (Translated by Boswell, P.G.H.).

Hossack, J.R., 1968. Pebble Deformation and Thrusting in the Bygdin Area, Southern Norway. Tectonophysics, 5:315-39.

1978. The Correction of Stratigraphic Sections for Tectonic Finite Strain in the Bygdin area, Norway. J . geol. Soc. Lond. 135:229-241.

1980. In : Park. R.G., A.G.M. Tectonic Studies Group. Keele. J. Struct. Geol. 1981, 3:188.

Hossack, J.R., Nickelsen, R.P. and Garton, M., 1981. The Geological Section From the Foreland up to the Jotun Sheet in the Valdres Area, Southern Norway. Terra. Cog. 1:52.

Hubbert, M.K. and Rubey, W.W., 1959. Role of Fluid Pressure in the Mechanics of Over-Thrust Faulting. Bull. Geol. Soc. Am., 70:115-206.

Hrouda, F., 1982. Magnetic Anisotropy of Rocks and Its Application in Geology and Geophysics. Geophysical Surveys, 5:37-82.

Hsu, K.J., 1969. Role of Cohesive Strength in the Mechanics of Overthrust Faulting and of Landsliding. Geol. Soc. Amer. Bull., 80:927-952.

Irving, E., 1957. The Origin of the Palaeomagnetism of the Torridonian Sandstone Series of Northwest Scotland. Phil. Trans. Roy. Soc. London. Ser. A, 250:100-10.

Irving, E. and Runcorn, S.K., 1957. Analysis of the Palaeomagnetisation of the Torridonian Sandstone Series of Northwest Scotland. Phil. Trans. Roy. Soc. London. Ser. A, 250:83-99.

Jelinek, V., 1981. Characterization of the Magnetic Fabric of Rocks. Tectonophysics, 79:533-557.

Johnson, M.R.W., 1955a. Tectonics and Metamorphism of Pre-Cambrian Rocks in Lochcarron and the Coulin Forest. Unpublished PhD Thesis University of London (Imperial College).

1955b. The Metamorphic History of the Precambrian Rocks of Lochcarron Wester Ross. Advanc. Sci. Lond., 12; 575-6.

1956. Conjugate Fold Systems in the Moine Thrust Zone in the Lochcarron and Coulin Forest Areas of Wester Ross. Geol. Mag., 93:345-350.

1957 The Structural Geology of the Moine Thrust Zone in Coulin Forest Wester Ross. Quart. J. Geol. Soc. Lond., 112:241-270.

1960a The Structural History of the Moine Thrust Zone at Lochcarron, Wester Ross. Trans. Roy. Soc. Edinb., 64: 139-168.

1960b Linear Structures in the Moine Thrust Belt of Northwest Scotland and Their Relation to the Caledonian Orogenesis. Int. Geol. Cong. Norden, Pt. XIX: 83-95.

Kanungo, D., 1956. The Structural Geology of the Torridonian, Lewisian and Moinian Rocks of the Area Between Plockton and the Kyle of Lochalsh in Wester Ross, Scotland. Unpublished PhD Thesis, University of London (Imperial College).

Kennedy, W.Q., 1954. The Tectonics of the Morar Anticline and the Problem of the Northwest Caledonian Front. Q. J . geol. Soc. Lond. 110:357-390.

Kligfield, R., Lowrie, W. and Dalziel, I.W.D., 199. Magnetic Susceptibility in the Sudbury Basin, Ontario. Tectonophysics, 24:115-131.

Kligfield, R., Pfiffner, A.and Lowrie, W., 1979. Strain and Magnetic Susceptibility Anisotropy of Fe-Rich Oolitic Limestones in Folds From the Central Swiss Alps. Trans. Am. Geophys. Union, 60:571(Abstract).

Kligfield, R., Owens, W.H. and Lowrie, W., 1981. Magnetic Susceptibility Anisotropy, Strain and Progressive Deformation in Permian Sediments From the Marritime Alps (France). Earth Planet Sci. Lett., 5:181-189.

Kligfield, R., Lowrie, W. and Pfiffner, A., 1982. Magnetic Properties of Deformed Oolite Limestones From the Swiss Alps : the Correlation of Magnetic Anisotropy and Strain. Eclogae geol. Helv., 75:127-157.

Kneen, S.J., 1976. The Relationship Between the Magnetic and Strain Fabrics in Some Haematite Bearing Slates. Earth and Planet. Sci. Lett., 31:413-416.

Knipe, R.J. and White, S.H., 1979. Deformation in Low Grade Shear Zones in the Old Red Sandstone, S.W. Wales. J. Struct. Geol., 1:53-66.

Kubler, B., 1968. Evaluation Quantitative du Metamorphisme par la Cristallinite de l'Illite. Bull. Centre. Rech. Pau. S.N.P.A., 7:385-397.

Kulling, O., 1961. On the Age and Tectonic Position of the Valdres Sparagmite. Geol. Foren. Stockholm Forhandl., 83:210-214.

Lisle, R.J., 1977a. Clatic Grain Shape and Orientation in Relation to Cleavage From the Aberystwyth Grits, Wales. Tectonphysics, 39:307-325.

1977b. Estimation of Tectonic Strain Ratio From the Mean Shape of Deformed Elliptical Markers. Geologie en Mijnbouw, 56:140-144.

1980. In Park., R.G., A.G.M., Tectonic Studies Group, Keele. J. Struct. Geol. 1981, 3:189.

Lister, G.S., 1979. Fabric Development in Shear Zones : Theoretical Controls and Observed Phenomena. J. Struct. Geol., 1:283-297.

Lloyd, G.E. and Ferguson, C.C., 1981. Boudinage Structure : Some New Interpretations Based on Elastic-Plastic Finite Element Simulations. J. Struct. Geol., 3:117-128.

Loeschke,J., 1967a. Zur Statigraphie und Petrographie des Valdre-Sparagmites und der Mellsenn-Gruppe bei Mellane/Valdres (Sud-Norwegen). Nor. Geol. Unders., 243:5-66.

1967b. Zur Petrographie des Valdres Sparagmites Zwischen Bitihorn und Langsuen/Valdres (Sud-Norwegen). Nor. Geol. Unders., 243:67-98.

Loeschke, J. and Nickelsen, R.P., 1968. On the Age and Tectonic Position of Valdres Sparagmite in Slidre (Southern Norway). N. Jb. Palaont. Abh., 131:337-367.

Lugeon, M., 1901. Les Grandes Nappes de Recouvrement des Alpes du Chablais et de Suise. Bull. Soc. geol. France, Ser. 4, I;723-823.

1903. Les Nappes de Recouvrement de In Tatra et l'origine des Klippes des Carpathes. Bull. Lab. Geol. etc., Univ Lausanne, W:1-51.

McClay, J.R., 1981. What is a Thrust? What is a Nappe?. In McClay K.R. and Price, N.J., (Eds) Thrust and Nappe Tectonics. Geological Society of London Special Publication No 9.

McClay, K.R. and Coward, M.P., 1981. The Moine Thrust Zone. An Overview. In McClay, K.R. and Price, N.J. (Eds) Thrust and Nappe Tectonics. Geological Society of London Special Publication No 9.

McClelland, E.A., 1976. A Palaeomagnetic Study of the Torridonian Sandstone Rocks of the Torridon Hills. N.W. Scotland. Unpublished MSc Thesis. University of Leeds.

McClelland-Brown, E.A., 1980. Palaeomagnetic Studies in Thermal Aureoles. Unpublished PhD Thesis. University of Leeds.

Mac Clintock, F.A. and Argon, A.S., 1966. Mechanical Behaviour of Materials. Reading, Massachussetts: Addison-Wesley.

McElhinny, M.W., 1967. Statistics of a Spherical Distribution. In Collinson, D.W., Creer, K.M. and Runcorn, S.K. (Eds). Elsevier, Amsterdam, 313-21.

1973. Palaeomagnetism and Plate Tectonics. Cambridge University Press.

MacIntyre, D.B., 1954. The Moine Thrust - Its Discovery, Age and Tectonic Significance. Proc. Geol. Assoc. 65: 203-223.

McLeish, A.J., 1971. Strain Analysis of Deformed Pipe Rock in the Moine Thrust Zone, Northwest Scotland. Tectonophysics, 12:469-503.

March, A., 1932. Mathematische Theorie der Redelung nach der Korngestalt bei affiener Deformation. Z. Kristallogr., 81:285-297.

Matthews, D.W. and Cheeney, R.F., 1968. The Metamorphic Evolution of the Moine Nappe in Skye. Scott. J. Geol. 4:20-30.

May, F., 1959. The Structural Geology of Lewisian and Moinian Rocks in the Area Between Stromeferry and Attadale Wester Ross Scotland. Unpublished PhD Thesis. University of London (Imperial College).

Milton, N.J., 1980. Thrusts and Related Structures in the Scandanavian Caledonides. Unpublished PhD Thesis. University of Wales (Cardiff).

Milton, N.J. and Chapman, T.J., 1979. Superposition of Plane Strain on an Initial Sedimentary Fabric : an Example from Laksefjord North Norway. J. Struct. Geol. 1:309-315.

Milton, N.J. and Williams, G.D., 1981. In McClay, K.R. and Price, N.J. (Eds), Thrust and Nappe Tectonics. Geological Society of London Special Publications No 9.

Neel, L., 1955. Some Theoretical Aspects of Rock Magnetism. Phil. Mag. Suppl. Adv. Phys., 4:191-243.

Nickelsen, R.P., 1967. The Structure of Mellene and Heggerberg, Valdres. Nor. Geol. Unders. 243:99-121.

1974. Geology of the Røssjøkollan-Dokkvatn Area, Oppland. Geol. Unders. 314:53-100.

Nickelsen, R.P., Garton, M. and Hossack, J.R., 1981. Late Pre-Cambrian to Ordovician Sedimentology and Stratigraphical Correlation of the Valdres and Synnfjell Thrust Sheets in the Valdres Area, Central Southern Norway. Terra. Cog., 1:61.

Oertel, G., 1970. Deformation of a Slaty, Lapillartuff in the Lake District, England. Geol. Soc. Am. Bull., 81:1173-1188.

1978. The Development of Slaty Cleavage in Part of the French Alps - Discussion. Tectonophysics, 47:185-191.

Owens, W.H., 1974. Representation of Finite Strain State by Three-Axis Planar Diagrams. Bull. geol. Soc. Am., 85:307-310.

Owens, W.H., 1974b. Mathematical Model Studies on Factors Affecting the Magnetic Anisotropy of Deformed Rocks. Tectonophysics, 24:115-131.

Owens, W.H. and Bamford, D., 1976. Magnetic, Seismic and Other Anisotropic Properties of Rock Fabrics. Phil. Trans. R. Soc. Lond., (A) 283:55-68.

Park, J.K., 1970. Acid Leaching of Red Beds, and its Application to the Relative Stability of the Red and Black Magnetic Components. Can. J. Earth Sci., 7: 1086-92.

Peach, B.N., Horne, J., Gunn, W., Clough, C.T. and Hinxman, L.W., 1907. The Geological Structure of the Northwest Highlands of Scotland. Mem. Geol. Surv. G.B.

Peach, C.J. and Lisle, R.J., 1979. A Fortran IV Program for the Analysis of Tectonic Strain Using Deformed Elliptical Markers. Computers and Geosciences, 5:325-334.

Phillips, F.C., 1939. The Micro-Fabric of Some Members of the Tarskavaig-Moine Series. Geological Magazine, 76:229-240.

Platt, J.P. and Vissers, R.L.M., 1980. Extensional Structures in Anisotropic Rocks. J. Struct. Geol. 2:397-410.

Potts. G.J., 1982. Finite Strains Within Recumbent Folds of the Kishorn Nappe, Northwest Scotland. Tectonophysics, 88:313-319.

Powell, C. McA., 1974. Timing of Slaty Cleavage During Folding of Pre-Cambrian Rocks, Northwest Tasmainian : Bulletin of the Geological Society of America . 83: 2149-2158.

Ragan, D.M., 1970. Structural Geology - an Introduction to Geometrical Techniques. Wiley and Sons Ltd..

Ramberg, H., 1964. Selective Buckling of Composite Layers with Contrasted Rheological Properties, a Theory for Simultaneous Formation of Several Orders of Folds. Tectonophysics, 1:307-341.

Ramsay, J.G., 1960. The Deformation of Early Linear Structures in Areas of Repeated Folding, J. Geol., 68:75-93.

1962. The Geometry and Mechanics of Formation of Similar Folds. J. Geol., 70:309-327.

1967. Folding and Fracturing of Rocks. McGraw-Hill, New York.

1969. The Measurement of Strain and Displacement in Orogenic Belts. In : Time and Place in Orogeny. Kent, P.E., Satterthwaite, G.E. and Spencer, A.M., (Eds). Geological Society of London Special Publication No. 3.

1974. Development of Chevron Folds. Geol. Soc. Am. Bull., 85:1741-1754.

Ramsay, J.G., 1980. Shear Zone Geometry : a Review. J. Struct. Geol., 2:83-99.

Ramsay, J.G., 1981. Tectonics of the Helvetic Nappes. in McClay, K.R. and Price, N.J., (Eds). Thrust and Nappe Tectonics. Geological Society of London Special publication No. 9.

Ramsay, J.G. and Graham, R.H., 1970. Strain Variations in Shear Belts. Can. J. Earth Sci, 7:786-813.

Ramsay, J.G. and Wood, D.S., 1973. The geometric Effects of Volume Change During Deformation Processes. Tectonophysics, 16:263-277.

Rathore, J.S., 1979. Magnetic Susceptibility Anisotropy in the Cambrian Slate Belts of North Wales and Correlation With Strain. Tectonophysics, 24:115-136.

1980. The Magnetic Fabrics of Some Slates From the Borrowdale Volcanic Group in the English Lake District and Their Correlations With Strain. Tectonophysics, 53:83-97.

Read, H.H. and Watson, J., 1962. Introduction to Geology Vol. 1 : Principals. Macmillan.

Rich, J.L., 1934. Mechanics of Low Angle Overthrust Faulting as Illustrated by Cumberland Thrust Block, Virginia, Kentucky, and Tennessee. Am. Assoc. Pet. Geol. Bull., 18:1584-1596.

Richey, J.E., 1935. British Regional Geology. Scotland : The Tertiary Volcanic Districts. H.M.S.O..

van Roermund, H., Lister, G.S. and Williams, P.F., 1979. Progressive Development of Quartz Fabrics in a Shear Zone From Monte Mucrone, Sesia-Lanzo Sone, Italian Alps. J. Struct. Geol. 1:43-52.

Schwerdtner, W.M., 1977. Geometric Interpretation of Regional Strain Analyses . Tectonophysics, 39:515-31.

Shimamoto, T. and Ikeda, Y., 1976. A Simple Algebraic Method of Strain Estimation From Deformed Ellipsoidal Objects. 1. Basic Theory. Tectonphysics, 36:315-337.

Siddans, A.W.B., 1976. Deformed Rocks and Their Textures. Phil. Trans. R. Soc. Lond., Ser. A, 283: 43-54.

1977. The Development of Slaty Cleavage in a Part of the French Alps. Tectonophysics, 39:533-557.

1978. The Development of Slaty Cleavage in a Part of the French Alps - a reply. Tectonophysics, 47:185-191.

1979. Deformation, Metamorphism and Texture Development in Permian Mudstones of the Glarus Alps. Eclogae. geol. Helv., 72-73:601-621.

Smoluchowski, M.S., 1909. Some Remarks on the Mechanics of Overthrusts. Geol. Mag., 6:204-205.

Soper, N.J. and Barber, A.J., 1979. Proterozoic Folds on the Northwest Caledonian Foreland. Scott. J. Geol. 15:1-11.

Strand, T., 1938. Nordre Etnedal. Beskrivelse til det geologiske grandteigskart. Nor. Geol. Unders., 152:71pp.

1951. Slidre. Beskrivelse til det geologiske grandteigskart. Nor Geol. Unders., 180:54pp.

1954. Aurdal. Beskrivelse til det geologiske grandteigskart. Nor. geol. Unders., 185:71pp.

1960. The pre-Devonian Rocks and Structures in the Region of Caledonian Deformation. In Holtedahl, O. (Ed) Geology of Norway. Norges. Geol. Unders., 208:170-284.

1962. On the Age and Tectonic Position of the Valdres Sparagmite. Geol. Foren. Forhandl., 84:230-231.

Sanderson, D.J., Andrews, J.R., Phillips, W.E.A. and Hutton, D.H.W., 1980. Deformation Studies in the Irish Caledonides. J. geol. Soc. London, 137:289-302.

Strand, T., 1964. Otta-dekket og Valdres gruppen i strokene langs Boverdalen og Leirdarlen. Norges. geol. Unders, 228:280-288.

Stewart, A.D., 1966. On The Correlation of the Torridonian Between Rhum and Skye. Geol. May., 103:432-439.

1969. Torridonian Rocks of Scotland Reviewed. In Kay, M., (Ed) North Atlantic-Geology and Continetal Drift. 559-608. Mem. Am. Assoc. Pet. Geol., 12.

Stewart, A.D. and Irving, E., 1974. Palaeomagnetism of Pre-Cambrian Sedimentary Rocks From N.W. Scotland and the Apparent Polar Wander Paths of Laurentia. Geophys. J. R. astr. Soc., 37:51-72.

Sutton, J. and Watson, J., 1960. Sedimentary Structures in the Epidotic Grits of Skye. Geol. Mag., 97:106-22.

1964. Some Aspects of Torridonian Stratigraphy in Skye. Proc. Geol. Assoc. London, 75:251-89.

Swett, K., 1969. Interpretation of Depositional and Diagenetic History of Cambro-Ordovician Sucession of N.W. Scotland. In : North Atlantic Geology and Continetal Drift (edited by Kay, M.) Mem. Am. Ass. Pet. Geol. 12:630-646.

Turnell, H.B., 1982. Palaeomagnetism of Lower Palaeozoic Intrusions in the Scottish Highlands. Unpublished PhD Thesis. University of Leeds.

Urrutia-Fucugauchi, J., 1980. On the Relationship Between the Magnetic and Strain Fabric in Slates and Possible Effects of Consistent Instrumental Discrepancies. Tectonophysics, 69:715-723.

van der Voo, R. and Channell, J.E.T., 1980. Palaeomagnetism In Orogenic Belts. Rev. Geolphys. and Space phys., 18: 455-481

van der Voo, R. and Grubbs, K.L., 1976. Structural Deformation of the Idaho-Wyoming Overthrust Belt, as Determined by Triasic Palaeomagnetism. Tectonophysics, 33:321-336.

Voight, B., 1976. Editor, Machanics of Thrust Faults and Decollement. Benchmark Papers in Geology/32 Dowden, Hutchinson and Ross Inc. U.S.A..

White, S., 1976. The Effects of Strain on the Microstructures, Fabrics and Deformation Mechanisms in Quartzite. Phil. Trans. R. Soc, London Ser. A 283:69-86.

Wilkinson, P., Soper, N.J. and Bell, A.M., 1975. Skolithus Pipes as a Strain Marker in Mylonites. Tectonophysics, 28:143-157.

Williams, G.D., 1979. Rotation of Contemporary Folds into the X Direction During Overthrust Processes in Laksefjord, Finnmark. Tectonophysics, 48:29-40.

Willis, B., 1891. The Mechanics of Appalacian Structure. U.S. Geol. Survey 13th Ann Rept., 1891-1892.

Wilson, R.L., Hall, J.M. and Dagley, P., 1981. The British Tertiary Igneous Province : Palaeomagnetism of the Dyke Swarm Along the Sleat Coast of Skye. Geophys. J.R. ast. Soc, 68:317-324.

Wood, D.S., Oertel, G., Singh, J. and Bennett, H.F., 1976. Strain and Anisotropy in Rocks. Phil. Trans. R. Soc. Lond. Ser. (A)., 283:27-42.

Zijderveld, J.D.A., 1967. Thermal Demagnetization by the Continuous Method In Collinson, D.W., Creer, K.M. and Runcorn,S. (Eds) Methods in Palaeomagnetism. Developments in Solid Eearth Geophysics No.3 Elsevier.

Tectonophysics, 88 (1982) 313–319
Elsevier Scientific Publishing Company, Amsterdam—Printed in The Netherlands

FINITE STRAINS WITHIN RECUMBENT FOLDS OF THE KISHORN NAPPE, NORTHWEST SCOTLAND

G.J. POTTS

Department of Earth Sciences, University of Leeds, Leeds (England)

(Submitted August 15, 1981; revised version received December 19, 1981)

ABSTRACT

Potts, G.J., 1982. Finite strains within recumbent folds of the Kishorn nappe, northwest Scotland. In: G.D. Williams (Editor), Strain within Thrust Belts. *Tectonophysics*, 88: 313–319.

This study is based on the Torridonian and Cambro-Ordovician rocks of the Kishorn Nappe on the Isle of Skye and the adjacent mainland of Scotland. Grain shape fabric, Skolithos pipe shape analysis and palaeomagnetic techniques have been used to give an indication of the strain distribution and possible mechanisms involved in the generation of the recumbent folds within the Kishorn Nappe. Results indicate that recumbent folding has occurred without internal deformation.

INTRODUCTION

Fold nappes have been recognised in many major mountain belts after they were first defined by Haug (1900). However, only recently have systematic attempts been made to quantify and analyse finite strains within both thrust and fold nappes (Cloos, 1947; Hossack, 1968; Pfiffner, 1977, 1980; Milton, 1980). This short paper is concerned with the strains produced by the process of recumbent folding in the Caledonian age, Kishorn Nappe of northern Scotland.

STRUCTURE OF THE KISHORN NAPPE

The Kishorn Nappe is the structurally lowest nappe at the southern end of the Moine Thrust zone of Northwest Scotland (Fig. 1). The nappe is named after the underlying thrust plane, the Kishorn Thrust which is taken to be the sole thrust in this southern region. It formed during the northwesterly directed thrust movement of the Moine Thrust zone and contains several recumbent folds. The Kishorn Nappe has been described by several authors, Peach et al. (1907), Bailey (1939, 1955), Kanungo (1956), Barber (1965), Coward and Whalley (1979) Potts (in press). At the southern end of the Moine Thrust zone a thick lower Torridonian sequence of

0040-1951/82/0000–0000/$02.75

sandstones and shales occurs, the Sleat Group (Stewart, 1966). The sequence was deposited on an eroded basement of Lewisian Gneiss. The Sleat Group is overlain by Middle Torridonian red sandstone of the Applecross Formation above which is a Cambro-Ordovician sequence of basal quartzite, bioturbated quartzite (Pipe Rock Member) and a mixed group of dolomitic shales and limestone (Peach et al., 1907).

Recently Potts (in press) has presented a model for the evolution of the Kishorn Nappe which suggests that early in the history of the nappe a fold train of northwesterly verging recumbent folds developed. The structurally highest of these recumbent folds is the Lochalsh Syncline which has a gently northwesterly dipping normal limb, to the west of Kyle village (Fig. 1) and an overturned limb to the east.

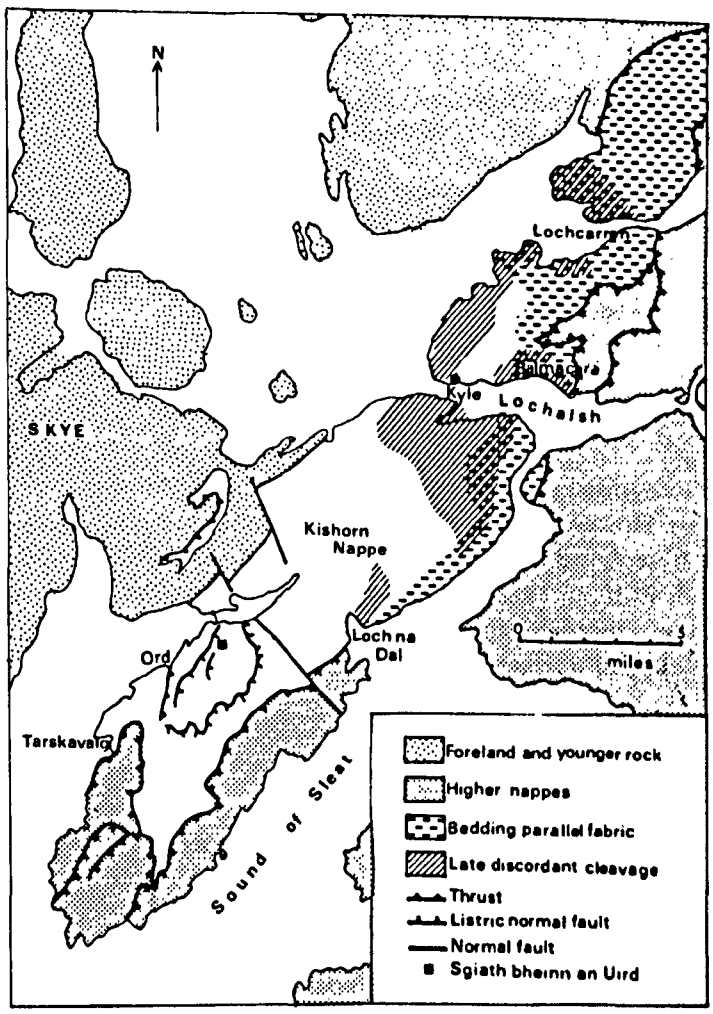

Fig. 1. Southern end of the Moine Thrust zone showing the sequence of thrust sheets and the distribution of cleavages within the Kishorn Nappe.

The dip of the inverted limb gradually decreases from around 70° to 20° but maintains an easterly to southeasterly dip. The axial trace of the fold may be followed southwards on to the Isle of Skye until it passes into the Sound of Sleat to the north of Loch na Dal (Peach et al., 1907; Sutton and Watson, 1964).

The normal limb of the Lochalsh Syncline forms the greater part of the Sleat Peninsula and around the villages of Ord and Tarskavaig (Fig. 1) the folds are complicated by further thrusting and faulting. To the west of Ord, an anticlinal fold was recognised by Clough in Peach et al. (1907) and Bailey (1939, 1955), who termed it the Ord Inversion, but Potts (in press) has renamed it the Eishort Anticline. It is a northwesterly verging recumbent anticline of Torridonian and Cambrian rocks and the axial trace may be followed from Tarskavaig to Ord by means of way up criteria. The fold is very tight to isoclinal and the limbs dip at about 30° to the southeast.

Within the Ord Window (Bailey, 1939, 1955), a synclinal fold has been recognized and termed the Ord Syncline. It was originally named by Bailey (op. cit) and Potts (in press) has shown that this major structure is present within all the Cambrian rocks to the east of Ord. The syncline has been disrupted by thrusting and normal faulting but flat lying normal limbs and moderately southeasterly dipping overturned limbs may be easily recognized.

The Ord Syncline forms the structurally lowest fold in the Kishorn Nappe and passes upwards into the Eishort Anticline and then into the Lochalsh Syncline. Results of studies made by the author on the age and distribution of cleavages throughout the fold train are summarized in Fig. 1. In the north, at Loch Carron, Lochalsh and the northern part of Sleat on the Isle of Syke, the earliest fabric is a linear, grain-shape fabric, in which the prolate grains tend to lie with their longest axes within the bedding plane. The fabric is restricted to the overturned limb and was first described by Peach et al. (1907). Kanungo (1956) considered it to be axial planar to the Lochalsh Syncline and Coward and Whalley (1979) came to the same conclusion. It is suggested that this fabric is not axial planar and is related to overturning of the inverted limb. A typical axial ratio for the strain ellipsoid obtained from grain measurements on this overturned limb is 3.2:2.0:1.0.

A southeasterly-dipping, spaced cleavage has been recognized which develops in rocks of the normal limb on the north coast of Sleat and at Lochalsh. Coward and Whalley (1979) considered this cleavage to be related to the axial plane cleavage of the Lochalsh Syncline. However, the cleavage is strongly developed on the normal limb of the Syncline, but it is only locally strong on the inverted limb. Eastwards, particularly on the inverted limb, an east to northeasterly dipping penetrative cleavage is seen. However, this cleavage consistently dips steeper than bedding and must post-date the main inversion (Coward and Whalley, 1979). In view of their similar orientation the author believes that this cleavage and the spaced cleavage are of comparable age and both post-date the main folding. This later cleavage may be followed on to Sleat where it is axial planar to minor folds of silty laminae and early bedding parallel slickensides. The slickensides consist of sheets of quartz fibres on

the bedding surface and presumably formed during the production of the Lochalsh fold. Similar structures have been recognized by Coward and Whalley (1979) around Balmacara village. Measurements of sheet length in the slickensides suggest that these minor folds represent approximately 27% shortening.

Axial planar cleavages may be seen to affect minor folds of the main Lochalsh Syncline (Kanungo, 1956; Potts, unpublished data) and it is thought that they represent the local accommodation of strains around these minor folds. The cleavages are seen at several localities but are of only local significance as minor folds are comparatively rare. To the south of Loch na Dal no cleavages have been recognized within the Kishorn Nappe.

STRAIN DETERMINATION—PIPES

On the west side of Sgiath bheinn an Uird (Fig. 1) a large hinge is exposed which represents a congruous minor fold on the overturned limb of the Ord Syncline (Potts, in press). The hinge is exposed in the Pipe Rock Member (Peach et al., 1907). The pipes are fossil worm burrows and are generally perpendicular to bedding and circular in cross-section when seen in an undeformed rock. There is no ductility contrast between them and the host rock and they form excellent strain markers. The author has applied R_f/ϕ analysis (Ramsay, 1967; Dunnet, 1969; Dunnet and Siddans, 1971) to the axial ratio and orientation of the pipe cross-sections on the

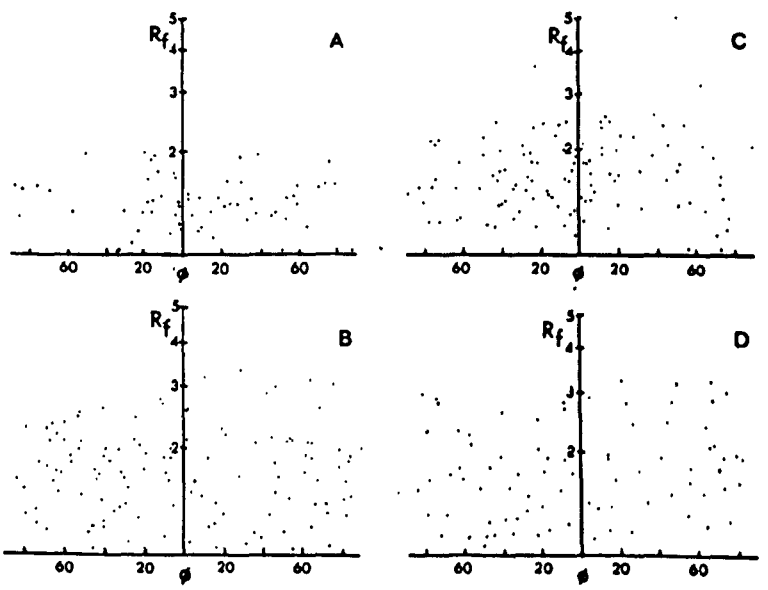

Fig. 2. A typical set of R_f/ϕ analyses taken from the hinge at Sgiath bheinn and Uird. A. Axial ratio and orientation of pipes on the bedding surface. B, C and D. Analysis of grain shape and orientation on three mutually perpendicular surfaces in the bed beneath. The bedding is vertical in this case.

bedding surface at several different dip values around the fold between 23°NW to 76°SE overturned. Corresponding analyses of grain shape and orientation were made in the bed beneath. A typical set of results characteristic of the whole group measured, is presented in Fig. 2. All diagrams of pipe cross section axial ratio and orientation show a complete spread of ϕ values from $-90°$ to $+90°$ suggesting that there was no deformation of the bedding surface and as the pipes are still normal to the bedding there are no bedding parallel ductile shear strains. Within the rock the quartz grains show no preferred orientation of long axes.

A state of no finite strain may exist due to the passage of the rocks along a complex strain path removing a pre-existing strain (Ramsay, 1967) but in thin-section the grains show few deformation microstructures which leads to the conclusion that the rocks record no or very little strain. It is apparent that the rocks attained their intensely folded state on Sleat with no internal deformation.

PALAEOMAGNETIC RESULTS

Within the Applecross Formation of the Eishort Anticline there are no comparable strain markers to the pipes and since the grains show little evidence of deformation an alternative method was applied to see the rocks have been deformed. Measurements were made to determine if the palaeomagnetic direction of Tor-

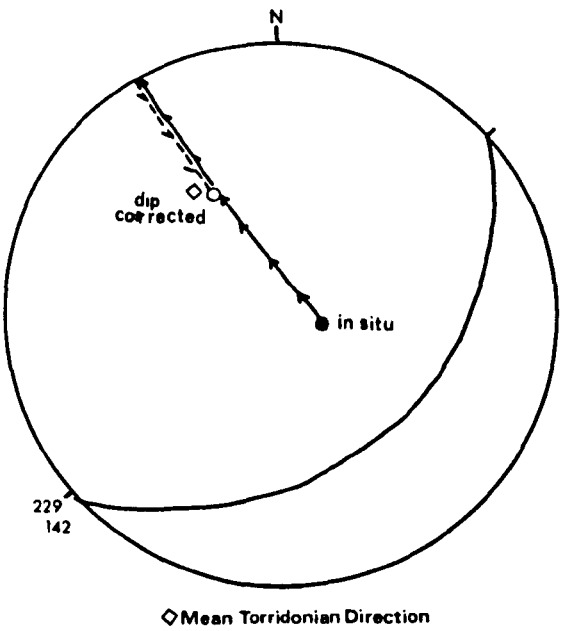

Fig. 3. Equal angle stereographic projection showing that simple rigid body rotation of the bedding about the strike restores a high blocking temperature component to its Torridonian position Stewart and Runcorn (1974).

ridonian age has been reorientated by the folding process. A result in which the measured direction can be restored to a Torridonian position by application of the Graham Fold Test (Graham, 1949) implies no strain. A result in which an angular correction is required for strain by techniques described by Ramsay (1967) implies that internal deformation of the rock has occurred.

During progressive stepwise demagnetization of palaeomagnetic sites in the Applecross Formation around the Eishort Anticline by thermal and alternating field techniques (McElhinny, 1973) a magnetization has been isolated for which a Torridonian direction may be inferred (Potts, unpublished data). In all cases, one of which is presented below (Fig. 3), all such Torridonian directions may be returned to their correct positions by simple rigid body rotation of the bedding about the strike (the fold axis is horizontal).

Consideration of errors involved in the method suggest that a 12° angular change is below the resolution of the technique. A detailed discussion will appear in a subsequent paper. Such a 12° change could allow some flexural flow or tangential longitudinal strain to pass undetected but the close correlation of the dip corrected magnetization direction to the true Torridonian direction (Fig. 3) together with the lack of deformation microstructures suggests that some of the beds in the Applecross Formation have suffered rotation without internal deformation.

CONCLUSION

The strongest fabric seen within the Kishorn Nappe cannot at present be related to the mechanism which produced the fold train. Further work is in progress on the origin of this bedding parallel fabric but since it is not present on the overturned limb of the Eishort Anticline it is not thought to be due to the folding process.

Strain analyses around the Ord Syncline and the Eishort Anticline record no strain, therefore a flexural slip model involving movement on the bedding surfaces is favoured in which the limbs of the fold reach their present position by rigid body rotation. This is in accord with previous work on the structurally higher Lochalsh Syncline (Coward and Whalley, 1979). However, if there is little strain distributed on the limbs of a fold then for geometrical reasons there must be a much greater concentration of strain within the hinge and this is not seen in either the Ord Syncline or the Eishort Anticline and this lack of strain is a problem which is at present unresolved.

The main period of internal deformation and consequential cleavage formation, recorded by the folding of the slickensides post dates the folding process. This work has shown that recumbent fold structures can be developed by thrust related processes with little or no internal deformation and that in more highly strained nappes many of the strains recorded by previous workers may be the response of variably orientated bedding to the later flattening or tightening of the fold structure and not a direct consequence of the folding process.

ACKNOWLEDGEMENTS

This work was carried out during a Natural Environment Research Council studentship at the Department of Earth Sciences, University of Leeds. My thanks are extended to all members of the Department who have provided assistance and discussion, in particular Drs. M.P. Coward and R.J. Knipe who read early manuscripts and to S. Potts for continued support and for typing of an early draft copy.

REFERENCES

Bailey, E.B., 1939. Caledonian tectonics and metamorphism in Skye. Bull. Geol. Surv. G. B., 2: 46–62.

Bailey, E.B., 1955. Moine tectonics and metamorphism in Skye. Trans. Edinb. Geol. Soc., 16: 93–166.

Barber, A.J., 1965. The history of the Moine Thrust zone, Lochcarron and Lochalsh, Scotland. Proc. Geol. Assoc., 76: 215–242.

Cloos, E., 1947. Oolite Deformation in South Mountain Fold, Maryland. Geol. Soc. Am. Bull., 58: 843–918.

Coward, M.P. and Whalley, J.S., 1979. Texture and fabric studies across the Kishorn Nappe, near Kyle of Lochalsh, Western Scotland. J. Struct. Geol., 1: 259–273.

Dunnet, D., 1969. A technique of finite strain analysis using elliptical particles. Tectonophysics, 7: 117–136.

Dunnet, D. and Siddans, A.W.B., 1971. Non-random sedimentary fabrics and their modification by strain. Tectonophysics, 12: 307–325.

Graham, J.W., 1949. The stability and significance of magnetism in sedimentary rocks. J. Geophys. Res., 54: 131–167.

Haug, E., 1900. Les géosyclinaux et les aires continentales. Contributions à l'étude des transgressions et des regressions marine. Bull. Soc. Géol. Fr., T. Ser., 28: 617–711.

Hossack, J.R., 1968. Pebble deformation and thrusting in the Bydin area (Southern Norway). Tectonophysics, 5: 315–339.

Kanungo, D., 1956. The Structural Geology of the Torridonian, Lewisian and Moinian Rocks of the Area between Plockton and Kyle of Lochalsh in Wester Ross, Scotland. Ph.D. Thesis, University of London (unpublished).

McElhinney, M.W., 1973. Palaeomagnetism and Plate Tectonics. Cambridge University Press, Cambridge.

Milton, N.J., 1980. Thrust Related Strain Studies in the Scandinavian Caledonides. Ph.D. Thesis, University of Wales (unpublished).

Peach, B.N., Horne, J., Gunn, W., Clough, C.T. and Hinxman, L.W., 1907. The geological structure of the northwest highlands of Scotland. Mem. Geol. Surv. G.B.

Pfiffner, O.A., 1977. Tektonische Untersuchungen im Infrahelvetikum der Ostschweiz. Mitt. Geol. Inst. Eidg. Tech. Hochsch. Univ. Zurich, N.F., 217: 1–432.

Pfiffner, O.A., 1980. Strain analysis in folds (Infahelvetic complex, Central Alps). Tectonophysics, 61: 337–362.

Potts, G.J., in prep. Revision of the Ord Window, Sleat, Isle of Skye. J. Geol. Soc. London.

Ramsay, J.G., 1967. Folding and Fracturing of Rocks. McGraw-Hill, New York, N.Y., 568 pp.

Stewart, A.D., 1969. Torridonian rocks and Scotland reviewed. Mem. Am. Assoc. Pet. Geol., 12: 595–615.

Stewart, A.D., 1974. Geophys. J.R. Astron. Soc., 37: 51–72.

Sutton, J. and Watson, J. 1964. Some aspects of Torridonian Stratigraphy in Skye. Proc. Geol. Assoc. London, 74: 213–258.

Moane

Onyangen

Rabbalsvann &
Rabbalsvatnet

Rundemellen

Melletjednet

Store kalvemellin

Vesle Kalvemellin

Rognslifjell

Bergo

Langetjednet

Svartetjednet

Skarvemellen

Mellsenn

Valdres
Skiferbrud

1km

N

STRONDAFJORD FORMATION
MELLSENN GROUP
VALDRES SPARAGMITE
AXIAL TRACE

78
77
76
75
74
73
72
6
7
8
9
10
11
12
13
14
15
16

```
C                                                                       ELL00010
C     A PROGRAM TO DETERMINE THE LONG AND SHORT AXES                    ELL00020
C     OF A SUITE OF DEFORMED ELLIPSES. DATA IS OUTPUT AS LONG AXIS      ELL00030
C     SHORT AXIS, RATIO AND ANGLE. THE FOLLOWING ANGLES CONVENTION IS   ELL00040
C     USED THROUGHOUT,                                                  ELL00050
C              *                                                        ELL00060
C            *                                                          ELL00070
C          *                                                            ELL00080
C        *                     - VE                                      ELL00090
C      *                                                                ELL00100
C    *                                                                  ELL00110
C  *                                                                    ELL00120
C  ************************************************                    ELL00130
C  *                                                                    ELL00140
C    *                                                                  ELL00150
C      *                                                                ELL00160
C        *                   + VE                                      ELL00170
C          *                                                            ELL00180
C            *                                                          ELL00190
C                                                                       ELL00200
C     THE HARMONIC MEAN OF RF AND VECTOR MEAN PHI ARE DETERMINED FOR THEELL00210
C     WHOLE SUITE. THE PROGRAM IS DIMENSIONED FOR 500 ELLIPSES.         ELL00220
C                                                                       ELL00230
C     LANGUAGE: IBM STANDARD FORTRAN ON AMDAHL V7, UNIVERSITY OF LEEDS  ELL00240
C      COMPUTER SERVICES.                                               ELL00250
C                                                                       ELL00260
C                                                                       ELL00270
C     G.J.POTTS, STRUCTURAL LABORATORY, DEPT EARTH SCIENCES, UNIVERSITY ELL00280
C      OF LEEDS.                                                        ELL00290
C                                                                       ELL00300
C                                                                       ELL00310
C     INPUT REGUIRMENTS:                                                ELL00320
C                                                                       ELL00330
C     CARD 1 (A9)                                                       ELL00340
C       SPECIMEN REFERENCE FIRST EIGHT CHARACTERS SIGNIFICANT           ELL00350
C                                                                       ELL00360
C     CARD 2 (I3,X,I1)                                                  ELL00370
C      NUMBER OF ELLIPSES N, OPTION NOPT,                               ELL00380
C      FOR PHI + OR - 90 NOPT = 2                                       ELL00390
C      FOR PHI 0 TO 180  NOPT = 1                                       ELL00400
C                                                                       ELL00410
C     CARDS 3 TO N : SEE FORMAT 107                                     ELL00420
C      COORDINATE PAIRS FOR ELLIPSES EXTREMITIES, SEE BELOW             ELL00430
C                                                                       ELL00440
C     THE PROGRAM WAS DESIGNED TO RUN ON PAPER TAPE OUTPUT FROM THE     ELL00450
C     DIGICO PROGRAM COORDS 2 MK 1.1 14/11/75 A.W.B.SIDDANS AND EXPECTS ELL00460
C     INTERGER PAIRS AND A COORDINATE DIFFERENCE OF 0.1 MM.<            ELL00470
C     ALTERNATIVE COORDINATE DIFFERENCES MAY BE USED BY CHANGING THE    ELL00480
C     VALUE OF SCALE                                                    ELL00490
C     THE OUTPUT FROM COORDS 2 IS IN BLOCKS OF SIX IT IS THEREFORE      ELL00500
C     NECESSARY TO ENTER TWO NULL COORDINATE PAIRS WHEN USING THE DMAC  ELL00510
C     DIGITISING TABLE                                                  ELL00520
C                                                                       ELL00530
C                                                                       ELL00540
C                                                                       ELL00550
```

```
C                                                                       ELL00560
C                                                                       ELL00570
C                                                                       ELL00580
C                                                                       ELL00590
C                                                                       ELL00600
C                                                                       ELL00610
C                                          XC,YC *                      ELL00620
C                                                                       ELL00630
C                                                                       ELL00640
C                                    XB,YB *                            ELL00650
C                                                * XD,YD                ELL00660
C                                                                       ELL00670
C                                                                       ELL00680
C                                          * XA,YA                      ELL00690
C                                                                       ELL00700
C                                                                       ELL00710
C     THE EXTREMITIES OF THE ELLIPSE MUST BE DIGITISED IN THE ORDER     ELL00720
C     A TO D THE A COORDINATE PAIR HAVING THE SMALLER VALUE OF X        ELL00730
C     AND THE B COORDINATE PAIR HAVING THE LARGER VALUE OF Y.           ELL00740
C     THIS PROGRAM WAS MODIFIED TO RUN ON PAPER TAPE OUTPUT FROM THE    ELL00750
C     D-MAC TABLE AND EXPECTS 4 COORDINATE PAIRS OF INTEGERS.           ELL00760
C     THE REMAINING DATA IS IGNORED. THE PROGRAM COULD BE EXTENDED TO   ELL00770
C     SORT THE DATA POINTS BUT IN PRACTICE IT IS MORE IMPORTANT FOR     ELL00780
C     THE OPERATOR TO DEVELOP A PATTERN DURING DIGITISING.              ELL00790
C                                                                       ELL00800
      DIMENSION RF(500),PHI(500),X(500),Y(500),AAXIS(500),BAXIS(500)    ELL00810
      COMMON /GRAPH/ TITLE(20)                                          ELL00820
      COMMON /GREF/ XMAX,XMIN,YMAX,YMIN,INDX,INDY,IND,                  ELL00830
     1IDOT,ANSTR1,XXN,XXM,YYN,YYM                                       ELL00840
      INTEGER ANSTR1                                                    ELL00850
      CHARACTER*8 TITLE,HEAD(7),SHORT,AXIS,BLANK,ALONG,BLONG,RFT,PHIT   ELL00860
      SHORT="SHORT AX"                                                  ELL00870
      AXIS='IS    MM'                                                   ELL00880
      ALONG="LONG AXI"                                                  ELL00890
      BLONG="S     MM"                                                  ELL00900
      BLANK="        "                                                  ELL00910
      RFT='RF      '                                                    ELL00920
      PHIT="PHI     "                                                   ELL00930
      XXN=0.0                                                           ELL00940
      XXM=1.0                                                           ELL00950
      YYN=0.0                                                           ELL00960
      YYM=1.0                                                           ELL00970
      NSETS=1                                                           ELL00980
      WRITE(8,98)NSETS                                                  ELL00990
C     READ AND WRITE SPECIMEN HEADING                                   ELL01000
      READ(5,99)(HEAD(I),I=1,7)                                         ELL01010
      WRITE(7,100)                                                      ELL01020
      WRITE(7,101)(HEAD(I),I=1,7)                                       ELL01030
      WRITE(8,99)(HEAD(I),I=1,7)                                        ELL01040
      TITLE(1)=SHORT                                                    ELL01050
      TITLE(2)=AXIS                                                     ELL01060
      TITLE(3)=BLANK                                                    ELL01070
      TITLE(4)=ALONG                                                    ELL01080
      TITLE(5)=BLONG                                                    ELL01090
      TITLE(6)=BLANK                                                    ELL01100
```

```
      DO 30 I=1,7                                                        ELL01110
   30 TITLE(I+7)=HEAD(I)                                                 ELL01120
C     READ AND WRITE NUMBER OF ELLIPSES                                  ELL01130
      READ(5,102)N,NOPT                                                  ELL01140
      WRITE(7,103)N                                                      ELL01150
      WRITE(8,105)N                                                      ELL01160
      WRITE(7,106)                                                       ELL01170
C     SET COUNTS TO ZERO AND SET CONVERSION FACTOR                       ELL01180
      SCALE=500.0                                                        ELL01190
      TOTSIN=0.0                                                         ELL01200
      TOTCOS=0.0                                                         ELL01210
      TOTINV=0.0                                                         ELL01220
      NE=0                                                               ELL01230
      CONFAC=57.2957795                                                  ELL01240
C     READ DATA                                                          ELL01250
      DO 1 I=1,N                                                         ELL01260
      NE=NE+1                                                            ELL01270
      READ(5,107)IXA,IYA,IXB,IYB,IXC,IYC,IXD,IYD                         ELL01280
C     SET UP THE TRIANGLES AND DETERMINE PHI                             ELL01290
      J=IXC-IXA                                                          ELL01300
      O=FLOAT(J)                                                         ELL01310
      K=IYC-IYA                                                          ELL01320
      P=FLOAT(K)                                                         ELL01330
      L=IXD-IXB                                                          ELL01340
      Q=FLOAT(L)                                                         ELL01350
      M=IYB-IYD                                                          ELL01360
      R=FLOAT(M)                                                         ELL01370
      IF(O.EQ.0.0) GOTO 2                                                ELL01380
      PHIR=ATAN(P/O)*(-1.0)                                              ELL01390
      PHI(I)=PHIR*CONFAC                                                 ELL01400
      GOTO 3                                                             ELL01410
    2 PHI(I)=90.0                                                        ELL01420
    3 CONTINUE                                                           ELL01430
C     ASSIGN SIGN OF PHI ACCORDING TO OPTION                             ELL01440
      DO 4 II=1,N                                                        ELL01450
      IF(NOPT.EQ.1.AND.PHI(II).LT.0.0) PHI(II)=PHI(II)+180.0             ELL01460
    4 CONTINUE                                                           ELL01470
C     DETERMINE THE LONG AND SHORT AXES OF THE ELLIPSE                   ELL01480
      O=ABS(O)                                                           ELL01490
      P=ABS(P)                                                           ELL01500
      Q=ABS(Q)                                                           ELL01510
      R=ABS(R)                                                           ELL01520
      SQDAX1=P*P+O*O                                                     ELL01530
      CAXIS=SQRT(SQDAX1)                                                 ELL01540
      AAXIS(I)=CAXIS/SCALE                                               ELL01550
      SQDAX2=Q*Q+R*R                                                     ELL01560
      DAXIS=SQRT(SQDAX2)                                                 ELL01570
      BAXIS(I)=DAXIS/SCALE                                               ELL01580
      RF(I)=AAXIS(I)/BAXIS(I)                                            ELL01590
C     CHECK THAT RF ALWAYS GREATER THAN 1.0 AND ASSIGN APPROPRIATE ANGLE ELL01600
      IF(RF(I).LT.1.0) GOTO 22                                           ELL01610
      GOTO 23                                                            ELL01620
   22 RF(I)=1.0/RF(I)                                                    ELL01630
      IF(PHI(I).LT.0.0) GOTO 24                                          ELL01640
      PHI(I)=PHI(I)-90.0                                                 ELL01650
```

```
      IF(NOPT.EQ.1.AND.PHI(I).LT.0.0) PHI(I)=PHI(I)+180.0                ELL01660
      GOTO 23                                                            ELL01670
 24   PHI(I)=PHI(I)+90.0                                                 ELL01680
C     WRITE THE VALUES DETERMINED                                        ELL01690
 23   WRITE(7,108)NE,AAXIS(I),BAXIS(I),RF(I),PHI(I)                     ELL01700
      WRITE(8,109)RF(I),PHI(I)                                           ELL01710
C     CALCULATE VECTOR MEAN OF PHI AND HARMONIC MEAN OF RF               ELL01720
      TOTSIN=TOTSIN+SIN(PHIR)                                            ELL01730
      TOTCOS=TOTCOS+COS(PHIR)                                            ELL01740
   1  TOTINV=TOTINV+1.0/RF(I)                                            ELL01750
      RR=SQRT(TOTSIN*TOTSIN+TOTCOS*TOTCOS)                               ELL01760
      VR=ATAN(TOTSIN/TOTCOS)                                             ELL01770
      V=VR*CONFAC                                                        ELL01780
      IF(NOPT.EQ.1.AND.V.LT.0.0)V=V+180.0                                ELL01790
      HM=N/TOTINV                                                        ELL01800
C     WRITE OUT VECTOR MEANOF PHI AND HARMONIC MEAN OF RF                ELL01810
      WRITE(7,110)HM,V                                                   ELL01820
C     DRAW NECESSARY GRAPHS                                              ELL01830
      INDX=1                                                             ELL01840
      INDY=1                                                             ELL01850
      ANSTR1=1                                                           ELL01860
      IND=1                                                              ELL01870
      IDOT=245                                                           ELL01880
      DO 5 I=1,N                                                         ELL01890
      X(I)=BAXIS(I)                                                      ELL01900
      Y(I)=AAXIS(I)                                                      ELL01910
 5    CONTINUE                                                           ELL01920
      CALL AMAXN(X,N,WXMAX)                                              ELL01930
      CALL AMAXN(Y,N,WYMAX)                                              ELL01940
      IF(WXMAX.GT.WYMAX)GOTO 6                                           ELL01950
      WXMAX=WYMAX                                                        ELL01960
      GOTO 7                                                             ELL01970
 6    WYMAX=WXMAX                                                        ELL01980
 7    CONTINUE                                                           ELL01990
      XMAX=WXMAX                                                         ELL02000
      XMIN=0.0                                                           ELL02010
      YMAX=WYMAX                                                         ELL02020
      YMIN=0.0                                                           ELL02030
      CALL PAPER(1)                                                      ELL02040
      CALL PEN(3)                                                        ELL02050
      CALL CARGRF(X,Y,N)                                                 ELL02060
      INDY=2                                                             ELL02070
      DO 8 I=1,N                                                         ELL02080
      X(I)=PHI(I)                                                        ELL02090
      Y(I)=RF(I)                                                         ELL02100
 8    CONTINUE                                                           ELL02110
      CALL AMAXN(Y,N,WYMAX)                                              ELL02120
      YMAX=10.0                                                          ELL02130
      YMIN=1.0                                                           ELL02140
      IF(WYMAX.GT.YMAX)YMAX=WYMAX                                        ELL02150
      IF(NOPT.EQ.1)GOTO 10                                               ELL02160
      XMAX=90.0                                                          ELL02170
      XMIN=-90.0                                                         ELL02180
      GOTO 11                                                            ELL02190
 10   XMAX=180.0                                                         ELL02200
```

```
      XMIN=0.0                                                          ELL02210
   11 CONTINUE                                                          ELL02220
      TITLE(1)=PHIT                                                     ELL02230
      TITLE(2)=BLANK                                                    ELL02240
      TITLE(5)=BLANK                                                    ELL02250
      TITLE(4)=RFT                                                      ELL02260
      CALL CARGRF(X,Y,N)                                                ELL02270
      CALL GREND                                                        ELL02280
      STOP                                                              ELL02290
   98 FORMAT(I2)                                                        ELL02300
   99 FORMAT(7A8)                                                       ELL02310
  101 FORMAT(1X,7A8)                                                    ELL02320
  100 FORMAT(1H1)                                                       ELL02330
  102 FORMAT(I3,1X,I1)                                                  ELL02340
  103 FORMAT(1H0,2X,19HNUMBER OF ELLIPSES=,I3)                          ELL02350
  105 FORMAT(I3)                                                        ELL02360
  106 FORMAT(1H0,3HNUM,2X,6HA AXIS,4X,6HB AXIS,5X,5HRATIO,3X,5HANGLE)   ELL02370
  107 FORMAT(2I5,2X,2I5,2X,2I5,2X,2I5)                                  ELL02380
  108 FORMAT(1H0,I3,3F10.5,2X,F6.2)                                     ELL02390
  109 FORMAT(F5.2,F8.1)                                                 ELL02400
  110 FORMAT(1H0,14HHARMONIC MEAN=,F5.2,2X,6HVMPHI=,F6.2)               ELL02410
      END                                                               ELL02420
      SUBROUTINE AMAXN(X,N,XMAX)                                        ELL02430
      REAL*4 X(N)                                                       ELL02440
C                                                                       ELL02450
      KQ=1                                                              ELL02460
    2 KP=KQ                                                             ELL02470
    5 IF(KQ-N)3,4,4                                                     ELL02480
    3 KQ=KQ+1                                                           ELL02490
      IF(X(KP)-X(KQ))2,5,5                                              ELL02500
    4 XMAX=X(KP)                                                        ELL02510
      RETURN                                                            ELL02520
      END                                                               ELL02530
      SUBROUTINE AMINN(X,N,XMIN)                                        ELL02540
      REAL*4 X(N)                                                       ELL02550
C                                                                       ELL02560
      KQ=1                                                              ELL02570
    2 KP=KQ                                                             ELL02580
    5 IF(KQ-N)3,4,4                                                     ELL02590
    3 KQ=KQ+1                                                           ELL02600
      IF(X(KP)-X(KQ))5,5,2                                              ELL02610
    4 XMIN=X(KP)                                                        ELL02620
      RETURN                                                            ELL02630
      END                                                               ELL02640
      SUBROUTINE CARGRF(X,Y,N)                                          ELL02650
C     NEW IMPROVED CARGRF                                               ELL02660
C                                                                       ELL02670
C                                                                       ELL02680
C     FROM THE CALL CARGRF(X,Y,N) THIS PACKAGE PLOTS N POINTS           ELL02690
C     THE CARTESIAN COORDINATES OF THE ITH POINT BEING SPECIFIED AS      ELL02700
C     X(I),Y(I).                                                        ELL02710
C                                                                       ELL02720
C     THE TITLE IS READ IN VIA THE COMMON /GRAPH/.                      ELL02730
C     THE REAL*8 ARRAY IS DIVIDED THUS:                                 ELL02740
C                                                                       ELL02750
```

```
C                                                                       ELL02760
C     TITLE(1,2,3)  CONTAINS THE UNITS OF THE ABSCISSAE                 ELL02770
C                                                                       ELL02780
C     TITLE(4,5)    CONTAINS THE UNITS OF THE ORDINATE                  ELL02790
C                                                                       ELL02800
C     TITLE(6)      USUALLY BLANK                                       ELL02810
C                                                                       ELL02820
C     TITLE(7-14)   CONTAINS TITLE OF THE PLOT (64 CHARS)               ELL02830
C                                                                       ELL02840
C     TITLE(15-20)  NOT USED                                            ELL02850
C                                                                       ELL02860
C     THE PLOTTING OPTIONS ARE CONTAINED IN THE COMMON /GREF/.          ELL02870
C     THESE ARE:                                                        ELL02880
C                                                                       ELL02890
C     XMAX ) SET BOTH EQUAL IF PROGRAM TO CHOOSE THE ABSCISSAE          ELL02900
C     XMIN ) SCALE, OTHERWISE SET TO CHOSEN PSPACE OF ABSCISSAE SCALE   ELL02910
C     YMAX ) SET BOTH EQUAL IF PROGRAM TO CHOOSE THE ORDINATE SCALE     ELL02920
C     YMIN ) OTHERWISE SET TO CHOSEN VALUES OF ORDINATE SCALE           ELL02930
C                                                                       ELL02940
C     INDX IS AN INDICATOR FOR PLOTTING THE ABSCISSAE ON A LOG SCALE    ELL02950
C     INDX=1 ABSCISSAE ON LINEAR SCALE                                  ELL02960
C     INDX=2 ABSCISSAE ON LOG SCALE                                     ELL02970
C     INDY IS A SIMILAR INDICATOR FOR THE ORDINATE SCALE                ELL02980
C                                                                       ELL02990
C        DON'T REQUEST LOG AXES IF ANY DATA ARE -VE....                 ELL03000
C        ---------------------------------------------                  ELL03010
C                                                                       ELL03020
C     IND = 0  CALL NEW FRAME.  PLOT AXES AND TITLE ONLY                ELL03030
C     IND = 1 CALL ANOTHER FRAME.  PLOT ALL DATA                        ELL03040
C     IND = 2 PLOTS ON THE CURRENT FRAME WITH NEW AXES                  ELL03050
C     IND = 3 PLOTS ON THE CURRENT FRAME WITH THE SAME AXES             ELL03060
C     IND = 4 PLOTS AXES AND TITLE ONLY ON CURRENT FRAME                ELL03070
C                                                                       ELL03080
C     IDOT IS THE CODE OF THE REQUIRED PLOTTING SYMBOL                  ELL03090
C                                                                       ELL03100
C     ANSTR1=1 POINTS NOT JOINED                                        ELL03110
C     ANSTR1=2 POINTS JOINED WITHOUT MARKING DATA POINTS                ELL03120
C     ANSTR1=3 POINTS JOINED AND DATA POINTS MARKED                     ELL03130
C     ANSTR1=4 POINTS JOINED BY SMOOTH FIT                              ELL03140
C                                                                       ELL03150
C     THE PHYSICAL AREA OF THE PLOT IS (XXN,XXM,YYN,YYM)                ELL03160
C                                                                       ELL03170
      DIMENSION X(N),Y(N)                                               ELL03180
      COMMON /GRAPH/ TITLE(20)                                          ELL03190
      COMMON /GREF/ XMAX,XMIN,YMAX,YMIN,INDX,INDY,IND,                  ELL03200
     1IDOT,ANSTR1,XXN,XXM,YYN,YYM                                       ELL03210
      REAL*8 TITLE                                                      ELL03220
      INTEGER ANSTR1                                                    ELL03230
C                                                                       ELL03240
C                                                                       ELL03250
      XC(A1,A2,A3,A4)=(A1-A2)/(A3-A4)                                   ELL03260
      IF(IND.LT.0.OR.IND.GT.4)IND=1                                     ELL03270
      IF(INDX.NE.2)INDX=1                                               ELL03280
      IF(INDY.NE.2)INDY=1                                               ELL03290
      IF(ANSTR1.LT.1.OR.ANSTR1.GT.4)ANSTR1=2                            ELL03300
```

```
C                                                                       ELL03310
C FIND MAX AND MIN OF AXES                                              ELL03320
C                                                                       ELL03330
      IF(XMAX-XMIN)110,120,110                                          ELL03340
  110 XMX=XMAX                                                          ELL03350
      XMN=XMIN                                                          ELL03360
      GO TO 130                                                         ELL03370
  120 CALL AMAXN(X,N,XMX)                                               ELL03380
      CALL AMINN(X,N,XMN)                                               ELL03390
  130 IF(YMAX-YMIN)140,150,140                                          ELL03400
  140 YMX=YMAX                                                          ELL03410
      YMN=YMIN                                                          ELL03420
      GO TO 160                                                         ELL03430
  150 CALL AMAXN(Y,N,YMX)                                               ELL03440
      CALL AMINN(Y,N,YMN)                                               ELL03450
C                                                                       ELL03460
C TO CHECK IF ASSIGNED LOG AXES, NO VALUES ARE NEGATIVE                 ELL03470
C                                                                       ELL03480
  160 GOTO(162,161),INDX                                                ELL03490
  161 IF(XMN.LE.0.)GOTO900                                              ELL03500
  162 GOTO(164,163),INDY                                                ELL03510
  163 IF(YMN.LE.0.)GOTO900                                              ELL03520
C                                                                       ELL03530
C TO ASSIGN REGIONS, CHECK FOR MINS LT 0, AND PLOT THE CURVES           ELL03540
C                                                                       ELL03550
  164 IF(IND.LE.1)CALL FRAME                                            ELL03560
      XXX=XXM-XXN                                                       ELL03570
      YYY=YYM-YYN                                                       ELL03580
      X1=XXN+XXX*.15                                                    ELL03590
      X2=XXN+XXX*.85                                                    ELL03600
      Y1=YYN+YYY*.15                                                    ELL03610
      Y2=YYN+YYY*.85                                                    ELL03620
      XV=XMN                                                            ELL03630
      IF(XV.LT.0.)XV=0.                                                 ELL03640
      IF(XMX.LT.0.)XV=XMX                                               ELL03650
      YV=YMN                                                            ELL03660
      IF(YV.LT.0.)YV=0.                                                 ELL03670
      IF(YMX.LT.0.)YV=YMX                                               ELL03680
      PTX=(YMX-YMN)/100.                                                ELL03690
      CALL PSPACE(X1,X2,Y1,Y2)                                          ELL03700
      GOTO (20,10),INDX                                                 ELL03710
   10 IF(INDY.EQ.1)GOTO30                                               ELL03720
      CALL MAPXYL(XMN,XMX,YMN,YMX)                                      ELL03730
      GOTO50                                                            ELL03740
   30 CALL MAPXL(XMN,XMX,YMN,YMX)                                       ELL03750
      GOTO50                                                            ELL03760
   20 IF(INDY.EQ.1)GOTO40                                               ELL03770
      CALL MAPYL(XMN,XMX,YMN,YMX)                                       ELL03780
      GOTO50                                                            ELL03790
   40 CALL MAP(XMN,XMX,YMN,YMX)                                         ELL03800
   50 IF(IND.LT.1.OR.IND.GT.3)GOTO170                                   ELL03810
      GOTO(220,230,220,240),ANSTR1                                      ELL03820
  220 CALL CTRSIZ(PTX)                                                  ELL03830
      IF(INDY.EQ.2)CALL CTRMAG(10)                                      ELL03840
      DO 215 I=1,N                                                      ELL03850
```

```
  215 CALL PLOTNC(X(I),Y(I),IDOT)                                    ELL03860
      IF(ANSIR1.NE.3)GOTO170                                         ELL03870
  230 CALL POINT(X(1),Y(1))                                          ELL03880
      DO 271 I=1,N                                                   ELL03890
  271 CALL JOIN(X(I),Y(I))                                           ELL03900
      GOTO170                                                        ELL03910
  240 CALL CURVE0(X,Y,1,N)                                           ELL03920
C                                                                    ELL03930
C                                                                    ELL03940
C AXIS DRAWING CALLS....LIBRARY ROUTINES NOT EMPLOYED FOR            ELL03950
C  EXPONENTIAL ANNOTATION OF AXES.                                   ELL03960
C                                                                    ELL03970
  170 IF(IND.GT.2)GOTO800                                            ELL03980
      IF(INDX.EQ.2)GOTO190                                           ELL03990
      CALL CTRSIZ(PTX*1.5)                                           ELL04000
      IF(INDY.EQ.2)CALL CTRMAG(12)                                   ELL04010
      IF((XMN-XMN).LE.9999.)GOTO189                                  ELL04020
      XGRD=(XMX-XMN)/6.                                              ELL04030
      YY=(YMX-YMN)/7.                                                ELL04040
      YPIP=YY*0.1                                                    ELL04050
      DO 171 I=1,5                                                   ELL04060
      PT=XGRD*I+XMN                                                  ELL04070
      CALL POINT(PT,YV)                                              ELL04080
  171 CALL JOIN(PT,YPIP)                                             ELL04090
      CALL POINT(XMN,YV)                                             ELL04100
      CALL JOIN(XMX,YV)                                              ELL04110
      X1=X1-XXX*.1                                                   ELL04120
      CALL PSPACE(X1,X2,YYN,Y2)                                      ELL04130
      CALL MAP(XMN,XMX,0.,0.85)                                      ELL04140
      YCOR=XC(.7,0.,YMX,YMN)*(YV-YMN)                                ELL04150
      CALL CTRSIZ(.006)                                              ELL04160
      DO 172 I=1,5                                                   ELL04170
      PT=XGRD*I+XMN                                                  ELL04180
  172 CALL PLOTNE(PT,(.07+YCOR),PT,2)                                ELL04190
C                                                                    ELL04200
C RESTORE PLOTTING AREA                                              ELL04210
C                                                                    ELL04220
      X1=X1+XXX*.1                                                   ELL04230
      CALL PSPACE(X1,X2,Y1,Y2)                                       ELL04240
      CALL MAP(XMN,XMX,YMN,YMX)                                      ELL04250
      GOTO200                                                        ELL04260
  189 DX=(XMX-XMN)*10.                                               ELL04270
      IX=DX/10                                                       ELL04280
      DX=FLOAT(IX)/10.                                               ELL04290
      CALL XAXISI(DX)                                                ELL04300
      GOTO200                                                        ELL04310
  190 IF(INDX.EQ.INDY)GOTO191                                        ELL04320
      CALL XAXISL                                                    ELL04330
      GOTO201                                                        ELL04340
  191 CALL AXEXYL                                                    ELL04350
      GOTO301                                                        ELL04360
  200 IF(INDY.EQ.2)GOTO300                                           ELL04370
  201 CALL CTRSIZ(PTX*1.5)                                           ELL04380
      IF(INDX.EQ.2)CALL CTRMAG(12)                                   ELL04390
      IF((YMX-YMN).LE.9999.)GOTO299                                  ELL04400
```

```
      YGRD=(YMX-YMN)/6.                                          ELL04410
      XX=(XMX-XMN)/7.                                            ELL04420
      XPIP=XX*0.1                                                ELL04430
      DO 205 I=1,5                                               ELL04440
      PT=YGRD*I+YMN                                              ELL04450
      CALL POINT(XV,PT)                                          ELL04460
  205 CALL JOIN(XPIP,PT)                                         ELL04470
      CALL POINT(XV,YMN)                                         ELL04480
      CALL JOIN(XV,YMX)                                          ELL04490
      CALL PSPACE(XXN,X2,Y1,Y2)                                  ELL04500
      CALL MAP(0.,.85,YMN,YMX)                                   ELL04510
      XCOR=XC(.7,0.,XMX,XMN)*(XV-XMN)                            ELL04520
      CALL CTRSIZ(.075*YGRD)                                     ELL04530
      DO 210 I=1,5                                               ELL04540
      PT=YGRD*I+YMN                                              ELL04550
  210 CALL PLOTNE((.11+XCOR),PT,PT,2)                            ELL04560
      GOTO301                                                    ELL04570
  299 DY=(YMX-YMN)*10.                                           ELL04580
      IX=DY/10                                                   ELL04590
      DY=FLOAT(IX)/10.                                           ELL04600
      CALL YAXISI(DY)                                            ELL04610
      GOTO301                                                    ELL04620
  300 CALL YAXISL                                                ELL04630
C                                                                ELL04640
C ANNOTATE GRAPH                                                 ELL04650
C                                                                ELL04660
  301 XCOR=XC(7.,0.,XMX,XMN)*(XV-XMN)                            ELL04670
      YCOR=XC(7.,0.,YMX,YMN)*(YV-YMN)                            ELL04680
      IF(XMX.LT.0)XCOR=0                                         ELL04690
      IF(YMX.LT.0)YCOR=0                                         ELL04700
      CALL PSPACE(XXN,XXM,YYN,YYM)                               ELL04710
      CALL MAP(0.0,10.0,0.0,10.0)                                ELL04720
      CALL CTRSIZ(.2)                                            ELL04730
      CALL CTROBL(1.3)                                           ELL04740
      CALL PLOTCS(6.5,(0.65+YCOR),TITLE(1),8)                    ELL04750
      CALL TYPECS(TITLE(2),8)                                    ELL04760
      CALL TYPECS(TITLE(3),8)                                    ELL04770
      CALL POSITN((.85+XCOR),8.1)                                ELL04780
      CALL CTRORI(270.)                                          ELL04790
      CALL CTRANG(90.)                                           ELL04800
      CALL TYPECS(TITLE(4),8)                                    ELL04810
      CALL TYPECS(TITLE(5),8)                                    ELL04820
      CALL CTRORI(0.)                                            ELL04830
      CALL CTRANG(0.)                                            ELL04840
      CALL CTROBL(1.)                                            ELL04850
      CALL CTRSIZ(.3)                                            ELL04860
      CALL PLOTCS(2.,9.15,TITLE(6),8)                            ELL04870
      CALL ITALIC(1)                                             ELL04880
      DO 700 I=7,14                                              ELL04890
  700 CALL TYPECS(TITLE(I),8)                                    ELL04900
      CALL ITALIC(0)                                             ELL04910
C                                                                ELL04920
  800 RETURN                                                     ELL04930
  900 WRITE(6,1000)                                              ELL04940
 1000 FORMAT(' GRAPH PLOT ABANDONED - ATTEMPT TO DRAW LOG AXES',  ELL04950
```

```
*       /' IC NEGATIVE DATA POINTS. CHECK DATA OR INDX/Y')          ELL04960
      RETURN                                                        ELL04970
      END                                                           ELL04980
```

PRINT COMPLETED AT 18:35:25 FOR USER: EAR6MPC DIST: EAR6MPC

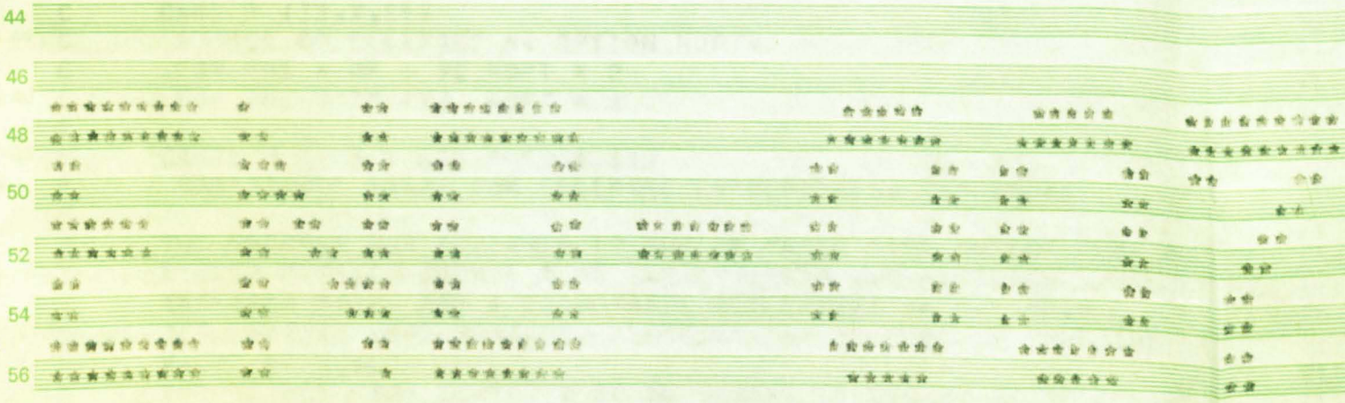

Fig 2.C.8

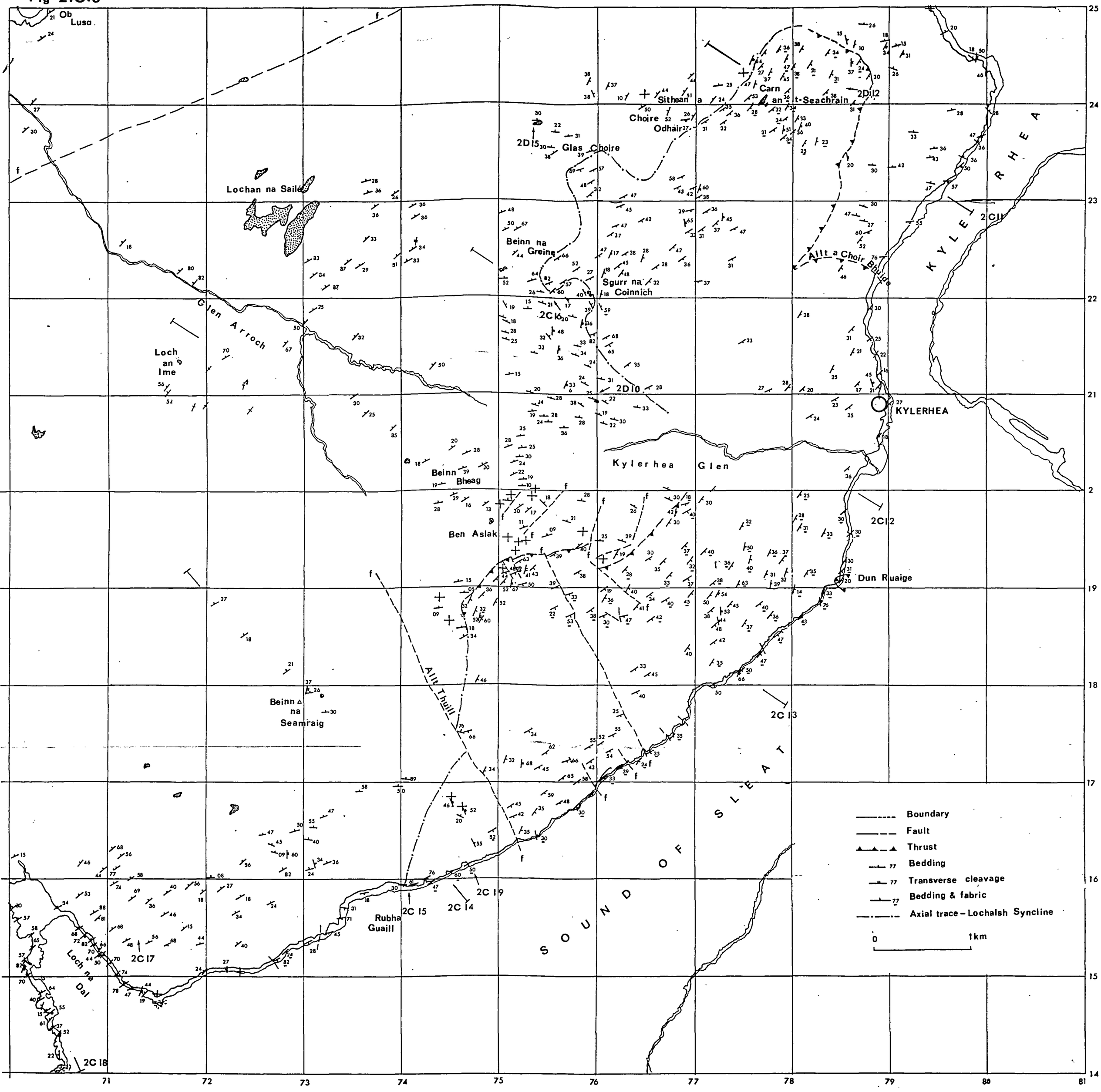
Ob Lusa
Lochan na Saile
Glen Arroch
Loch an Ime
Beinn na Greine
2D15
Glas Choire
Choire Odhair
Sithean a Carn an t-Seachrain
2D12
Sgurr na Coinnich
2C16
2D10
Allt a Choir Bhuidhe
KYLE RHEA
2C11
KYLERHEA
Kylerhea Glen
Beinn Bheag
Ben Aslak
2C12
Dun Ruaige
Allt Thuill
Beinn na Seamraig
2C13
SOUND OF SLEAT
2C19
2C14
2C15
Rubha Guaill
2C17
Loch na Dal
2C18
Boundary
Fault
Thrust
Bedding
Transverse cleavage
Bedding & fabric
Axial trace – Lochalsh Syncline
0
1km
71
72
73
74
75
76
77
78
79
80
81
25
24
23
22
21
2
19
18
17
16
15
14

LOCHALSH

An Dubh Aird

2C7

2C5
2C3

PLOCKTON

Craig

4A1.2

2C7

2D9
2C6
2C3

Port Cam

2D7

Dorch

Gleannan

2F3

Loch Iain Oig

Sgurr Beag

BALMACARA

Balmacara Thrust

2C7

KYLE

2C7

Ard Hill

L O C H A L S H

Cnoc na Loch

2C4

Loch na Beiste Fault

Fault

Boundary

Thrust

Bedding

Bedding & fabric

Mylonitic fabric

Transverse & Axial planar Cleavage

Epidotic Grit

Lewisian

Axial trace – Lochalsh Syncline

0 1 km

35
34
33
32
31
30
29

75
76
77
78
79
80
81
82
83